

Quantum Information and Quantum Gravity in Anti-De Sitter and Cosmological Spacetimes

Dissertation
zur
Erlangung des Doktorgrades (Dr. rer. nat.)
der
Mathematisch-Naturwissenschaftlichen Fakultät
der
Rheinischen Friedrich-Wilhelms-Universität Bonn

von
Joshua Kames-King
aus
Slough, UK

Bonn, 22.09.2022

Angefertigt mit Genehmigung der Mathematisch-Naturwissenschaftlichen Fakultät der Rheinischen
Friedrich-Wilhelms-Universität Bonn

1. Gutachter: Priv. Doz. Stefan Förste
2. Gutachterin: Prof. Dr. Albrecht Klemm

Tag der Promotion: 22.09.2022
Erscheinungsjahr: 2022

Für Mama und Oma.

Acknowledgements

First of all I would like to give special thanks to Stefan Förste for his supervision during my PhD studies. It was and is a huge pleasure working with him and learning from his sharp perception. I especially appreciate the tolerance to all of my numerous silly questions! Furthermore the friendly atmosphere is not only conducive to great discussions but allowed me to develop independently and pursue my own vision. Moreover, I am very grateful for the help in making career decisions. In a similar spirit I would also like to thank Hans Jockers for many hours of discussions, great collaborations and his input in my decisions. I would also like to thank Albrecht Klemm for being my second referee again and all current and former members of his string theory group for many interesting discussions. My thanks go to Mahsa Barzegar, Kilian Bönisch, Cesar Fierro Cota, Fabian Fischbach, Andreas Gerhardus, Thaisa Guio, Abhinav Joshi, Marvin Kohlmann, Urmi Ninad, Reza Safari, Thorsten Schimannek. I would also like to thank other current and former members of the Bethe Center such as Dominik Köhler, Hans Peter Nilles, Saurabh Natu and Saurabh Nangia, Jonas Schneegans, Iris Golla, Ruben Campos Delgado. Here I would especially like to highlight Christoph Liyanage, Christoph Nega and Andreas Gerhardus for all the fun times. I also want to thank everybody "behind the scenes": Christa Börsch, Petra Weiß, Andreas Wisskirchen, Patrizia Zündorf. Without you the BCTP would fall apart. I will miss this place.

As time moved on I had the pleasure of also visiting different universities and institutes. I would like to thank the Kavli Institute for Theoretical Physics and Lars Bildsten for hospitality and David Gross for mentorship in the Graduate Fellowship program. I would also like to thank Erik Verlinde and Evita Verheijden and the University of Amsterdam for hospitality and great collaborations.

My gratitude also goes out to those collaborators, whom I have not yet mentioned. In no particular order: Mohsen Alishahiha, Souvik Banerjee, Max Wiesner, Julian Sonner, Pranjal Nayak, Adrian Sanchez-Garrido, Alexandros Kanargias, Bob Knighton, Misha Usatyuk. I learned a lot from all of you.

Finally, my biggest thank is to my family. I would like to thank my father Andrew and Tante Uschi for support. And of course Oma and Mama for enduring support, love and encouragement. I would also like to thank Antonia for providing the right kind of distraction and making life even more enjoyable.

Summary

The holographic principle constitutes a guiding principle for the construction of a quantum theory of gravity. While the final goal is the application of such a theory to our own universe, the most concrete instantiation of the holographic principle derives from string theory on Anti-de Sitter (AdS) spacetimes: the AdS/CFT correspondence. It is this framework with which most of this thesis is concerned. In the first part of this work we consider a supersymmetric extension of a prominent two-dimensional duality: JT gravity on AdS_2 and the SYK model. We first demonstrate that the derivation of the Schwarzian boundary action may be generalised to the $\mathcal{N} = (2)$ super-Schwarzian. We show that the analysis of low-energy modes on a 1/4 BPS background on AdS_4 reduces to the calculation of matter coupled to the super-Schwarzian as determined from $\mathcal{N} = (2, 2)$ JT supergravity. We continue in the framework of JT gravity. More specifically we consider a duality between JT gravity on hyperbolic Riemann surfaces (with an arbitrary number of genera and asymptotic boundaries) and the genus expansion of a specific double-scaled matrix integral. In the language of topological gravity we show how the theory may be generalised to arbitrary deformations and how such deformations affect the spectral form factor. We then move on to the analysis of a specific quantum information quantity in the context of the AdS/CFT correspondence: complexity. We demonstrate that the universal Lloyd's bound, an upper bound on information processing, implies that complexity as a holographic probe may not penetrate behind the inner horizon of a charged black hole. Moreover, we also show how to define complexity non-perturbatively via a replica trick in JT gravity. This resolves an issue regarding the dangerous late time growth of the variance of complexity.

Finally, we move on to considering a toy model both of our past inflationary universe and our dark energy dominated current universe: de Sitter spacetime. In this context we show that for a specific state, the Unruh-de Sitter state, which is analagous to black hole evaporation for a cosmological spacetime, the past cosmological horizon becomes a holographic screen. Furthermore, we calculate the fine-grained entropy showing that information may not be recovered.

List of Publications

This thesis is based on the following publications:

- **No Page Curves for the de Sitter Horizon**, *J. Kames-King, E. Verheijden, E. Verlinde*, In: *JHEP*, DOI: 10.1007/JHEP03(2022)040, arXiv: 2108.09318 [hep-th]
- **Deformations of JT gravity via topological gravity and applications**, *S. Förste, H. Jockers, J. Kames-King, A. Kanargias*, In: *JHEP* 11 (2021) 154, DOI: 10.1007/JHEP11(2021)154, arXiv: 2107.02773 [hep-th]
- **Complexity as a holographic dual of strong cosmic censorship**, *M. Alishahiha, S. Banerjee, E. Loos, J. Kames-King*, In: *Phys.Rev.D* 105 (2022) 2, DOI: 10.1103/PhysRevD.105.026001, arXiv: 2106.14578 [hep-th]
- **Supersymmetric black holes and the SJT/nSCFT₁ correspondence**, *S. Förste, J. Kames-King, A. Gerhardus*, In: *JHEP* 01 (2021) 186, DOI: 10.1007/JHEP01(2021)186, arXiv: 2007.12393 [hep-th]
- **Towards the Holographic Dual of $\mathcal{N} = 2$ SYK**, *S. Förste, J. Kames-King, M. Wiesner*, In: *JHEP* 03 (2018) 028, DOI: 10.1007/JHEP03(2018)028, arXiv: 1712.07398 [hep-th]

and the preprint:

- **Complexity via Replica Trick**, *M. Alishahiha, S. Banerjee, J. Kames-King*, DOI: 10.1007/JHEP08(2022)181, arXiv: 2205.01150 [hep-th]

Contents

1	Introduction	1
1.1	The (big) Questions	1
1.2	General Arguments for the Holographic Principle	2
1.3	AdS/CFT Correspondence	3
1.3.1	String Theory and Large n Gauge Theories	4
1.3.2	Statement of the Correspondence	5
1.3.3	AdS/CFT and the Holographic Principle	6
1.3.4	Black Holes	8
1.4	Chaos, Random Matrix Theory and JT Gravity	8
1.4.1	Classical Chaos	8
1.4.2	Classical Thermalisation	10
1.4.3	Quantum Chaos and Random Matrix Theory	11
1.4.4	Eigenstate Thermalisation Hypothesis	15
1.4.5	Gravity as a chaotic Theory	16
1.4.6	AdS/CFT vs. Chaos Universality	16
1.4.7	JT Gravity on the Disk	18
1.4.8	Non-Perturbative Effects in JT Gravity	20
1.4.9	Discretised Surfaces and Random Matrices	23
1.5	Quantum Information: Complexity	27
1.5.1	What is Complexity? Part 1	27
1.5.2	Quantum Information Primer	28
1.5.3	What is Complexity? Part 2	30
1.5.4	Holographic Complexity	31
1.5.5	The Plateau via JT Gravity	33
1.6	Cosmology, our Universe and De Sitter	35
1.6.1	Covariant Entropy Bound	36
1.6.2	The Holographic Principle in Cosmology	37
2	JT Supergravity Part 1	41
3	JT Supergravity Part 2	65
4	JT Gravity/Matrix Model Duality	111
5	Quantum Information: Complexity	157
6	Quantum Information: Complexity in JT Gravity	173

7	Cosmology	205
8	Conclusion	239
8.1	Summary and Outlook	239
	Bibliography	243
	List of Figures	253
	List of Tables	255

Introduction

In this introductory section we will preface the main topics of this thesis and establish results which are part of the body of literature relevant to the work described here. While many details are given, the main emphasis here is on the larger, conceptual framework. More specifically the questions we want to answer in this section are the following:

- What are the big problems of theoretical physics and how do we plan to tackle them?
- What is the holographic principle?
- What is the AdS/CFT correspondence?
- What is a quantum chaotic system and why do we consider gravity to be chaotic?
- What is computational complexity and how does it appear in a holographic context?
- Why does JT gravity follow the expectations of a chaotic system both with respect to spectral statistics and also with respect to complexity at late times?
- What is the state of our universe and how may we think about it holographically?

The introductory section of this thesis is to large parts based on review articles. The sections explicitly dealing with the holographic principle, namely sections [1.2](#), [1.3.3](#), [1.6.1](#) and [1.6.2](#) are based on [\[1\]](#). The section dealing with generalities of quantum chaos and its realisation in gravitational contexts, section [1.4](#), is based on [\[2\]](#), [\[3\]](#), [\[4\]](#) and [\[5\]](#). The theory of computational complexity and its holographic realisation is introduced in section [5](#) and is based on [\[6\]](#), [\[7\]](#) and [\[8\]](#). We will cite original publications in the sections themselves.

1.1 The (big) Questions

Some of the biggest questions of modern theoretical physics are the following: what is the nature of the interior of a black hole? How did the universe begin? Are the singularities of general relativity resolved at the quantum level? Does the evaporation of a black hole occur in a unitary manner? These

are expressly gravitational questions. One hope of resolving these questions comes in the form of string theory. While there has been remarkable success on many fronts, many of the aforementioned questions are very difficult to tackle in a full-blown string theory framework. For this reason much recent work has been performed via low-dimensional toy models and more effective approaches. However, without a complete UV description, there must be a guiding principle. There are general arguments suggesting that for a quantum theory, the description of a volume of space may be described at a fundamental level, by the area encompassing that volume. The most explicit realisation of this principle comes from string theory: the AdS/CFT correspondence [9–12], which posits an equivalence between string theory on asymptotically Anti-de Sitter (AdS) spaces and conformal field theories (CFT), considered to be living on the boundary of the AdS space. As this gives an explicit definition of quantum gravity for AdS spacetimes, it is believed that formulating the above big questions in a holographic manner is essential in solving them. AdS/CFT therefore represents a well-understood setting in which to analyse important theoretical problems.

1.2 General Arguments for the Holographic Principle

In order to furnish some intuition, let us review the physical principles generally suggesting the holographic principle. For a quantum-mechanical system the number of degrees of freedom N is defined to be the logarithm of the dimension of the Hilbert space $\dim(\mathcal{H})$:

$$N = \ln \dim(\mathcal{H}) . \tag{1.1}$$

Let us now consider a spherical region of space with an arbitrary configuration of matter. On a fundamental level, how many degrees of freedom could such a system have? Naively, quantum field theory would lead to an infinite answer: $N \rightarrow \infty$. However, clearly we have to set a cutoff and hence specify a smallest possible length scale. The most natural possibility is the Planck length, $\ell_P = 1.6 \times 10^{-33}$ cm. We may therefore model our quantum field theory as individual harmonic oscillators on a Planck length grid and assume one oscillator per Planck volume. We take each oscillator to have n discrete states. As the oscillator spectrum is cut off at the Planck energy, the number of oscillators may not exceed the volume V of the system. Therefore the degrees of freedom are given as

$$N \sim \ln(n) V , \tag{1.2}$$

which seems to indicate a scaling with the volume. However, this is in tension with the principles of gravity. To demonstrate this, we will have to review some basic aspects of black hole thermodynamics. In [13] Hawking introduced the area theorem, which states that the area of a black hole horizon A may never decrease in time:

$$dA \geq 0 . \tag{1.3}$$

Clearly no classical process could violate (1.3) as no particles can escape a black hole. Particles falling into the black hole will lead to an increase of the black hole mass M , which in turn due to $A \sim M^2$ will lead to an increase of the area. Based on the similarity of (1.3) to the second law of thermodynamics, Bekenstein [14–16] suggested the following identification $S_{\text{BH}} = \frac{A}{4}$ and furthermore a generalisation of (1.3) to

$$dS_{\text{total}} \geq 0 , \tag{1.4}$$

with $S_{\text{total}} = S_{\text{BH}} + S_{\text{outside}}$. Equation (1.4) is called the generalised second law. The area theorem (1.3) leaves one issue untouched. Even though the area might increase via matter falling in, how is the entropy affected? The no-hair theorem guarantees that classically any kind of black hole is described completely by mass, angular momentum and charge [13, 17–20]. Throwing a high entropy system into a black hole would hence seemingly reduce the entropy of the universe as the black hole seems independent of the microstates of the high entropy box. The identification of the entropy of a black hole with its area and the generalised second law (1.4) seem to circumvent this as the reduction of matter entropy S_{outside} is compensated by the growth in area. This in itself however is not sufficient. Assuming the validity of equation (1.4), implies the Bekenstein bound for any matter system (in asymptotically flat space) [21]:¹

$$S = 2\pi ER, \quad (1.5)$$

where E is the mass-energy and R is the radius of smallest sphere that can hold the matter system. As the entropy S_{BH} is only sensitive to the increase of mass, which implies an increase in area, we could imagine a high entropy, low mass configuration which would violate (1.4). The bound (1.5) declares this scenario unphysical. Demanding gravitational stability ($R \geq 2E$) in (1.5) leads to

$$S = \frac{A}{4}. \quad (1.6)$$

We therefore arrive at the following conclusion. For a system of finite size and energy, the maximum amount of information required at the fundamental level can not exceed $\frac{A}{4}$, where A is the area enclosing the matter system. Furthermore, the bound is saturated for black holes. In contrast to (1.2) we conclude that

$$N = \frac{A}{4}. \quad (1.7)$$

How can we explain the discrepancy to (1.2)? In short, we had failed to include the demand of gravitational stability. The cutoff we imposed was that each Planck volume may at most contain one Planck mass, so implicitly the scaling $E \sim R^3$. However, as used in the derivation of (1.7) the bound for gravitational stability is $R \geq 2E$. The result (1.6) led to the proposal of the holographic principle [22, 23]:

A region with boundary of area A is fully described by no more than $A/4$ degrees of freedom, or about 1 bit of information per Planck area. A fundamental theory, unlike local field theory, should incorporate this counterintuitive result.

We have seen that for the reasoning of this fundamental principle, the inclusion of gravitational thinking was tantamount. Moreover, black holes play an important role.

1.3 AdS/CFT Correspondence

Before moving on to a more detailed description of the AdS/CFT duality as it originates from string theory, let us first state a general connection between gauge theories and string theory, which represents the fundament on which later developments were built.

¹ Indeed for this section we are considering asymptotically flat space in four dimensions.

1.3.1 String Theory and Large n Gauge Theories

For all gauge theories the rank of the gauge group n is a dimensionless parameter. It is therefore tempting to take parametric limits of this quantity. For $U(n)$ gauge theories 't Hooft proposed to perform an expansion for $n \rightarrow \infty$, which has proven remarkably useful. However, naively it might seem that $n \rightarrow \infty$ does not correspond to a sensible limit as the self-energy diverges. On closer inspection it is clear that the self-energy carries powers of $\lambda := g_{YM}^2 n$, where g_{YM} is the dimensionless coupling constant and in general that the partition function takes on the form [24]:

$$Z = \sum_{g \geq 0} n^{2-2g} f_g(\lambda). \quad (1.8)$$

Therefore the limit we should consider is actually

$$n \rightarrow \infty, \quad \lambda \text{ fixed}. \quad (1.9)$$

So far we have not explained why the partition function turns into (1.8) and what the parameter g means. Lets argue for this briefly. The Yang-mills action is given by (where we immediately use the 't Hooft parameter)

$$S_{YM} = -\frac{n}{2\lambda} \int d^4x \text{Tr} \left(F_{\mu\nu} F^{\mu\nu} \right), \quad (1.10)$$

where we temporarily work with $SU(n)$ such that the gluon fields are $n \times n$ matrices

$$\left(A_\mu \right)^{i\bar{j}}, \quad i, j = 1, \dots, n. \quad (1.11)$$

The Lagrangian (1.10) leads to the propagator

$$\langle A_\mu^{i\bar{j}}(x) A_\nu^{k\bar{l}}(y) \rangle = \Delta_{\mu\nu}(x-y) \left(\delta^{i\bar{l}} \delta^{j\bar{k}} - \frac{1}{n} \delta^{i\bar{j}} \delta^{k\bar{l}} \right), \quad (1.12)$$

which in the large n limit loses the second term (which also means we are then effectively working with $U(n)$). Without this term we can use the double-line notation shown in figure 1.1, where the lines represent the fundamental and anti-fundamental representations of the field in the adjoint representation [24]. As the same can be done for all vertices, all Feynman diagrams amount to closed, oriented Riemann surfaces. Counting the powers of n and λ can now be done diagrammatically and it can be shown that the vacuum diagrams with V vertices, E propagators and F loops have an expansion coefficient of the form

$$\left(\frac{\lambda}{n} \right)^E \left(\frac{n}{\lambda} \right)^V n^F = n^\chi \lambda^{E-V}, \quad (1.13)$$

where we have introduced the Euler number $\chi = V - E + F$, which for closed compact surfaces amounts to $\chi = 2 - 2g$ with g being the number of handles. This leads to the expression (1.8). A closer look at (1.8) suggests that we may rewrite this expression suggestively as

$$Z = \sum_{g \geq 0} g_s^{2g-2} Z_g. \quad (1.14)$$

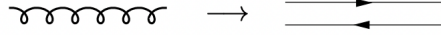


Figure 1.1: The large n limit of a $SU(n)$ gluon propagator depicted in terms of double-line notation first introduced in [24]. Figure taken from [25].

where we have made the identification $g_s = \frac{1}{n}$. The form (1.14) is very much reminiscent of the string theory loop expansion. We can therefore see that Feynman diagrams of gauge theory in a certain limit are equivalent to surfaces representing interacting strings. While this is a perturbative statement on the level of asymptotic expansions, it hints at a deep connection between gauge theories and string theory. The limit (1.9) will therefore play an important role in the construction of the AdS/CFT correspondence as we will see in the next section. We will also see similar ideas regarding surfaces and genus expansions in the context of two-dimensional gravity in section 1.4.9, where we will be somewhat more explicit in the derivation of the large n limit.

1.3.2 Statement of the Correspondence

Consider n coincident, parallel D_3 -branes in ten-dimensional spacetime. Naturally these objects are extended in a $(3 + 1)$ -dimensional hyperplane but localised at the same position in six-dimensional transverse space. Generally we would expect open string excitations of the D_3 -branes, closed string excitations on spacetime and open-closed interactions. We may take a low energy limit $\alpha' \rightarrow 0$, which decouples open-closed interactions. Moreover, massive modes and higher derivative terms are neglected and we encounter a bulk description in terms of free supergravity type IIB and four-dimensional $U(n)$ gauge theory on the D_3 -branes. To be clear, we obtain two non-interacting theories:

- free supergravity in the bulk ,
- $\mathcal{N} = 4$, four-dimensional $U(n)$ super Yang-Mills .

We may however also consider a different part of the parameter space, in which we have to take into account the backreaction of the branes. Let us take the limit introduced in section 1.3.1, $ng_{YM}^2 \gg 1$. As was shown in [26], now the D_3 -branes amount to extreme RR-charged black p-branes with a metric of the form:

$$ds^2 = \frac{1}{H^{\frac{1}{2}}} \eta_{\mu\nu} dx^\mu dx^\nu + H^{\frac{1}{2}} \left(dr^2 + r^2 d\Omega_5^2 \right) , \quad (1.15)$$

with the harmonic function $H = 1 + \frac{L^4}{r^4}$ with $L^4 = 4\pi g_s \ell_s^4 n$ and η of course being the flat space metric. In this context, at low energies we again arrive at two different sets of non-interacting theories. There are of course low-energy modes propagating far away from the branes which are hence described by free supergravity. However additionally there are also low-energy modes close to the horizon, which propagate on a metric, which is the near-horizon limit of (1.15). This region is obtained by $\frac{r}{L} \ll 1$, such that we arrive at

$$ds^2 = \frac{r^2}{L^2} d\vec{x}^2 + \frac{L^2}{r^2} dr^2 + L^2 d\Omega_5^2 . \quad (1.16)$$

This is the metric of $AdS_5 \times S^5$. Therefore we end up with two different theories describing the two different types of low-energy excitations

- free supergravity in the bulk ,
- supergravity type IIB on $AdS_5 \times S^5$.

Therefore the correspondence states that the (super-)gravitational theory obtained on $AdS_5 \times S^5$ is non-perturbatively defined by a 3 + 1-dimensional conformal field theory, namely supersymmetric Yang-Mills with a $U(n)$ gauge group. We can say more however. The perturbative regimes of the two theories do not overlap. The two dimensionless ratios are related as [9]:

$$\frac{L^4}{\ell_s^4} = 4\pi g_s n = g_{YM}^2 n = \lambda, \quad (1.17)$$

where to be clear L is the AdS and sphere lengthscale in (1.16), ℓ_s the string length, g_s the string coupling and g_{YM} , n and λ are gauge theory parameters introduced in section 1.3.1. Equation (1.17) illustrates that when we are in the limit of a simple, perturbative gauge theory description, therefore $\lambda \ll 1$, stringy effects become important. Moreover, we also learn that when we assume the gauge theory to be strongly coupled, therefore $\lambda \gg 1$, we have a simple classical supergravity description in the bulk. Hence “we can use string theory to learn about gauge theory, and we can use gauge theory to learn about string theory” [27]. In its strongest form the correspondence is believed to hold for arbitrary values of n . While the original top-down example of AdS_5/CFT_4 is best understood, in recent times a lot of progress has been made in bottom-up constructions. General symmetry arguments already hint at the fact that the ideas regarding AdS_5/CFT_4 can be generalised to a universal correspondence AdS_d/CFT_{d-1} [28]:

Isometries of AdS_d :

$$\mathcal{L}_{\zeta_1} g_{AdS} = 0.$$

Conformal isometries of $(d - 1)$ -dimensional flat space:

$$\mathcal{L}_{\zeta_2} \eta = \Omega \eta.$$

The framework of AdS/CFT is built on the fact, that these algebras are equivalent. This implies that states in these two theories can be matched. This is a more “bottom-up” view of AdS/CFT, whereas the original example is “top-down”. For the original example, the conformal group $SO(2, 4)$ and the R-symmetry group $SO(6)$ are realised as Killing symmetries on the $AdS_5 \times S^5$ background.

1.3.3 AdS/CFT and the Holographic Principle

How does the dual theory furnish the holographic principle we introduced earlier? In what way does it avoid the naive quantum field theory result (1.2)? To answer this question we have to calculate the degrees of freedom of this dual theory and compare with the boundary area in Planck units. Naively the degrees of freedom are infinite (due to the UV-divergent modes), however the same holds true for the area. Following [29], we focus solely on the AdS_5 part of (1.16) and perform a coordinate

transformation to arrive at the following metric:²

$$ds^2 = L^2 \left[- \left(\frac{1+u^2}{1-u^2} \right)^2 + \frac{4}{(1-u^2)^2} (du^2 + u^2 d\Omega_3^2) \right], \quad (1.18)$$

where the boundary is now at $u = 1$ and the interior at $0 \leq u < 1$. We regularise the bulk spacetime by introduction of an IR cutoff truncating the bulk: $u^2 = 1 - \epsilon$. For the gauge theory this is actually a UV cutoff. The regularised area of the sphere is given by

$$A \sim \frac{R^3}{\epsilon^3}. \quad (1.19)$$

Now we must compare (1.19) to the number of degrees of freedom of the field theory living on the regularised sphere. As the total number of cells of the discretised sphere is $\sim \epsilon^{-3}$ and the number of field theory degrees of freedom for $U(n)$ is of order n^2 , the total number of degrees of freedom amounts to

$$\begin{aligned} N &= \frac{n^2}{\epsilon^3} \\ &= \frac{An^2}{R^3}. \end{aligned} \quad (1.20)$$

The correspondence [9] requires the relationship (1.17), which in the conventions of [29] is:

$$L = \ell_s (ng_s)^{1/4}. \quad (1.21)$$

Using this we can rewrite (1.20) as

$$N = \frac{A}{G_5}, \quad (1.22)$$

where we have identified $G_5 = \ell_s^8 g_s^2 L^{-5}$. With respect to the holographic bound, Anti-de Sitter spacetimes display two crucial features related to the existence of a timelike (conformal) boundary, which make it predisposed for a holographic description:

- There exist spacelike slices of the spacetime allowing for a description at the boundary in terms of degrees of freedom not exceeding the area of the boundary of these slices A .
- The evolution between different spacelike slices at different times is given in terms of a unitary CFT decoupled from gravitational fields.

These features conform with the use of a spacelike entropy bound as proposed in (1.6), such that all considerations take place at a fixed time. For arbitrary situations as in cosmology, a covariant entropy bound is appropriate.

² A similar argument may of course also be used in the complete ten-dimensional spacetime [1].

1.3.4 Black Holes

Of course the identification of the entropy of a black hole with its area poses a new puzzle: what is the microscopic origin of the entropy? What are the underlying microstates? By the inclusion of quantum field theory effects on a curved background, Hawking famously showed that black holes radiate via a quantum process [30, 31]. Remarkably the temperature T is exactly in accordance with a first law of thermodynamics [32]

$$dM = T dS_{\text{BH}}. \quad (1.23)$$

However, the blackbody radiation T of the black hole implicates a tension between quantum field theory and gravity. The entropy of the radiation seems to imply an ever-increasing Hilbert space in contradiction with the finite size implied by $S_{\text{BH}} = \frac{A}{4}$. Therefore the resolution of this paradox is seen as central in the construction of a theory of quantum gravity. While in principle the AdS/CFT correspondence seems to already solve this paradox as any black hole in Anti-de Sitter is identical to some unitary quantum field theory, figuring out the details on how exactly information is localised in a gravitational theory is still a point of ongoing research.

1.4 Chaos, Random Matrix Theory and JT Gravity

In this section we will argue why we should think of gravity as a chaotic theory and furthermore how the universal behaviour of quantum chaotic systems allows us to determine general expectations for theories of quantum gravity. Furthermore we will briefly explain how JT gravity follows these expectations.

1.4.1 Classical Chaos

While in general there is no agreed upon definition of quantum chaos, at least in the classical case there are simple characteristics which may be defined. Let us however first define what an integrable system is. For classical systems we may think about phase space trajectories. A system with a Hamiltonian $H(\vec{p}, \vec{q})$ expressed in terms of the canonical coordinates $q = (q_1, \dots, q_N)$ and momenta $\vec{p} = (p_1, \dots, p_N)$ is called integrable if there are N independent conserved quantities \vec{I} (for a system of N degrees of freedom)[33]:

$$\{I_j, H\} = 0, \quad \{I_j, I_k\} = 0, \quad (1.24)$$

where we have used the Poisson bracket

$$\{f, g\} = \sum_{j=1, \dots, N} \frac{\partial f}{\partial q_j} \frac{\partial g}{\partial p_j} - \frac{\partial f}{\partial p_j} \frac{\partial g}{\partial q_j}. \quad (1.25)$$

For such a system the Liouville-Arnold Theorem states that there exists a canonical transformation to action angle variables $(\vec{p}, \vec{q}) \rightarrow (\vec{I}, \Theta)$, such that $H(\vec{I}, \Theta)$ [33]. The equations of motion are of course trivial: $I_j = \text{const.}$ and $\Theta_j(t) = \Omega_j t + \Theta_j(0)$. On the contrary, chaotic systems exhibit exponential sensitivity of the motion of trajectories in phase space to small perturbations. Therefore under a change of initial conditions $q_0 \rightarrow q_0 + \delta q_0$ (we take $q_0 := q(t=0)$) we observe a new trajectory

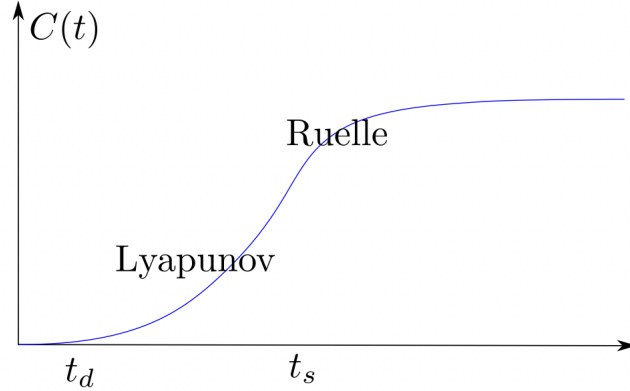


Figure 1.2: Schematic depiction of $C(t)$ (as defined in (1.29)) for a chaotic system. Following a short "collision time" $t_d \sim \beta$, $C(t)$ enters a regime of exponential Lyapunov growth. This ends at the scrambling time t_s (1.31). Thereafter $C(t)$ saturates to the late-time average. Figure taken from [4].

$q(t) \rightarrow q(t) + \delta q(t)$, such that

$$\frac{\partial q(t)}{\partial q_0} = \{q(t), p(0)\} \sim e^{\lambda_L t}, \quad (1.26)$$

where λ_L is the so-called Lyapunov exponent. For a system with a semi-classical regime ($\hbar \ll 1$), we may use an approach pioneered in [34] and advanced in [35–37]. The Poisson bracket is approximated by a commutator such that for our purposes we may take:

$$\{q(t), p(0)\} \rightarrow \frac{1}{i\hbar} [\hat{q}(t), \hat{p}(0)]. \quad (1.27)$$

As we are usually interested in thermal states the following quantity seems promising:

$$C(t) = \langle -[\hat{q}(t), \hat{p}(0)]^2 \rangle_\beta, \quad (1.28)$$

with $\langle \rangle_\beta = \text{Tr} \frac{e^{-\beta H}}{Z}$. More generally we could consider two arbitrary Hermitian operators, such that (1.28) generalises to

$$C(t) = \langle -[\hat{W}(t), \hat{V}(0)]^2 \rangle_\beta. \quad (1.29)$$

The square is taken here to avoid phase cancellation.

$$C(t) = 2 - 2\langle W(t)V(0)W(t)V(0) \rangle_\beta. \quad (1.30)$$

The typical behaviour of a chaotic system is depicted in figure 1.2. After a short time $t_d \sim \beta$ we observe a region of Lyapunov exponential growth. At the so-called scrambling time

$$t_s \sim \frac{1}{\lambda_L} \log \left(\frac{1}{\hbar} \right) \quad (1.31)$$

the commutator achieves macroscopic values $\mathcal{O}(1)$. The final region is the Ruelle region, which amounts to a saturation of $C(t)$ to its late-time average. All of the relevant information is encoded in the out-of-time-ordered correlator (OTOC)

$$\text{OTOC}(t) = \langle W(t)V(0)W(t)V(0) \rangle_{\beta}. \quad (1.32)$$

Let us now gain some intuition for the behaviour depicted in figure 1.2. The OTOC may be rewritten as the inner product of two states:

$$\text{OTOC}(t) = \langle \psi_2 | \psi_1 \rangle, \quad (1.33)$$

with

$$|\psi_1\rangle = W(t)V(0)|\beta\rangle, \quad (1.34)$$

$$|\psi_2\rangle = V(0)W(t)|\beta\rangle, \quad (1.35)$$

with $|\beta\rangle$ a thermal state defined by $e^{-\beta H}$. The OTOC must vanish at late times to achieve the saturation of $C(t)$ at the value 2.³ We can quickly see that this is in accordance with $[V(0), W(t)] \neq 0$, which intuitively means that early measurements of $V(0)$ affect later measurements of $W(t)$, which in turn implies that $\langle \psi_2 | \psi_1 \rangle \approx 0$ as $|\psi_1\rangle$ and $|\psi_2\rangle$ have a negligible superposition. This guarantees the saturation to $C(t) \approx 2$. This may also be nicely understood in the language of operator growth:

$$\begin{aligned} W(t) &= e^{iHt}W(0)e^{-iHt} \\ &= \sum_{k=0}^{\infty} \frac{(-it)^k}{k!} [H, W(0)]_k, \end{aligned} \quad (1.36)$$

where we use the definition $[X, Y]_k = [X, [X, Y]_{k-1}]$ and $[X, Y]_0 = Y$ and we have used the Baker-Campbell-Hausdorff formula. From (1.36) we can observe that for chaotic systems at each step in time the operator $W(t)$ becomes more complicated and the number of non-zero commutators with other operators grows as time evolves. This can for example be nicely checked with Ising-like models or spin chains [36].

1.4.2 Classical Thermalisation

Chaotic behaviour can both be a consequence of a complicated Hamiltonian or of a thermal heat bath with the later case perhaps being more relevant in a holographic context. Consider the phase space of a closed, classical system with a complete description in terms of canonical coordinates and momenta. As time progresses and the system evolves it will move in phase space. Due to energy conservation the path it traces out will be a surface of constant energy. We define a system to be ergodic if it gets arbitrarily close to every point of phase space (with the constant energy constraint fulfilled)[38]. In turn ergodic systems, given long enough time, will meet every point of the constant energy surface. Now Liouville's theorem states a relationship between time and phase space. More explicitly, the system will spend "equal times in equal phase space volumes". We are usually interested in time

³ "Late times" refers to the saturation of $C(t)$ here. In later sections, such as section 1.4.6, we also use the terminology of "late times", which then will refer to times after the Thouless time, which is defined as the time at which RMT behaviour is attained.

averages of observables $O(t)$ over timescales T with the final goal of taking T to infinity. The above logic implies that the time average may be replaced by a phase space calculation [38]:

$$\langle O \rangle_T = \frac{\int_S O(\Gamma) d\Gamma}{\int_S d\Gamma}, \quad (1.37)$$

where the constant energy surface is denoted by S and the phase space curve by Γ . This is exactly how averages are found in the microcanonical ensemble. Classically, we speak of thermalisation if (1.37) holds, therefore if the long-time average equals the microcanonical one. How does this apply to realistic physical systems? It is generally believed that for large systems, therefore $N \rightarrow \infty$, (1.37) is a good approximation. It should also be noted that ergodicity and chaos are not equivalent, however in practice most systems with a large number of degrees of freedom are both ergodic and chaotic. Especially in a holographic context, the entropy of a black hole is considered to be huge. The approach to thermal equilibrium, therefore the independence of initial conditions, can be given a more quantitative form in the following manner. We can introduce a thermal two-point function

$$G(t) = \langle q(t)q(0) \rangle_\beta - \langle q(t) \rangle_\beta^2, \quad (1.38)$$

with the generally expected behaviour

$$G(t) \sim \sum_j b_j e^{-\mu_j t}, \quad (1.39)$$

where b_j are some real constants but μ_j are complex and therefore correspond to resonances. At late times the behaviour is controlled by the smallest μ_j . If we apply a semi-classical analysis as in the previous section, then the objects of interest are the two-point correlators $\langle V(t)V(0) \rangle$. The dissipation time t_d we introduced in the previous section characterises the exponential decay of these correlators, i.e.

$$\langle V(t)V(0) \rangle \sim e^{-\frac{t}{t_d}}. \quad (1.40)$$

In a holographic context Ruelle resonances appear as quasi-normal modes of black holes with $\text{Im}(\omega) \sim t_d^{-1}$ and $t_d \sim \beta$ [39, 40].

1.4.3 Quantum Chaos and Random Matrix Theory

Naturally for a quantum mechanical system the above definitions with respect to phase space become ill-defined as the notion of a phase space trajectory can not be constructed due to the uncertainty principle. Furthermore the linearity of the Schrödinger equation does not allow for exponentially departing wavefunction trajectories under perturbation. However, originally in the setting of nuclear physics [41–44], so-called random matrix theory (RMT) was developed, which defines a notion of quantum chaos. The basic idea is that rather than trying to find the exact eigenspectra of highly complex Hamiltonians, one should instead probe their statistics. Furthermore, a microcanonical ensemble may be defined for which the density of states becomes constant and importantly the Hamiltonian will be *random*. Therefore under consideration of the symmetries of the original Hamiltonian, the analysis of statistical properties of random Hamiltonians may be used to deduce statistical statements about eigenstates and energy levels. Let us now elucidate some of the most

important RMT concepts by use of a 2×2 Hamiltonian theory. For any random matrix theory we have to specify the probability distribution from which the matrix is drawn. We consider a simple example with a Gaussian distribution with zero mean and variance σ [45–47]:

$$\hat{H} = \begin{pmatrix} \epsilon_1 & \frac{V}{\sqrt{2}} \\ \frac{V^*}{\sqrt{2}} & \epsilon_2 \end{pmatrix}. \quad (1.41)$$

Diagonalising the Hamiltonian gives the eigenvalues E_1 and E_2

$$E_{1,2} = \frac{\epsilon_1 + \epsilon_2}{2} \pm \frac{1}{2} \sqrt{(\epsilon_1 - \epsilon_2)^2 + 2|V|^2}. \quad (1.42)$$

We can already note the following by inspecting (1.42) closer: E_1 and E_2 due to V never cross each other. This phenomenon is known as *eigenvalue repulsion*. For a system with time-reversal symmetry \hat{H} is a real matrix with $V^* = V$. We now want to calculate the statistical properties of the level separation in terms of the energy difference, therefore $P(\omega) := P(E_1 - E_2)$. This amounts to the integration (for the real case)

$$P(\omega) = \frac{1}{(2\pi)^{3/2} \sigma^3} \int d\epsilon_1 \int d\epsilon_2 \int dV \exp\left(-\frac{-\epsilon_1^2 + \epsilon_2^2 + V^2}{2\sigma^2}\right) \delta\left(\sqrt{(\epsilon_1 - \epsilon_2)^2 + 2V^2} - \omega\right). \quad (1.43)$$

By use of spherical coordinates this gives the result

$$P(\omega) = \frac{\omega}{2\sigma^2} \exp\left(\frac{-\omega^2}{4\sigma^2}\right). \quad (1.44)$$

For the case without time reversal we arrive at

$$P(\omega) = \frac{\omega^2}{2\sqrt{2}\sigma^3} \exp\left(\frac{-\omega^2}{4\sigma^2}\right). \quad (1.45)$$

Note the following behaviour for both expressions given for $P(\omega)$.

- Level repulsion is again manifest as $P(\omega) \rightarrow 0$ for $\omega \rightarrow 0$.
- We also observe Gaussian decay for large ω .

The above expressions (1.44) and (1.45) generalise to Wigner's surmise:

$$P(\omega) = N_\beta \omega^\beta \exp\left(-M_\beta \omega^2\right), \quad (1.46)$$

with $\beta = 1$ being the time-reversal case, also called the Gaussian orthogonal ensemble (GOE) and $\beta = 2$ corresponding to the non time-reversal invariant case, also known as the Gaussian unitary ensemble (GUE). There is also a third ensemble with $\beta = 4$, called the Gaussian symplectic ensemble (GSE), which is invariant under symplectic transformations. The three aforementioned ensembles

from which the matrices themselves are drawn from, are of the form

$$\begin{aligned}
 P(\hat{H}) &\sim \exp(-\text{Tr} V(\hat{H})) \\
 &= \exp\left(-\frac{\beta}{2a} \text{Tr}(\hat{H}^2)\right) \\
 &= \exp\left(-\frac{\beta}{2a} \sum_{i,j} H_{ij} H_{ji}\right), \tag{1.47}
 \end{aligned}$$

which fulfills

- invariance under a rotation of basis $H \rightarrow gHg^{-1}$,
- a Hermitian matrix $H = H^\dagger$,
- a Gaussian potential $V(H) \sim H^2$.

Such random matrix ensembles are known as Wigner-Dyson ensembles. Although we have depicted a Gaussian structure in (1.47), the same concepts can be generalised to non-Gaussian measures. In the more general case of matrices of larger dimension than 2, the analytic form for the level separation can not be found, however it obeys a form similar to (1.46). Above we have seen three random matrix ensembles classified with respect to their symmetry group G . There are however all in all 10 ensembles. Four further ensembles can be constructed by considering the same simple symmetry groups with H being a second rank tensor [48, 49]. Briefly, for $G = U(L)$, H can either be symmetric or antisymmetric. For $G = O(L)$, H is antisymmetric and for $G = SP(L)$, H is symmetric. Three additional cases can be constructed by taking the products $U(L) \times U(L)$, $O(L) \times O(L)$ and $SP(L) \times SP(L)$, such that H is now a bifundamental. Mixed products of different groups are not permitted as the bifundamental would have more than L degrees of freedom. What is the relationship of such ensembles to individual quantum systems? The answer comes in form of the Bohigas-Giannoni-Schmit (BGS) conjecture [50]. BGS discovered that for single particle systems (in the context of Sinai billiards) for a sufficiently narrow high-energy window, the level statistics are described by the GOE distribution. This leads to the more general conjecture that for a system with a classical chaotic limit, the quantum energy level statistics will follow a Wigner-Dyson distribution (in a certain energy window). Therefore if a Wigner-Dyson distribution is observed, we speak of quantum chaos (even if there may not be a classical limit). We should also clearly delineate between actual physical Hamiltonians and those drawn from the ensemble. For most Hamiltonians due to locality we expect the matrix to be more sparse than random matrix Hamiltonians, such that it may not be clear how these things are related. There are two points to be made here. First, while indeed a random matrix is generally a dense matrix and a physical Hamiltonian generally more sparse, the eigenspectrum of the physical Hamiltonian still displays Wigner-Dyson statistics. These statistics in the random matrix theory are worked out in a fixed basis. If we were to diagonalise with respect to any specific random matrix, the physical statements would still hold for the ensemble overall. Secondly, there is a sense in which the sensitivity to initial conditions we had declared a signature of classical chaos, generalises to quantum chaos. Following ref. [46], it can be seen that if a physical (chaotic) Hamiltonian is perturbed it will generally take on the structure of a random matrix if written in the basis of the unperturbed eigenstates.

Let us now make some concrete statements about observables in RMT. We consider the observable \hat{O} , which therefore as a Hermitian operator may be written in the form

$$\hat{O} = \sum_j O_j |j\rangle\langle j|, \quad (1.48)$$

with $\hat{O}|j\rangle = O_j|j\rangle$. We can calculate matrix elements of this observable

$$\begin{aligned} O_{mn} &= \langle m|\hat{O}|n\rangle \\ &= \sum_i (\psi_i^m)^* \psi_i^n, \end{aligned} \quad (1.49)$$

where we have introduced the notation $\psi_i^m := \langle i|m\rangle$. What can we say about ψ_i^m in RMT? The joint probability distribution of eigenvector components takes on the form [51]:

$$P_{\text{GUE}}(\psi_1, \dots, \psi_N) \sim \delta\left(\sum_j |\psi_j|^2 - 1\right), \quad (1.50)$$

where the ψ_j are wavefunction components in some fixed basis. Intuitively (1.50) implies that eigenvectors of random matrices are random unit vectors. Therefore if we average over random eigenkets, we get

$$\overline{(\psi_i^m)^* \psi_j^n} = \frac{1}{N} \delta_{mn} \delta_{ij}, \quad (1.51)$$

in leading order in the Hilbert space dimension N . Equation (1.51) implies different results for off-diagonal and diagonal elements, namely:

$$\overline{O_{mn}} = \frac{\delta_{mn}}{N} \sum_i O_i := \bar{O}, \quad (1.52)$$

where we have also introduced new notation. We may also think about fluctuations by calculating the variance around (1.52), which again will give different results for diagonal and off-diagonal elements. For diagonal elements we get:

$$\overline{O_{mm}^2} - \overline{O_{mm}}^2 = \frac{3 - \beta}{N} \overline{O^2}, \quad (1.53)$$

where β refers to the different ensembles defined below (1.46). For off-diagonal elements we have:

$$\overline{O_{mn}^2} - \overline{O_{mn}}^2 = \frac{1}{N} \overline{O^2}. \quad (1.54)$$

From (1.52) in combination with (1.53) and (1.54) we arrive at the following ansatz in leading order in $\frac{1}{N}$:

$$O_{mn} \approx \bar{O} \delta_{mn} + \sqrt{\frac{\overline{O^2}}{N}} R_{mn}, \quad (1.55)$$

where we take R_{mn} to be the components of a random matrix from a Gaussian ensemble appropriately chosen with respect to symmetries. The ansatz (1.55) reproduces the previous equations. For large

enough systems (essentially large enough matrices) (1.55) holds for observables of fixed, chaotic Hamiltonians. We may also ask the question what integrability looks like at the quantum level. The answer is given by the Berry-Tabor conjecture, which states that the (quantum) energy levels behave like a sequence of independent random variables, if the classical system is integrable [52]. Therefore in contrast to the eigenvalue repulsion of (1.46), here the energy levels are just random numbers, which implies that energy level separation ω should follow a Poisson distribution

$$P(\omega) = \exp(-\omega) . \quad (1.56)$$

1.4.4 Eigenstate Thermalisation Hypothesis

Let us now upgrade our notion of thermalisation to the quantum realm. Consider a closed quantum system in the pure state $|\psi_0\rangle = |\psi(t=0)\rangle$ with a time-independent Hamiltonian \hat{H} with $\hat{H}|m\rangle = E_M|m\rangle$, then the time-evolved state is given by the well-known expression

$$|\psi(t)\rangle = \sum_m c_m e^{-\frac{iE_m t}{\hbar}} |m\rangle , \quad (1.57)$$

with $c_m = \langle m|\psi_0\rangle$. Then for an observable

$$O(t) := \langle \psi(t) | \hat{O} | \psi(t) \rangle , \quad (1.58)$$

we arrive at

$$O(t) = \sum_m |c_m|^2 O_{mm} + \sum_{m \neq n} c_m^* c_n e^{\frac{i(E_m - E_n)t}{\hbar}} O_{mn} . \quad (1.59)$$

We say that \hat{O} thermalises if the average expectation values agree with microcanonical predictions (after some time) and fluctuations around this value are negligible. Therefore thermalisation implies that the long-time average of (1.59) agrees with the microcanonical ensemble. Now the long-time average $\langle O(t) \rangle_{\text{LT}}$ of (1.59) is merely the first term. We already know what the behaviour of RMT observables is from (1.55). If we apply this in (1.59) and take the long-time average, we get:

$$\langle O(t) \rangle_{\text{LT}} = \bar{O} , \quad (1.60)$$

such that we see that for RMT quantum thermalisation holds. However, in actual physical systems relaxation times depend on the observable under consideration and are also temperature dependent. To account for this, a specific generalisation of RMT behaviour is required [53–55]:

$$O_{mn} = O(E) \delta_{mn} + e^{-\frac{S(E)}{2}} f(E, \omega) R_{mn} , \quad (1.61)$$

with $E = (E_m + E_n)/2$, $\omega = E_n - E_m$ and $e^{S(E)}$. $O(E)$ and $f(E, \omega)$ are smooth functions of (ω, E) . The so-called eigenstate thermalisation hypothesis (ETH) ansatz, equation (1.61), is a generalisation of RMT in the following sense. The diagonal elements are smooth functions of the energy and the off-diagonal elements now include thermal fluctuations with $f(E, \omega)$ also being a smooth function. However, if we fix on the narrowest energy Window, called the Thouless energy E_T , ETH can be shown to reduce to RMT. This might seem to seriously constrain the applicability of RMT technology as the energy level separation must be $\omega < E_T$ for RMT to be a valid approach in the description of a

single quantum chaotic system. However note that as a system size increases, energy level spacings decrease, such that there are still an exponential number of energy levels to which RMT applies. Also note that by Fourier transforming from energy to time, it is clear that late times of chaotic systems are well-described by RMT (after the Thouless *time*). We will see in section 1.4.6, that late times are especially difficult to probe correctly in a holographic context as they require non-perturbative effects.

1.4.5 Gravity as a chaotic Theory

We will now argue qualitatively that we should think of (Einstein) gravity as a (maximally) chaotic theory by reviewing various results in the literature [35–37, 56, 57]. As gravity allows for black holes, which are both thermal and have a large number of degrees of freedom, it might seem obvious at this point, which is why we will not be too explicit. Let us therefore summarily state that for large n gauge theories, which are holographically described by Einstein gravity, via the use of the AdS/CFT dictionary (which translates the operator language of sections 1.4.1 and 1.4.2 to semi-classical gravitational calculations in AdS), the Lyapunov exponent can shown to be given by the following expression:

$$\lambda_L = 2\pi T, \quad (1.62)$$

and therefore the scrambling time

$$t_s = \frac{1}{2\pi T} \log \left(\frac{1}{\hbar} \right). \quad (1.63)$$

Now a priori the Lyapunov exponent might not seem to carry any additional information (apart from the fact that the system indeed follows the exponential behaviour depicted in fig. 1.2). However, the seminal paper [58] illustrates why (1.62) is a remarkable result. More explicitly, reference [58] conjectures the existence of a universal bound for λ_L :

$$\lambda_L \leq 2\pi T \frac{k_B}{\hbar}, \quad (1.64)$$

where we introduced units for the moment. This bound is understood to hold not just for holographic systems but any kind of system.⁴ Therefore, (1.62) not only tells us that Einstein gravity is chaotic but actually maximally chaotic and that black holes are the fastest scramblers and therefore in some sense the most chaotic system [59].

1.4.6 AdS/CFT vs. Chaos Universality

Let us now continue in the setting of AdS/CFT for the moment. If we consider an AdS_{d+1} spacetime, the holographic dual is a CFT defined on $R \times S^{d-1}$. We can quickly see that a tension between these two (supposedly equivalent descriptions) appears in the case of a thermal state for the CFT and an eternal AdS black hole in the bulk [60]. We may calculate the thermal boundary correlator in the

⁴ With a certain set of constraints. There must be some parametric distance between scrambling and dissipation time. Moreover, there are also some constraints with respect to the locality of the system [58].

canonical ensemble as

$$\begin{aligned} G_\beta(t) &= \frac{1}{Z(\beta)} \text{Tr} \left[e^{-\beta H} \mathcal{O}(t) \mathcal{O}(0) \right], \\ &= \frac{1}{Z(\beta)} \sum_{i,j=1}^N |\mathcal{O}_{i,j}|^2 e^{-\beta E_n} e^{it(E_m - E_n)}, \end{aligned} \quad (1.65)$$

where we have assumed the thermal partition function (and density matrix) $Z(\beta) = \text{Tr}[e^{-\beta H}]$, and a hermitian operator \mathcal{O} with unitary evolution $e^{itH} \mathcal{O}(0) e^{-itH}$. For early times, we can consider the oscillation of the phases to be small and therefore the double sums over energy eigenstates may be approximated by integrals over the density of states. If we consider \mathcal{O} to fulfill the ETH, therefore \mathcal{O} to be a simple operator and the system to be chaotic, we find exponential decay at early times [39]

$$G_\beta(t) = e^{-\frac{4\pi t}{\beta}}. \quad (1.66)$$

However, at late times the discreteness of the boundary theory becomes manifest as the phases of (1.65) oscillate and the correlator is exponentially small in the system size but fluctuates erratically around a non-zero value. The ETH, equation (1.61), states that ultimately the diagonal elements vary smoothly as a function of energy with the difference between neighbouring eigenvalues at late times becoming exponentially small. Therefore it is often convenient to introduce the so-called spectral form factor, which is a simplification of (1.65) which allows for the extraction of universal behaviour. It essentially amounts to focusing on the oscillating phases of (1.65) by stripping off the matrix elements. It is defined in the following way:⁵

$$\begin{aligned} \text{SFF}_\beta(t) &:= \left| \frac{Z(\beta + it)}{Z(\beta)} \right|^2 \\ &= \frac{1}{Z(\beta)^2} \sum_{m,n} e^{-\beta(E_m + E_n)} e^{i(E_m - E_n)t}. \end{aligned} \quad (1.67)$$

What is the expectation for very late times? For this we should think about the long time average

$$\lim_{t^* \rightarrow \infty} \frac{1}{t^*} \int_0^{t^*} \text{SFF}_\beta(t) dt = \frac{Z(2\beta)}{Z(\beta)^2}, \quad (1.68)$$

where we have assumed that there are no degeneracies in the spectrum and also that $E_n = E_m$ as suggested by ETH. Equation (1.68) implies that at late times the SFF (1.67) takes on a constant value (i.e. independent of time) with a size set by the degrees of freedom of the system. This constant value is referred to as the ‘‘plateau’’ and is a hallmark of unitarity. If we take S_0 to refer to the entropy, then $Z(\beta) \sim e^{S_0}$, such that we see that (1.68) scales as e^{-S_0} . Moreover, if the discrete sum in (1.67) is replaced by a smooth density the late time average (1.68) vanishes, such that we see that the late time behaviour is sensitive to discreteness. This is of course in stark contrast to results in the context of perturbative gravity on black hole backgrounds. As shown in [60], the corresponding thermal two-point function or spectral form factor exponentially decays, such that

⁵ First introduced in a holographic context in [61].

(1.68) is invisible in perturbative gravitational calculations. We can understand why. In a holographic context, $S_0 \sim \frac{1}{G_N}$, such that (1.68) requires non-perturbative effects. It is therefore also clear why it is universally difficult to describe gravitational systems in accordance with quantum mechanical principles: non-perturbative effects are essential in observing traces of discreteness. The SFF (1.67) is a good indicator in understanding gravitational systems. For chaotic systems, the SFF actually follows a universal structure dictated by random matrix statistics. As can for example be understood via the Efetov sigma model approach to quantum chaos [62–64], for random matrices the SFF follows a “dip-ramp-plateau” structure. This behaviour is shown in figure 1.3 for the concrete example of the SYK model, which is not a RMT but a quantum chaotic system. As the “ramp” corresponds to the eigenvalue repulsion we introduced in section 1.4.3, we can clearly see the appearance of RMT behaviour in figure 1.3. The full derivation of “dip-ramp-plateau” requires the introduction of various technicalities, such that we will just state that the connected two-point function for the density of states of a RMT is given as [44, 65, 66]:⁶

$$\langle \rho(E_1)\rho(E_2) \rangle_{\text{conn.}} = -\frac{\sin^2(L\rho_0(E_2)(E_1 - E_2))}{\pi(E_1 - E_2)^2}, \quad (1.69)$$

which when Fourier transformed gives the “dip-ramp-plateau” structure (L is the size of the matrix). Therefore, while behaviour before the Thouless time depends on the specific system, for any chaotic theory we expect the behaviour in time to follow (for sufficiently late times) the aforementioned description. The numerator of (1.69) may of course be rewritten as the sum of a 1 and an exponential structure $\exp(-2iL(E_1 - E_2)\rho_0(E_2))$. Therefore the “ramp”, which is just the denominator of (1.69), can be achieved in the matrix model via a perturbative saddlepoint expansion, whereas the full structure of (1.69) requires the so-called Andreev-Altschuler instanton, which furnishes the non-perturbative exponential in L [67]. However, in gravity this becomes exponentially more difficult as we generally expect $L \sim e^{S_0}$ and therefore late times require doubly non-perturbative effects. If we are to think of gravity as a chaotic theory, as argued in section 1.4.5, we should expect that it follows the universal behaviour of (1.69) in the microcanonical setting (or the “dip-ramp-plateau” structure in the canonical ensemble). In the concrete setting of AdS_2 this expectation is even more explicit. It is usually conjectured that the SYK model constitutes the dual to JT gravity on AdS_2 . As seen in figure 1.3, the SYK model attains RMT behaviour at sufficiently late times, such that it is expected that the same should hold for JT gravity.

1.4.7 JT Gravity on the Disk

Let us now introduce a theory of gravity in two dimensions, called JT gravity, which, as we shall see, furnishes a spectrum which extends beyond the early time decaying behaviour but follows chaos universality due to the inclusion of gravitationally non-perturbative effects. The action in Euclidean

⁶ The exact expression is for a GUE ensemble.

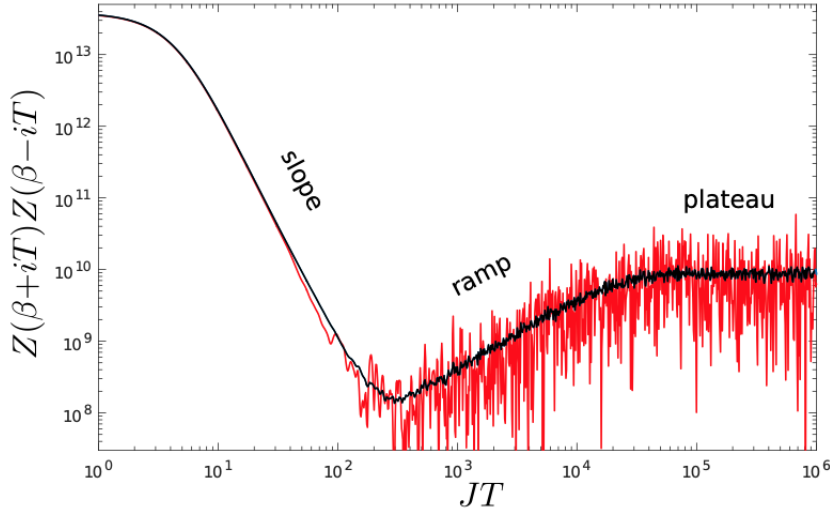


Figure 1.3: Here we see the *log-log* plot of the spectral form factor (as defined in (1.67)) for the SYK model [68]. More concretely, the parameters of the depicted SYK model are: $q = 4$, $N = 34$, $\beta\mathcal{J} = 5$, where q specifies the number of fermions (randomly) interacting with each other, N specifies the total number of fermions, β is the inverse temperature and finally J is the coupling. The x-axis labelling T refers to the time. Both a single SYK model sample (red) and a disorder average over 90 samples (black) are depicted. Figure taken from [68].

AdS₂ is given by the following expression [69–73]:

$$S = -\frac{\phi_0}{16\pi G_N} \left[\int_{\mathcal{M}} d^2x \sqrt{g} R + 2 \int_{\partial\mathcal{M}} du K \right] - \frac{1}{16\pi G_N} \left[\int_{\mathcal{M}} d^2x \phi \sqrt{g} (R + 2) + 2 \int_{\partial\mathcal{M}} du \phi_b K \right], \quad (1.70)$$

where R is the Ricci scalar, g the corresponding metric, K the extrinsic curvature, ϕ a dilaton field, ϕ_b its boundary value and ϕ_0 a constant fixing the groundstate entropy of the system. As we are in two dimensions the first line of (1.70) is the topological Gauss-Bonnet term, and therefore determines the Euler characteristic χ of the underlying surface and does not give a dynamical equation of motion but respects the conformal symmetry of AdS₂. As such, this line essentially describes a CFT₁ fixed point, which is why the second line is added, breaking the exact conformal symmetry. The dilaton ϕ acts as a Lagrange multiplier fixing the metric to hyperbolic curvature. The asymptotic boundary length may be regularised and fixed to a specific length by the following boundary condition [71]:

$$g|_{\text{bdy.}} = \frac{1}{\epsilon^2}, \quad \frac{1}{\epsilon^2} = g_{uu} = \frac{t'^2 + y'^2}{y^2}, \quad (1.71)$$

which may be solved for

$$y = \epsilon t' + \mathcal{O}(\epsilon^3). \quad (1.72)$$

Now different $t(u)$ constitute different regularised cutouts of AdS_2 . There is an underlying asymptotic symmetry corresponding to the only gravitational degree of freedom of this system. This symmetry acts as

$$\zeta^t = \epsilon(t), \quad \zeta^y = y\epsilon'(t). \quad (1.73)$$

While in general different $t(u)$ correspond to different situations, global translations and rotations keep the system invariant such that $SL(2, \mathbb{R})$ acting on $t(u)$ is preserved:

$$\hat{t}(u) = \frac{at(u) + b}{ct(u) + d}. \quad (1.74)$$

In addition to the hyperbolic constraint on the Ricci scalar, the variation of the metric gives

$$T_{\mu\nu}^\phi = \frac{1}{8\pi G} (\nabla_\mu \nabla_\nu \phi - g_{\mu\nu} \nabla^2 \phi + g_{\mu\nu} \phi) = 0. \quad (1.75)$$

As the only degree of freedom is situated on the asymptotic boundary, it may be expressed via K , which with the boundary conditions (1.71) and the solution (1.72) amounts to

$$S = -\frac{1}{8\pi G} \int du \phi_r(u) \text{Schw.}[t, u], \quad (1.76)$$

where we have introduced the Schwarzian derivative

$$\text{Schw.}[t, u] = \frac{t'''}{t'} - \frac{3}{2} \left(\frac{t''}{t'} \right)^2. \quad (1.77)$$

The action (1.76) may be interpreted as the Nambu-Goto action of the boundary graviton. As was shown in [74] (and via different methods also in [68, 75–78]) the Schwarzian action (1.76) localises to the following expression:

$$Z_{\text{Disk}}(\beta) = \frac{e^{\frac{\pi^2}{\beta}}}{4\sqrt{\pi}\beta^{3/2}}. \quad (1.78)$$

It can easily be seen that (1.78) amounts to decaying behaviour. In light of section 1.4.6, we take this as an indication that non-perturbative effects must be included. Geometrically speaking, the hyperbolic disk is not enough. This intuition was strengthened in [79], where it was shown that a Euclidean two-boundary wormhole geometry creates the “ramp”.

1.4.8 Non-Perturbative Effects in JT Gravity

Again, let us note that the field ϕ acts as a constraint fixing the geometry to be hyperbolic. The full functional integral (therefore beyond the disk) should include hyperbolic Riemann surfaces of arbitrary genus and an arbitrary number of asymptotic boundaries, with the weighting of these surfaces given in terms of the Gauss-Bonnet term. Of course on each surface we have to perform the integration over metric fluctuations. We will give the procedure here schematically and refer to the original publication [80] for more details. As noted above, the full functional integral F amounts to

$$F = \int \mathcal{D}(\text{geometry}) \mathcal{D}\phi e^{-S}, \quad (1.79)$$

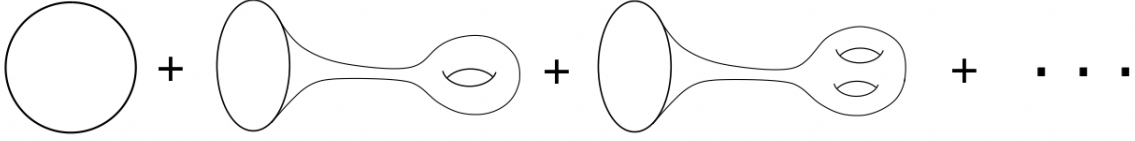


Figure 1.4: Depicted are the surfaces contributing to the single boundary partition function, which amounts to (1.82). These surfaces consist of one asymptotic boundary but an arbitrary genus g . Furthermore as the Euler characteristic is $\chi = 1 - 2g$, the weighting is $e^{(1-2g)S_0}$. Figure taken from [80].

where S refers to (1.70). We allow for multiple asymptotic boundaries with the same boundary conditions (1.71) at each. It can then be shown that a single contribution of n asymptotic boundaries and genus g has the form

$$Z_{g,n}(\beta_1, \dots, \beta_n) = \int \mathcal{D}(\text{bulk moduli space}) \mathcal{D}(\text{boundary fluctuations}) e^{\int_{\partial M} \phi_b \sqrt{h} (K-1)}. \quad (1.80)$$

The overall form of the connected partition function is

$$\langle Z(\beta_1) \dots Z(\beta_n) \rangle_{\text{conn.}} = \sum_{g=0}^{\infty} e^{S_0(2-2g-n)} Z_{g,n}(\beta_1, \dots, \beta_n), \quad (1.81)$$

with the contributions (1.80) weighted by the Euler characteristic. A structure of the form (1.81) necessarily includes gravitationally non-perturbative effects due to the presence of effects with $O(\exp(-S_0))$ and keeping in mind that $G_N \sim \frac{1}{S_0}$. Equation (1.80) tells us that the integration over the metric reduces to the integration of the Schwarzian degree of freedom, already performed in [74], and then an integration over the bulk moduli. The latter contribution arises as the geometries we are considering are more complicated hyperbolic Riemann surfaces, which exhibit a moduli space, whereas the hyperbolic disk does not. Let us see how this works for a single asymptotic boundary. The topologies contributing to the partition function $Z(\beta)$ are shown in fig.1.4. Every surface with $g \geq 1$ we can split into two parts. The length of a minimal geodesic running around the neck of the geometry is labeled b , see fig.1.5. Therefore we see that the full geometry consists of a “trumpet” made of a single geodesic and a single asymptotic boundary and a further geometry which is made of a single geodesic boundary and an arbitrary number of genera. These two geometries are glued together to a single hyperbolic Riemann surface by integrating over the hyperbolic moduli space volume $V_{g,1}(b)$ and an invariant measure. Therefore for a single boundary we get

$$\langle Z(\beta) \rangle = e^{S_0} Z_{\text{disk}}(\beta) + \sum_{g=0}^{\infty} e^{(1-2g)S_0} \int_0^{\infty} db b V_{g,1}(b) Z_{\text{trumpet}}(\beta, b). \quad (1.82)$$

For multiple boundaries (1.80) analogously gives

$$Z_{g,n}(\beta_1, \dots, \beta_n) = \int_0^{\infty} db_1 \dots \int_0^{\infty} db_n V_{g,n}(b_1, \dots, b_n) Z_{\text{trumpet}}(\beta_1, b_1) \dots Z_{\text{trumpet}}(\beta_n, b_n) \quad (1.83)$$

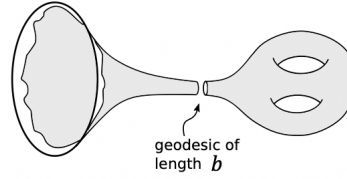


Figure 1.5: Depiction of the contribution $Z_{g=2, n=1}$ to (1.81). The path integral over ϕ constrains in each topological class to $R = -2$ surfaces. The path integral over the metric reduces to an integral over metric fluctuations on the asymptotic boundary (pictured on the left here) and a finite-dimensional integral over geometric moduli. We may think of the entire surface as the trumpet glued to a Riemann surface with geodesic boundary of length b and $g = 2$. The gluing has two parameters, the length b and a twist, both of which have to be integrated over. This procedure leads for the case of a single boundary to the expression (1.82). Figure taken from [80].

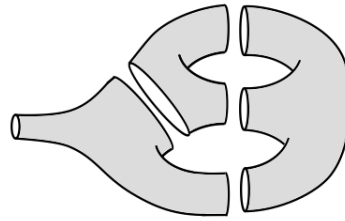


Figure 1.6: Schematic depiction of the “pants” approach used in constructing hyperbolic Riemann surfaces with boundary and arbitrary genus. Each pair of pants amounts to a $g = 0$ surface with three geodesic boundaries. For the contributions to the path integral (1.80), the moduli space of bordered Riemann surfaces $\mathcal{M}_{g,n}(b_1, \dots, b_n)$ up to arbitrary values is required. While in principle this may be calculated via the integral over the so-called Weil-Petersson symplectic form (restricted to a fundamental domain), in the seminal result of [81], it was shown that these volumes obey a recursion relation. Figure taken from [80].

Here Z_{trumpet} refers to the partition function on the “trumpet”, which localises to the expression

$$Z_{\text{trumpet}}(\beta) = \frac{e^{-\frac{b^2}{4\beta}}}{\sqrt{\pi\beta}} . \tag{1.84}$$

The hyperbolic Riemann surfaces without asymptotic boundary may be constructed via a “pants” construction as shown in fig.1.6. These “pants” are therefore the elementary building blocks. Remarkably, the moduli space volumes $V_{g,n}$ fulfill a recursion relation [81], which was later shown to determine the “topological recursion” of a specific matrix integral [82]. In [80] it was shown, based on this fact, that the partition function (1.81) corresponds to the genus expansion of a double-scaled matrix integral with the spectral curve:

$$y = \frac{\sin(2\pi z)}{4\pi} , z^2 = -E . \tag{1.85}$$

Hence the matrix integral is the non-perturbative completion of the gravitational theory. We therefore

have encountered a theory of (quantum) gravity following RMT universality. This is surely progress, however we have identified (1.81) as an observable in an ensemble of quantum mechanical systems. While indeed there should still be one underlying unique theory furnishing RMT statistics in some ergodic limit, it is unclear how to define such a theory. This is an open question. Moreover, it should also be noted that the surfaces included in the partition function do not constitute actual solutions to the equations of motion (beyond the disk) as (1.75) is not fulfilled. However, it can be shown that the two-boundary $g = 0$ wormhole is a solution in the microcanonical ensemble [79]. It is therefore not straightforward to generalise these ideas to higher dimensions, such as AdS_3 , although there is one proposal [83].

1.4.9 Discretised Surfaces and Random Matrices

Let us now come to an older approach to two-dimensional quantum gravity in terms of matrix theory. This approach also shares connections with JT gravity as first discovered in [80]. We may think of two-dimensional quantum gravity as “zero dimensional” string theory and therefore use the partition function

$$Z = \sum_g \int \mathcal{D}g e^{-\beta A + \gamma \chi}, \quad (1.86)$$

where A is the area, χ the Euler characteristic and β, γ are couplings. Eq. (1.86) is a theory of surfaces. One approach to such a theory was hinted at already in section 1.3.1 where it was explained that diagrams of $U(n)$ gauge theories amount to Riemann surfaces in the large n limit. We will consider a discretisation of (1.86) and then take an appropriately defined continuous limit. This will amount to a genus expansion of a matrix integral. In order to explain how surfaces are linked to matrices, let us take a step back. Consider an integral of the form

$$\int_{-\infty}^{\infty} \frac{d\phi}{\sqrt{2\pi}} e^{-\phi^2/2} \phi^{2k}, \quad (1.87)$$

where ϕ is merely a number. There is a useful trick to calculate such integrals. Take

$$\begin{aligned} & \int_{-\infty}^{\infty} \frac{d\phi}{\sqrt{2\pi}} e^{-\phi^2/2} \phi^{2k} \\ &= \frac{\partial^{2k}}{\partial J^{2k}} \int_{-\infty}^{\infty} \frac{d\phi}{\sqrt{2\pi}} e^{-\phi^2/2 + J\phi} \Big|_{\phi=0}. \end{aligned} \quad (1.88)$$

We can complete the square to show

$$\int_{-\infty}^{\infty} \frac{d\phi}{\sqrt{2\pi}} e^{-\phi^2/2 + J\phi} = e^{J^2/2}. \quad (1.89)$$



Figure 1.7: Depiction of Feynman diagrams corresponding to the theory defined in (1.91). The left panel shows the propagator and the right shows the vertex. Figure taken from [5].

Therefore eq.(1.88) amounts to

$$\begin{aligned} & \int_{-\infty}^{\infty} \frac{d\phi}{\sqrt{2\pi}} e^{-\phi^2/2} \phi^{2k} \\ &= \frac{\partial^{2k}}{\partial J^{2k}} e^{J^2/2} \Big|_{J=0} = \frac{(2k)!}{2^k k!}. \end{aligned} \quad (1.90)$$

A common situation in quantum field theory is of course the presence of an interaction term, such that we actually require an integration of the form

$$\int_{-\infty}^{\infty} \frac{d\phi}{\sqrt{2\pi}} e^{-\phi^2/2 + \lambda/4! \phi^4}. \quad (1.91)$$

This is already encompassed by $k = 2n$ in equation (1.88) with $n \in \mathbf{N}$:

$$\begin{aligned} & \frac{\lambda^n}{n!} \int_{-\infty}^{\infty} \frac{d\phi}{\sqrt{2\pi}} \left(\frac{\phi^k}{k!} \right)^n \\ &= \frac{\lambda^n}{n! k!} \left(\frac{\partial^k}{\partial J^k} \right)^n e^{J^2/2} \Big|_{J=0}. \end{aligned} \quad (1.92)$$

Diagrammatically (1.92) counts the number of distinct ways $4n$ objects, which themselves have four emerging lines, can be grouped. Connecting the lines corresponds to an insertion of a propagator, which is trivial though in this case. Taking the large n limit is not sufficient to create a Riemann surface though as this requires the graphs to become Ribbon graphs, see section 1.3.1. The idea is to replace scalars with Hermitian matrices, which carry enough structure. Therefore, we now consider integrals of the following form

$$\begin{aligned} & \int e^{-\text{Tr} \frac{H^2}{2}} H_{j_1}^{i_1} \dots H_{j_n}^{i_n} \\ &= \frac{\partial}{\partial J_{j_1}^{i_1}} \dots \frac{\partial}{\partial J_{j_n}^{i_n}} e^{J^2/2} \Big|_{J=0}. \end{aligned} \quad (1.93)$$

Now to calculate quantities such as

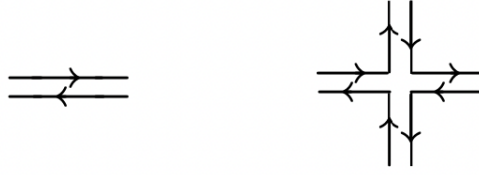


Figure 1.8: Depiction of Feynman diagrams corresponding to the theory defined in(1.94). We are using a double-line representation of the matrix indices. On the left panel we see the propagator and on the right the vertex. Figure taken from [5].

$$\frac{\lambda^n}{n!} \int dH e^{-\text{Tr} \frac{H^2}{2}} (\text{Tr} H^A)^n, \quad (1.94)$$

n vertices are laid down and connected via propagators. As upper and lower indices correspond to fundamental and antifundamental representations, we are introducing a “thickened” structure (called double-line notation in [24]), which will allow to associate a Riemann surface. Propagators and vertices are shown in fig.1.8. Now integrals such as (1.94) allow for a discretisation of the surfaces defined in the theory (1.86) as the surfaces can be constructed by the polygons corresponding to the vertices connected by propagators. It is customary to perform a triangulation of surfaces as depicted in fig.1.9.⁷ Therefore, we assume the full partition function to be of the form

$$e^Z = \int dH e^{-\frac{1}{2} \text{Tr} H^2 + \frac{\lambda}{\sqrt{n}} \text{Tr} H^3}. \quad (1.95)$$

The term of order λ^n now amounts to the number of diagrams with n 3-point vertices. Now the logic of section 1.3.1 can be applied. Therefore each diagram contributes a power of n according to topology of the surface it is drawn on. Therefore it is then also clear that Z is expanded in powers of n such as (1.8). For $n \rightarrow \infty$, genus zero surfaces, so-called planar diagrams, dominate. In order to furnish a uniform continuum of different genus contributions, one defines a double-scaling limit [84–86]. The idea is to take the limit $n \rightarrow \infty$ in combination with the tuning of the coupling g to a critical value $g \rightarrow g_c$. It can be shown that as the genus g contribution is given by

$$Z_g(g) \sim (g - g_c)^{(2-\gamma)\frac{\kappa}{2}}, \quad (1.96)$$

an overall expansion of the following form is achieved

$$Z = \sum_g \kappa^{2g-2} f_g, \quad (1.97)$$

with

$$\kappa^{-1} := n(g - g_c)^{(2-\gamma)/2}. \quad (1.98)$$

⁷ Whereas (1.94) would provide surfaces created by rectangles.

While we have immediately jumped to a matrix model description of (1.86), let us also describe how a continuum Liouville approach to the action may be used as this will be relevant to describe the relationship to the JT theory defined in section 1.4.8. Of course it is conjectured that the matrix model description and the pure worldsheet description are equivalent.⁸ So-called minimal string theory amounts to coupling the gravitational theory described above to a (p, q) minimal model CFT, that is a two-dimensional CFT with finitely many irreducible representations and a central charge of the form⁹

$$c = 1 - \frac{6(p - q)^2}{pq} < 1. \quad (1.99)$$

After gauge-fixing, this theory can be rewritten as a Liouville gravitational mode ϕ , a minimal model and the standard bc ghosts with the coupling fixed in such a manner that overall the condition $c_{\text{sum}} = 0$ is intact. Here c is the combined central charge. Let us now focus on $(2, 2m - 1)$, which is the unitary subset of the abovementioned minimal CFTs. Now importantly it can be shown that Z_0 takes on a form in agreement with (1.96) and furthermore, that in this approach

$$\gamma = \frac{1}{12} \left(c - 1 - \sqrt{(c - 1)(c - 25)} \right) = -\frac{1}{m}, \quad (1.100)$$

where c refers to the central charge of the minimal model. We therefore recover pure gravity (therefore the theory (1.86)), $c = 0$, as the case $m = 2$. Note that each individual minimal string theory implies a different γ in (1.96). How are minimal string theories realised in the matrix model language? In short, the $q = 2m - 1$ minimal string is realised as the m -th multicritical model of a one-matrix integral [87, 88]. That is, we consider a matrix model of the form

$$Z = \int dH \exp(V(H)), \quad (1.101)$$

and consider a double scaling procedure as mentioned above. For a first order critical point we arrive at pure gravity, whereas higher critical points of the potential in the double-scaling procedure amount minimal string theories. The most general solution of the one-matrix integral can be written as perturbations of pure gravity, i.e. [89]

$$S = S_{\text{grav.}} + \sum_{k \geq 0} t_k \int d\zeta^2 \sqrt{g} \mathcal{O}_k, \quad (1.102)$$

where the scaling parameters t_k (coupled to operators \mathcal{O}_k) allow the theory to interpolate between the critical points. Moreover, in the seminal papers [90, 91], Witten showed that the structure underlying the operators (1.102) can be interpreted in terms of a topological field theory, denoted topological gravity. More precisely, this theory calculates intersection numbers on the moduli space of Riemann surfaces with arbitrary genus. In the context of this thesis, it is important to mention that, as first shown in [80], JT gravity may be described as a limit of minimal string theory or as a coupling of infinitely many minimal string theories. It is this approach, the language of topological gravity, we use extensively in chapter 4. However, it is still a point of ongoing research to understand how

⁸ We are exclusively focusing on bosonic constructions here.

⁹ We are therefore strictly speaking immediately considering the worldsheet approach to a slightly more general theory than (1.86), namely one which is deformed by minimal matter.

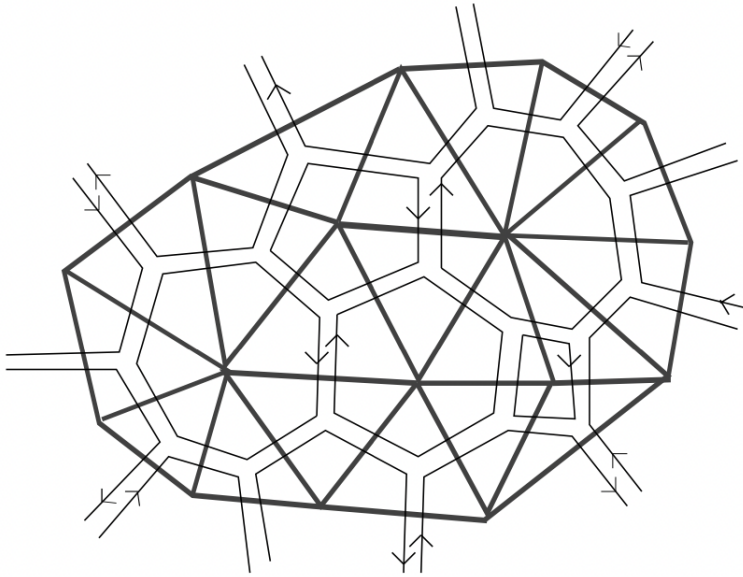


Figure 1.9: A random matrix triangulation of the theory of surfaces defined in (1.86) by the matrix integral (1.95). Figure taken from [5].

the geometric picture in terms of triangulations of Riemann surfaces is related to the hyperbolic geometries used in JT gravity.

1.5 Quantum Information: Complexity

Many recent developments with regard to quantum gravity (mostly in the context of AdS/CFT) focus on the description of gravitational phenomena in terms of quantum information quantities. One of the most commonly studied properties of quantum mechanical systems is complexity.

1.5.1 What is Complexity? Part 1

Computational complexity theory describes the inherent difficulty of computational problems. In the context of quantum mechanical theories, it estimates the difficulty of constructing a specific state in terms of simple operations, so-called *gates* [92]. While it is quite obvious in a purely quantum mechanical setting, why such a quantity plays an important role, it may not be so clear in a holographic setting. The connection is that there is mounting evidence that complexity may be related to the growing spatial volume of the black hole interior [93–96]. The intuition for this link is based on the following facts. The growth of the black hole interior continues past thermal equilibrium, whereas most holographic probes saturate at equilibrium time. However, complexity can be shown to display a similar late time growth as we will see below. It is for this reason that this quantum information quantity is connected to the interior of a black hole. In order to give a precise, microscopic definition, we first have to introduce some concepts from quantum information theory.

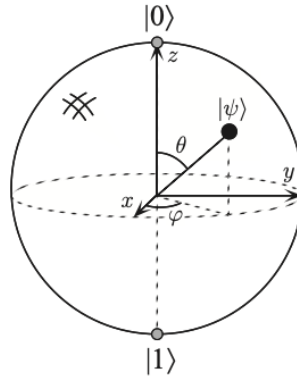


Figure 1.10: The Bloch sphere (Riemann sphere) geometrically represents the pure states of the qubit (1.105). Without loss of generality, north and south pole correspond to the mutually orthogonal states $|0\rangle$ and $|1\rangle$ respectively. Each point on the sphere represents a state of the two-dimensional system. Figure taken from [8].

1.5.2 Quantum Information Primer

In contrast to classical bits which either contain the state 0 or 1, a qubit is a superposition of states:

$$|\Psi\rangle = \alpha|0\rangle + \beta|1\rangle, \quad (1.103)$$

with α, β complex numbers. As the qubit is measured the result may either be 0 with α^2 probability or 1 with β^2 probability. The probabilities must add up:

$$|\alpha|^2 + |\beta|^2 = 1. \quad (1.104)$$

Therefore, one parametrisation of the qubit is given as:¹⁰

$$|\Psi\rangle = \cos\left(\frac{\theta}{2}\right)|0\rangle + e^{i\phi}\sin\left(\frac{\theta}{2}\right)|1\rangle, \quad 0 \leq \theta \leq \pi, 0 \leq \phi < 2\pi, \quad (1.105)$$

which is called the Bloch sphere representation as can be understood via figure 1.10. In this abstract language we may consider a quantum computer to be built out of a quantum circuit, consisting of wires, carrying the information, and logic gates manipulating the information. In accordance with one of the foundational principles of quantum mechanics the logic gates amount to unitary operators, such that (1.104) is preserved. For a single qubit, the operators move the qubit on the Bloch sphere in the language of (1.105), such that there is a representation of these operators in terms of matrices of $SU(2)$, which is generated by the Pauli matrices. For example the NOT gate amounts to σ_x and acts as

$$\sigma_x \begin{bmatrix} \alpha \\ \beta \end{bmatrix} = \begin{bmatrix} \beta \\ \alpha \end{bmatrix}. \quad (1.106)$$

¹⁰ Here we introduced a further constraint, reducing one degree of freedom. This comes from the fact that we are interested in scalar products for which overall phases drop out.

It is clear from the structure of (1.106) that the NOT gate implements logical negation. Let us introduce two additional gates, which are of great importance:

$$H = \frac{1}{\sqrt{2}} \begin{pmatrix} 1 & 1 \\ 1 & -1 \end{pmatrix}, \quad T = \begin{pmatrix} e^{-i\pi/8} & 0 \\ 0 & e^{i\pi/8} \end{pmatrix}. \quad (1.107)$$

The H gate is often called the Hadamard gate and the T gate the $\pi/8$ phase gate. Their meaning will become more apparent later. One important question is: given an arbitrary, unitary operator, can it be constructed using a specified, finite set of gates? Let us first understand how large the space of such operators is. For N qubits, the space of unitary operators is $SU(2^N)$. Now the volume of $SU(n)$ is [97]:

$$V(SU(n)) = \frac{2\pi \frac{(n+2)(n-1)}{2}}{1! \dots (n-1)!}, \quad (1.108)$$

with the dimension being $n^2 - 1$. How difficult is it to pick out one specific element? We can find an answer by discretising. We identify the number of different unitary operators with the number of ϵ -balls B_ϵ of dimension $n^2 - 1$ in $SU(n)$. The volume of such an ϵ -ball is given by:

$$V(B_\epsilon) = \frac{(\sqrt{\pi}\epsilon)^{n^2-1}}{\left(\frac{n^2-1}{2}\right)!}, \quad (1.109)$$

where the flat space result for the volume was used as ϵ is of course considered small. Therefore we then approximate the number of unitaries (where ϵ functions as a tolerance) by

$$\begin{aligned} \frac{V(SU(n))}{V(B_\epsilon)} &\sim \left(\frac{n}{\epsilon^2}\right)^{\frac{n^2}{2}} \\ &= \left(\frac{2^N}{\epsilon^2}\right)^{\frac{4^N}{2}}, \end{aligned} \quad (1.110)$$

where Stirling's approximation was used. Taking the logarithm of this we get

$$\log\left(\frac{V(SU(n))}{V(B_\epsilon)}\right) = \frac{4^N N}{2} \log(2) + 4^N \log\left(\frac{1}{\epsilon}\right). \quad (1.111)$$

In (1.111) we observe an exponential dependence on the size of the system and a logarithmic dependence on the tolerance. But what does it mean to approximate a unitary operator? Let us suppose that U, V are two unitary operators on the same state space with U being the target operator. By use of the operator norm, we can define the error to be

$$E(U, V) := \max_{\Psi} \|(U - V)|\Psi\rangle\|, \quad (1.112)$$

where the maximisation occurs over all states $|\Psi\rangle$. Let us now come back to the single qubit case and clarify the significance of H and T as defined in (1.107). It is well-known that any element of $SU(2)$

may be written as

$$R_{\vec{n}}(\theta) = e^{-i\theta\vec{n}\vec{\sigma}} . \quad (1.113)$$

Furthermore, it can be shown that

$$THTH = R_{\vec{n}}(\theta) . \quad (1.114)$$

Quite remarkably, it may also be shown that in the sense of (1.112), H and T together constitute *universal gates*. That means that any unitary operator (acting on a single qubit) may be constructed in finitely many steps within a specified tolerance. Therefore

$$E(U, R_{\vec{n}}(\theta)^{n_1} H R_{\vec{n}}(\theta)^{n_2} H R_{\vec{n}}(\theta)^{n_3}) < \epsilon . \quad (1.115)$$

For the actual proof we refer to [8]. For two-qubit systems H and T alone are not sufficient anymore. However, two facts allow for a remarkable generalisation.

- Any arbitrary, unitary matrix on a Hilbert space of arbitrarily many qubits can be written as a product of matrices only acting non-trivially on a two-qubit subspace (so-called *two-level* matrices).
- An arbitrary two-level operator can be constructed via single qubit operators and a two-qubit CNOT gate.

These two facts together tell us that H , T and CNOT together are universal. Any unitary operator acting on K qubits can be constructed up to arbitrary tolerance by these gates. The CNOT gate has the following form

$$\text{CNOT} = \frac{1}{2}(1^{(1)} + \sigma_z^{(1)}) \otimes 1^{(2)} + \frac{1}{2}(1^{(1)} - \sigma_z^{(1)}) \otimes \sigma_x^{(2)} . \quad (1.116)$$

The CNOT gate flips the second qubit if and only if the first qubit is in the state 1.

1.5.3 What is Complexity? Part 2

As we have established how an arbitrary unitary operator can be approximated, we can now define a notion of complexity [7]:

Quantum computational complexity $C(U)$ of an operator U is the minimal number n , such that $\|U - \prod_{i=1}^n U_i\| < \epsilon$, where the U_i belong to a set of allowed gates.

We see that $C(U)$ will depend on the tolerance ϵ , the gates we allow and the system size. We can deduce that for a set of p gates, the number of possible circuits with m elements is at most p^m , which implies that the number of unitary operators with $C(U) = m$ is bounded by p^m . By use of the formula (1.111) we see that it is exponentially difficult to simulate most operators. The above notion of complexity is with respect to operators. We can however also define state complexity [7]:

Quantum computational complexity of a state is defined by the minimal operator complexity over all operators which produce a given target state $|\psi_T\rangle$ starting with a simple reference state $|\psi_R\rangle$, i.e.,

$$C(|\psi_T\rangle) = \min_{U|\psi_R\rangle=|\psi_T\rangle} C(U) . \quad (1.117)$$

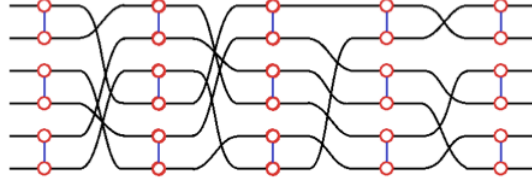


Figure 1.11: Depiction of the evolution of complexity for a N qubit model with a k -local (chaotic) Hamiltonian under the assumption that $k \ll N$. We can imagine time going from left to right, therefore e^{iHt} acting on the system. The specific setting shown here, has $N = 6$ and $k = 2$ and there are no restrictions on spatial locality, therefore the system is all-to-all. Figure taken from [6].

It can be shown that for the state complexity the qualitative expectations coincide with those for operator complexity. Therefore the number of states in the projective Hilbert space is exponential in n and logarithmic in ϵ . This is actually a common occurrence in this field. Many definitions of complexity may be defined, however, they usually converge to a similar general expected behaviour, see reference [98] in the holographic context.

1.5.4 Holographic Complexity

Having established black holes as quantum chaotic systems in 1.4.5, we can determine expectations by considering a toy model of a fast scrambling system. We model the evolution of Hamiltonian system by a discrete quantum circuit as pictured in figure 1.11. For our purposes this is a natural setting as unitary operators correspond to time evolution operators, which means we can translate the group-theoretic language used previously to actual time-dependence. Importantly, we consider a k -local Hamiltonian, which means that each gate only acts on k of the total N qubits at each discrete moment of time. As we are considering a chaotic, fast scrambling system, we assume that the partition of the qubits changes at each step and is all-to-all (no spatial locality as a qubit can move from one gate to any other). This means that all the qubits interact. After n steps of discrete time evolution, the number of unitaries which can be reached is:

$$\left(\frac{N!}{(N/k)!(k!)^{N/k}} \right)^n \approx \exp \left(n \frac{k-1}{k} N \log(N) \right), \quad (1.118)$$

which is of course a function of n as we consider k and N fixed. At early times, by which we mean n not being of exponential size, (1.118) is a lot smaller than (1.111). The complexity takes on the form

$$C = \frac{nN}{k}. \quad (1.119)$$

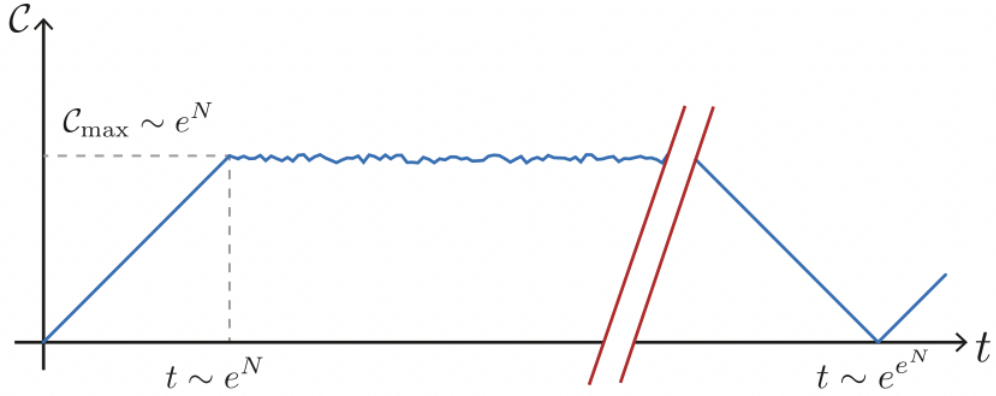


Figure 1.12: Schematic depiction of the evolution of complexity for a chaotic system in time. We observe early linear growth exponential in the degrees of freedom and a late time saturation to a constant value. Quantum recurrence is expected to occur on a doubly exponential timescale [6, 7]. Figure taken from [7].

We observe a linear growth in time. The linear growth continues until the entire group has been explored. This happens at the discrete time $n = O(2^{2N})$. At this point the complexity saturates. On doubly exponential time-scales it is expected that quantum recurrence occurs. Just as for the SFF, defined in section 1.4.6, here too we observe a “ramp” and a “plateau”. In a holographic context, which will elaborate upon below, it is expected that the timescales introduced in the qubit setting of figure 1.12 are translated via $N \sim S_0$. Let us now comment on how it is believed that the state complexity of the dual theory translates to bulk geometric quantities, an idea which was first proposed in [93]. Two proposals have been made:

- “Complexity=Volume” (CV)

Let Σ denote a spatial slice of the AdS boundary, then the complexity C_V of the state is given by [94]:

$$C_V = \frac{\text{Vol}(\mathcal{N})}{G_N L_{\text{AdS}}}, \quad (1.120)$$

where \mathcal{N} is a slice of maximal volume with $\partial\mathcal{N} = \Sigma$

- “Complexity=Action” (CA)

The complexity of the state is equal to the on-shell action on a Wheeler-DeWitt (WDW) patch [95, 96]:

$$C_A = \frac{S_{\text{WDW}}}{\pi\hbar}, \quad (1.121)$$

where the WDW patch is the domain of dependence of a Cauchy slice in the bulk anchored to the boundary at Σ .

Let us briefly go through the example of a two-sided eternal black hole in AdS via the CV proposal following [94, 99]. This spacetime has the metric:

$$ds^2 = -f(r)dt^2 + \frac{dr^2}{f(r)} + r^2 d\Omega_{d-2}^2, \quad (1.122)$$

$$f(r) = 1 + \frac{r^2}{L_{AdS}^2} - \frac{\mu}{r^{d-2}}, \quad (1.123)$$

where μ is a parameter related to the mass. The maximum volume may be calculated by extremising the volume functional:

$$\text{Vol}(\mathcal{N}) = \omega_{d-1} \int dr r^{d-1} \sqrt{f(r)t'(r)^2 + \frac{1}{f(r)}}. \quad (1.124)$$

Analytically continuing the expression (1.124) to Eddington-Finkelstein coordinates (as the slice goes behind the horizon) gives the expression

$$\frac{dC_V}{d\tau} = \frac{8\pi}{(d-1)} M, \quad (1.125)$$

for late times. Let us briefly also state the result from the CA approach [95]:

$$\frac{dC_A}{d\tau} = \frac{2M}{\pi}. \quad (1.126)$$

We note that both proposals reproduce the linearly growing ‘‘ramp’’ and therefore match expectations, namely (1.119), in a qualitative sense. However, the approaches seem to disagree on the exact prefactor. It is in general not clear how the circuit time maps to physical time, such that precise factors should not be taken seriously anyway. The important takeaway therefore is that the ‘‘ramp’’ is reproduced via semi-classical, perturbative analysis and also that there are various candidates for complexity agreeing qualitatively.¹¹

1.5.5 The Plateau via JT Gravity

While much research has been done on the early initial growth of complexity, the ‘‘ramp’’, the creation of the plateau has been elusive until recently. We will now outline how the non-perturbative (in G_N) nature of JT gravity as defined in [80] has led to a new quantity named ‘‘spectral complexity’’ which conforms with expectations beyond the ramp as it furnishes the ‘‘plateau’’. The reference [100] specifies an approach which may be considered a variant of the CV proposal in the context of higher genus surfaces as they appear in JT gravity. It is proposed that the volume of the black hole interior

¹¹ We are calling the linearly increasing section of 1.12 the ‘‘ramp’’ in analogy with the spectral form factor. However, note that in a holographic setting the complexity ramp is due to classical effects as explained in the main text, whereas the spectral form factor ramp requires non-perturbative effects in JT gravity.

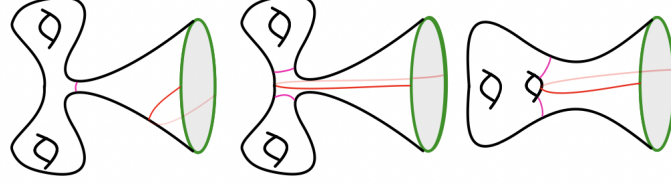


Figure 1.13: The three different surface topologies, which contribute to the calculation of $\langle \text{Tr}_\beta(\chi(x_1)\chi(x_2)) \rangle$ in the context of JT gravity. In red we see the boundary-to-boundary geodesic which furnishes these topologies in the path integral and leads to the moduli space structure of (1.130). Green depicts the asymptotic AdS boundary with graviton fluctuations. In purple we see the closed geodesics along which the wavefunctions are glued and therefore in the formula (1.130) amounts to the b_1 and b_2 integrations. Figure taken from [100].

(which in two dimensions is just a length) is to be identified with the following quantity:

$$\langle \ell \rangle = \lim_{\Delta \rightarrow 0} \left\langle \sum_{\gamma} \ell_{\gamma} e^{-\Delta \ell_{\gamma}} \right\rangle_{\text{JT}}, \quad (1.127)$$

where γ denotes self-intersecting geodesics, Δ is a regulator and $\langle \rangle_{\text{JT}}$ means that the sum is evaluated in the theory of JT gravity [80]. In practice (1.131) is determined by calculating

$$\langle \ell(t) \rangle = - \lim_{\Delta \rightarrow 0} \frac{\langle \chi_L(t) \chi_R(0) \rangle_{\text{non-int.}}}{\partial \Delta}, \quad (1.128)$$

where $\langle \chi_L(t) \chi_R(0) \rangle_{\text{non-int.}}$ is calculated in the Euclidean JT theory and then analytically continued to real time. In the probe limit the Euclidean quantity is

$$\langle \text{Tr}_\beta(\chi(x_1)\chi(x_2)) \rangle = \sum_{\mathcal{M}} \sum_{\gamma} \langle \text{Tr}_\beta e^{-\Delta \ell_{\gamma}} \rangle_{\mathcal{M}}, \quad (1.129)$$

where the sum over \mathcal{M} denotes a sum over all surfaces (with the same boundary condition) and the sum over γ corresponds to a sum over all geodesics connecting the points x_1 and x_2 , where each geodesic exhibits length ℓ_{γ} . The calculation of $\langle \text{Tr}_\beta(\chi(x_1)\chi(x_2)) \rangle_{\text{non-int.}}$ in the context of JT gravity of course involves a sum over hyperbolic Riemann surfaces with an infinite number of boundary-to-boundary geodesics. Ref. [101] states that the integral over the moduli space in the presence of these geodesics may be rewritten, such that we end up with the following expression for the genus g contribution [100]:

$$\begin{aligned} \langle \text{Tr}_\beta(\chi(x_1)\chi(x_2)) \rangle_{\text{non-int.}} &\sim e^{S_0(1-2g)} \int d\ell e^{\ell} \int db_1 b_1 db_2 b_2 \Psi_{\text{trumpet},x}(\ell, b_1) \Psi_{\text{trumpet},\beta-x}(\ell, b_2) e^{-\Delta \ell} \\ &[V_{g-1,2}(b_1, b_2) + \sum_{h \geq 0} V_{g-h,1}(b_1) V_{h,1}(b_2)]. \end{aligned} \quad (1.130)$$

Let us now elaborate schematically how this structure arises and what the individual ingredients refer to. As shown in fig. 1.13 for the $g = 2$ contribution. There are in principle an infinite number of geodesics running from the boundary to itself in the sum (1.129). We can however distinguish

between those geodesics which cut the surface into two disconnected individual surfaces each with one asymptotic boundary and those geodesics which cut the surface in such a manner that there is one connected surface with two asymptotic boundaries. This explains the structure of the moduli space volumes in (1.130). This cutting procedure therefore means we are dealing with surfaces which have a geodesic boundary, denoted with b and a geodesic of fixed length ℓ glued to the asymptotic boundary. From [78, 101, 102] the correct wavefunctional for these structures, here denoted as $\Psi_{\text{trumpet},x}$, is known as well as the integration measure e^ℓ . After integrating, analytically continuing and then using (1.128) we arrive at the expression:

$$\langle \ell(t) \rangle = -\frac{2e^{-S_0}}{Z(\beta)} \int_0^\infty \frac{\langle \rho(s_1)\rho(s_2) \rangle}{\bar{s} \sinh(2\pi\bar{s})\omega \sinh(\pi\omega)} \exp\left(-\beta\left(\frac{\bar{s}^2}{2} + \frac{\omega^2}{8}\right) - i\bar{s}\omega t\right). \quad (1.131)$$

with the definitions $\omega := s_1 - s_2$, $\bar{s} := \frac{s_1+s_2}{2}$ and $s_{1,2} := \sqrt{E_{1,2}}$. As also emphasised in ref. [100], equation (1.131) constitutes a new quantity which may be calculated for any quantum system. Due to its relation to the two-point function it is named ‘‘spectral complexity’’ in [100]. By use of (1.69) it can then be shown that indeed (1.131) for JT follows the expectations outlined earlier and furnishes a plateau. The proposal for ‘‘spectral complexity’’ can be further probed by calculating the variance. Following the procedure of [100] this leads to some tension as at late times the variance does not saturate but exhibits linear growth. This of course means that the variance is of the same size as the signal (at $t \sim e^{S_0}$). We will tackle this point in chapter 6.

1.6 Cosmology, our Universe and De Sitter

While AdS/CFT should by any estimation be considered a remarkable success of modern theoretical physics, our actual universe does not seem to be in accord with a negative cosmological constant. To the contrary actually, there is observational evidence for two distinct periods of exponential expansion. Chronologically first comes inflation [103–105], which is believed to have occurred 10^{-34} seconds after the big bang. Inflation is also believed to have furnished both the observed large-scale homogeneity of our universe and also allowed for tiny fluctuations which finally lead to the formation of structure. The cosmic microwave background (CMB), which is the afterglow of the big bang [106], while largely homogeneous, exhibits temperature fluctuations of order 10^{-5} . According to inflation these fluctuations are related to the formation of structure. Therefore, one of the most important questions is to understand what the microscopic origin of these fluctuations is. This is a true quantum gravity question and therefore should be amenable to some holographic analysis. In many models of inflation the universe is modelled by a de Sitter universe. With respect to this inflationary phase we are ‘‘meta-observers’’ observing the inflationary period ‘‘after’’ future infinity \mathcal{I}^+ . The second instance of a period of exponential expansion is the dark energy dominated present. The universe is currently expanding and remarkably it is also expanding at an accelerating pace [107, 108]. Moreover, observations seem to indicate that we are currently entering a phase which is dominated by a small, but positive cosmological constant. There are quite general arguments that this implies that we are asymptoting towards a de Sitter universe. Furthermore, we are surrounded by a cosmological horizon, which is similar in nature to an event horizon and therefore also brings similar problems as those alluded to in section 1.3.4 [109].

1.6.1 Covariant Entropy Bound

We have emphasised that in any effective approach to gravitational problems one of the most important guidelines is the holographic principle. Furthermore, in AdS/CFT we have seen that a dual theory, a conformal field theory, generally amounts to a microscopic definition of the gravitational theory and that this dual theory arises at the conformal boundary, where gravity decouples. Moreover, this theory exhibits redundant degrees of freedom such that the entropy bound is respected. If we take these results as lessons to be applied in the cosmological context, we would expect that gravitational results may be rephrased in the form of some proper microscopic theory respecting the holographic bound. If we drop the assumptions of asymptotic flatness, spherical symmetry and gravitational stability used in section 1.2, we would naively generalise (1.6) to

$$S(V) \leq \frac{A[B(V)]}{4}, \quad (1.132)$$

where V is a compact portion on a spacelike slice of some spacetime \mathcal{M} , $S(V)$ the matter entropy of all matter systems in V , B the boundary of V and A the area of this boundary. However, there are examples for which (1.132) does not hold. One such example is our universe as modeled by an FLRW universe expanding in time [110]. It is clear that we must look for a covariant entropy bound.¹² The covariant entropy bound is the following [111]:

$$S[L(B)] \leq \frac{A(B)}{4}, \quad (1.133)$$

where $L(B)$ is any light-sheet of a two-dimensional, spatial surface B . The new ingredient of (1.133) is the prescription of what entropy is bounded, as $S[L(B)]$ is now defined on space-time region (and therefore not a purely spatial region as in (1.132)), namely the null surface $L(B)$, which we will now briefly explain. For a given spatial surface B there are four orthogonal null directions (four families of light-rays): future directed ingoing, future directed outgoing, past directed ingoing, and past directed outgoing, which we label by F_1, \dots, F_4 . In fig. 1.14 an intuitive depiction of these four light-rays is given for the case of B being a spherical surface. Let us illustrate why these definitions are needed for the case of B being a spherical room. Clearly, as this is a weakly gravitating region we expect the area of B to give the entropy of the room inside. Therefore the spherical walls bounding the potential entropy. What we are therefore looking for is a choice of two of the four light-rays which covariantly defines "inside". Moreover, this may only be a local condition. Following ref [111], "inside" may be defined as the direction in which the cross-directional area decreases (along some affine parameter). Therefore, the construction we define is:

$$\theta(\lambda) \leq 0, \quad (1.134)$$

where λ is an affine parameter of the light-rays generating the F_i and $\theta(\lambda)$ is the *expansion* defined as

$$\theta(\lambda) = \frac{dA/d\lambda}{A}. \quad (1.135)$$

¹² One could also consider the construction of a bound involving energy as in (1.5), however local energy is not well-defined in general relativity, whereas area can always be covariantly defined.

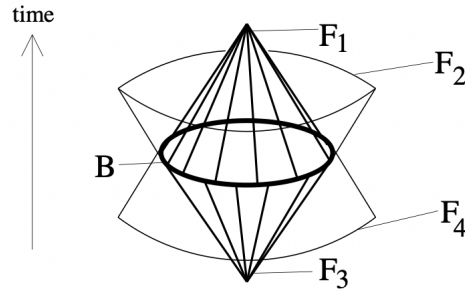


Figure 1.14: There are four null hypersurfaces F_1, \dots, F_4 orthogonal to the spherical surface B . Whereas F_1 and F_3 exhibit negative expansion, F_2 and F_4 have positive expansion and are therefore not relevant to the entropy bound. F_1 and F_3 are denoted as light-sheets and may be used in (1.133). Figure taken from [1].

Therefore of the four light-rays orthogonally projecting away from B we take those which are non-expanding via the definition (1.134) to be “inside”. We can then construct a null hypersurface L , called a lightsheet by following the light-rays until a boundary or a singularity is reached or until (1.134) is violated. The conjecture (1.133) then states that the entropy on the lightsheet will not exceed $\frac{A(B)}{4}$. Having laid the conceptual framework for the rest of section 1.6, let us concisely add some caveats and details as to when the Bekenstein bound (1.5), the generalised second law (1.4) and the covariant entropy bound (1.133) hold. It might be tempting to think that certain constraints on the matter configuration must hold for these equations. In the realm of (quantum) field theory there are multiple possible conditions, which are labelled as *energy conditions*. For example, the original proposal for the covariant entropy bound, as brought forth in [111], was based on the assumption of the dominant energy condition. This requires for the energy momentum tensor that $T^{\mu\nu}v_\mu v_\nu \geq 0$ for all timelike v_μ . However, for proper quantum fields such an energy condition can be violated locally by for example the Casimir effect. Moreover, perhaps more pertinent to the discussions here, for evaporating event horizons the null energy condition, and therefore also the dominant energy condition, is violated. In general, quantum effects may lead to violations of such conditions. However, remarkably under some mild assumptions the laws outlined in 1.2 and here still hold or can be given a quantum improvement, such that they hold.¹³ For example in some situations the generalised second law is actually proven to arbitrary quantum order, see for example [112]. Here merely the validity of semi-classical gravity, that is the use of a quantum energy momentum tensor $\langle T^{\mu\nu} \rangle$ for matter and the existence of a consistent regularisation scheme for the generalised entropy (plus some very mild symmetry assumptions) are assumed. In [113], it was shown that the Bekenstein bound holds for the relative entropy between states in Minkowski space without further constraining the matter content. The covariant entropy bound and the focussing theorem, which we did not discuss here but is closely related, can be generalised to quantum versions as shown in [114].

1.6.2 The Holographic Principle in Cosmology

Although the previous section holds for arbitrary spacetimes it is at this point not quite clear how such considerations may help in the construction of holography for cosmological scenarios. However, the

¹³ Similarly to the jump from the second law to the generalised second law.

covariant entropy bound actually already implicitly allows for the definition of a holographic screen for arbitrary spacetimes [115]. This would therefore answer the question: where is the information stored in cosmological spacetimes? The idea is to "invert" the covariant entropy bound by first foliating the spacetime into a one-parameter family of null hypersurfaces. Then each null hypersurface can be followed along its generators in direction of non-negative expansion right until it becomes negative (or it reaches a boundary). This procedure is called *projection*. To each slice we can therefore associate a $(D - 2)$ -dimensional surface and therefore each family forms a $(D - 1)$ -dimensional surface either embedded in the spacetime itself or on the boundary, which we call the holographic screen. Note that of course we could stop at any point following a non-negative expansion and we would have found a light-ray to which we can associate a covariant entropy bound. However, the procedure we have given here gives a *preferred* holographic screen, which acts as a screen in two directions and is therefore especially powerful in describing the spacetime. For a spherically symmetric spacetime this procedure simplifies via Penrose diagrams, which we will demonstrate for the most pertinent case, namely a dS spacetime. The spacetime must be divided into "wedges" as in the left panel of figure 1.15. These "wedges" indicate the change in the area of the sphere (therefore the expansion) with the legs showing the direction of negative expansion. On each lightcone each point must be projected along the direction of the tip of the wedge until the wedge flips or a boundary of spacetime is reached. For dS this actually furnishes two possible holographic screens: the conformal boundary or the cosmological horizon. In the middle panel we see that if we restrict to the observable region of dS (which is either the upper or the lower triangle) then either observer may be holographically described by either future infinity or past infinity. Remarkably, for the same two sets of observers either the past or future cosmological horizon is also a candidate. This would also seem to imply that the full eternal dS spacetime may either be described by both conformal boundaries or both past and future cosmological horizons. While the former approach due to its similarity to AdS/CFT has been brought forth in [116–118], the latter approach has gained more traction recently, see for example [119]. As we explore in the main text of this thesis, more precisely chapter 7, the complication at the cosmological horizon is of course that gravity does not fully decouple. However, we explore a specific state, which might be relevant to inflationary scenarios, in which backreaction allows for a fully decoupled description.

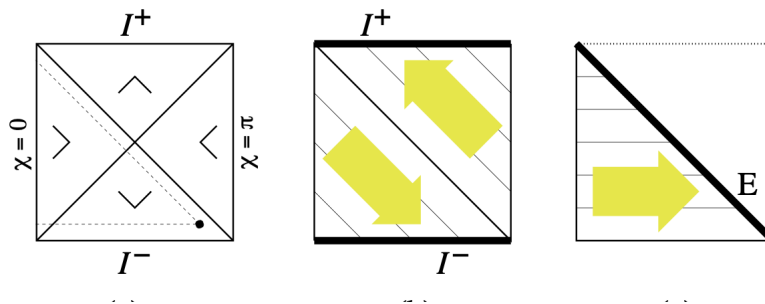


Figure 1.15: Penrose diagram of dS. The diagonal lines in the left panel are horizons dividing the spacetime into four regions corresponding to the different behaviour of changes to the area of S^{D-2} spheres. The legs of “wedges” indicate the direction of negative expansion. In the middle panel we see diagonal lines which correspond to a null foliation of spacetime in terms of past light cones of an observer on the north pole and future light cones for an observer on the south pole. We see that the projection, which runs along the tip of the nose gives two options for an holographic screen. In the middle we see that the spacetime may be projected onto a screen at both conformal boundaries \mathcal{I}^+ and \mathcal{I}^- or as in the panel on the right. Here, we see the north pole observer projected onto the cosmological horizon. Figure taken from [115].

JT Supergravity Part 1

This chapter has already been published as [120]:

Towards the Holographic Dual of $\mathcal{N} = 2$ SYK, *S. Förste, J. Kames-King, M. Wiesner*, In: *JHEP* 03 (2018) 028, arXiv: 1712.07398 [hep-th]

This chapter deals with a supersymmetric generalisation of the JT theory introduced in section 1.4.7. More explicitly, we show how to construct $\mathcal{N} = (2, 2)$ JT (axial) supergravity by gauging the local $U_A(1)$ tangent space group and solving the torsion constraints. We show how this theory reduces to the boundary $\mathcal{N} = 2$ super-Schwarzian. All of the above is done in an explicit superspace formalism using superconformal gauge. This is the starting point of a duality between $\mathcal{N} = (2, 2)$ JT (axial) supergravity and the $\mathcal{N} = 2$ supersymmetric SYK model [121]. A supersymmetric setting of the type discussed here may be more amenable to an inclusion into some higher-dimensional string theory setting.

In detail, we start by constructing the appropriate $\mathcal{N} = (2, 2)$ theory of supergravity. This amounts to a choice of superalgebra. By gauging the $U_A(1)$ tangent space group we are focusing on axial supergravity, which implies a specific spinorial covariant derivative structure. In addition, torsion constraints must be solved to furnish a physical supergravity theory. We choose to solve the torsion constraints in superconformal gauge. Furthermore, the superalgebra must be given a covariant form in terms of the covariant derivatives on superspace. We see that in this minimal theory the gravity supermultiplet is split up into a chiral and an anti-chiral superfield. The multiplet includes the supercurvature, a $U_A(1)$ field strength and the gravitini. As we are using superconformal gauge, the supercurvature amounts to a function of the superconformal Weyl factor. In addition, as we are describing a JT theory of supergravity, we introduce a dilaton superfield, which naturally also exhibits chiral/anti-chiral structure on superspace. The dilaton multiplet includes a complex scalar dilaton field and the fermionic dilatini fields. Of course we also add the extrinsic curvature as a superfield at the boundary. Naturally, this a priori appears as a chiral and anti-chiral superfield. As a check of the consistency of the theory in superspace, we may consider x-space projections. In an appropriate limit the standard bosonic JT theory should be recovered. If we are considering classical backgrounds such as AdS_2 , the fermionic contributions should be set to zero. Therefore considering only the bosonic

terms in the x-space projection we arrive at a generalisation of JT gravity with a complex curvature constraint, a complex dilaton and a $U_A(1)$ field strength. Considering real curvature constraints sets the field strength to zero. Assuming a real dilaton then reduces the action to the standard JT theory of section 1.4.7. As the superconformal factor plays an important role, it is determined in two ways. First, it can be shown that demanding a real, negative hyperbolic value for the supercurvature, gives a Liouville equation for the leading bosonic term of the superconformal Weyl factor, which itself in superspace appears as a chiral/anti-chiral superfield structure. This Liouville equation can then be solved, which fixes this leading component. The second approach is based on solving Killing spinor equations. We demand a background of maximal supersymmetry, that is the existence of four supercharges in line with [122]. This firstly implies a zero $U_A(1)$ field strength. Moreover, the resulting Killing spinors can then be shown to generate the isometries of AdS_2 . The resulting superconformal Weyl factor is in agreement with the previously determined expression. Now that we have determined how the classical AdS_2 background appears in this superspace construction, we can now move to the main focus of this publication, namely the emergence of a super-Schwarzian. The boundary condition of a boundary curve of constant length (discussed in section 1.4.7) is readily generalised to superspace. We observe that the boundary exhibits $\mathcal{N} = (1, 1)$ supersymmetry. The boundary conditions determine the extrinsic supercurvature which is shown to be the $\mathcal{N} = 2$ super-Schwarzian. As the boundary is generalised to a boundary superspace, the number of fluctuations is also enlarged compared to the standard Schwarzian. Concretely, there are two fermions and two bosons. These constitute the supergravity multiplet at the boundary. We conclude by performing a simple consistency check.

The author contributed to all conceptual discussions regarding this publication. In addition the author performed all calculations apart from the determination of the superconformal factor via the Killing spinor equations.

Towards the holographic dual of $\mathcal{N} = 2$ SYK

Stefan Förste, Joshua Kames-King and Max Wiesner

*Bethe Center for Theoretical Physics and Physikalisches Institut der Universität Bonn,
Nussallee 12, 53115 Bonn, Germany*

E-mail: forste@th.physik.uni-bonn.de, jvakk@yahoo.com,
wiesner@physik.uni-bonn.de

ABSTRACT: The gravitational part of the holographic dual to the SYK model has been conjectured to be Jackiw-Teitelboim (JT) gravity. In this paper we construct an AdS_2 background in $\mathcal{N} = (2, 2)$ JT gravity and show that the gravitational dynamics are — as in the $\mathcal{N} = 0$ and $\mathcal{N} = 1$ cases — fully captured by the extrinsic curvature as an effective boundary action. This boundary term is given by the super-Schwarzian of the $\mathcal{N} = 2$ SYK model, thereby providing further evidence of the JT/SYK duality. The chirality of this SYK model is reproduced by the inherent chirality of axial $\mathcal{N} = (2, 2)$ supergravity.

KEYWORDS: 2D Gravity, AdS-CFT Correspondence, Extended Supersymmetry

ARXIV EPRINT: [1712.07398](https://arxiv.org/abs/1712.07398)

Contents

1	Introduction	1
2	$\mathcal{N} = (2, 2)$ supergravity	2
3	$\mathcal{N} = (2, 2)$ Jackiw-Teitelboim action	5
4	Determination of the superconformal factor	8
5	Effective action: appearance of the super-Schwarzian	11
6	Consistency check	15
7	Summary and conclusions	16

1 Introduction

The Sachdev-Ye-Kitaev (SYK) model [1–7] is conformally (i.e. reparametrisation) invariant in the IR. The breaking of conformal symmetry results in an effective Lagrangian for time reparametrisations which is given by the Schwarzian. Models without random couplings sharing this property have been constructed and studied in e.g. [8–18]. There are various other mutations of the SYK model, for instance, higher dimensional analogs have been proposed in [19–21], complex versions are studied e.g. in [19, 22, 23], more than one flavour and non Abelian global symmetries have been investigated in [24–27]. For the present paper the supersymmetric versions constructed in [28] are most relevant. For variations and further aspects of supersymmetric SYK models see [29–41]. Now, superreparametrisations are an exact symmetry only in the infrared limit, and their breaking gives rise to an effective super-Schwarzian action.

The holographic dual is believed to contain some version of dilatonic 2d gravity arising quite universally in compactifications from higher dimensions [42]. Moreover, near the horizon of an AdS_2 black hole, corresponding to the IR of SYK, solutions of the dilaton are nearly constant. Approximating to linear order in non constant contributions leads to Jackiw-Teitelboim (JT) gravity [43, 44], for a recent review see [45]. JT gravity has been corroborated as the gravitational dual of the SYK model e.g. by deriving the Schwarzian as an effective action for the UV regulator curve [46–49]. Liouville theory instead of JT gravity has been considered in [50]. A three dimensional holographic dual has, however, been advocated in a series of papers [51–53]. Corrections to JT gravity have been recently proposed in [54]. Gathering information about the holographic dual beyond the gravitational sector has been the subject of [55, 56].

To start extending these investigations to supersymmetric versions of SYK it was shown in [57] that an $\mathcal{N} = (1, 1)$ supersymmetric version of JT gravity [58] supplemented with the appropriate boundary term leads to the $\mathcal{N} = 1$ super-Schwarzian as an effective action for the UV regulator curve. In the present paper we will extend this further to $\mathcal{N} = (2, 2)$ JT gravity.

The paper is organised as follows. In section 2 we collect some results on $\mathcal{N} = (2, 2)$ supergravity in superconformal gauge. Section 3 deals with the $\mathcal{N} = (2, 2)$ extension of JT gravity. The Gibbons-Hawking-York term is added. In section 4 the superconformal gauge is solved for AdS_2 as a supersymmetric background. The main result, the super-Schwarzian as effective Lagrangian of the boundary curve, is obtained in section 5. In section 6, a consistency check will be performed. Our results are summarised in section 7.

2 $\mathcal{N} = (2, 2)$ supergravity

In this section, we collect some information about extended $\mathcal{N} = (2, 2)$ supersymmetry and supergravity in two dimensions. Useful references are [59–64]. The two dimensional rigid $\mathcal{N} = (2, 2)$ superspace is given by the coset space [60]

$$\frac{(2, 2)\text{Supergroup}}{\text{Lorentz} \otimes U_A(1) \otimes U_V(1)},$$

with coordinates

$$z^\pi = (z, \theta^+, \bar{\theta}^+; \bar{z}, \theta^-, \bar{\theta}^-)$$

and covariant derivatives

$$\begin{aligned} \partial_z, & \quad D_+ = \frac{\partial}{\partial\theta^+} + \frac{1}{2}\bar{\theta}^+\partial_z, & \quad \bar{D}_+ = \frac{\partial}{\partial\bar{\theta}^+} + \frac{1}{2}\theta^+\partial_z, \\ \partial_{\bar{z}}, & \quad D_- = \frac{\partial}{\partial\theta^-} + \frac{1}{2}\bar{\theta}^-\partial_{\bar{z}}, & \quad \bar{D}_- = \frac{\partial}{\partial\bar{\theta}^-} + \frac{1}{2}\theta^-\partial_{\bar{z}}. \end{aligned}$$

They satisfy the anticommutation relations

$$\{D_+, \bar{D}_+\} = \partial_z, \quad \{D_-, \bar{D}_-\} = \partial_{\bar{z}}.$$

There are two versions of minimal $\mathcal{N} = 2$ supergravity, which can be obtained from the nonminimal $U_A(1) \otimes U_V(1)$ by gauging either the $U_A(1)$ or $U_V(1)$ factor of the tangent space symmetry group [61]. Here we will focus on the axial version of minimal $\mathcal{N} = 2$ sugra with gauged $U_A(1)$, which can also be obtained by dimensionally reducing $\mathcal{N} = 1$ sugra in $d = 4$. Accordingly, the tangent space symmetry group consists of the 2D Lorentz group and the gauged $U_A(1)$ factor.

The spinorial covariant derivatives in the minimal theory are given by

$$\nabla_\alpha = E_\alpha + \Omega_\alpha \mathcal{J} + \Sigma_\alpha \mathcal{Y}, \tag{2.1}$$

where $\alpha = \pm$ is a flat space spinor index and \mathcal{J}, \mathcal{Y} are respectively the Lorentz and $U_A(1)$ generators with corresponding connections Ω_α and Σ_α . For the complex conjugates and vector derivatives similar relations hold.

The Lorentz and $U_A(1)$ generators form together with the four supercharges Q^+ , Q^- , \bar{Q}^+ , \bar{Q}^- our SUSY algebra [60]:

$$\begin{aligned}
 [Q_+, \mathcal{Y}] &= -Q_+, & [\bar{Q}_+, \mathcal{Y}] &= \bar{Q}_+, \\
 [Q_-, \mathcal{Y}] &= Q_-, & [\bar{Q}_-, \mathcal{Y}] &= -\bar{Q}_-, \\
 [Q_+, \mathcal{J}] &= \frac{i}{2}Q_+, & [\bar{Q}_+, \mathcal{J}] &= \frac{i}{2}\bar{Q}_+, \\
 [Q_-, \mathcal{J}] &= -\frac{i}{2}Q_-, & [\bar{Q}_-, \mathcal{J}] &= -\frac{i}{2}\bar{Q}_-.
 \end{aligned}
 \tag{2.2}$$

Therefore Majorana constraints are implemented by the following constraint on Weyl spinors in Euclidean space:

$$(Q_+)^* = \bar{Q}_-, \quad (Q_-)^* = \bar{Q}_+. \tag{2.3}$$

For convenience, we introduce the following linear combination of the tangent group generators:

$$M \equiv \mathcal{J} - \frac{i}{2}\mathcal{Y}, \tag{2.4}$$

$$\bar{M} \equiv \mathcal{J} + \frac{i}{2}\mathcal{Y}. \tag{2.5}$$

In order to get a physical sugra theory, torsion constraints have to be imposed. In our case, the relevant constraints are given by

$$\begin{aligned}
 \{\nabla_{\pm}, \nabla_{\pm}\} &= 0, \quad \text{and} \quad \{\nabla_+, \nabla_-\} = -\frac{1}{2}\bar{R}\bar{M}, \\
 \{\bar{\nabla}_{\pm}, \bar{\nabla}_{\pm}\} &= 0, \quad \text{and} \quad \{\bar{\nabla}_+, \bar{\nabla}_-\} = -\frac{1}{2}RM, \\
 \{\nabla_+, \bar{\nabla}_-\} &= 0, \quad \text{and} \quad \{\bar{\nabla}_+, \nabla_-\} = 0,
 \end{aligned}
 \tag{2.6}$$

where R is the chiral and \bar{R} the anti-chiral curvature supermultiplet. These supermultiplets contain in their two θ component the usual bosonic scalar curvature \mathcal{R} as well as the $U_A(1)$ field strength \mathcal{F} as can be most easily displayed in a Wess-Zumino gauge [62]: the components of the supercurvature multiplets can be expressed through the components of the supergravity multiplet, namely the vielbein e_a^m , the gravitini ψ_a^α and the two auxiliary fields S and \bar{S} . These fields are defined by the leading components of the vector covariant derivatives

$$\begin{aligned}
 \nabla_a| &= \mathbf{D}_a + \psi_a^\alpha \nabla_\alpha| + \psi_a^{\dot{\alpha}} \nabla_{\dot{\alpha}}| \\
 &= \mathbf{D}_a + \psi_a^\alpha \partial_\alpha + \psi_a^{\dot{\alpha}} \partial_{\dot{\alpha}},
 \end{aligned}
 \tag{2.7}$$

where $|$ sets $\theta^+ = \theta^- = \bar{\theta}^+ = \bar{\theta}^- = 0$ and

$$\mathbf{D}_a = e_a + \Omega_a \mathcal{J} + \Sigma_a \mathcal{Y}. \tag{2.8}$$

The leading components of the curvature supermultiplets are given by

$$R| = S, \quad \bar{R}| = \bar{S}. \quad (2.9)$$

The higher order components can be determined by looking at

$$\begin{aligned} [\nabla_l, \nabla_{\bar{l}}] = & -\frac{i}{2} [(\nabla_- R)\nabla_+ + (\nabla_+ R)\nabla_- + (\bar{\nabla}_- \bar{R})\bar{\nabla}_+ + (\bar{\nabla}_+ \bar{R})\bar{\nabla}_-] \\ & + \frac{1}{2} \left[\bar{\nabla}_- \bar{\nabla}_+ \bar{R} + \frac{i}{2} \bar{R}R \right] \bar{M} + \frac{1}{2} \left[\nabla_- \nabla_+ R + \frac{i}{2} \bar{R}R \right] M. \end{aligned} \quad (2.10)$$

In the following, we will make use of the notation

$$\bar{\nabla}^2 \equiv \bar{\nabla}_+ \bar{\nabla}_-, \quad \nabla^2 \equiv \nabla_+ \nabla_-. \quad (2.11)$$

We can insert (2.7) into the commutator $[\nabla_l, \nabla_{\bar{l}}]$, use

$$[\nabla_l, \nabla_{\bar{l}}] | = [\nabla_l |, \nabla_{\bar{l}} |] + \psi_l^\alpha \nabla_\alpha \nabla_{\bar{l}} | + \psi_{\bar{l}}^{\dot{\alpha}} \nabla_{\dot{\alpha}} \nabla_l | - \psi_l^\alpha \nabla_\alpha \nabla_l | - \psi_{\bar{l}}^{\dot{\alpha}} \nabla_{\dot{\alpha}} \nabla_l |, \quad (2.12)$$

and read off the other components of R and \bar{R} . The calculation is rather tedious and since we are only interested in a certain classical background solution, we set the gravitini to zero and the only relevant component of the supercurvature is the $\theta^+ \theta^-$ component. This component depends on the $U_A(1)$ field strength \mathcal{F} and the scalar curvature \mathcal{R} and is of the form

$$\left(\nabla^2 R + \frac{i}{2} \bar{R}R \right) | = -i(\mathcal{R} + i\mathcal{F}), \quad (2.13)$$

$$\left(\bar{\nabla}^2 \bar{R} + \frac{i}{2} \bar{R}R \right) | = -i(\mathcal{R} - i\mathcal{F}), \quad (2.14)$$

if the gravitini are set to zero.

Coming back to the torsion constraints (2.6), these are most easily solved in super-conformal gauge in terms of a chiral field σ and an anti-chiral field $\bar{\sigma}$. The solution of the torsion constraints is then given by

$$\begin{aligned} \nabla_+ &= e^{\bar{\sigma}} (D_+ + i(D_+ \sigma) \bar{M}), \\ \nabla_- &= e^{\bar{\sigma}} (D_- - i(D_- \sigma) \bar{M}), \\ \bar{\nabla}_+ &= e^{\sigma} (\bar{D}_+ + i(\bar{D}_+ \bar{\sigma}) M), \\ \bar{\nabla}_- &= e^{\sigma} (\bar{D}_- - i(\bar{D}_- \bar{\sigma}) M). \end{aligned} \quad (2.15)$$

The vector derivatives are

$$\begin{aligned} \nabla_l = \{ \nabla_+, \bar{\nabla}_+ \} = & e^{\sigma + \bar{\sigma}} [(\partial_z + 2(D_+ \sigma) \bar{D}_+ + 2(\bar{D}_+ \bar{\sigma}) D_+ \\ & + i(\partial_z \bar{\sigma} + 2(D_+ \sigma) (\bar{D}_+ \bar{\sigma})) M + i(\partial_z \sigma + 2(\bar{D}_+ \bar{\sigma}) (D_+ \sigma)) \bar{M}], \end{aligned} \quad (2.16)$$

$$\begin{aligned} \nabla_{\bar{l}} = \{ \nabla_-, \bar{\nabla}_- \} = & e^{\sigma + \bar{\sigma}} [(\partial_{\bar{z}} + 2(D_- \sigma) \bar{D}_- + 2(\bar{D}_- \bar{\sigma}) D_- \\ & - i(\partial_{\bar{z}} \bar{\sigma} + 2(D_- \sigma) (\bar{D}_- \bar{\sigma})) M - i(\partial_{\bar{z}} \sigma + 2(\bar{D}_- \bar{\sigma}) (D_- \sigma)) \bar{M}]. \end{aligned} \quad (2.17)$$

The connection and vielbein components can be read off by comparing our expressions for the covariant derivatives with (2.1). One gets for the Lorentz connection

$$\begin{aligned}
 \Omega_l &= i\partial_z(\sigma + \bar{\sigma})e^{\sigma+\bar{\sigma}}, \\
 \Omega_{\bar{l}} &= -i\partial_{\bar{z}}(\sigma + \bar{\sigma})e^{\sigma+\bar{\sigma}}, \\
 \Omega_+ &= ie^{\bar{\sigma}}(D_+\sigma) \quad \text{and} \quad \bar{\Omega}_+ = ie^{\sigma}(\bar{D}_+\bar{\sigma}), \\
 \Omega_- &= -ie^{\bar{\sigma}}(D_-\sigma) \quad \text{and} \quad \bar{\Omega}_- = -ie^{\sigma}(\bar{D}_-\bar{\sigma}).
 \end{aligned} \tag{2.18}$$

The holomorphic part of the vielbein is given by

$$E_A{}^\pi = \begin{pmatrix} (1 + (D_+\sigma)\theta^+ + (\bar{D}_+\bar{\sigma})\bar{\theta}^+) e^{\sigma+\bar{\sigma}} & 2e^{\sigma+\bar{\sigma}}(\bar{D}_+\bar{\sigma}) & 2e^{\sigma+\bar{\sigma}}(D_+\sigma) \\ \frac{1}{2}e^{\bar{\sigma}}\bar{\theta}^+ & e^{\bar{\sigma}} & 0 \\ \frac{1}{2}e^{\sigma}\theta^+ & 0 & e^{\sigma} \end{pmatrix} \tag{2.19}$$

and the inverse

$$E_\pi{}^A = \begin{pmatrix} e^{-(\sigma+\bar{\sigma})} & -2(\bar{D}_+\bar{\sigma})e^{-\bar{\sigma}} & -2(D_+\sigma)e^{-\sigma} \\ -\frac{\bar{\theta}^+}{2}e^{-(\sigma+\bar{\sigma})} & e^{-\bar{\sigma}}(1 + \bar{\theta}^+(\bar{D}_+\bar{\sigma})) & e^{-\sigma}\theta^+(\bar{D}_+\bar{\sigma}) \\ -\frac{\theta^+}{2}e^{-(\sigma+\bar{\sigma})} & e^{-\bar{\sigma}}\bar{\theta}^+(D_+\sigma) & e^{-\sigma}(1 + \theta^+(D_+\sigma)) \end{pmatrix}, \tag{2.20}$$

with analogous expressions for the antiholomorphic part. Finally, the supercurvature is given by

$$R = 4ie^{2\sigma}(\bar{D}_+\bar{D}_-\bar{\sigma}), \tag{2.21}$$

$$\bar{R} = 4ie^{2\bar{\sigma}}(D_+D_-\sigma), \tag{2.22}$$

which are thus respectively a chiral and an anti-chiral superfield.

3 $\mathcal{N} = (2, 2)$ Jackiw-Teitelboim action

In the following, we want to consider the $\mathcal{N} = (2, 2)$ generalisation to JT gravity. First, we consider the action for pure supergravity supplemented with a Gibbons-Hawking-York term,

$$S = -\frac{\Phi_0}{16\pi G_N} \left[\int_{\mathcal{M}} d^2z d^2\theta \mathcal{E}^{-1} R + \int_{\mathcal{M}} d^2z d^2\bar{\theta} \bar{\mathcal{E}}^{-1} \bar{R} + 2 \int_{\partial\mathcal{M}} dud\vartheta K + 2 \int_{\partial\mathcal{M}} dud\bar{\vartheta} \bar{K} \right]. \tag{3.1}$$

Here, respectively R and \bar{R} are the chiral and anti-chiral curvature superfields (2.21), (2.22), \mathcal{E} and $\bar{\mathcal{E}}$ are the chiral and anti-chiral density which are needed to get well-defined (anti-)chiral integrals. We comment on the projection to x -space at the end of this section. Furthermore, Φ_0 is a constant which can be interpreted as a constant dilaton, K is the extrinsic curvature associated to the chiral bulk supercurvature and \bar{K} is the anti-chiral extrinsic curvature coming from the anti-chiral bulk supercurvature. These two extrinsic

curvatures can be calculated from the $\mathcal{N} = (1, 1)$ expressions [57]

$$K = \frac{T^A \bar{D}_T n_A}{T^A T_A}, \tag{3.2}$$

$$\bar{K} = \frac{T^A D_T n_A}{T^A T_A}, \tag{3.3}$$

where $A = l, \bar{l}$. Furthermore, T is the tangent vector along the boundary, n the normal vector satisfying $T^A n_A = 0$ and $n^A n_A = 1$ and the derivatives \bar{D}_T and D_T are defined as

$$D_T n_A = D n_A + \left(D z^\xi \Omega_\xi \mathcal{J} \right) n_A, \tag{3.4}$$

$$\bar{D}_T n_A = \bar{D} n_A + \left(\bar{D} z^\xi \Omega_\xi \mathcal{J} \right) n_A. \tag{3.5}$$

The supersymmetric generalisations (3.2) and (3.3) of the extrinsic curvature are chosen such that transformations of the derivatives D and \bar{D} , which replace the derivative ∂_u in the bosonic extrinsic curvature, cancel the Berezinian of the (anti-) chiral superspace measure (cf. [28]). In the following, it will be useful to express K and \bar{K} as a more general boundary superfield \mathcal{K} in order to couple the extrinsic curvature to superfields without definite chirality (as e.g. the dilaton at the boundary). We therefore define the overall extrinsic curvature \mathcal{K} through the condition

$$\int_{\partial\mathcal{M}} dud\vartheta d\bar{\vartheta} \mathcal{K} \stackrel{!}{=} \int_{\partial\mathcal{M}} dud\vartheta K + \int_{\partial\mathcal{M}} dud\bar{\vartheta} \bar{K}. \tag{3.6}$$

One could also try to directly find an expression for \mathcal{K} by searching for a generalisation of the derivative ∂_u appearing in the bosonic extrinsic curvature which cancels the Berezinian of the full $d = 1$ superspace measure upon transformations. However, there is no obvious expression involving the covariant derivatives D and \bar{D} and generalising ∂_u that satisfies this condition since the Berezinian of the full superspace measure equals one. Therefore, we have to take the detour and calculate \mathcal{K} via K and \bar{K} .

Now, we can use \mathcal{K} to define the supersymmetric $\mathcal{N} = (2, 2)$ generalisation of the JT action. This action reads

$$S = - \frac{1}{16\pi G_N} \left[\int_{\mathcal{M}} d^2z d^2\theta \mathcal{E}^{-1} \Phi (R - \alpha) + \int_{\mathcal{M}} d^2z d^2\bar{\theta} \bar{\mathcal{E}}^{-1} \bar{\Phi} (\bar{R} - \alpha) + 2 \int_{\partial\mathcal{M}} dud\vartheta d\bar{\vartheta} (\Phi_b + \bar{\Phi}_b) \mathcal{K} \right], \tag{3.7}$$

where Φ and $\bar{\Phi}$ are respectively the chiral and anti-chiral dilaton superfields, which serve as Lagrange multipliers imposing the constraints $R = \bar{R} = \alpha$. As we will soon see, the choice $\alpha = -2$ corresponds to an AdS background which we will use from now on. Moreover, Φ_b and $\bar{\Phi}_b$ are the respective boundary values of the chiral and anti-chiral dilatons. Imposing the supercurvature constraints yields the effective action for the boundary degrees of freedom

$$S_{\text{eff}} = - \frac{1}{8\pi G_N} \int_{\partial\mathcal{M}} dud\vartheta d\bar{\vartheta} (\Phi_b + \bar{\Phi}_b) \mathcal{K}. \tag{3.8}$$

One can check that the action above is indeed a supersymmetric generalisation of the bosonic JT action by considering the action in x -space, i.e. performing the integrals over the Grassmann variables. To do this, one has to know how to deal with the chiral density. The procedure to find the expression for the chiral density is explained in detail in [62]: if a Lagrangian \mathcal{L} is considered, the chiral projection has to take the form

$$\int d^2z d^2\theta d^2\bar{\theta} E^{-1} \mathcal{L} = \int d^2z d^2\theta \mathcal{E}^{-1} \bar{\nabla}^2 \mathcal{L}|_{\bar{\theta}=0} \tag{3.9}$$

$$= \int d^2z e^{-1} [\nabla^2 + X^+ \nabla_+ + X^- \nabla_- + Y] \bar{\nabla}^2 \mathcal{L}|_{\theta=\bar{\theta}=0}, \tag{3.10}$$

where $e = \det(e_a{}^m)$ and the coefficients X^+ , X^- and Y have to be determined. They can be found from the requirement that the transformation of the full superspace integral to the x -space integral should not depend on whether one has a chiral integral or an anti-chiral integral in the intermediate step. As in [62] this condition can be implemented for e.g. the kinetic term of a chiral field with $\mathcal{L} = \bar{\Phi}\Phi$ by choosing X^+ , X^- and Y s.t. the resulting x -space integral is symmetric in barred and unbarred quantities.

The calculation is tedious and since we are interested in a classical background solution, we set the gravitini to zero again. In that case, we obtain

$$X^+ = X^- = 0, \quad Y = \frac{i}{2} \bar{R}| = \frac{i}{2} \bar{S}, \tag{3.11}$$

$$\bar{X}^+ = \bar{X}^- = 0, \quad \bar{Y} = \frac{i}{2} R| = \frac{i}{2} S, \tag{3.12}$$

where \bar{X}^+ , \bar{X}^- and \bar{Y} are the corresponding quantities for the anti-chiral density projection formula.

Having the explicit formula for the (anti-)chiral projections, we can now proceed to find the x -space action of our particular supergravity setup. Let us for the moment only consider the bulk part of the action. We start with the supersymmetric Einstein-Hilbert action which now reads:

$$\begin{aligned} S_{EH} &= -\frac{\Phi_0}{16\pi G_N} \left[\int_{\mathcal{M}} d^2z d^2\theta \mathcal{E}^{-1} R + \int_{\mathcal{M}} d^2z d^2\bar{\theta} \bar{\mathcal{E}}^{-1} \bar{R} \right] \\ &= -\frac{\Phi_0}{16\pi G_N} \left[\int_{\mathcal{M}} d^2z e^{-1} \left(\nabla^2 + \frac{i}{2} \bar{S} \right) R| + \int_{\mathcal{M}} d^2z e^{-1} \left(\bar{\nabla}^2 + \frac{i}{2} S \right) \bar{R}| \right] \\ &= -\frac{\Phi_0}{16\pi G_N} \left[\int_{\mathcal{M}} d^2z e^{-1} (-i(\mathcal{R} + i\mathcal{F})) + \int_{\mathcal{M}} d^2z e^{-1} (-i(\mathcal{R} - i\mathcal{F})) \right] \\ &= +\frac{i\Phi_0}{8\pi G_N} \int_{\mathcal{M}} d^2z e^{-1} \mathcal{R}, \end{aligned} \tag{3.13}$$

where we made use of (2.13), (2.14). Thus, this part of the action, together with the extrinsic curvature term just gives the Euler characteristic of \mathcal{M} times an overall prefactor.

The second part of the bulk action is given by the JT term, which reads (using the

chiral projection formula)

$$\begin{aligned}
 S_{JT} &= -\frac{1}{16\pi G_N} \left[\int_{\mathcal{M}} d^2z d^2\theta \mathcal{E}^{-1} \Phi(R+2) + \int_{\mathcal{M}} d^2z d^2\bar{\theta} \bar{\mathcal{E}}^{-1} \bar{\Phi}(\bar{R}+2) \right] \\
 &= -\frac{1}{16\pi G_N} \left[\int_{\mathcal{M}} d^2z e^{-1} \left(\nabla^2 + \frac{i}{2} \bar{S} \right) \Phi(R+2) + \int_{\mathcal{M}} d^2z e^{-1} \left(\bar{\nabla}^2 + \frac{i}{2} S \right) \bar{\Phi}(\bar{R}+2) \right] \\
 &= \frac{i}{16\pi G_N} \int_{\mathcal{M}} d^2z e^{-1} [\varphi(\mathcal{R}+i\mathcal{F}) + \bar{\varphi}(\mathcal{R}-i\mathcal{F}) - \bar{S}\varphi - S\bar{\varphi} + iB(S+2) + i\bar{B}(\bar{S}+2)] ,
 \end{aligned} \tag{3.14}$$

where we used (2.13) and (2.14) as well as the component expansion of the dilaton superfield

$$\Phi = \varphi + \theta^\alpha \lambda_\alpha + \theta^+ \theta^- B, \quad \text{and} \quad \bar{\Phi} = \bar{\varphi} + \bar{\theta}^\alpha \bar{\lambda}_\alpha + \bar{\theta}^+ \bar{\theta}^- \bar{B}. \tag{3.15}$$

If we consider the variations of this JT action w.r.t. the auxiliary supergravity fields S and \bar{S} , we get the relations

$$B = i\bar{\varphi} \quad \text{and} \quad \bar{B} = i\varphi. \tag{3.16}$$

Further variations w.r.t. the auxiliary dilaton fields B and \bar{B} yield the bosonic JT action

$$S_{JT} = \frac{i}{16\pi G_N} \int_{\mathcal{M}} d^2z e^{-1} [\varphi(\mathcal{R} + i\mathcal{F} + 2) + \bar{\varphi}(\mathcal{R} - i\mathcal{F} + 2)] , \tag{3.17}$$

which upon variation w.r.t. φ and $\bar{\varphi}$ gives indeed an AdS background with vanishing field strength \mathcal{F} .

Finally, variations w.r.t. the vielbein give an energy momentum tensor similar to the bosonic case in [48]. Thus, one possible solution for φ and $\bar{\varphi}$ is given by the dilaton solution found in that reference. This implies in particular that $\varphi = \bar{\varphi}$.

4 Determination of the superconformal factor

A crucial step for calculating the extrinsic curvature is to find an expression for the (anti-)chiral superconformal field σ ($\bar{\sigma}$), which can be done in two different ways: on the one hand, one can consider (2.21), (2.22) and solve for σ and $\bar{\sigma}$ using the constraint $R = \bar{R} = -2$. On the other hand one can calculate σ and $\bar{\sigma}$ using the Killing spinors of AdS₂. Since the final result for the extrinsic curvature and thus the effective boundary action crucially depends on the result for σ and $\bar{\sigma}$, we will present both ways in order to check our findings.

First, we solve the supercurvature constraints (2.21) and (2.22) for the superconformal factors σ and $\bar{\sigma}$. Since σ is a chiral superfield it can be written in the chiral basis $z_c = z + \frac{1}{2}\theta^+\bar{\theta}^+$ and $\bar{z}_c = \bar{z} + \frac{1}{2}\theta^-\bar{\theta}^-$ as

$$\sigma = \phi(z_c, \bar{z}_c) + \theta^+\theta^- w(z, \bar{z}). \tag{4.1}$$

Here, ϕ and w are functions of the superspace variables which we will determine later on. Accordingly, the anti-chiral field $\bar{\sigma}$ can be written in terms of the anti-chiral basis $z_{ac} = z - \frac{1}{2}\theta^+\bar{\theta}^+$ and $\bar{z}_{ac} = \bar{z} - \frac{1}{2}\theta^-\bar{\theta}^-$ as

$$\bar{\sigma} = \bar{\phi}(z_{ac}, \bar{z}_{ac}) + \bar{\theta}^+\bar{\theta}^- \bar{w}(z, \bar{z}). \tag{4.2}$$

According to (2.22) $\bar{R} = -2$ yields

$$w = \frac{-i}{2} e^{-2\bar{\phi}}, \quad (4.3)$$

$$0 = 2w\bar{w} - \partial_z \partial_{\bar{z}} \phi. \quad (4.4)$$

The second equation has the form of a Liouville equation. Since we are interested in an AdS background geometry, we impose

$$\bar{\phi} = \phi = -\frac{1}{2} \log \left(\frac{1}{2y} \right), \quad (4.5)$$

where $z = t + iy$. With this input, (4.4) can be solved by setting

$$\bar{w} = \frac{-i}{2} e^{-2\phi}. \quad (4.6)$$

Note that this implies $R = -2$, in accordance with the remaining supercurvature constraint.

After expanding the chiral basis, the superconformal factors will be given by

$$\sigma = -\frac{1}{2} \log \left(\frac{1}{\beta y} \right) + \frac{i}{8y} \theta^+ \bar{\theta}^+ - \frac{i}{8y} \theta^- \bar{\theta}^- - \frac{i}{4y} \theta^+ \theta^- - \frac{1}{32y^2} \theta^- \bar{\theta}^- \theta^+ \bar{\theta}^+, \quad (4.7)$$

$$\bar{\sigma} = -\frac{1}{2} \log \left(\frac{1}{\beta y} \right) - \frac{i}{8y} \theta^+ \bar{\theta}^+ + \frac{i}{8y} \theta^- \bar{\theta}^- - \frac{i}{4y} \bar{\theta}^+ \bar{\theta}^- - \frac{1}{32y^2} \theta^- \bar{\theta}^- \theta^+ \bar{\theta}^+. \quad (4.8)$$

We see that σ and $\bar{\sigma}$ are not complex conjugates of each other, thereby making AdS₂ a non-unitary background. For our further deliberations we should corroborate the result for the superconformal factors. More precisely, the result of non-unitarity should be confirmed by other means. We opt to perform a short classification of $\mathcal{N} = (2, 2)$ supersymmetric backgrounds by calculation of Killing spinors. The following analysis closely follows the steps given in appendix D of [64]. Since we chose different conventions for our superspace it is useful to re-derive their results for our setup.

Recall, that due to conformal flatness of two-dimensional supergravity, the background geometry is entirely encoded in the conformal factors $e^{-2\sigma}$ and $e^{-2\bar{\sigma}}$. Thus, the relevant fields that we have to consider in order to determine the Killing spinors ϵ and $\bar{\epsilon}$ of supersymmetry variations are just the chiral σ field and the anti-chiral $\bar{\sigma}$ field. To obtain the background geometry, the fermionic components of σ and $\bar{\sigma}$ are set to zero.

As in [64] the standard restriction for supersymmetry can be written as

$$\partial_z \epsilon^- = \partial_z \bar{\epsilon}^- = 0, \quad \text{and} \quad \partial_{\bar{z}} \epsilon^+ = \partial_{\bar{z}} \bar{\epsilon}^+ = 0. \quad (4.9)$$

Further restrictions on the Killing spinors come from the requirement, that the fermionic components of the conformal factors $e^{-2\sigma}$ and $e^{-2\bar{\sigma}}$ remain zero under local supersymmetry transformations. In the following, we will work in the chiral basis as introduced above (4.1). With our conventions these conditions can be written as

$$\partial_{z_c} \left(\bar{\epsilon}^+ e^{-2\phi} \right) - 2\epsilon^- w e^{-2\phi} = 0, \quad \partial_{\bar{z}_c} \left(\bar{\epsilon}^- e^{-2\phi} \right) + 2\epsilon^+ w e^{-2\phi} = 0, \quad (4.10)$$

$$\partial_{z_{ac}} \left(\epsilon^+ e^{-2\bar{\phi}} \right) - 2\bar{\epsilon}^- \bar{w} e^{-2\bar{\phi}} = 0, \quad \partial_{\bar{z}_{ac}} \left(\epsilon^- e^{-2\bar{\phi}} \right) + 2\bar{\epsilon}^+ \bar{w} e^{-2\bar{\phi}} = 0, \quad (4.11)$$

where we inserted $\sigma = \phi + \theta^+ \theta^- w$ and $\bar{\sigma} = \bar{\phi} + \bar{\theta}^+ \bar{\theta}^- \bar{w}$. The classification of backgrounds preserving different numbers of supercharges can now be carried out along the lines of [64].

For a background preserving one supercharge with a particular $U_A(1)$ charge, we can e.g. choose the Killing spinor $(\epsilon_1^+, \bar{\epsilon}_1^-)$ to be non-zero with the other Killing spinor components zero. Solving (4.10), (4.11) algebraically, we get

$$w = \frac{1}{2} \frac{\bar{\epsilon}_1^-}{\epsilon_1^+} \partial_{\bar{z}_c} (2\phi - \log \bar{\epsilon}_1^-) , \tag{4.12}$$

$$\bar{w} = -\frac{1}{2} \frac{\epsilon_1^+}{\bar{\epsilon}_1^-} \partial_{z_{ac}} (2\bar{\phi} - \log \epsilon_1^+) . \tag{4.13}$$

If the background should also preserve a second supercharge of the opposite $U_A(1)$ charge, there should also exist a second non-zero Killing spinor $(\epsilon_2^-, \bar{\epsilon}_2^+)$. Solving (4.10), (4.11) with this Killing spinor yields results similar to (4.12), (4.13). Consistency of the two solutions requires

$$(\bar{\epsilon}_1^- \epsilon_2^- \partial_{z_{ac}} + \bar{\epsilon}_2^+ \epsilon_1^+ \partial_{z_{ac}}) (2\bar{\phi} + \log \epsilon_1^+ \epsilon_2^-) = 0 , \tag{4.14}$$

with a similar expression for z_c and ϕ . Thus, $\bar{\phi}$ is invariant under the vector $v = \bar{\epsilon}_1^- \epsilon_2^- \partial_{z_{ac}} + \bar{\epsilon}_2^+ \epsilon_1^+ \partial_{z_{ac}}$ up to a superconformal transformation.

As shown in e.g. [63], maximally four supercharges are preserved if and only if the background space is maximally symmetric and the $U_A(1)$ gauge field has zero field strength. Thus, with (4.12), (4.13) the w and \bar{w} fields can be expressed in terms of the bosonic conformal factor ϕ . Since we are interested in an AdS background, we know that $\phi = -\frac{1}{2} \log \left(\frac{1}{2y_c} \right)$ and $\bar{\phi} = -\frac{1}{2} \log \left(\frac{1}{2y_{ac}} \right)$. In that case indeed a set of four Killing spinors satisfying (4.14) can be found. These are

$$\zeta \equiv \begin{pmatrix} \epsilon^+ \\ \bar{\epsilon}^- \end{pmatrix} = \frac{1}{2} \begin{pmatrix} -1 \\ 1 \end{pmatrix} , \quad \bar{\zeta} \equiv \begin{pmatrix} \epsilon^- \\ \bar{\epsilon}^+ \end{pmatrix} = \frac{1}{2} \begin{pmatrix} -1 \\ 1 \end{pmatrix} , \tag{4.15}$$

and

$$\eta \equiv \begin{pmatrix} \epsilon^+ \\ \bar{\epsilon}^- \end{pmatrix} = \frac{1}{2} \begin{pmatrix} -z \\ \bar{z} \end{pmatrix} , \quad \bar{\eta} \equiv \begin{pmatrix} \epsilon^- \\ \bar{\epsilon}^+ \end{pmatrix} = \frac{1}{2} \begin{pmatrix} -\bar{z} \\ z \end{pmatrix} , \tag{4.16}$$

where we used a bar to distinguish Killing spinors with opposite $U_A(1)$ charge. Indeed, with these four Killing spinors, one can now calculate the three Killing vectors $\zeta \gamma^\mu \bar{\zeta} \partial_\mu$, $\eta \gamma^\mu \bar{\eta} \partial_\mu$ and $\eta \gamma^\mu \bar{\zeta} \partial_\mu$ to be

$$L_{-1} \equiv \zeta \gamma^\mu \bar{\zeta} \partial_\mu = -\frac{1}{2} (\partial_z + \partial_{\bar{z}}) , \tag{4.17}$$

$$L_0 \equiv \eta \gamma^\mu \bar{\zeta} \partial_\mu = -\frac{1}{2} (z \partial_z + \bar{z} \partial_{\bar{z}}) , \tag{4.18}$$

$$L_1 \equiv \eta \gamma^\mu \bar{\eta} \partial_\mu = -\frac{1}{2} (z^2 \partial_z + \bar{z}^2 \partial_{\bar{z}}) , \tag{4.19}$$

which are precisely the Killing vectors of AdS₂. At the boundary ($y \rightarrow 0$) they correctly reduce to the global conformal transformations

$$L_0 \rightarrow -t\partial_t, \quad L_{-1} \rightarrow -\partial_t, \quad L_1 \rightarrow -t^2\partial_t. \quad (4.20)$$

Now one can take any Killing spinor out of (4.15), (4.16) to calculate w and \bar{w} . The results for σ and $\bar{\sigma}$ are

$$\sigma = -\frac{1}{2} \log \left(\frac{1}{2y_c} \right) - \frac{i}{4y_c} \theta^+ \theta^-, \quad (4.21)$$

$$\bar{\sigma} = -\frac{1}{2} \log \left(\frac{1}{2y_{ac}} \right) - \frac{i}{4y_{ac}} \bar{\theta}^+ \bar{\theta}^-. \quad (4.22)$$

These results obtained by considering the Killing spinors perfectly coincide with our solution for σ and $\bar{\sigma}$ (4.7), (4.8) as obtained from the requirement $\bar{R} = R = -2$. In particular, this shows again that our background is non-unitary since σ and $\bar{\sigma}$ are not complex conjugates of each other.

5 Effective action: appearance of the super-Schwarzian

Only boundary curves of constant arc length are considered in the calculation of the effective action [48, 57],

$$\frac{du^2 + \bar{\vartheta} d\vartheta du + \vartheta d\bar{\vartheta} du + \frac{1}{2} \vartheta \bar{\vartheta} d\vartheta d\bar{\vartheta}}{4\epsilon^2} = \left(dz^\xi E_\xi^l dz^\pi E_\pi^{\bar{l}} \right) \Big|_{\text{pull-back}}. \quad (5.1)$$

This results in the constraints

$$Dz = \frac{1}{2} (\bar{\theta}^+ (D\theta^+) + \theta^+ (D\bar{\theta}^+)) , \quad \bar{D}z = \frac{1}{2} (\theta^+ (\bar{D}\bar{\theta}^+) + \bar{\theta}^+ (\bar{D}\theta^+)) , \quad (5.2)$$

$$D\bar{z} = \frac{1}{2} (\theta^- (D\bar{\theta}^-) + \bar{\theta}^- (D\theta^-)) , \quad \bar{D}\bar{z} = \frac{1}{2} (\bar{\theta}^- (\bar{D}\theta^-) + \theta^- (\bar{D}\bar{\theta}^-)) , \quad (5.3)$$

where we defined one dimensional supercovariant derivatives as in [28] (up to factors of one half due to differences in conventions),

$$D = \frac{\partial}{\partial \vartheta} + \frac{\bar{\vartheta}}{2} \frac{\partial}{\partial u} , \quad \bar{D} = \frac{\partial}{\partial \bar{\vartheta}} + \frac{\vartheta}{2} \frac{\partial}{\partial u} \quad (5.4)$$

In addition to (5.2) and (5.3), we impose the following chirality conditions

$$D\theta^- = D\bar{\theta}^+ = \bar{D}\theta^+ = \bar{D}\bar{\theta}^- = 0. \quad (5.5)$$

Equations (5.2), (5.3) and (5.5) are equivalent to the $\mathcal{N} = 2$ superconformal transformations of [28]. The bulk variables correspond to super-reparametrisations of the boundary. Furthermore, the conformal factor has to satisfy

$$e^{2(\sigma+\bar{\sigma})} = 4\epsilon^2 [(D\theta^+)(D\bar{\theta}^-)(\bar{D}\theta^-)(\bar{D}\bar{\theta}^+)] . \quad (5.6)$$

Together with (4.7), (4.8) this leads to

$$y = \text{Im } z = \epsilon [(D\theta^+)(D\bar{\theta}^-)(\bar{D}\theta^-)(\bar{D}\bar{\theta}^+)]^{1/2} + \frac{i}{4} (\theta^+\theta^- + \bar{\theta}^+\bar{\theta}^-). \quad (5.7)$$

Now, we can calculate the chiral and anti-chiral part of the extrinsic curvature given in (3.2) and (3.3). The tangent vector for the boundary can be evaluated using

$$T^l = (\partial_u z^\xi) E_\xi^l, \quad (5.8)$$

$$T^{\bar{l}} = (\partial_u z^\xi) E_\xi^{\bar{l}}, \quad (5.9)$$

leading to

$$T^l = e^{-(\sigma+\bar{\sigma})} [(D\theta^+)(\bar{D}\bar{\theta}^+)], \quad (5.10)$$

$$T^{\bar{l}} = e^{-(\sigma+\bar{\sigma})} [(D\bar{\theta}^-)(\bar{D}\theta^-)], \quad (5.11)$$

and

$$n_l = -\frac{i}{2} \left(\frac{(D\bar{\theta}^-)(\bar{D}\theta^-)}{(D\theta^+)(\bar{D}\bar{\theta}^+)} \right)^{1/2}, \quad (5.12)$$

$$n_{\bar{l}} = +\frac{i}{2} \left(\frac{(D\theta^+)(\bar{D}\bar{\theta}^+)}{(D\bar{\theta}^-)(\bar{D}\theta^-)} \right)^{1/2}. \quad (5.13)$$

Hence, the contribution to the anti-chiral extrinsic supercurvature \bar{K} which does not include the connection is given by

$$\frac{T^l Dn_l + T^{\bar{l}} Dn_{\bar{l}}}{T^2} = i\epsilon \left[\frac{(\bar{\theta}^+)' }{(\bar{D}\bar{\theta}^+)} - \frac{(\theta^-)' }{(\bar{D}\theta^-)} \right], \quad (5.14)$$

with a similar expression for the chiral extrinsic supercurvature K . Here, the prime indicates derivatives with respect to u . For the part of \bar{K} containing the connection, we first observe that the Lorentz generators applied to n_l and $n_{\bar{l}}$ give

$$[\mathcal{J}, n_{\bar{l}}] = in_{\bar{l}}, \quad [\mathcal{J}, n_l] = -in_l. \quad (5.15)$$

Thus, the contribution to \bar{K} containing the connection part is given by

$$\begin{aligned} & \frac{1}{T^2} T^A (Dz^\xi \Omega_\xi) J n_A \\ &= -2\epsilon (Dz^\xi \Omega_\xi) \end{aligned} \quad (5.16)$$

$$= \frac{1}{2 [(D\theta^+)(D\bar{\theta}^-)(\bar{D}\theta^-)(\bar{D}\bar{\theta}^+)]^{1/2}} [(D\theta^+)(\bar{\theta}^+ - \theta^-) + (D\bar{\theta}^-)(\theta^- - \bar{\theta}^+)]. \quad (5.17)$$

Having the general expression for the extrinsic curvature, we want to make contact to the boundary theory. The $\mathcal{N} = (2, 2)$ supersymmetry of the bulk reduces to $\mathcal{N} = (1, 1)$ supersymmetry on the boundary. We therefore need an expression for the bulk variables

at the boundary in terms of the boundary degrees of freedom. To zeroth order the solution to (5.1) after imposing (5.2), (5.3) reads

$$\theta^+ = \bar{\theta}^- = \xi, \quad \theta^- = \bar{\theta}^+ = \bar{\xi}, \quad \text{Im}z = \epsilon(D\xi)(\bar{D}\bar{\xi}). \quad (5.18)$$

In that case, (5.5) reduces to

$$D\bar{\xi} = \bar{D}\xi = 0. \quad (5.19)$$

We also need the corrections in ϵ to these solutions. We choose the ansatz

$$\theta^+ = \xi - i\epsilon\rho, \quad \bar{\theta}^+ = \bar{\xi} + i\epsilon\bar{\rho}, \quad (5.20)$$

$$\theta^- = \bar{\xi} - i\epsilon\bar{\rho}, \quad \bar{\theta}^- = \xi + i\epsilon\rho. \quad (5.21)$$

With this ansatz, (5.2), (5.3) can be solved by

$$\rho = -\xi' \quad \text{and} \quad \bar{\rho} = \bar{\xi}'. \quad (5.22)$$

Thus, the boundary solution of $\theta^+, \theta^-, \bar{\theta}^+, \bar{\theta}^-$ has the form of a Taylor expansion of e.g. $\theta^+(u + i\epsilon, \vartheta, \bar{\vartheta})$ around $\epsilon = 0$, with $\theta^+(u, \vartheta, \bar{\vartheta}) = \xi$ and similarly for the other Grassmann coordinates.

With this solution, the extrinsic curvature is given by

$$\bar{K} = -2\epsilon^2 \left[\frac{\bar{\xi}''}{\bar{D}\bar{\xi}} - \frac{\bar{\xi}'(\bar{D}\bar{\xi}')}{(\bar{D}\bar{\xi})^2} + \left(\frac{(D\xi')\bar{\xi}'}{(D\xi)(\bar{D}\bar{\xi})} \right) \right], \quad (5.23)$$

$$K = -2\epsilon^2 \left[\frac{\xi''}{D\xi} - \frac{\xi'(D\xi')}{(D\xi)^2} + \left(\frac{(\bar{D}\bar{\xi}')\xi'}{(D\xi)(\bar{D}\bar{\xi})} \right) \right]. \quad (5.24)$$

The next step is to find the overall extrinsic curvature \mathcal{K} as defined in (3.6). The following identity proves useful

$$\int du d\vartheta d\bar{\vartheta} f(u, \vartheta, \bar{\vartheta}) = \int du_c d\vartheta (\bar{D}f) \left(u + \frac{\vartheta\bar{\vartheta}}{2}, \vartheta \right) = - \int du_{ac} d\bar{\vartheta} (Df) \left(u - \frac{\vartheta\bar{\vartheta}}{2}, \bar{\vartheta} \right), \quad (5.25)$$

where $du \simeq du_{c/ac} = d(u \pm \frac{1}{2}\vartheta\bar{\vartheta})$ denote chiral and anti-chiral measures. To check this formula it is best to expand the superfield f into components

$$f(u, \vartheta, \bar{\vartheta}) = g(u) + \vartheta\bar{\zeta}(u) + \bar{\vartheta}\zeta(u) + \vartheta\bar{\vartheta}h(u). \quad (5.26)$$

Then one gets

$$\int du d\vartheta d\bar{\vartheta} f(u, \vartheta, \bar{\vartheta}) = - \int du h. \quad (5.27)$$

whereas for the second integral one gets

$$\int du_c d\vartheta (\bar{D}f) \left(u + \frac{\vartheta\bar{\vartheta}}{2}, \vartheta \right) = \int du_c d\vartheta \left[\zeta(u_c) + \vartheta \left(\frac{g'(u_c)}{2} - h(u_c) \right) \right] = - \int du h. \quad (5.28)$$

In the second step the first term has been killed by the $d\vartheta$ integral and the second term gave rise to a du_c integral over a derivative, leaving only the third contribution in agreement with (5.27). The other equality in (5.25) can be seen analogously.

Note that \bar{K} and K in (5.23), (5.24) can be expressed as derivatives,

$$\bar{K} = -2\epsilon^2 D \left(\frac{(\bar{D}\bar{\xi}')}{\bar{D}\bar{\xi}} - \frac{\xi'\bar{\xi}'}{(D\xi)(\bar{D}\bar{\xi})} \right), \quad (5.29)$$

$$K = -2\epsilon^2 \bar{D} \left(\frac{(D\xi')}{D\xi} + \frac{\xi'\bar{\xi}'}{(D\xi)(\bar{D}\bar{\xi})} \right). \quad (5.30)$$

This result can now be plugged into the Gibbons-Hawking-York term in (3.1):

$$S_{\text{GH}} = -\frac{1}{8\pi G_N \epsilon^2} \int_{\partial\mathcal{M}} dud\bar{v} \left[-2\epsilon^2 D \left(\frac{(\bar{D}\bar{\xi}')}{\bar{D}\bar{\xi}} - \frac{\xi'\bar{\xi}'}{(D\xi)(\bar{D}\bar{\xi})} \right) \right] \\ - \frac{1}{8\pi G_N \epsilon^2} \int_{\partial\mathcal{M}} dud\vartheta \left[-2\epsilon^2 \bar{D} \left(\frac{(D\xi')}{D\xi} + \frac{\xi'\bar{\xi}'}{(D\xi)(\bar{D}\bar{\xi})} \right) \right], \quad (5.31)$$

where the $1/\epsilon^2$ factor arises due to the ϵ factor in the flat space vielbein (5.1) [57]. With (5.25) each integral in the above expression can be expressed as an integral over the total superspace. Comparing with (3.6) yields

$$\mathcal{K} = 2\epsilon^2 \text{Schw}(t, \xi, \bar{\xi}; u, \vartheta, \bar{\vartheta}). \quad (5.32)$$

where

$$\text{Schw}(t, \xi, \bar{\xi}; u, \vartheta, \bar{\vartheta}) = \frac{(\bar{D}\bar{\xi}')}{\bar{D}\bar{\xi}} - \frac{(D\xi')}{D\xi} - 2 \frac{\xi'\bar{\xi}'}{(D\xi)(\bar{D}\bar{\xi})} \quad (5.33)$$

denotes the super-Schwarzian. With this expression for the extrinsic curvature, we get for the effective boundary action in (3.8)

$$S_{\text{eff}} = -\frac{1}{4\pi G_N} \int_{\partial\mathcal{M}} dud\vartheta d\bar{\vartheta} (\Phi_b + \bar{\Phi}_b) \text{Schw}(t, \xi, \bar{\xi}; u, \vartheta, \bar{\vartheta}), \quad (5.34)$$

which can be further simplified by noting that only the leading components φ of the dilaton supermultiplets contribute at the boundary, since for the two θ components of the dilaton, at the boundary we have at zeroth order in ϵ the relation

$$(\Phi + \bar{\Phi})_b \supset i(\varphi\theta^+\theta^- + \varphi\bar{\theta}^+\bar{\theta}^-)_b = i\varphi_b(\xi\bar{\xi} + \bar{\xi}\xi) = 0, \quad (5.35)$$

where φ_b is the value of the leading component at the boundary and we used that the chiral and the anti-chiral dilaton superfields have the same leading component on-shell

$$S_{\text{eff}} = -\frac{1}{2\pi G_N} \int_{\partial\mathcal{M}} dud\vartheta d\bar{\vartheta} \varphi_b \text{Schw}(t, \xi, \bar{\xi}; u, \vartheta, \bar{\vartheta}). \quad (5.36)$$

We close this section by briefly commenting on the physical interpretation of the action considered here (cf. e.g. [28, 45] for the bosonic case). The entire action reads

$$S = -\frac{\Phi_0}{16\pi G_N} \left[\int_{\mathcal{M}} d^2z d^2\theta \mathcal{E}^{-1} R + \int_{\mathcal{M}} d^2z d^2\bar{\theta} \bar{\mathcal{E}}^{-1} \bar{R} + 2 \int_{\partial\mathcal{M}} dud\vartheta d\bar{\vartheta} \mathcal{K} \right] \\ - \frac{\bar{\Phi}_0}{16\pi G_N} \left[\int_{\mathcal{M}} d^2z d^2\theta \mathcal{E}^{-1} \Phi(R+2) + \int_{\mathcal{M}} d^2z d^2\bar{\theta} \bar{\mathcal{E}}^{-1} \bar{\Phi}(\bar{R}+2) \right. \\ \left. + 2 \int_{\partial\mathcal{M}} dud\vartheta d\bar{\vartheta} (\Phi_b + \bar{\Phi}_b) \mathcal{K} \right]. \quad (5.37)$$

The manifold \mathcal{M} is obtained by cutting out a line given by coordinates $t(u, \vartheta, \bar{\vartheta})$, $y(u, \vartheta, \bar{\vartheta})$, $\theta^+(u, \vartheta, \bar{\vartheta})$, $\theta^-(u, \vartheta, \bar{\vartheta})$, $\bar{\theta}^+(u, \vartheta, \bar{\vartheta})$ and $\bar{\theta}^-(u, \vartheta, \bar{\vartheta})$ corresponding to the boundary $\partial\mathcal{M}$. The parameters u , ϑ , $\bar{\vartheta}$ are the coordinates of the one-dimensional $\mathcal{N} = (1, 1)$ superspace at this boundary. Different boundaries are related via superreparametrisations of the one-dimensional superspace. We saw earlier that the first line of (5.37) is just topological and corresponds to the Euler characteristic of \mathcal{M} which is not altered by superreparametrisations. Thus, we have a large symmetry group consisting of all superreparametrisations that do not violate the chirality constraints on the superfields in (5.2)–(5.5). We derived in (5.20)–(5.22), under the assumption of the chirality constraints, that our reparametrisations satisfy

$$\theta^+ = \xi(u, \vartheta, \bar{\vartheta}) + i\epsilon\xi'(u, \vartheta, \bar{\vartheta}), \quad \bar{\theta}^+ = \bar{\xi}(u, \vartheta, \bar{\vartheta}) + i\epsilon\bar{\xi}'(u, \vartheta, \bar{\vartheta}), \quad (5.38)$$

$$\theta^- = \bar{\xi}(u, \vartheta, \bar{\vartheta}) - i\epsilon\bar{\xi}'(u, \vartheta, \bar{\vartheta}), \quad \bar{\theta}^- = \xi(u, \vartheta, \bar{\vartheta}) - i\epsilon\xi'(u, \vartheta, \bar{\vartheta}), \quad (5.39)$$

$$y = \epsilon(D\xi)(\bar{D}\bar{\xi}) - \frac{\epsilon}{2}(\xi\bar{\xi}' + \bar{\xi}\xi'). \quad (5.40)$$

Since superreparametrisations of the one-dimensional superspace in general map a given boundary to a completely different one, we have a spontaneous breaking of the entire superreparametrisation symmetry to the subgroup $SU(1, 1|1)$ of global reparametrisations that leave the boundaries invariant [28]. As in the bosonic case the other reparametrisations can be interpreted as Goldstone modes.

The part of the action in (5.37) involving the dilaton now explicitly breaks this symmetry since its boundary term gives a non-zero action for the superreparametrisations, namely the Schwarzian action in (5.36) which vanishes only for $SU(1, 1|1)$ reparametrisations [28].

6 Consistency check

Here, we perform the following consistency check. The Gibbons-Hawking-York term should ensure that Dirichlet conditions on field variations should not lead to further boundary conditions on 2d fields. Hence, any solution to the bulk equations should be viable. In particular it can be seen that plugging a bulk solution of the dilaton into the effective action (5.35) and taking variations with respect to superreparametrisations yields zero. For cases with less supersymmetry this has been done in [48, 57]. In particular, in [57] superreparametrisations have been expressed in terms of unconstrained bosonic and fermionic degrees of freedom with respect to which the variation has been considered. Already there, this procedure turned out to give rather lengthy expressions. In the $\mathcal{N} = 2$ case the complexity of this calculation grows further [65]. Fortunately, there is a shortcut which could have been used also in [57]. The underlying trick can be found e.g. in chapter 4 of [66]. Using the anomalous chain rule, the variation of the Schwarzian can be linearised. For $\mathcal{N} = 2$ the details are as follows,

$$\begin{aligned} \delta\text{Schw}(t, \xi, \bar{\xi}; u, \vartheta, \bar{\vartheta}) &\equiv \text{Schw}(t + \delta t, \xi + \delta\xi, \bar{\xi} + \delta\bar{\xi}; u, \vartheta, \bar{\vartheta}) - \text{Schw}(t, \xi, \bar{\xi}; u, \vartheta, \bar{\vartheta}) \\ &= D\xi\bar{D}\bar{\xi}\text{Schw}(t + \delta t, \xi + \delta\xi, \bar{\xi} + \delta\bar{\xi}; t, \xi, \bar{\xi}) \\ &= D\xi\bar{D}\bar{\xi}(\partial_t\bar{D}_\xi\delta\bar{\xi} - \partial_t D_\xi\delta\xi). \end{aligned} \quad (6.1)$$

The next steps are to replace bosonic derivatives by anti-commutators of supercovariant derivatives and use

$$D_\xi = (D\xi)^{-1} D \quad , \quad \bar{D}_\xi = (\bar{D}\bar{\xi})^{-1} \bar{D}.$$

For the variation of (5.36) one gets

$$\delta S \sim \int dud\vartheta d\bar{\vartheta} \left\{ \delta\bar{\xi} \bar{D} \left(\frac{1}{\bar{D}\bar{\xi}} D \left(\frac{1}{D\xi} \bar{D} (\varphi_b D\xi) \right) \right) - \delta\xi D \left(\frac{1}{D\xi} \bar{D} \left(\frac{1}{\bar{D}\bar{\xi}} D (\varphi_b \bar{D}\bar{\xi}) \right) \right) \right\} \quad (6.2)$$

From the discussion in section 3 one can see that φ_b is given by the $\mathcal{N} = 0$ solution [48], multiplied with appropriate powers of ϵ , evaluated at the boundary

$$\varphi_b = \frac{\alpha + \beta t + \gamma t^2}{D\xi \bar{D}\bar{\xi}}, \quad (6.3)$$

with

$$2Dt = \bar{\xi} D\xi \quad , \quad 2\bar{D}t = \xi \bar{D}\bar{\xi}. \quad (6.4)$$

Plugging this into (6.2) and using the chirality conditions (5.19) yields

$$\delta S_{\text{eff}} \sim \gamma \int dud\vartheta d\bar{\vartheta} (\xi \delta\bar{\xi} - \bar{\xi} \delta\xi). \quad (6.5)$$

With (5.25) and the variation of (6.4) this can be brought into the form

$$\delta S_{\text{eff}} \sim \int dud\vartheta \bar{D}\delta t = \int du\delta t' = 0. \quad (6.6)$$

7 Summary and conclusions

In the present paper, we argued that the gravitational part of the holographic dual to the $\mathcal{N} = 2$ supersymmetric SYK model is given by an $\mathcal{N} = (2, 2)$ supersymmetric JT action. We elaborated on the construction of this supersymmetric extension including also a Gibbons-Hawking-York boundary term. The main part of the calculation was done in superconformal gauge. The superconformal factors can be determined in two ways giving the same result. First, one can solve the constraints of constant supercurvatures. On the other hand imposing the existence of four unbroken supersymmetries together with an AdS_2 metric yields the same superconformal factors. Symmetry breaking patterns due to a UV regulator curve match those of the SYK model. Further, we showed that the effective Lagrangian of those curves is given by the super-Schwarzian in agreement with the result [28] for SYK. The chirality of the SYK model emerges from the chirality of the two separate extrinsic curvature fields in our gravitational setup. As a consistency check we plugged a known dilaton solution into the effective boundary action. Its variation with respect to super-reparametrisations vanishes.

It would be interesting to see whether there are corrections towards deviation from JT. For $\mathcal{N} = 0$ such corrections have been proposed in [54]. Also the reconstruction of a more complete holographic dual along the lines of [55, 56] should be extended to supersymmetric

models. In particular the addition of matter and its backreaction should be considered. The dilaton equations of motion will be affected [42]. Insisting on a constant dilaton along the boundary will change the boundary supercurve. It is expected that the same change of the boundary curve will be obtained when supplementing the super-Schwarzian by a term coupling the boundary values of matter to the boundary curve [48]. A further subject of future research will be to study if JT supergravity admits more general dilaton bulk solutions than the one considered here. Less supercharges than in the constant dilaton case will be preserved.

Supersymmetric JT gravity might also be considered in the context of $d = 4$ black hole physics with extended supersymmetry. In particular, the qualitative difference between $\mathcal{N} = 1$ and $\mathcal{N} = 2$ SYK, the non-perturbative SUSY breaking of the former [28], should be relevant in this setting.

Acknowledgments

We thank Iris Golla and Hans Jockers for useful discussions. This work was supported by the SFB-Transregio TR33 “The Dark Universe” (Deutsche Forschungsgemeinschaft) and by “Bonn-Cologne Graduate School for Physics and Astronomy” (BCGS).

Open Access. This article is distributed under the terms of the Creative Commons Attribution License ([CC-BY 4.0](https://creativecommons.org/licenses/by/4.0/)), which permits any use, distribution and reproduction in any medium, provided the original author(s) and source are credited.

References

- [1] S. Sachdev and J. Ye, *Gapless spin fluid ground state in a random, quantum Heisenberg magnet*, *Phys. Rev. Lett.* **70** (1993) 3339 [[cond-mat/9212030](https://arxiv.org/abs/cond-mat/9212030)] [[INSPIRE](#)].
- [2] A. Kitaev, *A simple model of quantum holography*, talk given at the *KITP Program: entanglement in strongly-correlated quantum matter*, April 6–July 2, University of California, U.S.A. (2015), [part 1](#) and [part 2](#) available online.
- [3] S. Sachdev, *Holographic metals and the fractionalized Fermi liquid*, *Phys. Rev. Lett.* **105** (2010) 151602 [[arXiv:1006.3794](https://arxiv.org/abs/1006.3794)] [[INSPIRE](#)].
- [4] S. Sachdev, *Bekenstein-Hawking entropy and strange metals*, *Phys. Rev.* **X 5** (2015) 041025 [[arXiv:1506.05111](https://arxiv.org/abs/1506.05111)] [[INSPIRE](#)].
- [5] J. Polchinski and V. Rosenhaus, *The spectrum in the Sachdev-Ye-Kitaev model*, *JHEP* **04** (2016) 001 [[arXiv:1601.06768](https://arxiv.org/abs/1601.06768)] [[INSPIRE](#)].
- [6] A. Jevicki and K. Suzuki, *Bi-local holography in the SYK model: perturbations*, *JHEP* **11** (2016) 046 [[arXiv:1608.07567](https://arxiv.org/abs/1608.07567)] [[INSPIRE](#)].
- [7] J. Maldacena and D. Stanford, *Remarks on the Sachdev-Ye-Kitaev model*, *Phys. Rev.* **D 94** (2016) 106002 [[arXiv:1604.07818](https://arxiv.org/abs/1604.07818)] [[INSPIRE](#)].
- [8] R. Gurau, *The complete $1/N$ expansion of a SYK-like tensor model*, *Nucl. Phys.* **B 916** (2017) 386 [[arXiv:1611.04032](https://arxiv.org/abs/1611.04032)] [[INSPIRE](#)].
- [9] E. Witten, *An SYK-like model without disorder*, [arXiv:1610.09758](https://arxiv.org/abs/1610.09758) [[INSPIRE](#)].

- [10] I.R. Klebanov and G. Tarnopolsky, *Uncolored random tensors, melon diagrams and the Sachdev-Ye-Kitaev models*, *Phys. Rev. D* **95** (2017) 046004 [[arXiv:1611.08915](#)] [[INSPIRE](#)].
- [11] C. Krishnan, S. Sanyal and P.N. Bala Subramanian, *Quantum chaos and holographic tensor models*, *JHEP* **03** (2017) 056 [[arXiv:1612.06330](#)] [[INSPIRE](#)].
- [12] C. Krishnan, K.V.P. Kumar and S. Sanyal, *Random matrices and holographic tensor models*, *JHEP* **06** (2017) 036 [[arXiv:1703.08155](#)] [[INSPIRE](#)].
- [13] C. Peng, *Vector models and generalized SYK models*, *JHEP* **05** (2017) 129 [[arXiv:1704.04223](#)] [[INSPIRE](#)].
- [14] P. Narayan and J. Yoon, *SYK-like Tensor Models on the Lattice*, *JHEP* **08** (2017) 083 [[arXiv:1705.01554](#)] [[INSPIRE](#)].
- [15] C. Krishnan and K.V.P. Kumar, *Towards a finite- N hologram*, *JHEP* **10** (2017) 099 [[arXiv:1706.05364](#)] [[INSPIRE](#)].
- [16] S. Choudhury et al., *Notes on melonic $O(N)^{q-1}$ tensor models*, [arXiv:1707.09352](#) [[INSPIRE](#)].
- [17] C. Krishnan, K.V. Pavan Kumar and D. Rosa, *Contrasting SYK-like models*, *JHEP* **01** (2018) 064 [[arXiv:1709.06498](#)] [[INSPIRE](#)].
- [18] J. Ben Geloun and V. Rivasseau, *A renormalizable SYK-type tensor field theory*, [arXiv:1711.05967](#) [[INSPIRE](#)].
- [19] R.A. Davison et al., *Thermoelectric transport in disordered metals without quasiparticles: the Sachdev-Ye-Kitaev models and holography*, *Phys. Rev. B* **95** (2017) 155131 [[arXiv:1612.00849](#)] [[INSPIRE](#)].
- [20] M. Berkooz, P. Narayan, M. Rozali and J. Simón, *Comments on the random Thirring model*, *JHEP* **09** (2017) 057 [[arXiv:1702.05105](#)] [[INSPIRE](#)].
- [21] G. Turiaci and H. Verlinde, *Towards a 2d QFT analog of the SYK model*, *JHEP* **10** (2017) 167 [[arXiv:1701.00528](#)] [[INSPIRE](#)].
- [22] K. Bulycheva, *A note on the SYK model with complex fermions*, *JHEP* **12** (2017) 069 [[arXiv:1706.07411](#)] [[INSPIRE](#)].
- [23] R. Bhattacharya, S. Chakrabarti, D.P. Jatkar and A. Kundu, *SYK model, chaos and conserved charge*, *JHEP* **11** (2017) 180 [[arXiv:1709.07613](#)] [[INSPIRE](#)].
- [24] D.J. Gross and V. Rosenhaus, *A generalization of Sachdev-Ye-Kitaev*, *JHEP* **02** (2017) 093 [[arXiv:1610.01569](#)] [[INSPIRE](#)].
- [25] J. Yoon, *SYK models and SYK-like tensor models with global symmetry*, *JHEP* **10** (2017) 183 [[arXiv:1707.01740](#)] [[INSPIRE](#)].
- [26] Y. Chen, H. Zhai and P. Zhang, *Tunable quantum chaos in the Sachdev-Ye-Kitaev model coupled to a thermal bath*, *JHEP* **07** (2017) 150 [[arXiv:1705.09818](#)] [[INSPIRE](#)].
- [27] P. Zhang, *Dispersive Sachdev-Ye-Kitaev model: band structure and quantum chaos*, *Phys. Rev. B* **96** (2017) 205138 [[arXiv:1707.09589](#)] [[INSPIRE](#)].
- [28] W. Fu, D. Gaiotto, J. Maldacena and S. Sachdev, *Supersymmetric Sachdev-Ye-Kitaev models*, *Phys. Rev. D* **95** (2017) 026009 [*Addendum ibid.* **D 95** (2017) 069904] [[arXiv:1610.08917](#)] [[INSPIRE](#)].

- [29] T. Nishinaka and S. Terashima, *A note on Sachdev–Ye–Kitaev like model without random coupling*, *Nucl. Phys. B* **926** (2018) 321 [[arXiv:1611.10290](#)] [[INSPIRE](#)].
- [30] N. Sannomiya, H. Katsura and Y. Nakayama, *Supersymmetry breaking and Nambu–Goldstone fermions with cubic dispersion*, *Phys. Rev. D* **95** (2017) 065001 [[arXiv:1612.02285](#)] [[INSPIRE](#)].
- [31] C. Peng, M. Spradlin and A. Volovich, *A supersymmetric SYK-like tensor model*, *JHEP* **05** (2017) 062 [[arXiv:1612.03851](#)] [[INSPIRE](#)].
- [32] T. Li, J. Liu, Y. Xin and Y. Zhou, *Supersymmetric SYK model and random matrix theory*, *JHEP* **06** (2017) 111 [[arXiv:1702.01738](#)] [[INSPIRE](#)].
- [33] D. Stanford and E. Witten, *Fermionic localization of the Schwarzian theory*, *JHEP* **10** (2017) 008 [[arXiv:1703.04612](#)] [[INSPIRE](#)].
- [34] T.G. Mertens, G.J. Turiaci and H.L. Verlinde, *Solving the Schwarzian via the conformal bootstrap*, *JHEP* **08** (2017) 136 [[arXiv:1705.08408](#)] [[INSPIRE](#)].
- [35] T. Kanazawa and T. Wettig, *Complete random matrix classification of SYK models with $\mathcal{N} = 0, 1$ and 2 supersymmetry*, *JHEP* **09** (2017) 050 [[arXiv:1706.03044](#)] [[INSPIRE](#)].
- [36] J. Murugan, D. Stanford and E. Witten, *More on supersymmetric and 2d analogs of the SYK model*, *JHEP* **08** (2017) 146 [[arXiv:1706.05362](#)] [[INSPIRE](#)].
- [37] J. Yoon, *Supersymmetric SYK model: bi-local collective superfield/supermatrix formulation*, *JHEP* **10** (2017) 172 [[arXiv:1706.05914](#)] [[INSPIRE](#)].
- [38] C. Peng, M. Spradlin and A. Volovich, *Correlators in the $\mathcal{N} = 2$ Supersymmetric SYK Model*, *JHEP* **10** (2017) 202 [[arXiv:1706.06078](#)] [[INSPIRE](#)].
- [39] N. Hunter-Jones, J. Liu and Y. Zhou, *On thermalization in the SYK and supersymmetric SYK models*, *JHEP* **02** (2018) 142 [[arXiv:1710.03012](#)] [[INSPIRE](#)].
- [40] N. Hunter-Jones and J. Liu, *Chaos and random matrices in supersymmetric SYK*, [arXiv:1710.08184](#) [[INSPIRE](#)].
- [41] P. Narayan and J. Yoon, *Supersymmetric SYK model with global symmetry*, [arXiv:1712.02647](#) [[INSPIRE](#)].
- [42] A. Almheiri and J. Polchinski, *Models of AdS_2 backreaction and holography*, *JHEP* **11** (2015) 014 [[arXiv:1402.6334](#)] [[INSPIRE](#)].
- [43] R. Jackiw, *Lower dimensional gravity*, *Nucl. Phys. B* **252** (1985) 343 [[INSPIRE](#)].
- [44] C. Teitelboim, *Gravitation and Hamiltonian structure in two space-time dimensions*, *Phys. Lett. B* **126** (1983) 41.
- [45] G. Sárosi, *AdS_2 holography and the SYK model*, [arXiv:1711.08482](#) [[INSPIRE](#)].
- [46] G. Turiaci and H. Verlinde, *On CFT and quantum chaos*, *JHEP* **12** (2016) 110 [[arXiv:1603.03020](#)] [[INSPIRE](#)].
- [47] K. Jensen, *Chaos in AdS_2 holography*, *Phys. Rev. Lett.* **117** (2016) 111601 [[arXiv:1605.06098](#)] [[INSPIRE](#)].
- [48] J. Maldacena, D. Stanford and Z. Yang, *Conformal symmetry and its breaking in two dimensional Nearly Anti-de-Sitter space*, *PTEP* **2016** (2016) 12C104 [[arXiv:1606.01857](#)] [[INSPIRE](#)].

- [49] M. Cvetič and I. Papadimitriou, *AdS₂ holographic dictionary*, *JHEP* **12** (2016) 008 [Erratum *ibid.* **01** (2017) 120] [[arXiv:1608.07018](#)] [[INSPIRE](#)].
- [50] G. Mandal, P. Nayak and S.R. Wadia, *Coadjoint orbit action of Virasoro group and two-dimensional quantum gravity dual to SYK/tensor models*, *JHEP* **11** (2017) 046 [[arXiv:1702.04266](#)] [[INSPIRE](#)].
- [51] S.R. Das, A. Jevicki and K. Suzuki, *Three dimensional view of the SYK/AdS duality*, *JHEP* **09** (2017) 017 [[arXiv:1704.07208](#)] [[INSPIRE](#)].
- [52] S.R. Das, A. Ghosh, A. Jevicki and K. Suzuki, *Three dimensional view of arbitrary q SYK models*, [arXiv:1711.09839](#) [[INSPIRE](#)].
- [53] S.R. Das, A. Ghosh, A. Jevicki and K. Suzuki, *Space-time in the SYK model*, [arXiv:1712.02725](#) [[INSPIRE](#)].
- [54] A. Kitaev and S.J. Suh, *The soft mode in the Sachdev-Ye-Kitaev model and its gravity dual*, [arXiv:1711.08467](#) [[INSPIRE](#)].
- [55] D.J. Gross and V. Rosenhaus, *The bulk dual of SYK: cubic couplings*, *JHEP* **05** (2017) 092 [[arXiv:1702.08016](#)] [[INSPIRE](#)].
- [56] D.J. Gross and V. Rosenhaus, *All point correlation functions in SYK*, *JHEP* **12** (2017) 148 [[arXiv:1710.08113](#)] [[INSPIRE](#)].
- [57] S. Förste and I. Golla, *Nearly AdS₂ SUGRA and the super-Schwarzian*, *Phys. Lett. B* **771** (2017) 157 [[arXiv:1703.10969](#)] [[INSPIRE](#)].
- [58] A.H. Chamseddine, *Superstrings in arbitrary dimensions*, *Phys. Lett. B* **258** (1991) 97 [[INSPIRE](#)].
- [59] P.S. Howe and G. Papadopoulos, *N = 2, D = 2 supergeometry*, *Class. Quant. Grav.* **4** (1987) 11 [[INSPIRE](#)].
- [60] P.C. West, *Introduction to supersymmetry and supergravity*, World Scientific, Singapore (1990).
- [61] M.T. Grisaru and M.E. Wehlau, *Prepotentials for (2, 2) supergravity*, *Int. J. Mod. Phys. A* **10** (1995) 753 [[hep-th/9409043](#)] [[INSPIRE](#)].
- [62] M.T. Grisaru and M.E. Wehlau, *Superspace measures, invariant actions and component projection formulae for (2, 2) supergravity*, *Nucl. Phys. B* **457** (1995) 219 [[hep-th/9508139](#)] [[INSPIRE](#)].
- [63] C. Closset and S. Cremonesi, *Comments on $\mathcal{N} = (2, 2)$ supersymmetry on two-manifolds*, *JHEP* **07** (2014) 075 [[arXiv:1404.2636](#)] [[INSPIRE](#)].
- [64] J. Gomis et al., *Anomalies, conformal manifolds and spheres*, *JHEP* **03** (2016) 022 [[arXiv:1509.08511](#)] [[INSPIRE](#)].
- [65] J. Kames-King, *Constructing the supergravity dual of the $\mathcal{N} = 2$ SYK model*, Master Thesis, Bonn University, Bonn, Germany (2018), to appear.
- [66] R. Blumenhagen, D. Lüst and S. Theisen, *Basic concepts of string theory*, Springer, Germany (2013).

JT Supergravity Part 2

This chapter has already been published as [123]:

Supersymmetric black holes and the SJT/nSCFT₁ correspondence, *S. Förste, J. Kames-King, A. Gerhardus*, In: *JHEP* 01 (2021) 186, arXiv: 2007.12393 [hep-th]

This chapter deals with the connection between a four-dimensional $\mathcal{N} = 2$ supergravity theory and the two-dimensional axial $\mathcal{N} = (2, 2)$ JT supergravity theory. Essentially, we are considering a supersymmetric generalisation of the reference [124]. We consider the addition of supersymmetric matter in both theories. In the former setting we mainly work in the near-horizon limit, which amounts to a BPS enhanced $AdS_2 \times S^2$ background. This region of spacetime captures the low-energy dynamics of the matter fluctuations. For the two-dimensional theory we also consider the addition of matter, such that one arrives at a boundary theory involving the $\mathcal{N} = 2$ super-Schwarzian coupled to matter fluctuations. We compare the resulting theories in two ways. First by dimensionally reducing and directly comparing the resulting Lagrangians. Secondly, by calculating the holographic four-point function and comparing the results. After appropriate field matching between the theories, we find agreement. This demonstrates the usefulness of the super-Schwarzian approach. In addition, it would seem that supersymmetric approaches to these low-dimensional settings would allow for an embedding into string theory.

In detail, we start by reviewing and in addition constructing a specific four-dimensional solution of $\mathcal{N} = 2$, $d = 4$ supergravity based on important previous references [125, 126]. We consider a magnetically charged black hole of 1/4 BPS symmetry, which means that two Killing spinors are preserved. At the horizon, supersymmetry is enhanced to 1/2 BPS, which may be dimensionally reduced to two dimensions with resulting $\mathcal{N} = (2, 2)$ supersymmetry. This allows us to relate four and two dimensions in the way we propose. On the aforementioned background we consider additional matter fluctuations. As we want to preserve supersymmetry we consider the addition of a hypermultiplet of four real scalars and two chiral fermions in four dimensions. We check that there are still solutions of the supersymmetry equations preserving the same amount of supersymmetry as before. Demanding the BPS equations to be unaffected implies specific moment maps and vacuum expectation values for the hyperscalars. In the four-dimensional setup we perform two calculations on the near

horizon region, which is of the form $AdS_2 \times S^2$ and still exhibits 1/2 BPS. We perform a dimensional reduction on the sphere of matter, gauge and gravity fluctuations. In order to arrive at a consistent structure in line with two-dimensional supersymmetry, the gravitini must fulfill additional projection conditions. The dilaton in the standard bosonic setting is identified in the process of dimensional reduction as an angular metric component fluctuating on the four-dimensional spacetime. Therefore in our setting the two-dimensional dilaton multiplet is identified with spherical metric fluctuation components and in addition with spherical gravitini components. We also consider the calculation of the holographic four-point function. Our approach is to consider the matter linearly coupled to metric, gravitini and gauge field fluctuations and to successively integrate out these exact fluctuations. As we are doing this in a low energy limit, this four-point function is captured by calculations in the near horizon region. In the second half of the paper, we want to see how much of the four-dimensional low-energy physics can be captured by the $\mathcal{N} = 2$ super-Schwarzian, which is a boundary reduction of $\mathcal{N} = (2, 2)$ JT super-gravity, which we introduced in chapter 2. In addition to the super-Schwarzian we of course also have to consider matter fluctuations. We must consider a (covariantly) twisted chiral multiplet as matter as this kind of multiplet is charged under $U_A(1)$. Interestingly, the D-term already breaks superconformal symmetry and leads to massive matter (this was already observed in [127]). We observe that at leading order the actions from the two-dimensional theory match with the dimensionally reduced result. For the four-point function we first reduce the matter action from the bulk to the boundary as the matter couples to the boundary fluctuations. Finally, we show that the result for the four-point functions can be made to match when associating specific fields to each other. This matching is somewhat subtle as the four-dimensional theory is considered in a Lorentzian setting and the two-dimensional theory on an Euclidean background.

The author contributed to all conceptual discussions regarding this publication. The author performed all calculations apart from those in sections 3.6 and 3.7.

Supersymmetric black holes and the SJT/nSCFT₁ correspondence

Stefan Förste,^a Andreas Gerhardus^{b,1} and Joshua Kames-King^a

^a*Bethe Center for Theoretical Physics and Physikalisches Institut der Universität Bonn,
Nussallee 12, Bonn 53115, Germany*

^b*German Aerospace Center, Institute of Data Science,
Mülzerstrasse 3, Jena 07745, Germany*

E-mail: forste@th.physik.uni-bonn.de, andreas.gerhardus@gmx.de,
jvakk@yahoo.com

ABSTRACT: We consider 1/4 BPS black hole solutions of $\mathcal{N} = 2$ gauged supergravity in AdS_4 . The near horizon geometry is $AdS_2 \times S^2$ and supersymmetry is enhanced. In the first part of the paper we choose a moment map, which allows the embedding of this supergravity solution into a sugra theory with a hypermultiplet. We then perform the s-wave reduction of this theory at the horizon and determine the dilaton multiplet, which couples to both metric and gravitino fluctuations. In the second part we work with Euclidean axial $\mathcal{N} = (2, 2)$ JT supergravity and show how to add gauged matter in form of covariantly twisted chiral and anti-chiral multiplets. We demonstrate how to reduce the on-shell action to boundary superspace. We compare both theories and calculate the fourpoint function by integrating out gravitons, gravitini and photons for the s-wave setting and by use of the Super-Schwarzian modes in the JT theory.

KEYWORDS: 2D Gravity, AdS-CFT Correspondence, Black Holes, Supergravity Models

ARXIV EPRINT: [2007.12393](https://arxiv.org/abs/2007.12393)

¹AG contributed to this work while he was still at the Bethe Center for Theoretical Physics and the Physikalisches Institut der Universität Bonn.

Contents

1	Introduction	2
2	A supersymmetric black hole in 4d	3
2.1	Solution without hypermultiplets	3
2.2	Solution with a universal hypermultiplet	6
2.3	Dimensional reduction with hypermultiplet as source	8
2.3.1	Gravity sector	9
2.3.2	Matter sector	12
2.3.3	Linearized coupling	14
2.4	Four-point function	16
2.4.1	Integrating out gravitons	16
2.4.2	Integrating out gaugefields	17
2.4.3	Integrating out gravitini	18
3	Supersymmetric JT	21
3.1	Minimal $2d$ $\mathcal{N} = (2, 2)$ supergravity	21
3.2	$\mathcal{N} = (2, 2)$ JT supergravity	23
3.2.1	Graviphoton kinetic term	23
3.2.2	JT supergravity and the super-Schwarzian	24
3.3	Matter coupled to $2d$ $\mathcal{N} = (2, 2)$ supergravity	25
3.3.1	Chiral vs. twisted chiral	25
3.3.2	Supersymmetric action	25
3.3.3	X -space	26
3.3.4	Breaking superconformal symmetry	27
3.4	Equations of motion and currents	27
3.4.1	Symmetry currents	28
3.5	Comparison to four-dimensional model	29
3.6	Super-Schwarzian coupled to matter	29
3.6.1	On-shell action	30
3.6.2	Boundary super-space, two-point function	31
3.7	Four-point function/integrating out the fluctuations	34
4	Discussion	36
A	Four-dimensional supergravity conventions	38

1 Introduction

In the present paper we will carry out a supersymmetric extension of studies presented in [1, 2]. Extremal black holes contain an AdS_2 factor in the near horizon limit in which finite energy excitations decouple [3]. In order to capture also those it has been proposed in [4] to add Jackiw-Teitelboim gravity [5, 6] to the bulk action. By integrating out bulk fields this can be related to an effective one dimensional theory whose Lagrangian is given by the Schwarzian derivative of the boundary curve [7–10]. This is also the effective Lagrangian arising in the strong coupling limit of the SYK model [11–13]. (For reviews on the SYK/JT correspondence see e.g. [14, 15].) In the present paper we will be interested in supersymmetric extensions. On the SYK side $\mathcal{N} \in \{1, 2\}$ extensions have been presented in [17]. The effective Lagrangian at strong coupling is given by the corresponding super-Schwarzian derivatives. The $\mathcal{N} = (1, 1)$ extension of JT gravity on manifolds without a boundary is given in [16]. The inclusion of a boundary term, the extension to $\mathcal{N} = (2, 2)$ and the relation to super-Schwarzians is presented in [18–20]. In the present paper, we will be interested in the $\mathcal{N} = (2, 2)$ configuration of which further aspects have been studied in e.g. in [21–33].

In [1, 2] (see also e.g. [34, 35]) the relation of the $nAdS_2/nCFT_1$ correspondence to higher dimensional black holes is investigated in more detail. In [1] an extremal and near extremal Reissner Nordström AdS_4 black hole are considered. The authors compute the four point function of conformal primaries in a dual CFT_3 in different ways. Following [36] by adding a probe massive free scalar (dual to the primary under consideration) and integrating out the induced metric perturbations. This yields an expression quartic in the scalars (quadratic in energy momentum tensor components) i.e. quartic in the sources for the primaries in the dual CFT_3 . Dimensional reduction (for spherically symmetric configurations and small frequencies) relates this calculation to a calculation performed in the $nAdS_2/nCFT_1$ scheme. Results obtained by integrating out Schwarzian modes match.

In the present paper we will consider a 1/4 BPS solution of gauged $\mathcal{N} = 2$ 4d supergravity [37, 38]. This solution represents a magnetically charged black hole with AdS_4 asymptotics. In the near horizon limit supersymmetry is enhanced corresponding to $\mathcal{N} = (2, 2)$ in two dimensions. The probe should now not only preserve spherical symmetry but also supersymmetry. This can be achieved by adding a hypermultiplet along the lines of [39].

The paper is organised as follows. Section two is devoted to the four dimensional picture and its near horizon reduction. In section 2.1 we review the sugra solution [37, 38] which does not contain hypermultiplets. This solution represents a black hole with AdS_4 asymptotics and an $AdS_2 \times S^2$ near horizon geometry. General techniques for adding a hypermultiplet [39] are applied in section 2.2. Section 2.3 discusses the dimensional reduction in the near horizon limit, in s -wave approximation. In section 2.4 we compute four point functions in a dual CFT following [1, 36]. That is, we integrate out metric fluctuations, gravitini fluctuations and gauge field fluctuations in a limit in which first corrections to the S^2 radius have been added to the near horizon limit. For the gravitini we have to impose further projections such that super currents are conserved in that limit.

Section three is devoted to the $nAdS_2/nSCFT_1$ perspective on the considerations of section two. A natural choice for the two dimensional theory would be what we obtained

from dimensional reduction in the near horizon region of the four dimensional black hole solution. However, we will twist this slightly. Firstly, we switch to Euclidean signature corresponding to the choice in [20]. Another twist is performed for the following reason. We want to associate the integrating out of bulk modes (such as the graviton) to integrating out super-Schwarzian modes in the effective one dimensional dual. One of the super-Schwarzian modes corresponds to the two dimensional graviphoton. This is the gauge field of a Kaluza-Klein $U(1)$ when reducing from four to two dimensions. (The four dimensional $\mathcal{N} = 1$ gravity multiplet does not contain a graviphoton.) The fluctuating hypermultiplet in the four dimensional setup is charged under a combination of the $\mathcal{N} = 2$ graviphoton and an extra $U(1)$. In two dimensions this will correspond to an extra vector multiplet. We twist the charge of the probe matter in two dimensions such that it is charged under the graviphoton instead of an extra $U(1)$. In sections 3.1 and 3.2 we review the $\mathcal{N} = (2, 2)$ extensions of JT gravity [20]. After that, in section 3.3 we add a covariantly twisted chiral and anti-chiral multiplet describing probe matter. These have the same amount of degrees of freedom and the same mass as what we obtained from dimensional reduction of half the four dimensional hypermultiplet. But the covariantly twisted multiplets are charged under the two dimensional graviphoton. Conserved currents (energy momentum tensor, supercurrent, gauge current) share the same conservation laws with the dimensionally reduced ones and are associated to each other. Some further aspects of the relation between dimensionally reduced four dimensional theory and the considered two dimensional theory are mentioned in section 3.5. In section 3.6 the one dimensional holographic dual is considered. Supergravity is replaced by super reparametrisations with a super-Schwarzian action. Matter is coupled in a supersymmetric generalisation of the way it is presented in [8]. That is, we write down a term which generates the $\mathcal{N} = 2$ superconformal two point functions of operators being dual to the bulk matter, in the zero temperature case. By applying a general super reparametrisation on that expression one generates the couplings to the super-Schwarzian modes. By integrating out (linearised) super-Schwarzian modes we obtain the expression generating four point functions of the dual superconformal operator, in section 3.7. We express these generating functionals as two dimensional integrals containing the conserved 2d currents. Then they can be matched with the findings of section 2.4. We obtain agreement if we impose the same additional projection condition on the supercurrent as in 2.4.

In section 4, we summarize the results and discuss possible future directions. In an appendix A we list some of the used conventions.

2 A supersymmetric black hole in 4d

2.1 Solution without hypermultiplets

In this subsection we recapitulate the 1/4 BPS magnetically charged black hole solution [37, 38] of $\mathcal{N} = 2$ gauged supergravity (for a review see [41–44]). Our conventions follow [44, 46] and are summarized in appendix A. Pure gauged supergravity allows only for AdS_4 ‘black holes’ with a naked singularity [40].

We will first consider a solution to a theory containing the supergravity and a vector multiplet. The supergravity multiplet accomodates the vielbein e_μ^α , two gravitini ψ_μ^A , $A \in \{1, 2\}$, and a graviphoton A_μ^0 . The vector multiplet consists of a vector A_μ^1 two gauginos λ^A and a complex scalar z . The bosonic part of the supersymmetric Lagrangian is given by

$$\mathcal{L} = \frac{1}{2}R(e) + g_{zz^*}\partial^\mu z\partial_\mu z^* + I_{\Lambda\Sigma}F_{\mu\nu}^\Lambda F^{\Sigma\mu\nu} + \frac{1}{2}R_{\Lambda\Sigma}\epsilon^{\mu\nu\rho\sigma}F_{\mu\nu}^\Lambda F_{\rho\sigma}^\Sigma - g^2V(z, z^*). \quad (2.1)$$

Here, $R(e)$ is the scalar curvature and g_{zz^*} is the metric on a special Kähler manifold on which the scalar of the vector multiplet takes values. On a special Kähler manifold there are holomorphic sections $(X^\Lambda(z), F_\Lambda(z))$ where in our case $\Lambda \in \{0, 1\}$. Further, $F_\Lambda = \partial F/\partial X^\Lambda$ where for the explicit solution in [37, 38] the prepotential

$$F = -2i\sqrt{X^0(X^1)^3} \quad (2.2)$$

is chosen. $R_{\Lambda\Sigma}$ and $I_{\Lambda\Sigma}$ denote real respectively imaginary part of the period matrix

$$\mathcal{N}_{\Lambda\Sigma} = \left(\frac{\partial F_\Sigma}{\partial X^\Lambda}\right)^* + 2i\frac{\text{Im}(F_{\Lambda\Gamma})X^\Gamma\text{Im}(F_{\Sigma\Delta})X^\Delta}{X^E\text{Im}(F_{EZ})X^Z}. \quad (2.3)$$

with $F_{\Lambda\Sigma} = \partial F_\Sigma/\partial X^\Lambda$. The Kähler metric is expressed in terms of the Kähler potential

$$g_{zz^*} = \partial_z\partial_{z^*}\mathcal{K}, \quad \text{with} \quad \mathcal{K} = -\log\left[i\left((X^\Lambda)^*F_\Lambda - X^\Lambda(F_\Lambda)^*\right)\right]. \quad (2.4)$$

The scalar potential, finally, is given by

$$V = \left(g^{zz^*}f_z^\Lambda(f_z^\Sigma)^* - 3(L^\Lambda)^*L^\Sigma\right)\xi_\Lambda\xi_\Sigma, \\ \text{with } f_z^\Lambda = e^{\frac{\kappa}{2}}(\partial_z + (\partial_z\mathcal{K}))X^\Lambda, \quad L^\Lambda = e^{\frac{\kappa}{2}}X^\Lambda, \quad (2.5)$$

and the real constants ξ^Λ are called Fayet-Iliopoulos (FI) parameters (characterising under which U(1) the gravitini are charged). The explicit solution we are going to consider is a magnetically charged black hole. The metric is given by

$$ds^2 = U^2(r)dt^2 - U^{-2}(r)dr^2 - b^2(r)(d\theta^2 + \sin^2\theta d\varphi^2), \quad (2.6)$$

where U and b will be specified shortly. The non vanishing vierbein and spin connection components are,

$$e_\mu^\alpha = \text{diag}(U(r), 1/U(r), b(r), b(r)\sin\theta), \quad \omega_t^{01} = U\partial_r U, \quad \omega_\theta^{12} = -U\partial_r b, \\ \omega_\varphi^{13} = -(U\partial_r b)\sin\theta, \quad \omega_\varphi^{23} = -\cos\theta. \quad (2.7)$$

The gauge fields have only non vanishing φ components

$$A_\varphi^\Lambda = -p^\Lambda\cos\theta, \quad (2.8)$$

and hence the field strengths are

$$F_{tr}^\Lambda = 0, \quad F_{\theta\varphi}^\Lambda = \frac{p^\Lambda}{2}\sin\theta. \quad (2.9)$$

Mostly we will work with the self-dual and anti-self dual field strengths defined as

$$F_{\mu\nu}^{\pm\Lambda} = \frac{1}{2} \left(F_{\mu\nu} \mp \frac{i}{2} \epsilon_{\mu\nu\rho\sigma} F^{\rho\sigma} \right). \quad (2.10)$$

The 1/4 BPS solution reported in [37, 38] has two Killing spinors

$$\epsilon_1 = \sqrt{U(r)} e^{-\frac{1}{4}(\partial_z \mathcal{K} \partial_r z - \partial_{z^*} \mathcal{K} \partial_r z^*)} \epsilon_1^0, \quad \epsilon_2 = \sqrt{U(r)} e^{-\frac{1}{4}(\partial_z \mathcal{K} \partial_r z - \partial_{z^*} \mathcal{K} \partial_r z^*)} \epsilon_2^0, \quad (2.11)$$

where the ϵ_A^0 are chiral constant spinors satisfying the projection condition

$$\epsilon_A = -\sigma^3_A{}^B \gamma_{01} \epsilon_B, \quad \epsilon_A = \epsilon_{AB} \gamma_0 \epsilon^B. \quad (2.12)$$

The scalar in the vector multiplet is given by $z = X^1/X^0$ with

$$X^0 = \pm \frac{1}{4\xi_0} - \frac{\xi_1 \beta^1}{r \xi_0}, \quad X^1 = \pm \frac{3}{4\xi_1} + \frac{\beta^1}{r} \quad (2.13)$$

with correlated signs. Asymptotically, at $r \rightarrow \infty$, $z \rightarrow \frac{3\xi_0}{\xi_1}$ becomes constant and so does the potential

$$V \rightarrow \Lambda_4 = -\frac{2g^2}{\sqrt{3}} \sqrt{\xi_0 \xi_1^3},$$

corresponding to the radius of asymptotic AdS_4 geometry. The metric components in (2.6) are given by

$$U^2 = e^{\mathcal{K}} \left(gr + \frac{1}{2gr} - \frac{16g}{3r} (\xi_1 \beta^1)^2 \right)^2, \quad b^2 = e^{-\mathcal{K}} r^2, \quad (2.14)$$

with

$$e^{\mathcal{K}} = \frac{1}{8\sqrt{(X^1)^3 X^0}} = \frac{2\sqrt{\xi_0 \xi_1^3} r^2}{\sqrt{(r \mp 4\xi_1 \beta^1) (3r \pm 4\xi_1 \beta^1)^3}}. \quad (2.15)$$

This is a geometry of a charged black hole, for which charges (see (2.8)) and mass, M , are all fixed in terms of the integration constant β_1 , explicitly

$$p^0 = \frac{\mp 1}{g\xi_0} \left(\frac{1}{8} + \frac{8(g\xi_1 \beta^1)^2}{3} \right), \quad p^1 = \frac{\mp 1}{g\xi_1} \left(\frac{3}{8} - \frac{8(g\xi_1 \beta^1)^2}{3} \right),$$

$$M = -\frac{128}{81} \Lambda_4 (\xi_1 \beta^1)^3. \quad (2.16)$$

The metric component U^2 has a double zero at $r = r_h$. The position of the horizon is

$$r_h = \sqrt{\frac{16}{3} (\xi_1 \beta^1)^2 - \frac{1}{2g^2}}. \quad (2.17)$$

The near horizon geometry is $AdS_2 \times S^2$ where the negative AdS_2 curvature overcompensates the S^2 curvature resulting in a negative net curvature. Supersymmetry is enhanced to 1/2 BPS corresponding to $\mathcal{N} = (2, 2)$ in two dimensions [50].

2.2 Solution with a universal hypermultiplet

In the spirit of [1] we want to switch on perturbations around a sugra solution and study the backreaction on the super geometry. We would like to do this in a supersymmetric way and to consider only spin zero and 1/2 fluctuations. We also want the perturbation to be charged under a U(1) gauge symmetry such that there is a corresponding backreaction. All this can be achieved by modifying the solution of the previous section to fit into a theory with a sugra, a vector and a hypermultiplet. How to perform such a modification in general has been worked out in [39]. The hypermultiplet consists of four real scalars q^a , $a \in \{1, 2, 3, 4\}$, and two chiral fermions ζ_α , $\alpha \in \{1, 2\}$. The four real scalars will be called

$$(q^1, q^2, q^3, q^4) = (R, u, v, D).$$

These take values on a quaternionic-Kähler manifold which in our example is chosen to be SU(2, 1)/U(2) with metric

$$ds^2 = h_{ab} q^a q^b = \frac{1}{R^2} \left(dR^2 + R (du^2 + dv^2) + \left(dD + \frac{1}{2} u dv - \frac{1}{2} v du \right)^2 \right). \quad (2.18)$$

The metric h_{ab} can be expressed in terms of vielbeins (for details and conventions see [41, 44])

$$h_{ab} = \mathcal{U}_a^{A\alpha} \mathcal{U}_b^{B\beta} \epsilon_{\beta\alpha} \epsilon_{AB}. \quad (2.19)$$

Indices A and α are raised and lowered with the two dimensional epsilon tensor or its transposed when they label bosonic quantities. For fermions these indices are raised and lowered by complex conjugation. A reality constraint on the vielbeins can be viewed as applying both rules simultaneously

$$\mathcal{U}_{a,A\alpha} = \left(\mathcal{U}_a^{A\alpha} \right)^* = \epsilon_{AB} \mathcal{U}_a^{B\beta} \epsilon_{\beta\alpha}. \quad (2.20)$$

For the metric (2.18) the non vanishing vielbein components are

$$\begin{aligned} \mathcal{U}_R^{12} = \mathcal{U}_R^{21} &= \frac{1}{\sqrt{2}R}, & \mathcal{U}_D^{12} = -\mathcal{U}_D^{21} &= \frac{i}{\sqrt{2}R}, \\ \mathcal{U}_u^{21} = -\mathcal{U}_u^{12} &= \frac{iv}{2\sqrt{2}R}, & \mathcal{U}_u^{11} = -\mathcal{U}_u^{22} &= \frac{1}{\sqrt{2}R}, \\ \mathcal{U}_v^{12} = -\mathcal{U}_v^{21} &= \frac{iu}{2\sqrt{2}R}, & \mathcal{U}_v^{11} = \mathcal{U}_v^{22} &= \frac{i}{\sqrt{2}R}. \end{aligned} \quad (2.21)$$

The solution of [37, 38] is invariant under the susy variations of the gravitino and the gaugino

$$\begin{aligned} \delta_\epsilon \psi_{\mu A} &= \nabla_\mu \epsilon_A + 2i F_{\mu\nu}^{\Lambda-} I_{\Lambda\Sigma} L^\Sigma + ig S_{AB} \gamma_\mu \epsilon^B, \\ \delta_\epsilon \lambda^{iA} &= i \partial_\mu z^i \gamma^\mu \epsilon^A + G_{\mu\nu}^{-i} \gamma^{\mu\nu} \epsilon^{AB} \epsilon_B + ig g^{i\bar{j}} \bar{f}_{\bar{j}}^\Lambda a_{\Lambda} \sigma_3^{AB} \epsilon_B, \end{aligned} \quad (2.22)$$

with

$$\begin{aligned} \nabla_\mu \epsilon_A &= \left(\partial_\mu - \frac{1}{4} \omega_\mu^{ab} \gamma_{ab} \right) \epsilon_A + \frac{i}{2} g a_\Lambda A_\mu^\Lambda \sigma_A^{3B} \epsilon_B, \\ G_{\Lambda\mu\nu} &= \text{Re}(\mathcal{N}_{\Lambda\Sigma}) F_{\mu\nu}^\Sigma - \frac{1}{2} \text{Im}(\mathcal{N}_{\Lambda\Sigma}) \epsilon_{\mu\nu\gamma\delta} F^{\Sigma\gamma\delta}, \end{aligned} \quad (2.23)$$

provided the following BPS conditions are satisfied,

$$\begin{aligned}
 U' &= -\frac{2L^\Lambda I_{\Lambda\Sigma} p^\Sigma}{b^2} \pm g a_\Lambda L^\Lambda, \\
 \frac{U}{b} b' &= \frac{2L^\Lambda I_{\Lambda\Sigma} p^\Sigma}{b^2} \pm g a_\Lambda L^\Lambda, \\
 g a_\Lambda p^\Lambda &= \mp 1.
 \end{aligned}
 \tag{2.24}$$

In addition to this we now demand invariance of the hyperino variation

$$\delta_\epsilon \zeta_\alpha = i \mathcal{U}_a^{\beta B} \nabla_\mu q^a \gamma^\mu \epsilon^A \epsilon_{AB} \mathcal{C}_{\alpha\beta} + 2g \mathcal{U}_{\alpha a}^A k_\Lambda^a \bar{L}^\Lambda \epsilon_A,
 \tag{2.25}$$

with

$$\nabla_\mu q = \left(\partial_\mu q + g A_\mu^\Lambda k_\Lambda^q \right).
 \tag{2.26}$$

Following the logic of [39] we keep $g_{\mu\nu}, F_{\mu\nu}^\Lambda, z$ the same as for [37, 38] such that (2.22) is still solved. Parameters are fixed by the requirement that (2.25) is also solved, implying the conditions [37–39]

$$k_\Lambda^a F_{\mu\nu}^\Lambda = 0, \quad P_\Lambda^x f_i^\Lambda = 0, \quad \epsilon^{xyz} P_\Lambda^y P_\Sigma^y L^\Lambda \bar{L}^\Sigma = 0, \quad k_\Lambda^a L^\Lambda = 0.
 \tag{2.27}$$

Here, k_Λ are Killing vectors tangent to the quaternionic-Kähler manifold resembling charge vectors of the gauged isometry. We consider the following Killing vectors

$$k_\Lambda = a_\Lambda (-v \partial_u + u \partial_v),
 \tag{2.28}$$

where a_Λ functions as the FI parameter, such that the black hole background is unchanged. These Killing vectors correspond to moment maps

$$P_\Lambda^x = a_\Lambda \left(\frac{v}{\sqrt{R}}, \frac{u}{\sqrt{R}}, 1 - \frac{u^2 + v^2}{4R} \right).
 \tag{2.29}$$

Plugging (2.28), (2.29) back into (2.27) and (2.22) we see that the following vevs are required for the hyperscalar

$$\langle u \rangle = \langle v \rangle = 0, \quad \langle R \rangle = \text{const.} \neq 0, \quad \langle D \rangle = \text{const.}
 \tag{2.30}$$

Later we will consider fluctuations of u and v . In a dimensionally reduced system these will be scalars of a matter multiplet which is charged under a $U(1)$ with gauge fields $A^\Lambda \sim a^\Lambda$. We will freeze R and D to their background values (2.30).

The BPS equations are not affected. In relating field strengths and mass matrices to geometrical quantities we will often need the two linear combinations of the first two BPS conditions (2.24)

$$\frac{U}{b} b' - U' = \frac{4L^\Lambda I_{\Lambda\Sigma} p^\Sigma}{b^2}, \quad U' + \frac{U}{b} b' = \pm 2g a_\Lambda L^\Lambda.
 \tag{2.31}$$

2.3 Dimensional reduction with hypermultiplet as source

We now perform the explicit s-wave reduction on the two-sphere in the near horizon geometry $AdS_2 \times S^2$. This will be carried out for the gravity multiplet, the hypermultiplet and the linearized supergravity theory coupled to the hypermultiplet as a source. The former should reproduce the JT supergravity theory in 2d and the latter should correspond to the linearized couplings in 2d. Performing this dimensional reduction will also reveal which four-dimensional fields constitute the dilaton multiplet.

While for a bosonic field the s-wave reduction may be implemented by assuming no dependence on spherical coordinates, for fermions an additional projection must be applied such that the degrees of freedom are reduced by half. The correct projection can for example be deduced by demanding that the vevs chosen for the hyperscalars R, D are kept intact by supersymmetry variations, such that no dynamical R, D fields are generated and hence u, v and half of the degrees of freedom of the hyperinos constitute a proper two-dimensional multiplet.

By use of

$$\delta q^a = \mathcal{U}_{\alpha A}^a (\bar{\zeta}^\alpha \epsilon^A + \mathcal{C}^{\alpha\beta} \epsilon^{AB} \bar{\zeta}_\beta \epsilon_B), \tag{2.32}$$

the equations $\delta R = 0$ and $\delta D = 0$ are only fulfilled if ζ^1 fulfills the same projection as ϵ^2 and ζ^2 the same as ϵ^1 (see the first condition in (2.12)). The projected spinors have only one independent component which motivates the replacement,

$$\zeta_1 \rightarrow \begin{pmatrix} 1 \\ i \\ i \\ 1 \end{pmatrix} \zeta_1, \quad \zeta_2 \rightarrow \begin{pmatrix} 1 \\ i \\ -i \\ -1 \end{pmatrix} \zeta_2, \tag{2.33}$$

where in abuse of notation we have given the Grassmann variables on the right hand side of (2.33) the same name as the four dimensional spinors on the left hand side.

The metric on $AdS_2 \times S^2$ is given by

$$ds^2 = \frac{r^2}{v_1^2} dt^2 - \frac{v_1^2}{r^2} dr^2 - v_2^2 (d\theta^2 + \sin^2 \theta d\varphi^2), \tag{2.34}$$

with the vielbein

$$e_\mu^a = \text{diag} \left(\frac{r}{v_1}, \frac{v_1}{r}, v_2, v_2 \sin \theta \right). \tag{2.35}$$

The non vanishing components of the spin connection are

$$\omega_t^{01} = \frac{r}{v_1^2}, \quad \omega_\varphi^{23} = -\cos \theta. \tag{2.36}$$

We also note that for product space geometries, the equations of motion and the dimensionally reduced action are equivalent for the case of Einstein gravity and Maxwell theory [45] (barring terms which have been neglected in the approximation with at most linear contributions of the dilaton multiplet to the action). For the gravitini this can be easily seen to also hold: the equations of motion derived from (2.48), (2.83) match the dimensionally reduced equations (2.102)–(2.107) in the near horizon limit up to contributions J_A^θ containing $\psi_{\theta,A}$.

2.3.1 Gravity sector

As a first step we reduce the kinetic terms for the gravitational multiplet, which encompasses the Einstein-Hilbert term, the linear combination of the field strengths, and the gravitinos.

The relevant parts of the action are [46]

$$S \supset \int d^4x \sqrt{-g} \left(-\frac{1}{2}R + i \left(\bar{\mathcal{N}}_{\Lambda\Sigma} F_{\mu\nu}^{-\Lambda} F^{-\Lambda\mu\nu} - \mathcal{N}_{\Lambda\Sigma} F_{\mu\nu}^{+\Lambda} F^{+\Lambda\mu\nu} \right) + \epsilon^{\mu\nu\lambda\sigma} \bar{\psi}_\mu^A \gamma_\sigma \nabla_\nu \psi_{\lambda A} + \text{h.c.} + F^{-\Lambda\mu\nu} \mathcal{I}_{\Lambda\Sigma} 4L^\Sigma \bar{\psi}_\mu^A \psi_\nu^B \epsilon_{AB} + g S_{AB} \bar{\psi}_\mu^A \gamma^{\mu\nu} \psi_\nu^B \right), \quad (2.37)$$

with the gravitino mass matrix defined as

$$S_{AB} = \frac{i}{2} (\sigma_x)_A^C \epsilon_{BC} P_\Lambda^x L^\Lambda = \frac{i}{2} (\sigma_{x_3})_A^C \epsilon_{BC} a_\Lambda L^\Lambda, \quad (2.38)$$

where our choice of moment map (2.29) was applied in the second step. The covariant derivative of the gravitino is given in (2.23). Furthermore, we also have to include the potential for the complex scalar in the vector multiplet linked to the FI gauging. In the full black hole solution it acts as the cosmological constant of AdS_4 . It is given by

$$V \supset -g^2 3L^\Lambda \bar{L}^\Sigma a_\Lambda a_\Sigma, \quad (2.39)$$

where the momentum map has already been expressed via the FI constants.

The dimensional reduction of the Einstein-Hilbert term to two dimensions was performed in [1]. Assuming a static, spherically symmetric metric and allowing for linear fluctuations of spherical metric components $h_{\varphi\varphi} = (\sin\theta)^2 h_{\theta\theta}$ leads to

$$4\pi v_2^2 \int d^2x \sqrt{-\hat{g}} \phi (R - \Lambda_2) + 8\pi v_2^2 \int_{\partial M} du \phi K, \quad (2.40)$$

where ϕ is identified with $h_{\theta\theta}$ and Dirichlet conditions are set for ϕ . It also should be mentioned that the effective two-dimensional cosmological constant Λ_2 is a combination of the magnetic part of the field strength of (2.37) with background value (2.9) and (2.39). In (2.40) we have also added a boundary term originating from dimensionally reducing a Gibbons-Hawking-York term [1]. In the following boundary terms will not be included.

Now we add fluctuations for the gauge fields in the gravity and vector multiplet along the $U(1)$ under which u and v are charged. Spherical symmetry is respected by setting the φ and θ components in the corresponding combination of gauge fields to zero. The resulting vector field provides an effective photon. Assuming $A_{\hat{\mu}}^\Lambda = A^\Lambda A_{\hat{\mu}}$ with $\hat{\mu} \in \{t, r\}$ and A^Λ denoting a constant direction within the two $U(1)$'s gives the two-dimensional kinetic term

$$\frac{1}{g_2^2} \int d^2x \sqrt{-\hat{g}} (1 + 2\phi) F_{\hat{\mu}\hat{\nu}} F^{\hat{\mu}\hat{\nu}}, \quad (2.41)$$

where $F_{\hat{\mu}\hat{\nu}}$ is the fieldstrength of $A_{\hat{\mu}}$ and

$$\frac{1}{g_2^2} = 4\pi v_2^2 A^\Lambda I_{\Lambda\Sigma} A^\Sigma \quad (2.42)$$

with $\mathcal{I}_{\Lambda\Sigma}$ being the imaginary part of the period matrix depending on the horizon values of the gauge scalars z . The fluctuating gauge field $A_{\hat{\mu}}$ will be called photon in the rest of the paper.

The gravitinos have to fulfill specific γ_{01} projections. The projection conditions on the hyperinos (with solutions (2.33)) induce projection conditions on the supercurrent. Since the supercurrent acts as the source of the gravitini, this further induces projection conditions on the gravitini via their equations of motion. From an s-wave perspective these projections are needed to lose the angular spin connection components and also to obtain two-dimensional mass terms. Furthermore, when working out all contributions to the gravitino terms of (2.37), one encounters couplings of ψ_r to ψ_t . These are not compatible with unbroken two dimensional $\mathcal{N} = (2, 2)$ supersymmetry. When applying the correct projection these kinds of terms vanish as we will see below. We must also apply a spherical projection on the gravitini in order to emulate the spherical symmetry, linking J_A^φ to J_A^θ . To be more precise, when expressing the supercurrents explicitly via the matter sector as in (2.75) spherical symmetry manifests as

$$J_A^\theta = -\sin\theta\gamma_{23}J_A^\varphi. \quad (2.43)$$

This should also be respected by the gravitino sector. All in all, we apply

$$\psi_{r/tA} = \gamma_{01}(\sigma^3)_A{}^B\psi_{r/tB}, \quad \psi_{\theta A} = -\gamma_{01}(\sigma^3)_A{}^B\psi_{\theta B}, \quad \psi_{\varphi A} = \sin\theta\gamma_{23}\psi_{\theta A}. \quad (2.44)$$

Let us first understand the general structure of the gravitino contribution to (2.37) while only applying the γ_{23} projection of (2.44). First, the field strength with its background value (2.9) effectively acts as a mass term because it can be rewritten via the first equation of (2.31) as a purely geometric term; the same is also true for the mass matrix contribution. This can be expressed geometrically via the second equation of (2.31). We assume no angular dependence of the gravitino components ψ_{tA}, ψ_{rA} and $\psi_{\theta A}$ ($\psi_{\varphi A}$ is fixed by (2.44)). Hence, we get the following expression for the kinetic terms of the gravitini

$$\begin{aligned} S \supset & \int d^4x e_\varphi^3 \bar{\psi}_t^A \left(-2\gamma_3 \partial_r \psi_{\theta A} + \frac{i}{r} \sigma_{AB}^3 \gamma^{02} \psi_\theta^B + \frac{iv_2}{2} \left(-\psi_r^B \epsilon_{AB} + \sigma_{AB}^3 \gamma^{01} \psi_r^B \right) \right) \\ & + \int d^4x e_\varphi^3 \bar{\psi}_r^A \left(2\gamma_3 \partial_t \psi_{\theta A} + \frac{r}{v_1^2} \left(-\gamma_{013} \psi_{\theta A} + i\sigma_{AB}^3 \gamma_{12} \psi_\theta^B \right) + \frac{iv_2}{2} \left(\psi_t^B \epsilon_{AB} - \sigma_{AB}^3 \gamma^{01} \psi_t^B \right) \right) \\ & + 2 \int d^4x e_\varphi^3 \bar{\psi}_\theta^A \left(\frac{v_1}{rv_2} \gamma_{123} \partial_t \psi_{\theta A} - \frac{r}{v_1 v_2} \gamma_{023} \partial_r \psi_{\theta A} - \gamma_3 \partial_t \psi_{rA} + \gamma_3 \partial_r \psi_{tA} \right. \\ & \quad \left. + \frac{1}{2v_1 v_2} \left(-\gamma_{023} \psi_{\theta A} - \gamma_{23} \psi_\theta^B \epsilon_{AB} - i\sigma_{AB}^3 \psi_\theta^B \right) \right. \\ & \quad \left. + \frac{r}{2v_1^2} \left(\gamma_{013} \psi_{rA} + i\sigma_{AB}^3 \gamma^{21} \psi_r^B \right) + \frac{i}{2r} \sigma_{AB}^3 \gamma^{20} \psi_t^B \right), \end{aligned} \quad (2.45)$$

where so far only the relationship of $\psi_{\varphi A}$ to $\psi_{\theta A}$ (2.44) has been used. Now we observe couplings of ψ_t to ψ_r , couplings of ψ_θ to ψ_t and ψ_r and also terms exclusively consisting of ψ_θ . As there is no kinetic term for the gravitini in two dimensions, any consistent dimensional reduction should exclude couplings of ψ_t to ψ_r . A close inspection of these terms in the first two lines of (2.45) shows that these terms vanish when applying (2.44).

After use of the γ_{01} projections in (2.45) the ψ_θ to ψ_θ couplings can be brought into the form,

$$8\pi \int d^2x \epsilon^{23\hat{\nu}\hat{\mu}} \left(\bar{\psi}_\theta^A \gamma_\nu \gamma_{23} \nabla_\mu \psi_{\theta A} \right). \quad (2.46)$$

In the purely gravitational sector a linearized approximation is used to arrive at the Jackiw-Teitelboim action, where the dilaton appears only as a Lagrange multiplier. This procedure can be emulated here by denoting ψ_θ as the dilatino mode. This immediately implies that the quadratic term (2.46) is to be neglected. In accordance, after applying the γ_{01} projections, the remaining terms of (2.45) consist purely of $\psi_{t/rA}$ couplings to $\psi_{\theta A}$. To be specific, we solve projection conditions (2.44) explicitly and replace four component spinors by a single Grassmann field according to

$$\begin{aligned} \psi_{t/r1} &\rightarrow \begin{pmatrix} 1 \\ i \\ -i \\ -1 \end{pmatrix} \psi_{t/r1}, & \psi_{t/r2} &\rightarrow \begin{pmatrix} 1 \\ i \\ i \\ 1 \end{pmatrix} \psi_{t/r2}, \\ \psi_{\theta 1} &\rightarrow \begin{pmatrix} 1 \\ i \\ i \\ 1 \end{pmatrix} \psi_{\theta 1}, & \psi_{\theta 2} &\rightarrow \begin{pmatrix} 1 \\ i \\ -i \\ -1 \end{pmatrix} \psi_{\theta 2}. \end{aligned} \quad (2.47)$$

We focus on all terms in which $\psi_{t/rA}$ and $\psi_{\theta A}$ mix and perform the spherical integration. In addition, we partially integrate those terms in which derivatives of $\psi_{\theta A}$ appear. In the resulting expression $\psi_{\theta A}$ solely represents a fermionic Lagrange multiplier. We just give the final answer in two-dimensional conventions ($z = t + y$, $\bar{z} = t - y$, $y = v_1^2/r$)

$$\begin{aligned} &32\pi v_2 \int dz d\bar{z} \left(\psi_{\theta 1} \left(\nabla_{\bar{z}} \psi_{z1}^* - \nabla_z \psi_{\bar{z}1}^* + \frac{i}{2y} \psi_{z2} \right) + \psi_{\theta 2} \left(\nabla_z \psi_{\bar{z}2}^* - \nabla_{\bar{z}} \psi_{z2}^* - \frac{i}{2y} \psi_{\bar{z}1} \right) + \text{h.c.} \right) \\ &= 32\pi v_2^2 \int dz d\bar{z} \left(\lambda_1 \left(\nabla_{\bar{z}} \psi_{z1}^* - \nabla_z \psi_{\bar{z}1}^* + \frac{i}{2y} \psi_{z2} \right) + \lambda_2 \left(\nabla_z \psi_{\bar{z}2}^* - \nabla_{\bar{z}} \psi_{z2}^* - \frac{i}{2y} \psi_{\bar{z}1} \right) + \text{h.c.} \right), \end{aligned} \quad (2.48)$$

where the covariant derivatives are given by

$$\nabla_z \psi_{\bar{z},A} = \partial_z \psi_{\bar{z},A} + \left(\sigma^3 \right)_A^B \frac{1}{4y} \psi_{\bar{z},B}, \quad \nabla_{\bar{z}} \psi_{z,A} = \partial_{\bar{z}} \psi_{z,A} + \left(\sigma^3 \right)_A^B \frac{1}{4y} \psi_{z,B}$$

and in the last two lines we have introduced the dilatino with $\psi_{\theta A} = e_\theta^2 \lambda_A$.

It should be noted that this procedure is quite natural from a supersymmetric perspective. Recall that for the gravitational sector the role of the dilaton was played by $h_{\theta\theta}$. Together with ψ_θ these should constitute the dilaton multiplet. So far however the degrees of freedom do not match up. Whereas the dilaton which naturally appears as the metric fluctuation $h_{\theta\theta}$ must be real, we have double the amount of degrees of freedom for the dilatino. In $\mathcal{N} = (2, 2)$ JT gravity there are two dilaton multiplets [20]. Here however we do not consider the full Kaluza-Klein reduction, which would furnish the $U(1)_A$ field

strength accompanied by the missing bosonic degree of freedom in the dilaton multiplet. Hence we must set reality conditions on the dilatino.

Setting $\lambda_1 = i\lambda_2^*$, we arrive at

$$32\pi v_2^2 \int dz d\bar{z} \lambda_1 \left(\nabla_{\bar{z}} (\psi_{z1}^* + i\psi_{z2}) - \nabla_z (\psi_{\bar{z}1}^* + i\psi_{\bar{z}2}) - \frac{1}{2y} (\psi_{z1} + i\psi_{\bar{z}2}) + \text{h.c.} \right). \quad (2.49)$$

The conditions for the dilatino modes are also applied when calculating the four-point function (2.110).

2.3.2 Matter sector

Now we consider the kinetic and mass terms of the hypermultiplet in the near horizon limit. These match the corresponding terms for the twisted chiral and anti-chiral multiplets in section 3.4.

The relevant terms of the $\mathcal{N} = 2$ Lagrangian are, the kinetic terms for our matter fields

$$\int d^4x \sqrt{-g} \left(h_{ab} \nabla_\mu q^a \nabla^\mu q^b - i \left(\bar{\zeta}^\alpha \gamma^\mu \nabla_\mu \zeta_\alpha - \text{h.c.} \right) \right), \quad (2.50)$$

with the general mass terms

$$\int d^4x \sqrt{-g} \left(g^2 4h_{ab} k_\Lambda^a k_\Sigma^b L^\Lambda \bar{L}^\Sigma + g M^{\alpha\beta} \bar{\zeta}_\alpha \zeta_\beta \right), \quad (2.51)$$

with the hyperino mass matrix defined as

$$M^{\alpha\beta} = -\mathcal{U}_a^{\alpha A} \mathcal{U}_b^{\beta B} \epsilon_{AB} \partial^a k_\Lambda^b L^\Lambda \quad (2.52)$$

and also a Pauli term

$$\int d^4x \sqrt{-g} F_{\mu\nu}^{-\Lambda} I_{\Lambda\Sigma} \bar{\zeta}_\alpha \gamma^{\mu\nu} \zeta_\gamma \mathcal{C}^{\alpha\gamma}, \quad (2.53)$$

which effectively acts as a mass term with the background value (2.9). For the vevs we have chosen for the hyperscalars (2.30) and the choice of moment map (2.29), the scalar mass terms of (2.51) amount to

$$\begin{aligned} g^2 (4h_{ab} k_\Lambda^a k_\Sigma^b) &= g^2 a_\Lambda a_\Sigma \frac{4}{R} (u^2 + v^2) \bar{L}^\Lambda L^\Sigma \\ &= (u^2 + v^2) U'^2, \end{aligned} \quad (2.54)$$

where for the last step the BPS conditions (2.24) were used. The covariant derivatives are given by

$$\nabla_\mu q = \left(\partial_\mu q + g A_\mu^\Lambda k_\Lambda^q \right), \quad \nabla_\mu \zeta_\alpha = \partial_\mu \zeta_\alpha - \frac{1}{4} \omega_\mu^{mn} \gamma_{mn} \zeta_\alpha + \Delta_{\mu\alpha}^\beta \zeta_\beta, \quad (2.55)$$

where for the hyperino covariant derivative we have already applied that the Kähler connection is zero. Furthermore, in our approximation (leaving out higher order interaction terms)

$$\Delta_\alpha^\beta \zeta_\beta = \mathcal{C}_{\beta\gamma} \Delta^{\alpha\gamma} = \mathcal{C}_{\beta\gamma} \left(g A^\Lambda \partial_a k_\Lambda^b \mathcal{U}^{a\alpha A} \mathcal{U}_{bA}^\beta \right). \quad (2.56)$$

For both the scalar fields and the fermions the coupling to the gauge fields occurs due to the last term in the covariant derivative. As we are considering electric fluctuations around the magnetic background of the solution, we will also assume general gauge fields $A_{\hat{\mu}}^{\Lambda}$, such that not only terms due to (2.8) will occur. In the s-wave approximation the A_{φ} couplings should drop out and only the couplings to $A_{\hat{\mu}}^{\Lambda}$ should appear in two dimensions. We will consider these effects, namely the linearized coupling to supergravity modes in the next section 2.3.3.

For the scalar field one straightforwardly arrives at

$$S \supset 4\pi v_2^2 \int d^2x \sqrt{-\hat{g}} \frac{1}{R} \left(\partial_{\mu} u \partial^{\mu} u + \partial_{\mu} v \partial^{\mu} v + (u^2 + v^2) U'^2 \right). \quad (2.57)$$

In the near horizon limit U' is constant and (2.57) resembles a free massive scalar on AdS_2 . This leads to the equations of motion

$$\frac{v_1^2}{r^2} \partial_t^2 u - \frac{r^2}{v_1^2} \partial_r^2 u - \frac{2r}{v_1^2} \partial_r u - \frac{2}{v_1} u = 0, \quad (2.58)$$

and the same with u replaced by v .

Solving (2.58) at large r leads to the solutions of the form

$$u \sim r^{-\Delta_{\pm}} \quad (2.59)$$

with

$$\Delta_{\pm} = \frac{1 \pm 3}{2}, \quad (2.60)$$

and the same for v . According to the AdS/CFT dictionary [47] u and v are dual to conformal primaries of dimension Δ_+ of the emergent CFT_1 . For the comparison with the two-dimensional results of section 3 it should also be noted that the scalar fields u, v always appear in complex linear combinations with the vevs chosen for the hypermultiplet sector, such that it is convenient to introduce the combinations

$$f := u - iv, \quad \bar{f} := u + iv. \quad (2.61)$$

The action for the complex scalars is

$$S \supset 4\pi v_2^2 \int d^2x \sqrt{-\hat{g}} \frac{1}{R} \left(\partial_{\mu} f \partial^{\mu} \bar{f} + (f \bar{f}) U'^2 \right). \quad (2.62)$$

For the hyperinos we impose the projections which led us to (2.47) earlier. Then terms in the Lagrangian including angular components of the spin connection drop out. To be more explicit, (2.50) includes terms of the form

$$-i \left(\bar{\zeta}^{\alpha} \gamma^{\theta} \nabla_{\theta} \zeta_{\alpha} + \bar{\zeta}^{\alpha} \gamma^{\varphi} \nabla_{\varphi} \zeta_{\alpha} \right), \quad (2.63)$$

which are set to zero since the γ_{01} projections commute with γ_{23} .

By use of $M^{12} = -ia_{\Lambda} L^{\Lambda}$, the background value of the field strength (2.9) and the BPS equations, (2.51) and (2.53) combine to a single effective mass term such that one ends up with the following two-dimensional Lagrangian for the hyperinos

$$S \supset 4\pi v_2^2 \int d^2x \sqrt{-\hat{g}} \left(-i \bar{\zeta}^{\alpha} \gamma^{\hat{\mu}} \nabla_{\hat{\mu}} \zeta_{\alpha} + U' \bar{\zeta}_1 \zeta_2 + \text{h.c.} \right). \quad (2.64)$$

Replacing ζ^α by the one component fields as in (2.33) and taking variational derivatives of (2.64) gives the following fermionic equations of motion

$$\partial_t \zeta^1 - \frac{r^2}{v_1^2} \partial_r \zeta^1 - \frac{r}{2v_1^2} \zeta^1 - \frac{ir}{v_1^2} \zeta_2 = 0, \quad \partial_t \zeta^2 + \frac{r^2}{v_1^2} \partial_r \zeta^2 + \frac{r}{2v_1^2} \zeta^2 + \frac{ir}{v_1^2} \zeta_1 = 0. \quad (2.65)$$

These describe free massive fermions on AdS_2 . For large r we arrive at a solution of the form (2.59) with

$$\Delta_\pm = \frac{1 \pm 2}{2}. \quad (2.66)$$

2.3.3 Linearized coupling

So far we have discussed the dimensional reduction of the fields of the supergravity theory itself, namely metric, photon and gravitinos and also of the matter on this specific background. In this section we want to dimensionally reduce the coupling of the photon and gravitino fluctuations to the matter. To be more explicit, we now perform the dimensional reduction of the part of the action, which quite heuristically may be written as

$$S \supset \int d^4x \sqrt{-g} \left(h_{\mu\nu} T^{\mu\nu} + \bar{\psi}_\mu^A J_\mu^A + \bar{J}_\mu^A \psi^\mu + A_\mu j_A^\mu \right). \quad (2.67)$$

As explained previously, due to covariance metric fluctuations are already coupled to matter fields, such that we will only mention this schematically. We have to allow for metric fluctuations in the spherical directions $h_{\varphi\varphi} = \sin^2 \theta h_{\theta\theta}$ and metric fluctuations in the AdS_2 direction $h_{\hat{\mu}\hat{\nu}}$ in (2.50), to arrive at a structure like the first term in (2.67). Now integrating over the spherical directions gives the two-dimensional action [1]

$$-4\pi v_2^2 \int d^2x \sqrt{-\hat{g}} \left(h_{\hat{\mu}\hat{\nu}} T^{\hat{\mu}\hat{\nu}} + 2\phi T^{\theta\theta} \right), \quad (2.68)$$

where the metric fluctuation $h_{\theta\theta}$ has been identified with the dilaton ϕ . The effective 2d energy-momentum conservation reads

$$v_1^4 \partial_t T_{tt} - r^2 \partial_r \left(r^2 T_{tr} \right) = 0, \quad v_1^4 \partial_t T_{tr} - r \partial_r \left(r^3 T_{rr} \right) - r v_1^4 T_{tt} = 0. \quad (2.69)$$

The coupling of matter fields to the considered $U(1)$ fluctuations (2.42) are contained in the covariant derivatives in (2.50) via (2.55).

Starting from (2.50) we arrive at

$$\begin{aligned} S \supset & -4\pi v_2^2 g \int d^2x \sqrt{-\hat{g}} \left(\bar{\zeta}^1 \gamma^\mu \zeta_1 - \bar{\zeta}^2 \gamma^\mu \zeta_2 - 2u \partial^\mu v + 2v \partial^\mu u \right) a_\Lambda A_\mu^\Lambda \\ & = -q_2 \int d^2x \sqrt{-\hat{g}} \left(\bar{\zeta}^1 \gamma^{\hat{\mu}} \zeta_1 - \bar{\zeta}^2 \gamma^{\hat{\mu}} \zeta_2 - 2u \partial^{\hat{\mu}} v + 2v \partial^{\hat{\mu}} u \right) A_{\hat{\mu}} \end{aligned} \quad (2.70)$$

where the charge q_2 is

$$q_2 = 4\pi v_2^2 g a_\Lambda A^\Lambda. \quad (2.71)$$

Notice also that the sum over $\mu \in \{t, r, \theta, \varphi\}$ is reduced to $\hat{\mu} \in \{t, r\}$ because u and v are taken to depend only on t and r and the ζ_A 's are eigenspinors of γ_{01} (which anticommutes with γ_{02} and γ_{03}).

We now express the four component spinors in (2.70) by their one component projections according to (2.33) and combine two real scalars into one complex scalar (2.61). Then (2.70) equals

$$\begin{aligned}
 & q_2 \int d^2x \sqrt{-\hat{g}} \left(-4iA_t e_0^t (\zeta_1^* \zeta_1 - \zeta_2^* \zeta_2) - 4iA_r e_1^r (-\zeta_1^* \zeta_1 - \zeta_2^* \zeta_2) \right) \\
 & + q_2 \int d^2x \sqrt{-\hat{g}} \left(-iA_{\hat{\mu}} \partial^{\hat{\mu}} \bar{f} f + iA_{\hat{\mu}} \partial^{\hat{\mu}} f \bar{f} \right).
 \end{aligned} \tag{2.72}$$

Taking the variational derivative of (2.70) with respect to $A_{\hat{\mu}}$ we arrive at the currents

$$\begin{aligned}
 j_t &= -iq_2 \left(f \partial_t \bar{f} - \bar{f} \partial_t f \right) + 4iq_2 \frac{r}{v_1} \left(-\zeta_1^* \zeta_1 + \zeta_2^* \zeta_2 \right), \\
 j_r &= -iq_2 \left(f \partial_r \bar{f} - \bar{f} \partial_r f \right) + 4iq_2 \frac{v_1}{r} \left(-\zeta_1^* \zeta_1 - \zeta_2^* \zeta_2 \right).
 \end{aligned} \tag{2.73}$$

The current conservation equation is given by

$$\partial_t j^t + \partial_r j^r = 0. \tag{2.74}$$

The coupling of gravitino to supercurrent can directly be read off from the general $\mathcal{N} = 2$ supergravity Lagrangian [46]

$$\int d^4x \sqrt{-g} \left(-2U_{aA\alpha} \nabla^\mu q^a \bar{\psi}_\mu^A \zeta^\alpha - 2U_{aA\alpha} \nabla_\mu q^a \bar{\psi}_\nu^A \gamma^{\mu\nu} \zeta_\alpha - 2giN_A^\alpha \bar{\psi}_\mu^A \gamma^\mu \zeta_\alpha \right), \tag{2.75}$$

with

$$N_\alpha^A = 2\mathcal{U}_{\alpha a}^A k_\Lambda^a \bar{L}^\Lambda. \tag{2.76}$$

For clarity we will give the individual supercurrents of (2.75) explicitly before moving to two-dimensional conventions. We will use the linear combinations (2.61) and explicit solutions to spinor projection conditions as in (2.33) and (2.47). Then we get one component supercurrents (for a relation to four component spinors see (2.101)),

$$\begin{aligned}
 J_1^t &= \frac{\sqrt{2}}{\sqrt{R}} \left(\frac{v_1^2}{r^2} \partial_t \chi + \partial_r \chi \right) \zeta^1 - \frac{i}{r} \chi \zeta_2, & J_2^t &= \frac{\sqrt{2}}{\sqrt{R}} \left(-\frac{v_1^2}{r^2} \partial_t \bar{\chi} + \partial_r \bar{\chi} \right) \zeta^2 - \frac{i}{r} \bar{\chi} \zeta_1, \\
 J_1^r &= \frac{\sqrt{2}}{\sqrt{R}} \left(-\partial_t \chi - \frac{r^2}{v_1^2} \partial_r \chi \right) \zeta^1 - ir \chi \zeta_2, & J_2^r &= \frac{\sqrt{2}}{\sqrt{R}} \left(-\partial_t \bar{\chi} + \frac{r^2}{v_1^2} \partial_r \bar{\chi} \right) \zeta^2 + iir \bar{\chi} \zeta_1.
 \end{aligned} \tag{2.77}$$

The supercurrent components satisfy conservation equations

$$\partial_t J_1^t + \partial_r J_1^r - \frac{r}{2v_1^2} \left(J_1^t - iJ_2^{t*} \right) + \frac{i}{2r} J_2^{r*} = 0, \tag{2.78}$$

$$\partial_t J_2^t + \partial_r J_2^r + \frac{r}{2v_1^2} \left(J_2^t - iJ_1^{t*} \right) - \frac{i}{2r} J_1^{r*} = 0. \tag{2.79}$$

For the angular components the following relation holds

$$J_A^\theta = -\sin \theta \gamma_{23} J_A^\varphi. \tag{2.80}$$

The explicit form is

$$J_1^\theta = \frac{\sqrt{2}}{\sqrt{R}} \left(\frac{v_1}{rb} \partial_t f - \frac{r}{v_1 b} \partial_r f \right) \zeta^1 + \frac{i}{b} f \zeta_2, \quad J_2^\theta = \frac{\sqrt{2}}{\sqrt{R}} \left(\frac{v_1}{rb} \partial_t f + \frac{r}{v_1 b} \partial_r f \right) \zeta^2 - \frac{i}{b} f \zeta_1. \quad (2.81)$$

Now we want to perform the dimensional reduction of the linearized supercurrent gravitino coupling which in terms of four component spinors reads

$$4\pi v_2^2 \int d^2x \sqrt{-\hat{g}} \left(\bar{\psi}_{\hat{\mu}}^A J_A^{\hat{\mu}} + 2\bar{\psi}_{\theta}^A J_A^\theta + \text{h.c.} \right). \quad (2.82)$$

Plugging in our explicit solutions to projection conditions in terms of one component Grassmann fields (see (2.33), (2.47) and (2.101)) yields

$$16\pi v_2^2 \int d^2x \left(\psi_{1\hat{\mu}}^* J_1^{\hat{\mu}} - \psi_{2\hat{\mu}}^* J_2^{\hat{\mu}} - 2\psi_{1\theta}^* J_1^\theta + 2\psi_{2\theta}^* J_2^\theta + \text{c.c.} \right). \quad (2.83)$$

with $\hat{\mu} \in \{r, t\}$. The $\psi_{A\hat{\mu}}$ are the gravitini of the (2, 2) SUGRA multiplet in 2d whereas $\psi_{\theta A}$ are the superpartners of the dilaton, the dilatini.

2.4 Four-point function

In this subsection we will compute four point functions in the spirit of [36]. We will turn on fluctuations in half of the hypermultiplet as described in section 2.3. This will backreact and create fluctuations for gravitons, gravitini and photons. By expressing these in terms of the hypermultiplet fluctuations and plugging that into the action one obtains terms which are quartic in the hypermultiplet fluctuations. According to the AdS/CFT dictionary those generate fourpoint functions in the dual CFT₃. In a certain limit these match fourpoint functions in the SYK model as was shown for gravitons and gauge fields in [1, 2]. This is because the region in which the geometry differs from $AdS_2 \times S^2$ contributes, in the considered low frequency approximation, only contact terms which will be neglected. In the dual CFT contact terms can be cancelled by local counterterms. In our case, the calculation corresponding to integrating out gravitons and photons is quite close to the one reported above. For this reason, we can be brief there. For the gravitini, the discussion will be more complicated and, indeed, we will be able only to match a subsector of the SYK result.

2.4.1 Integrating out gravitons

We consider metric fluctuations around our solution, impose spherical symmetry and fix diffeomorphisms, i.e. we consider [1],

$$ds^2 = U^2(r) (1 + h_{tt}(r, t)) dt^2 - U^{-2}(r) dr^2 - b^2(r) (1 + h_{\theta\theta}) (d\theta^2 + \sin^2 \theta d\varphi^2), \quad (2.84)$$

where $U(r)$ and $b(r)$ are solutions to the BPS equations (2.24) ensuring also that they solve Einstein's equations for the given background. For the computation of non-contact contributions to the fourpoint function only the region of spacetime in which the geometry can be nearly approximated by $AdS_2 \times S^2$ is relevant. Here, 'nearly' means that $U(r)$ is taken to its Maldacena limit

$$U(r) = \frac{r}{v_1} \quad (2.85)$$

where r has been shifted by r_h :

$$r - r_h \rightarrow r. \quad (2.86)$$

For the S^2 radius linear deviations from a constant are taken into account

$$b(r) = v_2 + r, \quad (2.87)$$

$$f(b) = f(v_2) + r f'(v_2), \quad (2.88)$$

where in the expansion (2.88) only the leading contribution is kept for each term. If no further derivatives w.r.t. r are considered this is the limit given in [1] (adopted to our notation)

$$U(r) = \frac{r}{v_1}, \quad b(r) = v_2, \quad b'(r) = 1. \quad (2.89)$$

After integrating over the S^2 the relevant part of the on-shell action is as in (2.68) with $\phi = h_{\theta\theta}$ and the metric fluctuations are to be replaced by the corresponding solutions of the linearised Einstein equations. This works in the same way as in [1]. The explicit form of the energy-momentum tensor does not matter, here. In our case it will have contributions from two real scalars u and v and also from the hyperinos satisfying the projection condition (2.33). What matters later is that $T^{\hat{\mu}\hat{\nu}}$ with $\hat{\mu}, \hat{\nu} \in \{0, 1\}$ matches the result from the twisted chiral multiplet to be discussed in section 3.3. It is perhaps worthwhile to point out that $T_{\theta\theta}$ is expressed in terms of $T_{\hat{\mu}\hat{\nu}}$ with $\hat{\mu}, \hat{\nu} \in \{0, 1\}$ by means of energy-momentum conservation. For this it is important to take the nearly $AdS_2 \times S^2$ limit (with $b'(r) = 1$) because in the original Maldacena limit $T_{\theta\theta}$ would decouple from the conservation law which would just be the two dimensional energy-momentum conservation.

The result for this sector of the on-shell action can be just copied from [1] (up to differences in the signature)

$$S_{g,os} \sim \int dt dr \left(\frac{r^2 v_2^3}{v_1^2} T_{rr} \frac{1}{\partial_t} T_{tr} + \frac{v_2^3 r}{v_1^2} T_{tr} \frac{1}{\partial_t^2} T_{tr} \right). \quad (2.90)$$

To explicitly compute the four point function one should employ holographic renormalization (for a review see [48]). For our purpose of comparing to results from integrating out super Schwarzian modes the regularised version ($r < \infty$) suffices.

2.4.2 Integrating out gaugefields

According to our discussion after (2.70) the angular components of the electromagnetic current vanish. Spherical symmetry imposes vanishing angular dependence on the gauge fields and we consider only fluctuations for A_t and A_r .

$$\partial_{\hat{\mu}} F^{\hat{\mu}\hat{\nu}} = g_2^2 j^{\hat{\mu}}, \quad (2.91)$$

where $j^{\hat{\mu}}$ is given in terms of hypermultiplet fluctuations (2.73). Following [2] we gauge fix $A_t = 0$ and solve (2.91) by

$$A_r = g_2^2 \frac{r}{v_1} \partial_t^{-2} j_r \quad (2.92)$$

resulting in the on-shell action

$$S_{A,os} \sim \int dr dt \left(\frac{r}{v_1} \right)^4 j_r \partial_t^{-2} j_r. \quad (2.93)$$

2.4.3 Integrating out gravitini

Integrating out the gravitini reflects some new aspects and we will be more detailed, here. We gauge fix

$$\psi_{tA} = 0, \quad A \in \{1, 2\}. \quad (2.94)$$

From spherical symmetry we deduced that J_A^φ is related to J_A^θ (2.43). This is compatible with the gravitini equations if we impose the last condition in (2.44). At the moment no near horizon limit is considered. Then the remaining gravitini equations of motion are from the variation of (2.37) plus (2.67) with respect to the gravitini

$$J_1^t = -\frac{2}{b}\gamma_3\partial_r\psi_{\theta 1} - \frac{b'}{b^2}\gamma_3\psi_{\theta 1} + \frac{b'U}{b}\gamma_{123}\psi_{r1} + i\left(\frac{U'}{Ub} + \frac{b'}{b^2}\right)\gamma_{02}\psi_{\theta 2}^* + \frac{i}{2}\left[\frac{Ub'}{b} - U' + \left(\frac{Ub'}{b} + U'\right)\gamma_{01}\right]\psi_{r2}^* \quad (2.95)$$

$$J_2^t = -\frac{2}{b}\gamma_3\partial_r\psi_{\theta 2} - \frac{b'}{b^2}\gamma_3\psi_{\theta 2} + \frac{b'U}{b}\gamma_{123}\psi_{r2} + i\left(\frac{U'}{Ub} + \frac{b'}{b^2}\right)\gamma_{02}\psi_{\theta 1}^* + \frac{i}{2}\left[U' - \frac{Ub'}{b} + \left(\frac{Ub'}{b} + U'\right)\gamma_{01}\right]\psi_{r1}^* \quad (2.96)$$

$$J_1^r = \frac{2}{b}\gamma_3\partial_t\psi_{\theta 1} - \left(\frac{UU'}{b} + \frac{U^2b'}{b^2}\right)\gamma_{013}\psi_{\theta 1} - i\left(\frac{UU'}{b} + \frac{U^2b'}{b^2}\right)\gamma_{12}\psi_{\theta 2}^* \quad (2.97)$$

$$J_2^r = \frac{2}{b}\gamma_3\partial_t\psi_{\theta 2} - \left(\frac{UU'}{b} + \frac{U^2b'}{b^2}\right)\gamma_{013}\psi_{\theta 2} - i\left(\frac{UU'}{b} + \frac{U^2b'}{b^2}\right)\gamma_{12}\psi_{\theta 1}^* \quad (2.98)$$

$$J_1^\theta = -\frac{1}{b}\gamma_3\partial_t\psi_{r1} + \left(\frac{UU'}{2b} + \frac{U^2b'}{2b^2}\right)\gamma_{013}\psi_{r1} + \frac{1}{Ub^2}\gamma_{123}\partial_t\psi_{\theta 1} - \frac{U'}{2b^2}\gamma_{023}\psi_{\theta 1} - \frac{U}{b^2}\gamma_{023}\partial_r\psi_{\theta 1} + \left[\left(\frac{Ub'}{2b^3} - \frac{U'}{2b^2}\right)\gamma_{23} + i\left(\frac{Ub'}{2b^3} + \frac{U'}{2b^2}\right)\right]\psi_{\theta 2}^* + i\left(\frac{UU'}{2b} + \frac{U^2b'}{2b^2}\right)\gamma_{12}\psi_{r2}^* \quad (2.99)$$

$$J_2^\theta = -\frac{1}{b}\gamma_3\partial_t\psi_{r2} + \left(\frac{UU'}{2b} + \frac{U^2b'}{2b^2}\right)\gamma_{013}\psi_{r2} + \frac{1}{Ub^2}\gamma_{123}\partial_t\psi_{\theta 2} - \frac{U'}{2b^2}\gamma_{023}\psi_{\theta 2} - \frac{U}{b^2}\gamma_{023}\partial_r\psi_{\theta 2} - \left[\left(\frac{Ub'}{2b^3} - \frac{U'}{2b^2}\right)\gamma_{23} - i\left(\frac{Ub'}{2b^3} + \frac{U'}{2b^2}\right)\right]\psi_{\theta 1}^* + i\left(\frac{UU'}{2b} + \frac{U^2b'}{2b^2}\right)\gamma_{12}\psi_{r1}^*. \quad (2.100)$$

In the following we will reduce these four component spinor equations each to a one component equation. In (2.33) we had reduced the four component hyperinos to one component by imposing that the frozen scalars R and D do not change under susy transformation (together with chirality). This amounts to a reduction of the supercurrents (other

projections will vanish) which we denote as

$$\begin{aligned}
 J_1^{t/r} &\rightarrow \begin{pmatrix} 1 \\ -i \\ -i \\ 1 \end{pmatrix} J_1^{t/r}, & J_2^{t/r} &\rightarrow \begin{pmatrix} 1 \\ -i \\ i \\ -1 \end{pmatrix} J_2^{t/r}, \\
 J_1^\theta &\rightarrow \begin{pmatrix} 1 \\ -i \\ i \\ -1 \end{pmatrix} J_1^\theta, & J_2^\theta &\rightarrow \begin{pmatrix} 1 \\ -i \\ -i \\ 1 \end{pmatrix} J_2^\theta.
 \end{aligned} \tag{2.101}$$

For the gravitini we keep only those components whose equations are sourced by the projected supercurrents. This amounts to imposing projection conditions (2.44) or explicitly to replace four component spinors by one component ones according to (2.47). In the following we will use one component spinors only. For those, the remaining non trivial gravitini equations read

$$J_1^t = \frac{2}{b} \partial_r \psi_{\theta 1} + \frac{b'}{b^2} \psi_{\theta 1} - \frac{b'U}{b} \psi_{r1} - i \left(\frac{U'}{Ub} + \frac{b'}{b^2} \right) \psi_{\theta 2}^* + i \frac{Ub'}{b} \psi_{r2}^*, \tag{2.102}$$

$$J_2^t = \frac{2}{b} \partial_r \psi_{\theta 2} + \frac{b'}{b^2} \psi_{\theta 2} + \frac{b'U}{b} \psi_{r2} - i \left(\frac{U'}{Ub} + \frac{b'}{b^2} \right) \psi_{\theta 1}^* - i \frac{Ub'}{b} \psi_{r1}^*, \tag{2.103}$$

$$J_1^r = -\frac{2}{b} \partial_t \psi_{\theta 1} + \left(\frac{UU'}{b} + \frac{U^2 b'}{b^2} \right) \psi_{\theta 1} - i \left(\frac{UU'}{b} + \frac{U^2 b'}{b^2} \right) \psi_{\theta 2}^*, \tag{2.104}$$

$$J_2^r = -\frac{2}{b} \partial_t \psi_{\theta 2} - \left(\frac{UU'}{b} + \frac{U^2 b'}{b^2} \right) \psi_{\theta 2} + i \left(\frac{UU'}{b} + \frac{U^2 b'}{b^2} \right) \psi_{\theta 1}^*, \tag{2.105}$$

$$\begin{aligned}
 J_1^\theta &= \frac{1}{b} \partial_t \psi_{r1} + \left(\frac{UU'}{2b} + \frac{U^2 b'}{2b^2} \right) \psi_{r1} + \frac{1}{Ub^2} \partial_t \psi_{\theta 1} - \frac{U'}{2b^2} \psi_{\theta 1} - \frac{U}{b^2} \partial_r \psi_{\theta 1} + \\
 &+ i \frac{Ub'}{b^3} \psi_{\theta 2}^* - \frac{i}{2} \left(\frac{UU'}{b} + \frac{U^2 b'}{b^2} \right) \psi_{r2}^*,
 \end{aligned} \tag{2.106}$$

$$\begin{aligned}
 J_2^\theta &= \frac{1}{b} \partial_t \psi_{r2} - \left(\frac{UU'}{2b} + \frac{U^2 b'}{2b^2} \right) \psi_{r2} - \frac{1}{Ub^2} \partial_t \psi_{\theta 2} - \frac{U'}{2b^2} \psi_{\theta 2} - \frac{U}{b^2} \partial_r \psi_{\theta 2} + \\
 &+ i \frac{Ub'}{b^3} \psi_{\theta 1}^* + \frac{i}{2} \left(\frac{UU'}{b} + \frac{U^2 b'}{b^2} \right) \psi_{r1}^*.
 \end{aligned} \tag{2.107}$$

From this set of equations one can derive the following conservation laws

$$\begin{aligned}
 \partial_t J_1^t + \partial_r J_1^r - \frac{UU'}{2} (J_1^t - iJ_2^{t*}) + \frac{2b'}{b} J_1^r - i \frac{U'}{2U} J_2^{r*} + Ub' (J_1^\theta - iJ_2^{\theta*}) \\
 = \left(\frac{UU'b'}{b^2} + \frac{U^2 b''}{b^2} + \frac{UU''}{b} - \frac{U^2 b'^2}{b^3} \right) (\psi_{\theta 1} - i\psi_{\theta 2}^*),
 \end{aligned} \tag{2.108}$$

$$\begin{aligned}
 i(\partial_t J_2^{t*} + \partial_r J_2^{r*}) - \frac{UU'}{2} (J_1^t - iJ_2^{t*}) - \frac{U'}{2U} J_1^r + i \frac{2b'}{b} J_2^{r*} + Ub' (J_1^\theta - iJ_2^{\theta*}) \\
 = \left(\frac{UU'b'}{b^2} + \frac{U^2 b''}{b^2} + \frac{UU''}{b} - \frac{U^2 b'^2}{b^3} \right) (\psi_{\theta 1} - i\psi_{\theta 2}^*).
 \end{aligned} \tag{2.109}$$

Due to the non-vanishing right hand sides in (2.108) and (2.109) these may not look like proper conservation laws. However, imposing the BPS conditions (2.24) it is not difficult to check that the right hand sides vanish. For us there remains a problem, though. In the limit (2.89) the right hand sides do not vanish. This is because the limit is not consistent with the BPS conditions (for consistency one would have to include corrections to U , i.e. the AdS_2 geometry, which we do not want to consider). Another, more technical, problem is that the J_A^θ enter only in the combination $J_1^\theta - iJ_2^{\theta*}$. This means, that one cannot use conservation laws to express the other combination, $J_1^\theta + iJ_2^{\theta*}$, in terms of J_A^t and J_A^r . This does not pose an immediate problem. However, when we will later integrate over the super-Schwarzian modes in section 3.7 we will find that the result can be expressed by 2d supercurrents only. The dilatino source corresponding to J_A^θ will not appear. Both these problems can be addressed by restricting ourselves to a subsector

$$\psi_{\theta 1} - i\psi_{\theta 2}^* = 0. \tag{2.110}$$

Such a constraint puts the right hand sides of (2.108) and (2.109) to zero and also solves our second problem since, in the on shell action, $J_1^\theta + iJ_2^{\theta*}$ couples just to the l.h.s. of (2.110). From the gravitini equations (2.104) and (2.105) we learn that (2.110) constrains

$$J_1^r - iJ_2^{r*} = 0. \tag{2.111}$$

After imposing spherical symmetry, the projections (2.101), (2.47) and the restriction (2.110) (implying (2.111)) the relevant part of the on-shell action takes the form

$$\int d^4x \sqrt{-g} (\bar{\psi}_\mu^A J_A^\mu + \text{h.c.}) \rightarrow S_{\psi, \text{os}} \sim \int dr dt \left[(J_1^r + iJ_2^{r*})^* (\psi_{1r} - i\psi_{2r}^*) - 2 (J_1^\theta - iJ_2^{\theta*})^* (\psi_{1\theta} + i\psi_{2\theta}^*) + \text{c.c.} \right] \tag{2.112}$$

where on the r.h.s. of (2.112) one component fields appear. This can now be computed along the following steps. First one expresses J_A^r by the gravitini equations (2.104) and (2.105). The appearing time derivatives of ψ_{Ar} can be expressed by means of gravitini equations (2.106), (2.107). Taking also the limit (2.89) one arrives at

$$S_{\psi, \text{os}} \sim \int dt dr \left[(\psi_{\theta 1} + i\psi_{\theta 2}^*)^* \left(J_1^\theta - iJ_2^{\theta*} + \frac{v_1}{2rv_2^2} \partial_t (\psi_{\theta 1} + i\psi_{\theta 2}^*) \right) + \text{c.c.} \right] \tag{2.113}$$

The $\psi_{\theta A}$ can be expressed as solutions to (2.104) and (2.105)

$$\psi_{\theta 1} + i\psi_{\theta 2}^* = -\frac{v_2}{2} \partial_t^{-1} (J_1^r + iJ_2^{r*}), \tag{2.114}$$

whereas the combination of J_A^θ can be replaced by means of the conservation laws (2.108), (2.109). The final result reads

$$S_{\psi, \text{os}} \sim \int dt dr \left\{ v_2 (J_1^r + iJ_2^{r*})^* \times \partial_t^{-1} \left[\frac{1}{v_1} (J_1^t - iJ_2^{t*}) - \left(\frac{2v_1}{r} \partial_r + \frac{v_1}{r^2} \right) (J_1^r + iJ_2^{r*}) \right] + \text{c.c.} \right\} \tag{2.115}$$

where contact terms have been omitted. Notice that, when we go to the near horizon limit (with $b' = 0$), the last two terms in (2.115) can be expressed via the conservation equations (2.78), (2.79) as a time derivative of a current component. Therefore, they give rise to contact terms in that limit. The result (2.115) will be matched with one obtained by integrating out super-Schwarzian modes in section 3.7.

3 Supersymmetric JT

In this section we would like to compare our results from the near horizon considerations of the AdS_4 supersymmetric black hole to a two dimensional configuration relating supersymmetric JT gravity to the super-Schwarzian effective theory on the boundary. We will consider Euclidean signature and take for the AdS_2 metric

$$ds^2 = \frac{dzd\bar{z}}{y^2} = \frac{dx^2 + dy^2}{y^2}, \quad z = x + iy. \tag{3.1}$$

The coordinate x can be viewed as Euclidean time. For the matter multiplet we will not take directly what we get from dimensional reduction of half the hyper multiplet which we turned on as a probe in the previous section. Instead, we will use two twisted chiral respectively anti-chiral multiplets. They share many features with the probe of the previous section. The major difference is that they are not charged under an extra $U(1)$ but under the $U(1)$ mediated by the 2d graviphoton. This would correspond to a Kaluza Klein $U(1)$ in the dimensional reduction setup. The reason is that integrating out the graviphoton can be directly associated to integrating out a bosonic mode in super reparametrisations of the boundary. The dynamics of this boundary mode is contained in an effective super-Schwarzian action. If instead, we considered the original $U(1)$ gauge field we would need to add an extra phase mode to the boundary as it was done in [2]. This would correspond to a straightforward repetition of the calculation presented in [2]. In the following, we will match results on a qualitative level not taking into account numerical factors. Further we will not identify 2d probe fields with 4d probes but rather present a map between conserved currents.

3.1 Minimal $2d \mathcal{N} = (2, 2)$ supergravity

In this section we summarize the Euclidean $2d \mathcal{N} = (2, 2)$ supergravity construction of [20].

With superspace coordinates

$$z^\pi = (z, \theta^+, \bar{\theta}^+; \bar{z}, \theta^-, \bar{\theta}^-) \tag{3.2}$$

we have rigid superspace derivatives

$$\partial_z, \quad D_+ = \frac{\partial}{\partial\theta^+} + \frac{1}{2}\bar{\theta}^+\partial_z, \quad \bar{D}_+ = \frac{\partial}{\partial\bar{\theta}^+} + \frac{1}{2}\theta^+\partial_z, \tag{3.3}$$

$$\partial_{\bar{z}}, \quad D_- = \frac{\partial}{\partial\theta^-} + \frac{1}{2}\bar{\theta}^-\partial_{\bar{z}}, \quad \bar{D}_- = \frac{\partial}{\partial\bar{\theta}^-} + \frac{1}{2}\theta^-\partial_{\bar{z}}, \tag{3.4}$$

which fulfil the anticommutation relations

$$\{D_+, \bar{D}_+\} = \partial_z, \quad \{D_-, \bar{D}_-\} = \partial_{\bar{z}}. \quad (3.5)$$

In general complex conjugation for fermionic quantities such as the supercharges is given by

$$(Q_+)^* = \bar{Q}_-, \quad (Q_-)^* = \bar{Q}_+. \quad (3.6)$$

Applying axial torsion constraints and solving them in conformal gauge gives the following supercovariant derivatives

$$\begin{aligned} \nabla_+ &= e^{\bar{\sigma}} \left(D_+ + i(D_+\sigma) \bar{M} \right), \\ \nabla_- &= e^{\bar{\sigma}} \left(D_- - i(D_-\sigma) \bar{M} \right), \\ \bar{\nabla}_+ &= e^{\sigma} \left(\bar{D}_+ + i(\bar{D}_+\bar{\sigma}) M \right), \\ \bar{\nabla}_- &= e^{\sigma} \left(\bar{D}_- - i(\bar{D}_-\bar{\sigma}) M \right). \end{aligned} \quad (3.7)$$

Here, $\sigma, \bar{\sigma}$ refer to the conformal factors since in $U(1)_A$ supergravity the geometric quantities are given in terms of chiral/anti-chiral fields. M, \bar{M} are convenient linear combinations of the Lorentz and $U(1)_A$ generators.

The superconformal factor takes on the following form on the AdS_2 geometry,

$$\sigma = -\frac{1}{2} \log \left(\frac{1}{2y_c} \right) - \frac{i}{4y_c} \theta^+ \theta^-, \quad (3.8)$$

where y_c refers to the chiral basis. It is important to note here that the auxiliary field of the gravity multiplet, which appears as the field multiplying the $\theta^+ \theta^-$ factor in (3.8) takes on a non-zero vev. We will see in section 3.3 that this will furnish the mass of the probe matter.

While the starting point of our considerations will indeed be the superspace described above, it is important to see how the structures of (3.7) map onto x -space quantities as the actual physical calculations will take place there.

The x -space covariant derivative, which can be deduced by projecting out superspace coordinates in (3.7) is of the form

$$\nabla_\mu = \partial_\mu + \mathcal{J} \Omega_\mu + \frac{\mathcal{Y}}{2} A_\mu, \quad (3.9)$$

where \mathcal{J}, \mathcal{Y} refer to the Lorentz and $U(1)_A$ generator respectively and Ω_μ and A_μ are the spin connection and graviphoton gauge field. Both Ω_μ and A_μ are of course implied by the bosonic term of the superconformal factor. Ω_μ is determined by the real part of $\sigma|$, A_μ by the imaginary part of $\sigma|$, where $|$ denotes the projection on the leading component of a multiplet. For the background (3.8) the imaginary part of $\sigma|$ is zero, however we must allow for fluctuations later. In section 3.3 it will be explained how (3.9) acts on the individual component fields of the matter multiplets.

3.2 $\mathcal{N} = (2, 2)$ JT supergravity

The first term of our two-dimensional action, is the $\mathcal{N} = (2, 2)$ JT action, which leaving out the topological term, is given by [20]:

$$S = -\frac{1}{16\pi G_N} \left[\int_{\mathcal{M}} d^2z d^2\theta \mathcal{E}^{-1} \Phi (R + 2) + \text{h.c.} + 2 \int_{\partial\mathcal{M}} dud\vartheta d\bar{\vartheta} (\Phi_b + \bar{\Phi}_b) \mathcal{K} \right]. \quad (3.10)$$

\mathcal{E}^{-1} refers to the chiral density, which is needed to correctly define chiral superspace integration, R to the chiral supercurvature and \mathcal{K} to the extrinsic supercurvature. Furthermore, the dilaton naturally also appears as a chiral and anti-chiral field with the field content $\Phi \supset \varphi, \lambda_\alpha, B$ and $\bar{\Phi} \supset \bar{\varphi}, \bar{\lambda}_\alpha, \bar{B}$.

We should also think about what (3.10) implies in x -space and how it can be related to the four-dimensional model of the previous section. We repeat the analysis of [20] for the bosonic fields: the variations with respect to the supergravity auxiliary fields fix the dilaton auxiliary fields to be related to the dynamical bosonic field of the dilaton, such that one ends up with the following bosonic part of the JT action in x -space

$$S_{\text{JT,bos.}} = \frac{i}{16\pi G_N} \int dzd\bar{z} \sqrt{g} (\varphi (\mathcal{R} + i\mathcal{F} + 2) + \bar{\varphi} (\mathcal{R} - i\mathcal{F} + 2)). \quad (3.11)$$

Recall, that the supersymmetric JT action not only furnishes a dynamical term for metric fluctuations, it also allows the gravitino to acquire a kinetic term, as the standard gravitino term vanishes in two dimensions. In superconformal gauge the gravitino appears as the fermionic components of the conformal factor. The coupling of dilatino to gravitino is

$$\begin{aligned} S_{\text{JT,ferm.}} = & \frac{1}{2\pi G_N} \int dzd\bar{z} \left[\lambda_+ \left(\nabla_{\bar{z}} \psi_{\bar{+}z} - \nabla_z \psi_{\bar{+}\bar{z}} + \frac{i}{2y} \psi_{-z} \right) + \right. \\ & + \lambda_- \left(\nabla_z \psi_{-z} - \nabla_{\bar{z}} \psi_{-z} - \frac{i}{2y} \psi_{+z} \right) + \bar{\lambda}_+ \left(\nabla_z \psi_{+z} - \nabla_{\bar{z}} \psi_{+z} + \frac{i}{2y} \psi_{-z} \right) + \\ & \left. + \bar{\lambda}_- \left(\nabla_{\bar{z}} \psi_{-z} - \nabla_z \psi_{-z} - \frac{i}{2y} \psi_{\bar{+}z} \right) \right]. \quad (3.12) \end{aligned}$$

Assuming real curvature constraints in (3.11) implies $\varphi = \bar{\varphi}$ and hence a real Lagrange multiplier coupled to the Ricci scalar, which is just the canonical form of the JT action. In order for dilaton degrees of freedom to match, reality constraints have to be applied to the dilatino modes. We apply Majorana conditions, which in our conventions amount to $\lambda_+ = \bar{\lambda}_+$ and $\lambda_- = \bar{\lambda}_-$. This results in

$$\begin{aligned} S_{\text{JT,ferm.}} = & \frac{1}{4\pi G_N} \int dzd\bar{z} \left[\lambda_+ \left(\nabla_{\bar{z}} \psi_{\bar{+}z} - \nabla_z \psi_{\bar{+}\bar{z}} + \frac{i}{2y} \psi_{-z} + \nabla_z \psi_{+z} - \nabla_{\bar{z}} \psi_{+z} + \frac{i}{2y} \psi_{-z} \right) \right. \\ & \left. + \lambda_- \left(\nabla_z \psi_{-z} - \nabla_{\bar{z}} \psi_{-z} - \frac{i}{2y} \psi_{+z} + \nabla_{\bar{z}} \psi_{-z} - \nabla_z \psi_{-z} - \frac{i}{2y} \psi_{\bar{+}z} \right) \right]. \quad (3.13) \end{aligned}$$

3.2.1 Graviphoton kinetic term

As we have introduced a gauge field in the covariant derivatives and will treat gauged matter below, we should also add a kinetic term for the gauge field. First consider the

supersymmetric Gauss-Bonnet term

$$S = -\frac{1}{16\pi G_N} \int_{\mathcal{M}} d^2z d^2\theta \mathcal{E}^{-1} R + \text{h.c.} \quad (3.14)$$

Here, when moving to x -space, the field strength drops out and one recovers the standard Gauss-Bonnet term. Therefore a further term is required in order for a kinetic term for the gauge field to appear,

$$S = -\frac{1}{2\pi G_N} \int_{\mathcal{M}} d^2z d^2\theta d^2\bar{\theta} R \bar{R}. \quad (3.15)$$

Integrating to x -space gives

$$S = -\frac{i}{4\pi G_N} \int_{\mathcal{M}} d^2z \sqrt{g} F_{z\bar{z}} F^{z\bar{z}}, \quad (3.16)$$

where the curvature \mathcal{R} drops out. Here, we should specify exactly how the superconformal factor is related to the graviphoton.

In general $\text{Im}(\sigma)|$ constitutes the gauge field in Lorentz gauge $A_\mu = \epsilon_{\mu\nu} \partial^\nu \text{Im}(\sigma)|$.

Hence,

$$\partial_z \text{Im}(\sigma)| = -\frac{1}{2} A_z, \quad \partial_z \text{Im}(\bar{\sigma})| = \frac{1}{2} A_z, \quad (3.17)$$

and also

$$\partial \bar{\partial} \text{Im}(\sigma)| = \frac{1}{4} F_{z\bar{z}}. \quad (3.18)$$

From a two-dimensional perspective the term (3.16) will reduce to the kinetic term of the internal $U(1)_A$ mode at the boundary and from a four-dimensional perspective this term corresponds to the Kaluza-Klein field strength.

3.2.2 JT supergravity and the super-Schwarzian

Just as delineated in [8] integrating out the dilaton as a Lagrange multiplier, constrains the geometry to AdS_2 , while at the same time reducing the action to an integral over the boundary, which in our supersymmetric case is [20]

$$S_{\text{eff}} = -\frac{1}{8\pi G_N} \int_{\partial\mathcal{M}} du d\vartheta d\bar{\vartheta} (\Phi_b + \bar{\Phi}_b) \mathcal{K}. \quad (3.19)$$

Setting Dirichlet conditions for the dilaton and calculating the supercurvature then leaves us with the explicit form for the effective action of the system:

$$S_{\text{eff}} = -\frac{1}{2\pi G_N} \int_{\partial\mathcal{M}} du d\vartheta d\bar{\vartheta} \varphi_b \text{Schw} \left(t, \xi, \bar{\xi}; u, \vartheta, \bar{\vartheta} \right), \quad (3.20)$$

where φ_b is the boundary value for the leading component of Φ and $\text{Schw} \left(t, \xi, \bar{\xi}; u, \vartheta, \bar{\vartheta} \right)$ refers to the $\mathcal{N} = 2$ super-Schwarzian, which is defined by

$$\text{Schw} \left(x, \xi, \bar{\xi}; u, \vartheta, \bar{\vartheta} \right) = \frac{(D_{\bar{\vartheta}} \bar{\xi}')}{D_{\bar{\vartheta}} \xi} - \frac{(D_{\vartheta} \xi')}{D_{\vartheta} \bar{\xi}} - 2 \frac{\xi' \bar{\xi}'}{(D_{\vartheta} \xi)(D_{\bar{\vartheta}} \bar{\xi})}, \quad (3.21)$$

with $\xi, \bar{\xi}$ general super-reparametrisations of the boundary and $u, \vartheta, \bar{\vartheta}$ the boundary superspace coordinates. The super-reparametrisations are subject to superconformal constraints (3.65).

Whereas for the bosonic case the Schwarzian action describes the soft mode of reparametrisations of time, here the situation is generalised to superspace. The super-Schwarzian constitutes the effective action of reparametrisations of time, and the fermionic coordinates of the boundary superspace.

It should be mentioned that the x -space expressions for the kinetic terms of the gravity multiplet given in the previous sections could also be reduced to boundary expressions individually. Here, we have assumed the super-Schwarzian as the boundary effective action due to the arguments presented in [20] and then projected down to x -space. Alternatively, it should in principle also be possible to perform everything entirely in superspace.

3.3 Matter coupled to $2d \mathcal{N} = (2, 2)$ supergravity

Now we also want to add supersymmetric matter to the JT supergravity theory. This is done by straightforwardly adding a matter term, such that the matter field only couples to the metric and not the dilaton. The field can then be considered to be moving on a pure AdS_2 geometry, such that the usual AdS/CFT dictionary can be applied.

Hence, we must only work out what the coupling of the superconformal factor to a locally supersymmetric matter multiplet in superspace amounts to in components in x -space.

3.3.1 Chiral vs. twisted chiral

For global supersymmetry, there are two main ways to build symmetric theories: setting chiral constraints or setting twisted chiral constraints on a general superfield. While the former is charged under $U(1)_V$ and uncharged under $U(1)_A$, the opposite is true for the latter. Since we are interested in constructing matter gauged under the graviphoton of the super-curvature multiplet, which can be related to a bosonic mode in super-reparameterisations of the boundary, we must set twisted chiral constraints given by

$$\bar{D}_+\chi = 0, \quad D_-\chi = 0. \tag{3.22}$$

Here a crucial difference arises to the Lorentzian case [49]. Whereas complex conjugation of (3.22) implies the conditions for the associated twisted anti-chiral field for Lorentzian signature, here, due to the complex conjugation properties elucidated in section 3.1 we obtain the same constraints on the complex conjugated field, such that the usual kinetic action would vanish. This implies that we have to choose χ to be real.

3.3.2 Supersymmetric action

For our analysis we must construct superfields which are covariantly twisted chiral, which means that they fulfil the generalisation of (3.22) to curved space. Such that a covariantly twisted chiral field is given by

$$\bar{\nabla}_+\chi_{\text{cov}} = 0, \quad \nabla_-\chi_{\text{cov}} = 0, \tag{3.23}$$

and a covariantly twisted anti-chiral field by

$$\bar{\nabla}_- \bar{\chi}_{\text{cov}} = 0, \quad \nabla_+ \bar{\chi}_{\text{cov}} = 0. \quad (3.24)$$

Note that the notation $\bar{\chi}$ here does not refer to complex conjugation. The solution of the constraints (3.23) and (3.24) depends on the charge of the superfield, which we choose to be

$$[M, \chi] = -i\chi, \quad [M, \bar{\chi}] = i\bar{\chi}. \quad (3.25)$$

In superconformal gauge we arrive at the following expressions for the definition of our covariant fields

$$\chi_{\text{cov.}} = e^{-\sigma - \bar{\sigma}} \chi, \quad \bar{\chi}_{\text{cov.}} = e^{-\sigma - \bar{\sigma}} \bar{\chi}. \quad (3.26)$$

The formal expression for the D-term is

$$\int dz d\bar{z} d^2\theta d^2\bar{\theta} E^{-1} \chi_{\text{cov}} \bar{\chi}_{\text{cov}}. \quad (3.27)$$

As we will see below, there will be no need to add another probe term.

3.3.3 X-space

We also have to define how the physical fields, which will appear in x -space after superspace integration are defined.

The most convenient way to do this is by the projection method:

$$\chi_{\text{cov}}| = f \quad \bar{\chi}_{\text{cov}}| = \bar{f} \quad (3.28)$$

$$\nabla_+ \chi_{\text{cov}} = \zeta_+ \quad \nabla_- \chi_{\text{cov}} = \zeta_- \quad (3.29)$$

$$\bar{\nabla}_- \chi_{\text{cov}} = \bar{\zeta}_- \quad \bar{\nabla}_+ \bar{\chi}_{\text{cov}} = \bar{\zeta}_+ \quad (3.30)$$

$$\frac{1}{2}[\nabla_+, \bar{\nabla}_-] \chi_{\text{cov}} = F \quad \frac{1}{2}[\bar{\nabla}_+, \nabla_-] \bar{\chi}_{\text{cov}} = \bar{F}. \quad (3.31)$$

We should also translate the superspace charge (3.25) into $U(1)_A$ and Lorentz charges in x -space for the individual component fields (3.28).

For the bosonic components

$$[\mathcal{Y}, f] = 2 \quad [\mathcal{Y}, \bar{f}] = 2, \quad (3.32)$$

and for the fermionic fields

$$[\mathcal{Y}, \zeta_- / \zeta_+] = \zeta_- / \zeta_+. \quad (3.33)$$

For the Lorentz charge we naturally get

$$[\mathcal{J}, \bar{\zeta}_+ / \zeta_+] = -\frac{i}{2} \bar{\zeta}_+ / \zeta_+ \quad (3.34)$$

$$[\mathcal{J}, \bar{\zeta}_- / \zeta_-] = \frac{i}{2} \bar{\zeta}_- / \zeta_-. \quad (3.35)$$

This determines (3.9). In conformal gauge for (3.8) we have $\Omega_{z/\bar{z}} = \frac{1}{2y}$.

3.3.4 Breaking superconformal symmetry

We can now just take the formal expression (3.27) and perform the integration via the chiral density method and then project onto the physical x -space fields via (3.28). So far it would seem that as we have only included a D-term, we still have to add an F-term in order to add masses to the fields and break conformal symmetry. However, as we will see, the gauging itself breaks superconformal symmetry. This is due to a theorem first noted in [51]:

In 2D, if the spin-0 field of a matter supermultiplet carries a non-trivial realization of an internal symmetry charge that is gauged by a spin-1 field in the superconformal multiplet, the action for the spin-0 field is neither conformally nor superconformally invariant.

For the specific case at hand this occurs because in the component expansion of (3.27) the matter fields couple to the supergravity auxiliary field of (3.8). Therefore the masses are determined by the curvature itself.

3.4 Equations of motion and currents

Now performing the integration of (3.27) in superspace and then using (3.28) we arrive at the two-dimensional matter action for the probe multiplet

$$\begin{aligned} \frac{i}{2} \int dzd\bar{z} \left[(\partial f) (\bar{\partial} \bar{f}) + (\bar{\partial} f) (\partial \bar{f}) + \frac{1}{y^2} f \bar{f} - \frac{1}{2y} \bar{\zeta}_- \partial \zeta_- - \bar{\zeta}_+ \bar{\partial} \zeta_+ - i \frac{1}{2y^2} \bar{\zeta}_- \bar{\zeta}_+ + \right. \\ \left. + f A_z \bar{\partial} \bar{f} + f A_{\bar{z}} \partial \bar{f} + \frac{3}{2y} A_z \zeta_- \bar{\zeta}_+ + \right. \\ \left. + \bar{\psi}^{+z} (\bar{\zeta}_+ \partial \bar{f}) - i \bar{\psi}^{+\bar{z}} (e_{\bar{z}}^{\bar{l}} \bar{\zeta}_- \bar{f}) + \bar{\psi}^{-\bar{z}} (\bar{\zeta}_- \bar{\partial} f) + i \bar{\psi}^{-z} (e_z^l \zeta_+ f) + \text{h.c.} \right]. \end{aligned} \quad (3.36)$$

The first line represents the kinetic terms, the second line the linearized coupling to the gauge field and the last line the linearized coupling to the gravitinos.

Now focussing on the kinetic terms for a moment we can derive the equations of motion, which take on a simple form by use of (3.9).

For the bosons

$$\partial \bar{\partial} f = \frac{1}{2y^2} f, \quad (3.37)$$

$$\partial \bar{\partial} \bar{f} = \frac{1}{2y^2} \bar{f}, \quad (3.38)$$

and for the fermions

$$\nabla_{\bar{z}} \zeta_+ = i e_{\bar{z}}^{\bar{l}} \bar{\zeta}_-, \quad (3.39)$$

$$\nabla_z \zeta_- = -i e_z^l \bar{\zeta}_+. \quad (3.40)$$

For bosons we can immediately solve the equations asymptotically, which lead to normalizable mode y^{Δ_+} and non-normalizable mode y^{Δ_-} with

$$\Delta_{\pm} = \frac{1 \pm 3}{2}. \quad (3.41)$$

Iteration of (3.39) with the complex conjugate of (3.39) (and vice versa) provides corresponding asymptotics for fermions with

$$\Delta_{\pm} = \frac{1 \pm 2}{2}. \tag{3.42}$$

3.4.1 Symmetry currents

It is now also important for us to write out the symmetry currents of the two-dimensional action. There are currents linked to energy-momentum, $U(1)_A$ and supersymmetry conservation. In principle the currents constitute a multiplet in superspace. More precisely, as we are breaking superconformal symmetry we are essentially introducing a multiplet of superconformal anomalies, which together with the multiplet of superconformal currents fulfill a conservation equation in superspace. For our purposes we are only interested in x -space expressions. A purely superconformal current such as the superstring fulfills the algebraic constraints

$$T_{\mu}^{\mu} = 0 \quad (\gamma^{\mu} S_{\mu})_{\alpha} = 0, \tag{3.43}$$

As we have essentially gauged the tangent space group of the $\mathcal{N} = (2, 2)$ superstring and also added massive perturbations, we will have corrections to (3.43). The energy-momentum tensor acquires a non-zero trace and for the supercurrent, the components $S_{+\bar{z}}, S_{-z}$ and their complex conjugates become non-zero.

In a linearized approach we can derive the $U(1)_A$ current by taking the variational derivative of (3.36) with respect to the gauge field, which leads to

$$j_z^A = \frac{1}{2} (\bar{f} \partial f - f \partial \bar{f}) + \frac{3}{4y} \zeta_+ \bar{\zeta}_+, \quad j_{\bar{z}}^A = \frac{1}{2} (\bar{f} \bar{\partial} f - f \bar{\partial} \bar{f}) - \frac{3}{4y} \zeta_- \bar{\zeta}_-, \tag{3.44}$$

where the A denotes the axial nature of these currents. The conservation equation is given by

$$\partial j_{\bar{z}}^A + \bar{\partial} j_z^A = 0. \tag{3.45}$$

Due to the internal $U(1)_A$ charge the supercurrents split up into a parts consisting of $f, \zeta_+, \bar{\zeta}_-$ and a part, which includes $\bar{f}, \zeta_-, \bar{\zeta}_+$.

The former being

$$\begin{aligned} S_{\bar{+}z} &= \zeta_+ \partial f, & S_{-\bar{z}} &= \bar{\zeta}_- \bar{\partial} f, \\ S_{\bar{+}\bar{z}} &= -i e_{\bar{z}}^{\bar{l}} \bar{\zeta}_- f, & S_{-z} &= i e_z^l \zeta_+ f. \end{aligned} \tag{3.46}$$

and the latter

$$\begin{aligned} S_{+z} &= \bar{\zeta}_+ \partial \bar{f}, & S_{-\bar{z}} &= \zeta_- \bar{\partial} \bar{f}, \\ S_{+\bar{z}} &= -i e_{\bar{z}}^{\bar{l}} \bar{\zeta}_- \bar{f}, & S_{-z} &= i e_z^l \zeta_+ \bar{f}. \end{aligned} \tag{3.47}$$

The conservation equations are

$$\begin{aligned} \bar{\partial} S_{\bar{+}z} + \partial S_{\bar{+}\bar{z}} - \frac{i}{4y} (S_{\bar{+}z} + S_{\bar{+}\bar{z}}) + \frac{i}{2y} S_{-\bar{z}} &= 0, \\ \bar{\partial} S_{-z} + \partial S_{-\bar{z}} + \frac{i}{4y} (S_{-z} + S_{-\bar{z}}) - \frac{i}{2y} S_{+z} &= 0. \end{aligned} \tag{3.48}$$

The energy-momentum tensor is most conveniently expressed by splitting it up into fermionic and bosonic contributions. For the bosons we have

$$\begin{aligned} T_B^{zz} &= -4y^4 \partial f \partial \bar{f}, & T_B^{\bar{z}\bar{z}} &= -4y^4 \bar{\partial} f \bar{\partial} \bar{f}, \\ T_B^{z\bar{z}} &= 2y^2 f \bar{f}, \end{aligned} \tag{3.49}$$

and for the fermions

$$\begin{aligned} T_F^{zz} &= y^3 (\zeta_+ \partial \bar{\zeta}_+ + \bar{\zeta}_+ \partial \zeta_+), & T_F^{\bar{z}\bar{z}} &= y^3 (\zeta_- \bar{\partial} \bar{\zeta}_- + \bar{\zeta}_- \bar{\partial} \zeta_-), \\ T_F^{z\bar{z}} &= -iy^2 (\zeta_- \zeta_+). \end{aligned} \tag{3.50}$$

Now for the combined energy momentum Tensor $T_{\mu\nu} := T_{B;\mu\nu} + T_{F;\mu\nu}$ the conservation equations are

$$\partial_x T_{xx} + \partial_y T_{xy} = 0, \quad \partial_x T_{xy} + \partial_y T_{yy} + \frac{1}{y} (T_{xx} + T_{yy}) = 0. \tag{3.51}$$

3.5 Comparison to four-dimensional model

We see that at leading order we can let the JT model acquire the same form as the dimensionally reduced model. For the gravity multiplet it is important to note that for the JT term we have a priori already made an assumption by restricting the supercurvature to a real number: $\Phi(R+2)$. This forces a real dilaton and hence also real dilatino structures. In principle one could allow the supercurvature to be a general complex number, which would fix the field strength to a specific value. In comparison the dimensionally reduced model naturally assumes a real dilaton.

Furthermore, for the matter sector we recover behaviour already noticed in [1]. In the dimensionally reduced model, an additional source dilaton coupling $\phi T^{\theta\theta}$ appears, which constitutes a deviation from pure JT behaviour as one does not consider matter to dilaton couplings in that approach. Here, we acquire an additional dilatino to supercurrent coupling: $\bar{\psi}_\theta^A S_A^\theta$. Also, the field strength comes with the standard kinetic term and a linear dilaton coupling, whereas the two-dimensional approach just yields the former. There is a further deviation related to the different signatures. Recall, that the four-dimensional calculations are performed in Lorentzian signature, whereas the two-dimensional model is Euclidean. In order to add gauged matter, we had to use covariantly twisted chiral and anti-chiral multiplets, which was only possible by applying an additional reality condition. Hence, for two dimensions f and \bar{f} are not linked by complex conjugation and as such are real, whereas for the dimensionally reduced model we had complex bosons. However, the current conservations still match between the two approaches as do the masses.

3.6 Super-Schwarzian coupled to matter

Our general approach will follow the steps outlined in [1]. We work out the on-shell action of the two-dimensional probe matter, such that it reduces to a boundary two-point form coupled to fluctuations of the boundary. There are additional complications for the case at hand as the boundary two-point function only takes on an elegant form in superspace. Hence, we work out what the general form of two-point function should be at the boundary due to

symmetry restrictions. Then for a general multiplet we allow for superspace fluctuations in this two-point function, and match the resulting x -space expressions to the on-shell action of the bulk pulled back to the boundary.

Furthermore, we can now calculate the four-point function by combining the previous result with the effective Schwarzian action and integrating out the fluctuations.

To recapitulate, we do the following: work out the probe on-shell action implied by (3.36) and reduce to the boundary. This will then be matched with a general result for the boundary two-point form in superspace dictated by symmetry considerations. This superspace action will then in conjunction with (3.20) be used to integrate out the fluctuations.

3.6.1 On-shell action

Now we want to determine the on-shell action, which will just reduce to a boundary expression. A regularised solution to (3.37) is

$$f(y, \omega) = e^{-(y-\epsilon)|\omega|} \frac{1+y|\omega|}{y(1+\epsilon|\omega|)} f(\omega), \tag{3.52}$$

where a Fourier transform replacing Euclidean time x by ω has been performed. Solution (3.52) is unique in that it is regular at $y \rightarrow \infty$ and satisfies the boundary condition

$$f(\epsilon, \omega) = \frac{1}{\epsilon} f(\omega)$$

for some given $f(\omega)$. The solution of $\bar{f}(y, \omega)$ is the same with $f(\omega)$ replaced by $\bar{f}(\omega)$. Note, that for more generic masses solution (3.52) is expressed in terms of modified Bessel functions [52].

Analogously the solutions to (3.39) and (3.40) are given by

$$\begin{aligned} \zeta_+(y, \omega) &= e^{(\epsilon-y)|\omega|} \frac{(1+\omega y+y|\omega|)\zeta(\omega)}{\sqrt{y}(1+\epsilon|\omega|)}, & \bar{\zeta}_-(y, \omega) &= -e^{(\epsilon-y)|\omega|} \frac{(1-\omega y+y|\omega|)\zeta(\omega)}{\sqrt{y}(1+\epsilon|\omega|)} \\ \zeta_-(y, \omega) &= e^{(\epsilon-y)|\omega|} \frac{(1-\omega y+y|\omega|)\bar{\zeta}(\omega)}{\sqrt{y}(1+\epsilon|\omega|)}, & \bar{\zeta}_+(y, \omega) &= -e^{(\epsilon-y)|\omega|} \frac{(1+\omega y+y|\omega|)\bar{\zeta}(\omega)}{\sqrt{y}(1+\epsilon|\omega|)}. \end{aligned} \tag{3.53}$$

As can easily be seen from (3.53), at the boundary there will only be two fermionic degrees of freedom. Let us note the explicit boundary behaviour of the solutions above. The bosonic boundary behaviour is

$$f(y, \omega) \sim f(\omega) \left(\frac{1}{y} + \frac{\epsilon^2 \omega^2}{2y} - \frac{1}{2} \omega^2 y - \frac{\epsilon^3 \omega^2 |\omega|}{3y} + \frac{1}{3} \omega^2 y^2 \right), \tag{3.54}$$

with the analogous behaviour for $\bar{f}(y, \omega)$. For the fermions we get

$$\zeta_+(y, \omega) \sim \zeta(\omega) \left(\frac{1}{\sqrt{y}} + \omega \sqrt{y} + \frac{\epsilon^2 \omega^2}{2\sqrt{y}} - \frac{1}{2} \omega^2 y^{3/2} - \omega |\omega| y^{3/2} \right), \tag{3.55}$$

$$\zeta_-(y, \omega) \sim \bar{\zeta}(\omega) \left(\frac{1}{\sqrt{y}} - \omega \sqrt{y} + \frac{\epsilon^2 \omega^2}{2\sqrt{y}} - \frac{1}{2} \omega^2 y^{3/2} + \omega |\omega| y^{3/2} \right). \tag{3.56}$$

We define the following quantities for which frequency dependence is replaced by dependence on Euclidean time

$$\begin{aligned}
 f_{\Delta_-}(x) &= \int d\omega e^{i\omega x} f(\omega), & \bar{f}_{\Delta_-}(x) &= \int d\omega e^{i\omega x} \bar{f}(\omega), \\
 f_{\Delta_+}(x) &= \int dx' \frac{f_{\Delta_-}(x')}{[x-x']^4}, & \bar{f}_{\Delta_+}(f) &= \int dx' \frac{\bar{f}_{\Delta_-}(x')}{[x-x']^4},
 \end{aligned}
 \tag{3.57}$$

and similarly for the fermions

$$\begin{aligned}
 \zeta_{\Delta_-}(x) &= \int d\omega e^{i\omega x} \zeta(\omega), & \bar{\zeta}_{\Delta_-}(x) &= \int d\omega e^{i\omega x} \bar{\zeta}(\omega), \\
 \zeta_{\Delta_+}(x) &= \int dx' \frac{\zeta_{\Delta_-}(x')}{[x-x']^3}, & \bar{\zeta}_{\Delta_+}(x) &= \int dx' \frac{\bar{\zeta}_{\Delta_-}(x')}{[x-x']^3}.
 \end{aligned}
 \tag{3.58}$$

In terms of (3.57), (3.58) the boundary behaviour (3.54), (3.55) amounts to (a dot denotes a derivative w.r.t. Euclidian time x)

$$f(y, \omega) \sim \frac{f_{\Delta_-}(x)}{y} - \frac{2\epsilon^3 f_{\Delta_+}(x)}{\pi y} + \frac{2y^2 f_{\Delta_+}(x)}{\pi} - \frac{\epsilon^2 \dot{f}_{\Delta_-}(x)}{2y} + \dots
 \tag{3.59}$$

and for the fermions

$$\begin{aligned}
 \zeta_+(y, x) &\sim \frac{\zeta_{\Delta_-}(x)}{\sqrt{y}} + \frac{2iy^{3/2}\zeta_{\Delta_+}(x)}{\pi} - i\sqrt{y}\dot{\zeta}_{\Delta_-} + \frac{2\epsilon^3\dot{\zeta}_{\Delta_+}}{3\pi\sqrt{y}} + \dots, \\
 \zeta_-(y, x) &\sim \frac{\bar{\zeta}_{\Delta_-}(x)}{\sqrt{y}} - \frac{2iy^{3/2}\bar{\zeta}_{\Delta_+}(x)}{\pi} + i\sqrt{y}\dot{\bar{\zeta}}_{\Delta_-} + \frac{2\epsilon^3\dot{\bar{\zeta}}_{\Delta_+}}{3\pi\sqrt{y}} + \dots.
 \end{aligned}
 \tag{3.60}$$

3.6.2 Boundary super-space, two-point function

In superspace, the on-shell action should reduce to the form of a superconformal two-point function. Therefore one must only know what the supertranslation invariant interval on the boundary is and also the structure of chiral or anti-chiral multiplet to give the correct form of the boundary two-point function. The boundary superspace was constructed in the context of the $\mathcal{N} = 2$ SYK model [17]. The super-derivatives are in our conventions

$$D_{\vartheta} = \partial_{\vartheta} + \frac{1}{2}\bar{\vartheta}\partial_u, \quad D_{\bar{\vartheta}} = \partial_{\bar{\vartheta}} + \frac{1}{2}\vartheta\partial_u,
 \tag{3.61}$$

with the anticommutation relations

$$\{D_{\vartheta}, \bar{D}_{\bar{\vartheta}}\} = \partial_u.
 \tag{3.62}$$

Chirality constraints can then be imposed via

$$D_{\vartheta}\bar{\chi} = 0, \quad D_{\bar{\vartheta}}\chi = 0.
 \tag{3.63}$$

Here $\chi, \bar{\chi}$ are general boundary superfields. The $\mathcal{N} = 2$ superreparametrisations

$$(u, \vartheta, \bar{\vartheta}) \rightarrow (x(u, \vartheta, \bar{\vartheta}), \xi(u, \vartheta, \bar{\vartheta}), \bar{\xi}(u, \vartheta, \bar{\vartheta})),
 \tag{3.64}$$

are constrained by

$$D_{\vartheta}\bar{\xi} = 0, \quad D_{\vartheta}x(u) = \frac{1}{2}\bar{\xi}D_{\vartheta}\xi, \quad D_{\bar{\vartheta}}\xi = 0, \quad D_{\bar{\vartheta}}x(u) = \frac{1}{2}\xi D_{\bar{\vartheta}}\bar{\xi}. \quad (3.65)$$

Their dynamics are effectively described by the super-Schwarzian (3.21). One can solve (3.65) for a general component structure (x denotes Euclidean time)

$$\begin{aligned} x(u) &= u + \epsilon(u) + \frac{1}{2}[\vartheta\bar{\eta}(u) + \vartheta\eta(u)] \\ \xi(u) &= \eta(u) + \vartheta \left[1 + \sigma(u) + \frac{1}{2}\dot{\epsilon}(u) \right] + \frac{1}{2}\vartheta\bar{\vartheta}\dot{\eta}(u), \\ \bar{\xi}(u) &= \bar{\eta}(u) + \bar{\vartheta} \left[1 - \sigma(u) + \frac{1}{2}\dot{\epsilon}(u) \right] - \frac{1}{2}\vartheta\bar{\vartheta}\dot{\bar{\eta}}(u). \end{aligned} \quad (3.66)$$

We observe that the superreparametrisations can be expressed in x -space via four individual modes $\epsilon, \eta, \bar{\eta}, \sigma$. The first, $\epsilon(u)$, is the single gravitational mode, which also appears in the purely bosonic setting and as such is the boundary fluctuation, which is linked to the energy-momentum coupling of the bulk on-shell action. In a similar spirit, σ represents the boundary degree of freedom of gauge fluctuations $A_{z/\bar{z}}$ and $\eta, \bar{\eta}$ constitute boundary gravitinos and are hence linked to the supercurrent.

In order to find the supertranslation invariant boundary superspace structure, we demand the following

$$D'_{\vartheta}\Delta_{\text{bdy.}} = D_{\bar{\vartheta}}\Delta_{\text{bdy.}} = 0. \quad (3.67)$$

The unique solution is [28]

$$\Delta_{\text{bdy.}} = [u - u'] - \frac{1}{2}[\vartheta\bar{\vartheta} + \vartheta'\bar{\vartheta}' + 2\bar{\vartheta}\vartheta']. \quad (3.68)$$

We can include fluctuations of the boundary super-curve by employing the relations (3.66)

$$\Delta_{\text{bdy.}} = [t(u) - t'(u')] - \frac{1}{2}[\xi(u)\bar{\xi}(u) + \xi'(u')\bar{\xi}'(u') + 2\bar{\xi}(u)\xi'(u')]. \quad (3.69)$$

We also have to define a boundary multiplet which should have a matter content consistent with the boundary expansions of the bulk matter multiplet. Hence, we define a chiral and an anti-chiral multiplet (with respect to the boundary derivatives). Both will consist of the on-shell boundary degrees of freedom worked out in the previous section. Hence, for the chiral multiplet we have $(\chi_{\text{bdy.}} \supset f_{\Delta_-}, \zeta_{\Delta_-})$ and for the anti-chiral one $(\bar{\chi}_{\text{bdy.}} \supset \bar{f}_{\Delta_-}, \bar{\zeta}_{\Delta_-})$

$$\chi_{\text{bdy.}}(u_C) = f_{\Delta_-}(u_C) + \sqrt{2}\vartheta\zeta_{\Delta_-}(u_C), \quad (3.70)$$

$$\bar{\chi}_{\text{bdy.}}(u_{AC}) = \bar{f}_{\Delta_-}(u_{AC}) - \sqrt{2}\bar{\vartheta}\bar{\zeta}_{\Delta_-}(u_{AC}). \quad (3.71)$$

We end up with the following boundary two-point function coupled to super-curve fluctuations¹

$$S_{\chi_{\text{bdy.}}} = \int dud\vartheta du'd\bar{\vartheta}' \frac{[D_{\bar{\vartheta}}\xi(u)]^3 [D'_{\vartheta}\xi'(u')]^3}{\Delta_{\text{bdy.}}^3} \chi_{\text{bdy.}}(u) \bar{\chi}_{\text{bdy.}}(u'). \quad (3.72)$$

¹Here, we assume that there is no mixing with any other dimension two operator. If there was such a mixing we would have to add terms in which one of the χ 's is replaced by the corresponding boundary mode. Indeed, there is another dimension two operator associated to the dilaton [10]. Since the 2d action does not contain terms linear in the twisted multiplet fields and there is no direct coupling to the dilaton we do not see how a corresponding mixing could arise in an on-shell action.

Plugging in the structure (3.66) and performing the superspace integration of (3.72) will give boundary couplings of the x -space matter fields to the fluctuations of (3.66). These are quite lengthy expressions. Therefore, we give each matter coupling to one of the four fluctuations individually.

Matching to bulk. The internal σ mode is coupled in the following way:

$$\frac{\delta S_{\chi^{\text{bdy.}}}}{\delta \sigma} = 6 \left(\bar{f}_{\Delta-} f_{\Delta+} - f_{\Delta-} \bar{f}_{\Delta+} + \zeta_{\Delta-} \bar{\zeta}_{\Delta+} - \bar{\zeta}_{\Delta-} \zeta_{\Delta+} \right). \quad (3.73)$$

The first boundary gravitino mode coupling reads

$$\frac{\delta S_{\chi^{\text{bdy.}}}}{\delta \eta} = \sqrt{2} \left(2\bar{f}_{\Delta-} \dot{\zeta}_{\Delta+} - 3\bar{\chi}_{\Delta+} \bar{\zeta}_{\Delta-} + 3\dot{f}_{\Delta-} \bar{\zeta}_{\Delta+} \right), \quad (3.74)$$

and the second is

$$\frac{\delta S_{\chi^{\text{bdy.}}}}{\delta \bar{\eta}} = \sqrt{2} \left(-2\chi_{\Delta-} \dot{\zeta}_{\Delta+} + 3f_{\Delta+} \zeta_{\Delta-} + 3\dot{f}_{\Delta-} \zeta_{\Delta+} \right). \quad (3.75)$$

The boundary graviton couples according to

$$\begin{aligned} \frac{\delta S_{\chi^{\text{bdy.}}}}{\delta \epsilon} = & -3 \left(f_{\Delta-} \dot{f}_{\Delta+} + \bar{f}_{\Delta-} \dot{f}_{\Delta+} + 2f_{\Delta+} \dot{f}_{\Delta-} + 2\bar{f}_{\Delta+} \dot{f}_{\Delta-} \right) \\ & + \left(3\bar{\zeta}_{\Delta+} \dot{\zeta}_{\Delta-} + 3\zeta_{\Delta+} \dot{\zeta}_{\Delta-} - \bar{\zeta}_{\Delta-} \dot{\zeta}_{\Delta+} - \zeta_{\Delta-} \dot{\zeta}_{\Delta+} \right). \end{aligned} \quad (3.76)$$

In order to match the expressions with the four-dimensional results we must first express the Schwarzsian couplings via the on-shell symmetry currents (3.44), (3.46), (3.49), (3.50).

The boundary expressions are

$$\begin{aligned} T_{xx}^{\text{bdy.}} &= -\frac{3}{y\pi} \left(f_{\Delta-} \bar{f}_{\Delta+} + \bar{f}_{\Delta-} f_{\Delta+} \right), \\ T_{xy}^{\text{bdy.}} &= \frac{1}{\pi} \left(-3f_{\Delta+} \dot{f}_{\Delta-} - 3\bar{f}_{\Delta+} \dot{f}_{\Delta-} + \bar{\zeta}_{\Delta-} \dot{\zeta}_{\Delta+} + \zeta_{\Delta-} \dot{\zeta}_{\Delta+} + \zeta_{\Delta+} \dot{\zeta}_{\Delta-} \right), \\ T_{yy}^{\text{bdy.}} &= \frac{1}{\pi y} \left(3f_{\Delta-} \bar{f}_{\Delta+} + 3\bar{f}_{\Delta-} f_{\Delta+} + 2\bar{\zeta}_{\Delta-} \zeta_{\Delta+} + 2\zeta_{\Delta-} \bar{\zeta}_{\Delta+} \right). \end{aligned} \quad (3.77)$$

We can now express (3.76) as

$$\frac{\delta S_{\chi^{\text{bdy.}}}}{\delta \epsilon} = \pi (T_{ty} - y \partial_t T_{yy}). \quad (3.78)$$

The boundary expressions for the supercurrent components are

$$\begin{aligned} S_{+z}^{\text{bdy.}} &= \frac{\bar{f}_{\Delta-} \bar{\zeta}_{\Delta+}}{\sqrt{y}\pi} + 3i \frac{\sqrt{y} \bar{\zeta}_{\Delta+} \bar{f}_{\Delta-}}{\pi} - i \frac{\sqrt{y} \bar{\zeta}_{\Delta+} \dot{f}_{\Delta-}}{\pi}, & S_{-z}^{\text{bdy.}} &= -\frac{\bar{f}_{\Delta-} \bar{\zeta}_{\Delta+}}{\sqrt{y}\pi}, \\ S_{-\bar{z}}^{\text{bdy.}} &= -\frac{\bar{f}_{\Delta-} \bar{\zeta}_{\Delta+}}{\sqrt{y}\pi} + 3i \frac{\sqrt{y} \bar{\zeta}_{\Delta+} \bar{f}_{\Delta+}}{\pi} - i \frac{\sqrt{y} \bar{\zeta}_{\Delta+} \dot{f}_{\Delta-}}{\pi}, & S_{+\bar{z}}^{\text{bdy.}} &= \frac{\bar{\chi}_{\Delta-} \bar{\zeta}_{\Delta+}}{\sqrt{y}\pi}, \\ S_{+\bar{z}}^{\text{bdy.}} &= -\frac{f_{\Delta-} \zeta_{\Delta+}}{\sqrt{y}\pi} - 3i \frac{\sqrt{y} \zeta_{\Delta-} \bar{f}_{\Delta+}}{\pi} + i \frac{\sqrt{y} \zeta_{\Delta+} \dot{f}_{\Delta-}}{\pi}, & S_{+\bar{z}}^{\text{bdy.}} &= \frac{f_{\Delta-} \zeta_{\Delta+}}{\sqrt{y}\pi}, \\ S_{-\bar{z}}^{\text{bdy.}} &= \frac{f_{\Delta-} \zeta_{\Delta+}}{\sqrt{y}\pi} - 3i \frac{\sqrt{y} \zeta_{\Delta-} f_{\Delta+}}{\pi} + i \frac{\sqrt{y} \zeta_{\Delta+} \dot{f}_{\Delta-}}{\pi}, & S_{-z}^{\text{bdy.}} &= -\frac{f_{\Delta-} \zeta_{\Delta+}}{\sqrt{y}\pi}. \end{aligned} \quad (3.79)$$

Equations (3.79) allow us to rewrite (3.74)

$$\frac{\delta S_{f_{\text{bdy.}}}}{\delta \eta} = \frac{\pi}{\sqrt{2y}} \left(i(S_{+z} - S_{+\bar{z}} - S_{-z} + S_{-\bar{z}}) + y \partial_t (S_{+z} - S_{+\bar{z}} + S_{-z} - S_{-\bar{z}}) \right). \quad (3.80)$$

Similarly for $\bar{\eta}$ we get

$$\frac{\delta S_{\chi_{\text{bdy.}}}}{\delta \bar{\eta}} = \frac{\pi}{\sqrt{2y}} \left(i(S_{\bar{+}z} - S_{\bar{+}\bar{z}} - S_{-z} + S_{-\bar{z}}) + y \partial_t (S_{\bar{+}z} - S_{\bar{+}\bar{z}} + S_{-z} - S_{-\bar{z}}) \right). \quad (3.81)$$

The values of the gauge current at the boundary are

$$\begin{aligned} j_z^A &= \frac{3i}{2\pi} \left(f_{\Delta-} \bar{f}_{\Delta+} - f_{\Delta-} \bar{f}_{\Delta+} + \bar{\zeta}_{\Delta-} \zeta_{\Delta+} - \zeta_{\Delta-} \bar{\zeta}_{\Delta+} \right), \\ j_{\bar{z}}^A &= -j_z. \end{aligned} \quad (3.82)$$

This allows us to express (3.73) as

$$\frac{\delta S_{\chi_{\text{bdy.}}}}{\delta \sigma} = 2\pi j_y^A. \quad (3.83)$$

3.7 Four-point function/integrating out the fluctuations

To the action (3.72) we must also add the super-Schwarzian (3.21). This is a quite lengthy expression. Fortunately, we only have to consider expressions at most quadratic in the fields appearing on the r.h.s. of (3.66), leading to

$$S_{\text{Schw}} = \int du \left[-\frac{1}{2} \ddot{\epsilon}(u)^2 + 2\sigma \ddot{\sigma}(u) - 4\eta \ddot{\eta}(u) - 4\bar{\eta} \ddot{\bar{\eta}}(u) \right]. \quad (3.84)$$

We now have to work out the equations of motion of the fluctuations in order to integrate them out. We get contributions from the kinetic terms (3.84) and from the coupling of these modes to matter, which was worked out in the previous subsection. The general form for the resulting on-shell action is

$$\begin{aligned} S &= \int du \left[\left(\partial_u^{-4} \frac{\delta S_{\chi_{\text{bdy.}}}}{\delta \epsilon} \right) \left(\frac{\delta S_{\chi_{\text{bdy.}}}}{\delta \epsilon} \right) - \frac{1}{4} \left(\partial_u^{-2} \frac{\delta S_{\chi_{\text{bdy.}}}}{\delta \sigma} \right) \left(\frac{\delta S_{\chi_{\text{bdy.}}}}{\delta \sigma} \right) \right. \\ &\quad \left. + \frac{1}{4} \left(\partial_u^{-3} \frac{\delta S_{\chi_{\text{bdy.}}}}{\delta \bar{\eta}} \right) \left(\frac{\delta S_{\chi_{\text{bdy.}}}}{\delta \bar{\eta}} \right) + \frac{1}{4} \left(\partial_u^{-3} \frac{\delta S_{\chi_{\text{bdy.}}}}{\delta \eta} \right) \left(\frac{\delta S_{\chi_{\text{bdy.}}}}{\delta \eta} \right) \right], \end{aligned} \quad (3.85)$$

For comparison with results from the 4d calculation performed in section 2.4 we would like to rewrite these expressions in terms of two dimensional integrals. To this end, one inserts a ‘constructive identity’, $\int dy \partial_y$, and employs conservation equations [1]. This works well for the first, third and fourth term in (3.85) leading to

$$S_\epsilon = -\frac{\pi^2}{4} \int dx dy y^2 \left(\partial_x^{-2} T_{xx} \right) (2T_{xy} - 2y \partial_x T_{yy}), \quad (3.86)$$

$$\begin{aligned} S_{\eta\bar{\eta}} &= \frac{\pi^2 i}{8} \int dx dy \left(\partial_x^{-1} (S_{+z} + S_{+\bar{z}} + S_{-z} + S_{-\bar{z}}) (S_{\bar{+}z} - S_{\bar{+}\bar{z}} - S_{-z} + S_{-\bar{z}}) \right) \\ &\quad + \frac{\pi^2 i}{8} \int dx dy \left(\partial_x^{-1} (S_{\bar{+}z} + S_{\bar{+}\bar{z}} + S_{-z} + S_{-\bar{z}}) (S_{+z} - S_{+\bar{z}} - S_{-z} + S_{-\bar{z}}) \right). \end{aligned} \quad (3.87)$$

For the contribution corresponding to integrating out the gauge field there is a subtlety which has been pointed out in [2]. In our approximation ($\omega y \ll 1$) j_y^A does not depend on y , and therefore inserting $\int dy \partial_y$ on $j_y^A \partial_x^{-2} j_y^A$ would return zero. The authors of [2] considered just a charged scalar. Their argument is based on the observation that the current contains the scalar and its complex conjugate in an antisymmetrised way. Therefore, only products between different modes in an expansion like (3.54) contribute. At the given approximation this includes the first two lowest powers in y yielding a factor of y (since $\Delta_+ + \Delta_- = 1$). Another factor of $1/y$ appears due to a y derivative (in the first term on the r.h.s. of (3.44)). The same arguments also apply to the fermionic contributions to the gauge current (where the derivative w.r.t. y has been replaced by a division by y). In summary, the second term in (3.85) can be rewritten as (for further details see [2])

$$S_\sigma = -\pi^2 v_2 \int dx dy \sqrt{g} (g^{yy})^2 j_y^A \partial_x^{-2} j_y^A. \tag{3.88}$$

Now, we would like to compare this to the results of section 2.4.3. To this end, we replace the presently used 2d metric by one with the AdS_2 radius restored and an additional overall sign ($z = x + iy$)

$$ds^2 = -v_1^2 \frac{dz d\bar{z}}{y^2}. \tag{3.89}$$

This changes, at most, a numerical factor in front of (3.86), (3.87) and (3.88). To make contact with the 4d near horizon AdS_2 factor in (2.6) with $U(r) = v_1/r$ (and $b = v_2, b' = 0$) we perform the following coordinate transformation (including a Wick rotation)

$$x = -\frac{i}{v_1} t, \quad y = \frac{v_1}{r}. \tag{3.90}$$

Then energy momentum conservation (3.51) matches the one obtained in the near horizon dimensional reduction (2.69). This motivates us to associate the involved energy momentum tensors (up to an overall factor which would not change conservation laws). Indeed, applying (3.90) on the corresponding part of the on-shell action S_ϵ in (3.86) matches the 4d near horizon result (2.90). The same observation holds for the $U(1)$ currents with conservation laws (3.45) respectively (2.74). The onshell actions (3.88) and (2.93) agree as well.

For the gravitini sector the situation is more complicated. Performing a Wick rotation on spinorcomponents (such as the supercurrent) can be more involved (see e.g. [53–55]). In our setup, where we have projected everything to one component spinors the problem shows up as follows. Performing the transformation (3.90) on the equations (3.48) as well as on their complex conjugates will result in four equations which are not anymore pairwise related by complex conjugation. We proceed as follows. We just perform (3.90) on the two equations written explicitly in (3.48), resulting in

$$\partial_t S_+^t + \partial_r S_+^r - \frac{r}{2v_1^2} (S_+^t - S_-^t) - \frac{1}{2r} S_-^r = 0, \tag{3.91}$$

$$\partial_t S_-^t + \partial_r S_-^r + \frac{r}{2v_1^2} (S_-^t - S_+^t) - \frac{1}{2r} S_+^r = 0. \tag{3.92}$$

These, we compare to (2.78) and its complex conjugate. This suggests the following association

$$\begin{aligned} S_+^t &= iJ_1^t, & S_+^r &= iJ_1^r, & S_+^t &= iJ_1^{t*}, & S_+^r &= iJ_1^{r*}, \\ S_-^t &= -J_2^t, & S_-^r &= J_2^r, & S_-^t &= -J_2^{t*}, & S_-^r &= J_2^{r*}. \end{aligned} \quad (3.93)$$

Then (2.79) and its complex conjugate should map the set of conservation laws obtained from complex conjugation of (3.91) and (3.92). This indeed happens if we apply the following rules for taking the complex conjugate of (3.91) and (3.92) ($\alpha \in \{t, r\}$),

$$(S_+^\alpha)^* = S_-^\alpha, \quad (S_-^\alpha)^* = S_+^\alpha, \quad \partial_t^* = -\partial_t. \quad (3.94)$$

The relation between the current components is the same as it would be without performing a Wick rotation. Therefore one should take the complex conjugate of the coordinate transformation (3.90) justifying the last assignment in (3.94). Note also, that the prescription (3.94) does not apply to the right hand sides of (3.93). That means in particular that after the replacement (3.93) the onshell action (3.86) is not manifestly real anymore. Therefore we add its complex conjugate by hand. Finally, we arrive at

$$\begin{aligned} S_{\eta\bar{\eta}} \sim \int dudr & \left[(J_1^r - iJ_2^{r*})^* \partial_t^{-1} (J_1^t + iJ_2^{t*}) + \right. \\ & \left. + (J_1^r + iJ_2^{r*})^* \partial_t^{-1} (J_1^t - iJ_2^{t*}) + \text{c.c.} \right], \end{aligned} \quad (3.95)$$

where now complex conjugation relates 4d components ($(J_A^\mu)^* = J_A^{\mu*}$). To compare with results from section 2.4.3 we impose (2.111) which removes the first contribution to (3.95). Further we notice that (2.78) and (2.79) imply

$$\left(\frac{2}{r} \partial_r + \frac{1}{r^2} \right) (J_1^r + iJ_2^{r*}) = -\frac{2}{r} \partial_t (J_1^t + iJ_2^{t*}) \quad (3.96)$$

giving rise to a contact term in the near horizon limit. Hence, our expressions (2.115) and (3.95) match within the given restriction (2.111).

4 Discussion

Summary. In the first half of the paper we embedded the solution of [37, 38] into a supergravity solution with the same amount of susy encompassing a hypermultiplet. This requires the choice of a moment map (and a corresponding Killing vector on the quaternion manifold) and choice of vacuum expectation values for the four hyperscalars. As a next step the dimensional reduction (in s-wave approximation) of the supergravity theory is performed in the near horizon limit, hence on $AdS_2 \times S^2$. To be more exact, we include fluctuations of photon, metric, gravitini and of the matter multiplet. For the latter we only let half of the hypermultiplet fluctuate, namely u, v and one projection of the hyperinos, such that we acquire a proper two-dimensional multiplet. Contributions containing the background magnetic fieldstrength or the angular components of the spin connection drop out due to the spherical integration, the BPS conditions and the choice of projection, such that a fully two-dimensional theory is furnished. The effective two-dimensional cosmological constant is given by a linear combination of the magnetic charge and the FI constants. We observe the dilaton coupled to metric fluctuations, an electric field strength term, an

electric field strength to dilaton coupling and gravitini fluctuations coupled to the dilatini. The spherical fluctuations $h_{\theta\theta}, \psi_{\theta 1}, \psi_{\theta 2}$ constitute the dilaton multiplet. Furthermore, we also see that deviations from pure JT supergravity occur due to additional source to dilaton multiplet couplings. We also calculate the four-point function in a dual CFT following the general prescription [36] within the same limits as discussed in [1].

In the second half of the paper we repeat the construction of [20] for $\mathcal{N} = (2, 2)$ Euclidean JT supergravity, while allowing the gravitini and graviphoton field strength to fluctuate. We focus on real supercurvature constraints, which take out half the degrees of freedom of the dilaton multiplet. Gauged matter can be added in form of a covariantly twisted chiral and anti-chiral multiplet and additional reality constraints due to the Euclidean signature. Somewhat unusually only a D-term is necessary to enable gauged, massive matter fields. The masses are determined by the curvature, such that they agree with the dimensionally reduced near-horizon theory. The D-term furthermore gives a linearized supergravity theory. Taking variational derivatives with respect to graviphoton, metric and gravitini furnishes symmetry currents. We show how the on-shell action of the matter coupled to the gravity multiplet fluctuations may be described via the boundary superspace two-point function. Then in combination with the super-Schwarzian up to quadratic order, we may integrate out the gravity multiplet fluctuations, such that we end up with a four point function described in terms of the currents. We compare our results with the computation obtained in the near horizon calculation of the four dimensional theory in which next to leading corrections to the S^2 radius have been taken into account. When expressed in terms of energy-momentum tensor and gauge current the results match. For the contribution containing the supercurrent the situation is a bit more involved. The limit in which only corrections to the S^2 radius are considered is not compatible with BPS conditions. Supercurrents are only conserved if we impose an additional projection. Up to terms vanishing under that projection results from integrating out the fermionic super-Schwarzian mode match the four dimensional calculation.

$\mathcal{N} = (2, 2)$ JT quantum supergravity. As mentioned above, $\mathcal{N} = (2, 2)$ JT supergravity encompasses a larger space of options than might be guessed when just performing the s-wave reduction. The dimensionally reduced theory naturally assumes a real dilaton and hence half the degrees of freedom available to the most general two-dimensional theory. A priori the two-dimensional theory might use $\Phi(R + \alpha)$, with α being a general complex number. This would fix the graviphoton to a specific background value. It would be interesting to explore the full range of solutions of this theory.

This is especially interesting with respect to the results of [56, 57]. By use of [56, 58] calculated exact partition functions for JT gravity with arbitrary genus and arbitrary number of asymptotic boundaries. The partition functions are (non-uniquely) non-perturbatively completed by a genus expansion of a specific matrix integral. While [57] extended these results to the $\mathcal{N} = 1$ case,² it would be interesting to see the extension to $\mathcal{N} = 2$ for the aforementioned reasons, although it is not quite clear how feasible this is.

²Supersymmetric extensions of JT gravity have been considered in this context also in [59–61].

Localization. As we have constructed a Euclidean off-shell formulation of an $\mathcal{N} = 2$ supergravity theory coupled to matter, it is natural to consider localization techniques. For the general Schwarzian theory this was performed in [21] for the bosonic case and also $\mathcal{N} = 1$ and $\mathcal{N} = 2$. It would be interesting to first of all, localize the minimal sugra theory on the AdS_2 background. The assumption would be that this should in leading order match the Schwarzian result for the partition function with differences perhaps arising in higher order corrections. Then one might attempt to perform this while also including the chiral twisted multiplet.

Other settings. We have chosen the specific background of [37, 38] as the near horizon enhancement matches with the two-dimensional theory first presented in [20] and for the fact that the AdS_4 asymptotics of [37, 38] allow for the construction of a four-dimensional four point function via the AdS/CFT dictionary. However, the most common four dimensional BPS solutions exhibit Minkowski asymptotics with near horizon enhancement to full BPS. It would be interesting to try and understand if these kind of solutions can be described via super-Schwarzian asymptotics.

Acknowledgments

We would like to thank Max Wiesner for collaboration on this project at the initial stage. Preliminary results had been reported in [62]. We would also like to thank Hans Jockers and Jun Nian for numerous discussions and Kyril Hristov for correspondence. This work was supported by “Bonn-Cologne Graduate School for Physics and Astronomy” (BCGS).

A Four-dimensional supergravity conventions

In this appendix, we summarize the most important conventions taken from [41, 44]. We use the mostly minus form of the Minkowski metric $\eta_{ab} = \text{diag}(1, -1, -1, -1)$. The flat space Dirac algebra of the γ -matrices is

$$\{\gamma_a, \gamma_b\} \equiv 2\eta_{ab}, \tag{A.1}$$

with γ_{ab} given by the commutator

$$\gamma_{ab} \equiv \frac{1}{2} [\gamma_a, \gamma_b]. \tag{A.2}$$

The chirality matrix is defined as

$$\gamma_5 \equiv -i\gamma_0\gamma_1\gamma_2\gamma_3 = i\gamma^0\gamma^1\gamma^2\gamma^3. \tag{A.3}$$

The γ matrices are chosen to be purely imaginary $(\gamma_\mu)^* = -\gamma_\mu$ and furthermore

$$\gamma_0^\dagger = \gamma_0, \quad \gamma_0\gamma_i^\dagger\gamma_0 = \gamma_i, \quad \gamma_5^\dagger = \gamma_5, \quad i = 1, 2, 3. \tag{A.4}$$

The γ_5 eigenvalues of the fermions are

$$\gamma_5 \begin{pmatrix} \psi_A^\mu \\ \lambda^{iA} \\ \zeta_\alpha \end{pmatrix} = \begin{pmatrix} \psi_A^\mu \\ \lambda^{iA} \\ \zeta_\alpha \end{pmatrix}, \quad (\text{A.5})$$

$$\gamma_5 \begin{pmatrix} \psi^{\mu A} \\ \lambda_A^i \\ \zeta^\alpha \end{pmatrix} = - \begin{pmatrix} \psi^{\mu A} \\ \lambda_A^i \\ \zeta^\alpha \end{pmatrix}, \quad (\text{A.6})$$

where ψ_A^μ is the gravitino, λ^{iA} the gaugino and ζ_α the hyperino. For this choice of γ_5 for chiral fermions we get

$$\lambda_A^* = \lambda^A, \quad \psi_{\mu A}^* = \psi_\mu^A, \quad \zeta_\alpha^* = \zeta^\alpha. \quad (\text{A.7})$$

In terms of the Pauli matrices the representation of the γ -matrices is

$$\gamma^0 = \begin{pmatrix} 0 & \sigma^2 \\ \sigma^2 & 0 \end{pmatrix}, \quad \gamma^1 = \begin{pmatrix} i\sigma^3 & 0 \\ 0 & i\sigma^3 \end{pmatrix}, \quad \gamma^2 = \begin{pmatrix} 0 & -\sigma^2 \\ \sigma^2 & 0 \end{pmatrix}, \quad \gamma^3 = \begin{pmatrix} -i\sigma^1 & 0 \\ 0 & -i\sigma^1 \end{pmatrix}, \quad (\text{A.8})$$

where σ^i , $i = 1, 2, 3$ denote the Pauli matrices,

$$(\sigma^1)_A{}^B = \begin{pmatrix} 0 & 1 \\ 1 & 0 \end{pmatrix}, \quad (\sigma^2)_A{}^B = \begin{pmatrix} 0 & -i \\ i & 0 \end{pmatrix}, \quad (\sigma^3)_A{}^B = \begin{pmatrix} 1 & 0 \\ 0 & -1 \end{pmatrix}. \quad (\text{A.9})$$

The SU(2) indices A, B are raised and lowered via the antisymmetric matrix

$$\epsilon_{AB} = \begin{pmatrix} 0 & 1 \\ -1 & 0 \end{pmatrix}, \quad \epsilon^{AB} = \begin{pmatrix} 0 & 1 \\ -1 & 0 \end{pmatrix}$$

such that we get

$$(\sigma^1)_{AB} = \begin{pmatrix} 1 & 0 \\ 0 & -1 \end{pmatrix}, \quad (\sigma^2)_{AB} = \begin{pmatrix} -i & 0 \\ 0 & -i \end{pmatrix}, \quad (\sigma^3)_{AB} = \begin{pmatrix} 0 & -1 \\ -1 & 0 \end{pmatrix} \quad (\text{A.10})$$

and

$$(\sigma^1)^{AB} = \begin{pmatrix} -1 & 0 \\ 0 & 1 \end{pmatrix}, \quad (\sigma^2)^{AB} = \begin{pmatrix} -i & 0 \\ 0 & -i \end{pmatrix}, \quad (\sigma^3)^{AB} = \begin{pmatrix} 0 & 1 \\ 1 & 0 \end{pmatrix}. \quad (\text{A.11})$$

In the hypermultiplet sector the indices α, β are raised and lowered via the antisymmetric symplectic matrix $\mathbb{C}_{\alpha\beta}$

$$\mathbb{C}_{\alpha\beta} = \begin{pmatrix} 0 & -1 \\ 1 & 0 \end{pmatrix}. \quad (\text{A.12})$$

With the charge conjugation matrix

$$C = i\gamma_0, \quad (\text{A.13})$$

and

$$\overline{\lambda}_A = i(\lambda_A)^T \gamma_0, \quad (\text{A.14})$$

chiral fermions satisfy

$$(\overline{\lambda}_A)^* = \overline{\lambda}^A. \quad (\text{A.15})$$

Open Access. This article is distributed under the terms of the Creative Commons Attribution License ([CC-BY 4.0](https://creativecommons.org/licenses/by/4.0/)), which permits any use, distribution and reproduction in any medium, provided the original author(s) and source are credited.

References

- [1] P. Nayak, A. Shukla, R.M. Soni, S.P. Trivedi and V. Vishal, *On the Dynamics of Near-Extremal Black Holes*, *JHEP* **09** (2018) 048 [[arXiv:1802.09547](https://arxiv.org/abs/1802.09547)] [[INSPIRE](#)].
- [2] U. Moitra, S.P. Trivedi and V. Vishal, *Extremal and near-extremal black holes and near- CFT_1* , *JHEP* **07** (2019) 055 [[arXiv:1808.08239](https://arxiv.org/abs/1808.08239)] [[INSPIRE](#)].
- [3] J.M. Maldacena, J. Michelson and A. Strominger, *Anti-de Sitter fragmentation*, *JHEP* **02** (1999) 011 [[hep-th/9812073](https://arxiv.org/abs/hep-th/9812073)] [[INSPIRE](#)].
- [4] A. Almheiri and J. Polchinski, *Models of AdS_2 backreaction and holography*, *JHEP* **11** (2015) 014 [[arXiv:1402.6334](https://arxiv.org/abs/1402.6334)] [[INSPIRE](#)].
- [5] R. Jackiw, *Lower Dimensional Gravity*, *Nucl. Phys. B* **252** (1985) 343 [[INSPIRE](#)].
- [6] C. Teitelboim, *Gravitation and Hamiltonian Structure in Two Space-Time Dimensions*, *Phys. Lett. B* **126** (1983) 41 [[INSPIRE](#)].
- [7] K. Jensen, *Chaos in AdS_2 Holography*, *Phys. Rev. Lett.* **117** (2016) 111601 [[arXiv:1605.06098](https://arxiv.org/abs/1605.06098)] [[INSPIRE](#)].
- [8] J. Maldacena, D. Stanford and Z. Yang, *Conformal symmetry and its breaking in two dimensional Nearly Anti-de-Sitter space*, *Prog. Theor. Exp. Phys.* **2016** (2016) 12C104 [[arXiv:1606.01857](https://arxiv.org/abs/1606.01857)] [[INSPIRE](#)].
- [9] J. Engelsöy, T.G. Mertens and H. Verlinde, *An investigation of AdS_2 backreaction and holography*, *JHEP* **07** (2016) 139 [[arXiv:1606.03438](https://arxiv.org/abs/1606.03438)] [[INSPIRE](#)].
- [10] M. Cvetič and I. Papadimitriou, *AdS_2 holographic dictionary*, *JHEP* **12** (2016) 008 [Erratum *JHEP* **01** (2017) 120] [[arXiv:1608.07018](https://arxiv.org/abs/1608.07018)] [[INSPIRE](#)].
- [11] S. Sachdev and J. Ye, *Gapless spin fluid ground state in a random, quantum Heisenberg magnet*, *Phys. Rev. Lett.* **70** (1993) 3339 [[cond-mat/9212030](https://arxiv.org/abs/cond-mat/9212030)] [[INSPIRE](#)].
- [12] A. Kitaev, *A Simple Model Of Quantum Holography*, talks given at the *Entanglement in Strongly-Correlated Quantum Matter*, KITP, Santa Barbara, CA, U.S.A., 6 April–2 July 2015 and online at <http://online.kitp.ucsb.edu/online/entangled15/kitaev/> and <http://online.kitp.ucsb.edu/online/entangled15/kitaev2/>.
- [13] J. Maldacena and D. Stanford, *Remarks on the Sachdev-Ye-Kitaev model*, *Phys. Rev. D* **94** (2016) 106002 [[arXiv:1604.07818](https://arxiv.org/abs/1604.07818)] [[INSPIRE](#)].
- [14] G. Sárosi, *AdS_2 holography and the SYK model*, *PoS Modave2017* (2018) 001 [[arXiv:1711.08482](https://arxiv.org/abs/1711.08482)] [[INSPIRE](#)].
- [15] V. Rosenhaus, *An introduction to the SYK model*, *J. Phys. A* **52** (2019) 323001 [[arXiv:1807.03334](https://arxiv.org/abs/1807.03334)] [[INSPIRE](#)].
- [16] A.H. Chamseddine, *Superstrings in arbitrary dimensions*, *Phys. Lett. B* **258** (1991) 97 [[INSPIRE](#)].

- [17] W. Fu, D. Gaiotto, J. Maldacena and S. Sachdev, *Supersymmetric Sachdev-Ye-Kitaev models*, *Phys. Rev. D* **95** (2017) 026009 [*Erratum ibid.* **95** (2017) 069904] [[arXiv:1610.08917](#)] [[INSPIRE](#)].
- [18] M. Astorino, S. Cacciatori, D. Klemm and D. Zanon, *AdS₂ supergravity and superconformal quantum mechanics*, *Annals Phys.* **304** (2003) 128 [[hep-th/0212096](#)] [[INSPIRE](#)].
- [19] S. Förste and I. Golla, *Nearly AdS₂ SUGRA and the super-Schwarzian*, *Phys. Lett. B* **771** (2017) 157 [[arXiv:1703.10969](#)] [[INSPIRE](#)].
- [20] S. Förste, J. Kames-King and M. Wiesner, *Towards the Holographic Dual of N = 2 SYK*, *JHEP* **03** (2018) 028 [[arXiv:1712.07398](#)] [[INSPIRE](#)].
- [21] D. Stanford and E. Witten, *Fermionic Localization of the Schwarzian Theory*, *JHEP* **10** (2017) 008 [[arXiv:1703.04612](#)] [[INSPIRE](#)].
- [22] T.G. Mertens, G.J. Turiaci and H.L. Verlinde, *Solving the Schwarzian via the Conformal Bootstrap*, *JHEP* **08** (2017) 136 [[arXiv:1705.08408](#)] [[INSPIRE](#)].
- [23] T. Kanazawa and T. Wettig, *Complete random matrix classification of SYK models with $\mathcal{N} = 0, 1$ and 2 supersymmetry*, *JHEP* **09** (2017) 050 [[arXiv:1706.03044](#)] [[INSPIRE](#)].
- [24] J. Murugan, D. Stanford and E. Witten, *More on Supersymmetric and 2d Analogs of the SYK Model*, *JHEP* **08** (2017) 146 [[arXiv:1706.05362](#)] [[INSPIRE](#)].
- [25] J. Yoon, *Supersymmetric SYK Model: Bi-local Collective Superfield/Supermatrix Formulation*, *JHEP* **10** (2017) 172 [[arXiv:1706.05914](#)] [[INSPIRE](#)].
- [26] N. Sannomiya, H. Katsura and Y. Nakayama, *Supersymmetry breaking and Nambu-Goldstone fermions with cubic dispersion*, *Phys. Rev. D* **95** (2017) 065001 [[arXiv:1612.02285](#)] [[INSPIRE](#)].
- [27] C. Peng, M. Spradlin and A. Volovich, *Correlators in the $\mathcal{N} = 2$ Supersymmetric SYK Model*, *JHEP* **10** (2017) 202 [[arXiv:1706.06078](#)] [[INSPIRE](#)].
- [28] K. Bulycheva, *$\mathcal{N} = 2$ SYK model in the superspace formalism*, *JHEP* **04** (2018) 036 [[arXiv:1801.09006](#)] [[INSPIRE](#)].
- [29] C. Peng, *$\mathcal{N} = (0, 2)$ SYK, Chaos and Higher-Spins*, *JHEP* **12** (2018) 065 [[arXiv:1805.09325](#)] [[INSPIRE](#)].
- [30] C.-M. Chang, S. Colin-Ellerin and M. Rangamani, *On Melonic Supertensor Models*, *JHEP* **10** (2018) 157 [[arXiv:1806.09903](#)] [[INSPIRE](#)].
- [31] M. Cárdenas, O. Fuentealba, H.A. González, D. Grumiller, C. Valcárcel and D. Vassilevich, *Boundary theories for dilaton supergravity in 2D*, *JHEP* **11** (2018) 077 [[arXiv:1809.07208](#)] [[INSPIRE](#)].
- [32] M. Berkooz, N. Brukner, V. Narovlansky and A. Raz, *The double scaled limit of Super-Symmetric SYK models*, *JHEP* **12** (2020) 110 [[arXiv:2003.04405](#)] [[INSPIRE](#)].
- [33] C. Peng and S. Stanojevic, *Soft modes in $\mathcal{N} = 2$ SYK model*, [arXiv:2006.13961](#) [[INSPIRE](#)].
- [34] A. Castro, F. Larsen and I. Papadimitriou, *5D rotating black holes and the nAdS₂/nCFT₁ correspondence*, *JHEP* **10** (2018) 042 [[arXiv:1807.06988](#)] [[INSPIRE](#)].
- [35] U. Moitra, S.K. Sake, S.P. Trivedi and V. Vishal, *Jackiw-Teitelboim Gravity and Rotating Black Holes*, *JHEP* **11** (2019) 047 [[arXiv:1905.10378](#)] [[INSPIRE](#)].

- [36] H. Liu and A.A. Tseytlin, *On four point functions in the CFT/AdS correspondence*, *Phys. Rev. D* **59** (1999) 086002 [[hep-th/9807097](#)] [[INSPIRE](#)].
- [37] S.L. Cacciatori and D. Klemm, *Supersymmetric AdS₄ black holes and attractors*, *JHEP* **01** (2010) 085 [[arXiv:0911.4926](#)] [[INSPIRE](#)].
- [38] K. Hristov and S. Vandoren, *Static supersymmetric black holes in AdS₄ with spherical symmetry*, *JHEP* **04** (2011) 047 [[arXiv:1012.4314](#)] [[INSPIRE](#)].
- [39] K. Hristov, H. Looyestijn and S. Vandoren, *BPS black holes in N = 2 D = 4 gauged supergravities*, *JHEP* **08** (2010) 103 [[arXiv:1005.3650](#)] [[INSPIRE](#)].
- [40] L.J. Romans, *Supersymmetric, cold and lukewarm black holes in cosmological Einstein-Maxwell theory*, *Nucl. Phys. B* **383** (1992) 395 [[hep-th/9203018](#)] [[INSPIRE](#)].
- [41] L. Andrianopoli et al., *N = 2 supergravity and N = 2 superYang-Mills theory on general scalar manifolds: Symplectic covariance, gaugings and the momentum map*, *J. Geom. Phys.* **23** (1997) 111 [[hep-th/9605032](#)] [[INSPIRE](#)].
- [42] D.Z. Freedman and A. Van Proeyen, *Supergravity*, Cambridge University Press, Cambridge U.K. (2015) [ISBN: 9781139368063, 9780521194013] [[INSPIRE](#)].
- [43] T. Ortin, *Gravity and Strings*, in *Cambridge Monographs on Mathematical Physics*, Cambridge University Press, Cambridge U.K. (2015) [ISBN: 9780521768139, 9780521768139, 9781316235799] [[INSPIRE](#)].
- [44] K. Hristov, *Lessons from the Vacuum Structure of 4d N = 2 Supergravity*, Ph.D. Thesis, Utrecht University, Utrecht The Netherlands (2012) [[arXiv:1207.3830](#)] [[INSPIRE](#)].
- [45] B. Gouteraux, J. Smolic, M. Smolic, K. Skenderis and M. Taylor, *Holography for Einstein-Maxwell-dilaton theories from generalized dimensional reduction*, *JHEP* **01** (2012) 089 [[arXiv:1110.2320](#)] [[INSPIRE](#)].
- [46] L. Andrianopoli et al., *N = 2 supergravity and N = 2 superYang-Mills theory on general scalar manifolds: Symplectic covariance, gaugings and the momentum map*, *J. Geom. Phys.* **23** (1997) 111 [[hep-th/9605032](#)] [[INSPIRE](#)].
- [47] E. Witten, *Anti-de Sitter space and holography*, *Adv. Theor. Math. Phys.* **2** (1998) 253 [[hep-th/9802150](#)] [[INSPIRE](#)].
- [48] K. Skenderis, *Lecture notes on holographic renormalization*, *Class. Quant. Grav.* **19** (2002) 5849 [[hep-th/0209067](#)] [[INSPIRE](#)].
- [49] C.M. Hull, U. Lindström, L. Melo dos Santos, R. von Unge and M. Zabzine, *Euclidean Supersymmetry, Twisting and Topological σ -models*, *JHEP* **06** (2008) 031 [[arXiv:0805.3321](#)] [[INSPIRE](#)].
- [50] B. de Wit and M. van Zalk, *Electric and magnetic charges in N = 2 conformal supergravity theories*, *JHEP* **10** (2011) 050 [[arXiv:1107.3305](#)] [[INSPIRE](#)].
- [51] S.J. Gates Jr., M.T. Grisaru and M.E. Wehlau, *A Study of general 2D, N = 2 matter coupled to supergravity in superspace*, *Nucl. Phys. B* **460** (1996) 579 [[hep-th/9509021](#)] [[INSPIRE](#)].
- [52] D.Z. Freedman, S.D. Mathur, A. Matusis and L. Rastelli, *Correlation functions in the CFT_d/AdS_{d+1} correspondence*, *Nucl. Phys. B* **546** (1999) 96 [[hep-th/9804058](#)] [[INSPIRE](#)].
- [53] K. Osterwalder and R. Schrader, *Feynman-Kac formula for Euclidean Fermi and Bose fields*, *Phys. Rev. Lett.* **29** (1972) 1423 [[INSPIRE](#)].

- [54] H. Nicolai, *A Possible constructive approach to $(\text{super-}\phi^3)_4$: (I). Euclidean formulation of the model*, *Nucl. Phys. B* **140** (1978) 294 [INSPIRE].
- [55] P. van Nieuwenhuizen and A. Waldron, *On Euclidean spinors and Wick rotations*, *Phys. Lett. B* **389** (1996) 29 [hep-th/9608174] [INSPIRE].
- [56] P. Saad, S.H. Shenker and D. Stanford, *JT gravity as a matrix integral*, [arXiv:1903.11115](#) [INSPIRE].
- [57] D. Stanford and E. Witten, *JT Gravity and the Ensembles of Random Matrix Theory*, [arXiv:1907.03363](#) [INSPIRE].
- [58] M. Mirzakhani, *Simple geodesics and Weil-Petersson volumes of moduli spaces of bordered Riemann surfaces*, *Invent. Math.* **167** (2006) 179 [INSPIRE].
- [59] C.V. Johnson, *JT Supergravity, Minimal Strings, and Matrix Models*, [arXiv:2005.01893](#) [INSPIRE].
- [60] C.V. Johnson, *Explorations of Non-Perturbative JT Gravity and Supergravity*, [arXiv:2006.10959](#) [INSPIRE].
- [61] T.G. Mertens, *Degenerate operators in JT and Liouville (super)gravity*, [arXiv:2007.00998](#) [INSPIRE].
- [62] M. Wiesner, *Dilaton Supergravity and Near-Horizon Dynamics of Supersymmetric Black Holes*, Master Thesis, Bonn University, Bonn Germany (2018).

JT Gravity/Matrix Model Duality

This chapter has already been published as [128]:

Deformations of JT gravity via topological gravity and applications, *S. Förste, H. Jockers, J. Kames-King, A. Kanargias*, In: *JHEP* 11 (2021) 154, arXiv: 2107.02773 [hep-th]

This chapter deals with the non-perturbatively defined theory of JT gravity as elaborated upon in section 1.4.8. Here, we are interested in using the methods of topological gravity to generalise JT gravity and construct new results for JT gravity in the presence of defects, which was first considered in [129, 130]. Topological gravity exhibits an underlying integrable KdV structure, which fixes the structure of the partition function in terms of the couplings t_k . We may think of these couplings as the “target space”, whereas the standard JT parameters, the asymptotic boundary length β and its analytic continuation to Lorentzian time t are “worldsheet” parameters. We use the KdV structure to generalise the JT theory to potentially arbitrary deformations. We emphasise that in principle there should be a dictionary between these deformations and a dilaton potential $U(\phi)$, although this is difficult to specify exactly. Conical defects are recovered as a tractable example. We use a low-energy expansion scheme to show the appearance of a plateau in the spectral form factor, therefore the appearance of chaos universality in terms of the “worldsheet” theory. Furthermore, we also comment on JT gravity approaches involving conical defects on de Sitter spacetime. Both topological gravity and minimal models are introduced in 1.4.9.

In detail, we start by reviewing how the Weil-Petersson volume is related to the theory of intersection numbers, which is defined on the moduli space of smooth curves with marked points. We show how JT gravity in the presence of conical defects may be recovered as a specific coupling of topological gravity. We move on from this specific example to generalising to arbitrary couplings. More specifically, the underlying, integrable KdV structure of topological gravity fixes the general form of the genus expansion. We use this to explicitly generalise the JT partition function to potentially arbitrary couplings, of which standard JT gravity as introduced in section 1.4.8 and JT gravity with conical defects are specific examples. To be precise the deformations of JT gravity are parametrised as deformations of the $(2, 2p - 1)$ minimal string theories in the large p limit. It is not in all generality clear, which specific values are actualised in the JT theory. One would suspect that there exists

a dictionary between deformations of the dilaton potential to deformations of the aforementioned couplings. It would also seem that the asymptotic behaviour of the deformations is linked to the asymptotic behaviour of the dilaton potential for large values of ϕ . We then move on to use a specific low temperature expansion scheme of the partition function to furnish new results for JT gravity in the presence of conical defects. This approach essentially amounts to considering all genus contributions at a fixed energy. This therefore allows the approximate appearance of effects, which are usually considered to be in the realm of (doubly) non-perturbative physics of the asymptotic genus expansion series. We put these results to use in section 4 of this publication, where we analyse the spectral form factor in detail. This quantity is explained in section 1.4. Interestingly the low temperature expansion shows the emergence of the plateau and the dependence of the spectral form factor on the underlying parameters. In addition we discover a Hawking-Page phase transition between connected and disconnected geometries similar to the generally observed behaviour of reference [10]. At low temperatures the connected geometries dominate, whereas at high temperatures disconnected geometries are dominant. We conclude by commenting on JT gravity on de Sitter spacetime. We emphasise that a recent approach would seem to rely on conical Weil-Petersson volumes being analytic continuations of Weil-Petersson volumes with geodesic boundaries, which does not seem to be the case in all generality.

The author contributed to all conceptual discussions regarding this publication. The author performed the calculations of sections 3 and 5. In addition the author suggested to consider the analysis of the spectral form factor in section 4. Moreover, the author performed most calculations of section 2.3.

Deformations of JT gravity via topological gravity and applications

Stefan Förste,^a Hans Jockers,^b Joshua Kames-King^{a,c} and Alexandros Kanargias^a

^a*Bethe Center for Theoretical Physics and Physikalisches Institut der Universität Bonn, Nussallee 12, 53115 Bonn, Germany*

^b*PRISMA+ Cluster of Excellence and Institute for Physics, Johannes Gutenberg-Universität, Staudinger Weg 7, 55128 Mainz, Germany*

^c*Kavli Institute for Theoretical Physics, University of California, Santa Barbara, CA93106, U.S.A.*

E-mail: forste@th.physik.uni-bonn.de, jockers@uni-mainz.de, jvakk@yahoo.com, kanargias@physik.uni-bonn.de

ABSTRACT: We study the duality between JT gravity and the double-scaled matrix model including their respective deformations. For these deformed theories we relate the thermal partition function to the generating function of topological gravity correlators that are determined as solutions to the KdV hierarchy. We specialise to those deformations of JT gravity coupled to a gas of defects, which conforms with known results in the literature. We express the (asymptotic) thermal partition functions in a low temperature limit, in which non-perturbative corrections are suppressed and the thermal partition function becomes exact. In this limit we demonstrate that there is a Hawking-Page phase transition between connected and disconnected surfaces for this instance of JT gravity with a transition temperature affected by the presence of defects. Furthermore, the calculated spectral form factors show the qualitative behaviour expected for a Hawking-Page phase transition. The considered deformations cause the ramp to be shifted along the real time axis. Finally, we comment on recent results related to conical Weil-Petersson volumes and the analytic continuation to two-dimensional de Sitter space.

KEYWORDS: 2D Gravity, AdS-CFT Correspondence, Integrable Hierarchies, Matrix Models

ARXIV EPRINT: [2107.02773](https://arxiv.org/abs/2107.02773)

Contents

1	Introduction	1
2	JT gravity, deformed JT gravity and topological gravity	4
2.1	Weil-Petersson volumes of hyperbolic Riemann surfaces	5
2.2	Deformations of JT gravity from minimal strings	8
2.3	JT gravity interacting with a gas of defects	9
2.4	KdV hierarchy and off-shell partition functions	13
2.5	Partition functions with leading order off-shell couplings	18
3	Low temperature expansion	26
3.1	Low temperature limit	27
3.2	Low temperature expansion schemes	29
3.3	Low temperature expansion schemes for multiple boundaries	32
4	Phase transition and spectral form factor	32
5	Some comments on two-dimensional de Sitter space	36
6	Conclusion and outlook	37

1 Introduction

Jackiw-Teitelboim (JT) gravity is a simple model of two-dimensional quantum gravity on backgrounds of constant curvature such as anti-de Sitter spaces AdS_2 [1–6]. It consists of a real scalar field ϕ coupled to gravity with the Euclidean action on a Riemann surface Σ being

$$\begin{aligned}
 I_{\text{JT}} = & -\frac{S_0}{2} \left(\frac{1}{2} \int_{\Sigma} d^2x \sqrt{g} R + \int_{\partial\Sigma} dx \sqrt{h} K \right) \\
 & - \frac{1}{2} \int_{\Sigma} d^2x \sqrt{g} \phi (R + 2) + \int_{\partial\Sigma} dx \sqrt{h} \phi (K - 1),
 \end{aligned} \tag{1.1}$$

where R is the Ricci scalar, $g_{\mu\nu}$ the metric, K is the trace of the extrinsic curvature at the boundary $\partial\Sigma$, and $h_{\mu\nu}$ is the boundary metric induced from $g_{\mu\nu}$. The sum of the first two terms is proportional to the Euler characteristic of the surface Σ , which in a black hole context represents the ground-state entropy and for the full gravitational path integral weighs the contribution of geometries in terms of the coupling S_0 . The third term sets the constraint of only considering hyperbolic Riemann surfaces

$$R(x) + 2 = 0, \tag{1.2}$$

and the last term contains a Gibbons-Hawking-York boundary term together with a counterterm that ensures a finite result when removing the regularisation of the position of the AdS_2 boundary. This term captures the Schwarzian dynamics of reparametrisations at the boundary. JT gravity has been used as a gravitational model in the AdS_2/CFT_1 correspondence and in a broader context it encapsulates the low-energy dynamics of near-extremal black holes [7, 8]. It can also be linked to the Sachdev-Ye-Kitaev model [9, 10] because its low-energy sector is described by the Schwarzian theory and in a certain limit the thermal partition functions agree [10, 11].

In the remarkable work [12] Saad, Shenker and Stanford demonstrate that extending the gravitational sector to include geometries consisting of arbitrary number of boundaries and also arbitrary genera furnishes a partition function equivalent to a specific double-scaled Hermitian matrix theory. This duality can be stated as

$$Z(\beta_1, \dots, \beta_n) \cong \langle \text{Tr} e^{-\beta_1 H} \dots \text{Tr} e^{-\beta_n H} \rangle_{\text{MM}} . \tag{1.3}$$

Here the left hand side is the connected thermal partition function $Z(\beta_1, \dots, \beta_n)$ of JT gravity for geometries with n asymptotic boundary components characterised by their inverse temperatures β_i , $i = 1, \dots, n$. The right hand side is the corresponding correlator of the dual Hermitian matrix integral. Interestingly, these correlators enjoy an interpretation as observables in an ensemble of quantum mechanical systems whose random Hamiltonians H are given by Hermitian matrices H of the matrix model [12].¹ This duality is generalised in ref. [14], where extensions of JT gravity are associated to other matrix models [15–17].

The arguments for the proposed duality in ref. [12] rely on two crucial facts: firstly, as can be seen for the disk, the path integral of the Schwarzian theory localises [18]. Secondly, the contributions of Riemann surfaces of higher genera to the JT gravity path integral reduce to a Schwarzian theory at each boundary component together with an integration over suitable moduli spaces of hyperbolic Riemann surfaces. The latter contributions give rise to Weil-Peterson volumes on the associated moduli spaces of stable curves that — as proven in ref. [19] — obey the same recursion relations as appear in the context of the specific double-scaled Hermitian matrix integral, which in turn suggests the proposed correspondence (1.3). The duality (1.3) as spelt out above is a priori established perturbatively, i.e. on the level of an asymptotic genus expansion. In addition, there are also non-perturbative contributions [12], and hence the matrix model can be viewed as a (non-unique) non-perturbative completion of the genus expansion of JT gravity. A proposal to deal with potential non-perturbative instabilities is developed in refs. [20–22].

In this work we focus on the structure of deformations to JT gravity and the resulting modifications to the thermal partition functions appearing on the left hand side of the duality (1.3). A particular deformation to JT gravity can be incorporated by adding a scalar potential $U(\phi)$ to the Lagrangian of the action (1.1) of the form [23, 24]

$$U(\phi) = 2\epsilon e^{-(2\pi-\alpha)\phi}, \quad 0 < \alpha < \pi . \tag{1.4}$$

¹According to ref. [13], the intriguing appearance of an ensemble of quantum mechanical systems can also be argued for via the relationship of JT gravity to the Sachdev-Ye-Kitaev model.

This potential does not affect the asymptotic boundary conditions and the gravitational path integral can be evaluated perturbatively in the coupling ϵ [24]. Carrying out the path integral over the scalar field ϕ at the perturbative order ϵ^k changes the constraint (1.2) to [23, 25]

$$R(x) + 2 = 2 \sum_{j=1}^k (2\pi - \alpha) \delta^{(2)}(x - x_j), \tag{1.5}$$

with a remaining integral of the positions x_1, \dots, x_k over the Riemann surface Σ . Thus the constraint (1.5) at the given perturbative order ϵ^k with the two-dimensional δ -distributions introduces on the hyperbolic surfaces k conical singularities at the points x_1, \dots, x_k with identification angle α . As a result, perturbatively the path integral of JT gravity with the potential (1.4) can be interpreted as a sum over all possible hyperbolic Riemann surfaces Σ with any number of conical singularities with identification angles α at arbitrary positions on Σ . Furthermore, we can interpret the deformation (1.4) as coupling JT gravity to a gas of defects characterized by the coupling constant ϵ and the identification angle α [23, 24]. The structure can readily be generalised to an arbitrary finite number (possibly even to an infinite number or to a continuous family) of defect species with individual couplings ϵ_j and identification angles α_j [23, 24], such that a more general class of deformations to JT gravity can be realised.

Instead of directly studying deformations to JT gravity via scalar potentials of the type (1.4), we use the connection to two-dimensional topological gravity [26] and the related formulation in terms of moduli spaces of stable curves [27, 28]. Previously, this approach has been prominently employed in this context, for instance, in refs. [12, 24, 29–31]. Upon identifying deformations to JT gravity with solutions to the KdV hierarchy (which play a central role in topological gravity, see e.g. ref. [32]) and using well-established matrix model techniques [33–36], we can study a rather general class of deformations to JT gravity. From this perspective topological gravity and hence JT gravity with deformations can be identified with certain minimal string theories and deformations thereof [35, 37, 38]. Already in ref. [12] it is observed that JT gravity can be viewed as the large $p \rightarrow +\infty$ limit of the $(2, 2p - 1)$ minimal string theory with the associated couplings t_k given by [20, 29]

$$t_0 = t_1 = 0, \quad t_k = \gamma_k \quad \text{with} \quad \gamma_k = \frac{(-1)^k}{(k-1)!} \quad \text{for} \quad k = 2, 3, \dots \tag{1.6}$$

These values for the couplings t_k relate to a specific solution to the above mentioned KdV hierarchy. In this work we study deformations to JT gravity by considering more general solutions to the KdV hierarchy, which on the level of the couplings t_k amounts to deforming them as

$$t_k = \gamma_k + \delta_k \quad \text{for} \quad k = 0, 1, 2, \dots \tag{1.7}$$

For particular choices of δ_k — as established in refs. [23, 24] and as discussed in detail in the main text — this description realises JT gravity interacting with a gas of defects as described by the scalar potential (1.4) and generalisations thereof discussed in ref. [24]. Inspired by the work of Okuyama and Sakai we thoroughly investigate the relationship

between general deformations δ_k and the specific deformations that are attributed to the interaction of JT gravity with a gas of defects.

Moreover, we turn to some applications of our general results. First of all, we analyse the low temperature behaviour of the calculated thermal partition functions using techniques developed in refs. [29, 30]. At low temperatures the (asymptotic) genus expansion of the thermal partition function can be given an exact analytic expression [30, 39], because non-perturbative corrections are suppressed in the performed low temperature double scaling limit. This allows us to study in this low temperature regime Hawking-Page phase transitions and the features of spectral form factors as functions of the deformation parameters with the help of numerical methods. As a second application, we comment on a further instance of JT gravity, which requires the inclusion of Riemann surfaces with conical singularities, namely the wavefunction of the universe for JT gravity in de Sitter space [40, 41]. This striking connection relies on subtleties of the analytic continuation from sharp to blunt defects or equivalently from small identification angles to large identification angles.

The structure of the paper is as follows: in section 2 we first set the stage for the forthcoming analysis and introduce well-established physical and mathematical tools to study correlation functions in topological gravity. Then, applying techniques developed in ref. [29], as a genus expansion we calculate for deformed theories of JT gravity (asymptotic) thermal partition functions (with one or several asymptotic boundary components). The studied class of deformations is suitable to describe interactions of JT gravity with defects. In section 3 we turn to the low temperature expansion of the thermal partition function, which can be computed exactly at leading order in temperature [29–31]. For certain physical applications this analysis is more natural than the previously discussed asymptotic genus expansion because the expansion in temperature naturally sets an energy scale for the accessible states in the computed thermal partition functions. Using the computed low energy limit of the partition functions for JT gravity coupled to a gas of defects, we show in section 4 that there is a Hawking-Page phase transition. We numerically compute the associated critical temperature as a function of the deficit coupling constant, and we also analyse the spectral form factor. We find that in the given low temperature approximation the time scale for the onset of the plateau exhibits a simple behaviour in terms of the deficit coupling, which conforms with the observed Hawking-Page phase transition. In section 5 we make some basic comments on the connection between the wavefunction of the universe for JT gravity on de Sitter space dS_2 and the Weil-Petersson volumes of the associated Riemann surfaces with conical singularities in the light of the recent work [42]. Finally, in section 6 we present our conclusions, where we discuss our results and present some outlook for further investigations.

While completing this work, ref. [43] appeared, which has certain overlap with some of our discussions in section 2.

2 JT gravity, deformed JT gravity and topological gravity

In this section we aim to describe JT gravity together with deformations in terms of two-dimensional topological gravity. The works [29, 30] by Okuyama and Sakai establish a

direct link between the partition functions of JT gravity and correlation functions in topological gravity. Deforming JT gravity from interactions with defects (as established in refs. [23, 24]) yields another instance of two-dimensional topological gravity with modified coupling parameters. While we are indeed interested in JT gravity coupled to a gas of defects, we study deformations to JT gravity in a more general setting. By using the results of ref. [32] we construct thermal partition functions for deformed theories of JT gravity, which at any intermediate stage of their derivation can be specialised to particular deformed JT gravity theories (such as JT gravity interacting with defects). Our approach could offer a starting point towards a dictionary between specific values for the couplings in two-dimensional topological gravity and deformations attributed to scalar potentials added to the JT gravity action, such as the potential (1.4) for deformations arising from defect interactions.²

In part this section uses and reviews some well-established mathematical tools from the intersection theory on the moduli spaces of stable curves to derive the thermal partition functions of deformed JT gravity. The reader not interested in these derivations should skip these technical details and instead view this section as a collocation of expressions for thermal partition functions and related quantities, which are used in later sections of this work.

2.1 Weil-Petersson volumes of hyperbolic Riemann surfaces

To set the stage and to introduce the used notation, we first collect some mathematical preliminaries on the Weil-Petersson volumes of hyperbolic Riemann surfaces with geodesic boundary components and conical singularities from the perspective of intersection theory on the moduli spaces of stable curves.

Let $\mathcal{M}_{g,n}$ be the moduli space of smooth curves of genus g with n distinct marked points. By construction the moduli space $\mathcal{M}_{g,n}$ is not compact, as it contains neither the limiting curve with a handle degenerating to a nodal point nor the limit as two marked points collide. The Deligne-Mumford compactification $\overline{\mathcal{M}}_{g,n}$ includes the above mentioned limits in terms of stable curves with nodal singularities. The resulting moduli space of stable curves is well-defined to parametrise curves with marked points that do not admit any continuous automorphisms. That is to say $\overline{\mathcal{M}}_{g,n}$ is defined for genus $g \geq 2$ and any number of marked points, for genus one with at least one marked point, and for genus zero with at least three marked points. The complex dimensions of these moduli spaces are given by

$$\dim_{\mathbb{C}} \overline{\mathcal{M}}_{g,n} = 3g - 3 + n . \tag{2.1}$$

The moduli space of stable curves $\overline{\mathcal{M}}_{g,n}$ comes equipped with several natural cohomology classes. To each marked point p_i , $i = 1, \dots, n$, on the curve C_g one associates at the point p_i the complex cotangent line $T_{p_i}^* C_g$, which patches together to a line bundle \mathcal{L}_i on $\overline{\mathcal{M}}_{g,n}$. The first Chern class of this line bundle realises a cohomology class on $\overline{\mathcal{M}}_{g,n}$

²Results in a similar vein of thought are reported in ref. [42] as well. See also ref. [44] for a discussion along these lines from the minimal string theory perspective.

denoted by

$$\psi_i = c_1(\mathcal{L}_i) \in H^2(\overline{\mathcal{M}}_{g,n}, \mathbb{Q}) . \quad (2.2)$$

The other for us relevant cohomology class is the first Miller-Morita-Mumford class κ_1 , which arises in a similar fashion. Consider the forgetful map $\pi : \overline{\mathcal{M}}_{g,n+1} \rightarrow \overline{\mathcal{M}}_{g,n}$ that omits the $(n+1)$ -th marked point. Then the cohomology class κ_1 is given by [45, 46]

$$\kappa_1 = \pi_*(c_1(\mathcal{L}_{n+1})^2) + \sum_{i=1}^n \psi_i \in H^2(\overline{\mathcal{M}}_{g,n}, \mathbb{Q}) , \quad (2.3)$$

where the push-forward π_* can heuristically be thought of as integrating over the fiber of the map π . The class κ_1 is proportional to the Weil-Petersson Kähler form ω_{WP} [47]

$$\omega_{\text{WP}} = 2\pi^2 \kappa_1 . \quad (2.4)$$

Upon integrating such cohomology classes over $\overline{\mathcal{M}}_{g,n}$ we obtain (rational) intersection numbers that are collected in correlators. The correlators of particular interest to us are given by

$$\left\langle \kappa_1^\ell \tau_{d_1} \dots \tau_{d_n} \right\rangle_{g,n} = \int_{\overline{\mathcal{M}}_{g,n}} \kappa_1^\ell \psi_1^{d_1} \dots \psi_n^{d_n} , \quad \ell, d_1, \dots, d_n \in \mathbb{Z}_{\geq 0} , \quad (2.5)$$

where the classes τ_{d_i} are the conventional abbreviations for $\psi_i^{d_i}$ arising from the i -th marked point. The defined correlators are only non-vanishing if the integrated class represents a (non-zero) top class of $\overline{\mathcal{M}}_{g,n}$, which together with eq. (2.1) amounts to the selection rule

$$\left\langle \kappa_1^\ell \tau_{d_1} \dots \tau_{d_n} \right\rangle_{g,n} \neq 0 \quad \Rightarrow \quad \ell + d_1 + \dots + d_n = 3g - 3 + n . \quad (2.6)$$

For these correlators we introduce the generating functions [26]

$$F(\{t_k\}) = \sum_{g=0}^{+\infty} g_s^{2g} \left\langle e^{\sum_{d=0}^{\infty} t_d \tau_d} \right\rangle_g = \sum_{g=0}^{+\infty} g_s^{2g} \sum_{\{n_d\}} \left(\prod_{d=0}^{\infty} \frac{t_d^{n_d}}{n_d!} \right) \langle \tau_0^{n_0} \tau_1^{n_1} \dots \rangle_g , \quad (2.7)$$

and

$$G(s, \{t_k\}) = \sum_{g=0}^{+\infty} g_s^{2g} \left\langle e^{s\kappa_1 + \sum_{d=0}^{\infty} t_d \tau_d} \right\rangle_g = \sum_{g=0}^{+\infty} \sum_{m=0}^{+\infty} \frac{g_s^{2g} s^m}{m!} \sum_{\{n_d\}} \left(\prod_{d=0}^{\infty} \frac{t_d^{n_d}}{n_d!} \right) \langle \kappa_1^m \tau_0^{n_0} \tau_1^{n_1} \dots \rangle_g , \quad (2.8)$$

in terms of the genus expansion parameter g_s and the couplings $\{t_d\}$. Due to the relation (2.3) the two generating functions are not independent but instead are related as [46, 48, 49]

$$G(s, \{t_k\}) = F(\{t_k + \gamma_k\}) , \quad \gamma_0 = \gamma_1 = 0 , \quad \gamma_k = \frac{(-1)^k}{(k-1)!} s^{k-1} . \quad (2.9)$$

As the first Miller-Morita-Mumford class κ_1 is proportional to the Weil-Petersson Kähler form ω_{WP} (cf. eq. (2.4)), the function $G(2\pi^2, \{t_k = 0\})$ evaluated at $t_k = 0$ readily

becomes the generating function of the Weil-Petersson volumes V_g of the moduli space of genus g curves (for $g \geq 2$) without any marked points, i.e.

$$G(2\pi^2, \{t_k = 0\}) = \sum_{g=2}^{+\infty} g_s^{2g} \int_{\overline{\mathcal{M}}_{g,0}} e^{\omega_{\text{WP}}} = \sum_{g=2}^{+\infty} g_s^{2g} \int_{\overline{\mathcal{M}}_{g,0}} \text{vol}_{\text{WP}} = \sum_{g=2}^{+\infty} g_s^{2g} V_g. \quad (2.10)$$

Here vol_{WP} is the Weil-Petersson volume form of the $(3g - 3)$ -dimensional moduli space $\overline{\mathcal{M}}_{g,0}$.

As shown in the seminal work [50] by Mirzakhani, the Weil-Petersson volume of a hyperbolic Riemann surfaces of genus g with n geodesic boundary components of length $\vec{b} = (b_1, \dots, b_n)$ reads in terms of the previously defined cohomology classes on $\overline{\mathcal{M}}_{g,n}$

$$V_{g,\vec{b}} = \int_{\overline{\mathcal{M}}_{g,n}} e^{\omega_{\text{WP}} + \frac{1}{2} \sum_{\ell=1}^n b_\ell^2 \psi_\ell} = \left\langle e^{2\pi^2 \kappa_1 + \frac{1}{2} \sum_{\ell=1}^n b_\ell^2 \psi_\ell} \right\rangle_{g,n}. \quad (2.11)$$

For hyperbolic Riemann surfaces with geodesic boundary components of uniform length b , using eq. (2.5) it is straightforward to verify that the volumes $V_{g,(b,\dots,b)}$ are generated by

$$G(2\pi^2, \{t_k = \frac{b^{2k}}{2^k k!} \delta\}) = \sum_g g_s^{2g} \sum_{i=0}^{+\infty} \frac{\delta^i}{i!} V_{g,\underbrace{(b,\dots,b)}_{i \text{ times}}}, \quad (2.12)$$

or upon rescaling all cohomology classes with a non-zero factor λ we obtain with eq. (2.1) the generating function

$$G(2\pi^2 \lambda, \{t_k = \frac{\lambda^k b^{2k}}{2^k k!} \delta\}) = \sum_g \frac{g_s^{2g}}{\lambda^3} \sum_{i=0}^{+\infty} \frac{(\lambda \delta)^i}{i!} \lambda^{3g} V_{g,\underbrace{(b,\dots,b)}_{i \text{ times}}}. \quad (2.13)$$

For this generating function of Weil-Petersson volumes (and similarly for all other generating functions of Weil-Petersson volumes to be defined in the following), the volumes $V_{g,(b,\dots,b)}$ that are not in accord with the selection rule (2.6) are set to zero.³ Furthermore, for boundary components with p distinct geodesic length b_1, \dots, b_p , this generating function readily generalises to

$$G\left(2\pi^2 \lambda, \left\{t_k = \sum_{i=1}^p \frac{\lambda^k b_i^{2k}}{2^k k!} \delta_j\right\}\right) = \sum_g \frac{g_s^{2g}}{\lambda^3} \sum_{i_1, \dots, i_p=0}^{+\infty} \left(\prod_{s=1}^p \frac{(\lambda \delta_s)^{i_s}}{i_s!}\right) \lambda^{3g} V_{g,\underbrace{(b_1, \dots, b_1, \dots, b_p, \dots, b_p)}_{\substack{i_1 \text{ times} \\ i_p \text{ times}}}}. \quad (2.14)$$

Finally, a hyperbolic Riemann surface with a conical singularity with identification angle α can simply be obtained by replacing the argument b of a boundary component by $i\alpha$ (for the identification angles in the range $0 < \alpha_i < \pi$).⁴ Thus, the Weil-Petersson volume $V_{g,\vec{b},\vec{\alpha}}$ of a

³This in particular implies that the Weil-Petersson volumes are only non-vanishing for stable curves, with the only exception being the Weil-Petersson volume V_1 for $g = 1$ and $n = 0$, which is either set to zero or to a constant, see for instance the discussion in ref. [26]. In this work, however, the volume V_1 is not relevant as we only consider Riemann surfaces with at least one boundary component.

⁴The identification angle α of a conical singularity corresponds to the deficit angle $2\pi - \alpha$ of the singularity.

hyperbolic Riemann surface with boundary components of geodesic lengths $\vec{b} = (b_1, \dots, b_p)$ and together with conical singularities $\vec{\alpha} = (\alpha_1, \dots, \alpha_q)$ is given by

$$V_{g, \vec{b}, \vec{\alpha}} = V_{g, (b_1, \dots, b_p, i\alpha_1, \dots, i\alpha_q)} \cdot \quad (2.15)$$

Moreover, the generating function for hyperbolic Riemann surfaces with boundary components of geodesic lengths b_1, \dots, b_p and conical singularities of with identification angles $\alpha_1, \dots, \alpha_q$ becomes in terms of the non-zero parameter λ

$$\begin{aligned} G\left(2\pi^2\lambda, \left\{t_k = \sum_{i=1}^p \frac{\lambda^k b_i^{2k}}{2^k k!} \delta_i + \sum_{j=1}^q \frac{\lambda^k (-\alpha_j^2)^k}{2^k k!} \epsilon_j\right\}\right) & \quad (2.16) \\ &= \sum_g \frac{g_s^{2g}}{\lambda^3} \sum_{\substack{i_1, \dots, i_p=0 \\ j_1, \dots, j_q=0}}^{+\infty} \left(\prod_{s=1}^p \frac{(\lambda \delta_s)^{i_s}}{i_s!} \prod_{t=1}^q \frac{(\lambda \epsilon_t)^{j_t}}{j_t!} \right) \\ & \quad \times \lambda^{3g} V_{g, (\underbrace{b_1, \dots, b_1}_{i_1 \text{ times}}, \dots, \underbrace{b_p, \dots, b_p}_{i_p \text{ times}}, \underbrace{\alpha_1, \dots, \alpha_1}_{j_1 \text{ times}}, \dots, \underbrace{\alpha_q, \dots, \alpha_q}_{j_q \text{ times}})} \end{aligned}$$

2.2 Deformations of JT gravity from minimal strings

Before delving into the technical computation of the thermal partition functions of JT gravity with deformations, in this subsection we briefly spell out the connections among topological gravity, minimal string theories, and JT gravity. This puts the forthcoming analysis into a broader context.

Saad, Shenker and Stanford already point out that standard JT gravity relates to the large p limit of the $(2, 2p - 1)$ minimal string theory [12]. Such minimal string theories in turn enjoy a dual matrix model formulation [35, 51, 52], which for finite p comes with a finite number of coupling parameters. In the large p limit, however, an infinite (but countable) number of couplings occur, which for standard JT gravity are set to specific non-zero values. Furthermore, this infinite number of couplings relate to observables and their correlators in two-dimensional topological gravity, as introduced in the previous subsection.

In the following, as in ref. [29], using the connection to topological gravity we want to compute thermal partition functions as a function of this infinite number of couplings in order to describe JT gravity and deformations thereof. In other words, instead of solely focussing on particular deformation backgrounds — such as JT gravity without deformations or JT gravity interacting with a gas of defects — we parametrise generic deformations to JT gravity in terms of deformations of the $(2, 2p - 1)$ minimal string theories in the large p limit, using the results of ref. [32].

Starting from a JT gravity action formulation the values of the deformation parameters are ultimately determined from the constraints obtained from integrating out the scalar dilaton field. For instance, JT gravity coupled to a gas of defects yields the constraint (1.4), which is dual to specific values of the topological gravity coupling parameters. For a given JT gravity action functional — such as JT gravity interacting with defects — we refer to coupling values that fulfill these constraints as on-shell couplings and couplings that deviate from this critical condition as off-shell couplings (adapting to a terminology introduced in ref. [29]).

Turning this argument around, we can now ask whether specific values for these couplings correspond to a legitimate action functional of a deformed theory of JT gravity. Intriguingly, as discussed in the following both JT gravity and JT gravity coupled to defects give rise to on-shell couplings that are governed by Bessel functions [20, 23, 24, 29]. The problem of establishing a dictionary between these deformation spaces raises the question to what extent other transcendental functions for on-shell couplings are linked to action functionals of deformed JT gravity theories (see, e.g. ref. [53] for the realisation of JT supergravity). For finite p the $(2, 2p - 1)$ minimal string theories possess a finite dimensional deformation space resulting from finitely many couplings t_k . In the considered limit $p \rightarrow \infty$, the deformations δ_k in eq. (1.7) can be characterized by their asymptotic behaviour for large k . The values for the couplings t_k for undeformed JT gravity are suppressed factorially (cf. eq. (1.6)). For deformations arising from a gas of defects (at least for only finitely many types of defect species) the asymptotic behaviour of the couplings t_k for large k remains the same. On the level of the action functional of JT gravity such deformations give rise to a scalar potential (1.4) that is exponentially suppressed for large positive values of the dilaton ϕ . In general, we expect that the asymptotic behaviour of the scalar potential $U(\phi)$ for large ϕ relates to the asymptotic behaviour of the deformations δ_k for large k .⁵ Describing this duality beyond the discussed asymptotic growth behaviours seems a challenging task, which is beyond the scope of this work. Nevertheless, we hope that the description of generic deformations in the context of $(2, 2p - 1)$ minimal string theories in the large p limit presented here proves useful from the JT gravity perspective as well.

2.3 JT gravity interacting with a gas of defects

We now study JT gravity interacting with a gas of defects, which is geometrically described in terms of Riemann surfaces with conical singularities [23, 24]. That is to say, we consider the partition function of JT gravity with contributions from hyperbolic Riemann surfaces with asymptotic boundary conditions together with an arbitrary number of conical singularities and at arbitrary genus. The relevant path integrals localise on the Weil-Petersson volumes of hyperbolic Riemann surfaces with geodesic boundary components and conical defects, folded with the path integral of the Schwarzian theory describing the one-dimensional action at the asymptotic boundaries [12]. For a single asymptotic boundary component the resulting partition function reads [23, 24]

$$\begin{aligned}
 Z(\beta) = & e^{S_0} Z^{\text{disk}}(\beta) + e^{S_0} \sum_{j=1}^r \epsilon_j Z^{\text{disk}}(\beta, \alpha_j) \\
 & + \sum_{g,n=0}^{\infty} e^{(1-2g)S_0} \sum_{j_1, \dots, j_n=1}^r \frac{\epsilon_{j_1} \cdots \epsilon_{j_n}}{n!} \int_0^\infty db b Z^{\text{trumpet}}(\beta, b) V_{g,b,(\alpha_{j_1}, \dots, \alpha_{j_n})} . \quad (2.17)
 \end{aligned}$$

Here the parameters ϵ_j , $j = 1, \dots, r$, are the coupling constants to the r distinct defect types that are characterised by the identification angles α_j of their associated conical singularities

⁵Ref. [44] makes an interesting proposal for a correspondence between a certain limit of Liouville theory coupled to matter and JT gravity with a $\sinh(\phi)$ -dilaton potential with a different asymptotic behaviour for $\phi \rightarrow +\infty$ (see also ref. [54]).

on the hyperbolic Riemann surfaces. Furthermore, β is the inverse temperature attributed to the configurations of wiggles at the asymptotic boundary of the hyperbolic Riemann surfaces. The distinct topologies of Riemann surfaces are weighted by the action S_0 that relates to the gravitational coupling G_N as $G_N \sim 1/S_0$. Hence, the partition function is a non-perturbative expansion in the gravitational coupling G_N of JT gravity [12]. The first two terms in this expansion capture the contributions of disks with no conical singularities and a single conical singularity, respectively. The remaining topologies appear in the second line.⁶ The individual terms in this expansion are computed as [12, 18, 25]

$$Z^{\text{disk}}(\beta) = \frac{\gamma^{\frac{3}{2}} e^{\frac{2\pi^2\gamma}{\beta}}}{(2\pi)^{\frac{1}{2}} \beta^{\frac{3}{2}}}, \quad Z^{\text{disk}}(\beta, \alpha_j) = \frac{\gamma^{\frac{1}{2}} e^{\frac{\gamma\alpha_j^2}{2\beta}}}{(2\pi\beta)^{\frac{1}{2}}}, \quad Z^{\text{trumpet}}(\beta, b) = \frac{\gamma^{\frac{1}{2}} e^{-\frac{\gamma b^2}{2\beta}}}{(2\pi\beta)^{\frac{1}{2}}}, \quad (2.18)$$

where γ is the coupling constant to the one-dimensional Schwarzian action.

First we observe that the summation over defects in eq. (2.17) can be rewritten as

$$\sum_{n=0}^{+\infty} \sum_{j_1, \dots, j_n=1}^r \frac{\epsilon_{j_1} \cdots \epsilon_{j_n}}{n!} V_{g,b,(\alpha_{j_1}, \dots, \alpha_{j_n})} = \sum_{n_1, \dots, n_r=0}^{+\infty} \left(\prod_{j=1}^r \frac{\epsilon_j^{n_j}}{n_j!} \right) V_{g,b,(\underbrace{\alpha_1, \dots, \alpha_1}_{n_1 \text{ times}}, \dots, \underbrace{\alpha_r, \dots, \alpha_r}_{n_r \text{ times}})}. \quad (2.19)$$

Summed over all genera g we readily express the volumes $V_{g,b,(\alpha_{j_1}, \dots, \alpha_{j_n})}$ in terms of the generating function (2.16) as

$$\begin{aligned} & \sum_{g,n=0}^{+\infty} g_s^{2g} \sum_{j_1, \dots, j_n=1}^r \frac{\epsilon_{j_1} \cdots \epsilon_{j_n}}{n!} \lambda^{3g} V_{g,b,(\alpha_{j_1}, \dots, \alpha_{j_n})} \\ &= \lambda^2 \frac{\partial}{\partial \delta} G \left(2\pi^2 \lambda, \left\{ t_k = \frac{\lambda^k b^{2k}}{2^k k!} \delta + \sum_{j=1}^r \frac{\lambda^{k-1} (-\alpha_j^2)^k}{2^k k!} \epsilon_j \right\} \right) \Bigg|_{\delta=0} \\ &= \sum_{\ell} \frac{b^{2\ell} \lambda^{\ell+2}}{2^{\ell} \ell!} \frac{\partial}{\partial t_{\ell}} G \left(2\pi^2 \lambda, \left\{ t_k = \sum_{j=1}^r \frac{\lambda^{k-1} (-\alpha_j^2)^k}{2^k k!} \epsilon_j \right\} \right). \end{aligned} \quad (2.20)$$

We insert this expression into eq. (2.17) with the relation

$$e^{-S_0} = \lambda^{\frac{3}{2}} g_s, \quad (2.21)$$

and carry out the integration over the geodesic boundary lengths in eq. (2.17) using

$$\int_0^{\infty} db b^{2n+1} e^{-\frac{\gamma b^2}{2\beta}} = \frac{n!}{2} \left(\frac{2\beta}{\gamma} \right)^{n+1}. \quad (2.22)$$

Then we arrive for the partition function $Z(\beta)$ at

$$Z(\beta) = \frac{1}{\sqrt{2\pi g_s}} \left(\frac{\gamma}{\lambda\beta} \right)^{\frac{3}{2}} \left(e^{\frac{2\pi^2\gamma}{\beta}} + \frac{\beta}{\gamma} \sum_{j=1}^r \epsilon_j e^{\frac{\gamma\alpha_j^2}{2\beta}} + \sum_{\ell=0}^{+\infty} \left(\frac{\lambda\beta}{\gamma} \right)^{\ell+2} \frac{\partial}{\partial t_{\ell}} G(2\pi^2 \lambda, \{t_k = \delta_k\}) \right), \quad (2.23)$$

⁶Due to the selection rules (2.6) for non-vanishing Weil-Petersson volumes $V_{g,b,\bar{a}}$, the second line of eq. (2.17) does not contain a contribution from disks without any or with a single conical singularity.

with

$$\delta_k = \sum_j \delta_{k,j}, \quad \delta_{k,j} = \frac{\lambda^{k-1}(-\alpha_j^2)^k}{2^k k!} \epsilon_j. \quad (2.24)$$

Note that only the last term of the partition function $Z(\beta)$ given in eq. (2.23) is mapped to the topological correlators (2.5), whereas the first two terms associated to disk topologies capture the semi-classical contributions to the partition function in the presence of a gas of defects.

It is straightforward to generalise the partition function $Z(\beta)$ to geometries with multiple asymptotic boundaries [23, 24]. For m boundaries we define the partition function of connected hyperbolic Riemann surfaces by $Z(\beta_1, \dots, \beta_m)$, where the inverse temperatures β_1, \dots, β_m describe the thermodynamics of the wiggles at the m distinct asymptotic boundary components.

Similarly as for the partition function $Z(\beta)$ of a single asymptotic boundary, the partition function $Z(\beta_1, \beta_2)$ with two asymptotic boundaries splits into two pieces

$$Z(\beta_1, \beta_2) = Z(\beta_1, \beta_2)^{\text{non-top.}} + Z(\beta_1, \beta_2)^{\text{top.}}. \quad (2.25)$$

The first term does not relate to topological correlators (2.5), while the second term arises from an integral transformation of the Weil-Petersson volumes of hyperbolic Riemann surfaces with two geodesic boundary components that are computable in terms of topological correlators, cf. eqs. (2.11) and (2.15). The non-topological piece $Z(\beta_1, \beta_2)^{\text{non-top.}}$ receives only a contribution at genus zero from the topology of a cylinder (without any conical singularities). Using eqs. (2.18) and (2.22), this cylindrical contribution is obtained by gluing two trumpets along their geodesic boundary components, as computed in ref. [12]

$$Z(\beta_1, \beta_2)^{\text{non-top.}} = \int_0^\infty db b Z^{\text{trumpet}}(\beta_1, b) Z^{\text{trumpet}}(\beta_2, b) = \frac{\sqrt{\beta_1 \beta_2}}{2\pi \beta_1 + 2\pi \beta_2}. \quad (2.26)$$

The selection rule (2.6) implies that the partition functions $Z(\beta_1, \dots, \beta_m)$ with $m > 2$ receive only contributions of the topological type, i.e.

$$Z(\beta_1, \dots, \beta_m) = Z(\beta_1, \dots, \beta_m)^{\text{top.}} \quad \text{for } m > 2. \quad (2.27)$$

For any $m \geq 1$ the topological part of the partition function $Z(\beta_1, \dots, \beta_m)$ reads

$$\begin{aligned} Z(\beta_1, \dots, \beta_m)^{\text{top.}} &= \sum_{g,n=0}^\infty e^{(2-2g-m)S_0} \sum_{j_1, \dots, j_n=1}^r \frac{\epsilon_{j_1} \cdots \epsilon_{j_n}}{n!} \\ &\times \prod_{i=1}^m \int_0^\infty db_i b_i Z^{\text{trumpet}}(\beta_i, b_i) V_{g, (b_1, \dots, b_m), (\alpha_{j_1}, \dots, \alpha_{j_n})}. \end{aligned} \quad (2.28)$$

Analogously to the formula (2.20) for a single boundary component, we express the volumes $V_{g, (b_1, \dots, b_m), (\alpha_{j_1}, \dots, \alpha_{j_n})}$ in terms of the generating function (2.16) as

$$\begin{aligned} \sum_{g,n} g_s^{2g} \sum_{j_1, \dots, j_n=1}^r \lambda^{3g} \frac{\epsilon_{j_1} \cdots \epsilon_{j_n}}{n!} V_{g, (b_1, \dots, b_m), (\alpha_{j_1}, \dots, \alpha_{j_n})} \\ = \lambda^{3-m} \prod_{i=1}^m \left(\sum_{\ell=0}^{+\infty} \frac{b_i^{2\ell} \lambda^\ell}{2^\ell \ell!} \frac{\partial}{\partial t_\ell} \right) G \left(2\pi^2 \lambda, \left\{ t_k = \sum_{j=1}^r \frac{\lambda^{k-1} (-\alpha_j^2)^k}{2^k k!} \epsilon_j \right\} \right). \end{aligned} \quad (2.29)$$

Inserting this expression into eq. (2.28) and carrying out the integrals (2.22), we obtain

$$Z(\beta_1, \dots, \beta_m)^{\text{top.}} = \frac{1}{g_s^2} \mathcal{B}(\beta_1) \cdots \mathcal{B}(\beta_m) G(2\pi^2 \lambda, \{t_k = \delta_k\}) \quad \text{for } m \geq 1, \quad (2.30)$$

with δ_k as defined in eq. (2.24) and in terms of the differential operator

$$\mathcal{B}(\beta) = g_s \sqrt{\frac{\lambda \beta}{2\pi \gamma}} \sum_{\ell=0}^{+\infty} \left(\frac{\lambda \beta}{\gamma} \right)^\ell \frac{\partial}{\partial t_\ell}. \quad (2.31)$$

It is shown in ref. [30] that the differential operator $\mathcal{B}(\beta)$ creates an asymptotic boundary component at temperature β . It is universal in the sense that without any modifications it also creates asymptotic boundary components in the presence of defects. The operator $\mathcal{B}(\beta)$ as a function of β relates to the operator in ref. [55], which in the context of two-dimensional topological gravity creates in a surface a hole of specified boundary length. Therefore, we refer to $\mathcal{B}(\beta)$ as the boundary creation operator.

The obtained simple forms (2.23) and (2.30) of the partition function $Z(\beta)$ and its multi-boundary generalisations $Z(\beta_1, \dots, \beta_m)$ in the presence of a gas of defects have a nice interpretation from the topological gravity perspective. The Weil-Petersson volumes (2.11) are computed with the Kähler class $2\pi^2 \kappa_1$ on the moduli spaces $\overline{\mathcal{M}}_{g,n}$ [50]. The generating function $G(2\pi^2 \lambda, \{t_k\})$ now expresses these volumes (as functions of the scaling and genus expansion parameters λ and g_s) in terms of the shifted generating function $F(\{t_k + \gamma_k\})$ of topological gravity according to eq. (2.9). As explained in refs. [12, 29], JT gravity can be interpreted as topological gravity with non-vanishing background parameters $\{\gamma_k\}$. Including now a gas of defects (characterised by their couplings ϵ_j and identification angles α_j) further deforms the background couplings $\{\gamma_k\}$. The leading order contribution arises from single-defect interactions while the higher order corrections are due to multi-defect interactions. These order-by-order contributions can be viewed as a Taylor expansion about the JT gravity background parameters $\{\gamma_k\}$, which altogether sum up to the deformation $\{\gamma_k + \delta_k\}$. Thus, JT gravity interacting with a gas of defects yields yet other expansion points of the generating function $F(\{t_k\})$. It would be interesting to see if there are special expansion points that are singled out from the topological gravity point of view.

As in ref. [29], in the following we set the coupling γ and the scaling parameter λ to the convenient values

$$\lambda = \gamma = \frac{1}{2\pi^2}. \quad (2.32)$$

Then the boundary creation operator $\mathcal{B}(\beta)$ and the background parameters δ_k simplify to

$$\mathcal{B}(\beta) = g_s \sqrt{\frac{\beta}{2\pi}} \sum_{\ell=0}^{+\infty} \beta^\ell \frac{\partial}{\partial t_\ell}, \quad \delta_k = \sum_j \left(-\frac{\alpha_j^2}{4\pi^2} \right)^k \frac{2\pi^2 \epsilon_j}{k!}, \quad (2.33)$$

and the partition functions become

$$Z(\beta) = \frac{1}{\sqrt{2\pi} g_s \beta^{\frac{3}{2}}} \left(e^{\frac{1}{\beta}} + 2\pi^2 \beta \sum_{j=1}^r \epsilon_j e^{\frac{\alpha_j^2}{4\pi^2 \beta}} \right) + \frac{1}{g_s^2} \mathcal{B}(\beta) G(1, \{t_k = \delta_k\}),$$

$$\begin{aligned}
 Z(\beta_1, \beta_2) &= \frac{\sqrt{\beta_1 \beta_2}}{2\pi\beta_1 + 2\pi\beta_2} + \frac{1}{g_s^2} \mathcal{B}(\beta_1) \mathcal{B}(\beta_2) G(1, \{t_k = \delta_k\}), \\
 Z(\beta_1, \dots, \beta_m) &= \frac{1}{g_s^2} \mathcal{B}(\beta_1) \cdots \mathcal{B}(\beta_m) G(1, \{t_k = \delta_k\}) \quad \text{for } m \geq 3,
 \end{aligned}
 \tag{2.34}$$

where the first two partition functions receive both non-topological and topological contributions.

2.4 KdV hierarchy and off-shell partition functions

As conjectured by Witten [26] and proven by Kontsevich [27] the generating function $F(\{t_k\})$ of correlators in topological gravity defined in eq. (2.7) arises as a solution to the KdV hierarchy as follows. Let us define

$$u(\{t_k\}) = \frac{\partial^2}{\partial t_0^2} F(\{t_k\}). \tag{2.35}$$

The function $u(\{t_k\})$ is a tau function to the KdV hierarchy, i.e. it solves the system of graded partial differential equations

$$\partial_k u = \partial_0 \mathcal{R}_{k+1}(u, \partial_0 u, \partial_0^2 u, \dots) \quad \text{with} \quad \partial_k \equiv \frac{\partial}{\partial t_k}, \quad k = 0, 1, 2, 3, \dots \tag{2.36}$$

Here \mathcal{R}_k , $k = 1, 2, 3, \dots$, are the Gelfand-Dikii polynomials [56], which are polynomials in the derivatives $\partial_0^\ell u(\{t_k\})$, $\ell = 0, 1, 2, \dots$ of $u(\{t_k\})$, and depend on the parameter g_s . Together with the condition $\mathcal{R}_k(\{\partial_0^\ell u \equiv 0\}) = 0$ they are defined with the initial polynomial $\mathcal{R}_1 = u$ recursively as [56]

$$\partial_0 \mathcal{R}_{k+1} = \frac{1}{2k+1} \left(2u(\partial_0 \mathcal{R}_k) + (\partial_0 u) \mathcal{R}_k + \frac{g_s^2}{4} \partial_0^3 \mathcal{R}_k \right). \tag{2.37}$$

The first three Gelfand-Dikii polynomials read

$$\mathcal{R}_1 = u, \quad \mathcal{R}_2 = \frac{u^2}{2} + \frac{g_s^2}{12} \partial_0^2 u, \quad \mathcal{R}_3 = \frac{u^3}{3!} + \frac{g_s^2}{24} (2u \partial_0^2 u + (\partial_0 u)^2) + \frac{g_s^4}{240} \partial_0^4 u. \tag{2.38}$$

The leading order term of the Gelfand-Dikii polynomials is given by

$$\mathcal{R}_k|_{g_s=0} = \frac{u^k}{k!}, \tag{2.39}$$

independent of any derivatives $\partial_0 u(\{t_k\})$, $\partial_0^2 u(\{t_k\})$, $\partial_0^3 u(\{t_k\})$, \dots

As the KdV hierarchy (2.36) depends only implicitly on the couplings t_k , the function $v(\{t_k\}) = \partial_0^2 F(\{t_k + \Delta t_k\})$ is a tau function for any set of constants $\{\Delta t_k\}$. In particular, a tau function arises from the generating function $G(s, \{t_k\})$ of Weil-Petersson volumes (cf. eq. (2.9)) and from the generating function $H(\{t_k\})$ of correlators on hyperbolic Riemann surfaces with conical singularities given by

$$H(\{t_k\}) = G(1, \{t_k + \delta_k\}) = F(\{t_k + \gamma_k + \delta_k\}), \tag{2.40}$$

in terms of the constants $\Delta t_k = \gamma_k + \delta_k$, cf. eqs. (2.9) and (2.33).

The particular tau function $u(\{t_k\})$ of topological gravity and hence the tau function $v(\{t_k\})$ with the shifted couplings obey the string equation [57]

$$\partial_0 u = 1 + \sum_{k=1}^{+\infty} t_k \partial_k u, \quad \partial_0 v = 1 + \sum_{k=1}^{+\infty} (t_k + \Delta t_k) \partial_k v. \quad (2.41)$$

The string equation together with the KdV hierarchy determine unambiguously the tau functions $u(\{t_k\})$ and $v(\{t_k\})$ [26]. The string equation can be viewed as the initial condition specifying a unique solution to the KdV hierarchy.

The partition functions $Z(\beta_1, \dots, \beta_m)$ defined in eq. (2.34) do not depend on the coupling parameters $\{t_k\}$ appearing in the definition of $H(\{t_k\})$. Instead the generating function $H(\{t_k\})$ is evaluated at the specific values $t_k = 0$ (corresponding to $t_k = \gamma_k + \delta_k$ in terms of the generating functions $F(\{t_k\})$). We can define partition functions $Z^F(\{t_k\}; \beta_1, \dots, \beta_m)$ based on $F(\{t_k\})$ or alternatively the partition functions $Z^H(\{t_k\}; \beta_1, \dots, \beta_m)$ based on $H(\{t_k\})$ depending on $\{t_k\}$ by generalising the topological part in eqs. (2.34) to

$$\begin{aligned} Z^F(\{t_k\}; \beta_1, \dots, \beta_m)^{\text{top.}} &= \frac{1}{g_s^2} \mathcal{B}(\beta_1) \cdots \mathcal{B}(\beta_m) F(\{t_k\}), \\ Z^H(\{t_k\}; \beta_1, \dots, \beta_m)^{\text{top.}} &= \frac{1}{g_s^2} \mathcal{B}(\beta_1) \cdots \mathcal{B}(\beta_m) H(\{t_k\}). \end{aligned} \quad (2.42)$$

Following ref. [29] we refer to $Z^F(\{t_k\}; \beta_1, \dots, \beta_m)$ and $Z^H(\{t_k\}; \beta_1, \dots, \beta_m)$ as the off-shell partition functions, and upon specialising to suitable values for the couplings $\{t_k\}$ — denoted as on-shell values — we get back the result $Z(\beta_1, \dots, \beta_m)$ referred to as the on-shell partition function, i.e.

$$\begin{aligned} Z(\beta_1, \dots, \beta_m) &= Z^F(\{t_k = \gamma_k + \delta_k\}; \beta_1, \dots, \beta_m), \\ Z(\beta_1, \dots, \beta_m) &= Z^H(\{t_k = 0\}; \beta_1, \dots, \beta_m). \end{aligned} \quad (2.43)$$

These two classes of off-shell partition functions enjoy distinct interpretations. Whereas the off-shell partition function $Z^F(\{t_k\}; \beta_1, \dots, \beta_m)$ is defined in the setting of topological gravity in the context of intersection theory on the moduli spaces of stable curves [26, 27], the partition functions $Z^H(\{t_k\}; \beta_1, \dots, \beta_m)$ directly relate to correlators on hyperbolic Riemann surfaces (possibly coupled to a gas of defects as described by the constants $\{\delta_k\}$) in the context of JT gravity [12, 29]. These two classes of off-shell partition functions are related as $Z^F(\{\gamma_k + \delta_k + t_k\}; \beta_1, \dots, \beta_m) = Z^H(\{t_k\}; \beta_1, \dots, \beta_m)$.

Let us now determine the introduced off-shell partition functions explicitly. The tau function (2.35) and the generating function $F(\{t_k\})$ enjoy the genus expansion

$$u(\{t_k\}) = \sum_{\ell=0}^{+\infty} g_s^{2\ell} u_\ell(\{t_k\}), \quad F(\{t_k\}) = \sum_{\ell=0}^{+\infty} g_s^{2\ell} F_\ell(\{t_k\}), \quad (2.44)$$

such that $F_g = \partial_0^2 u_g$. The KdV hierarchy (2.36) with eq. (2.39) and the string equation (2.41) imply for the genus zero contribution the partial differential equations

$$\partial_k u_0 = \frac{\partial_0 u_0^{k+1}}{(k+1)!}, \quad \partial_0 u_0 = 1 + \sum_{k=1}^{+\infty} t_k \partial_k u_0. \quad (2.45)$$

Defining the series

$$I_n(u_0, \{t_k\}) = \sum_{k=0}^{+\infty} t_{k+n} \frac{u_0^k}{k!} \quad \text{for } n = 0, 1, 2, \dots, \quad (2.46)$$

and using the partial differential equations (2.45), Itzykson and Zuber show for the genus zero part $u_0(\{t_k\})$ of the tau function $u(\{t_k\})$ the remarkable functional relation [32]

$$u_0 - I_0(u_0, \{t_k\}) = 0. \quad (2.47)$$

With the ansatz $u_0(\{t_k\}) = \sum_{N=0}^{+\infty} \sum_{\sum n_k=N} u_{0, \{n_k\}} t_0^{1-N+\sum kn_k} (t_1^{n_1} t_2^{n_2} \dots)$ summed over non-negative integral sets $\{n_k\}$, one readily determines order-by-order the formal expansion in the coupling parameters $\{t_k\}$

$$u_0(\{t_k\}) = t_0 + t_0 t_1 + \left(t_0 t_1^2 + \frac{1}{2} t_0^2 t_2 \right) + \left(t_0 t_1^3 + \frac{3}{2} t_0^2 t_1 t_2 + \frac{1}{6} t_0^3 t_3 \right) + \dots \quad (2.48)$$

Imposing the correct boundary conditions, the function u_0 integrates to [32]

$$F_0(u_0, \{t_k\}) = \frac{u_0^3}{3!} - \sum_{k=0}^{+\infty} t_k \frac{u_0^{k+2}}{(k+2)k!} + \frac{1}{2} \sum_{k=0}^{+\infty} \frac{u_0^{k+1}}{k+1} \sum_{n=0}^k \frac{t_n t_{k-n}}{n!(k-n)!}. \quad (2.49)$$

Furthermore, observing that the functions (2.46) obey the differential identities

$$\partial_0 I_0 = \frac{1}{1 - I_1}, \quad \partial_0 I_k = \frac{I_{k+1}}{1 - I_1} \quad \text{for } k \geq 1 \quad (2.50)$$

Itzykson and Zuber establish that the KdV hierarchy implies at higher genus the finite non-trivial expansions [32]

$$u_g = (1 - I_1)^{g-1} \sum_{\sum_{k=2}^{3g} (k-1)\ell_k=3g-1} u_{g, \{\ell_k\}} \left(\frac{I_2}{(1 - I_1)^2} \right)^{\ell_2} \dots \left(\frac{I_{3g}}{(1 - I_1)^{3g}} \right)^{\ell_{3g}}. \quad (2.51)$$

Inserting this ansatz into the KdV hierarchy (2.36) (recursively in the genus) determines unambiguously the numerical coefficients $u_{g, \{\ell_k\}}$, for instance up to genus $g = 2$ we arrive at

$$u_1 = \frac{1}{12} \left(\frac{I_2}{(1 - I_1)^2} \right)^2 + \frac{1}{24} \frac{I_3}{(1 - I_1)^3}, \quad (2.52)$$

$$u_2 = (1 - I_1) \left(\frac{49I_2^5}{288(1 - I_1)^{10}} + \frac{11I_3I_2^3}{36(1 - I_1)^9} + \frac{7I_4I_2^2}{96(1 - I_1)^8} + \frac{109I_3^2I_2}{1152(1 - I_1)^8} \right. \\ \left. + \frac{I_5I_2}{90(1 - I_1)^7} + \frac{17I_3I_4}{960(1 - I_1)^7} + \frac{I_6}{1152(1 - I_1)^6} \right). \quad (2.53)$$

At genus one $u_1(\{t_k\})$ integrates to

$$F_1 = -\frac{1}{24} \log(1 - I_1). \quad (2.54)$$

The generating functions F_g for $g > 1$ enjoy yet again an expansion of the form [32]

$$F_g = (1 - I_1)^{g-1} \sum_{\sum_{k=2}^{3g-2} (k-1)\ell_k = 3g-3} f_{g, \{\ell_k\}} \left(\frac{I_2}{(1 - I_1)^2} \right)^{\ell_2} \cdots \left(\frac{I_{3g-2}}{(1 - I_1)^{3g-2}} \right)^{\ell_{3g-2}}, \quad (2.55)$$

in terms of the finitely many coefficients $f_{g, \{\ell_k\}}$ (with the subscript $\{\ell_k\} = \{\ell_2, \ell_3, \dots\}$). In particular, with eq. (2.53) we find for $g = 2$ the numerical coefficients

$$f_{2, \{3\}} = \frac{7}{1440}, \quad f_{2, \{1,1\}} = \frac{29}{5760}, \quad f_{2, \{0,0,1\}} = \frac{1}{1152}, \quad (2.56)$$

and we arrive at

$$F_2 = \frac{7}{1440} \frac{I_2^3}{(1 - I_1)^5} + \frac{29}{5760} \frac{I_2 I_3}{(1 - I_1)^4} + \frac{1}{1152} \frac{I_4}{(1 - I_1)^3}. \quad (2.57)$$

Thus, the method of Itzykson and Zuber — expressing the tau function $u(\{t_k\})$ and hence the generating function $F(\{t_k\})$ in terms of the functions $I_n(u_0, \{t_k\})$ — offers a very powerful method to compute the generating function $F(\{t_k\})$ order-by-order as a genus expansion [32]. Upon inserting the expression (2.48) to the desired order, one can readily read off the correlators of topological gravity explicitly.

Solving the KdV hierarchy in terms of the functions I_n allows us to derive a universal expression for the off-shell partition functions (2.42) with arbitrary shifts $\{\Delta t_k\}$ in the coupling parameters $\{t_k\}$. The defined off-shell partition functions (2.42) are derived from the generating function $F(F_0, \{I_n\}) = F_0 + \sum_{g=1}^{+\infty} g_s^{2g} F_g(\{I_n\})$, which — if expressed in terms of $F_0(u_0(\{t_k\}), \{t_k\})$ and $I_n(u_0(\{t_k\}), \{t_k\})$, $n = 1, 2, 3, \dots$ — only implicitly depend on the couplings $\{t_k\}$. Computing the action of the boundary creation operators (2.33) on the functions F_0 yields

$$\begin{aligned} \mathcal{B}(\beta)F_0 &= \frac{g_s}{\sqrt{2\pi}\beta^{\frac{3}{2}}} \left(e^{\beta I_0} (1 - \beta I_0) - 1 + \sum_{k, \ell=0}^{+\infty} \frac{I_0^{k+\ell+1}}{k + \ell + 1} \frac{\beta^{k+2} t_\ell}{k! \ell!} \right), \\ \mathcal{B}(\beta_1)\mathcal{B}(\beta_2)F_0 &= \frac{g_s^2 \sqrt{\beta_1 \beta_2}}{2\pi\beta_1 + 2\pi\beta_2} \left(e^{(\beta_1 + \beta_2)I_0} - 1 \right), \end{aligned} \quad (2.58)$$

whereas for I_n we find

$$\mathcal{B}(\beta)I_0 = g_s \sqrt{\frac{\beta}{2\pi}} \frac{e^{\beta I_0}}{1 - I_1}, \quad \mathcal{B}(\beta)I_k = g_s \sqrt{\frac{\beta}{2\pi}} e^{\beta I_0} \left(\beta^k + \frac{I_{k+1}}{(1 - I_1)} \right) \quad \text{for } k \geq 1. \quad (2.59)$$

As a consequence of these derivative rules — except for the leading genus zero contribution to the partition function with one asymptotic boundary — the off-shell partition functions (2.42) are universally expressible in terms of the functions I_n , i.e.

$$\begin{aligned} Z(\{\mathcal{B}(\beta)F_0, I_n\}; \beta)^{\text{top.}} &= \frac{1}{g_s^2} \mathcal{B}(\beta)F(\{t_k\}) = \frac{1}{g_s^2} \mathcal{B}(\beta)F_0 + Z^{(g>0)}(\{I_n\}; \beta)^{\text{top.}}, \\ Z(\{I_n\}; \beta_1, \dots, \beta_m)^{\text{top.}} &= \frac{1}{g_s^2} \mathcal{B}(\beta_1) \cdots \mathcal{B}(\beta_m)F(\{t_k\}) \quad \text{for } m > 1. \end{aligned} \quad (2.60)$$

In particular, the partition function with a single asymptotic boundary component enjoys the genus expansion

$$Z(\{\mathcal{B}(\beta)F_0, I_n\}; \beta)^{\text{top.}} = \frac{1}{g_s^2} \mathcal{B}(\beta)F_0 + \sqrt{\frac{\beta}{2\pi}} e^{\beta I_0} \sum_{g=1}^{+\infty} g_s^{2g-1} (1-I_1)^{g-1} Z_g(\{I_n\}, \beta), \quad (2.61)$$

where

$$Z_1 = \frac{1}{24} \left(\frac{\beta}{1-I_1} + \frac{I_2}{(1-I_1)^2} \right), \quad (2.62)$$

and for $g > 0$

$$Z_g = \sum_{\sum_{k=2}^{3g-2} (k-1)\ell_k = 3g-3} f_{g, \{\ell_k\}} \sum_{s=2}^{3g-2} \ell_s \left(\frac{1+2s}{3(1-I_1)} \left(\beta + \frac{I_2}{1-I_1} \right) + \frac{I_{s+1}}{I_s(1-I_1)} + \frac{\beta^s}{I_s} \right) \cdot \left(\frac{I_2}{(1-I_1)^2} \right)^{\ell_2} \cdots \left(\frac{I_{3g-2}}{(1-I_1)^{3g-2}} \right)^{\ell_{3g-2}}, \quad (2.63)$$

in terms of the constants $f_{g, \{\ell_k\}}$ defined in eq. (2.55). With eq. (2.62) and inserting (2.56) into Z_2 we find explicitly up to genus two

$$\begin{aligned} Z^{(g>0)}(\{I_n\}; \beta)^{\text{top.}} &= \frac{g_s}{24} \sqrt{\frac{\beta}{2\pi}} e^{\beta I_0} \left(\frac{\beta}{1-I_1} + \frac{I_2}{(1-I_1)^2} \right) \\ &+ \frac{g_s^3}{5760} \sqrt{\frac{\beta}{2\pi}} e^{\beta I_0} \left(\frac{5\beta^4}{(1-I_1)^4} + \frac{29\beta^3 I_2 + 29\beta^2 I_3 + 15\beta I_4 + 5I_5}{(1-I_1)^5} \right. \\ &+ \frac{84\beta^2 I_2^2 + 116\beta I_3 I_2 + 44I_4 I_2 + 29I_3^2}{(1-I_1)^6} + \frac{20I_2^2(7\beta I_2 + 10I_3)}{(1-I_1)^7} \\ &\left. + \frac{140I_2^4}{(1-I_1)^8} \right) + \dots \end{aligned} \quad (2.64)$$

Similar formulas can be worked out for the universal partition functions with several asymptotic boundary components, namely

$$Z(\{I_n\}; \beta_1, \dots, \beta_m)^{\text{top.}} = \prod_{i=1}^m \left(e^{\beta_i I_0} \sqrt{\frac{\beta_i}{2\pi}} \right) \sum_{g=0}^{\infty} g_s^{2g+m-2} (1-I_1)^{g-1} Z_g(\{I_n\}, \beta_1, \dots, \beta_m), \quad (2.65)$$

where

$$\mathcal{B}(\beta_1) \cdots \mathcal{B}(\beta_m) F_g = \frac{g_s \sqrt{\beta_1 \cdots \beta_m}}{(2\pi)^{\frac{m}{2}}} e^{(\beta_1 + \dots + \beta_m) I_0} (1-I_1)^{g-1} Z_g(\{I_n\}, \beta_1, \dots, \beta_m). \quad (2.66)$$

In particular for two asymptotic boundary components the leading order contributions are given by

$$\begin{aligned} Z(\{I_n\}; \beta_1, \beta_2) &= \frac{\sqrt{\beta_1 \beta_2}}{2\pi \beta_1 + 2\pi \beta_2} e^{(\beta_1 + \beta_2) I_0} + \frac{g_s^2 \sqrt{\beta_1 \beta_2}}{48\pi} e^{(\beta_1 + \beta_2) I_0} \left(\frac{\beta_1^2 + \beta_1 \beta_2 + \beta_2^2}{(1-I_1)^2} \right. \\ &\left. + \frac{2(\beta_1 + \beta_2) I_2 + I_3}{(1-I_1)^3} + \frac{2I_2^2}{(1-I_1)^4} \right) + \dots, \end{aligned} \quad (2.67)$$

including the semi-classical contribution, cf. eq. (2.34). Thus, any of the off-shell or on-shell partition functions defined in eqs. (2.42) and (2.43) can be obtained from the universal partition functions (2.60) upon inserting $I_n(\{t_k\}, u_0(\{t_k\}))$ with suitable values for the couplings $\{t_k\}$. For instance, inserting $I_n(\{t_k + \gamma_k + \delta_k\}, u_0(\{t_k + \gamma_k + \delta_k\}))$ we obtain the off-shell partition functions $Z^H(\{t_k\}; \beta_1, \dots, \beta_m)$, whereas for $I_n(\{\gamma_k + \delta_k\}, u_0(\{\gamma_k + \delta_k\}))$ we arrive at the on-shell partition functions $Z(\beta_1, \dots, \beta_m)$. In the next section, we focus on the partition functions $Z(t_0, t_1; \beta_1, \dots, \beta_m)$ studied in refs. [29, 30], where we assign on-shell values to the couplings t_k , $k = 2, 3, 4, \dots$, while keeping the first two couplings t_0 and t_1 off-shell [58].

While the presented genus expansion in the coupling $g_s \sim e^{-1/G_N}$ is non-perturbative in the gravitational coupling G_N of JT gravity, it is perturbative in the dual matrix model formulation, where the expansion parameter g_s describes quantum fluctuations about the classical energy density of states [12, 20]. In fact the discussed partition functions $Z(\{I_n\}; \beta_1, \dots, \beta_m)$ are divergent series in g_s due to the factorial growth $(2g)!$ of the contributions at order g_s^{2g} [12, 58]. Therefore, the partition functions $Z(\{I_n\}; \beta_1, \dots, \beta_m)$ are asymptotic series that require a non-perturbative completion arising from non-perturbative effects of the order e^{-1/g_s} . For further details on this issue and the possible emergence of non-perturbative instabilities, we refer the reader to refs. [12, 20] and the solutions proposed in refs. [20–22].

2.5 Partition functions with leading order off-shell couplings

In the spirit of refs. [29, 30] let us now consider the partition functions $Z(t_0, t_1; \beta_1, \dots, \beta_m)$ with only the couplings t_0 and t_1 taken to be off-shell. Then the partition functions for JT gravity coupled to a gas of defects are defined as

$$Z(t_0, t_1; \beta_1, \dots, \beta_m) \equiv Z(\{t_0, t_1, t_{k \geq 2} = \gamma_k + \delta_k\}; \beta_1, \dots, \beta_m), \quad (2.68)$$

where setting $t_0 = \delta_0$ and $t_1 = \delta_1$ yields the on-shell partition functions in all couplings. Analogously, we can define the function $u(t_0, t_1)$ and the generating function $F(t_0, t_1)$ obtained by evaluating the couplings $t_{k \geq 2}$ of the tau function $u(\{t_k\})$ and of the generating function $F(\{t_k\})$ at their on-shell values, i.e.

$$u(t_0, t_1) = u(\{t_0, t_1, t_{k \geq 2} = \gamma_k + \delta_k\}), \quad F(t_0, t_1) = F(\{t_0, t_1, t_{k \geq 2} = \gamma_k + \delta_k\}), \quad (2.69)$$

with

$$u(t_0, t_1) = \partial_0^2 F(t_0, t_1). \quad (2.70)$$

All these functions can respectively be obtained from their universal expressions (2.60), (2.51), and (2.55) by inserting the on-shell values of the couplings $t_{k \geq 2}$ into the functions I_n . The function $u(t_0, t_1)$ fulfils the first partial differential equation of the KdV hierarchy (2.36), which is just the non-linear partial differential KdV equation, i.e.,

$$\partial_1 u = u \partial_0 u + \frac{g_s^2}{12} \partial_0^3 u. \quad (2.71)$$

With t_0 and t_1 off-shell we observe that the function I_1 depends only on t_1 and $u_0 \equiv I_0$, while I_n for $n \geq 2$ are series in u_0 without an explicit dependence on t_0 and t_1 . Therefore, it is convenient to introduce new (formal) variables (y, t) given by [29, 58]

$$y = u_0, \quad t = 1 - I_1. \quad (2.72)$$

Since I_n for $n \geq 2$ is only a function of y , we obtain from the universal tau function (2.51) and the universal generating function (2.55) the asymptotic series

$$u(y, t) = y + \sum_{g=1}^{\infty} g_s^{2g} u_g(y, t), \quad u_g(y, t) = \sum_{k=2g+1}^{5g-1} u_{g,k}(y) t^{-k}, \quad (2.73)$$

and

$$F(y, t) = F_0(y, t) - \frac{g_s^2}{24} \log t + \sum_{g=2}^{\infty} g_s^{2g} F_g(y, t), \quad F_g(y, t) = \sum_{k=2g-1}^{5g-5} F_{g,k}(y, t) t^{-k}. \quad (2.74)$$

The coefficient functions $u_g(y, t)$ (for $g \geq 1$) and $F_g(y, t)$ (for $g \geq 2$) are Laurent polynomials in the variable t , where the range for the powers of t is a consequence of the restricted sums in eqs. (2.51) and (2.55). The degrees of these Laurent polynomials conform with the structure derived by Zograf for the specific on-shell couplings $t_k = \gamma_k$ for $k \geq 2$ [58]. Furthermore, at genus one the logarithmic contribution to $F(y, t)$ arises from eq. (2.54), whereas with eq. (2.49) the genus zero contribution becomes

$$F_0(y, t) = \frac{1}{6} y^3 t^2 + \frac{1}{6} y^2 t \sum_{k=2}^{+\infty} \frac{y^k (2k+5)(\gamma_k + \delta_k)}{(k+2)(k+1)(k-2)!} + \frac{1}{6} y \left(\sum_{k=2}^{+\infty} \frac{y^k (\gamma_k + \delta_k)}{(k+1)(k-2)!} \right)^2 + \sum_{k=4}^{+\infty} \frac{y^{k+1}}{3(k+1)(k+2)!} \sum_{n=2}^{k-2} \binom{k+4}{n+2} \binom{n}{2} \binom{k-n}{2} (\gamma_n + \delta_n)(\gamma_{k-n} + \delta_{k-n}). \quad (2.75)$$

Let us now turn to the partition function $Z(t_0, t_1; \beta)$ with a single asymptotic boundary. Since the couplings $t_{k \geq 2}$ are taken on-shell we cannot obtain $Z(t_0, t_1; \beta)$ by acting with the boundary creation operator $\mathcal{B}(\beta)$ on the generating function $F(t_0, t_1)$ because the boundary operator $\mathcal{B}(\beta)$ contains derivatives with respect to those parameters that have been fixed to their on-shell values. Thus, either we compute $Z(t_0, t_1; \beta)$ from the universal partition function (2.60) or we determine a differential equation with $Z(t_0, t_1; \beta)$ as its solution. For the latter approach we follow the authors of ref. [29]. Note that the partial derivatives ∂_k for $k \geq 2$ appearing in the boundary operator $\mathcal{B}(\beta)$ can be rewritten in terms of derivatives with respect to ∂_0 due to the KdV hierarchy (2.36), namely

$$\partial_0 Z(t_0, t_1; \beta) = \frac{1}{g_s^2} \mathcal{B}(\beta) \partial_0 F(\{t_k\}) \Big|_{\{t_{k \geq 2} = \gamma_k + \delta_k\}} = -\frac{1}{g_s \sqrt{2\pi\beta}} + W(t_0, t_1; \beta), \quad (2.76)$$

with the definition

$$W(t_0, t_1; \beta) = \frac{1}{g_s \sqrt{2\pi\beta}} \sum_{\ell=0}^{+\infty} \beta^\ell \mathcal{R}_\ell, \quad (2.77)$$

in terms of the Gelfand-Dikii polynomials (2.38) and $\mathcal{R}_0 = 1$. The key observation of ref. [29] is now that the Gelfand-Dikii polynomials obey the non-trivial relation⁷

$$\partial_1 \mathcal{R}_k = u \partial_0 \mathcal{R}_k + \frac{g_s^2}{12} \partial_0^3 \mathcal{R}_k, \quad (2.78)$$

which immediately implies the differential equation

$$\partial_1 W(t_0, t_1; \beta) = u \partial_0 W(t_0, t_1; \beta) + \frac{g_s^2}{12} \partial_0^3 W(t_0, t_1; \beta). \quad (2.79)$$

The partition function $Z(t_0, t_1; \beta)$ can now be determined from this differential equation for $W(t_0, t_1; \beta)$. The function $W(t_0, t_1; \beta)$ is an interesting quantity by itself, see for instance the discussion in ref. [29].

Upon expressing the couplings (t_0, t_1) in terms of the variables (y, t) defined in eq. (2.72), the function $W(y, t; \beta)$ enjoys the asymptotic genus expansion

$$W(y, t; \beta) = \frac{e^{\beta y}}{\sqrt{2\pi\beta}} \sum_{g=0}^{+\infty} g_s^{2g-1} W_g(y, t; \beta), \quad (2.80)$$

where — due to the definition $\mathcal{R}_0 = 1$ and due to the leading order behaviour (2.39) of the Gelfand-Dikii polynomials — the genus zero contribution reads

$$W_0(y, t; \beta) = 1. \quad (2.81)$$

By inserting the variables (2.72) into the t_0 -derivative of the universal expressions (2.63), we find that the higher genus contributions $W_g(y, t; \beta)$ are polynomials in t^{-1} with coefficient functions in terms of y and β of the form

$$W_g(y, t; \beta) = \sum_{k=2g}^{5g-1} W_{g,k}(y; \beta) t^{-k} \quad \text{for } g \geq 1. \quad (2.82)$$

Inserting the asymptotic expansion (2.80) into the partial differential equation yields the recursion differential equation [29]

$$\partial_t W_g = - \sum_{h=0}^{g-1} u_{g-h} \nabla(\beta) W_h - \frac{1}{12} \nabla(\beta)^3 W_{g-1}, \quad (2.83)$$

with the linear differential operators

$$\nabla(\beta) = \partial_0 + \frac{\beta}{t} = \frac{1}{t} (-I_2 \partial_t + D_y), \quad D_y = \partial_y + \beta. \quad (2.84)$$

Furthermore, inserting the expansion (2.82) into the differential recursion relation and carrying out a few steps of algebra yields recursion relations for the Laurent modes $W_{g,k}(y; \beta)$. With the initial genus zero contribution (2.81) we arrive for genus $g = 1$ at⁸

$$W_{1,k} = \frac{\beta}{k} u_{1,k} + \frac{\beta^3}{24} \delta_{k,2} + \frac{1}{36} (3I_2 \beta^2 + I_3 \beta) \delta_{k,3} + \frac{\beta}{16} I_2^2 \delta_{k,4} \quad \text{for } k = 2, 3, 4, \quad (2.85)$$

⁷This relation can directly be proven by induction with respect to the index k of the Gelfand-Dikii polynomials \mathcal{R}_k . The induction step is performed by applying the recursion relation (2.37) of the Gelfand-Dikii polynomials.

⁸Note that the polynomial structure (2.82) of $W_g(y, t; \beta)$ fixes the constant of integration in the differential recursion relation (2.83) with respect to t unambiguously.

which explicitly becomes with eq. (2.52)

$$W_1(y, t; \beta) = \frac{\beta^3}{24t^2} + \frac{\beta}{24t^3} (2\beta I_2 + I_3) + \frac{\beta}{12t^4} I_2^2. \quad (2.86)$$

Furthermore, for $g \geq 2$ and $k = 2g + 1, \dots, 5g - 1$ we arrive at the lengthy but straightforwardly applicable recursion relation

$$\begin{aligned} W_{g,k} = & \sum_{h=1}^{g-1} \sum_{n=2h}^{5h-1} \left(\frac{n}{k} I_2 u_{g-h,k-n-1} W_{h,n} + \frac{1}{k} u_{g-h,k-n} D_y W_{h,n} \right) + \frac{\beta}{k} u_{g,k} \\ & + \frac{1}{12k} \left[D_y^3 W_{g-1,k-2} + \left(3(k-2) I_2 D_y^2 + (3k-8) I_3 D_y + (k-3) I_4 \right) W_{g-1,k-3} \right. \\ & \quad + \left(3(k^2 - 5k + 5) I_2^2 D_y + (k-4)(3k-5) I_2 I_3 \right) W_{g-1,k-4} \\ & \quad \left. + (k-5)(k-3)(k-1) I_2^3 W_{g-1,k-5} \right], \end{aligned} \quad (2.87)$$

where we set $W_{h,n} \equiv 0$ for $n \notin \{2h, \dots, 5h-1\}$ and $u_{h,n} \equiv 0$ for $n \notin \{2h+1, \dots, 5h-1\}$. In particular, for genus two we readily compute

$$\begin{aligned} W_2(y, t; \beta) = & \frac{\beta}{5760} \left(\frac{5\beta^5}{t^4} + \frac{44\beta^4 I_2 + 58\beta^3 I_3 + 44\beta^2 I_4 + 20\beta I_5 + 5I_6}{t^5} \right. \\ & + \frac{200\beta^3 I_2^2 + 400\beta^2 I_2 I_3 + 145\beta I_3^2 + 220\beta I_2 I_4 + 102 I_3 I_4 + 64 I_2 I_5}{t^6} \\ & + \frac{5 I_2 (112\beta^2 I_2^2 + 240\beta I_3 I_2 + 84 I_4 I_2 + 109 I_3^2)}{t^7} \\ & \left. + \frac{20 I_2^3 (49\beta I_2 + 88 I_3)}{t^8} + \frac{980 I_2^5}{t^9} \right). \end{aligned} \quad (2.88)$$

With the help of these recursion formulas we are now in a position to deduce the partition function $Z(y, t; \beta)$ with one asymptotic boundary component as well. The general structure (2.63) implies for the partition function the asymptotic series⁹

$$Z(y, t; \beta) = \sum_{g=0}^{+\infty} g_s^{2g-1} \tilde{Z}_g(y, t; \beta). \quad (2.89)$$

The genus zero part splits into the semi-classical and topological contributions

$$\tilde{Z}_0(y, t; \beta) = \tilde{Z}_0^{\text{semi.}}(y, t; \beta) + \tilde{Z}_0^{\text{top.}}(y, t; \beta), \quad (2.90)$$

where — using eqs. (2.33) and (2.34)— the semi-classical part is given by

$$\begin{aligned} \tilde{Z}_0^{\text{semi.}}(y, t; \beta) = & \frac{t(1+y\beta)}{\sqrt{2\pi}\beta^{\frac{3}{2}}} + \frac{1}{\sqrt{2\pi}\beta} \sum_{k=2}^{+\infty} \frac{y^k (\gamma_k + \delta_k)}{k(k-2)!} \\ & + \frac{1}{\sqrt{2\pi}\beta^{\frac{3}{2}}} \sum_{k=2}^{+\infty} \frac{y^{k-1} (\gamma_k + \delta_k)}{(k-1)!} + \frac{1}{\sqrt{2\pi}\beta} \sum_{k=2}^{+\infty} \frac{\delta_k + \gamma_k}{(-\beta)^k}, \end{aligned} \quad (2.91)$$

⁹Note that the newly introduced contributions \tilde{Z}_g to the partition function differ from the definition of Z_g given in eq. (2.61) by a normalisation.

and where — according to eq. (2.58) — the topological part reads

$$\begin{aligned} \tilde{Z}_0(y, t; \beta)^{\text{top.}} &= \frac{t}{\sqrt{2\pi\beta^{\frac{3}{2}}}} \left(e^{\beta y} - (1 + y\beta) \right) - \frac{e^{\beta y}}{\sqrt{2\pi\beta}} \sum_{k=2}^{+\infty} \frac{y^k (\gamma_k + \delta_k)}{k!} \\ &\quad - \frac{1}{\sqrt{2\pi\beta}} \sum_{k=2}^{+\infty} \frac{y^k (\gamma_k + \delta_k)}{k(k-2)!} + \frac{e^{\beta y} - 1}{\sqrt{2\pi\beta^{\frac{3}{2}}}} \sum_{k=2}^{+\infty} \frac{y^{k-1} (\gamma_k + \delta_k)}{(k-1)!} \\ &\quad + \frac{1}{\sqrt{2\pi\beta^{\frac{3}{2}}}} \sum_{k=0}^{+\infty} \sum_{\ell=2}^{+\infty} \frac{y^{k+\ell+1} \beta^{k+2}}{(k+\ell+1)!} \binom{k+\ell}{k} (\gamma_\ell + \delta_\ell). \end{aligned} \quad (2.92)$$

Therefore, the total genus zero contribution becomes

$$\begin{aligned} \tilde{Z}_0(y, t; \beta) &= \frac{e^{\beta y}}{\sqrt{2\pi\beta^{\frac{3}{2}}}} \left(t - \beta \sum_{k=2}^{+\infty} \frac{y^k (\gamma_k + \delta_k)}{k!} + \sum_{k=2}^{+\infty} \frac{y^{k-1} (\gamma_k + \delta_k)}{(k-1)!} \right) \\ &\quad + \frac{1}{\sqrt{2\pi\beta^{\frac{3}{2}}}} \sum_{k=0}^{+\infty} \sum_{\ell=2}^{+\infty} \frac{y^{k+\ell+1} \beta^{k+2}}{(k+\ell+1)!} \binom{k+\ell}{k} (\gamma_\ell + \delta_\ell) + \frac{1}{\sqrt{2\pi\beta}} \sum_{k=2}^{+\infty} \frac{\delta_k + \gamma_k}{(-\beta)^k}. \end{aligned} \quad (2.93)$$

For the higher genus contributions we arrive with eq. (2.63) at the polynomials in t^{-1}

$$\tilde{Z}_g(y, t; \beta) = \frac{e^{\beta y}}{\sqrt{2\pi\beta^{\frac{3}{2}}}} \sum_{k=2g-1}^{5g-3} Z_{g,k}(y; \beta) t^{-k} \quad \text{for } g \geq 1. \quad (2.94)$$

Thus, employing the derived recursion relations for $W_{g,k}(y; \beta)$ we can determine $Z_g(y, t; \beta)$ recursively upon integrating eq. (2.76). Note that the constants of integration at each order in g_s are unambiguously determined by the general structure (2.94). Explicitly, we find for genus one — in agreement with eq. (2.62) — the result

$$\tilde{Z}_1(y, t; \beta) = \frac{e^{\beta y}}{24\sqrt{2\pi\beta}} \left(\frac{\beta^2}{t} + \frac{\beta I_2}{t^2} \right), \quad (2.95)$$

whereas for genus two — in agreement with eq. (2.64) — we obtain

$$\begin{aligned} \tilde{Z}_2(y, t; \beta) &= \frac{\sqrt{\beta} e^{\beta y}}{5760\sqrt{2\pi}} \left(\frac{5\beta^4}{t^3} + \frac{29\beta^3 I_2 + 29\beta^2 I_3 + 15\beta I_4 + 5I_5}{t^4} \right. \\ &\quad \left. + \frac{84\beta^2 I_2^2 + 116\beta I_3 I_2 + 44I_4 I_2 + 29I_3^2}{t^5} + \frac{20I_2^2(7\beta I_2 + 10I_3)}{t^6} + \frac{140\beta I_2^4}{t^7} \right). \end{aligned} \quad (2.96)$$

Let us give an alternative perspective on the partition function $Z(y, t; \beta)$ in terms of the associated Schrödinger problem [33, 35, 36]

$$\mathcal{H}\psi_E(t_0, t_1) = E\psi_E(t_0, t_1) \quad \text{with} \quad \mathcal{H} = \hbar^2 \partial_0^2 + u(t_0, t_1), \quad (2.97)$$

with $\hbar = \frac{g_s}{\sqrt{2}}$, Hamilton operator \mathcal{H} , and the wavefunctions $\psi_E(t_0, t_1)$, which are eigenfunctions with energy eigenvalue E . Here the partially on-shell tau function $u(t_0, t_1)$ becomes the potential of the Schrödinger equation, and the partition function can be written as

$$Z(y, t; \beta) = \int dE e^{-\beta E} \rho(E; y, t), \quad (2.98)$$

in terms of the spectral density $\rho(E; y, t)$ of the energy eigenvalues of the Hamilton operator \mathcal{H} . This formulation offers a framework for a non-perturbative description in the genus expansion g_s . However, since in our context the tau function $u(t_0, t_1)$ itself is only given as an asymptotic series in g_s , setting up the appropriate non-perturbatively exact Schrödinger problem is nevertheless a difficult task. This question has been discussed and analysed with numerical methods in refs. [20–22]. Here we only focus on the leading order contribution at genus zero, which predicts the integral representation

$$\tilde{Z}_0(y, t; \beta) = \int dE e^{-\beta E} \rho_0(E; y, t), \tag{2.99}$$

in terms of the genus zero spectral density $\rho_0(E; y, t)$. To verify this prediction explicitly, we first express the genus zero partition function (2.93) as

$$\tilde{Z}_0 = \frac{e^{\beta y}}{\sqrt{2\pi\beta^{\frac{3}{2}}}} (t + J'(y)) - \frac{e^{\beta y}}{\sqrt{2\pi\beta}} J(y) + \sqrt{\frac{\beta}{2\pi}} \int_{-\infty}^y dv e^{v\beta} J(v), \tag{2.100}$$

in terms of the function

$$J(y) = \sum_{k=2}^{+\infty} \frac{y^k (\gamma_k + \delta_k)}{k!}. \tag{2.101}$$

Here we assume that the function $J(v)$ is continuously differentiable in the interval $(-\infty, y)$, and that the stated integral (for $\beta > 0$) is finite. Performing an integration by parts and using the integral identities

$$\sqrt{\frac{\pi}{\beta}} e^{\beta z} = \int_{-z}^{+\infty} dE \frac{e^{-\beta E}}{\sqrt{E+z}}, \quad \frac{\sqrt{\pi}}{2\beta^{\frac{3}{2}}} e^{\beta z} = \int_{-z}^{+\infty} dE e^{-\beta E} \sqrt{E+z}, \tag{2.102}$$

we arrive at the expression

$$\tilde{Z}_0(y, t; \beta) = \int_{-y}^{+\infty} dE e^{-\beta E} \rho_0(E; y, t), \tag{2.103}$$

in terms of the (genus zero) spectral density

$$\rho_0(E; y, t) = \frac{\sqrt{2}}{\pi} \sqrt{E+y} (t + J'(y)) - \frac{1}{\sqrt{2\pi}} \int_{-y}^E dv \frac{J'(-v)}{\sqrt{E-v}}. \tag{2.104}$$

The obtained result agrees with the expected structure of the partition function obtained from the associated Schrödinger problem. Note that the obtained function $\rho_0(E; y, t)$ enjoys only the interpretation as a spectral density, if it is non-negative over the energy range $(-y, +\infty)$. The conditions $J'(y) \geq -t$ and $J'(v) \geq 0$ for $v \in (-y, +\infty)$ are sufficient to ensure a non-negative spectral density function (in the genus zero approximation). For some energy ranges E in the interval $(-y, +\infty)$ we seemingly arrive at a negative function $\rho_0(E; y, t)$. However, as on the classical level a Hawking-Page like first order phase transition can be observed when varying the potential (1.4) [59], it might be expected that here too, a phase transition occurs preventing the aforementioned negativity of the spectral density function. In ref. [60] this was only observed to be true for a specific class

of models for which $U(0) = 0$ with $U(\phi)$ (again referring to eq. (1.4)), while a larger class of models, namely those for which $U(0) \neq 0$, are declared both perturbatively and non-perturbatively unstable.

For energies E close to the negative coupling $-y$ the calculated energy density $\rho_0(E; y, t)$ behaves as

$$\rho_0(E; y, t) = \frac{\sqrt{2t}}{\pi} \sqrt{E + y} + \mathcal{O}(|E - E_0|^{\frac{3}{2}}) . \quad (2.105)$$

Therefore, we can interpret the negative coupling $-y$ as the (semi-classical) ground state energy of the Schrödinger problem. In particular, for JT gravity in the absence of defects the on-shell value of y becomes zero, and hence the ground state energy vanishes. Coupling JT gravity to a gas of defect, however, yields a non-vanishing on-shell value for y according to eqs. (2.33) and (2.72), which therefore results in a non-trivial shift of the ground state energy. This observation is in agreement with the results obtained in refs. [23, 24], and we get back to this point in the explicit example below and in section 3.

Finally, let us illustrate the structure of the partially off-shell partition function $Z(y, t; \beta)$ for JT gravity interacting with a single defect type specified by the coupling ϵ and identification angle α . Then — according to eqs. (2.9) and (2.33) — the on-shell couplings t_k for $k \geq 2$ become

$$t_k = \frac{(-1)^k}{(k-1)!} + \left(-\frac{\alpha^2}{4\pi^2}\right)^k \frac{2\pi^2\epsilon}{k!} \quad \text{for } k \geq 2, \quad (2.106)$$

whereas the remaining unfixed couplings t_0 and t_1 acquire their on-shell values upon setting

$$(t_0, t_1)|_{\text{on-shell}} = 2\pi^2\epsilon \left(1, -\frac{\alpha^2}{4\pi^2}\right) . \quad (2.107)$$

The on-shell values of the variables (y, t) defined in terms of (t_0, t_1) in eq. (2.72) are governed by the functional relations

$$\begin{aligned} 0 &= -\sqrt{y} \mathcal{J}_1(2\sqrt{y})|_{\text{on-shell}} + (2\pi^2\epsilon) \mathcal{J}_0\left(\frac{\alpha\sqrt{y}}{\pi}\right)\Big|_{\text{on-shell}} , \\ t|_{\text{on-shell}} &= \mathcal{J}_0(2\sqrt{y})|_{\text{on-shell}} + (2\pi^2\epsilon) \frac{\alpha}{2\pi\sqrt{y}} \mathcal{J}_1\left(\frac{\alpha\sqrt{y}}{\pi}\right)\Big|_{\text{on-shell}} , \end{aligned} \quad (2.108)$$

in terms of the Bessel functions $\mathcal{J}_\nu(x)$ of the first kind

$$\mathcal{J}_\nu(x) = \left(\frac{x}{2}\right)^\nu \sum_{k=0}^{+\infty} \frac{(-1)^k}{\Gamma(\nu+k+1)k!} \left(\frac{x^2}{4}\right)^k , \quad \mathcal{J}_{-n}(x) \equiv (-1)^n \mathcal{J}_n(x) \text{ for integer } n . \quad (2.109)$$

In the limit of vanishing defect interaction $\epsilon \rightarrow 0$ the functional relations (2.108) have the on-shell solution $(y, t)|_{\text{on-shell}} = (0, 1)$ in accord with ref. [29]. Solving for $(y, t)|_{\text{on-shell}}$ in the vicinity of $(0, 1)$ for small ϵ with the implicit function theorem, we obtain for (y, t) the

on-shell expansion in the first few orders

$$\begin{aligned}
 y|_{\text{on-shell}} &= 2\pi^2\epsilon + \pi^2(2\pi^2 - \alpha^2)\epsilon^2 + \frac{\pi^2(15\alpha^4 - 72\pi^2\alpha^2 + 80\pi^4)}{24}\epsilon^3 + \dots, \\
 t|_{\text{on-shell}} &= 1 + \frac{\alpha^2 - 4\pi^2}{2}\epsilon - \frac{\alpha^4 - 8\pi^2\alpha^2 + 8\pi^4}{8}\epsilon^2 \\
 &\quad + \frac{21\alpha^6 - 216\pi^2\alpha^4 + 576\pi^4\alpha^2 - 448\pi^6}{288}\epsilon^3 + \dots.
 \end{aligned}
 \tag{2.110}$$

According to eq. (2.105) these on-shell values give rise to a non-vanishing ground state energy, which to leading order in ϵ reads

$$E_0 = -2\pi^2\epsilon + \mathcal{O}(\epsilon^2). \tag{2.111}$$

Furthermore, inserting the on-shell couplings (2.106) into the functions I_n for $n \geq 2$ yields in terms of the Bessel function (2.109) the expressions

$$I_n(y) = \frac{(-1)^n}{(\sqrt{y})^{n-1}} \mathcal{J}_{n-1}(2\sqrt{y}) + (2\pi^2\epsilon) \left(-\frac{\alpha}{2\pi\sqrt{y}}\right)^n \mathcal{J}_n\left(\frac{\alpha\sqrt{y}}{\pi}\right) \quad \text{for } n \geq 2. \tag{2.112}$$

Similarly, the function $J'(y)$ defined via eq. (2.101) becomes

$$J'(y) = 1 + 2\pi^2\epsilon \frac{\alpha^2}{4\pi^2} - \mathcal{J}_0(2\sqrt{y}) - (2\pi^2\epsilon) \frac{\alpha}{2\pi\sqrt{y}} \mathcal{J}_1\left(\frac{\alpha\sqrt{y}}{\pi}\right). \tag{2.113}$$

Thus — according to eq. (2.104) — the genus zero contribution of the spectral density is given in terms of the Bessel functions \mathcal{J}_0 and \mathcal{J}_1 and the modified Bessel functions \mathcal{I}_0 and \mathcal{I}_1 by

$$\rho_0(E; y, t) = \frac{1}{\sqrt{2}\pi} \int_{-y}^E dv \frac{\mathcal{I}_0(2\sqrt{v}) + (2\pi^2\epsilon) \frac{\alpha}{2\pi\sqrt{v}} \mathcal{I}_1\left(\frac{\alpha\sqrt{v}}{\pi}\right)}{\sqrt{E-v}} \tag{2.114}$$

with the modified Bessel functions defined as $\mathcal{I}_\nu(x) = i^{-\nu} \mathcal{J}_\nu(ix)$. This result is in agreement with refs. [23, 24]. Finally, upon inserting the expressions (2.112) into the general genus one and genus two results (2.95) and (2.96), we arrive at $Z_1(y, t; \beta)$ and $Z_2(y, t; \beta)$ in terms of Bessel functions. Expanding these results to leading order in the coupling ϵ we respectively obtain

$$\begin{aligned}
 \tilde{Z}_1(y, t; \beta) \Big|_{y=2\pi^2\epsilon + \mathcal{O}(\epsilon^2), t=1 + \frac{1}{2}(\alpha^2 - 4\pi^2)\epsilon + \mathcal{O}(\epsilon^2)} \\
 = \frac{\beta^{\frac{3}{2}} e^{2\pi^2\epsilon\beta}}{\sqrt{2\pi}} \left(\frac{1}{24} - \frac{\alpha^2\epsilon}{48} + \frac{\pi^2\epsilon}{12} \right) \\
 + \frac{\beta^{\frac{1}{2}} e^{2\pi^2\epsilon\beta}}{\sqrt{2\pi}} \left(\frac{1}{24} + \frac{\alpha^4\epsilon}{384\pi^2} - \frac{\alpha^2\epsilon}{24} + \frac{\pi^2\epsilon}{8} \right) + \mathcal{O}(\epsilon^2),
 \end{aligned}
 \tag{2.115}$$

and

$$\begin{aligned}
 \tilde{Z}_2(y, t; \beta) \Big|_{y=2\pi^2\epsilon+\mathcal{O}(\epsilon^2), t=1+\frac{1}{2}(\alpha^2-4\pi^2)\epsilon+\mathcal{O}(\epsilon^2)} & \\
 = \frac{\beta^{\frac{9}{2}}e^{2\pi^2\epsilon\beta}}{\sqrt{2\pi}} \left(\frac{1}{1152} - \frac{\alpha^2\epsilon}{768} + \frac{\pi^2\epsilon}{192} \right) & + \frac{\beta^{\frac{7}{2}}e^{2\pi^2\epsilon\beta}}{\sqrt{2\pi}} \left(\frac{29}{5760} + \frac{29\alpha^4\epsilon}{92160\pi^2} - \frac{29\alpha^2\epsilon}{2880} + \frac{203\pi^2\epsilon}{5760} \right) \\
 + \frac{\beta^{\frac{5}{2}}e^{2\pi^2\epsilon\beta}}{\sqrt{2\pi}} \left(\frac{139}{11520} - \frac{29\alpha^6\epsilon}{1105920\pi^4} + \frac{7\alpha^4\epsilon}{3840\pi^2} - \frac{181\alpha^2\epsilon}{5760} + \frac{1697\pi^2\epsilon}{17280} \right) & \\
 + \frac{\beta^{\frac{3}{2}}e^{2\pi^2\epsilon\beta}}{\sqrt{2\pi}} \left(\frac{449}{11520} + \frac{\alpha^8\epsilon}{1179648\pi^6} - \frac{29\alpha^6\epsilon}{276480\pi^4} + \frac{461\alpha^4\epsilon}{46080\pi^2} - \frac{77\alpha^2\epsilon}{576} + \frac{5269\pi^2\epsilon}{13824} \right) & \\
 + \frac{\beta^{\frac{1}{2}}e^{2\pi^2\epsilon\beta}}{\sqrt{2\pi}} \left(-\frac{137}{9216} - \frac{\alpha^{10}\epsilon}{70778880\pi^8} + \frac{11\alpha^8\epsilon}{4423680\pi^6} - \frac{19\alpha^6\epsilon}{122880\pi^4} - \frac{289\alpha^4\epsilon}{138240\pi^2} \right. & \\
 \left. + \frac{1267\alpha^2\epsilon}{27648} - \frac{3239\pi^2\epsilon}{23040} \right) + \mathcal{O}(\epsilon^2). & \tag{2.116}
 \end{aligned}$$

We observe that at every order in the inverse temperature β , there are contributions from the interaction with the defects already at the linear order in the defect coupling ϵ . Therefore, it is obvious that the dynamics of JT gravity are strongly influenced by the interaction with defects.

Finally, let us remark that the generalisation to multiple species of defects (with defect couplings ϵ_j and identification angles α_j) is straightforward. Namely, the on-shell values of the couplings (y, t) of eq. (2.110) generalise to

$$\begin{aligned}
 y|_{\text{on-shell}} &= 2\pi^2 \sum_j \epsilon_j + \sum_{j,k} \left(2\pi^4 - \frac{1}{2}\pi^2\alpha_j^2 - \frac{1}{2}\pi^2\alpha_k^2 \right) \epsilon_j \epsilon_k + \dots, \\
 t|_{\text{on-shell}} &= 1 + \sum_j \frac{\alpha_j^2 - 4\pi^2}{2} \epsilon_j - \sum_{j,k} \frac{\alpha_k^4 + \alpha_j^4 - 8\pi^2(\alpha_k^2 + \alpha_j^2) + 16\pi^4}{16} \epsilon_j \epsilon_k + \dots.
 \end{aligned} \tag{2.117}$$

Furthermore, the functions (2.112) and (2.113) now become

$$\begin{aligned}
 I_n(y) &= \frac{(-1)^n}{(\sqrt{y})^{n-1}} \mathcal{J}_{n-1}(2\sqrt{y}) + 2\pi^2 \sum_j \epsilon_j \left(-\frac{\alpha_j}{2\pi\sqrt{y}} \right)^n \mathcal{J}_n \left(\frac{\alpha_j\sqrt{y}}{\pi} \right) \quad \text{for } n \geq 2, \\
 J'(y) &= 1 + 2\pi^2 \sum_j \epsilon_j \frac{\alpha_j^2}{4\pi^2} - \mathcal{J}_0(2\sqrt{y}) - 2\pi^2 \sum_j \epsilon_j \frac{\alpha_j}{2\pi\sqrt{y}} \mathcal{J}_1 \left(\frac{\alpha_j\sqrt{y}}{\pi} \right).
 \end{aligned} \tag{2.118}$$

With these expressions at hand one can again readily compute order-by-order in the genus expansion parameter g_s the partition function of JT gravity coupled to several species of defects.

3 Low temperature expansion

So far the partition function has been organised as a genus expansion. That is to say, for any given genus different powers of the temperature T contribute in combination with

different powers of the defect couplings ϵ_j . The contribution to the thermal partition functions at each genus are multiplied by polynomials in the inverse temperature $\beta = 1/T$. Hence the magnitude of these polynomials are bounded for high temperatures, and the genus expansion in g_s is sensible in the high temperature regime. However, this expansion breaks down in the low temperature limit $\beta \rightarrow +\infty$ unless we keep $g_s\beta^{3/2}$ fixed. Then the perturbative genus expansion remains finite and can be summed exactly [29–31]. This double scaling limit implies for the genus expansion parameter $g_s \rightarrow 0^+$, and as a consequence the non-perturbative corrections of the type $\sim e^{-1/g_s}$ vanish in this limit.

To study in the following in the described low temperature limit the interaction of JT gravity with a gas of defects, the couplings ϵ_j — which are the characteristic energy scales of the defect, see, e.g., eq. (2.111) — must be comparable to the low temperature scale T . Therefore, we additionally require that for $\beta \rightarrow +\infty$ the products $\beta\epsilon_j$ remain constant as well. This limit also implies that non-perturbative corrections of the type $\sim e^{-1/|\epsilon_j|}$ are exponentially suppressed.

3.1 Low temperature limit

Let us consider the low temperature expansion of JT gravity coupled to a gas of defects of a single species type characterised by the defect coupling ϵ and the identification angle α . To this end, we want to compute the partition functions $Z(\beta_1, \dots, \beta_m)$ defined in eq. (2.34) in the double scaling limit

$$\beta_i \rightarrow +\infty \quad \text{with} \quad g_s\beta_i^{3/2} = \text{const.}, \quad \epsilon\beta_i = \text{const.} \quad \text{for all} \quad i = 1, \dots, m, \quad (3.1)$$

with distinct inverse temperatures β_i for the individual boundary components.¹⁰ The inverse temperatures of the boundary components are conveniently described in terms of the universal inverse temperature scale β and the dimensionless constants

$$\mathbf{b}_i = \frac{\beta_i}{\beta}. \quad (3.2)$$

Then the above limit becomes $\beta \rightarrow +\infty$ for constant positive values \mathbf{b}_i while keeping $g_s\beta^{3/2}$ and $\epsilon\beta$ fixed.

In the limit (3.1) (the topological part of) the partition function of eq. (2.34) becomes

$$\begin{aligned} & Z(\beta_1, \dots, \beta_m)^{\text{top.}} \\ &= \frac{1}{g_s^2} \mathcal{B}(\beta_1) \cdots \mathcal{B}(\beta_m) G(1, \{t_k = \delta_k\}) \\ &= \sum_{g,n=0}^{+\infty} \frac{(g_s\beta^{\frac{3}{2}})^{2g-2+m} (\epsilon\beta)^n}{(2\pi)^{\frac{m}{2}}} \\ &\quad \cdot \sum_{\ell_1, \dots, \ell_m=0}^{+\infty} \beta^{\ell_1+\dots+\ell_m-m-n-3g+3} \mathbf{b}_1^{\ell_1+\frac{1}{2}} \cdots \mathbf{b}_m^{\ell_m+\frac{1}{2}} \partial_{\ell_1} \cdots \partial_{\ell_m} G_{g,m+n}(\{t_k\}) \Big|_{t_k=\delta_k/\epsilon}, \end{aligned} \quad (3.3)$$

¹⁰In the absence of defects the low temperature limit of the partition function $Z(\beta_1, \beta_2)$ was previously derived in ref. [30]. For the uniform limit $\beta \rightarrow +\infty$ with $\beta = \beta_1 = \dots = \beta_m$ the low temperature limit of the partition functions together with defects has been first reported in ref. [31].

with the generating function $G(1, \{t_k\}) = \sum_{g,n} g_s^{2g} G_{g,n}(\{t_k\})$ decomposed into the contributions $G_{g,n}$ indexed by their genus g and their number of marked points n . Imposing now the selection rule (2.6) and inserting $\delta_0 = 2\pi^2\epsilon$, we arrive at

$$Z(\beta_1, \dots, \beta_m)^{\text{top.}} = \sum_{g,n=0}^{+\infty} \frac{(g_s \beta^{\frac{3}{2}})^{2g-2+m} (2\pi^2\epsilon\beta)^n}{(2\pi)^{\frac{m}{2}} n!} \cdot \sum_{\ell_1, \dots, \ell_m=0}^{+\infty} \mathbf{b}_1^{\ell_1+\frac{1}{2}} \dots \mathbf{b}_m^{\ell_m+\frac{1}{2}} \langle \tau_0^n \tau_{\ell_1} \dots \tau_{\ell_m} \rangle_g + \mathcal{O}(\beta^{-1}), \quad (3.4)$$

in terms of the non-vanishing correlators (2.5) on the moduli space of stable curves $\overline{\mathcal{M}}_{g,m+n}$ of genus g with $m+n$ marked points.¹¹ The string equation of topological correlators implies (except for the genus zero correlator $\langle \tau_0 \tau_0 \tau_0 \rangle_0 = 1$) [26]

$$\langle \tau_0^n \tau_{\ell_1} \dots \tau_{\ell_m} \rangle_g = \sum_{p_1+\dots+p_m=n} \frac{n!}{p_1! \dots p_m!} \langle \tau_{\ell_1-p_1} \dots \tau_{\ell_m-p_m} \rangle_g, \quad (3.5)$$

where $\langle \tau_{a_1} \dots \tau_{a_m} \rangle_g = 0$ if any $a_i, i = 1, \dots, m$, is negative.

Following ref. [30], we express the low temperature limit by applying the results of ref. [39]. Namely, let us define the generating function \mathcal{F} of topological correlators with m marked points as

$$\begin{aligned} \mathcal{F}(x) &= \frac{1}{x^2} + \sum_{\ell=0}^{+\infty} \sum_{g=1}^{+\infty} x^\ell \langle \tau_\ell \rangle_g, \\ \mathcal{F}(x_1, x_2) &= \frac{1}{x_1 + x_2} + \sum_{\ell_1, \ell_2=0}^{+\infty} \sum_{g=1}^{+\infty} x_1^{\ell_1} x_2^{\ell_2} \langle \tau_{\ell_1} \tau_{\ell_2} \rangle_g, \\ \mathcal{F}(x_1, \dots, x_m) &= \sum_{\ell_1, \dots, \ell_m=0}^{+\infty} \sum_{g=0}^{+\infty} x_1^{\ell_1} \dots x_m^{\ell_m} \langle \tau_{\ell_1} \dots \tau_{\ell_m} \rangle_g \quad \text{for } m \geq 3. \end{aligned} \quad (3.6)$$

Using these expressions with the string equation (3.5) and formula $\langle \tau_{\alpha_1} \dots \tau_{\alpha_n} \rangle_0 = \frac{(n-3)!}{\alpha_1! \dots \alpha_n!}$ we arrive from eq. (3.4) (for any $m \geq 1$) at

$$Z(\beta_1, \dots, \beta_m) = \prod_{i=1}^m \sqrt{\frac{g_s^{\frac{2}{3}} \beta_i}{2\pi}} e^{2\pi^2 \epsilon \beta_i} \mathcal{F}(g_s^{2/3} \beta_1, \dots, g_s^{2/3} \beta_m) + \mathcal{O}(\beta^{-1}), \quad (3.7)$$

because $Z(\beta_1, \dots, \beta_m)^{\text{top.}} = Z(\beta_1, \dots, \beta_m)$ for $m > 2$ while the semi-classical terms of the partition functions $Z(\beta_1)$ and $Z(\beta_1, \beta_2)$ are included in the leading non-polynomial terms in $\mathcal{F}(x)$ and $\mathcal{F}(x_1, x_2)$, respectively.

For this generating functions Okounkov has developed a remarkable formula spelt out in ref. [39], namely

$$\mathcal{F}(x_1, \dots, x_m) = \frac{(2\pi)^{m/2}}{\sqrt{x_1 \dots x_m}} \mathcal{G}(2^{-1/3} x_1, \dots, 2^{-1/3} x_m), \quad (3.8)$$

¹¹The correction terms $\mathcal{O}(\beta^{-1})$ depend on the genus expansion parameter g_s and the coupling ϵ in such a way that in the double scaling limit (3.1) they approach zero at least with the rate $\sim 1/\beta$.

where

$$\mathcal{G}(x_1, \dots, x_m) = \sum_{\alpha \in \Pi_m} \frac{(-1)^{\ell(\alpha)+1}}{\ell(\alpha)} \sum_{\sigma \in S_{\ell(\alpha)}} \mathcal{E}(\sigma(x_\alpha)) . \quad (3.9)$$

Here the first sum is taken over the partitions Π_m of the set $\{1, \dots, m\}$ with m elements where the individual partitions α characterised by their length $\ell(\alpha)$. Furthermore, to each partition α of length $\ell(\alpha)$ is assigned a vector x_α of length $\ell(\alpha)$, where the individual entries of x_α are in turn given by sums of the variables x_i indexed by the subsets in α . For example the partition $\alpha = \{\{1, 3, 6\}, \{2\}, \{4, 5\}\} \in \Pi_6$ of length $\ell(\alpha) = 3$ yields the vector $x_\alpha = (x_1 + x_3 + x_6, x_2, x_4 + x_5)$. The second sum runs over the permutations σ in the symmetric group $S_{\ell(\alpha)}$ of size $\ell(\alpha)$, where $\sigma(x_\alpha)$ permutes the entries of the vector x_α of length $\ell(\alpha)$. Finally, the function $\mathcal{E}(x_1, \dots, x_\ell)$ is defined as

$$\mathcal{E}(x_1, \dots, x_\ell) = \frac{1}{2^{\ell} \pi^{\ell/2}} \frac{e^{\frac{1}{12} \sum_{i=1}^{\ell} x_i^3}}{\sqrt{x_1 \cdots x_\ell}} \int_{y_i \geq 0} dy_1 \cdots dy_\ell e^{-\sum_{i=1}^{\ell} \frac{(y_i - y_{i+1})^2}{4x_i} - \sum_{i=1}^{\ell} \frac{y_i + y_{i+1}}{2} x_i} , \quad (3.10)$$

with $y_{\ell+1} \equiv y_1$. For further details on the function $\mathcal{G}(x_1, \dots, x_m)$ see the original definitions in refs. [39].

Using the integral formulation of the generating functions \mathcal{F} , in the low temperature limit the partition function $Z(\beta)$ is calculated to be

$$Z(\beta) = \frac{e^{\frac{g_s^2}{24} \beta^3 + 2\pi^2 \epsilon \beta}}{\sqrt{2\pi} g_s \beta^{\frac{3}{2}}} + \mathcal{O}(\beta^{-1}) , \quad (3.11)$$

while the partition function $Z(\beta_1, \beta_2)$ becomes

$$Z(\beta_1, \beta_2) = \frac{e^{\frac{g_s^2}{24} (\beta_1 + \beta_2)^3 + 2\pi^2 \epsilon (\beta_1 + \beta_2)}}{\sqrt{2\pi} g_s (\beta_1 + \beta_2)^{\frac{3}{2}}} \operatorname{erf}(2^{-3/2} g_s \sqrt{\beta_1 \beta_2 (\beta_1 + \beta_2)}) + \mathcal{O}(\beta^{-1}) , \quad (3.12)$$

in terms of the error function

$$\operatorname{erf}(x) = \frac{2}{\sqrt{\pi}} \int_0^x du e^{-u^2} = \frac{2}{\sqrt{\pi}} \left(x - \frac{x^3}{3} + \frac{x^5}{10} - \dots \right) . \quad (3.13)$$

3.2 Low temperature expansion schemes

The corrections $\mathcal{O}(\beta^{-1})$ to the low temperature limit in eq. (3.7) are perturbatively included order-by-order by evaluating the subleading terms of eq. (3.3). For explicitness we focus on the partition function $Z(T)$ with a single boundary component with temperature $T \equiv \beta^{-1}$, and we want to study its low temperature corrections

$$Z(\epsilon; T) = \frac{T^{\frac{3}{2}} e^{\frac{g_s^2}{24T^3} + \frac{2\pi^2 \epsilon}{T}}}{\sqrt{2\pi} g_s} \mathcal{Z}_\epsilon(T) \quad \text{where} \quad \mathcal{Z}_\epsilon(T) = \sum_{\ell=0}^{+\infty} T^\ell z_\ell(g_s \beta^{3/2}, \epsilon \beta) . \quad (3.14)$$

The coefficient functions z_ℓ do not depend on the temperature T in the applied double scaling limit (3.1). By including these perturbative temperature corrections to all orders,

the partition function becomes an asymptotic series in T , i.e., the series does not contain any non-perturbative corrections that vanish in the limit $T \rightarrow 0$.

Compared to the (asymptotic) genus expansion studied in detail in section 2, the low temperature expansion (3.14) is more natural from a physics point of view, as for many physical problems one is interested in the result up to a certain energy scale. In particular, we see that by only taking the leading order contribution (3.11) we can immediately read off the threshold energy (2.111). Note, however, that since the coupling ϵ approaches zero in the low energy limit $T \rightarrow 0$, the ground state energy and the subleading temperature corrections in the expansion (3.14) depend on the details of the chosen double scaling limit. The limit (3.7) is naturally adapted to the defect coupling ϵ and the genus expansion parameter g_s . However, alternatively we can study other low temperature limits, where other ratios between physical parameters and the temperature T are kept constant. In the following, we refer to such different choices for the double scaling limits as distinct low temperature expansion schemes.

In addition to the scheme discussed in the previous subsection, we introduce the low temperature expansion scheme of ref. [29], which is naturally adapted to the variables (y, t) defined in eq. (2.72) by the double scaling limit

$$\beta \rightarrow +\infty \quad \text{with} \quad \frac{g_s \beta^{\frac{3}{2}}}{t} = \text{const.}, \quad y\beta = \text{const.} \quad . \quad (3.15)$$

Solving eq. (2.72) for small deformations δ_k , $k = 1, 2, 3, \dots$, away from pure JT gravity yields for the coupling parameters (y, t) appearing in the above limit the expansion

$$\begin{aligned} y &= \delta_0 + \frac{1}{2}(2\delta_0\delta_1 - \delta_0^2) + \dots, \\ t &= 1 - (\delta_0 + \delta_1) + (\delta_0^2 - \delta_0\delta_1 - \delta_0\delta_2) + \dots, \end{aligned} \quad (3.16)$$

which at leading order for a single defect become $y = 2\pi^2\epsilon + \mathcal{O}(\epsilon^2)$ and $t = 1 + \mathcal{O}(\epsilon)$ (cf. eq. (2.110)). This low temperature expansion scheme agrees at leading order in ϵ with the scheme (3.1), and in particular, upon inserting the on-shell values for (y, t) in the absence of defects, i.e., setting $\epsilon = 0$ such that $(y, t) = (0, 1)$, the two low temperature expansion schemes become the same.

In the latter scheme the (asymptotic) low temperature expansion of the partition function reads [29]

$$Z(y, t; T) = \frac{T^{\frac{3}{2}} e^{\frac{g_s^2}{24t^2 T^3} + \frac{y}{T}}}{\sqrt{2\pi} g_s} \mathcal{Z}_{y,t}(T) \quad \text{where} \quad \mathcal{Z}_{y,t}(T) = \sum_{\ell=0}^{+\infty} T^\ell z_\ell(y, t), \quad (3.17)$$

where the coefficient functions $z_\ell(y, t)$ now differ from the coefficient functions $z_\ell(g_s\beta^{3/2}, \epsilon\beta)$ in eq. (3.14) (even after inserting the functional relations among their respective arguments).¹²

¹²There is actually a subtlety here. While the coefficient functions $z_\ell(g_s\beta^{3/2}, \epsilon\beta)$ are temperature independent in the double scaling limit (3.1), the functions $z_\ell(y, t)$ are still temperature dependent in the limit (3.15). One can obviously define temperature independent coefficients in the latter case as well. However, as discussed in the following the coefficient functions $z_\ell(y, t)$ are conveniently computable and

For completeness, let us briefly review the strategy of ref. [29] to compute the coefficients $z_\ell(y, t)$. First of all, the coefficients $z_\ell(y, t)$ are conveniently determined from the low temperature expansion of the function $W(y, t; \beta)$ defined in eq. (2.80). Using the ansatz

$$W(y, t; T) = \sqrt{\frac{T}{4\pi}} e^{\frac{g_s^2}{24t^2 T^3} + \frac{y}{T}} \mathcal{W}_{y,t}(T) \quad \text{where} \quad \mathcal{W}_{y,t}(T) = \sum_{\ell=0}^{\infty} T^\ell w_\ell(y, t), \quad (3.18)$$

together with equation (2.83) yields the differential equation

$$\partial_t \mathcal{W}_{y,t} = \frac{g_s^2}{12t^3 T^3} \mathcal{W}_{y,t} - \sum_{g=1}^{\infty} g_s^{2g} u_g \nabla(T) \mathcal{W}_{y,t} + \frac{g_s^2}{12} \nabla(T)^3 \mathcal{W}_{y,t}, \quad (3.19)$$

in terms of the differential operator

$$\nabla(T) = \partial_0 + \frac{1}{tT} + \frac{g_s^2 I_2}{12t^4 T^3} = \frac{1}{t} (-I_2 \partial_t + D_y) + \frac{g_s^2 I_2}{12t^4 T^3}, \quad D_y = \partial_y + \frac{1}{T}, \quad (3.20)$$

which then recursively determines the coefficient functions $w_\ell(y, t)$.¹³ Finally, the relation (2.76) translates to

$$\mathcal{W}_{y,t} = T \nabla(T) \mathcal{Z}_{y,t}, \quad (3.21)$$

leading for the coefficient functions $z_\ell(y, t)$ to the recursion formula [29]

$$z_\ell = t \left(\ell! w_\ell - \ell \left(\nabla(T) - \frac{1}{tT} \right) z_{\ell-1} \right). \quad (3.22)$$

The first few coefficient functions z_ℓ are calculated to be

$$\begin{aligned} z_0 &= t, & z_1 &= \left(1 + \frac{g_s^4}{240t^4 T^6} \right) I_2, \\ z_2 &= \left(\frac{7g_s^4}{240t^5 T^6} + \frac{g_s^6}{576t^7 T^9} + \frac{g_s^8}{57600t^9 T^{12}} \right) I_2^2 \\ &\quad + \left(-2 + \frac{g_s^2}{12t^2 T^3} + \frac{g_s^4}{120t^4 T^6} + \frac{g_s^6}{3360t^6 T^9} \right) I_3. \end{aligned} \quad (3.23)$$

Let us point out some physical implications of the low temperature expansion scheme in the variables (y, t) . For the on-shell values (2.110) of (y, t) for JT gravity coupled to a gas of defect and compared to the expansion scheme (3.14), the low temperature expansion of the partition function depends on the identification angle α already at leading orders in the temperature T . Namely compared to the result (3.11) one finds upon inserting eq. (2.110) into the expansion (3.17)

$$Z(T) = \frac{\left(1 + \frac{\alpha^2 - 4\pi^2}{2} \epsilon + \dots \right) T^{\frac{3}{2}} e^{\frac{g_s^2}{24T^3} + \frac{g_s^2(4\pi^2 - \alpha^2)}{24T^3} \epsilon + \frac{2\pi^2}{T} \epsilon + \dots}}{\sqrt{2\pi} g_s} + \mathcal{O}(T), \quad (3.24)$$

where the dots ‘...’ indicate subleading terms in ϵ at order $\mathcal{O}(\epsilon^2)$.

comparable with ref. [29]. Truncating the infinite sum in $\mathcal{Z}_{y,t}$ at some finite value $\ell = N$ yields unambiguously the low temperature corrections up to order T^N in the discussed expansion scheme (because the temperature dependence only gives rise to corrections at order $\mathcal{O}(T^{N+1})$).

¹³The first few coefficient functions w_ℓ are calculated and spelled out explicitly in ref. [29].

The above analysis of the low temperature limit is general in the sense that we can consider other on-shell values for the couplings (y, t) (and also for the couplings $t_k = \gamma_k + \delta_k$ appearing implicitly in the expansion (3.17)). In particular, if we consider small deviations from the on-shell values $(y, t) = (1, 0)$ (and small perturbations δ_k for $k \geq 2$) of pure JT gravity, we can study the low temperature expansions of deformations to pure JT gravity together with their scheme dependence.

A particularly interesting example in this context is discussed in ref. [24], which corresponds to coupling JT gravity to a gas of defects with two types of defect species characterized by their couplings $\epsilon_1 = -\epsilon_2 = \epsilon$, which are aligned with opposite sign, and their respective identification angles α_1 and α_2 . On the one hand, for the low temperature double scaling limit (3.1) we arrive at

$$Z(T) = \frac{T^{\frac{3}{2}} e^{\frac{g_s^2}{24T^3}}}{\sqrt{2\pi} g_s} + \mathcal{O}(T), \tag{3.25}$$

which results in an expected vanishing threshold energy, cf. eq. (2.111). On the other hand the double scaling limit (3.15) yields

$$Z(T) = \frac{(1 + \frac{(\alpha_1^2 - \alpha_2^2)}{2}\epsilon + \dots) T^{\frac{3}{2}} e^{\frac{g_s^2}{24T^3} + \frac{g_s^2(\alpha_2^2 - \alpha_1^2)}{24T^3}\epsilon + \dots}}{\sqrt{2\pi} g_s} + \mathcal{O}(T), \tag{3.26}$$

where a non-trivial dependence on the identification angles α_1 and α_2 now enters because the couplings (y, t) govern the physical quantities that are kept constant in the double scaling limit (3.15).

3.3 Low temperature expansion schemes for multiple boundaries

Finally, let us remark that the low temperature discussion of the previous subsection can be repeated with multiple boundary components in the same way. The low temperature expansion in this case is studied by Okuyama and Sakai in ref. [30].

As a preparation for section 4, we just record here the result of the low temperature limit for the partition function $Z(\beta_1, \beta_2)$ with two boundary components with inverse temperatures β_1 and β_2 . Then the low temperature expansion scheme (3.15) generalises to the double scaling limit

$$\beta_i \rightarrow +\infty \quad \text{with} \quad \frac{g_s \beta_i^{\frac{3}{2}}}{t} = \text{const.}, \quad y\beta_i = \text{const.} \quad \text{for} \quad i = 1, 2, \tag{3.27}$$

which yields for the low temperature limit of the partition function $Z(\beta_1, \beta_2)$ the result [30]

$$Z(y, t; \beta_1, \beta_2) = \frac{t e^{\frac{g_s^2(\beta_1 + \beta_2)^3}{24t^2} + y(\beta_1 + \beta_2)}}{\sqrt{2\pi} g_s (\beta_1 + \beta_2)^{\frac{3}{2}}} \text{erf} \left(\frac{g_s}{2\sqrt{2}t} \sqrt{\beta_1 \beta_2 (\beta_1 + \beta_2)} \right) + \mathcal{O}(\beta_1^{-1}, \beta_2^{-1}). \tag{3.28}$$

4 Phase transition and spectral form factor

Using the low temperature limit of the partition functions $Z(y, t; \beta_1, \beta_2)$ and $Z(y, t; \beta)$ of the previous section and applying numerical methods, we study two well-established and



Figure 1. The left figure shows a disconnected geometry — here illustrated in terms of two AdS_2 disks at genus zero — that dominates the spectral form factor at early times τ , whereas the right figure depicts a connected geometry with two boundaries — shown is the double trumpet contribution — that becomes dominant at late times τ .

related phenomena, namely the phase transition [61, 62], which exchanges the dominance between the connected versus the disconnected geometries in the two boundary partition function, and the spectral form factor,¹⁴ which arises as a certain analytic continuation of the two-boundary partition function. In particular, we analyse the dependence of these quantities in the presence of defects.

Phase transition. There are two types of geometries that contribute to the two-point function. On the one hand there are geometries with two disconnected components, each with a single boundary component, and on the other hand there are connected geometries with two boundary components, as illustrated in figure 1 (where only the genus zero contributions are depicted for simplicity). At low temperatures we have according to eqs. (3.17) and (3.28) (in the chosen low temperature expansion scheme) the following two quantities

$$\begin{aligned}
 Z(y, t; \beta)^2 &= \frac{e^{2y\beta} e^{\frac{g_s^2 \beta^3}{12t^2}}}{2\pi g_s^2 \beta^3} t^2 + \mathcal{O}(\beta^{-1}), \\
 Z(y, t; \beta, \beta) &= \frac{e^{2y\beta} e^{\frac{\beta^3 g_s^2}{3t^2}}}{4\sqrt{\pi} \beta^{3/2} g_s} t \operatorname{erf}\left(\frac{\beta^{3/2} g_s}{2t}\right) + \mathcal{O}(\beta^{-1}).
 \end{aligned}
 \tag{4.1}$$

Independent of the specific choices for the on-shell values of the parameters (y, t) , we can make some quite general comments. Taking the ratio of the two-point contributions in eq. (4.1), the dependence on the shift in energy given by y drops out (at leading order in the temperature). Hence, the phase transition (and as a consequence also the spectral form factor introduced later) is determined by the off-shell parameter t . Explicitly analysing the ratio of the two contributions (4.1) in the low temperature regime yields with the dimensionless constant $c := g_s \beta^{3/2} / t$ the dimensionless (numerical) critical value c_{crit} . for the phase transition according to

$$\frac{Z(y, t; \beta, \beta)}{Z(y, t; \beta)^2} = 1 \Rightarrow \frac{1}{2} \sqrt{\pi} c e^{\frac{c^2}{4}} \operatorname{erf}\left(\frac{c}{2}\right) = 1 \Rightarrow c_{\text{crit}} \approx \pm 1.24013.
 \tag{4.2}$$

Let us now focus on JT gravity with defects. This means that we take (y, t) to their on-shell values (2.108) and that we work with the quantities in eq. (4.3), where the on-shell

¹⁴The spectral form factor was first introduced in the AdS/CFT context in ref. [63].

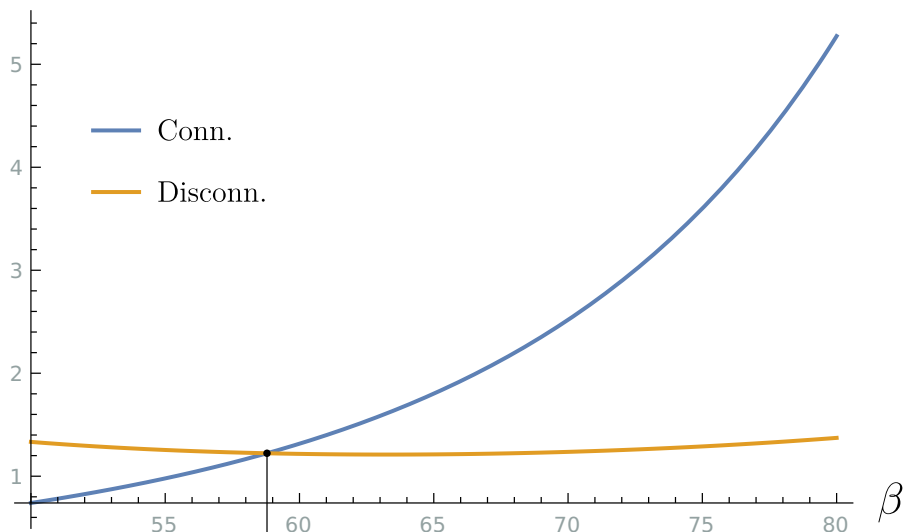


Figure 2. We plot the connected versus the disconnected geometry contributions of eq. (4.3). The identification angle α is fixed to $\alpha = \frac{\pi}{2}$, the defect amplitude is $\epsilon = 0.001$ and $g_s = 0.0027$. In the range of the plot we have a maximum of $\sim 4.2\%$ relative error, which measures the ratio of the terms ignored (order T^2) over the terms kept in the low temperature expansion.

values of (y, t) are found numerically for a given set of ϵ and α , i.e.

$$\begin{aligned}
 Z(\beta)^2 &= \frac{e^{2y\beta} e^{\frac{g_s^2 \beta^3}{12t^2}}}{2\pi g_s^2 \beta^3} t^2 \Bigg|_{y,t \text{ on-shell}}, \\
 Z(\beta, \beta) &= \frac{e^{2y\beta} e^{\frac{\beta^3 g_s^2}{3t^2}}}{4\sqrt{\pi} \beta^{3/2} g_s} t \operatorname{erf}\left(\frac{\beta^{3/2} g_s}{2t}\right) \Bigg|_{y,t \text{ on-shell}}.
 \end{aligned}
 \tag{4.3}$$

Keeping the above in mind, we plot the connected and disconnected parts of the two-point function in figure 2. We can see the general behaviour of JT gravity in the absence of defects is reproduced: at high temperatures the disconnected geometry dominates, whereas for low temperatures the connected part constitutes the more dominant contribution [22, 30]. This is the two-dimensional instantiation of a Hawking-Page phase transition [3, 64]. However, we should also notice that, as shown in figure 3, for larger ϵ , the phase transition occurs at a smaller value of β .

Spectral form factor. Now we come to the analysis of the spectral form factor $Z(\beta + i\tau, \beta - i\tau)$, which is a real function of the time τ defined via an analytic continuation of the two-point function $Z(\beta_1, \beta_2)$. The spectral form factor is essential in the analysis of quantum chaotic behaviour and plays an increasingly important role in the study of black hole physics [13]. For the case of JT gravity in the presence of defects the spectral form factor has not yet been analysed. The task is to understand the role of the parameter ϵ .

For large groups of systems obeying quite common assumptions (such as the eigenstate thermalisation hypothesis [65, 66]), one expects the spectral form factor to exhibit certain

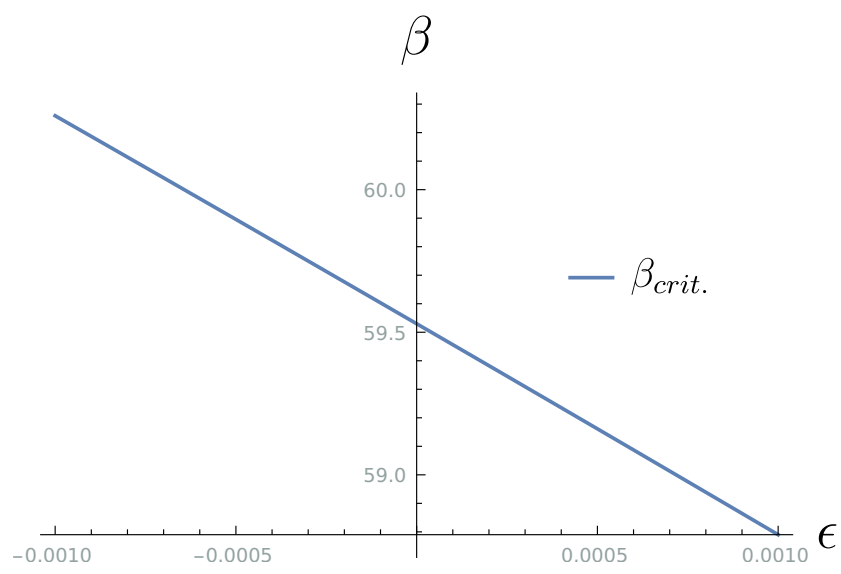


Figure 3. The phase transition temperature (the point for which $Z(\beta, \beta) = Z(\beta)^2$) as a function of the defect amplitude. The identification angle α is fixed to $\alpha = \frac{\pi}{2}$ and $g_s = 0.0027$.

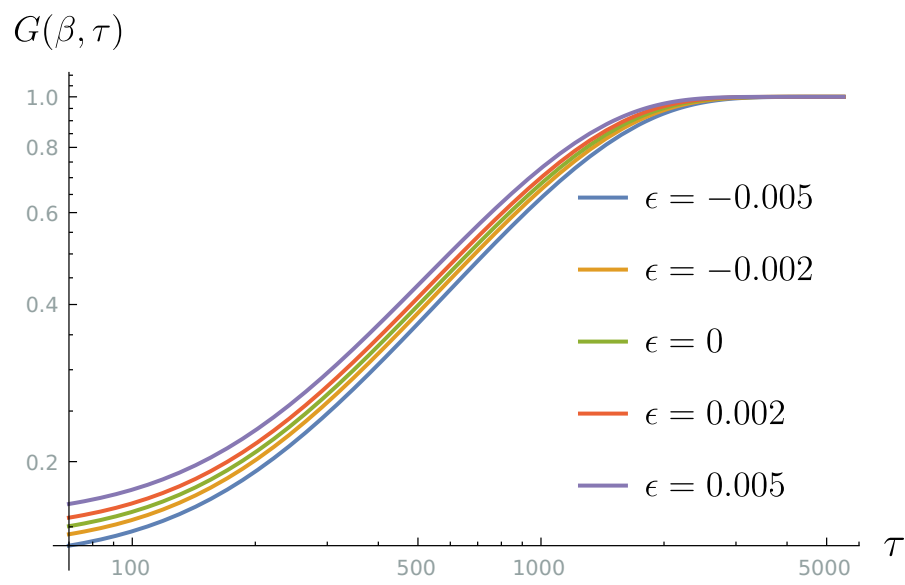


Figure 4. Shown is the spectral form factor for different values of ϵ with $g_s = \frac{1}{4 \cdot 180^{3/2}}$, $\beta = 180$, $\alpha = \pi/2$.

universal features. Early times are characterised by decay and hence a “slope”, followed by a rise and hence a “ramp”, and lastly at late times we encounter a “plateau” with fixed value given by the one-point function $Z(2\beta)$.¹⁵ Let us define the normalised spectral form factor in the following manner

$$G(\beta, \tau) := \frac{Z(\beta + i\tau, \beta - i\tau)}{Z(2\beta)} = \operatorname{erf} \left(\frac{\beta^{3/2} g_s \sqrt{\frac{\tau^2}{\beta^2} + 1}}{2t} \right), \quad (4.4)$$

where we are normalising with respect to the contribution $Z(2\beta)$ as this sets the height of the plateau. Due to the low temperature dominance of the connected contribution as outlined above, we would expect late times to be dominated by connected contributions. A closer look at eq. (4.1) shows that this is guaranteed by the functional form of both expressions. We are only considering connected geometries in eq. (4.4) as we are mainly interested in the ramp and plateau behaviour. We want to reiterate some statements of refs. [12, 30], which help in understanding the importance of the corrections outlined in section 3.1. The $g = 0$ part of the two-boundary correlator only furnishes the “ramp” behaviour as shown in ref. [61]. We can see that the approximation (3.1) already allows for the creation of the plateau [30]. Furthermore, if we work in the limit (3.15) both the phase transition and spectral form factor become sensitive to the presence of defects.

We note that the transition from ramp to plateau now depends on ϵ . More specifically, for larger values of ϵ we can move it to earlier times, whereas negative values moves it to later times, which mirrors the behaviour discovered for the phase transition.

We may also consider changes in the identification angle α while keeping ϵ fixed for both the phase transition and the spectral form factor. While the dependence on α within the range $0 \leq \alpha < \pi$ can be studied straightforwardly with the methods presented here, it would be even more interesting to consider changes in α over the full range of identification angles. This could possibly be achieved by implementing the results of ref. [42].

5 Some comments on two-dimensional de Sitter space

In both refs. [40, 41] a proposal is made for the application of the matrix model/JT duality to two-dimensional de Sitter space. The logic is the following: as Lorentzian de Sitter space can be analytically continued to Euclidean Anti-de Sitter space [67], in the two-dimensional setting there should exist a map translating the results for the partition function of ref. [12] to the wavefunction of the universe Ψ at future infinity \mathcal{I}^+ and past infinity \mathcal{I}^- [40, 41]. For the semi-classical contribution it can be shown that the wavefunction can be mapped to the disk result via the identification

$$\beta \rightarrow \begin{cases} -i\ell, & \text{future} \\ i\ell, & \text{past} \end{cases} \quad (5.1)$$

¹⁵The “plateau” cannot be obtained if the perturbative series is truncated at some finite g . To render an asymptotic series convergent non-perturbative contributions have to be taken into account [61]. In the zero temperature/zero coupling limit considered in ref. [29] and here the perturbative series converges.

where ℓ is the renormalised length of both the future and past circles. For higher genus contributions an approach was outlined in ref. [41], in which the boundary conditions inherited from de Sitter space require the analytic continuation of the geodesic length $b \rightarrow i\alpha$ such that this instance of JT gravity requires the inclusion of surfaces with conical singularities. Sticking to the one-point function for the moment, following ref. [41] the wave function on a single future boundary would be given by

$$\begin{aligned} \Psi(\ell) &= \frac{(2\pi^2)^{3/2}}{g_s} Z^{\text{disk}}(-i\ell) - \sum_{g=1}^{\infty} g_s^{2g-1} \int_0^{\infty} d\alpha \alpha \frac{e^{\frac{i\alpha^2}{4\pi^2\ell}}}{2\pi\sqrt{\pi}\sqrt{-i\ell}} V_{g,(i\alpha)} \\ &= \frac{(2\pi^2)^{3/2}}{g_s} Z^{\text{disk}}(-i\ell) + \frac{1}{g_s^2} B(-i\ell) F(\{\gamma_k\}) . \end{aligned} \tag{5.2}$$

which would indeed correspond to $Z(-i\ell)$. In general this approach implies that the mere analytic continuation (5.1) of the partition function of ref. [12] corresponds to the wave function Ψ , i.e.

$$\begin{aligned} \Psi_{\text{conn.}}(\ell_1, \dots, \ell_{n_+}, \ell_{n_++1}, \dots, \ell_{n_-}) \\ \cong \left\langle \text{tr} \left(e^{i\ell_1 H} \right) \dots \text{tr} \left(e^{i\ell_{n_+} H} \right) \text{tr} \left(e^{-i\ell_{n_++1} H} \right) \dots \text{tr} \left(e^{-i\ell_{n_-} H} \right) \right\rangle , \end{aligned} \tag{5.3}$$

However, as clearly stated in ref. [41], for eqs. (5.2) and (5.3) to hold in full generality it is necessary that the conical volumes are obtained from a mere analytic continuation as in eq. (2.15). This, however, is only established for $\alpha < \pi$, whereas the results of ref. [42] propose for general identification angles α an implicit definition of Weil-Petersson volumes that goes beyond the analytic continuation prescription of eq. (2.15). Hence, due to the integration range over α in eq. (5.2), the naive analytic continuation of the individual volumes $V_{g,(b)}$ of the (asymptotic) thermal partition function possibly requires a further modification to the approach of ref. [41] for the computation of the wavefunction Ψ .¹⁶ Moreover, the authors of ref. [41] show that eq. (5.3) may be derived from the approach of ref. [68], such that the wavefunction Ψ is also equivalent to the no-boundary wavefunction. Therefore, further investigation is required in order to understand in how far the correspondence of the Hartle-Hawking construction of ref. [68] and the approach of ref. [41] via continuation to Euclidean Anti-de Sitter space holds at the non-perturbative level and in how far the validity of eq. (5.3) is guaranteed beyond the semi-classical level.¹⁷

6 Conclusion and outlook

In this work we compute thermal partition functions of deformed JT gravity theories from solutions to the KdV hierarchy. These solutions govern the correlation functions of two-dimensional topological gravity, and — similarly as in ref. [29] — we describe both undeformed and a rather general class of deformed theories of JT gravity in terms of solutions

¹⁶Although it is not immediately clear if the path integral may be performed in the same manner as in ref. [41] for the volumes of ref. [42]. See comments in ref. [42].

¹⁷We would like to thank Joaquin Turiaci for valuable correspondence on these points.

to the KdV hierarchy. In refs. [23, 24] deformations of JT gravity are described by suitable scalar potentials that do not alter the asymptotic boundaries of the two-dimensional hyperbolic space-time geometries. It would be interesting to relate deformations arising from scalar potentials to solutions of the KdV hierarchy in the topological gravity description. While we can identify certain classes of deformations in both formulations — in particular those that arise from a gas of defects with a finite number of defect species — it would be interesting to investigate whether these two approaches towards deformations of JT gravity are actually in one-to-one correspondence. As both descriptions yield infinite dimensional deformation spaces, a meaningful comparison of the two approaches to the deformation problem presumably requires a careful treatment using methods of functional analysis.

Interestingly, both standard JT gravity and JT gravity interacting with a finite number of defect species are governed by spectral densities given in terms of (modified) Bessel functions, whereas for more general deformations other transcendental functions occur. Therefore, it would be interesting to understand in how far standard JT gravity and JT gravity interacting with a gas of defects are singled out from other solutions to the KdV hierarchy. For instance, the Witten-Kontsevich tau-function relates to the free energy of two-dimensional topological gravity [26, 27] and the Brézin-Gross-Witten tau-function describes JT supergravity [53]. Yet other tau-functions are discussed from the mathematical perspective in ref. [69]. As the connection between specific solutions to the KdV hierarchy and two-dimensional gravitational theories does not seem to be arbitrary, a systematic investigation of tau functions and the associated physical theories is an interesting idea to pursue.

As already addressed in ref. [12], the discussed solutions to the KdV hierarchy and the resulting thermal partition functions are asymptotic series in the genus expansion parameter g_s , which are only rendered to analytic functions once non-perturbative effects are taken into account. Therefore, a challenging task is to derive solutions to the KdV hierarchy that are analytic instead of just being an asymptotic series in the parameter g_s . In refs. [70, 71] a non-perturbative completion of the solutions to the KdV hierarchy is proposed that has recently been applied to JT gravity in an interesting series of works [20, 22, 60]. Both the results of ref. [29] and our work furnish an easy and systematic access to higher genus contributions, such that modern resurgence techniques could come into play to address non-perturbative effects in this context. Similar considerations in that direction are made in ref. [72] for JT gravity with a finite cutoff at the asymptotic space-time boundaries,¹⁸ where a Borel resummation can be performed for the asymptotic series with respect to the cutoff parameter.

Applying the approach developed by Okuyama and Sakai [29, 30], we compute in a certain low temperature limit the thermal partition functions (with one or more boundary components) for JT gravity with deformations such as those arising from the presence of a gas of defects. In this limit the studied thermal partition functions become exact because non-perturbative corrections are suppressed. We determine the critical temperature of the

¹⁸More work on JT gravity restricted to a finite AdS_2 subregion can be found in refs. [73, 74]. The general paradigm of finite cutoff AdS/CFT was first explored in ref. [75].

Hawking-Page phase transition as a function of the defect parameters by analysing the two-boundary partition function with numerical methods. Depending on the sign of the defect coupling constant we find that the phase transition either occurs at higher or lower temperatures. The spectral form factor exhibits a similar behaviour, namely the time scale for the onset of the plateau is shifted to earlier or later times depending on the sign of the defect coupling. While we expect that this behaviour of the phase transition and the spectral form factor as a function of the defect parameters does not change upon including further subleading temperature corrections, it is nevertheless desirable to include further terms in the low temperature expansion in order to reliably analyse the Hawking-Page phase transition and the spectral form factor as a function of the defect parameters at higher temperature scales. JT gravity in the presence of defects is linked to 3d gravity in the near-extremal limit, as reported in ref. [23]. It would be nice to understand and to interpret the changes in both the Hawking-Page phase transition and the spectral form factor more explicitly in that context.

We briefly comment on a possible matrix model/JT gravity duality for two-dimensional de Sitter backgrounds. Here we point out an apparent puzzle in light of the recent results of ref. [42], which suggest that the Weil-Petersson volumes in the presence of conical singularities with large identification angles are in general not obtained via analytic continuation from surfaces with conical singularities with small identification angles. As a consequence, computing the wave function of the universe for JT gravity on two-dimensional de Sitter by use of analytic continuation techniques may only be an approximation. It is, however, still possible that upon going beyond the study of asymptotic series the validity of this approach is nevertheless justified. We believe that this issue deserves further study.

Acknowledgments

We would like to thank Alexander Belavin, Clifford Johnson, Joaquin Turiaci, Kefeng Liu, and Hao Xu for discussions and correspondences. The work of H.J. is supported by the Cluster of Excellence “Precision Physics, Fundamental Interactions and Structure of Matter” (PRISMA+ — EXC 2118/1). The work of J.K.K. is supported in part by the Heising-Simons Foundation, the Simons Foundation, and National Science Foundation Grant No. NSF PHY-1748958. A.K. is supported by the “Onassis Foundation” as an “Onassis Scholar” (Scholarship ID: F ZO 030/2 (2020-2021)). S.F., J.K.K., and A.K. acknowledge support by the Bonn Cologne Graduate School of Physics and Astronomy (BCGS).

Open Access. This article is distributed under the terms of the Creative Commons Attribution License ([CC-BY 4.0](https://creativecommons.org/licenses/by/4.0/)), which permits any use, distribution and reproduction in any medium, provided the original author(s) and source are credited.

References

- [1] R. Jackiw, *Lower dimensional gravity*, *Nucl. Phys. B* **252** (1985) 343 [[INSPIRE](#)].
- [2] C. Teitelboim, *Gravitation and Hamiltonian structure in two space-time dimensions*, *Phys. Lett. B* **126** (1983) 41 [[INSPIRE](#)].

- [3] J. Maldacena, D. Stanford and Z. Yang, *Conformal symmetry and its breaking in two dimensional Nearly Anti-de-Sitter space*, *PTEP* **2016** (2016) 12C104 [[arXiv:1606.01857](#)] [[INSPIRE](#)].
- [4] A. Almheiri and J. Polchinski, *Models of AdS₂ backreaction and holography*, *JHEP* **11** (2015) 014 [[arXiv:1402.6334](#)] [[INSPIRE](#)].
- [5] K. Jensen, *Chaos in AdS₂ Holography*, *Phys. Rev. Lett.* **117** (2016) 111601 [[arXiv:1605.06098](#)] [[INSPIRE](#)].
- [6] J. Engelsöy, T.G. Mertens and H. Verlinde, *An investigation of AdS₂ backreaction and holography*, *JHEP* **07** (2016) 139 [[arXiv:1606.03438](#)] [[INSPIRE](#)].
- [7] P. Nayak, A. Shukla, R.M. Soni, S.P. Trivedi and V. Vishal, *On the dynamics of near-extremal black holes*, *JHEP* **09** (2018) 048 [[arXiv:1802.09547](#)] [[INSPIRE](#)].
- [8] G. Sárosi, *AdS₂ holography and the SYK model*, *PoS(Modave2017)001* [[arXiv:1711.08482](#)] [[INSPIRE](#)].
- [9] S. Sachdev and J. Ye, *Gapless spin fluid ground state in a random, quantum Heisenberg magnet*, *Phys. Rev. Lett.* **70** (1993) 3339 [[cond-mat/9212030](#)] [[INSPIRE](#)].
- [10] A. Kitaev and S.J. Suh, *The soft mode in the Sachdev-Ye-Kitaev model and its gravity dual*, *JHEP* **05** (2018) 183 [[arXiv:1711.08467](#)] [[INSPIRE](#)].
- [11] J. Maldacena and D. Stanford, *Remarks on the Sachdev-Ye-Kitaev model*, *Phys. Rev. D* **94** (2016) 106002 [[arXiv:1604.07818](#)] [[INSPIRE](#)].
- [12] P. Saad, S.H. Shenker and D. Stanford, *JT gravity as a matrix integral*, [arXiv:1903.11115](#) [[INSPIRE](#)].
- [13] J.S. Cotler et al., *Black holes and random matrices*, *JHEP* **05** (2017) 118 [Erratum *ibid.* **09** (2018) 002] [[arXiv:1611.04650](#)] [[INSPIRE](#)].
- [14] D. Stanford and E. Witten, *JT gravity and the ensembles of random matrix theory*, *Adv. Theor. Math. Phys.* **24** (2020) 1475 [[arXiv:1907.03363](#)] [[INSPIRE](#)].
- [15] F.J. Dyson, *Statistical theory of the energy levels of complex systems. I*, *J. Math. Phys.* **3** (1962) 140 [[INSPIRE](#)].
- [16] A. Altland and M.R. Zirnbauer, *Nonstandard symmetry classes in mesoscopic normal-superconducting hybrid structures*, *Phys. Rev. B* **55** (1997) 1142 [[cond-mat/9602137](#)] [[INSPIRE](#)].
- [17] M.R. Zirnbauer, *Riemannian symmetric superspaces and their origin in random-matrix theory*, *J. Math. Phys.* **37** (1996) 4986 [[math-ph/9808012](#)] [[INSPIRE](#)].
- [18] D. Stanford and E. Witten, *Fermionic localization of the Schwarzian theory*, *JHEP* **10** (2017) 008 [[arXiv:1703.04612](#)] [[INSPIRE](#)].
- [19] B. Eynard and N. Orantin, *Weil-Petersson volume of moduli spaces, Mirzakhani's recursion and matrix models*, [arXiv:0705.3600](#) [[INSPIRE](#)].
- [20] C.V. Johnson, *Nonperturbative Jackiw-Teitelboim gravity*, *Phys. Rev. D* **101** (2020) 106023 [[arXiv:1912.03637](#)] [[INSPIRE](#)].
- [21] C.V. Johnson, *Jackiw-Teitelboim supergravity, minimal strings, and matrix models*, *Phys. Rev. D* **103** (2021) 046012 [[arXiv:2005.01893](#)] [[INSPIRE](#)].

- [22] C.V. Johnson, *Explorations of nonperturbative Jackiw-Teitelboim gravity and supergravity*, *Phys. Rev. D* **103** (2021) 046013 [[arXiv:2006.10959](#)] [[INSPIRE](#)].
- [23] H. Maxfield and G.J. Turiaci, *The path integral of 3D gravity near extremality; or, JT gravity with defects as a matrix integral*, *JHEP* **01** (2021) 118 [[arXiv:2006.11317](#)] [[INSPIRE](#)].
- [24] E. Witten, *Matrix models and deformations of JT gravity*, *Proc. Roy. Soc. Lond. A* **476** (2020) 20200582 [[arXiv:2006.13414](#)] [[INSPIRE](#)].
- [25] T.G. Mertens and G.J. Turiaci, *Defects in Jackiw-Teitelboim quantum gravity*, *JHEP* **08** (2019) 127 [[arXiv:1904.05228](#)] [[INSPIRE](#)].
- [26] E. Witten, *Two-dimensional gravity and intersection theory on moduli space*, *Surveys Diff. Geom.* **1** (1991) 243 [[INSPIRE](#)].
- [27] M. Kontsevich, *Intersection theory on the moduli space of curves and the matrix Airy function*, *Commun. Math. Phys.* **147** (1992) 1 [[INSPIRE](#)].
- [28] M. Mirzakhani, *Simple geodesics and Weil-Petersson volumes of moduli spaces of bordered Riemann surfaces*, *Invent. Math.* **167** (2006) 179 [[INSPIRE](#)].
- [29] K. Okuyama and K. Sakai, *JT gravity, KdV equations and macroscopic loop operators*, *JHEP* **01** (2020) 156 [[arXiv:1911.01659](#)] [[INSPIRE](#)].
- [30] K. Okuyama and K. Sakai, *Multi-boundary correlators in JT gravity*, *JHEP* **08** (2020) 126 [[arXiv:2004.07555](#)] [[INSPIRE](#)].
- [31] M. Alishahiha, A. Faraji Astaneh, G. Jafari, A. Naseh and B. Taghavi, *Free energy for deformed Jackiw-Teitelboim gravity*, *Phys. Rev. D* **103** (2021) 046005 [[arXiv:2010.02016](#)] [[INSPIRE](#)].
- [32] C. Itzykson and J.B. Zuber, *Combinatorics of the modular group. 2. The Kontsevich integrals*, *Int. J. Mod. Phys. A* **7** (1992) 5661 [[hep-th/9201001](#)] [[INSPIRE](#)].
- [33] D.J. Gross and A.A. Migdal, *Nonperturbative two-dimensional quantum gravity*, *Phys. Rev. Lett.* **64** (1990) 127 [[INSPIRE](#)].
- [34] D.J. Gross and A.A. Migdal, *A nonperturbative treatment of two-dimensional quantum gravity*, *Nucl. Phys. B* **340** (1990) 333 [[INSPIRE](#)].
- [35] M.R. Douglas and S.H. Shenker, *Strings in less than one-dimension*, *Nucl. Phys. B* **335** (1990) 635 [[INSPIRE](#)].
- [36] E. Brézin and V.A. Kazakov, *Exactly solvable field theories of closed strings*, *Phys. Lett. B* **236** (1990) 144 [[INSPIRE](#)].
- [37] P.H. Ginsparg and G.W. Moore, *Lectures on 2D gravity and 2D string theory*, [hep-th/9304011](#) [[INSPIRE](#)].
- [38] A.A. Belavin and A.B. Zamolodchikov, *On correlation numbers in 2D minimal gravity and matrix models*, *J. Phys. A* **42** (2009) 304004 [[arXiv:0811.0450](#)] [[INSPIRE](#)].
- [39] A. Okounkov, *Generating functions for intersection numbers on moduli spaces of curves*, [math/0101201](#) [[INSPIRE](#)].
- [40] J. Maldacena, G.J. Turiaci and Z. Yang, *Two dimensional Nearly de Sitter gravity*, *JHEP* **01** (2021) 139 [[arXiv:1904.01911](#)] [[INSPIRE](#)].
- [41] J. Cotler, K. Jensen and A. Maloney, *Low-dimensional de Sitter quantum gravity*, *JHEP* **06** (2020) 048 [[arXiv:1905.03780](#)] [[INSPIRE](#)].

- [42] G.J. Turiaci, M. Usatyuk and W.W. Weng, *Dilaton-gravity, deformations of the minimal string, and matrix models*, [arXiv:2011.06038](#) [INSPIRE].
- [43] K. Okuyama and K. Sakai, *A proof of loop equations in 2d topological gravity*, *JHEP* **10** (2021) 107 [[arXiv:2106.05643](#)] [INSPIRE].
- [44] T.G. Mertens and G.J. Turiaci, *Liouville quantum gravity — Holography, JT and matrices*, *JHEP* **01** (2021) 073 [[arXiv:2006.07072](#)] [INSPIRE].
- [45] E. Arbarello and M. Cornalba, *Combinatorial and algebro-geometric cohomology classes on the moduli spaces of curves*, [alg-geom/9406008](#) [INSPIRE].
- [46] K. Liu and H. Xu, *Recursion formulae of higher Weil-Petersson volumes*, *Int. Math. Res. Not. IMRN* **5** (2009) 835 [[arXiv:0708.0565](#)].
- [47] S. Wolpert, *On the homology of the moduli space of stable curves*, *Ann. Math.* **118** (1983) 491.
- [48] M. Mulase and B. Safnuk, *Mirzakhani's recursion relations, Virasoro constraints and the KdV hierarchy*, [math/0601194](#) [INSPIRE].
- [49] R. Dijkgraaf and E. Witten, *Developments in topological gravity*, *Int. J. Mod. Phys. A* **33** (2018) 1830029 [[arXiv:1804.03275](#)] [INSPIRE].
- [50] M. Mirzakhani, *Weil-Petersson volumes and intersection theory on the moduli space of curves*, *J. Am. Math. Soc.* **20** (2007) 1 [INSPIRE].
- [51] V.A. Kazakov, *The appearance of matter fields from quantum fluctuations of 2D gravity*, *Mod. Phys. Lett. A* **4** (1989) 2125 [INSPIRE].
- [52] M. Staudacher, *The Yang-Lee edge singularity on a dynamical planar random surface*, *Nucl. Phys. B* **336** (1990) 349 [INSPIRE].
- [53] K. Okuyama and K. Sakai, *JT supergravity and Brezin-Gross-Witten tau-function*, *JHEP* **10** (2020) 160 [[arXiv:2007.09606](#)] [INSPIRE].
- [54] H. Kyono, S. Okumura and K. Yoshida, *Comments on 2D dilaton gravity system with a hyperbolic dilaton potential*, *Nucl. Phys. B* **923** (2017) 126 [[arXiv:1704.07410](#)] [INSPIRE].
- [55] G.W. Moore, N. Seiberg and M. Staudacher, *From loops to states in 2 – D quantum gravity*, *Nucl. Phys. B* **362** (1991) 665 [INSPIRE].
- [56] I.M. Gelfand and L.A. Dikii, *Asymptotic behavior of the resolvent of Sturm-Liouville equations and the algebra of the Korteweg-De Vries equations*, *Russ. Math. Surveys* **30** (1975) 77 [*Usp. Mat. Nauk* **30** (1975) 67] [INSPIRE].
- [57] R. Dijkgraaf, H.L. Verlinde and E.P. Verlinde, *Loop equations and Virasoro constraints in nonperturbative 2D quantum gravity*, *Nucl. Phys. B* **348** (1991) 435 [INSPIRE].
- [58] P. Zograf, *On the large genus asymptotics of Weil-Petersson volumes*, [arXiv:0812.0544](#) [INSPIRE].
- [59] E. Witten, *Deformations of JT gravity and phase transitions*, [arXiv:2006.03494](#) [INSPIRE].
- [60] C.V. Johnson and F. Rosso, *Solving puzzles in deformed JT gravity: phase transitions and non-perturbative effects*, *JHEP* **04** (2021) 030 [[arXiv:2011.06026](#)] [INSPIRE].
- [61] P. Saad, S.H. Shenker and D. Stanford, *A semiclassical ramp in SYK and in gravity*, [arXiv:1806.06840](#) [INSPIRE].
- [62] N. Engelhardt, S. Fischetti and A. Maloney, *Free energy from replica wormholes*, *Phys. Rev. D* **103** (2021) 046021 [[arXiv:2007.07444](#)] [INSPIRE].

- [63] K. Papadodimas and S. Raju, *Local operators in the eternal black hole*, *Phys. Rev. Lett.* **115** (2015) 211601 [[arXiv:1502.06692](#)] [[INSPIRE](#)].
- [64] E. Witten, *Anti-de Sitter space, thermal phase transition, and confinement in gauge theories*, *Adv. Theor. Math. Phys.* **2** (1998) 505 [[hep-th/9803131](#)] [[INSPIRE](#)].
- [65] M. Srednicki, *Chaos and quantum thermalization*, *Phys. Rev. E* **50** (1994) 888.
- [66] J.M. Deutsch, *Quantum statistical mechanics in a closed system*, *Phys. Rev. A* **43** (1991) 2046.
- [67] J. Maldacena, *Vacuum decay into Anti de Sitter space*, [arXiv:1012.0274](#) [[INSPIRE](#)].
- [68] J.B. Hartle and S.W. Hawking, *Wave function of the universe*, *Phys. Rev. D* **28** (1983) 2960 [[INSPIRE](#)].
- [69] B. Dubrovin, D. Yang and D. Zagier, *On tau-functions for the KdV hierarchy*, *Selecta Math.* **27** (2021) 12 [[arXiv:1812.08488](#)] [[INSPIRE](#)].
- [70] S. Dalley, C.V. Johnson and T.R. Morris, *Multicritical complex matrix models and nonperturbative 2D quantum gravity*, *Nucl. Phys. B* **368** (1992) 625 [[INSPIRE](#)].
- [71] S. Dalley, C.V. Johnson and T.R. Morris, *Nonperturbative two-dimensional quantum gravity*, *Nucl. Phys. B* **368** (1992) 655 [[INSPIRE](#)].
- [72] L. Griguolo, R. Panerai, J. Papalini and D. Seminara, *Nonperturbative effects and resurgence in JT gravity at finite cutoff*, [arXiv:2106.01375](#) [[INSPIRE](#)].
- [73] D.J. Gross, J. Kruthoff, A. Rolph and E. Shaghoulian, *$T\bar{T}$ in AdS_2 and quantum mechanics*, *Phys. Rev. D* **101** (2020) 026011 [[arXiv:1907.04873](#)] [[INSPIRE](#)].
- [74] L.V. Iliesiu, J. Kruthoff, G.J. Turiaci and H. Verlinde, *JT gravity at finite cutoff*, *SciPost Phys.* **9** (2020) 023 [[arXiv:2004.07242](#)] [[INSPIRE](#)].
- [75] L. McGough, M. Mezei and H. Verlinde, *Moving the CFT into the bulk with $T\bar{T}$* , *JHEP* **04** (2018) 010 [[arXiv:1611.03470](#)] [[INSPIRE](#)].

Quantum Information: Complexity

This chapter has already been published as [131]:

Complexity as a holographic dual of strong cosmic censorship, *M. Alishahiha, S. Banerjee, J. Kames-King, E. Loos*, In: *Phys.Rev.D* 105 (2022) 2, arXiv: 2106.14578 [hep-th]

This chapter deals with complexity for charged black branes in AdS. We use the CA proposal, which is explained in section 1.5.4. For charged black holes and black branes there is both an inner and an outer horizon. Complexity is a highly intriguing holographic probe as it is sensitive to behind-the-horizon physics of black holes. It is therefore clear that while complexity should “see” behind the outer horizon of charged black holes, it is a priori not obvious if complexity should be sensitive to physics behind the inner horizon too. We show that complexity may not penetrate the inner horizon in order to be consistent with Lloyd’s bound, which is a general bound on the computation speed of all physical systems. In addition, we specify a new expression for Lloyd’s bound on charged black hole backgrounds based on various reasonable arguments. Both complexity and the CA proposal are defined in section 1.5.

In detail, we start by applying the CA approach, which amounts to calculating the on-shell action on the Wheeler-DeWitt (WdW) patch of the spacetime under consideration. Here this is applied to the Einstein-Hilbert-Maxwell action on a charged black brane background. We consider two cutoffs. One of these is the usual holographic cutoff r_c . Therefore we can always consider the $r_c \rightarrow 0$ limit as the standard limit in holography or keep r_c finite for a broader $T\bar{T}$ approach. The other cutoff, which we denote by r_0 is behind the outer horizon. In principle there are two options for this second cutoff: behind the inner horizon or outside the inner horizon. As we will argue below, only the latter option is consistent with respect to Lloyd’s bound. Due to the lightlike boundaries of the WdW patch on which the on-shell action is calculated, special care must be taken of boundary contributions. More specifically in order to furnish finite and unique results, in addition to the Gibbons-Hawking boundary term, further counter terms are needed. For example, we need a term taking care of so-called joint points. These are points where the lightlike boundaries intersect a spacelike boundary, such as the behind-the-horizon cutoff or a timelike boundary, such as the holographic cutoff. As usual for complexity calculations, the on-shell action is evaluated in a late time limit, which results in an explicit

expression for the growth of complexity. At the same time we can use Lloyd's bound to furnish an expression for the growth of complexity. Lloyd's bound constitutes a general upper bound on the growth of complexity based on heuristic arguments about computational speed. We propose a new expression for this bound on charged black hole backgrounds based on simple consistency checks. In addition, the growth of complexity furnished by the bound can be matched to the previous expression we had extracted via the CA proposal by matching specific parameters. Namely, a specific relation between the holographic cutoff r_c and the behind-the-horizon cutoff r_0 must hold. This same relation may also be deduced by a different approach. We use a mirror operator construction of operators behind the black hole horizon in the spirit of the seminal approach outlined in references [132, 133]. One may argue for factorisation of partition functions defined on patches of the black hole background in the large N limit. More precisely, the partition function behind the outer horizon should be the product of the two partition functions outside the outer horizon (in the large N limit). This demand of factorisation leads to a relation between the cutoff parameters r_c and r_0 , which precisely agrees with the relation we had obtained earlier. This approach therefore gives an additional argument for our modified Lloyd's bound. Finally, we argue that setting the behind-the-horizon-cutoff behind the inner horizon is problematic as this would not allow Lloyd's bound to be saturated. Assuming the cutoff to lie behind the inner horizon, gives an expression for the late time growth of complexity, which is independent of the cutoff. As such this would violate our newly formulated Lloyd's bound. Complexity is therefore not able to penetrate the inner horizon. We interpret this as a holographic realisation of strong cosmic censorship for complexity.

The author contributed to all conceptual discussions regarding this publication. The author performed the calculations of sections 3 and 4.

Complexity as a holographic probe of strong cosmic censorshipMohsen Alishahiha^{1,*} Souvik Banerjee^{2,†} Joshua Kames-King^{3,4,‡} and Emma Loos^{2,§}¹*School of Physics, Institute for Research in Fundamental Sciences (IPM),
P.O. Box 19395-5531 Tehran, Iran*²*Institut für Theoretische Physik und Astrophysik, Julius-Maximilians-Universität Würzburg,
Am Hubland, 97074 Würzburg, Germany*³*Bethe Center for Theoretical Physics and Physikalisches Institut der Universität Bonn,
Nussallee 12, 53115 Bonn, Germany*⁴*Kavli Institute for Theoretical Physics, University of California,
Santa Barbara, California 93106, USA* (Received 4 July 2021; accepted 14 December 2021; published 3 January 2022)

Based on reasonable assumptions, we propose a new expression for Lloyd’s bound, which confines the complexity growth of charged black holes. We then revisit holographic complexity for charged black branes in the presence of a finite cutoff. Using the proposed Lloyd’s bound we find a relation between the UV and the behind the horizon cutoff. This is found to be consistent with the factorization of the partition function at leading order in large N . We argue that the result may be thought of as a holographic realization of strong cosmic censorship.

DOI: 10.1103/PhysRevD.105.026001

I. INTRODUCTION

In the past decade, there have been a lot of interesting developments in understanding and resolving puzzles related to the interior of black holes, the mysterious part of the spacetime hiding behind the black hole event horizon. In particular, in the context of the AdS/CFT correspondence, in which these paradoxes can be given a sharp form in terms of information processing of the boundary conformal field theory (CFT) [1–4], a lot of effort has been devoted towards resolving the aforementioned problems using the entanglement structure of spacetime [5,6]. Some of the resolutions are even instrumental in understanding the unique nature of entanglement in generic systems of quantum gravity [7,8].

These developments motivated a rigorous search for probes both sensitive to the interior of a black hole and which also systematically relate to the evolution of operators in the boundary CFT. Holographic complexity turned out to be one such probe. It was originally proposed in terms of an entangled pair of black holes [9]. The pair

exchanges information through a virtual wormhole structure, namely, the Einstein-Rosen (ER) bridge [10]. The bridge growing in time is identified as the holographic complexity growth in this set up. In an anti-de Sitter (AdS) black hole spacetime such a notion naturally relates the radial depth in the bulk spacetime to the growth of boundary operators. As a consequence, the black hole spacetime can be thought of as an onion shell-like structure with each radial slice corresponding to a particular complexity [9] of the dual boundary CFT. One efficient way to compute the complexity of a holographic state was proposed in [11,12]—the “complexity = action” (CA) conjecture. In this conjecture, the holographic complexity is given by the on-shell action on the Wheeler-DeWitt (WdW) patch which is the domain of dependence of any Cauchy surface in the bulk which intersects the asymptotic boundary on the time slice, Σ ,

$$\mathcal{C}(\Sigma) = \frac{\mathcal{I}_{\text{WdW}}}{\pi\hbar}. \quad (1.1)$$

One interesting tool to investigate the precise relation between complexity and radial depth in a black hole spacetime is the recently proposed duality between AdS spacetimes cut off at a finite radial distance and dual CFTs deformed by an irrelevant operator, known as the $T\bar{T}$ deformation [13–15]. $T\bar{T}$ is a certain quadratic combination of the stress-energy tensor of the boundary field theory [16–18]. This correspondence is very nontrivially supported by the matching of the energy spectrum measured by

*alishah@ipm.ir

†souvik.banerjee@physik.uni-wuerzburg.de

‡jvakk@yahoo.com

§emma.loos@physik.uni-wuerzburg.de

Published by the American Physical Society under the terms of the Creative Commons Attribution 4.0 International license. Further distribution of this work must maintain attribution to the author(s) and the published article’s title, journal citation, and DOI. Funded by SCOAP³.

an observer at a finite distance away from the black hole in AdS spacetime and that of a $T\bar{T}$ deformed CFT.¹

An attempt to explore the time evolution of holographic complexity for a black hole in AdS with a radial cutoff was made in [21]. It was shown that in order for this complexity to grow linearly with time with the coefficient approaching a constant value equal to twice the energy of the state, (this is known as the ‘‘Lloyd’s bound’’ in the literature [22]²) it is necessary to invoke a cutoff behind the horizon as well, with a value fixed by the boundary UV cutoff. The precise relation between the boundary cutoff and the cutoff behind the horizon has also been obtained in [21]. The corresponding relations between the two cutoffs for charged black holes and near extremal charged black branes in AdS were derived in [24] and in [25], respectively.

Intuitively the relation between the two cutoffs may be understood as follows. In the context of the CA proposal, the late time behavior of complexity growth is entirely given by the on-shell action evaluated on the intersection of the WdW patch with the future interior [26], leading to an observation that the late time behavior of holographic complexity is insensitive to the UV cutoff [21]. On the other hand according to Lloyd’s bound [22], the late time behavior of complexity growth is given in terms of the energy of the system that is sensitive to the finite UV cutoff. Therefore, while the physical charges are sensitive to a UV cutoff, the late time behavior of holographic complexity seems blind to the UV cutoff. A remedy to resolve this puzzle is to assume that the UV cutoff will induce a cutoff behind the horizon with a value fixed by the UV cutoff.

By relating the partition functions inside and outside of the horizon of an eternal black hole using the ‘‘mirror operator’’ construction of Papadodimas and Raju [5,6], the authors of [27] established that a cutoff at a finite radial distance does indeed imply a cutoff behind the horizon. This guarantees a bulk effective field theory at leading order in the $\frac{1}{N}$ expansion. Remarkably, the relation between the cutoffs obtained this way, exactly matches the one derived in [21], hinting at a deep connection between radial distance and complexity as well as with the black hole information paradox.

¹We note, however, that one should be careful once we are dealing with a gravity theory with a finite radial cutoff [19]. It has been shown that the $T\bar{T}$ deformation might be better described by imposing mixed boundary conditions at the asymptotic boundary [20].

²In the context of holographic complexity, it is known that Lloyd’s bound may actually be violated [23]. Nonetheless, the violation of Lloyd’s bound just modifies the relation between the cutoff behind the horizon and the UV cutoff at intermediate times, depending on whether at late times the bound is saturated from above or below. This does not, however, affect the main conclusion of our paper because in either case, the saturation is guaranteed at late times and the late time behavior of complexity growth is controlled by boundary physical charges whose values are affected by a finite UV cutoff.

In this paper we shall consider a charged, eternal black brane in AdS. It has an inner horizon in addition to its outer event horizon which makes the causal structure of such spacetime geometries even more rich and interesting. In particular, there has been a long-standing debate regarding the fate of an infalling observer after crossing the event horizon of such black holes. Whether the observer can also cross the inner horizon smoothly is a tricky question since this horizon, being a Cauchy horizon, does not guarantee a unique evolution of smooth initial data. This problem is resolved in classical gravity using the conjecture of ‘‘strong cosmic censorship’’ that predicts the eventual collapse of the inner horizon as soon as the infalling observer reaches it. This instability is an artefact of an infinite blue shift effect. It is, however, very difficult to prove this in general particularly beyond the regime of classical gravity. In recent work, [28], a quantum test in form of the behavior of boundary correlators was proposed in order to diagnose the smoothness of the inner horizon for charged AdS black holes.

In our study we will set the interior cutoff behind the event horizon but outside the inner horizon and derive a relation between the two cutoffs in two different ways; first by making use of complexity growth and secondly by using the validity of low-energy effective field theory and the factorization of the corresponding Hilbert space. We will then give a dual interpretation of our result in terms of the emergence of strong cosmic censorship.

On our way towards deriving the relation between the cutoffs, we will also address a long-standing issue regarding the bound on the late time growth of complexity. In the existing literature, there is no unique consensus on the generalization of Lloyd’s bound for a charged system. The reason for this apparent ambiguity is that, unlike the uncharged case, in the case of a charged black hole, this bound is hard to ‘‘derive’’ from first principles. There have been two proposals based on ‘‘natural expectations’’ [12,29]; however, both of them suffer from certain pathologies. The cutoff geometry makes this problem even more complicated. However, in our case since we compute the relation between the cutoffs in two different ways, it can be used as a very nice diagnostic of the correct Lloyd’s bound for a charged system. In fact, we will propose a new bound for charged black holes (branes) which apart from being consistent with several limits, namely, the zero cutoff and zero charge limits, is also free from the aforementioned issues associated with previous proposals.

The rest of the paper is organized as follows. In Sec. II we present the computation of the late-time growth of complexity in detail. Section III will be devoted to the discussion of the generalization of Lloyd’s bound to charged black branes. Here we will propose a new bound and compare it with the previously existing bounds in the literature. At the end of that section we will present the relation between the two cutoffs implied by the proposed

bound. In Sec. IV we will derive the relation between the cutoffs from a different perspective, namely from the factorization of the partition function. We will show that, provided we use the proposed Lloyd's bound, the relation between the cutoffs in both the approaches match exactly. Section V is reserved for the interpretation of our results, particularly, in terms of an emergent strong cosmic censorship. We will conclude in Sec. VI with some comments on the choice of ensembles and also some future outlooks.

II. COMPLEXITY OF A CHARGED BLACK BRANE WITH CUTOFF

In this section we shall study the complexity growth of an eternal charged black brane solution with a finite radial cutoff.³ To proceed, let us first fix our notation. We will consider the Einstein-Hilbert-Maxwell bulk action

$$S_{\text{bulk}} = \frac{1}{16\pi G_N} \int d^{d+2}x \sqrt{-g} \left(R - 2\Lambda - \frac{1}{2} F_{\mu\nu} F^{\mu\nu} \right), \quad (2.1)$$

for which eternal charged black brane solutions, for $d > 2$ may be given as follows⁴:

$$ds^2 = \frac{L^2}{r^2} \left(-f(r) dt^2 + \frac{dr^2}{f(r)} + \sum_{i=1}^d dx_i^2 \right), \quad \text{with} \quad (2.2)$$

$$f(r) = 1 - mr^{d+1} + Q^2 r^{2d}$$

and

$$A_t = \sqrt{\frac{d}{d-1}} Q L (r_+^{d-1} - r^{d-1}). \quad (2.3)$$

Here m and Q are related to the mass and the charge of the black brane, respectively. In particular, the total Arnowitt-Deser-Misner (ADM) charge of the system is given by

$$\mathcal{Q} = \oint *F = \sqrt{d(d-1)} \frac{V_d L^{d-1}}{8\pi G_N} Q, \quad (2.4)$$

where the d -form field, $*F$, is the Hodge dual of the electromagnetic field strength tensor $F_{\mu\nu} = \partial_\mu A_\nu - \partial_\nu A_\mu$. V_d denotes the transverse d -dimensional volume. G_N is the $(d+2)$ -dimensional Newton's constant and L is the AdS length scale.

³We note that the complexity of charged black holes in the presence of a finite cutoff has been already studied in [24] (see also [30]) and indeed most parts of this section are a review. Our aim is to present the results in a new, inspiring form.

⁴In what follows we only consider electric brane solutions in which the only nonzero components of the electromagnetic field strengths are F^{rt} and $F^{r\theta}$. We have also assumed the radial gauge, $A_r = 0$. For a complete discussion on these solutions and how to obtain them see [31].

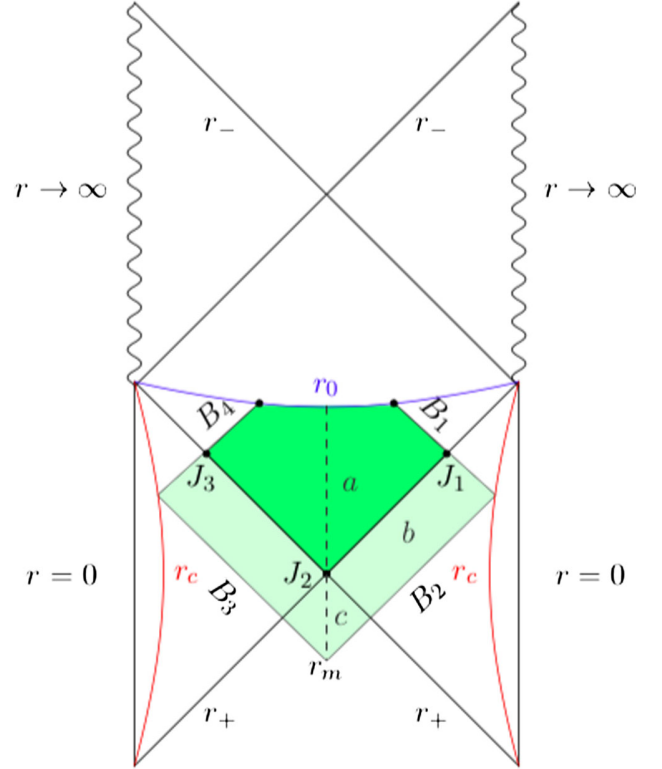


FIG. 1. The Penrose diagram of the eternal charged black brane with the WdW patch depicted in light green. The intersection of the WdW with the future interior is denoted in a darker green. We have also labeled the four lightlike boundaries by B_1, \dots, B_4 and denoted joint points of these boundaries with each other and with the spacelike surface r_0 by black dots. The three lightlike joint points are marked as J_1, J_2, J_3 . Moreover, we also introduce the three regions a, b, c , which break the WdW patch into simple contributions.

This geometry has two horizons, the outer horizon r_+ , and the inner horizon r_- , as depicted in the Penrose diagram in Fig. 1. They correspond to the positive real roots of the equation $f(r) = 0$, where $f(r)$ is the blackening factor given in (2.2). In our choice of coordinates in which the AdS boundary is located at $r = 0$, one has $r_+ < r_-$.

Furthermore, following [21], we introduce two cutoffs, the UV cutoff at $r = r_c$ and a cutoff at $r = r_0$ lying behind the outer horizon. We place our cutoff, r_0 in between the inner and the outer horizons, $r_+ < r_0 < r_-$. However, in principle, r_0 could also lie behind the inner horizon, $r_0 > r_-$. For the moment, this is only a choice, but we will elaborate upon and justify this in Sec. V.

Now we proceed to compute the late time growth of complexity in the charged black brane geometry with the aforementioned two cutoffs. We will use the CA proposal given in (1.1),⁵ which requires the evaluation of the on-shell

⁵Although the procedure of computing complexity using the CA proposal is, by now, quite standard, in order to be self-contained, we will present the computations in a rather detailed manner.

action on the WdW patch associated with a boundary state at a time, $\tau = t_L + t_R$. Here t_L is the time at the left boundary and t_R at the right boundary. The full WdW patch is the union of the dark and the light green regions in Fig. 1.⁶ As for the computations in this section, we will closely follow [21] (see also [24,25]).

In general, the action on the WdW patch contains the following pieces [32–34]

$$\mathcal{I}_{\text{WdW}} = I_{\text{bulk}} + I_{\text{GH}} + I_{\text{CT}} + I_j. \quad (2.5)$$

The individual terms on the right-hand side correspond to the on-shell bulk action, the Gibbons-Hawking surface terms, the counterterms, and the contributions coming from the joint points on the WdW patch, respectively. While the bulk contribution can be straightforwardly obtained by evaluating the on-shell bulk action (2.1) on the WdW patch, the boundary contributions are slightly subtle. One needs to specify the choice of ensemble at this point. We prefer to work in the grand canonical ensemble, which amounts to having a fixed chemical potential for the boundary CFT. For any other ensemble, one has to be careful about Maxwell boundary terms on different surfaces [31,35]. We postpone further discussion on this subtlety to Sec. VI.

While the Gibbons-Hawking term is required to achieve a well-defined variational principle, to guarantee finite free energies in respective regions of spacetime one needs to add further counterterms [36]. The explicit forms of these terms are given by⁷

$$I_{\text{GH}} = \pm \frac{1}{8\pi G} \int d^{d+1}x \sqrt{|h|} K, \quad (2.6)$$

$$I_{\text{CT}} = \mp \frac{1}{8\pi G} \int d^{d+1}x \sqrt{|h|} \frac{d}{L}. \quad (2.7)$$

Since the WdW patch possesses both spacelike and timelike boundary surfaces, we have to be careful about fixing the signs in front of (2.6) and (2.7). A timelike surface corresponds to the upper choice of sign, while for a spacelike one the lower sign is appropriate. For example, in our setup, the upper signs of both (2.6) and (2.7) are to be used for the cutoff at r_c , whereas the lower signs have to be used when dealing with the cutoff at r_0 .

The requirement of having boundary terms on the null boundaries can be avoided by simply choosing an affine parametrization of the null directions as we will do in what follows. However, for such boundaries, we do need to consider contributions to the action coming from joint

points. These are the points where two null boundaries intersect or a null boundary intersects with a spacelike or timelike boundary. The former case requires

$$I_j = \pm \frac{1}{8\pi G} \int d^d x \sqrt{\sigma} \log \frac{|v_1 \cdot v_2|}{2}, \quad (2.8)$$

where v_1 and v_2 are the null vectors of the two respective boundaries

$$v_1 = \alpha \left(-dt + \frac{dr}{f(r)} \right) \quad v_2 = \beta \left(dt + \frac{dr}{f(r)} \right). \quad (2.9)$$

Here, α and β are parameters, which must be introduced due to the ambiguous nature of the normalization of lightlike vectors. σ is the induced metric on this surface.

The latter case, namely the intersection of a lightlike boundary with either a spacelike or timelike boundary takes on a similar form

$$I_j = \pm \frac{1}{8\pi G} \int d^d x \sqrt{\sigma} \log n^\mu v_\mu, \quad (2.10)$$

where n^μ refers to the unit normal of the timelike/spacelike surface and where v_μ is as given in (2.9).

In order to evaluate these contributions explicitly, it is convenient to introduce the tortoise coordinate r^* as

$$r^* = - \int_r^\infty \frac{dr}{f(r)}, \quad (2.11)$$

in terms of which, from Fig. 1, we can read off the null boundaries of the WdW patch at late times as

$$\begin{aligned} B_1 : t = t_R + r^*(r_c) - r^*(r), \quad B_3 : t = -t_L + r^*(r_c) - r^*(r), \\ B_2 : t = t_R - r^*(r_c) + r^*(r), \quad B_4 : t = -t_L - r^*(r_c) + r^*(r). \end{aligned} \quad (2.12)$$

The action of the WdW patch only depends on the time $\tau = t_L + t_R$ and not on the individual boundary times, t_L and t_R . This follows trivially from the boost symmetry. Therefore, to simplify our computation, without any loss of generality, we can consider a time-symmetric configuration, namely, $t_L = t_R = \frac{\tau}{2}$. One could, in principle, also choose time-shifted configurations, but this would not affect the late time growth of complexity.

A. The bulk and the boundary contributions

In order to evaluate the bulk contribution along with the Gibbons-Hawking and the counterterms, we split up half the WdW patch into three regions, a , b , and c , as depicted in Fig. 1. The bulk and boundary terms of the full WdW patch will then be obtained by simply doubling the contributions.

⁶We are ultimately interested in the late-time behavior which means that we effectively restrict to the intersection of the WdW patch with the future interior. This region is highlighted as the dark green patch in Fig. 1.

⁷The same counterterm (2.7) also appears for a flat boundary metric in the context of holographic renormalization [37].

Let us first work through the bulk contributions. We work on the full WdW patch (the union of the dark and the light green regions) before reducing to the

intersection of WdW with the future interior. Evaluating the action, (2.1), on-shell in the three regions a , b , and c yields

$$\begin{aligned} I_{\text{bulk}}^a &= \frac{L^d V}{8\pi G} \int_{r_+}^{r_0} dr \int_0^{B_1} dt \left(-\frac{(d+1)}{r^{d+2}} + Q^2(d-1)r^{d-2} \right) \\ &= \frac{L^d V}{8\pi G} \int_{r_+}^{r_0} dr \left(-\frac{(d+1)}{r^{d+2}} + Q^2(d-1)r^{d-2} \right) \left(\frac{\tau}{2} + r^*(r_c) - r^*(r) \right), \end{aligned} \quad (2.13)$$

$$\begin{aligned} I_{\text{bulk}}^b &= \frac{L^d V}{8\pi G} \int_{r_c}^{r_+} dr \int_{B_2}^{B_1} dt \left(-\frac{(d+1)}{r^{d+2}} + Q^2(d-1)r^{d-2} \right) \\ &= \frac{L^d V}{8\pi G} \int_{r_c}^{r_+} dr \left(-\frac{(d+1)}{r^{d+2}} + Q^2(d-1)r^{d-2} \right) (r^*(r_c) - r^*(r)), \end{aligned} \quad (2.14)$$

$$\begin{aligned} I_{\text{bulk}}^c &= \frac{L^d V}{8\pi G} \int_{r_+}^{r_m} dr \int_{B_2}^0 dt \left(-\frac{(d+1)}{r^{d+2}} + Q^2(d-1)r^{d-2} \right) \\ &= \frac{L^d V}{8\pi G} \int_{r_+}^{r_m} dr \left(-\frac{(d+1)}{r^{d+2}} + Q^2(d-1)r^{d-2} \right) \left(-\frac{\tau}{2} + r^*(r_c) - r^*(r) \right). \end{aligned} \quad (2.15)$$

As stated above, for the full WdW patch these contributions have to be doubled. Note, that we are working in a late time approximation, $r_m \approx r_+$, such that (2.15) vanishes. Both the Gibbons-Hawking term (2.6) and the counterterm (2.7) do not contribute on the lightlike segments due to the affine parametrization we choose. However, both do appear at the spacelike cutoff surface located at r_0 . Here we get

$$\begin{aligned} I_{\text{GH}} &= -2 \times \frac{VL^d}{8\pi G} \int_0^{\tau/2} dt \left((d+1) \frac{1}{r_0^{d+1}} + Q^2 r_0^{d-1} \right. \\ &\quad \left. - \frac{1}{2} (d+1)m \right), \end{aligned} \quad (2.16)$$

$$I_{\text{CT}} = 2 \times \frac{VL^d}{8\pi G} \int_0^{\tau/2} dt \frac{d}{r_0^{d+1}} \sqrt{|f(r_0)|}. \quad (2.17)$$

The factors of 2 appearing in front of (2.16) and (2.17) follow from the same logic of doubling the contributions.

B. Contributions from the joint points

In Fig. 1, as far as the late time behavior is concerned, there are five joint point contributions, which we will evaluate using (2.8) and (2.10). In order to specify the location of these points it is useful to switch to the following coordinates [38]

$$u = -e^{-\frac{1}{2}f'(r_+)(r^*-t)}, \quad v = -e^{-\frac{1}{2}f'(r_+)(r^*+t)}. \quad (2.18)$$

In these coordinates the horizon is located at $uv = 0$ or equivalently $r^*(r_+) = -\infty$ on which three of the joint

points are located. However, since both $r^*(r_+)$ and $\log(f(r_+))$ diverge, we must introduce ϵ_u and ϵ_v , which can be interpreted as regularized locations of the horizon. The three lightlike joint points are then represented by

$$J_1 : (\epsilon_u, v_0), \quad J_2 : (\epsilon_u, \epsilon_v), \quad J_3 : (u_0, \epsilon_v), \quad (2.19)$$

where v_0 and u_0 designate the future interior null boundaries. We denote the corresponding radial coordinates by r_{u_0, ϵ_v} , r_{ϵ_u, v_0} , and $r_{\epsilon_u, \epsilon_v}$ respectively. Using (2.8), we can evaluate the contribution coming from these three joint points. Similarly, contributions from the other two joints located at the spacelike cutoff r_0 can be evaluated using (2.10). The total contribution from all five joint points is given by

$$\begin{aligned} I_j &= \frac{VL^d}{8\pi G} \left(\frac{\log \frac{\alpha\beta r_0^2}{L^2 |f(r_0)|}}{r_0^d} + \frac{\log \frac{\alpha\beta r_{\epsilon_u, \epsilon_v}^2}{L^2 |f(r_{\epsilon_u, \epsilon_v})|}}{r_{\epsilon_u, \epsilon_v}^d} \right. \\ &\quad \left. - \frac{\log \frac{\alpha\beta r_{u_0, \epsilon_v}^2}{L^2 |f(r_{u_0, \epsilon_v})|}}{r_{u_0, \epsilon_v}^d} - \frac{\log \frac{\alpha\beta r_{\epsilon_u, v_0}^2}{L^2 |f(r_{\epsilon_u, v_0})|}}{r_{\epsilon_u, v_0}^d} \right), \end{aligned} \quad (2.20)$$

where the first term corresponds to the two joint points at r_0 and the remaining three terms, to the lightlike joint points. We work in the approximation $r_{\epsilon_u, \epsilon_v} \approx r_+$, $r_{u_0, \epsilon_v} \approx r_+$ and $r_{\epsilon_u, v_0} \approx r_+$, such that (2.20) simplifies to

$$I_j = \frac{VL^d}{8\pi G} \left(\frac{\log |f(r_{\epsilon_u, v_0})| + \log |f(r_{u_0, \epsilon_v})| - \log |f(r_{\epsilon_u, \epsilon_v})|}{r_+^d} - \frac{\log \frac{\alpha\beta r_+^2}{L^2} - \log \frac{\alpha\beta r_0^2}{L^2 |f(r_0)|}}{r_+^d - r_0^d} \right). \quad (2.21)$$

Furthermore, in the limit, $uv \rightarrow 0$, $\log |f(r_{u,v})|$ appearing in (2.21) can be approximated as [38]

$$\log |f(r_{u,v})| = \log |uv| + c_0 + \mathcal{O}(uv), \quad (2.22)$$

where c_0 is an u, v independent function. This further simplifies (2.21) to

$$I_j = \frac{VL^d}{8\pi G} \left(\frac{\log |u_0 v_0| + c_0}{r_+^d} - \frac{\log |f(r_0)|}{r_0^d} - \frac{\log \frac{\alpha\beta r_+^2}{L^2}}{r_+^d} + \frac{\log \frac{\alpha\beta r_0^2}{L^2}}{r_0^d} \right). \quad (2.23)$$

The ambiguity in (2.23) due to the presence of the last two terms may in principle be removed by a further counterterm [25,34,39]. However, since we are only interested in the growth rate of complexity, we can ignore this issue since only the τ -dependent first term of (2.23) will contribute in this case.

C. The late time growth of complexity

Now that we have all the constituents appearing in (2.5), evaluated on shell, on the intersection of the WdW patch with the future interior, we can evaluate the late time growth of the action by taking derivatives of (2.13), (2.14), (2.16), (2.17), and (2.23) with respect to τ

$$\frac{dI_{\text{bulk}}}{d\tau} = \frac{L^d V}{8\pi G} \left(\frac{1}{r_0^{d+1}} - \frac{1}{r_+^{d+1}} + Q^2 (r_0^{d-1} - r_+^{d-1}) \right), \quad (2.24)$$

$$\frac{dI_{\text{GH}}}{d\tau} = \frac{L^d V}{8\pi G} \left(\frac{m}{2} (1+d) - \frac{(1+d)}{r_0^{d+1}} - Q^2 r_0^{d-1} \right), \quad (2.25)$$

$$\frac{dI_{\text{CT}}}{d\tau} = \frac{L^d V}{8\pi G} \left(\frac{d\sqrt{-f(r_0)}}{r_0^{d+1}} \right), \quad (2.26)$$

$$\frac{dI_j}{d\tau} = \frac{L^d V}{8\pi G} \left(\frac{(1+d)m}{2} - dQ^2 r_+^{d-1} \right). \quad (2.27)$$

On the other hand by making use of (1.1), one obtains the late time growth of complexity as follows:

$$\frac{dC}{d\tau} = \frac{L^d V}{8\pi^2 G \hbar} \left\{ (d+1)m - \frac{d}{r_0^{d+1}} \left(1 - \sqrt{-f(r_0)} \right) - \frac{1}{r_+^{d+1}} - Q^2 (d+1) r_+^{d-1} \right\}, \quad (2.28)$$

which could be further simplified, using $f(r_+) = 0$, to find

$$\frac{dC}{d\tau} = \frac{L^d V d}{8\pi^2 G \hbar} \left\{ \frac{1}{r_+^{d+1}} + \frac{1}{r_0^{d+1}} \left(\sqrt{-f(r_0)} - 1 \right) \right\}, \quad (2.29)$$

which has the same form as that of the neutral case (see [21]) and the only charge dependence comes from the blacking factor $f(r_0)$. It is evident that it reduces to that of the neutral case in the zero charge limit. On the other hand it is also clear that for $r_0 \rightarrow r_-$ it gives the standard expression for the late time growth of complexity of a charged black brane [23,29],

$$\frac{dC}{d\tau} = \frac{L^d V d}{8\pi^2 G \hbar} \left(\frac{1}{r_+^{d+1}} - \frac{1}{r_-^{d+1}} \right) = \frac{L^d V d}{8\pi^2 G \hbar} Q^2 (r_-^{d-1} - r_+^{d-1}). \quad (2.30)$$

It is believed that the late time behavior of complexity should be expressed in terms of conserved charges such as energy. Therefore there must be a relation between r_0 and the UV cutoff r_c , so that the above expression for the late time growth of complexity can be written entirely in terms of the conserved charges defined at the boundary. To find such a relation it is natural to use the Lloyd's bound. To do so, in the next section we revisit Lloyd's bound for charged black branes (black holes).

III. LLOYD'S BOUND AND BEHIND THE HORIZON CUTOFFS

Lloyd's bound constitutes an upper bound on the growth rate of the quantum complexity of any physical system [22]. Explicitly, it is given as

$$\frac{dC}{dt} \leq \frac{2\mathcal{E}}{\pi \hbar}, \quad (3.1)$$

\mathcal{E} being the energy of the system.

In [11,12] it was shown that the late time growth of the WdW action of a charge neutral AdS black hole satisfies the relation

$$\frac{dI_{\text{WdW}}}{d\tau} = 2\mathcal{E} = 2M, \quad (3.2)$$

which, in conjunction with (1.1), can be read as a statement on the saturation of Lloyd's bound (3.1). M here is the ADM mass of the black hole in AdS which in the context of the AdS/CFT correspondence can be identified with the energy of the boundary CFT.⁸

⁸Although we are calling it "Lloyd's bound" for historical reasons, more appropriately, we should think of this as a bound on holographic complexity given in terms of conserved quantities at the holographic boundary. In presence of a UV cutoff, this bound will, therefore, be sensitive to the cutoff.

They further proposed the generalization of Lloyd’s bound for a charged AdS black hole as

$$\left(\frac{dC}{dt}\right)_{\text{Lloyd}} \leq \frac{2}{\pi\hbar} \left[(\mathcal{E} - \mu Q) - (\mathcal{E} - \mu Q)_{\text{gs}} \right], \quad (3.3)$$

where the subscript *gs* denotes the ground state. Computing the growth explicitly and using the CA proposal, they concluded that while this bound is saturated for a small charged black hole, it is violated for finite sized charged black holes.

However, the authors of [29] showed explicitly that the claim of [11,12] was actually incorrect and even small charged black holes disobey the bound (3.3). This observation was quite intriguing because [11,12] attributed the saturation and violation of the bound, respectively, by small and finite-sized charged black holes to the fact that the bound could only be saturated in the supersymmetric limit and for UV complete holographic theories. This further fueled the possibility that the bound proposed in [11,12] was actually inappropriate.

Due to the fast scrambling nature of black holes,⁹ it is natural to expect that black holes should saturate the appropriately defined bound, irrespective of its size. In [29] a new version of the bound on charged black holes was proposed, namely

$$\frac{dC}{dt} \leq \frac{1}{\pi\hbar} [(\mathcal{E} - \mu_+ Q) - (\mathcal{E} - \mu_- Q)], \quad (3.4)$$

where \mathcal{E} is the total energy and Q is the ADM charge of the system given in (2.4). μ_{\pm} denote, “formally”, the chemical potentials associated with the two horizons, r_+ and r_- respectively. However, one might complain that this statement is a bit vague since the thermodynamics of the inner horizon is not a strictly well-understood concept, and rightly so. The way we should understand μ_- here is through the replacement $r_+ \rightarrow r_-$ in the expression for the CFT chemical potential μ_+ which is thermodynamically well defined. However, it is worth mentioning that, although μ_- cannot be interpreted as a chemical potential from the perspective of the boundary CFT, it can be reexpressed in terms of other well-defined boundary quantities using the expressions of ADM mass and charge in terms of r_+ and r_- [29].

While [29] explicitly established the saturation of the proposed Lloyd’s bound (3.4) for charged (and also rotating and Gauss-Bonnet) AdS black holes, they also showed how this proposal reduces to (3.2) in the uncharged limit. This limit is very interesting and follows from the fact that in the neutral limit, where $Q \rightarrow 0$ and $r_- \rightarrow \infty$ simultaneously, $\mu_+ Q \rightarrow 0$ and $\mu_- Q \rightarrow 2M$ while the energies \mathcal{E} cancel between the two terms.

⁹Black holes may be considered the fastest scramblers, see [40].

Although (3.4) conforms with the saturation of Lloyd’s bound for charged AdS black holes of any size, along with other categories of black holes, this is slightly unnatural. This can be understood from the limiting argument to the neutral case mentioned above. The contribution in this limit arises solely from the “-” side, namely from the term which modifies the original proposal for Lloyd’s bound because of the existence of the inner horizon. It is legitimate to expect that all such contributions coming from the “-” side will add up to zero in the neutral limit.

Moreover, due to this unnatural limiting behavior, it was argued that Eq. (3.4) is unable to accommodate the right expression for Lloyd’s bound when a finite cutoff is applied to the theory [24].¹⁰

Based on the above observations we would like to propose a new bound for the late time growth of complexity as follows:

$$\left(\frac{dC}{dt}\right)_{\text{bound}} = \frac{1}{\pi\hbar} [(2\mathcal{E}_+ - \mu_+ Q) - (2\mathcal{E}_- - \mu_- Q)], \quad (3.5)$$

with \pm denoting the quantities associated with the outer and inner horizons as before. It is then clear that in the zero-charge limit, the contributions coming from the “-” side will add up to zero and we are left with the contribution of the “+” side. Of course, for most cases in which $\mathcal{E}_+ = \mathcal{E}_-$ both proposals (3.4) and (3.5) result in the same expression for Lloyd’s bound. The difference shows up when $\mathcal{E}_+ \neq \mathcal{E}_-$, which may happen when we have a finite cutoff. Indeed, we will also see that the expression for Lloyd’s bound as given in (3.5) allows to consider the theory in the presence of finite cutoffs. As we mentioned before [following (3.4)], it is worth stressing once again that μ_- cannot be directly interpreted as a chemical potential. However, it is possible to express μ_- in terms of well-defined conserved charges of the boundary CFT [29].

To proceed we note that for the case in which there is no cutoff, the ADM energy can be directly computed from the on shell gravitational action as [31]

$$\mathcal{E}_0 = \frac{L^d V d}{16\pi G} m, \quad (3.6)$$

which is the same for both the inner and the outer horizon. Now if we consider the cutoff at $r = r_c$, the physical energy gets corrected by [15]

$$\frac{L^d V d}{16\pi G} m \rightarrow \frac{L^d V}{8\pi G} \frac{d}{r_c^{d+1}} \left(1 - \sqrt{|f(r_c)|} \right). \quad (3.7)$$

This can be derived in two steps, first by computing the bulk energy enclosed by the cutoff surface at $r = r_c$

¹⁰The authors of [24] used the equation (3.3) for Lloyd’s bound.

and then using the holographic dictionary for the cutoff AdS/ TT -deformed CFT correspondence to compute the boundary energy¹¹

$$\mathcal{E}_+ = \frac{L^d V d}{8\pi G r_c^{d+1}} \left(1 - \sqrt{|f(r_c)|}\right). \quad (3.8)$$

While the presence of the cutoff will only modify the energy contribution in the outside “+” region, the contribution coming from the “-” region will remain unaffected,

$$\mathcal{E}_- = \frac{L^d V d}{16\pi G} m. \quad (3.9)$$

This is supported by the zero charge limit in which, as we mentioned, one would naturally expect that the contribution of the “-” side should vanish in this limit.

We also need the contributions to Lloyd’s bound coming from the chemical potentials. Following our conventions in (2.2), (2.3), and in (2.4), the chemical potentials for the outer and the inner horizons are given by

$$\mu Q|_+ = \frac{L^d V d}{8\pi G} Q^2 r_+^{d-1}, \quad \mu Q|_- = \frac{L^d V d}{8\pi G} Q^2 r_-^{d-1}. \quad (3.10)$$

Now we are in a position to combine (3.8), (3.9) and (3.10) to evaluate the bound given in (3.5)

$$\begin{aligned} \left(\frac{dC}{d\tau}\right)_{\text{bound}} &= \frac{L^d V d}{8\pi^2 \hbar G} \left[2 \frac{1}{r_c^{d+1}} \left(1 - \sqrt{|f(r_c)|}\right) - Q^2 r_+^{d-1} \right] - \frac{L^d V d}{8\pi^2 \hbar G} [m - Q^2 r_-^{d-1}] \\ &= \frac{L^d V d}{8\pi^2 \hbar G} \left[\frac{2}{r_c^{d+1}} \left(1 - \sqrt{|f(r_c)|}\right) - m + Q^2 (r_-^{d-1} - r_+^{d-1}) \right]. \end{aligned} \quad (3.11)$$

From this expression, it is clear that in the limit $Q \rightarrow 0$, the full contribution coming from the “-” side, namely $(2\mathcal{E} - \mu Q)_-$, vanishes identically leaving only the contribution coming from the canonical energy \mathcal{E}_+ at the boundary. This leads to the expected result

$$\left(\frac{dC}{d\tau}\right)_{\text{bound}} = \frac{L^d V d}{8\pi^2 \hbar G} \left[\frac{2}{r_c^{d+1}} \left(1 - \sqrt{|f(r_c)|}\right) \right] = 2\mathcal{E}_+. \quad (3.12)$$

It is worth stressing again that both proposals for a suitable Lloyd’s bound for a charged black brane, the one considered in [29] and the other we proposed, namely, (3.5), reduce to the uncharged limit, (3.2). However, the limits are achieved in crucially different manners. Contrary to our case discussed above, in the neutral limit of [29], “-” quantities contribute.

A. Behind the horizon cutoff

Apart from our proposal being physically more reasonable, it will turn out that in the presence of cutoffs, our proposal is the apt one. Before justifying this in the following section, let us use our proposal to find the relation between the two cutoffs.

Equating (3.11) to the late time growth of complexity (2.29), one obtains a relation between r_c and r_0 as follows:

$$\frac{2}{r_c^{d+1}} \left(1 - \sqrt{|f(r_c)|}\right) - m = \frac{1}{r_-^{d+1}} + \frac{1}{r_0^{d+1}} \left(\sqrt{-f(r_0)} - 1\right). \quad (3.13)$$

To write this equation we have used the fact that

$$\frac{1}{r_+^{d+1}} - \frac{1}{r_-^{d+1}} = Q^2 (r_-^{d-1} - r_+^{d-1}). \quad (3.14)$$

In the next section, we will use a different approach to arrive at the result (3.13), which implicitly also verifies (3.5).

IV. FACTORIZATION OF THE PARTITION FUNCTION

In this section we will investigate the possibility of relating the UV and the behind the horizon cutoff from a completely different perspective. This study follows directly from the construction of interior operators in terms of those describing the exterior regions proposed in [5]. Actually, based on this fact one can argue that the partition function of the operators describing the interior of an eternal black hole is proportional to the product of partition functions of operators describing the left and right exteriors of the black hole [27]. At leading order this connection may be reduced to a relation between the on-shell actions evaluated on the inside and outside of the black hole.

Using this approach for neutral, eternal black holes one may find an expression for the cutoff behind the horizon which is the same as that obtained in the context of holographic complexity [27]. The aim of this section is to extend this study to charged black branes.

To proceed, we note that in regions I and III of the Penrose diagram depicted in Fig. 2, AdS/CFT provides us with a map allowing us to write down nonlocal CFT operators playing the role of the local bulk fields in these regions

¹¹See [15] for the details of this computation.

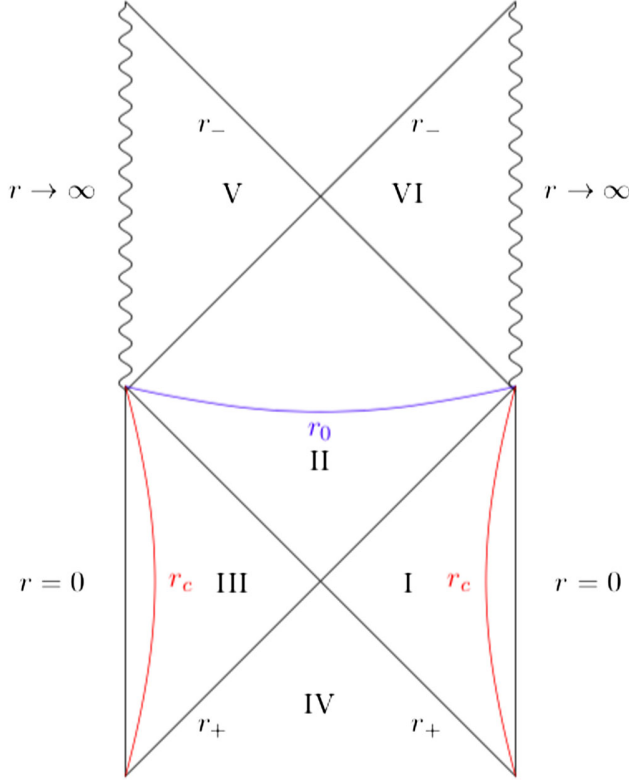


FIG. 2. Penrose diagram of the eternal, charged black brane. The radial cutoff in region *I* lies at $r = r_c$ and induces a cutoff behind the outer horizon at $r = r_0$.

$$\begin{aligned}\Phi_{\text{CFT}}^{\text{I}} &= \int_{\omega>0} \frac{d\omega d^d k}{(2\pi)^{d+1}} [\mathcal{O}_{\omega, \vec{k}} f_{\omega, \vec{k}}(t, \vec{x}, r) + \text{H.c.}], \\ \Phi_{\text{CFT}}^{\text{III}} &= \int_{\omega>0} \frac{d\omega d^d k}{(2\pi)^{d+1}} [\tilde{\mathcal{O}}_{\omega, \vec{k}} f_{\omega, \vec{k}}(t, \vec{x}, r) + \text{H.c.}],\end{aligned}\quad (4.1)$$

where $\mathcal{O}_{\omega, \vec{k}}$ and $\tilde{\mathcal{O}}_{\omega, \vec{k}}$ are Fourier transforms of generalized free fields in the CFT. These are special CFT operators whose n -point correlators factorize into 2-point correlators at leading order in the large N expansion [41]. The mode functions $f_{\omega, \vec{k}}$ are the solutions of the bulk equations of motion in these two regions subject to normalizability conditions at the respective boundaries.

On the other hand in the interior regions, such as II, representation of the local bulk field needs both sets of operators [5]

$$\begin{aligned}\Phi_{\text{CFT}}^{\text{II}} &= \int_{\omega>0} \frac{d\omega d^d k}{(2\pi)^{d+1}} [\mathcal{O}_{\omega, \vec{k}} g_{\omega, \vec{k}}(t, \vec{x}, r) \\ &+ \tilde{\mathcal{O}}_{\omega, \vec{k}} \tilde{g}_{\omega, \vec{k}}(t, \vec{x}, r) + \text{H.c.}],\end{aligned}\quad (4.2)$$

where $g_{\omega, \vec{k}}^i(t, \vec{x}, r)$ and $\tilde{g}_{\omega, \vec{k}}^i(t, \vec{x}, r)$ are bulk mode functions in respective regions. However, for the obvious reason that these regions cannot access the AdS boundaries, one cannot impose any boundary conditions on these solutions, and (4.2) follows naturally from the smoothness of the horizon [5] or equivalently, the entanglement structure of the dual CFT state [42]. It is worth mentioning that in the expansions (4.1) and (4.2), the bulk radial coordinate r , plays the role of a nonlocality parameter in the dual CFT.

Following [27], let us define the *restricted* partition function in which the integration is taken over the fields associated with regions I, II, or III of the corresponding eternal black hole

$$\mathcal{Z}^{(\alpha)} \propto \int \mathcal{D}\Phi^\alpha e^{-iS^{(\alpha)}[\Phi^\alpha]},\quad (4.3)$$

where $\alpha = \{\text{I, II, III}\}$. We can rewrite the path integral using the mode expansions in the respective regions which yield

$$\mathcal{Z}^{(\text{I})} \propto \int \mathcal{D}\mathcal{O}_{\omega, \vec{k}} \mathcal{D}\mathcal{O}_{-\omega, -\vec{k}} e^{-iS^{(\text{I})}[\mathcal{O}]},\quad (4.4)$$

$$\mathcal{Z}^{(\text{III})} \propto \int \mathcal{D}\tilde{\mathcal{O}}_{\omega, \vec{k}} \mathcal{D}\tilde{\mathcal{O}}_{-\omega, -\vec{k}} e^{-iS^{(\text{III})}[\tilde{\mathcal{O}}]},\quad (4.5)$$

$$\mathcal{Z}^{(\text{II})} \propto \int \mathcal{D}\mathcal{O}_{\omega, \vec{k}} \mathcal{D}\tilde{\mathcal{O}}_{\omega, \vec{k}} \mathcal{D}\mathcal{O}_{-\omega, -\vec{k}} \mathcal{D}\tilde{\mathcal{O}}_{-\omega, -\vec{k}} e^{-iS^{(\text{II})}[\mathcal{O}, \tilde{\mathcal{O}}]}.\quad (4.6)$$

In general the restricted partition function in region II, (4.6), does not factorize into the contributions coming from the modes \mathcal{O} and $\tilde{\mathcal{O}}$; $S^{(\text{II})}[\mathcal{O}, \tilde{\mathcal{O}}] \neq S^{(\text{I})}[\mathcal{O}] + S^{(\text{III})}[\tilde{\mathcal{O}}]$. However, we know that for generalized free fields, mixed correlators factorize at leading order of the $\frac{1}{N}$ expansion [41],

$$\begin{aligned}\langle \mathcal{O}_1 \mathcal{O}_2 \cdots \mathcal{O}_n \tilde{\mathcal{O}}_1 \tilde{\mathcal{O}}_2 \cdots \tilde{\mathcal{O}}_m \rangle &= \frac{1}{\mathcal{Z}^{(\text{II})}} \left. \frac{d^{n+m} \mathcal{Z}^{(\text{II})}}{dJ^n d\tilde{J}^m} \right|_{J=\tilde{J}=0} \\ &= \frac{1}{\mathcal{Z}^{(\text{I})}} \left. \frac{d^n \mathcal{Z}^{(\text{I})}}{dJ^n} \right|_{J=0} + \frac{1}{\mathcal{Z}^{(\text{III})}} \left. \frac{d^m \mathcal{Z}^{(\text{III})}}{d\tilde{J}^m} \right|_{\tilde{J}=0} + \mathcal{O}\left(\frac{1}{N}\right) \\ &= \langle \mathcal{O}_1 \mathcal{O}_2 \cdots \mathcal{O}_n \rangle \langle \tilde{\mathcal{O}}_1 \tilde{\mathcal{O}}_2 \cdots \tilde{\mathcal{O}}_m \rangle + \mathcal{O}\left(\frac{1}{N}\right).\end{aligned}\quad (4.7)$$

Therefore in the large N limit, one obtains a simple relation between the restricted partition functions at leading order of the $\frac{1}{N}$ expansion

$$\mathcal{Z}^{(II)} \propto \mathcal{Z}^{(I)} \mathcal{Z}^{(III)}. \quad (4.8)$$

Intuitively, the above equation indicates that in order to study region II, one needs twice the number of modes as those in region I. It is worth noting that since the operator (4.2) is a nonlocal operator in the dual field theory whose nonlocality parameter is given by the AdS radial coordinate, imposing any restriction on the nonlocality parameter (such as setting a UV cutoff) would restrict the range of the spacetime accessible to those fields defined behind the horizon.

Therefore, assuming that spacetime is cut off at the radial distance r_c , immediately and automatically implies that there should also be a second cutoff in region II, the region behind the outer horizon. This provides a justification for the existence of the interior cutoff “ r_0 ”, we introduced in the context of late time growth of the WdW action before. Furthermore, one can fix the proportionality constant in (4.8) and write down a relation involving the on-shell actions, in the respective regions of the Penrose diagram as

$$e^{i(S_{\text{cut-off}}^{(II)} - S_0^{(II)})} = e^{2i(S_{\text{cut-off}}^{(I)} - S_0^{(I)})}, \quad (4.9)$$

with $S_0^{(i)}$ denoting the on-shell action evaluated without a cutoff. In view of the fact that the original relation (4.8) was derived for generalized free fields, one might wonder at this point about how one can identify the restricted actions with the gravitational actions in respective regions.¹² An intuitive justification for doing this comes from the fact that at leading

order of $\frac{1}{N}$, the classical effective action is indeed given by the Einstein-Hilbert-Maxwell action, (2.1). The fluctuation of this action around the classical geometry given by (2.2) and (2.3) gives rise to the expectation value of the graviton field which can be treated as a generalized free field of the dual CFT. However, we should mention that this is only an intuitive argument and we do not have a concrete proof for the same. Rather we will consider this as a proposition motivated by [27] where the relation between the restricted gravitational actions led to a relation between two cutoffs in the case of an uncharged black brane which was found to be perfectly consistent with the well-accepted Lloyd’s bound in the uncharged case. It is legitimate to expect that the same should also work for our charged black brane.

Now we would like to use the relation (4.9) to determine the relation between the two cutoffs: the UV cutoff, r_c and the cutoff behind the horizon, r_0 . We will again assume the interior cutoff r_0 to lie between the inner and the outer horizons. Furthermore, here too we will compute the on-shell actions in the grand canonical ensemble. Also, as is standard procedure, in order to ensure finite free energies in all regions we are required to use both the Gibbons-Hawking terms and the counterterms which have the forms given in (2.6) and (2.7) respectively. With this, let us now write down the on-shell actions in different regions explicitly.

A. Region I: Outside the outer horizon

First we calculate the on-shell action in the region outside the outer horizon. This entails a radial integration from r_c to r_+ . The individual components of the on-shell action are given by

$$\begin{aligned} S_{\text{bulk}}^{(I)}(r_c) &= \frac{L^d V_d \tau}{8\pi G} \left(\frac{1}{r_+^{d+1}} + Q^2 r_+^{d-1} \right) - \frac{L^d V_d \tau}{8\pi G} \left(\frac{1}{r_c^{d+1}} + Q^2 r_c^{d-1} \right), \\ &= \frac{L^d V_d \tau}{8\pi G} m - \frac{L^d V_d \tau}{8\pi G} \left(\frac{1}{r_c^{d+1}} + Q^2 r_c^{d-1} \right), \\ S_{\text{GH}}^{(I)}(r_c) &= \frac{L^d V_d \tau}{8\pi G} \left(\frac{d+1}{r_c^{d+1}} + Q^2 r_c^{d-1} - \frac{d+1}{2} m \right), \\ S_{\text{CT}}^{(I)}(r_c) &= -\frac{L^d V_d \tau}{8\pi G} \frac{d}{r_c^{d+1}} \sqrt{f(r_c)}. \end{aligned} \quad (4.10)$$

Here, we have also introduced τ as a cutoff in time direction. By summing up the individual contributions we arrive at the total on-shell action in region I

$$\begin{aligned} S^{(I)}(r_c) &= S_{\text{bulk}}^{(I)}(r_c) + S_{\text{GH}}^{(I)}(r_c) + S_{\text{CT}}^{(I)}(r_c) \\ &= \frac{L^d V_d \tau}{16\pi G} (1-d)m + \frac{L^d V_d \tau}{8\pi G} \frac{d}{r_c^{d+1}} \left(1 - \sqrt{f(r_c)} \right). \end{aligned} \quad (4.11)$$

We now normalize this expression with respect to the no cutoff case. Hence, we subtract from (4.11), the asymptotic boundary limit, $r_c = \epsilon \rightarrow 0$, namely,

¹²We would like to thank the anonymous referee for bringing up this subtlety.

$$S^{(\text{I})}(\epsilon) = \frac{L^d V_d \tau}{16\pi G} m. \quad (4.12)$$

This yields

$$\begin{aligned} \Delta S^{(\text{I})} &= S^{(\text{I})}(r_c) - S^{(\text{I})}(\epsilon) \\ &= -\frac{L^d V_d \tau d}{16\pi G} m + \frac{L^d V_d \tau}{8\pi G} \frac{d}{r_c^{d+1}} \left(1 - \sqrt{f(r_c)}\right). \end{aligned} \quad (4.13)$$

B. Regions II: Between the two horizons

We now move to region II, which in principle runs from r_+ to r_- . However, we are assuming the existence of a cutoff situated between r_- and r_+ . Hence, we perform a radial integration from r_+ to r_0 . First note that without a cutoff, the bulk action in region II amounts to

$$\begin{aligned} S_{\text{bulk}}^{(\text{II})} &= \frac{L^d V_d \tau}{8\pi G} \left(\frac{1}{r_-^{d+1}} + Q^2 r_-^{d-1} \right) \\ &\quad - \frac{L^d V_d \tau}{8\pi G} \left(\frac{1}{r_+^{d+1}} + Q^2 r_+^{d-1} \right) = 0. \end{aligned} \quad (4.14)$$

However, if we set a cutoff at $r_0 < r_-$ this changes to

$$S_{\text{bulk}}^{(\text{II})}(r_0) = \frac{L^d V_d \tau}{8\pi G} \left(\frac{1}{r_0^{d+1}} + Q^2 r_0^{d-1} \right) - \frac{L^d V_d \tau}{8\pi G} m, \quad (4.15)$$

which, as expected, clearly vanishes as we set $r_0 = r_-$. Noting again the spacelike nature of the cutoff surface r_0 in region II, the contributions of the boundary terms (2.6), (2.7), are given by

$$\begin{aligned} S_{\text{GH}}^{(\text{II})}(r_0) &= -\frac{L^d V_d \tau}{8\pi G} \left(\frac{d+1}{r_0^{d+1}} + Q^2 r_0^{d-1} - \frac{d+1}{2} m \right), \\ S_{\text{CT}}^{(\text{II})}(r_0) &= \frac{L^d V_d \tau}{8\pi G} \frac{d}{r_0^{d+1}} \sqrt{-f(r_0)}. \end{aligned} \quad (4.16)$$

Hence, the full on-shell action in the interior for $r_0 < r_-$ is given by

$$\begin{aligned} S^{(\text{II})}(r_0) &= S_{\text{bulk}}^{(\text{II})}(r_0) + S_{\text{GH}}^{(\text{II})}(r_0) + S_{\text{CT}}^{(\text{II})}(r_0) \\ &= \frac{L^d V_d \tau}{16\pi G} (d-1)m + \frac{L^d V_d \tau}{8\pi G} \frac{d}{r_0^{d+1}} \left(\sqrt{-f(r_0)} - 1 \right). \end{aligned} \quad (4.17)$$

Just as we did for region I, we want to normalize the cutoff partition function by subtracting the asymptotic contribution, which for this case amounts to $r_0 = r_-$. Setting $r_0 = r_-$ makes the counter term and also the bulk contribution vanish, the Gibbons-Hawking term remains nonzero yielding the full on-shell action in this region without cutoff as

$$S^{(\text{II})}(r_-) = -\frac{L^d V_d \tau}{8\pi G} \left(\frac{d}{r_-^{d+1}} - \frac{d-1}{2} m \right). \quad (4.18)$$

One can then evaluate the difference $\Delta S^{(\text{II})}$ as

$$\begin{aligned} \Delta S^{(\text{II})} &= S^{(\text{II})}(r_0) - S^{(\text{II})}(r_-) \\ &= \frac{L^d V_d \tau d}{8\pi G} \left\{ \frac{1}{r_-^{d+1}} + \frac{1}{r_0^{d+1}} \left(\sqrt{-f(r_0)} - 1 \right) \right\}. \end{aligned} \quad (4.19)$$

We can now simply use (4.13) and (4.19) in (4.9) to find a relation between the two cutoffs, r_0 and r_c

$$\frac{2}{r_c^{d+1}} \left(1 - \sqrt{|f(r_c)|} \right) - m = \frac{1}{r_-^{d+1}} + \frac{1}{r_0^{d+1}} \left(\sqrt{-f(r_0)} - 1 \right). \quad (4.20)$$

This relation is identical to the one obtained by demanding the saturation of Lloyd's bound in (3.13). This matching is very much reminiscent of the chargeless case already noted in [27]. The charged scenario, in presence of the inner horizon will provide a new interpretation of this result.

V. TOWARDS A HOLOGRAPHIC REALIZATION OF STRONG COSMIC CENSORSHIP

Let us come back to the issue of the location of the cutoff r_0 . As stated previously, there are, in principle, two options in placing this cutoff. One may either put it between the inner and the outer horizons, or it may also be assumed to lie behind the inner horizon. In all our computations presented above, we chose the former option. Although this was only a choice initially, we will now argue that this choice leads to a self-consistent physical interpretation of our result.

It is worth mentioning here that in [25], the interior cutoff was assumed to lie behind the inner horizon.¹³ This leads to the late time growth of complexity being independent of this cutoff. Of course this was also consistent with Lloyd's bound (3.4) upon which this assumption was made. In this paper we have argued that this expression for Lloyd's bound exhibits certain unnatural features and therefore needs to be modified.

Moreover the assumption made in [25] results in inconsistencies if the growth has to approach and eventually saturate a bound at late times. This is because, whatever the correct bound is, it should depend on the physical, thermodynamical quantities of the boundary CFT and as we already saw, these quantities are explicitly dependent on the UV cutoff, r_c . As a result, there will be a mismatch of scales if we aim to construct an equation describing a bound, \mathcal{B} , on the growth of complexity, namely,

¹³We note however, that the main conclusion of that paper was not based on this assumption.

$$\frac{dC}{dt} \leq \mathcal{B}, \quad (5.1)$$

where the left-hand side of (5.1) will now be independent of any cutoff and the right-hand side will be dependent on r_c . One could argue that this might be the case if saturation is never met. However, it is quite unreasonable to expect such a situation for an AdS black hole due to the ‘‘fast scrambler’’ argument mentioned before.

Another interesting aspect of the setup considered in [25] is that it adds to an apparent ambiguity. While it was assumed that the late time growth of complexity is independent of the cutoff behind the horizon, in order to achieve the expected complexity growth for the near horizon AdS₂ region, one does need to consider the counterterms coming from the behind the horizon cutoff. Therefore, it turns out, in the setup of [25], this interior cutoff is very much essential but it is not clear how this should get fixed explicitly in terms of the UV cutoff, contrary to our expectations.

Having the interior cutoff between the two horizons solves all the aforementioned problems in a consistent way. With the interior cutoff placed between the inner and the outer horizons, the left-hand side of (5.1) depends on r_0 and the right-hand side, on r_c , thus providing the relation between the cutoffs. Moreover, we obtained exactly the same relation from the factorization of the partition function. As a consequence of having a well-defined bulk effective field theory, the factorization is expected to be obeyed at least when the cutoff is sufficiently close to the boundary of AdS.

The aforementioned arguments in favour of having the interior cutoff in between the inner and the outer horizons give us a hint about bulk reconstruction in AdS/CFT. The exact matching of the relation between the cutoffs makes it clear that complexity, as a probe, cannot penetrate the inner horizon of the black brane or black hole if it is to be consistent with the factorization of the Hilbert space at large N . It therefore indicates emergence of a holographic censorship in bulk reconstruction behind the inner horizon. One might naturally identify this as a version of strong cosmic censorship arising from holography.

VI. DISCUSSION AND OUTLOOK

In this work, we have revisited holographic complexity for charged black branes in the presence of a finite cutoff. We have seen that a UV finite cutoff enforces a cutoff behind the outer horizon, with an expression determined by the UV cutoff. This was shown in two ways.

First, by assuming that Lloyd’s bound is saturated for a charged black hole in the presence of a cutoff, we related conserved charges of this system to the late time growth of complexity. Here, interestingly, the charges are only sensitive to the UV cutoff, whereas the late-time behavior of holographic complexity seems blind to r_c . Assuming an

agreement to hold at late times forces a relation between the two cutoffs.

Secondly, we saw that the same relation may also be obtained using the leading-order factorization of the partition function in the $\frac{1}{N}$ expansion. Following Papadodimas-Raju’s construction of interior operators in terms of exterior operators, implies that behind the horizon, twice the number of modes are required.

A crucial point in order to make the overall setup consistent is to use the correct expression for Lloyd’s bound in terms of conserved charges such as the electric charge at the boundary. Although in the literature there are several proposals for Lloyd’s bound, they suffer from certain pathologies. Our proposal (3.5), in the neutral limit, reduces to the Schwarzschild case in a more natural way with the contributions arising solely from the outer horizon. Furthermore and perhaps more importantly, our proposed relation between the two cutoffs (3.13) as derived using our proposal for Lloyd’s bound, (3.5), guarantees an exact match with the relation obtained from the Papadodimas-Raju construction.

Our proposal for the expression of Lloyd’s bound (3.5), can be further generalized to systems with more physical conserved charges. For instance, in the case of a charged rotating system, it can be readily generalized to

$$\frac{dC}{dt} \leq \frac{1}{\pi\hbar} (2\mathcal{E} - \mu Q - \Omega J)_+ - (2\mathcal{E} - \mu Q - \Omega J)_-, \quad (6.1)$$

where J and Q are angular momentum and charge, and Ω and μ are their corresponding potentials.

In this paper we have only considered the case of an electric black brane, although we could have also considered dyonic black holes, in which the system carries both electric and magnetic charges. While in this case the final expressions become more involved, essentially the physical conclusions remain unchanged.

Moreover, in our computations, we have made a specific choice of ensemble. We are working in a grand canonical ensemble, in which the chemical potential μ is considered fixed. However, it is of course interesting to examine different choices of ensemble, specifically the canonical ensemble. This requires the addition of a boundary term to the action (2.1)

$$S_{\text{M,b}} = \frac{\gamma}{8\pi G} \int d^{d+1}x \sqrt{|h|} n_\mu F^{\mu\nu} A_\nu. \quad (6.2)$$

This generalizes our calculations to a larger choice of ensembles designated by values of γ , which is in the interval $[0, 1]$. $\gamma = 1$ corresponds to the canonical ensemble where the total charge Q is held fixed, while $\gamma = 0$ corresponds to the grand canonical ensemble where instead the chemical potential μ of the system is fixed and hence reduces to the approach outlined in this paper. Choices in between correspond to mixed ensembles. Holographic

complexity of charged black holes in the presence of this boundary term has been studied in [35,43].

The boundary term (6.2) would alter both the on-shell action computed on the WdW patch and also the computations of partition functions taking into account the effective field theory of the interior. Accordingly, the relations (3.13) and (4.20) between r_c and r_0 should be generalized to an arbitrary choice of ensemble. The natural question would then be if the relations obtained from the two approaches should agree for general γ or if this should only work for a specific choice of ensemble. We are investigating this issue and we hope to come back with a precise answer in a future publication. It will also be interesting to understand the near horizon, near extremal limit of the construction with arbitrary γ , as the presence of a boundary term of the form (6.2) was shown to be essential in this limit [25,43].

Assuming that the leading order factorization of the partition function works for arbitrary γ , following Sec. IV, the relation (4.20) generalizes to

$$\begin{aligned} & \frac{2}{r_c^{d+1}} \left(1 - \sqrt{|f(r_c)|} \right) - m \\ &= \frac{1}{r_-^{d+1}} + \frac{1}{r_0^{d+1}} \left(\sqrt{-f(r_0)} - 1 \right) \\ & \quad - \gamma Q^2 (r_0^{d-1} - r_-^{d-1} + 2r_c^{d-1}). \end{aligned} \quad (6.3)$$

It is interesting to see if this expression is consistent with the complexity computations for general ensembles.

Another aspect which we would like to investigate in the future is the “factorization puzzle”, namely, the apparent tension of the exact factorization of the boundary Hilbert space and the loss thereof due to bulk wormhole structures [44–48]. Following the connection between the bound on the late time growth of complexity and the factorization of the partition function that we developed in this work, it is of course highly interesting to see in how far the presence of bulk wormholes is captured by the growth of complexity. Particularly, connecting to the discussion above, it will be worth investigating if the ensemble dependence plays any crucial role here.

ACKNOWLEDGMENTS

We would like to thank Johanna Erdmenger, René Meyer, and Ali Naseh for several useful discussions. We would like to thank Johanna Erdmenger for comments on the manuscript. The work of S. B. is supported by the Alexander von Humboldt postdoctoral fellowship. The work of J. K.-K. was supported in part by the Heising-Simons Foundation, the Simons Foundation, and National Science Foundation Grant No. NSF PHY-1748958.

-
- [1] S. D. Mathur, The information paradox: A pedagogical introduction, *Classical Quantum Gravity* **26**, 224001 (2009).
 - [2] A. Almheiri, D. Marolf, J. Polchinski, and J. Sully, Black holes: Complementarity or firewalls?, *J. High Energy Phys.* **02** (2013) 062.
 - [3] A. Almheiri, D. Marolf, J. Polchinski, D. Stanford, and J. Sully, An apologia for firewalls, *J. High Energy Phys.* **09** (2013) 018.
 - [4] D. Marolf and J. Polchinski, Gauge/Gravity Duality and the Black Hole Interior, *Phys. Rev. Lett.* **111**, 171301 (2013).
 - [5] K. Papadodimas and S. Raju, An infalling observer in AdS/CFT, *J. High Energy Phys.* **10** (2013) 212.
 - [6] K. Papadodimas and S. Raju, State-dependent bulk-boundary maps and black hole complementarity, *Phys. Rev. D* **89**, 086010 (2014).
 - [7] S. Banerjee, J.-W. Bryan, K. Papadodimas, and S. Raju, A toy model of black hole complementarity, *J. High Energy Phys.* **05** (2016) 004.
 - [8] C. Chowdhury, O. Papadoulaki, and S. Raju, A physical protocol for observers near the boundary to obtain bulk information in quantum gravity, *SciPost Phys.* **10**, 106 (2021).
 - [9] L. Susskind, Computational complexity and black hole horizons, *Fortschr. Phys.* **64**, 44 (2016); **64**, 24 (2016).
 - [10] J. Maldacena and L. Susskind, Cool horizons for entangled black holes, *Fortschr. Phys.* **61**, 781 (2013).
 - [11] A. R. Brown, D. A. Roberts, L. Susskind, B. Swingle, and Y. Zhao, Holographic Complexity Equals Bulk Action?, *Phys. Rev. Lett.* **116**, 191301 (2016).
 - [12] A. R. Brown, D. A. Roberts, L. Susskind, B. Swingle, and Y. Zhao, Complexity, action, and black holes, *Phys. Rev. D* **93**, 086006 (2016).
 - [13] L. McGough, M. Mezei, and H. Verlinde, Moving the CFT into the bulk with $T\bar{T}$, *J. High Energy Phys.* **04** (2018) 010.
 - [14] M. Taylor, TT deformations in general dimensions, [arXiv:1805.10287](https://arxiv.org/abs/1805.10287).
 - [15] T. Hartman, J. Kruthoff, E. Shaghoulian, and A. Tajdini, Holography at finite cutoff with a T^2 deformation, *J. High Energy Phys.* **03** (2019) 004.
 - [16] A. B. Zamolodchikov, Expectation value of composite field T anti-T in two-dimensional quantum field theory, [arXiv: hep-th/0401146](https://arxiv.org/abs/hep-th/0401146).
 - [17] F. A. Smirnov and A. B. Zamolodchikov, On space of integrable quantum field theories, *Nucl. Phys.* **B915**, 363 (2017).
 - [18] A. Cavaglià, S. Negro, I. M. Szécsényi, and R. Tateo, $T\bar{T}$ -deformed 2D quantum field theories, *J. High Energy Phys.* **10** (2016) 112.

- [19] E. Witten, A note on boundary conditions in euclidean gravity, *Rev. Math. Phys.* **33**, 2140004 (2021).
- [20] M. Guica and R. Monten, $T\bar{T}$ and the mirage of a bulk cutoff, *SciPost Phys.* **10**, 024 (2021).
- [21] A. Akhavan, M. Alishahiha, A. Naseh, and H. Zolfi, Complexity and behind the horizon cut off, *J. High Energy Phys.* **12** (2018) 090.
- [22] S. Lloyd, Ultimate physical limits to computation, *Nature (London)* **406**, 1047 (2000).
- [23] D. Carmi, S. Chapman, H. Marrochio, R. C. Myers, and S. Sugishita, On the time dependence of holographic complexity, *J. High Energy Phys.* **11** (2017) 188.
- [24] S. S. Hashemi, G. Jafari, A. Naseh, and H. Zolfi, More on complexity in finite cut off geometry, *Phys. Lett. B* **797**, 134898 (2019).
- [25] M. Alishahiha, K. Babaei Velni, and M. R. Tanhayi, Complexity and near extremal charged black branes, *Ann. Phys. (Amsterdam)* **425**, 168398 (2021).
- [26] M. Alishahiha, K. Babaei Velni, and M. R. Mohammadi Mozaffar, Black hole subregion action and complexity, *Phys. Rev. D* **99**, 126016 (2019).
- [27] A. Akhavan and M. Alishahiha, An infalling observer and behind the horizon cutoff, *SciPost Phys.* **7**, 073 (2019).
- [28] K. Papadodimas, S. Raju, and P. Shrivastava, A simple quantum test for smooth horizons, *J. High Energy Phys.* **12** (2020) 003.
- [29] R.-G. Cai, S.-M. Ruan, S.-J. Wang, R.-Q. Yang, and R.-H. Peng, Action growth for AdS black holes, *J. High Energy Phys.* **09** (2016) 161.
- [30] H. Razaghian, Complexity growth of dyonic black holes with quartic field strength corrections, [arXiv:2009.03948](https://arxiv.org/abs/2009.03948).
- [31] A. Chamblin, R. Emparan, C. V. Johnson, and R. C. Myers, Charged AdS black holes and catastrophic holography, *Phys. Rev. D* **60**, 064018 (1999).
- [32] K. Parattu, S. Chakraborty, B. R. Majhi, and T. Padmanabhan, A boundary term for the gravitational action with null boundaries, *Gen. Relativ. Gravit.* **48**, 94 (2016).
- [33] K. Parattu, S. Chakraborty, and T. Padmanabhan, Variational principle for gravity with null and non -null boundaries: A unified boundary counter-term, *Eur. Phys. J. C* **76**, 129 (2016).
- [34] L. Lehner, R. C. Myers, E. Poisson, and R. D. Sorkin, Gravitational action with null boundaries, *Phys. Rev. D* **94**, 084046 (2016).
- [35] K. Goto, H. Marrochio, R. C. Myers, L. Queimada, and B. Yoshida, Holographic complexity equals which action?, *J. High Energy Phys.* **02** (2019) 160.
- [36] R. Emparan, C. V. Johnson, and R. C. Myers, Surface terms as counterterms in the AdS/CFT correspondence, *Phys. Rev. D* **60**, 104001 (1999).
- [37] S. de Haro, S. N. Solodukhin, and K. Skenderis, Holographic reconstruction of space-time and renormalization in the AdS/CFT correspondence, *Commun. Math. Phys.* **217**, 595 (2001).
- [38] C. A. Agón, M. Headrick, and B. Swingle, Subsystem complexity and holography, *J. High Energy Phys.* **02** (2019) 145.
- [39] A. Reynolds and S. F. Ross, Divergences in holographic complexity, *Classical Quantum Gravity* **34**, 105004 (2017).
- [40] Y. Sekino and L. Susskind, Fast scramblers, *J. High Energy Phys.* **10** (2008) 065.
- [41] S. El-Showk and K. Papadodimas, Emergent spacetime and holographic CFTs, *J. High Energy Phys.* **10** (2012) 106.
- [42] M. Van Raamsdonk, Comments on quantum gravity and entanglement, [arXiv:0907.2939](https://arxiv.org/abs/0907.2939).
- [43] A. R. Brown, H. Gharibyan, H. W. Lin, L. Susskind, L. Thorlacius, and Y. Zhao, Complexity of Jackiw-Teitelboim gravity, *Phys. Rev. D* **99**, 046016 (2019).
- [44] D. Harlow, Wormholes, emergent gauge fields, and the weak gravity conjecture, *J. High Energy Phys.* **01** (2016) 122.
- [45] D. Harlow and D. Jafferis, The factorization problem in Jackiw-Teitelboim gravity, *J. High Energy Phys.* **02** (2020) 177.
- [46] P. Saad, S. H. Shenker, and D. Stanford, JT gravity as a matrix integral, [arXiv:1903.11115](https://arxiv.org/abs/1903.11115).
- [47] P. Saad, S. H. Shenker, D. Stanford, and S. Yao, Wormholes without averaging, [arXiv:2103.16754](https://arxiv.org/abs/2103.16754).
- [48] H. Verlinde, Deconstructing the wormhole: Factorization, entanglement and decoherence, [arXiv:2105.02142](https://arxiv.org/abs/2105.02142).

Quantum Information: Complexity in JT Gravity

This chapter has already been published as [134]:

Complexity via Replica Trick, *M. Alishahiha, S. Banerjee, J. Kames-King*, arXiv: 2205.01150 [hep-th]

This chapter deals with the non-perturbatively defined approach to complexity as outlined in section 1.5.5. We reinterpret the results of that section in terms of a replica type formula. While this proposal implies the same late time behaviour for complexity, it furnishes an improved result for the variance, which no longer suffers from late time linear growth but saturates to a constant value. Moreover, we generalise the overall approach to one-sided black holes as modelled by JT gravity in the presence of an end-of-the-world brane.

In detail, we start by introducing JT gravity in the presence of an end-of-the-world brane. The introduction of such a brane amounts to modelling a one-sided black hole and therefore a pure state. This geometry arises as a \mathcal{Z}_2 quotient of the two-sided case, where the end-of-the-world brane constitutes a dynamical boundary (see references [60, 135]). The exact location depends on the mass of the brane. Canonical quantisation of this theory of gravity on the disk gives a specific wavefunction expression, which is the starting point of most considerations in this publication. The geodesic length running from the end-of-the-world brane to the asymptotically AdS boundary is the canonical basis of the Hilbert space underlying these L_2 -normalisable wavefunctions. We show how such a wavefunction can be calculated via the Euclidean JT path integral on different geometries. The trumpet geometry for example is important as higher genus topologies require this ingredient. As a side note, we show that the pure state we are describing still obeys the eigenstate thermalisation hypothesis (see section 1.4.4). This is to be expected as it is universally very difficult to distinguish a pure state from a typical thermal state. Moreover, we calculate both the partition function in the presence of an end-of-the-world brane and also matter correlation functions. The main result of this paper is the calculation of complexity in terms of a modified CV proposal (see section 1.5.5). First, we do not consider a specific maximum length geodesic as would be in line with the standard CV proposal. Due to the statistical nature of the JT path integral, we consider an infinite sum of geodesics in line with section 1.5.5. Geometrically this makes sense as there is no single, maximum geodesic on

geometries with handles. However, in contrast to section 1.5.5, we do not consider this length to be related to an analytically continued boundary-to-boundary two-point function. We instead argue that the length expectation value used for complexity, as an extensive quantity in an ensemble theory, is defined as a quenched expectation value (see also reference [136]). For the two-sided case this gives the same result for the complexity as shown in section 1.5.5. For the variance of complexity, that is the fluctuations of the plateau, we arrive at a pleasing conclusion. Our modified approach implies a different calculation for the connected contribution to the variance, which leads to the same behaviour in time as complexity itself. As complexity saturates in our proposal, so does the variance. While the complexity in the presence of an end-of-the-world brane involves lengthier expressions, the qualitative result, that is the time-dependence, is of the form as the two-sided case. In addition we perform a toy-model calculation of complexity involving dynamical end-of-the-world branes. This would mean that such branes may also appear as loops and additional boundaries of the involved Riemann surfaces. As directly working with dynamical end-of-the-world branes is a project in itself, the calculation was performed instead with so-called FZZT anti-branes. These objects are simpler to handle. Interestingly, there is a competition between the number of branes vs e^{S_0} similar to the behaviour of entanglement entropy in [137]. We conclude by calculating complexity in the presence of an UV cutoff, therefore in the framework of the $T\bar{T}$ deformation.

The author contributed to all conceptual discussions regarding this preprint. The author performed the calculations of sections 2.1, 2.2, 2.3, 2.4, 3, 5.2.

Complexity via Replica Trick

Mohsen Alishahiha,^a Souvik Banerjee,^{b,c} Joshua Kames-King^d

^a*School of Physics, Institute for Research in Fundamental Sciences (IPM),
P.O. Box 19395-5531, Tehran, Iran*

^b*Institut für Theoretische Physik und Astrophysik, Julius-Maximilians-Universität Würzburg,
Am Hubland, 97074 Würzburg, Germany*

^c*Würzburg-Dresden Cluster of Excellence ct.qmat*

^d*Bethe Center for Theoretical Physics and Physikalisches Institut der Universität Bonn, Nussallee
12, 53115 Bonn, Germany*

E-mail: alishah@ipm.ir, souvik.banerjee@physik.uni-wuerzburg.de,
jvakk@yahoo.com

ABSTRACT: We consider the complexity of a single-sided AdS black hole as modelled by an end-of-the-world brane. In addition we present multi-boundary partition functions and matter correlation functions for such a setting. We compute the complexity using a modified replica trick corresponding to the “quenched geodesic length” in JT gravity. The late time behaviour of complexity shows a saturation to a constant value of order e^{S_0} following a period of linear growth. Furthermore, we show that our approach leads to an improved result for the variance of complexity, namely it being time-independent at late times. We conclude by commenting on the introduction of dynamical end-of-the-world branes.

Contents

1	Introduction	1
2	Lorentzian JT gravity with EOW Branes and Wavefunctions	4
2.1	The classical solution	4
2.2	Quantisation in presence of a brane	4
2.3	The disk wavefunctions	7
2.4	The trumpet wavefunctions	8
2.5	Pure vs. Thermal States	10
3	Partition Function	12
4	Correlation Functions	13
5	The late time behaviour of complexity	15
5.1	The geodesic ℓ	16
5.2	The geodesic L	17
5.3	The variance of complexity	21
6	Conclusion and Outlook	22

1 Introduction

In the context of the AdS/CFT correspondence [1–3] it is believed that the interior of a black hole may be systematically studied via the notion of quantum computational complexity. This field of study quantifies the difficulty of constructing a specific “target state” by use of a simple set of “universal gates”. More specifically in a holographic setting it is conjectured that for a chaotic CFT the growth of complexity has a simple geometric description in terms of the growth of the black hole interior.

One of the arguments for this conjecture is that for a fast-scrambling system with finite entropy S , complexity is expected to grow for exponentially large times in the entropy, long after thermal equilibrium has been reached [4, 5]. Remarkably, the same growth holds for the black hole interior. Therefore a concrete instantiation of this conjectured duality is the “complexity=volume” (CV) conjecture, which proposes that the complexity equals the volume of a maximal slice in the black hole interior [4, 6]. There is also another competing proposal known as the “complexity=action” (CA) conjecture, in which the on-shell action on a Wheeler-de Witt patch is determined [7, 8].

We note however, that for chaotic Hamiltonians (as can, for example, be seen in simple circuit models) after the aforementioned period of growth, at times $t \sim (\mathcal{O}(e^S))$ we expect saturation to a plateau of size $C \sim (\mathcal{O}(e^S))$ [9–14]. While semi-classical contributions both in form of the CV and CA conjectures indeed furnish the period of growth, the saturation to the plateau, until recently, has been illusive.

To understand complexity better one may study this concept in Jackiw-Teitelboim (JT) gravity; a theory of two-dimensional dilaton gravity, including arbitrary genus, hyperbolic Riemann surfaces and therefore also exponentially small corrections to semi-classical gravity calculations [15–20]. Actually extending the gravitational sector by including such geometries with an arbitrary number of asymptotic boundaries and arbitrary genus corrects the partition function to be equivalent to a specific double-scaled Hermitian matrix integral. This implies that JT gravity follows RMT universality at late times and therefore exhibits spectral statistics with a dip-ramp-plateau structure [19–22].¹ By use of the same theory it has also been shown that the inclusion of higher topologies gives a unitary Page curve [25, 26].

Recently, holographic complexity was calculated in JT gravity using the CV conjecture in [27] where it was shown that including higher genus geometries (as mentioned above) gives the correct late-time behaviour for complexity. More precisely, in this paper the authors compute complexity in terms of a non-perturbative geodesic length in JT gravity as follows

$$\langle \ell \rangle = \lim_{\Delta \rightarrow 0} \left\langle \sum_{\gamma} \ell_{\gamma} e^{-\Delta \ell_{\gamma}} \right\rangle_{\text{JT}}, \quad (1.1)$$

where γ refers to non self-intersecting geodesics, Δ is a regulator and $\langle \rangle_{\text{JT}}$ a correlator in JT gravity defined over arbitrary genus. It is then argued that in practice (1.1) is calculated by

$$\langle \ell(t) \rangle = - \lim_{\Delta \rightarrow 0} \frac{\partial \langle \chi(t) \chi(0) \rangle_{\text{non-int.}}}{\partial \Delta}, \quad (1.2)$$

where $\langle \chi(t) \chi(0) \rangle_{\text{non-int.}}$ is obtained in the Euclidean JT theory and then analytically continued. Here Δ is the scaling dimension of the operator χ . Eq. (1.2) then of course involves (on surfaces with $g \geq 1$) an infinite number of geodesics which can be taken care of by the moduli space volume of hyperbolic surfaces [28]. It was, then, demonstrated that the above definition results in the following expression for complexity

$$\langle \ell(t) \rangle = - \frac{2e^{-S_0}}{Z(\beta)} \int_0^{\infty} \frac{\langle \rho(s_1) \rho(s_2) \rangle}{\bar{s} \sinh(2\pi \bar{s}) \omega \sinh(\pi \omega)} \exp \left(-\beta \left(\frac{\bar{s}^2}{2} + \frac{\omega^2}{8} \right) - i\bar{s}\omega t \right). \quad (1.3)$$

with the definitions of $\omega = s_1 - s_2$, $\bar{s} = \frac{s_1 + s_2}{2}$ and $s_{1,2} = \sqrt{E_{1,2}}$. The quantity (1.3) was called “spectral complexity” in [27], which can be calculated for any quantum theory by use of its spectral correlation $\langle \rho(s_1) \rho(s_2) \rangle$.

Due to the usual arguments regarding quantum chaos [29, 30], one would suspect that for chaotic systems, (1.3) would reduce to RMT predictions at late times. For the case of JT gravity, the spectral two-point function can be shown to take on the standard RMT sine-kernel structure [20, 22, 31] by use of doubly non-perturbative effects. This in turn leads to the aforementioned, expected behaviour for the quantity $\langle \ell(t) \rangle$: early linear growth followed by a late-time plateau saturation.

In the present work, we are interested in studying two aspects of complexity for JT gravity. First, we would like to use an approach which removes the worrisome behaviour of the variance obtained in [27], as we will explain in greater detail below. Secondly, we would like to study the introduction of an end-of-the-world (EOW) brane. Recently, these

¹For work on the relationship between chaos universality and Euclidean wormholes in higher dimensions see [23, 24].

objects have played a crucial role in understanding quantum aspects of black holes in a two-dimensional setting as they can be used to model black hole microstates in JT gravity [26]. Since a black hole with an EOW brane behind the horizon may be understood as a \mathbb{Z}_2 quotient of the two-sided scenario, it corresponds to a pure state [32, 33]. However, according to the eigenstate thermalisation hypothesis (ETH) [29, 30], a pure state is in many ways indistinguishable from a thermal state.

It is also worth mentioning that EOW branes may also be used in a dynamical manner, which means they appear as loops and are summed over in the path integral. In this approach they may provide an ingredient in defining a UV completion of JT gravity and solve the factorisation problem [34, 35].²

Motivated by this, we consider the computation of multi-boundary partition functions and matter correlation functions in the presence of an EOW brane. While we adopt the techniques developed in [20] and [39] respectively, the modified result we obtain due to the presence of the EOW brane is expected to represent the aforementioned quantities in a single-sided black hole geometry.

Indeed the main concern of the present paper is the computation of the late time behaviour of complexity. We define this as the geodesic length connecting the EOW brane and the asymptotic boundary.³ More concretely, this is calculated in JT gravity as a *quenched expectation value*. The qualitative behaviour remains the same as in the case of a two-sided black hole, namely, the complexity grows linearly at late times up to a time $t \sim e^{S_0}$ and subsequently saturates to a constant value. The value of this constant which is of $\mathcal{O}(e^{S_0})$ depends crucially on the tension of the EOW brane.

Although we adopt the non-perturbative definition⁴ of complexity from [27], we refrain from rewriting it in terms of the correlators as in (1.2). The reason is, although the quantity structurally looks similar to the aforementioned correlators, the limits on Δ appearing in the definition are counter-intuitive and do not agree with the standard geodesic approximation to the two-point function.

Therefore we rather use a modified version of the replica trick in order to compute the quenched expectation value of the length of the geodesic.⁵ This avoids the aforementioned ambiguity. Moreover using the definition of variance engendered by the modified replica approach, we observe time-independent results at late times both for the two-sided and the one-sided geometries. This is in contrast with the result for the variance presented in [27] where the complexity is defined in terms of a two-point function (1.2).

Our paper is organised as follows. We will start by introducing the theory of interest in section 2. By use of the quantisation procedure in the presence of a boundary brane [34], we construct various wavefunctions needed in building up different partition functions and of course the path integral, which describes the volume of the black hole interior for our setting. In this section we also consider matrix elements in the geodesic length basis on the Hilbert space produced by the EOW brane. More specifically, we calculate the off-diagonal elements showing that while we are describing a pure state, they still obey the ETH. In sections 3 and 4 we construct the multi-boundary partition function and the quantum gravity matter correlation functions respectively. We put the pieces together in section 5, where we compute the complexity using the definition mentioned above. Then

²For other approaches to possible non-perturbative completions of JT gravity see [36–38].

³In the Lorentzian picture this replaces the bridge-to-nowhere of [40].

⁴This is non-perturbative by virtue of an analytic continuation of the Euclidean path integral.

⁵Following [27], we only consider non self-intersecting geodesics.

we also consider the variance of this quantity. We conclude in section 6 with a couple of interesting questions and comments on work in progress.

2 Lorentzian JT gravity with EOW Branes and Wavefunctions

In this section we use the canonical quantisation procedure first introduced in [35], to construct different wavefunction expressions for JT gravity in the presence of an EOW brane. After reviewing the quantisation procedure in presence of a boundary brane [34], we generalise the construction to compute wavefunctions for different configurations of the EOW brane on the disk and then for the trumpet. These quantities are the essential building blocks in the calculation of correlation functions as well as complexity in our setup.

2.1 The classical solution

JT gravity is a two-dimensional theory of gravity with the Lorentzian action [15, 16]

$$S_{\text{JT}} = \frac{S_0}{2\pi} \left(\int \sqrt{-g} R + 2 \int \sqrt{|h|} K \right) + \int \sqrt{-g} \phi (R + 2) + 2 \int \sqrt{|h|} \phi (K - 1), \quad (2.1)$$

where the first term is the topological Gauss-Bonnet term and S_0 is the ground state entropy. In addition, we add the action of an EOW brane, which is of the form:

$$S_{\text{Brane}} = \mu \int_{\text{Brane}} ds, \quad (2.2)$$

with μ being the brane tension. In two spacetime dimensions, the eq (2.2) boils down to the action of a particle with mass μ . The overall action is given by

$$S = S_{\text{JT}} + S_{\text{Brane}}. \quad (2.3)$$

The corresponding equations of motion are

$$R + 2 = 0, \quad \nabla_\mu \nabla_\nu \phi - g_{\mu\nu} \nabla^2 \phi + g_{\mu\nu} \phi = 0. \quad (2.4)$$

At the asymptotic AdS boundary, the boundary conditions are set by fixing the induced metric and the dilaton value [17, 18, 41]

$$ds^2|_{\partial M} = -\frac{dt^2}{\epsilon^2}, \quad \phi|_{\partial M} = \frac{\phi_b}{\epsilon}, \quad (2.5)$$

where ϵ is a holographic renormalisation parameter and we are interested in the limit $\epsilon \rightarrow 0$. Additionally, at the EOW brane the following conditions are set [26]

$$K = 0, \quad \partial_n \phi = \mu. \quad (2.6)$$

Here ∂_n denotes the derivative normal to the EOW brane. The latter condition is essential in ensuring dynamical gravity on the EOW brane.

2.2 Quantisation in presence of a brane

Let us denote the normalised geodesic distance between the AdS boundary and the EOW brane by L . The Hilbert space may be constructed in terms of L_2 -normalisable functions of

L .⁶ As the system may be thought of as a particle in a Morse potential, the Hamiltonian amounts to [34]

$$H = \frac{2}{\phi_b} \left(\frac{P^2}{4} + \mu e^{-L} + e^{-2L} \right), \quad (2.7)$$

such that the Schrödinger equation is given by [34, 35]

$$(-\partial_L^2 + 4\mu e^{-L} + 4e^{-2L}) \psi_{\mu,E}(L) = 2E \psi_{\mu,E}(L). \quad (2.8)$$

In going from (2.7) to (2.8) we have set $\phi_b = 1$ and replaced $P \rightarrow -i\partial_L$. In solving (2.8), we are generally assuming $\mu > 0$. Setting $k^2 = 2E$ and $z = 4e^{-L}$ the corresponding normalised wavefunction [34] is⁷

$$\psi_{k,\mu}(z) = \sqrt{f_\mu(k)} \frac{W_{-\mu,ik}(z)}{\sqrt{z}}, \quad \text{with } f_\mu(k) = \gamma_\mu(k)r(k), \quad (2.9)$$

where we have defined

$$\gamma_\mu(k) = \left| \Gamma \left(\frac{1}{2} + \mu + ik \right) \right|^2, \quad r(k) = \frac{k \sinh(2\pi k)}{\pi^2}. \quad (2.10)$$

The normalisation of $\psi_{k,\mu}(z)$ requires the use of the orthogonality relation for Whittaker functions of the second kind of imaginary order [42]

$$\int_0^\infty \frac{dz}{z^2} W_{-\mu,ik}(z) W_{-\mu,ik'}(z) = \frac{1}{f_\mu(k)} \delta(k - k'). \quad (2.11)$$

The quantum mechanical propagator is [34]

$$G_\beta(z_1, z_2) = \langle L_2 | e^{-\beta H} | L_1 \rangle = \int dk e^{-\frac{\beta k^2}{2}} f_\mu(k) \frac{W_{-\mu,ik}(z_1)}{\sqrt{z_1}} \frac{W_{-\mu,ik}(z_2)}{\sqrt{z_2}}. \quad (2.12)$$

Let us now come to a more geometric description in terms of the Euclidean path integral of JT gravity. In the Euclidean picture, the time coordinate τ is periodic with $\tau \sim \tau + \beta$. The Euclidean action is given by

$$S = -\frac{S_0}{2\pi} \left(\int \sqrt{g} R + 2 \int \sqrt{|\hbar|} K \right) - \int \sqrt{g} \phi (R + 2) - 2 \int \sqrt{|\hbar|} \phi (K - 1), \quad (2.13)$$

where we set the following boundary conditions for an asymptotic AdS boundary

$$ds^2|_{\partial M} = \frac{d\tau^2}{\epsilon^2}, \quad \phi|_{\partial M} = \frac{\phi_b}{\epsilon}. \quad (2.14)$$

Again, the first term of (2.13) is purely topological and accounts for the Euler characteristic of the Riemann surface $\chi = 2 - 2g - n$, where g is the genus and n the number of boundaries. The integration over the dilaton localises the path integral to surfaces of con-

⁶This is referred to as the ‘‘L-basis’’ in [35]. The choice of this basis avoids the subtlety of defining a ‘‘time operator’’ whose dual Hamiltonian is bounded from below. Furthermore, this choice also allows for a full phase space \mathbb{R}^2 without any restrictions on the phase space coordinates.

⁷Due to the fact that $W_{a,b} = W_{a,-b}$ we are restricted to $k \geq 0$.

stant negative curvature with an asymptotic boundary length determined by the boundary conditions (2.14). The extrinsic curvature term gives a Schwarzian action to the asymptotic boundary fluctuations on the hyperbolic space [17, 18].

The complete path integral includes an integral over the moduli of such surfaces and the boundary fluctuations. Briefly stated, the higher genus surfaces for one asymptotic boundary may be viewed as consisting of two parts, namely, one asymptotic boundary of fixed length and a geodesic boundary of length b and a remaining genus g Riemann surface with geodesic boundary of the same length b . The genus expansion of JT then takes on the form [20]:

$$\langle Z(\beta) \rangle = e^{S_0} \hat{Z}_D(\beta) + \sum_{g=1} e^{(1-2g)S_0} \int_0^\infty b db V_{g,1}(b) \hat{Z}_T(\beta, b), \quad (2.15)$$

where $V_{g,1}$ is the Weil-Petersson volume of genus g and one geodesic boundary [28, 43] and the integration over b glues the two parts of the surface together. Here $\hat{Z}_D(\beta)$ refers to the disk topology partition function and $\hat{Z}_T(\beta, b)$ to the ‘‘trumpet’’ partition function [20, 44]

$$\hat{Z}_D(\beta) = \frac{e^{\frac{2\pi^2}{\beta}}}{\sqrt{2\pi}\beta^{3/2}}, \quad \hat{Z}_T(\beta, b) = \frac{e^{-\frac{b^2}{2\beta}}}{\sqrt{2\pi}\beta^{1/2}}. \quad (2.16)$$

This construction can be generalised to n asymptotic boundaries with the connected contribution being of the form [20]:

$$\langle Z(\beta_1) \dots Z(\beta_n) \rangle_C = \sum_{g=0} e^{(2-2g-n)S_0} \hat{Z}_{g,n}(\beta_1, \dots, \beta_n), \quad (2.17)$$

with the definition

$$\hat{Z}_{g,n}(\beta_1, \dots, \beta_n) = \int_0^\infty b_1 db_1 \dots b_n db_n V_{g,n}(b_1, \dots, b_n) \hat{Z}_T(\beta_1, b_1) \dots \hat{Z}_T(\beta_n, b_n). \quad (2.18)$$

Moreover, the hats, $\hat{}$ denote quantities without manifest topological weighting. Incorporating the latter, one defines $Z_D(\beta) = e^{S_0} \hat{Z}_D(\beta)$. In our construction, we additionally consider the addition of an EOW brane via the action (2.2) and the boundary conditions (2.6). This modifies the partition function as we explain in the next sections.

At various points we will compute the expectation value of geodesic length in the Euclidean JT path integral. In contrast to the disk, on hyperbolic surfaces of genus $g \geq 1$ there are an infinite number of geodesics. Let us consider the case of non self-intersecting geodesics as in [27]. The moduli space of hyperbolic, bordered Riemann surfaces $\mathcal{M}_{g,n}(b_1, \dots, b_n)$ comes with a symplectic form, the Weil-Petersson form $\Omega = \sum_{i=1}^{3g+n-3} db_i \wedge d\tau_i$, which in principle allows the calculation of the corresponding moduli space volume if restricted to a fundamental domain. Similarly, as first argued for in the $g = 1$ case in [21], and elaborated upon in [27, 45], the integral of the geodesics over moduli space may be calculated by modding via the mapping class group, which we denote $\text{MCG}_{g,n}$. This leads to the expression [21, 27, 27, 28]

$$\int_{\frac{\mathcal{M}_{g,1}}{\text{MCG}_{g,1}}} \Omega \sum_{\gamma} e^{-\Delta \ell_{\gamma}} = e^{-\Delta \ell} \int_{\frac{\mathcal{M}_{g-1,2}}{\text{MCG}_{g-1,2}}} \Omega + \sum_{h \geq 0} e^{-\Delta \ell} \int_{\frac{\mathcal{M}_{h,1}}{\text{MCG}_{h,1}}} \Omega \int_{\frac{\mathcal{M}_{g-h,1}}{\text{MCG}_{g-h,1}}} \Omega. \quad (2.19)$$

This formula may be visualised as cutting along the geodesic and considering the resulting geometries.

2.3 The disk wavefunctions

Let us start by quickly revisiting some results we need from the two-sided AdS system. A natural procedure to prepare the states in the Hilbert space of the two-sided system is via the Hartle- Hawking construction [35], which is depicted in fig.1(a).

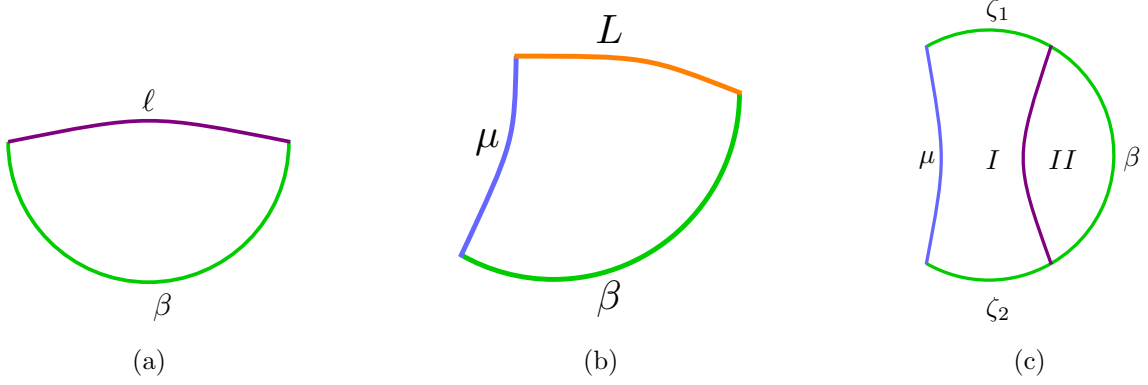


Figure 1: Three possible disk configurations corresponding to different wavefunctions. Figure (a) is the wavefunction of the Hartle-Hawking state of the two-sided AdS system in JT gravity. Figure (b) and figure (c) are two options in the presence of an EOW brane. While in figure (b) we see a geodesic connecting the EOW brane to the asymptotic boundary, for figure (c) the geodesic connects to two different points on the asymptotic boundary. An orange curve corresponds to the former geodesic and a violet curve to the latter. Green denotes an AdS boundary and blue an EOW brane, respectively.

We denote the fixed geodesic length between two parts of the AdS boundary by ℓ . Then the Hartle-Hawking wavefunction $\Phi_{D,\beta}(\ell)$ corresponds to the integral over all Euclidean geometries with disk topology and asymptotic AdS boundary of renormalised length β . Explicitly it amounts to

$$\Phi_D(\beta, \ell) = 2e^{S_0/2} \int_0^\infty dk e^{-\frac{\beta k^2}{2}} r(k) K_{2ik}(y), \quad (2.20)$$

where $y = 4e^{-\frac{\ell}{2}}$. In this formalism the disk partition function is given as

$$\begin{aligned} Z_D(\beta) &= \int_0^\infty \frac{dy}{y} \Phi_D(\beta/2, \ell) \Phi_D(\beta/2, \ell) = \frac{e^{S_0}}{2} \int_0^\infty dk e^{-\frac{\beta k^2}{2}} r(k) \\ &= e^{S_0} \int_0^\infty dE e^{-\beta E} \hat{\rho}_D(E), \end{aligned} \quad (2.21)$$

where $\hat{\rho}_D(E)$ is the disk density of states, which is given as [39, 44, 46–49]

$$\hat{\rho}_D(E) = \frac{\sinh(2\pi\sqrt{2E})}{2\pi^2}. \quad (2.22)$$

From (2.21) we see that the wavefunction is normalised in such a way to give the correct expression for (2.21) and (2.22).

Before moving on to more complicated hyperbolic surfaces, let us now introduce the EOW brane already in this setting and construct the disk wavefunction in its presence. We can interpret the resulting wavefunction as the Hartle-Hawking wavefunction in the L basis for the case of a one-sided black hole. This wavefunction is associated to a region enclosed by an asymptotically AdS boundary of renormalised length β , an EOW brane and a geodesic of length L connecting them.⁸ This configuration is depicted in fig.1(b).

We will denote the corresponding wavefunction by $\Psi_D(\beta, L)$ ⁹ which should satisfy

$$\int_0^\infty \frac{dz}{z} \Psi_D(\beta/2, L) \Psi_D(\beta/2, L) = \int_0^\infty \frac{dz_1}{z_1} \frac{dz_2}{z_2} \Psi_D(x, L_1) G_{\beta-2x}(z_1, z_2) \Psi_D(x, L_2), \quad (2.23)$$

where the variable of integration is $z = 4e^{-L}$. It is straightforward to see that (2.23) is fulfilled for the following expression

$$\Psi_D(\beta, L) = \frac{e^{S_0/2}}{\sqrt{2}} \int_0^\infty dk e^{-\frac{\beta k^2}{2}} \gamma_\mu(k) r(k) \frac{W_{-\mu, ik}(z)}{\sqrt{z}}. \quad (2.24)$$

The disk partition function in the presence of an EOW brane therefore amounts to

$$\begin{aligned} Z_{D,\mu}(\beta) &= \int_0^\infty \frac{dz}{z} \Psi_D(\beta/2, L) \Psi_D(\beta/2, L) = \frac{e^{S_0}}{2} \int_0^\infty dk e^{-\frac{\beta k^2}{2}} \gamma_\mu(k) r(k) \\ &= e^{S_0} \int_0^\infty dE e^{-\beta E} \gamma_\mu(E) \hat{\rho}_D(E), \end{aligned} \quad (2.25)$$

Comparing (2.25) to (2.21) we see that the effect of the EOW brane is encompassed by an additional Γ -function expression defined in (2.10). The above expressions also allow us to calculate the wavefunction $\Psi_D(\zeta_1, \zeta_2, \ell)$ for region I depicted in fig. 1(c): a region enclosed by an EOW brane and a geodesic connecting points on the asymptotic AdS boundary. This wavefunction can be derived from the identification,

$$Z_{D,\mu}(\beta) = \int_0^\infty \frac{dy}{y} \Psi_D(\zeta_1, \zeta_2, \ell) \Phi_D(\beta - \zeta_1 - \zeta_2, \ell), \quad (2.26)$$

by which, using (2.20), one arrives at

$$\Psi_D(\zeta_1, \zeta_2, \ell) = 2e^{S_0/2} \int_0^\infty dk e^{-\frac{k^2}{2}(\zeta_1 + \zeta_2)} \gamma_\mu(k) r(k) K_{2ik}(y). \quad (2.27)$$

2.4 The trumpet wavefunctions

The most important ingredients of our study are the wavefunctions on the trumpets whose asymptotic boundaries are either pinched off by the disk regions considered in fig.1 or replaced in some parts by the EOW brane.

While more complicated hyperbolic surfaces require the use of Riemann surfaces with geodesic boundaries, the simplest configuration on the trumpet is depicted in fig. 2(a).

⁸In contrast to the geodesic length connecting two points on the AdS boundary which we denoted by ℓ .

⁹We denote wavefunctions associated to the two-sided black hole via Φ and those in the presence of EOW branes by Ψ .

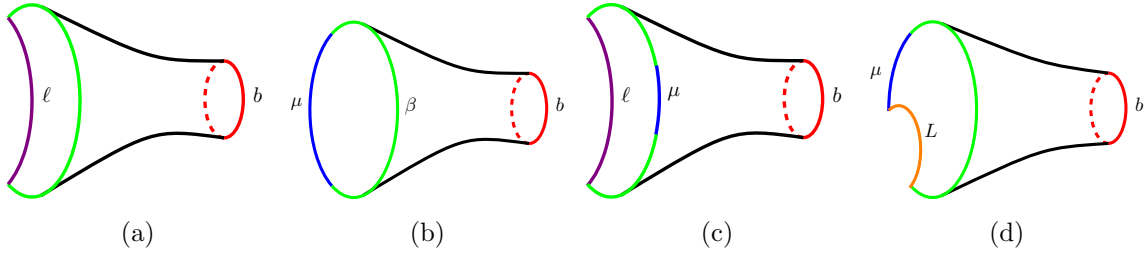


Figure 2: Four different possible trumpet geometries corresponding to four distinct wavefunctions. The closed geodesic boundary is depicted in red. In figure (a) we see the generalisation of the disk configuration, figure 1(a) to the trumpet. Figure (b) corresponds to the wavefunction on a trumpet geometry with both an EOW brane and an asymptotically AdS boundary. Figure (c) shows the wavefunction of a geodesic connecting two points on an asymptotically AdS boundary which contains an EOW brane. Lastly, in figure (d) we see a geodesic connecting EOW brane and AdS boundary on a trumpet geometry.

The corresponding wavefunction $\Phi_T(\beta, b, \ell)$ can be realised as the trumpet wavefunction pinched off by the disk wavefunction shown in fig. 1(a). This is obtained through the identity

$$\Phi_T(\beta, b) = \frac{1}{\pi} \int_0^\infty dk \cos(kb) e^{-\frac{\beta k^2}{2}} = \int_0^\infty \frac{dy}{y} \Phi_T(\beta - x, b, \ell) \Phi_D(x, \ell), \quad (2.28)$$

which results in

$$\Phi_T(\beta, b, \ell) = \frac{4e^{-S_0/2}}{\pi} \int_0^\infty dk e^{-\frac{\beta k^2}{2}} \cos(kb) K_{2ik}(y). \quad (2.29)$$

Let us now come to the geometry depicted in fig.2(b). This can be computed by gluing the above geometry with a region enclosed by a geodesic and EOW brane as shown in fig.1(c). This yields the wavefunction $\Psi_T(\beta, b)$ associated with this diagram

$$\Psi_T(\beta, b) = \int_0^\infty \frac{dy}{y} \Phi_T(\beta, b, \ell) \Psi_D(0, 0, \ell) = \frac{1}{\pi} \int_0^\infty dk \cos(kb) \gamma_\mu(k) e^{-\frac{\beta k^2}{2}}. \quad (2.30)$$

The wavefunction (2.30) is in a perfect agreement with the corresponding wavefunction presented in [34].

This in turn allows for the calculation of $\Psi_T(\zeta_1, \zeta_2, b, \ell)$, the wavefunction associated with fig.2(c) and obtained through the equation

$$\Psi_T(\beta, b) = \int_0^\infty \frac{dy}{y} \Psi_T(\zeta_1, \zeta_2, b, \ell) \Phi_D(\beta - \zeta_1 - \zeta_2, \ell). \quad (2.31)$$

Using (2.20) and (2.30), this yields

$$\Psi_T(\zeta_1, \zeta_2, b, \ell) = \frac{4e^{-S_0/2}}{\pi} \int_0^\infty dk \cos(kb) \gamma_\mu(k) e^{-\frac{k^2}{2}(\zeta_1 + \zeta_2)} K_{2ik}(y). \quad (2.32)$$

Finally, the wavefunction corresponding to the geometry shown in the panel (d) of fig.

2, namely a trumpet geometry with geodesic of length L from the EOW brane to the asymptotic boundary, can be computed by pinching-off the wavefunction $\Psi_D(\beta, L)$ from the above wavefunction. Therefore the structure

$$\Psi_T(\beta, b) = \int_0^\infty \frac{dz}{z} \Psi_T(\beta - x, b, L) \Psi_D(x, L), \quad (2.33)$$

by use of (2.24) results in the wavefunction

$$\Psi_T(\beta, b, L) = \frac{\sqrt{2}e^{-S_0/2}}{\pi} \int_0^\infty dk \cos(kb) \gamma_\mu(k) e^{-\frac{\beta k^2}{2}} z^{-1/2} W_{-\mu, ik}(z). \quad (2.34)$$

2.5 Pure vs. Thermal States

As already mentioned in the introduction, by considering an EOW brane we are describing a pure state. However, to establish its interpretation as a typical boundary state, it is essential to try and delineate differences to a thermal state. We can check the expectation value of the energy. Indeed at disk level this amounts to

$$\langle E \rangle = \frac{\int_0^\infty \frac{dz}{z} \Psi_D(\beta/2, L) H \Psi_D(\beta/2, L)}{\int_0^\infty \frac{dz}{z} \Psi_D(\beta/2, L) \Psi_D(\beta/2, L)}, \quad (2.35)$$

with H being the Hamiltonian defined in (2.7). As the corresponding system may be thought of as a particle in a Morse potential, by use of the Schrödinger equation, one arrives at

$$\langle E \rangle = -\frac{\partial}{\partial \beta} \ln Z_\mu(\beta), \quad (2.36)$$

which is in agreement with the expectation value of a thermal ensemble with temperature $\frac{1}{\beta}$. This may be readily generalised to higher genus. Therefore the wavefunctions in the presence of an EOW brane indeed correspond to states which are indistinguishable from thermal states.

On the other hand we note that the ETH delineates between diagonal and off-diagonal matrix elements. More explicitly, the matrix elements of observables in the eigenstate of the Hamiltonian are given by [50]

$$\mathcal{O}_{mn} = \mathcal{O}(\bar{E})\delta_{mn} + e^{-\frac{S(\bar{E})}{2}} f_{\mathcal{O}}(\bar{E}, \omega) R_{mn}, \quad (2.37)$$

where $\bar{E} = \frac{E_m + E_n}{2}$, $\omega = E_m - E_n$ and $S(\bar{E})$ is the entropy. Moreover, $\mathcal{O}(\bar{E})$ is the expectation value in the microcanonical ensemble, $f_{\mathcal{O}}(\bar{E}, \omega)$ is a smooth function and R_{mn} a random variable with zero mean and unit variance.

One observes that off-diagonal elements are suppressed by the Hilbert space size. In order to show that the wavefunction we consider also satisfies ETH, we need to calculate off-diagonal elements of the inner product in the length basis $|L\rangle$ used in the quantisation of (2.7). Actually the inner product we need for this analysis was already considered in [34], where the importance of higher topologies was stressed. First we need to define a building block, which is shown in fig.3. Denoting the corresponding wavefunction by $\Psi_T(b, L_1, L_2)$, one has

$$\Psi_T(\beta, b) = \int_0^\infty \frac{dz_1}{z_1} \frac{dz_2}{z_2} \Psi_D(\beta - x, L_1) \Psi_T(b, L_1, L_2) \Psi_D(x, L_2), \quad (2.38)$$

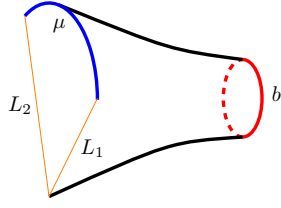


Figure 3: One important ingredient in the calculation of the leading order correction to the inner product $\langle L_1|L_2\rangle$ via Euclidean path integral. We see the two geodesics L_1 and L_2 in orange, the EOW brane in blue and a closed geodesic b in red. The wavefunction of this geometry is denoted by $\Psi_T(b, L_1, L_2)$. Topologies beyond the disk are important in recovering ETH-like behaviour.

which in combination with the expression (2.24) may be used to find

$$\Psi_T(b, L_1, L_2) = \frac{2e^{-S_0}}{\pi} \int_0^\infty dk \cos(kb) \gamma_\mu(k) (z_1 z_2)^{-1/2} W_{-\mu, ik}(z_1) W_{-\mu, ik}(z_2), \quad (2.39)$$

in agreement with the result obtained in [34]. The wavefunction (2.39) plays an important role in recovering ETH behaviour, as the standard canonical quantisation condition

$$\langle L_1|L_2\rangle = \delta(L_1 - L_2), \quad (2.40)$$

is corrected via higher genus contributions to the expression

$$\langle L_1|L_2\rangle = \delta(L_1 - L_2) + \int_0^\infty b db X(b) \Psi_T(b, L_1, L_2), \quad (2.41)$$

where we have introduced the notation $X(b)$ as in [34]. Here $X(b)$ is an integration measure which corresponds to all topologies ending on a single closed geodesic length b , such that the weighting by the Euler characteristic and the Weil-Petersson volumes are included in this quantity. We could also consider it to include an arbitrary number of EOW brane loops as in [34]. By use of (2.39), (2.41) takes on the form

$$\langle L_1|L_2\rangle = \delta(L_1 - L_2) + \frac{2e^{-S_0}}{\pi} \int_0^\infty dk \chi(k) \gamma_\mu(k) \frac{W_{-\mu, ik}(z_1) W_{-\mu, ik}(z_2)}{\sqrt{z_1 z_2}}, \quad (2.42)$$

where

$$\chi(k) = \int_0^\infty b db X(b) \cos(kb). \quad (2.43)$$

The leading contribution to the off-diagonal term comes from surfaces with genus one for which $\chi(k) \sim e^{-S_0}$, which results in

$$\langle L_1|L_2\rangle \approx \delta(L_1 - L_2) + (\dots)_{L_1, L_2} e^{-2S_0}, \quad (2.44)$$

in agreement with [51]. Here $(\dots)_{L_1, L_2}$ refers to the $g = 1$ contribution, where we have already pulled out the topological weighting. We therefore see that off-diagonal terms are suppressed exponentially just as in (2.37).

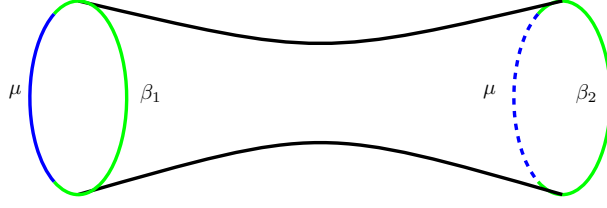


Figure 4: Two trumpet geometries glued together along their closed geodesic boundaries. This geometry corresponds to the connected part of the spectral form factor.

3 Partition Function

In this section we construct the partition function in the presence of an EOW brane via the wavefunction formalism developed in section 2. The most natural quantity to analyse is the two-point function or the spectral form factor. More specifically, we require the trumpet wavefunction (2.30). We may visualise the connected contribution to the two-point function as gluing two trumpet geometries of the type illustrated in fig.2(a) together along their closed geodesic boundaries, which results in the geometry shown in fig.4.

In analogy to (2.17), the overall contribution including connected and disconnected structures gives the following expression:

$$\begin{aligned}
& \langle Z(\beta_1)Z(\beta_2) \rangle_\mu \\
&= \int_0^\infty b_1 db_1 b_2 db_2 \Psi_T(\beta_1, b_1) X(b_1, b_2) \Psi_T(\beta_2, b_2) \\
&= \frac{e^{-S_0}}{\pi^2} \int_0^\infty dk_1 dk_2 e^{-\frac{\beta_1 k_1^2}{2} - \frac{\beta_2 k_2^2}{2}} \gamma_\mu(k_1) \gamma_\mu(k_2) \int_0^\infty b_1 db_1 b_2 db_2 X(b_1, b_2) \cos(k_1 b_1) \cos(k_2 b_2).
\end{aligned} \tag{3.1}$$

Here we have introduced the function $X(b_1, b_2)$ that denotes the topologically weighted sum over the Weil-Petersson volumes associated to surfaces with two geodesic boundaries parametrised by b_1 and b_2 . It is of the form

$$X(b_1, b_2) := \sum_{g=0} e^{(2-2g)S_0} \left(V_{g-1,2}(b_1, b_2) + \sum_{a \geq 0} V_{g-a,1}(b_1) V_{a,1}(b_2) \right). \tag{3.2}$$

We note that the first term of (3.2) corresponds to the connected contribution, whereas the second term corresponds to the disconnected contribution. There are two contributions in (3.1) which must be put in “by hand” as the moduli space volumes $V_{g=0,1}(b)$ and $V_{g=0,2}(b_1, b_2)$ in (3.2) are undefined.¹⁰ For the disconnected contributions involving $V_{g=0,1}(b)$, the correct result is given by (2.25) and the two boundary $g = 0$ connected contribution is defined as

$$Z(\beta_1, \beta_2)_{g=0, n=2, \mu} = \int_0^\infty b_1 db_1 b_2 db_2 \Psi_T(\beta_1, b_1) \Psi_T(\beta_2, b_2). \tag{3.3}$$

Comparing (3.1) to the two-sided expression of [20], one observes that the distinction to

¹⁰These two volumes constitute input values for the topological recursion [52, 53].

(3.1) lies in the factor $\gamma_\mu(k_1)\gamma_\mu(k_2)$. Analytically continuing (3.1) to the spectral form factor and rewriting in terms of energy variables one arrives at

$$\langle Z(\beta + it)Z(\beta - it) \rangle_\mu = \int_0^\infty dE_1 dE_2 e^{-\beta(E_1+E_2)-it(E_1-E_2)} \gamma_\mu(E_1)\gamma_\mu(E_2) \langle \rho(E_1)\rho(E_2) \rangle \quad (3.4)$$

where

$$\langle \rho(E_1)\rho(E_2) \rangle = \int b_1 db_1 b_2 db_2 X(b_1, b_2) \frac{\cos(b_1\sqrt{2E_1})\cos(b_2\sqrt{2E_2})}{2\pi^2\sqrt{E_1E_2}}, \quad (3.5)$$

which is the density of states corresponding to two boundary case of (2.17). At late times, the integral (3.4) is dominated by small energy ranges, and it can be shown that for $|E_1 - E_2| \ll 1$, non-perturbative contributions give the following expression for (3.5)[20]¹¹

$$\langle \rho(E_1)\rho(E_2) \rangle \approx e^{2S_0} \hat{\rho}_D(E_1)\hat{\rho}_D(E_2) + e^{S_0} \hat{\rho}_D(E_2)\delta(E_1 - E_2) - \frac{\sin^2(\pi e^{S_0} \hat{\rho}_D(E_2)(E_1 - E_2))}{\pi^2(E_1 - E_2)^2}, \quad (3.6)$$

where $\hat{\rho}_D(E)$ refers to the genus zero contribution to the density of states (2.22). The last term in (3.6) is the so-called sine-kernel. The non-perturbative nature of this contribution can be spotted by noting the factor of e^{S_0} inside the “sin”. As should be expected, plugging (3.6) into (3.4), gives a ramp-plateau structure for the connected and decaying behaviour for the disconnected contribution.

4 Correlation Functions

Following the procedure of [39] we will now determine full quantum gravity expressions for the matter correlation functions in the presence of an EOW brane. The idea of [39] is to construct a certain Kernel which can be used to dress quantum field theory correlation functions on AdS₂ to produce gravity correlators. For the two-sided case, the Kernel essentially amounts to the Hartle-Hawking wavefunction (2.20). More concretely, let us denote the coordinates by $\mathbf{x} = (\xi, x)$, where ξ is the holographic coordinate and x the boundary coordinate. The regularised geodesic distance between two points is given by

$$e^{\frac{\ell}{2}} = \frac{|x_1 - x_2|}{\sqrt{\xi_1 \xi_2}}. \quad (4.1)$$

In terms of this expression the Kernel is

$$K(u_{12}, \mathbf{x}_1, \mathbf{x}_2) = 2e^{S_0/2} \frac{4\sqrt{\xi_1 \xi_2}}{|x_1 - x_2|} \int_0^\infty dk e^{-\frac{u_{12}k^2}{2}} r(k) K_{2ik} \left(\frac{4\sqrt{\xi_1 \xi_2}}{|x_1 - x_2|} \right). \quad (4.2)$$

The quantum gravity correlators constructed in [39] then amount to

$$\begin{aligned} \langle \mathcal{O}_1(u_1) \cdots \mathcal{O}_n(u_n) \rangle_D &= \int_{x_1 > \cdots > x_n} \frac{\prod_i d\xi_i dx_i}{\text{Vol}(\text{SL}(2, R))} K(u_{12}, \mathbf{x}_1, \mathbf{x}_2) \cdots K(u_{1n}, \mathbf{x}_n, \mathbf{x}_1) \quad (4.3) \\ &\times \prod_i \xi_i^{\Delta_i - 2} \langle \mathcal{O}_1(x_1) \cdots \mathcal{O}_n(x_n) \rangle_{\text{CFT}}, \end{aligned}$$

¹¹See also [22] based on the elegant approach of [54, 55].

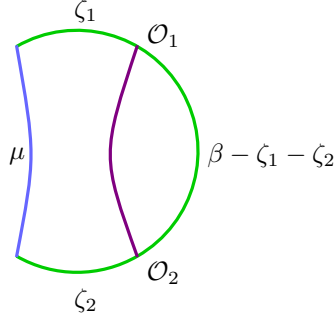


Figure 5: This figure corresponds to the two-point function of two operators \mathcal{O}_1 and \mathcal{O}_2 on the Euclidean disk in the presence of an EOW brane. The corresponding wavefunction is given in (2.27).

where Δ_i is the scaling dimension of the operator \mathcal{O}_i . $\text{Vol}(\text{SL}(2, R))$ reminds us that one needs to fix the $\text{SL}(2, R)$ gauge symmetry. In our case, while the general logic leading to the structure of (4.3) is preserved, now two different Kernels have to be used. In addition to (4.2), a Kernel must be introduced due to the presence of the EOW brane. A quick look at fig.5 suggests that this Kernel corresponds to the wavefunction (2.27), which results in the expression

$$M(\zeta_1, \zeta_2, \mathbf{x}_1, \mathbf{x}_2) = 2e^{S_0/2} \frac{4\sqrt{\xi_1\xi_2}}{|x_1 - x_2|} \int_0^\infty dk e^{-\frac{k^2}{2}(\zeta_1 + \zeta_2)} \gamma_\mu(k)r(k) K_{2ik} \left(\frac{4\sqrt{\xi_1\xi_2}}{|x_1 - x_2|} \right). \quad (4.4)$$

Using this kernel and (4.2) the quantum gravity correlators in the presence of an EOW brane is

$$\begin{aligned} \langle \mathcal{O}_1(u_1) \cdots \mathcal{O}_n(u_n) \rangle_{D, \mu} &= \int_{x_1 > \cdots > x_n} \frac{\prod_i d\xi_i dx_i}{\text{Vol}(\text{SL}(2, R))} K(u_{12}, \mathbf{x}_1, \mathbf{x}_2) \cdots K(u_{n-1n}, \mathbf{x}_{n-1}, \mathbf{x}_n) \\ &\times M(\zeta_1, \zeta_n, \mathbf{x}_n, \mathbf{x}_1) \prod_i \xi_i^{\Delta_i - 2} \langle \mathcal{O}_1(x_1) \cdots \mathcal{O}_n(x_n) \rangle_{\text{CFT}}. \end{aligned} \quad (4.5)$$

The above expressions are for disk topology as indicated by the index D . Let us briefly describe how to generalise to arbitrary topology by use of the two-point function as a concrete example. For the disk the two-point function is shown in fig.5. The variables of fig.5 are related to those of formula (4.5) via $u = \zeta_1 + \zeta_2$. Keeping in mind that the CFT two-point function is given by:

$$\langle \mathcal{O}_1(x_1) \mathcal{O}_2(x_2) \rangle = e^{-\Delta \ell}, \quad (4.6)$$

we arrive at the quantum gravity two-point function at disk level (according to (4.5))

$$\begin{aligned} \langle \mathcal{O}_1(\zeta_1 + \zeta_2) \mathcal{O}_2(0) \rangle_{D, \mu} &= \int_0^\infty \frac{dy}{y} \Phi_D(\beta - \zeta_1 - \zeta_2, \ell) \Psi_D(\zeta_1, \zeta_2, \ell) \left(\frac{y}{4} \right)^{2\Delta} \\ &= e^{S_0} \int_0^\infty dk_1 dk_2 e^{-\frac{k_1^2}{2}(\beta - u) - \frac{k_2^2}{2}u} r(k_1)r(k_2) \gamma_\mu(k_2) \mathcal{N}(\Delta, k_1, k_2), \end{aligned} \quad (4.7)$$

where

$$\mathcal{N}(\Delta, k_1, k_2) = 4 \int_0^\infty \frac{dy}{y} K_{2ik_1}(y) K_{2ik_2}(y) \left(\frac{y}{4}\right)^{2\Delta} = \frac{|\Gamma(\Delta + i(k_1 + k_2))\Gamma(\Delta + i(k_1 - k_2))|^2}{2^{2\Delta+1}\Gamma(2\Delta)}. \quad (4.8)$$

Comparing (4.7) to the expression for the two-sided AdS black hole [39] we again see the new factor $\gamma_\mu(k)$ due to the presence of the EOW brane.

In order to generalise (4.7) to higher genus, the wavefunctions (2.29) and (2.32) are needed. By making use of these wavefunctions and formula (2.19) the two-point function of arbitrary genus is

$$\begin{aligned} \langle \mathcal{O}_1(\zeta_1 + \zeta_2) \mathcal{O}_2(0) \rangle_\mu &= \int b_1 db_1 b_2 db_2 X(b_1, b_2) \quad (4.9) \\ &\quad \times \int_0^\infty \frac{dy}{y} \Phi_T(\beta - \zeta_1 - \zeta_2, b_1, \ell) \Psi_T(\zeta_1, \zeta_2, b_2, \ell) \left(\frac{y}{4}\right)^{2\Delta} \\ &= \frac{16e^{-S_0}}{\pi^2} \int_0^\infty dk_1 dk_2 \gamma_\mu(k_2) e^{-\frac{k_1^2}{2}(\beta-u) - \frac{k_2^2}{2}u} \mathcal{N}(\Delta, k_1, k_2) \\ &\quad \times \int b_1 db_1 b_2 db_2 X(b_1, b_2) \cos(k_2 b_2) \cos(k_1 b_1). \end{aligned}$$

We note, however, that the disk contribution is a particular case and it is understood that the genus zero contribution is defined to be (4.7). Altogether one gets

$$\langle \mathcal{O}_1(u) \mathcal{O}_2(0) \rangle_\mu = 16e^{-S_0} \int_0^\infty dE_1 dE_2 e^{-E_1(\beta-u) - E_2 u} \gamma_\mu(E_2) \langle \rho(E_1) \rho(E_2) \rangle \mathcal{N}(\Delta, E_1, E_2), \quad (4.10)$$

where we are using (3.5). The late-time behaviour of the two-point function amounts to considering the analytic continuation $u = \beta + it$, which gives

$$\langle \mathcal{O}_1(t) \mathcal{O}_2(0) \rangle_\mu = 16e^{-S_0} \int_0^\infty dE_1 dE_2 e^{-\frac{\beta}{2}(E_1+E_2) + it(E_1-E_2)} \gamma_\mu(E_2) \langle \rho(E_1) \rho(E_2) \rangle \mathcal{N}(\Delta, E_1, E_2). \quad (4.11)$$

Comparing this expression to (3.4) shows that the late-time behaviour is essentially the same as that of spectral form factor. Indeed as far as the ramp and the plateau are concerned the extra $\mathcal{N}(\Delta, E_1, E_2)$ plays no essential role.

5 The late time behaviour of complexity

In this section we would like to study the late time behaviour of complexity in our setup. It is conjectured that the holographic quantum complexity is given by the volume of the Einstein-Rosen bridge [6]. In our language in two dimensions it translates into the length of a geodesic connecting two boundaries. This definition was used to compute the late time behaviour of complexity of a two-sided black hole in [27]. In that work it was shown that the complexity exhibits linear growth at late times before it eventually saturates to a finite value. As detailed in the introduction, the most essential step in this construction was the use of the non-perturbative expression (3.6) to furnish the saturation at late times.

In this section we adopt the same logic to work out the late time behaviour of complexity for a single-sided black hole. Crucially however, we do not relate the geodesic length to a matter two-point function but use the quenched expectation value. For the calculation

of the complexity itself this leads to the same expressions for the two-sided case but a decisively different result for the variance. For the one-sided case, we need to compute the quenched expectation value of a geodesic suspended between the AdS boundary and the EOW brane. Note that, in our notation, classically the geodesic distance between boundary and EOW brane is denoted by $L = -\ln z/4$. The complexity is therefore proportional to the expectation value of the geodesic $\mathcal{C} \sim \langle L \rangle_{QG}$ in quantum gravity. It is also worth noting that in the present case one could also compute the expectation value of a geodesic length connecting two points on the boundary, $\langle \ell \rangle_{QG}$. In what follows we will study the time dependence of these quantities using the wavefunction formalism we developed in the previous sections.

5.1 The geodesic ℓ

To proceed, let us start with the geodesic ℓ which is used in the two-sided case and compute its “quantum expectation” value. At the disk level one has

$$\langle \ell(u) \rangle = -\frac{1}{Z_{D,\mu}(\beta)} \int_0^\infty \frac{dy}{y} \Psi_D(\zeta_1, \zeta_2, \ell) \Phi_D(\beta - u, \ell) \left(2 \ln \frac{y}{4}\right), \quad \text{with } u = \zeta_1 + \zeta_2. \quad (5.1)$$

To evaluate this quantity, we will use a trick which is inspired by the replica trick used *e.g.* in computing the quenched free energy. We write the logarithm in terms of the following limit¹²

$$\ln A = \lim_{N \rightarrow 0} \frac{A^N - 1}{N} = \lim_{N \rightarrow 0} \frac{d}{dN} A^N. \quad (5.2)$$

We normalise by multiplying with a factor of $Z_{D,\mu}^{-1}(\beta)$, where $Z_{D,\mu}(\beta)$ is the disk partition function, given in (2.25). Using this definition one may define complexity as

$$\langle \ell(u) \rangle = -\lim_{N \rightarrow 0} \frac{\langle y^{2N} \rangle_u - 1}{N}, \quad (5.3)$$

where

$$\langle y^{2N} \rangle_u = \frac{1}{Z_{D,\mu}(\beta)} \int_0^\infty \frac{dy}{y} \Psi_D(\zeta_1, \zeta_2, \ell) \Phi_D(\beta - u, \ell) \left(\frac{y}{4}\right)^{2N} \quad (5.4)$$

and it is understood that an analytic continuation must still be performed. Expressions such as (5.4) may then be calculated via (2.19). It is very interesting that in this context, the complexity, similar to entanglement entropy, can also be computed via a replica trick. To be clear, while the expression (5.4) is calculated in the Euclidean path integral, we have not explicitly shown the existence of replicated geometries. Perhaps one should take the validity of (5.4) as an indication on the existence of some kind of broader approach involving replica geometries. It is also worth noting that the above expression found by use of a replica trick is identical to the expression of the matter two-point function (4.7) with the identification of $\Delta = N$. However, although they are the same expression, conceptually they play different roles as (5.4) is used in (5.3). This is where our approach deviates significantly from [27].

Indeed, it is not clear if one could interpret (5.4) as a matter two-point function since the corresponding matter two-point function is obtained from an opposite limit, namely, in the limit of large scaling dimension. On the contrary, in our case, we need the limit, $N \rightarrow 0$

¹²In the context of JT gravity, see [56–59].

by which we lose the semiclassical interpretation of the two-point function. Nonetheless, as long as the computations are concerned, both yield the same result.

In particular from (4.7) by use of (2.19) one gets

$$\langle y^{2N} \rangle_u = \frac{e^{S_0}}{Z_{D,\mu}(\beta)} \int_0^\infty dk_1 dk_2 e^{-\frac{k_1^2}{2}(\beta-u) - \frac{k_2^2}{2}u} r(k_1)r(k_2) \gamma_\mu(k_2) \mathcal{N}(N, k_1, k_2). \quad (5.5)$$

Of course this expression in itself does not yet furnish late time linear growth as (5.5) is not the end of the story and needs to be plugged into the replica formula (5.3) and analytically continued to find complexity. Performing the analytic continuation $u = \frac{\beta}{2} + it$ and using energy variables we arrive at

$$\langle y^{2N} \rangle_t = \frac{e^{S_0}}{Z_{D,\mu}(\beta)} \int_0^\infty dE_1 dE_2 e^{-\frac{\beta}{2}(E_1+E_2) + i(E_1-E_2)t} \hat{\rho}_D(E_1)\hat{\rho}_D(E_2) \gamma_\mu(E_2) \mathcal{N}(N, E_1, E_2). \quad (5.6)$$

Now we have to simply plug this equation into the replica formula (5.3). Moreover since we are interested in the behaviour at late times, the main contribution should come from the coincident limit, $E_1 \rightarrow E_2$. In this limit, using the change of variables,

$$E = \frac{E_1 + E_2}{2}, \quad \omega = E_1 - E_2, \quad (5.7)$$

one gets

$$\langle \ell(t) \rangle \sim \text{const.} - \frac{e^{S_0}}{2\sqrt{2\pi}Z_{D,\mu}(\beta)} \int_0^\infty dE e^{-\beta E} \sqrt{E} \hat{\rho}_D(E) \gamma_\mu(E) \int_{-\infty}^\infty d\omega \frac{e^{i\omega t}}{\omega^2}, \quad (5.8)$$

which results in the linear growth $\langle \ell(t) \rangle \sim t$. Of course, one still needs to perform the integral over E , though we will not do it here. Here our aim was only to show that the linear growth at the disk level could be thought of as the consequence of our replica trick. Performing the calculation of the quenched length on a two-boundary topology and using (3.6) would lead to the results already obtained in [27] and we will therefore not do this explicitly.

5.2 The geodesic L

It is straightforward to compute the late time behaviour of the quantum expectation value of the length of the geodesic connecting a point on the boundary to one on the EOW brane

$$\langle L(u) \rangle = -\frac{1}{Z_{D,\mu}(\beta)} \int_0^\infty \frac{dz}{z} \Psi_D(\beta - u, L) \Psi_D(u, L) \ln \frac{z}{4} = -\lim_{N \rightarrow 0} \frac{\langle z^N \rangle_u - 1}{N}, \quad (5.9)$$

where

$$\begin{aligned} \langle z^N \rangle_u &= \frac{1}{Z_{D,\mu}(\beta)} \int_0^\infty \frac{dz}{z} \Psi_D(\beta - u, L) \Psi_D(u, L) \left(\frac{z}{4}\right)^N \\ &= \frac{e^{S_0}}{2Z_{D,\mu}(\beta)} \int_0^\infty dk_1 dk_2 e^{-\frac{k_1^2}{2}(\beta-u) - \frac{k_2^2}{2}u} \gamma_\mu(k_1)\gamma_\mu(k_2)r(k_1)r(k_2) \mathcal{M}(N, k_1, k_2). \end{aligned} \quad (5.10)$$

Here we have introduced

$$\mathcal{M}(N, k_1, k_2) = \int_0^\infty \frac{dz}{z^2} W_{-\mu, ik_1}(z) W_{-\mu, ik_2}(z) \left(\frac{z}{4}\right)^N. \quad (5.11)$$

At this point, one could perform a computation similar to what was done in the case of $\langle \ell(u) \rangle$ in the previous section to find the late time behavior of $\langle L(u) \rangle$. In general, we would expect to get the same linear growth as before, although in this case we will have to deal with the Whittaker functions. However, we will postpone this computation for a little while and will first study the higher genus corrections to the late time behaviour of complexity. The reason for changing the order of computation is as follows. The computation of complexity as the quantum expectation value of the geodesic length at the disk level yields a late time linear growth which keeps growing forever. However, on general grounds it is expected that complexity saturates at late times. Therefore the disk level computation should not constitute the entire story. It is natural to expect that the inclusion of higher topologies and connected geometries plays an important role. Thus, in order to see the saturation phase, one needs to compute the quantum expectation of geodesic length taking into account surfaces of higher genus [27]. By making use of the trumpet wavefunctions we have found in section 2.4, one has

$$\langle L(u) \rangle = -\frac{1}{Z_\mu(\beta)} \int b_1 db_1 b_2 db_2 X(b_1, b_2) \int_0^\infty \frac{dz}{z} \Psi_T(\beta - u, b_1, L) \Psi_T(u, b_2, L) \ln \frac{z}{4}, \quad (5.12)$$

where we have used the notation (3.2) again. In this case we compute the following quantity to be used in the replica formula

$$\langle z^N \rangle_u = \frac{1}{Z_\mu(\beta)} \int b_1 db_1 b_2 db_2 X(b_1, b_2) \int_0^\infty \frac{dz}{z} \Psi_T(\beta - u, b_1, L) \Psi_T(u, b_2, L) \left(\frac{z}{4}\right)^N. \quad (5.13)$$

Using equation (2.34) and expression (5.11) one finds

$$\begin{aligned} \langle z^N \rangle_u &= \frac{2e^{-S_0}}{\pi^2 Z_\mu(\beta)} \int_0^\infty dk_1 dk_2 e^{-\frac{k_1^2}{2}(\beta-u) - \frac{k_2^2}{2}u} \gamma_\mu(k_1) \gamma_\mu(k_2) \\ &\quad \times \int b_1 db_1 b_2 db_2 X(b_1, b_2) \cos(k_1 b_1) \cos(k_2 b_2) \mathcal{M}(N, k_1, k_2), \end{aligned} \quad (5.14)$$

which in the energy variable may be reexpressed as

$$\langle z^N \rangle_u = \frac{2e^{-S_0}}{Z_\mu(\beta)} \int_0^\infty dE_1 dE_2 e^{-E_1(\beta-u) - E_2 u} \gamma_\mu(E_1) \gamma_\mu(E_2) \langle \rho(E_1) \rho(E_2) \rangle \mathcal{M}(N, E_1, E_2), \quad (5.15)$$

$\langle \rho(E_1) \rho(E_2) \rangle$ being the spectral correlation. The main part of the above equation is $\mathcal{M}(N, E_1, E_2)$ which is an integral involving Whittaker functions. This can be evaluated

using the integral identity [60]

$$\begin{aligned}
\int_0^\infty x^{\rho-1} W_{k,m}(x) W_{\lambda,n}(x) &= \frac{\Gamma(2n) \Gamma(-m-n+\rho+1) \Gamma(m-n+\rho+1)}{\Gamma(n-\lambda+\frac{1}{2}) \Gamma(-k-n+\rho+\frac{3}{2})} \\
& {}_3F_2 \left(-n-\lambda+\frac{1}{2}, -m-n+\rho+1, m-n+\rho+1; 1-2n, -k-n+\rho+\frac{3}{2}; 1 \right) \\
& + \frac{\Gamma(-2n) \Gamma(-m+n+\rho+1) \Gamma(m+n+\rho+1)}{\Gamma(-n-\lambda+\frac{1}{2}) \Gamma(-k+n+\rho+\frac{3}{2})} \\
& {}_3F_2 \left(n-\lambda+\frac{1}{2}, -m+n+\rho+1, m+n+\rho+1; 2n+1, -k+n+\rho+\frac{3}{2}; 1 \right).
\end{aligned} \tag{5.16}$$

In order to evaluate the late time behaviour of complexity, the scheme is as follows. First we need to make the analytic continuation $u = \frac{\beta}{2} + it$ as before. Then plugging the resulting expression in the replica formula and taking the $N \rightarrow 0$, limit one can find the quantum expectation value of the geodesic length or equivalently, the complexity. Now since we are only interested in late time behaviour, the main contribution comes from the coincident limit, namely, $E_1 \rightarrow E_2$. It is convenient to use E and ω variables as defined in (5.7). Using (5.16) for our case, we get a nice expansion of the function $\mathcal{M}(N, E_1, E_2)$ in the limit $\omega \rightarrow 0$

$$\lim_{N \rightarrow 0} \frac{d}{dN} \mathcal{M}(N, E_1, E_2) = \frac{\sqrt{2E}}{2\pi\gamma_\mu(E)\hat{\rho}_D(E)} \frac{1}{\omega^2} + \text{local terms}. \tag{5.17}$$

However, in order to obtain the late time behaviour of complexity, we still need to perform the integrations over E and ω . Using this and the replica trick detailed above, one arrives at¹³

$$\begin{aligned}
\langle L(t) \rangle &= \text{const.} - \frac{e^{S_0}}{\pi Z_\mu(\beta)} \int_0^\infty dE e^{-\beta E} \sqrt{2E} \gamma_\mu(E) \hat{\rho}_D(E) \\
& \times \int_{-\infty}^\infty d\omega \frac{e^{i\omega t}}{\omega^2} \left(1 - \frac{\sin^2(\pi \hat{\rho}_D(E) e^{S_0} \omega)}{(\pi \hat{\rho}_D(E) e^{S_0} \omega)^2} \right).
\end{aligned} \tag{5.18}$$

It is worth stressing here that in order to derive the expression given in (5.18), one needs to take into account the non-perturbative effects explicitly through the sine-kernel appearing in the spectral correlation given in (3.6) [20].

It is now clear that the ω -integral may be performed exactly. In particular the expression in brackets on the right hand side of (5.18) corresponds to the disk contribution that results in linear growth. As was observed in [27], the disk linear growth is cancelled by the non-perturbative term as long as $2\pi\hat{\rho}_D(E)e^{S_0} \ll t$. It is easy to check that in this regime the integral vanishes identically.

On the other hand for $2\pi\hat{\rho}_D(E)e^{S_0} \gg t$, expanding the ‘‘sin’’-contribution in terms of

¹³Since we are interested in the time dependence of complexity, in this expression we have dropped a local term leading to a time independent term in the complexity and added all terms into the constant term. The corresponding term is divergent and has the form of $\delta(\omega)/\omega$.

exponentials and deforming the pole one finds [27]

$$\int_{-\infty}^{\infty} d\omega \frac{e^{i\omega t}}{\omega^2} \left(1 - \frac{\sin^2(\pi \hat{\rho}_D(E) e^{S_0} \omega)}{(\pi \hat{\rho}_D(E) e^{S_0} \omega)^2} \right) = \frac{2\pi^2 \hat{\rho}_D(E) e^{S_0}}{3} \left(1 - \frac{t}{2\pi \hat{\rho}_D(E) e^{S_0}} \right)^3. \quad (5.19)$$

Therefore overall

$$\langle L(t) \rangle = \text{const.} - \frac{2\pi e^{2S_0}}{3Z_\mu(\beta)} \int_{E_0}^{\infty} dE e^{-\beta E} \sqrt{2E} \gamma_\mu(E) \hat{\rho}_D^2(E) \left(1 - \frac{t}{2\pi \hat{\rho}_D(E) e^{S_0}} \right)^3. \quad (5.20)$$

Here E_0 is implicitly obtained via the equation $\pi \hat{\rho}_D(E_0) e^{S_0} = t$. Finally we have to perform the integral over E . To proceed, it is instructive to consider particular values of μ for which the above expression is simplified further. In what follows we will consider the case of $\mu = \frac{1}{2}$ as an illustrative example. In this case using the fact that

$$\gamma_{\frac{1}{2}}(E) = \frac{\pi \sqrt{2E}}{\sinh(\pi \sqrt{2E})}, \quad (5.21)$$

one gets

$$\langle L(t) \rangle = \text{const.} - \frac{4\pi^2 e^{2S_0}}{3Z_{\frac{1}{2}}(\beta)} \int_{E_0}^{\infty} dE e^{-\beta E} \frac{E \hat{\rho}_D^2(E)}{\sinh(\pi \sqrt{2E})} \left(1 - \frac{t}{2\pi \hat{\rho}_D(E) e^{S_0}} \right)^3, \quad (5.22)$$

where

$$Z_{\frac{1}{2}}(\beta) = e^{S_0} \int_0^{\infty} dE e^{-\beta E} \gamma_{\frac{1}{2}}(E) \hat{\rho}_D(E) = \frac{e^{\pi^2/2\beta} e^{S_0}}{\sqrt{2\pi} \beta^{3/2}} \left(1 + \frac{\pi^2}{\beta} \right). \quad (5.23)$$

For times $t \ll e^{S_0}$ one may expand the r.h.s of (5.22) and evaluate the integral which at leading order takes the form

$$\langle L(t) \rangle \approx \text{const.} - C_0 e^{S_0} + C_1 t, \quad (5.24)$$

where

$$C_0 = \frac{\pi^2 + 3\beta + 9e^{\frac{4\pi^2}{\beta}} (\beta + 3\pi^2)}{6\beta (\beta + \pi^2)},$$

$$C_1 = \frac{\sqrt{2} e^{-\frac{\pi^2}{2\beta}} \sqrt{\beta} (2\beta + \pi^2) + \pi^{3/2} (3\beta + \pi^2) \operatorname{erf}\left(\frac{\pi}{\sqrt{2}\sqrt{\beta}}\right)}{\sqrt{\pi} \beta (\beta + \pi^2)}. \quad (5.25)$$

For large t ($t \sim e^S$) the lower limit of the integral becomes large as well; $E_0 \rightarrow \infty$. Taking into account that the integrand itself has a factor of $e^{-\beta E}$ results in the fact that the integral decays and therefore the quantum expectation value of the geodesic length becomes constant. This can be interpreted as the saturation of complexity. For large t , one can estimate the rate by which the integral decays. For large t the lower limit of integral reads $E_0 = \frac{1}{8\pi^2} \ln^2(2\pi e^{-S_0} t)$. In this limit, approximating the ‘‘sinh’’ by an exponential

function one arrives at

$$\langle L(t) \rangle \approx \text{const.} - \frac{2\beta^{3/2} e^{-\frac{\pi^2}{2\beta}}}{3\pi^2 (\beta + \pi^2)} e^{S_0} e^{-\frac{\beta}{8\pi^2} \ln^2(2\pi e^{-S_0} t)} (e^{-S_0} t)^{3/2} \ln^2(2\pi e^{-S_0} t). \quad (5.26)$$

To summarise, our computation shows that the complexity grows linearly at late times up to $t \sim e^{S_0}$ and then saturates to a constant value of order e^{S_0} . Although we have demonstrated this behaviour explicitly only for a particular value of μ , the qualitative late time behaviour of complexity is the same for any value of μ .

5.3 The variance of complexity

Although the results of section 5 and the results of [27] exhibit late time behaviour in line with general expectations for complexity, this can be probed further by calculating the variance σ . Based on the procedure of computing the complexity in terms of the boundary-to-boundary two-point function, the variance of complexity has been evaluated in [27] where it was observed that the fluctuations exhibit linear growth at late times that is in tension with general expectations. In particular, this becomes especially problematic as the “noise” grows to the same size as the “signal” at $t \sim e^{2S_0}$.

Here we would like to use our approach based on the replica trick to compute the variance. To proceed let us focus on the two-sided case first to draw a direct comparison. Its generalisation to the one-sided case is then evident.

The variance has the structure

$$\sigma_\ell^2 = \langle \ell^2(u) \rangle - \langle \ell(u) \rangle^2 = \langle \ell^2(u) \rangle_C, \quad (5.27)$$

where we denote the connected contribution by C. Now in line with the rest of this section, it is clear that the quantity we have to determine is

$$\langle \ell^2(u) \rangle_C = \frac{4}{Z(\beta)} \int_0^\infty db_1 b_1 db_2 b_2 X(b_1, b_2) \int_0^\infty \frac{dy}{y} \Phi_T(\beta - u, b_1, \ell) \Phi_T(u, b_2, \ell) \left(\ln \frac{y}{4} \right)^2. \quad (5.28)$$

In order to calculate this we have to apply a replica type formula. We utilise the simple relation

$$\ln^2 A = \lim_{N \rightarrow 0} \frac{d^2}{dN^2} A^N. \quad (5.29)$$

By which the equation (5.28) may be recast into the following form

$$\begin{aligned} \langle \ell^2(u) \rangle_C &= \frac{1}{Z(\beta)} \lim_{N \rightarrow 0} \frac{d^2}{dN^2} \int_0^\infty b_1 db_2 b_2 db_2 X(b_1, b_2) \\ &\quad \times \int_0^\infty \frac{dy}{y} \Phi_T(\beta - u, b_1, \ell) \Phi_T(u, b_2, \ell) \left(\frac{y}{4} \right)^{2N}. \end{aligned} \quad (5.30)$$

This of course has a structure similar to the calculations of sections 5.1 and 5.2 and it is therefore clear that by making use of the trumpet wavefunction (2.29) one arrives at

$$\langle \ell^2(u) \rangle_C = \frac{4e^{-S_0}}{Z(\beta)} \int_0^\infty dE_1 dE_2 e^{-E_1(\beta-u)-E_2 u} \langle \rho(E_1) \rho(E_2) \rangle \left(\lim_{N \rightarrow 0} \frac{d^2}{dN^2} \mathcal{N}(N, E_1, E_2) \right), \quad (5.31)$$

which we analytically continue to

$$\langle \ell^2(t) \rangle_C = \frac{4e^{-S_0}}{Z(\beta)} \int_0^\infty dE \int_{-\infty}^\infty d\omega e^{-\beta E + i\omega t} \langle \rho(E + \frac{\omega}{2}) \rho(E - \frac{\omega}{2}) \rangle \left(\lim_{N \rightarrow 0} \frac{d^2}{dN^2} \mathcal{N}(N, E, \omega) \right), \quad (5.32)$$

where we are using the coordinates (5.7). At late times, taking the limit $\omega \rightarrow 0$, we have

$$\lim_{N \rightarrow 0} \frac{d^2}{dN^2} \mathcal{N}(N, E, \omega) = \frac{\sqrt{E}}{8\pi \hat{\rho}_D(E)} \left(\psi(2i\sqrt{2E}) + \psi(-2i\sqrt{2E}) - \ln 4 \right) \frac{1}{\omega^2} + \mathcal{O}(\omega^0), \quad (5.33)$$

where we have introduced the Polygamma function $\psi(x)$. This may then be used together with (3.6) to arrive at the final result

$$\begin{aligned} \langle \ell^2(t) \rangle_C &= \frac{e^{S_0}}{2\pi Z_D(\beta)} \int_0^\infty dE e^{-\beta E} \left(\psi(2i\sqrt{2E}) + \psi(-2i\sqrt{2E}) - \ln 4 \right) \hat{\rho}_D(E) \sqrt{E} \\ &\quad \times \int_{-\infty}^\infty d\omega \frac{e^{i\omega t}}{\omega^2} \left(1 - \frac{\sin^2(\pi \hat{\rho}_D(E) e^{S_0} \omega)}{(\pi \hat{\rho}_D(E) e^{S_0} \omega)^2} \right). \end{aligned} \quad (5.34)$$

We can see that the ω integration is of the same form as the one which appears in the calculation of the complexity itself.¹⁴ Indeed the only difference is the additional Polygamma structure. This is a pleasing result. The expression (5.34) circumvents the problematic late time growth of noise observed in [27]. The result saturates to a constant value and we therefore recover time-independent fluctuations before the recurrence time. We also observe that (5.34) implies a signal-to-noise ratio of order $\sim e^{-\frac{S_0}{2}}$ at $t \sim e^{S_0}$.

For the one-sided black hole the procedure is the same and indeed we recover a similar expression with a rather more complicated E -dependent function that comes from the fact that

$$\lim_{N \rightarrow 0} \frac{d^2}{dN^2} \mathcal{M}(N, E, \omega) = \frac{1}{\hat{\rho}_D(E)} \frac{F(E, \mu)}{\omega^2} + \mathcal{O}(\omega^0), \quad (5.35)$$

where we introduced $F(E, \mu)$, which is a complicated function of E and μ containing hypergeometric and polygamma functions and their derivatives.

6 Conclusion and Outlook

In this work, we have considered a fixed EOW brane which plays the role of a cutoff by removing a part of boundary. This setup provides a holographic model for a one-sided black hole. We have computed the multi-boundary partition functions and the matter correlation functions in this model. However, the most important result in this work is the computation of complexity.

To compute complexity we have employed a modified version of the well-known replica trick used to study the quenched free energy. This avoids the ambiguity of defining complexity in terms of boundary-to-boundary correlation functions as advocated for in [27]. The

¹⁴Note that in this expression we have not considered a contact term that is proportional to a delta function. As we mentioned in the calculation of complexity, this term being of the form of $\delta(\omega)/\omega$ leads to a time independent term which does not contribute to complexity growth. In the present case this term gives a divergent term which could be removed by subtracting $\ell(0)$. Although it is important to consider this term in the computation of variance, since our aim was to show how the replica trick results in a reasonable variance, we have just considered $\ell^2(t)$ and dropped the corresponding term by hand.

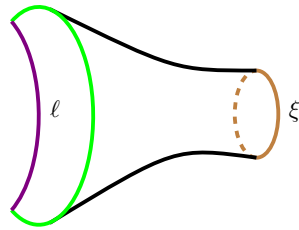


Figure 6: Trumpet capped by the FZZT brane shown by a brown circle and parametrized by ξ .

tension between the limit of scaling dimensions and the geodesic approximation is therefore not present in this work. We have retrieved the expected non-perturbative plateau regime in the late time growth of complexity, which follows an early period of perturbative linear growth in time. Although the result is qualitatively similar to that of a two-sided black hole, except for the coefficients being sensitive to the tension of the EOW brane now, the replica trick employed in our work yields a more satisfactory result for the variance. The emergence of only time-independent fluctuations in the variance compared to the late-time linear growth of [27] would seem an advancement in the calculation of the black hole volume in JT gravity. Of course in our approach the geometric picture is less obvious.

We will now conclude with a couple of interesting and related questions which are in progress.

Dynamical EOW branes So far we have considered a fixed EOW brane without any associated dynamics. However, it is interesting to consider a dynamical EOW brane. This requires considering a certain EOW brane that contributes to the path integral. In other words, one could imagine a general hypersurface with some of geodesics capped by EOW branes.

To start with we can start with a toy model where the geodesic of a trumpet geometry is capped off by an Fateev-Zamolodchikov-Zamolodchikov-Teschner (FZZT) anti-brane [61, 62] as shown in fig. 6. Following the prescription of [63], what we need to do is insert a factor of $-\frac{1}{b}e^{-\xi b}$ in the path integral on a trumpet with parameter b .

In order to see the effect of this brane on the behaviour of complexity as a function of time, following the procedure we adopted for the EOW brane, one first needs to construct the corresponding wavefunction in presence of the FZZT anti-brane. In what follows, for simplicity, we shall consider two-sided black holes. Starting from $\Phi_T(\beta, b, \ell)$ given in (2.29), one can compute the wavefunction associated with fig. 6 as

$$\Phi_T(\beta, \ell) = - \int_0^\infty db e^{-\xi b} \Phi_T(\beta, b, \ell) = - \frac{4e^{-S_0/2}}{\pi} \int_0^\infty dk e^{-\frac{\beta k^2}{2}} \frac{\xi}{\xi^2 + k^2} K_{2ik}(y). \quad (6.1)$$

With this result in hand, we need to employ our modified replica method defined

through (5.3) which yields, at late time,

$$\langle \ell(t) \rangle = \text{Const.} + \frac{1}{\pi^3 \tilde{Z}(\beta)} \int_0^\infty \frac{dE}{2E} e^{-\beta E} \left[\pi \xi \kappa \frac{2\sqrt{2E} \hat{\rho}_D(E)}{\xi^2 + 2E} - \frac{\kappa^2 \xi^2 e^{-S_0}}{(\xi^2 + 2E)^2} \right] \times \frac{\sqrt{2E}}{\hat{\rho}_D(E)} \int_{-\infty}^\infty d\omega \frac{e^{i\omega t}}{\omega^2}, \quad (6.2)$$

where κ is the number of FZZT anti-branes. Since we are only interested in the late time behaviour, we have used the E and ω variables (5.7) in the coincident limit, $E_1 \rightarrow E_2$.

The ω -integral of (6.2) can be readily performed and yields

$$\langle \ell(t) \rangle = \text{Const.} - \frac{t}{\pi^2 \tilde{Z}(\beta)} \int_0^\infty \frac{dE}{2E} e^{-\beta E} \left[\pi \xi \kappa \frac{2\sqrt{2E} \hat{\rho}_D(E)}{\xi^2 + 2E} - \frac{\kappa^2 \xi^2 e^{-S_0}}{(\xi^2 + 2E)^2} \right] \frac{\sqrt{E}}{\hat{\rho}_D(E)}. \quad (6.3)$$

From (6.3) it is clear that whether the above contribution results in a decreasing or increasing behaviour of complexity at late times depends on the E integral. Note that the disk contribution is proportional to e^{S_0} whereas the above contribution is given in terms of the number of branes κ , therefore one might naively expect an interesting competition between κ and e^{S_0} that is similar to that of entanglement entropy. We hope to report the final conclusion, both for the two-sided and one-sided black hole geometries, soon [64]. We expect this computation to shed light on the physical interpretation of the replica procedure we employed to compute complexity.

UV cutoff In this paper we discussed EOW branes playing the role of cutoffs. In the Lorentzian version of the theory, the cutoff EOW brane lies behind the event horizon of the black hole. In holographic theories, there is an interesting correspondence between a UV cutoff near the boundary of AdS spacetime and a conformal field theory deformed by a particular irrelevant operator quadratic in the stress-energy tensor [65–67], namely, the $T\bar{T}$ deformation [68–70]. The wavefunction technique we used for the EOW brane will also be useful in computing complexity for a $T\bar{T}$ -deformed CFT.

The partition function of $T\bar{T}$ deformed JT gravity may be written as [71]

$$Z_{D,\lambda}(\beta) = \int_{-\infty}^\infty dE e^{-\beta f(E)} \hat{\rho}_D(E), \quad (6.4)$$

where $f(E) = \frac{1 - \sqrt{1 - 8\lambda E}}{4\lambda}$, λ is the deformation parameter and E , the energy of the undeformed theory. Clearly for $\lambda \rightarrow 0$ one finds the standard partition function.

Our aim is to compute the complexity for this deformed version of JT gravity. As mentioned above, we will use the wavefunction formalism. To do so, one needs to write down the corresponding disk wave function for the deformed theory. Using the formalism developed in [71] for $\lambda < 0$ one can easily find the deformed wavefunction as

$$\Phi_{D,\lambda}(\beta, \ell) = 4e^{S_0/2} \int_0^\infty dE e^{-\beta f(E)} \hat{\rho}_D(E) K_{2i\sqrt{2E}}(y). \quad (6.5)$$

which exactly reproduces the partition function (6.4).

Once we have the wavefunction (6.5), we can once again use the modified replica method (5.3) to compute complexity. In the late time limit, using the coincident variables

(5.7), we obtain

$$\langle \ell(t) \rangle \sim \text{const.} - \frac{2e^{S_0}}{\sqrt{2\pi Z_\lambda(\beta)}} \int_0^\infty dE e^{-\beta f(E)} \sqrt{E} \hat{\rho}_D(E) \int_{-\infty}^\infty d\omega \frac{e^{\frac{i t \omega}{\sqrt{1-8\lambda E}}}}{\omega^2}. \quad (6.6)$$

The integral over ω can be performed exactly and we arrive at the following expression at late time showing linear growth of complexity, as expected from the disk level computation.

$$\langle \ell(t) \rangle \sim \text{const.} + \frac{2e^{S_0 t}}{\sqrt{2} Z_\lambda(\beta)} \int_0^\infty dE e^{-\beta f(E)} \frac{\sqrt{E} \hat{\rho}_D(E)}{\sqrt{1-8\lambda E}}. \quad (6.7)$$

While obtaining the plateau regime of complexity in this setup can be done straightforwardly by adding higher genus contributions as before, it will be interesting to study the saturation of complexity in this deformed JT setup in presence of an EOW brane. We postpone this for future work.

Acknowledgments

We would like to thank Moritz Dorband, Johanna Erdmenger and Misha Usatyuk for helpful discussions.

References

- [1] J.M. Maldacena, *The Large N limit of superconformal field theories and supergravity*, *Adv. Theor. Math. Phys.* **2** (1998) 231 [[hep-th/9711200](#)].
- [2] E. Witten, *Anti-de Sitter space and holography*, *Adv. Theor. Math. Phys.* **2** (1998) 253 [[hep-th/9802150](#)].
- [3] S.S. Gubser, I.R. Klebanov and A.M. Polyakov, *Gauge theory correlators from noncritical string theory*, *Phys. Lett. B* **428** (1998) 105 [[hep-th/9802109](#)].
- [4] L. Susskind, *Computational Complexity and Black Hole Horizons*, *Fortsch. Phys.* **64** (2016) 24 [[1403.5695](#)].
- [5] L. Susskind, *Three Lectures on Complexity and Black Holes*, SpringerBriefs in Physics, Springer, 10, 2018, DOI [[1810.11563](#)].
- [6] D. Stanford and L. Susskind, *Complexity and Shock Wave Geometries*, *Phys. Rev. D* **90** (2014) 126007 [[1406.2678](#)].
- [7] A.R. Brown, D.A. Roberts, L. Susskind, B. Swingle and Y. Zhao, *Holographic Complexity Equals Bulk Action?*, *Phys. Rev. Lett.* **116** (2016) 191301 [[1509.07876](#)].
- [8] A.R. Brown, D.A. Roberts, L. Susskind, B. Swingle and Y. Zhao, *Complexity, action, and black holes*, *Phys. Rev. D* **93** (2016) 086006 [[1512.04993](#)].
- [9] L. Susskind, *The Typical-State Paradox: Diagnosing Horizons with Complexity*, *Fortsch. Phys.* **64** (2016) 84 [[1507.02287](#)].
- [10] A.R. Brown, L. Susskind and Y. Zhao, *Quantum Complexity and Negative Curvature*, *Phys. Rev. D* **95** (2017) 045010 [[1608.02612](#)].
- [11] V. Balasubramanian, M. Decross, A. Kar and O. Parrikar, *Quantum Complexity of Time Evolution with Chaotic Hamiltonians*, *JHEP* **01** (2020) 134 [[1905.05765](#)].
- [12] L. Susskind, *Black Holes at Exp-time*, [2006.01280](#).

- [13] V. Balasubramanian, M. DeCross, A. Kar, Y.C. Li and O. Parrikar, *Complexity growth in integrable and chaotic models*, *JHEP* **07** (2021) 011 [2101.02209].
- [14] J. Haferkamp, P. Faist, N.B.T. Kothakonda, J. Eisert and N.Y. Halpern, *Linear growth of quantum circuit complexity*, 2106.05305.
- [15] C. Teitelboim, *Gravitation and Hamiltonian Structure in Two Space-Time Dimensions*, *Phys. Lett. B* **126** (1983) 41.
- [16] R. Jackiw, *Lower Dimensional Gravity*, *Nucl. Phys. B* **252** (1985) 343.
- [17] J. Maldacena, D. Stanford and Z. Yang, *Conformal symmetry and its breaking in two dimensional Nearly Anti-de-Sitter space*, *PTEP* **2016** (2016) 12C104 [1606.01857].
- [18] J. Engelsöy, T.G. Mertens and H. Verlinde, *An investigation of AdS₂ backreaction and holography*, *JHEP* **07** (2016) 139 [1606.03438].
- [19] P. Saad, S.H. Shenker and D. Stanford, *A semiclassical ramp in SYK and in gravity*, 1806.06840.
- [20] P. Saad, S.H. Shenker and D. Stanford, *JT gravity as a matrix integral*, 1903.11115.
- [21] P. Saad, *Late Time Correlation Functions, Baby Universes, and ETH in JT Gravity*, 1910.10311.
- [22] A. Altland and J. Sonner, *Late time physics of holographic quantum chaos*, *SciPost Phys.* **11** (2021) 034 [2008.02271].
- [23] A. Belin and J. de Boer, *Random statistics of OPE coefficients and Euclidean wormholes*, *Class. Quant. Grav.* **38** (2021) 164001 [2006.05499].
- [24] J. Cotler and K. Jensen, *AdS₃ gravity and random CFT*, *JHEP* **04** (2021) 033 [2006.08648].
- [25] A. Almheiri, T. Hartman, J. Maldacena, E. Shaghoulian and A. Tajdini, *Replica Wormholes and the Entropy of Hawking Radiation*, *JHEP* **05** (2020) 013 [1911.12333].
- [26] G. Penington, S.H. Shenker, D. Stanford and Z. Yang, *Replica wormholes and the black hole interior*, 1911.11977.
- [27] L.V. Iliesiu, M. Mezei and G. Sárosi, *The volume of the black hole interior at late times*, 2107.06286.
- [28] M. Mirzakhani, *Simple geodesics and Weil-Petersson volumes of moduli spaces of bordered Riemann surfaces*, *Invent. Math.* **167** (2006) 179.
- [29] J.M. Deutsch, *Quantum statistical mechanics in a closed system*, *Phys. Rev. A* **43** (1991) 2046.
- [30] M. Srednicki, *Chaos and quantum thermalization*, *Phys. Rev. E* **50** (1994) 888.
- [31] K. Okuyama and K. Sakai, *Multi-boundary correlators in JT gravity*, *JHEP* **08** (2020) 126 [2004.07555].
- [32] I. Kourkoulou and J. Maldacena, *Pure states in the SYK model and nearly-AdS₂ gravity*, 1707.02325.
- [33] J.M. Maldacena, *Eternal black holes in anti-de Sitter*, *JHEP* **04** (2003) 021 [hep-th/0106112].
- [34] P. Gao, D.L. Jafferis and D.K. Kolchmeyer, *An effective matrix model for dynamical end of the world branes in Jackiw-Teitelboim gravity*, *JHEP* **01** (2022) 038 [2104.01184].
- [35] D. Harlow and D. Jafferis, *The Factorization Problem in Jackiw-Teitelboim Gravity*, *JHEP* **02** (2020) 177 [1804.01081].
- [36] C.V. Johnson, *Nonperturbative Jackiw-Teitelboim gravity*, *Phys. Rev. D* **101** (2020) 106023 [1912.03637].

- [37] C.V. Johnson, *Explorations of nonperturbative Jackiw-Teitelboim gravity and supergravity*, *Phys. Rev. D* **103** (2021) 046013 [2006.10959].
- [38] C.V. Johnson, *The Microstate Physics of JT Gravity and Supergravity*, 2201.11942.
- [39] Z. Yang, *The Quantum Gravity Dynamics of Near Extremal Black Holes*, *JHEP* **05** (2019) 205 [1809.08647].
- [40] L. Susskind and Y. Zhao, *Switchbacks and the Bridge to Nowhere*, 1408.2823.
- [41] K. Jensen, *Chaos in AdS₂ Holography*, *Phys. Rev. Lett.* **117** (2016) 111601 [1605.06098].
- [42] R. Szmytkowski and S. Bielski, *An orthogonality relation for the whittaker functions of the second kind of imaginary order*, 0910.1492.
- [43] B. Eynard and N. Orantin, *Weil-Petersson volume of moduli spaces, Mirzakhani's recursion and matrix models*, 0705.3600.
- [44] D. Stanford and E. Witten, *Fermionic Localization of the Schwarzian Theory*, *JHEP* **10** (2017) 008 [1703.04612].
- [45] A. Blommaert, *Dissecting the ensemble in JT gravity*, 2006.13971.
- [46] J.S. Cotler, G. Gur-Ari, M. Hanada, J. Polchinski, P. Saad, S.H. Shenker et al., *Black Holes and Random Matrices*, *JHEP* **05** (2017) 118 [1611.04650].
- [47] D. Bagrets, A. Altland and A. Kamenev, *Power-law out of time order correlation functions in the SYK model*, *Nucl. Phys. B* **921** (2017) 727 [1702.08902].
- [48] T.G. Mertens, G.J. Turiaci and H.L. Verlinde, *Solving the Schwarzian via the Conformal Bootstrap*, *JHEP* **08** (2017) 136 [1705.08408].
- [49] A. Kitaev and S.J. Suh, *Statistical mechanics of a two-dimensional black hole*, *JHEP* **05** (2019) 198 [1808.07032].
- [50] M. Srednicki, *The approach to thermal equilibrium in quantized chaotic systems*, *Journal of Physics A: Mathematical and General* **32** (1999) 1163–1175.
- [51] M. Miyaji, T. Takayanagi and T. Ugajin, *Spectrum of End of the World Branes in Holographic BCFTs*, *JHEP* **06** (2021) 023 [2103.06893].
- [52] B. Eynard, *Topological expansion for the 1-Hermitian matrix model correlation functions*, *JHEP* **11** (2004) 031 [hep-th/0407261].
- [53] B. Eynard and N. Orantin, *Invariants of algebraic curves and topological expansion*, *Commun. Num. Theor. Phys.* **1** (2007) 347 [math-ph/0702045].
- [54] F. Wegner, *The mobility edge problem: Continuous symmetry and a conjecture*, *Zeitschrift für Physik B Condensed Matter* **35** (1979) 207.
- [55] K.B. Efetov, *Supersymmetry and theory of disordered metals*, *Adv. Phys.* **32** (1983) 53.
- [56] N. Engelhardt, S. Fischetti and A. Maloney, *Free energy from replica wormholes*, *Phys. Rev. D* **103** (2021) 046021 [2007.07444].
- [57] C.V. Johnson, *Low Energy Thermodynamics of JT Gravity and Supergravity*, 2008.13120.
- [58] C.V. Johnson, *On the Quenched Free Energy of JT Gravity and Supergravity*, 2104.02733.
- [59] M. Alishahiha, A. Faraji Astaneh, G. Jafari, A. Naseh and B. Taghavi, *Free energy for deformed Jackiw-Teitelboim gravity*, *Phys. Rev. D* **103** (2021) 046005 [2010.02016].
- [60] I.S. Gradshteyn, I.M. Ryzhik, D. Zwillinger and V. Moll, *Table of integrals, series, and products; 8th ed.*, Academic Press, Amsterdam (Sep, 2014), 0123849330.
- [61] V. Fateev, A.B. Zamolodchikov and A.B. Zamolodchikov, *Boundary Liouville field theory. 1. Boundary state and boundary two point function*, hep-th/0001012.

- [62] J. Teschner, *Remarks on Liouville theory with boundary*, *PoS tnr2000* (2000) 041 [[hep-th/0009138](#)].
- [63] K. Okuyama and K. Sakai, *FZZT branes in JT gravity and topological gravity*, *JHEP* **09** (2021) 191 [[2108.03876](#)].
- [64] M. Alishahiha, S. Banerjee and J. Kames-King, *To appear soon*, .
- [65] L. McGough, M. Mezei and H. Verlinde, *Moving the CFT into the bulk with $T\bar{T}$* , *JHEP* **04** (2018) 010 [[1611.03470](#)].
- [66] M. Taylor, *TT deformations in general dimensions*, [1805.10287](#).
- [67] T. Hartman, J. Kruthoff, E. Shaghoulian and A. Tajdini, *Holography at finite cutoff with a T^2 deformation*, *JHEP* **03** (2019) 004 [[1807.11401](#)].
- [68] A.B. Zamolodchikov, *Expectation value of composite field T anti- T in two-dimensional quantum field theory*, [hep-th/0401146](#).
- [69] F.A. Smirnov and A.B. Zamolodchikov, *On space of integrable quantum field theories*, *Nucl. Phys. B* **915** (2017) 363 [[1608.05499](#)].
- [70] A. Cavaglià, S. Negro, I.M. Szécsényi and R. Tateo, *$T\bar{T}$ -deformed 2D Quantum Field Theories*, *JHEP* **10** (2016) 112 [[1608.05534](#)].
- [71] L.V. Iliesiu, J. Kruthoff, G.J. Turiaci and H. Verlinde, *JT gravity at finite cutoff*, *SciPost Phys.* **9** (2020) 023 [[2004.07242](#)].

Cosmology

This chapter has already been published as [138]:

No Page Curves for the de Sitter Horizon, *J. Kames-King, E. Verheijden, E. Verlinde*, In: *JHEP*, arXiv: 2108.09318 [hep-th]

This chapter deals with quantum information in de Sitter. More concretely, we calculate the behaviour of entanglement entropy of the evaporating de Sitter horizon both at future infinity and at the cosmological horizon. In order to do this we set a state, which is analogous to black hole evaporation for a cosmic horizon, which was first considered in the reference [139]. Backreaction allows a holographic description at the horizon. Why de Sitter is relevant to our universe is explained in 1.6 and ideas on how to think of de Sitter in a holographic manner are also explained in section 1.6.

In detail, we start by performing a partial dimensional reduction of three-dimensional de Sitter space to two-dimensional de Sitter space. By “partial” we mean that we do not reduce over the complete angular coordinate. The dimensional reduction leads to a two-dimensional JT gravity theory with a positive cosmological constant. The extrinsic curvature plays an important role as in principle it leads to a Schwarzian action both at future infinity and past infinity if the boundary conditions explained in section 1.4.7 are used. We then consider the addition of matter. More specifically we use conformal matter, which we interpret as the Hawking radiation of the cosmological horizon. Different choices for the expectation value of the energy-momentum tensor of the conformal matter correspond to different physical situations with regard to the Hawking radiation. Usually the Bunch-Davies state is chosen for the radiation, which amounts to considering the static patch to be in thermal equilibrium. The static observer sees the same amount of in- and outgoing radiation. However, we choose to consider the Unruh state. This state is out-of-equilibrium, which means that the static observer will see only incoming radiation. Therefore it is analogous to black hole evaporation for this cosmological scenario. In principle one could also consider only outgoing radiation or a linear combination of Bunch-Davies and Unruh. The energy-momentum tensor is singular at the past cosmological horizon, such that past infinity should not be considered to be part of this spacetime anymore. In order to arrive at an understanding as to what this implies at future infinity we solve the Schwarzian equations of motion in presence of the matter conformal field theory. This leads to a linear solution for the dilaton in terms of

the future boundary coordinate. As the dilaton amounts to the angular coordinate, this may be interpreted to mean that the radiation “moves along” the direction of partial reduction in this evaporating scenario. It is also interesting to note that the entropy of the static patch appears as conserved ADM momentum here. As the dilaton solution becomes dynamical due to the Unruh state, we can easily read off that the ADM momentum becomes dynamical and therefore also the entropy. The backreaction can also be solved for the dilaton in the static patch due to the simple structure of JT gravity. Remarkably, it can be seen that the dilaton diverges infinitely at the past cosmological horizon, which implies that gravity decouples in this region, making it suitable to play the role of a holographic screen (also see comments in section 1.6.2). Remarkably, the dilaton reproduces the same linear solution mentioned above but in terms of a static patch lightlike coordinate. In the final section, we calculate the fine-grained entropy at the two regions for which gravity decouples: future infinity and the past cosmological horizon. We see that at future infinity we naturally get a Page curve without the need for the island formula. We take this to mean that future infinity being behind the cosmological horizon is a naturally pure observer. In contrast for the static patch, we see standard thermal growth. We argue that in principle one could consider the existence of an island which would lead to a pure Page curve. However, times after the Page time should be considered unphysical in any case. As can be seen via the singularity theorem, at the Page time a trapped region forms preventing the recovery of the radiation. In addition, at future infinity a singularity forms. Therefore, information recovery does not seem possible for this state in de Sitter spacetime.

The author contributed to all conceptual discussions regarding this publication. The author performed the calculations of sections 2.1, 2.2, 2.3, 3.1 and 5.2.

No Page curves for the de Sitter horizon

Joshua Kames-King,^{a,c} Evita M.H. Verheijden^b and Erik P. Verlinde^b

^a*Bethe Center for Theoretical Physics & Physikalisches Institut der Universität Bonn,
Nussallee 12, 53115 Bonn, Germany*

^b*Institute of Physics & Delta Institute for Theoretical Physics, University of Amsterdam,
Science Park 904, 1090 GL Amsterdam, The Netherlands*

^c*Kavli Institute for Theoretical Physics, University of California,
Santa Barbara, CA93106, U.S.A.*

E-mail: jvakk@yahoo.com, e.m.h.verheijden@uva.nl, e.p.verlinde@uva.nl

ABSTRACT: We investigate the fine-grained entropy of the de Sitter cosmological horizon. Starting from three-dimensional pure de Sitter space, we consider a partial reduction approach, which supplies an auxiliary system acting as a heat bath both at \mathcal{I}^+ and inside the static patch. This allows us to study the time-dependent entropy of radiation collected for both observers in the out-of-equilibrium Unruh-de Sitter state, analogous to black hole evaporation for a cosmological horizon. Central to our analysis in the static patch is the identification of a weakly gravitating region close to the past cosmological horizon; this is suggestive of a relation between observables at future infinity and inside the static patch. We find that in principle, while the meta-observer at \mathcal{I}^+ naturally observes a pure state, the static patch observer requires the use of the island formula to reproduce a unitary Page curve. However, in practice, catastrophic backreaction occurs at the Page time, and neither observer will see unitary evaporation.

KEYWORDS: 2D Gravity, Models of Quantum Gravity

ARXIV EPRINT: [2108.09318](https://arxiv.org/abs/2108.09318)

Contents

1	Introduction	1
2	JT gravity on dS_2 from dS_3	5
2.1	Dimensional reduction from 3D Einstein to JT gravity	5
2.2	Two-dimensional bulk dynamics	7
2.3	Boundary action and renormalised dilaton	8
3	Adding matter: a dynamical boundary dilaton	10
3.1	Matter and the Unruh state	10
3.2	Estimates on the de Sitter lifetime	13
4	The static patch	14
4.1	The bulk dilaton solution	15
4.2	The cosmological horizon and quantum mechanics	15
5	Fine-grained entropy calculations	16
5.1	Entropy computed at \mathcal{I}^+	17
5.2	Entropy computed inside the static patch	19
5.3	Backreaction considerations: formation of a trapped region	21
6	Discussion	23
6.1	Quantum mechanics and the island	23
6.2	Information recovery	24
6.3	Inflationary perspective	24
A	Coordinate systems	25

1 Introduction

One of the greatest puzzles posed by our Universe — which we to good approximation believe to be described by de Sitter space — is a proper understanding of the cosmological horizon that surrounds any observer. The cosmological horizon of such a static observer exhibits thermodynamic properties similar to a black hole horizon [1]. One of the subtle obscurities is the entropy associated to the cosmological horizon, and in particular the fact that it appears to be finite. This seems to imply a finite-dimensional Hilbert space, which is in direct contradiction with the infinite-dimensional degrees of freedom of effective field theory on a de Sitter background [2–8]. This discrepancy constitutes a significant problem, as not only the early Universe but also the current Universe at large scales is approximated by de Sitter space. While a complete microscopic understanding would require a full

quantum gravity approach, here we follow a semi-classical approximation very much in the spirit of recent developments in a black hole context [9–16]. In practice this means that, while the exact microscopic state may be unknown, there is still a procedure to calculate the fine-grained entropy.

Until recently it was not known how unitary evolution of an evaporating black hole could be aligned with the apparently ever-increasing entropy of Hawking radiation. In a series of breakthroughs it was shown that the Quantum Extremal Surface (QES) of a non-gravitating region entangled with a gravitational system undergoes a phase transition at the Page time: the empty surface jumps to a surface just behind the horizon. This implies that the Hawking radiation follows the Page curve in accordance with unitarity [17, 18]. This result is now seen as an instantiation of a more general rule:¹

$$S_{\text{QG}}[\text{Rad}] = \min_I \left\{ \text{ext}_I \left[S_{\text{SCG}}[\text{Rad} \cup I] + \frac{\text{Area}[\partial I]}{4G} \right] \right\}. \quad (1.1)$$

This so-called ‘island rule’ tells us that the calculation of the fine-grained entropy must allow for the existence of disconnected regions or ‘islands’. To compute the entropy of Hawking radiation in quantum gravity (QG), we should include “quantum extremal islands” in our semi-classical entropy calculation (SCG). These islands can minimize the entropy, e.g. an island just inside the black hole horizon will include Hawking partners of the radiation. The price to pay is the area of the island. Finally, one has to extremize and minimize over all possible islands.

The island rule has been used to reproduce the Page curve for various black hole solutions [21–30]. We would like to use these developments to learn more about the cosmological horizon. More specifically, we extend the procedure of [31], in which the evaporation of two-dimensional black holes in JT gravity on AdS₂ was studied from a three-dimensional point of view, to de Sitter space. In the original setup, the authors effectively divided the BTZ black hole into two parts. In one of these, they integrated out the angular coordinate, thereby reducing it to a black hole in AdS₂ JT gravity. In the other part, the holographic coordinate was integrated out, thereby obtaining the dual CFT (which took on the role of the ‘bath’). The evaporation of the 2D black hole effectively corresponds to changing the location of the dividing line. The entropy of a region in the bath can then be computed using geodesics in the three-dimensional BTZ geometry; this reproduces the Page curve for the bath entropy.

One might wonder if a similar approach could lead to new insights on the nature of the de Sitter entropy. A natural starting place would be to consider JT gravity in de Sitter [32–34]. There has been some work on entanglement islands in a cosmological setup, see e.g. [35–38]. In particular, [39] provides a complementary perspective to the approach we will take, which we outline below.

Our approach. We will start from pure (empty) dS₃ and perform a similar trick as explained above. A partial dimensional reduction of dS₃ along the angular direction φ divides the three-dimensional spacetime into two. Up to some value of the angular coordinate

¹We are neglecting (potential) subtleties here about the use of the island rule in a gravitating system, see [19, 20].

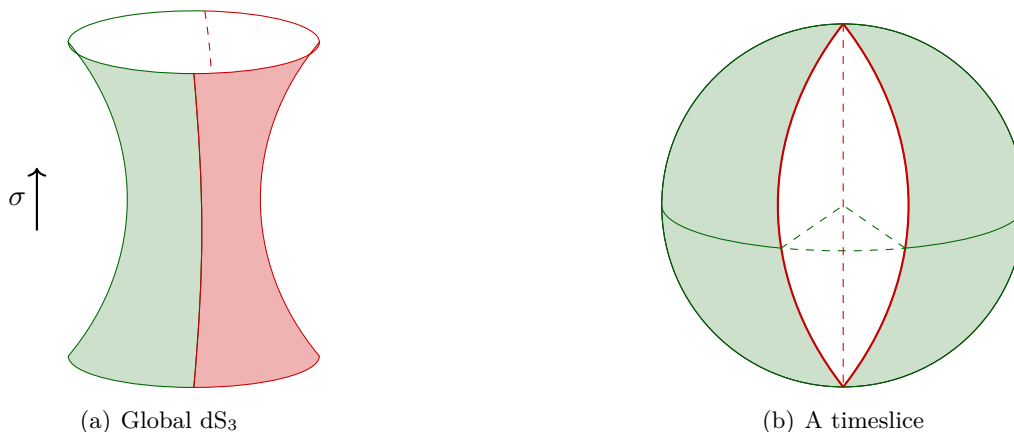


Figure 1. Global de Sitter is the surface of the hyperboloid (a). Time flows upwards; one angular coordinate is suppressed, such that each time-slice is actually a two-sphere (b). We split the spacetime into two, reducing over the red part to get JT gravity on dS_2 . The green part is the remainder of dS_3 , which takes on the role of the bath.

the system is described by dynamical gravity: JT gravity on dS_2 . The remainder of the three-dimensional spacetime will take on the role of the thermal ‘bath’ for the radiation of the cosmological horizon. To be precise, in our two-dimensional set-up we will identify two regions where gravity is weakly coupled; these regions may be considered non-dynamical and are thus good regions to collect radiation. We will then compute the fine-grained entropy of radiation collected in these regions by embedding them in the three-dimensional geometry. In this sense, we will refer to the remainder of the three-dimensional spacetime as the non-gravitating ‘bath’. The full (global) setup is depicted in figure 1.

Motivated by recent results in the context of evaporating black holes, we will consider an out-of-equilibrium thermal state corresponding to the evaporation of the cosmological horizon. As shown in [40], this so called Unruh-de Sitter state amounts to demanding a positive net incoming energy flux on the static patch, breaking the isometries preserved in the standard Bunch-Davies vacuum. The Schwarzian dynamics of \mathcal{I}^+ , established in [32, 33], allow for the calculation of the backreaction of the assumed matter configuration on the boundary dilaton, which becomes a function of the single boundary variable u at future infinity.² From the three-dimensional perspective the renormalised boundary dilaton corresponds to the angle of the dimensional reduction, $\Phi_r \sim 2\pi\alpha$, such that the backreaction of the Unruh-de Sitter state imbues the full three-dimensional setup with a dependence on u . In the partial reduction the entropy of the cosmological horizon is

$$S_{dS,\alpha} = \frac{\pi\alpha\ell}{2G^{(3)}}, \tag{1.2}$$

where α is the parameter determining the reduction angle. From (1.2) we see that a dynamical boundary dilaton $\Phi_r(u) \sim \alpha(u)$ not only amounts to dynamical evolution of the

²Although u appears as a spacelike coordinate at future infinity, we will often denote a function of this variable as ‘time-dependent’. We do so because we take the results of section 4 to mean that in the static patch functions of u become functions of the proper static patch time.

dividing line between the thermal bath and gravity, but also to a decreasing entropy. As depicted in figure 4 and figure 6 of section 5, in the three-dimensional picture we think of this dynamical change as the evaporation of the radiation into the bath.

Note that in [31], it was the mass of the BTZ black hole that became time-dependent, and consequently the entropy; however, empty de Sitter only exhibits a single (fixed) length scale. We can still introduce a time-dependent entropy if we allow for time-dependence in α and hence consider $(\alpha \ell)$ as an effective time-dependent de Sitter length.

While the behaviour of $\alpha(u)$ can indeed be determined at the future boundary, we will also find that we can recover the same behaviour by use of an explicit bulk solution at the cosmological horizon in the static patch. This allows us to address an important subtlety that arises for the de Sitter case: we can make a choice of observer. Whereas the static observer is surrounded by a cosmological horizon and as such experiences a thermal bath, we can also define a ‘meta-observer’ at future infinity, who can observe the wavefunction of the universe as they have access to distances larger than the Hubble scale [2, 41]. From a cosmological perspective we can (approximately) be described as a static observer currently entering a new de Sitter phase. However, we may also be considered meta-observers with respect to our inflationary past [42].

As our construction creates a thermal bath in both the static patch and at future infinity of the two-dimensional de Sitter space, we can perform calculations for both observers. These are complementary views and we give results for the entropy of the collected radiation with respect to both. As a second subtlety, we must take into account the lifetime of the backreacted solution. In a semi-classical setting, various arguments have been made about the lifetime of de Sitter. We will consider how these approaches bound our results. Furthermore, as we are considering an out-of-equilibrium state, we should expect the lifetime to be drastically reduced and even a singularity to arise [39]. These considerations naturally will reduce the domain of validity of the entropy computations.

This paper is organised as follows. In section 2 we discuss how to obtain JT gravity on two-dimensional de Sitter from a three-dimensional Einstein-Hilbert action in de Sitter. We discuss the two-dimensional bulk equations of motion, and then comment on the boundary action and the dilaton at future infinity. In section 3 we introduce dynamics by considering the effect of adding matter to our configuration. Specifying the Unruh-de Sitter state, we find a dynamical boundary dilaton $\Phi_r(u)$. This allows us to estimate the lifetime of our setup, and we comment on the timescales relevant to our problem. We also calculate the backreacted bulk dilaton in section 4. We discover that the gravitational coupling becomes weak at the past horizon. Remarkably, the explicit backreacted bulk dilaton exhibits the same behaviour close to the past cosmological horizon in terms of the static patch time t as the boundary dilaton does in terms of u . In section 5 we move on to the calculation of the entanglement entropy of the radiation as a function of our boundary time u and of the static patch time t . We explain why our setup naturally supplies an auxiliary system at both \mathcal{I}^+ and in the static patch, and we compute the fine-grained entropy in both regions. While for \mathcal{I}^+ we recover unitary behaviour without the use of an island, the static patch requires a more involved argument and, implicitly, the existence of an island. This agrees with intuition due to the different locations of these regions with

respect to the cosmological horizon. The meta-observer is in causal contact with behind the horizon degrees of freedom, whereas the static patch observer represents a thermal observer. However, the aforementioned finite lifetime of the Unruh de Sitter state corresponds to the occurrence of a trapped region at the Page time. Therefore information recovery does not seem possible for the evaporating de Sitter horizon.

2 JT gravity on dS_2 from dS_3

As outlined in the introduction, we start with three-dimensional gravity on pure de Sitter space. The first step is to perform a partial dimensional reduction on the spherical coordinate φ . This means we consider the upper value of the spherical integration of φ to be given in terms of a new parameter $\alpha \in (0, 1]$. As we will see below, α is closely related to the dilaton in two dimensions.

2.1 Dimensional reduction from 3D Einstein to JT gravity

Our starting point is given by the three-dimensional action

$$S = \frac{1}{16\pi G^{(3)}} \int d^3x \sqrt{-g^{(3)}} \left(R^{(3)} - \frac{2}{\ell^2} \right) - \frac{1}{8\pi G^{(3)}} \int d^2x \sqrt{-h^{(3)}} \left(K^{(3)} - 1 \right), \quad (2.1)$$

where the last term is the Gibbons-Hawking boundary term. Here $K^{(3)}$ plays an important role as it will furnish the Schwarzian boundary action at future infinity \mathcal{I}^+ . The Einstein equations give $R^{(3)} = \frac{6}{\ell^2}$.

We collect different coordinate systems for de Sitter space in appendix A. Here, we single out two important systems we will use: global and static coordinates. In global conformal coordinates, three-dimensional de Sitter space is given by:

$$ds_3^2 = \frac{\ell^2}{\cos^2 \sigma} \left(-d\sigma^2 + d\theta^2 + \sin^2 \theta d\varphi^2 \right), \quad (2.2)$$

where $\sigma \in (-\frac{\pi}{2}, \frac{\pi}{2})$, $\theta \in [0, \pi]$ and $\varphi \in [0, 2\pi)$. The corresponding Penrose diagram is a square, see figure 2. No single observer can access the full geometry and there is no global timelike Killing vector.

The so-called static patch is the region accessible to a single observer living on one of the poles of the S^2 . For this region, the $SO(1, 3)$ isometry group gives rise to a manifest t -translation, such that we arrive at a time-independent metric, given by:

$$ds_3^2 = - \left(1 - \frac{r^2}{\ell^2} \right) dt^2 + \left(1 - \frac{r^2}{\ell^2} \right)^{-1} dr^2 + r^2 d\varphi^2, \quad (2.3)$$

with $r \in [0, \ell]$. Note that the same angle φ appears in both (2.2) and (2.3). The static coordinates cover only the right (orange) diamond of figure 2. The null surface at $r = \ell$ surrounding the observer at all times is known as the cosmological horizon. The temperature associated to this horizon is

$$T_{\text{dS}} = \frac{1}{2\pi\ell}, \quad (2.4)$$

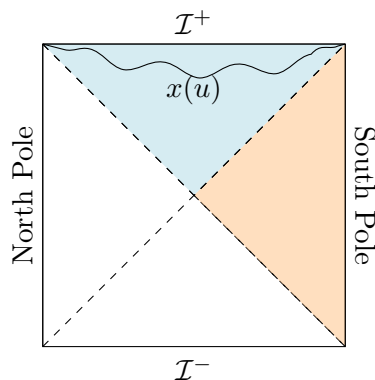


Figure 2. The Penrose diagram of three-dimensional de Sitter. Each point represents a circle. The static patch for an observer at the south pole is indicated in orange; the dashed lines are the horizons. The Milne (future) patch is indicated in blue. We will make use of the fluctuating boundary geometry at \mathcal{I}^+ described by a Schwarzian action. \mathcal{I}^- does not play a role in our considerations as we consider a quantum state that is singular at the past horizon.

which is a fixed quantity. The corresponding Gibbons-Hawking entropy is given by

$$S_{\text{dS}} = \frac{\pi \ell}{2G^{(3)}}. \tag{2.5}$$

As outlined in the introduction, we consider a partial reduction ansatz by considering an upper value of the spherical coordinate φ in the spherical integration to be given as $2\pi\alpha$, $\alpha \in (0, 1]$, which then means that the Gibbons-Hawking entropy is given as (1.2), which we repeat here for convenience:

$$S_{\text{dS},\alpha} = \frac{\pi\alpha\ell}{2G^{(3)}} = \frac{\pi\alpha}{2G^{(2)}}, \tag{2.6}$$

where we identified $G^{(3)} = \ell G^{(2)}$ and we will from now on denote $G^{(2)}$ simply as G . We are interested in considering the evolution of (2.6) by allowing for time-dependence in α . We will see below that the dilaton of the JT theory we acquire in two dimensions is intimately linked to this angle α . From the two-dimensional perspective, any backreaction is captured by the dilaton. Hence, it is clear that setting a two-dimensional Unruh-de Sitter state will not only lead to a time-dependent dilaton solution, but also from the higher-dimensional perspective lead to a dynamical change of (2.6) as desired.

Let us now turn to the details of the dimensional reduction. We assume an ansatz of the form

$$ds_3^2 = g_{ij}^{(2)} dx^i dx^j + \phi^2(x^i) \ell^2 d\varphi^2. \tag{2.7}$$

Under the assumption of an asymptotic boundary, by use of the following identities

$$\begin{aligned} R^{(3)} &= R^{(2)} - \frac{2}{\phi} \square^{(2)} \phi, \\ K^{(3)} &= K^{(2)} + \frac{1}{\phi} n^\mu \nabla_\mu^{(2)} \phi, \end{aligned} \tag{2.8}$$

and by integrating the spherical coordinate as outlined below (2.5), we find

$$S = \frac{2\pi\alpha\ell}{16\pi G^{(3)}} \int d^2x \sqrt{-g^{(2)}} \phi \left(R^{(2)} - \frac{2}{\ell^2} \right) - \frac{2\pi\alpha\ell}{8\pi G^{(3)}} \int dx \sqrt{-h^{(2)}} \phi_b \left(K^{(2)} - 1 \right). \quad (2.9)$$

We have implicitly identified $\ell_3 = \ell_2 \equiv \ell$. Using again $G^{(3)} = \ell G$, we conclude

$$\Phi = 2\pi\alpha\phi, \quad (2.10)$$

such that we arrive at the JT gravity action

$$S = \frac{1}{16\pi G} \int d^2x \sqrt{-g^{(2)}} \Phi \left(R^{(2)} - \frac{2}{\ell^2} \right) - \frac{1}{8\pi G} \int dx \sqrt{-h^{(2)}} \Phi_b \left(K^{(2)} - 1 \right). \quad (2.11)$$

Here Φ_b denotes the boundary value of Φ . In the dimensionally reduced language of (2.11) we recover the global metric (2.2) by

$$ds_2^2 = \frac{\ell^2}{\cos^2 \sigma} \left(-d\sigma^2 + d\theta^2 \right), \quad \Phi = 2\pi\alpha \frac{\sin \theta}{\cos \sigma}. \quad (2.12)$$

The extrinsic curvature $K^{(2)}$ plays a pivotal role in our approach, but we will postpone our discussion of it to section 2.3. First, we will expand on the bulk dynamics in section 2.2. Before we do so, we wish to point out that in (2.11) we do not recover the Gauss-Bonnet term ordinarily used in JT gravity. This term, in an AdS context proportional to the ground state entropy of an extremal, higher-dimensional black hole, usually allows for negative values of the dilaton Φ while still maintaining positive values for the total entropy $\Phi_0 + \Phi$. In that case, the Penrose diagram of dS_2 ‘doubles’ and allows for two horizons located at $r = \pm\ell$. The second horizon is often interpreted as a black hole horizon, and this geometry then serves as a lower-dimensional toy model for Schwarzschild-de Sitter. We are instead interested in studying ‘pure’ de Sitter, and hence will stick to figure 2 also for the two-dimensional model, as we interpret this as inherited from the three-dimensional de Sitter spacetime. This agrees with the absence of Φ_0 in (2.11).

2.2 Two-dimensional bulk dynamics

To study the two-dimensional bulk dynamics, it is convenient to switch to conformal gauge and employ general lightcone coordinates (x^+, x^-) :

$$ds_2^2 = -e^{2\omega(x^+, x^-)} dx^+ dx^-. \quad (2.13)$$

In these coordinates the bulk equations of motion amount to [36, 43]

$$\begin{aligned} \partial_+ \partial_- \omega &= \frac{1}{4\ell^2} e^{2\omega}, \\ -\partial_{\pm}^2 \Phi + 2\partial_{\pm} \omega \partial_{\pm} \Phi &= 8\pi G \langle T_{x^{\pm} x^{\pm}} \rangle, \\ 2\partial_- \partial_+ \Phi - \frac{1}{\ell^2} e^{2\omega} \Phi &= 16\pi G \langle T_{x^+ x^-} \rangle. \end{aligned} \quad (2.14)$$

Let us now comment on different solutions to (2.14) in vacuum. As shown in appendix A, we can introduce null coordinates σ^\pm such that the static patch metric (2.3) is given by

$$e^{2\omega(\sigma^+, \sigma^-)} = \frac{1}{\cosh^2\left(\frac{\sigma^+ - \sigma^-}{2\ell}\right)}, \quad \Phi = 2\pi\alpha \frac{1}{\tanh\left(\frac{\sigma^+ + \sigma^-}{2\ell}\right)}. \quad (2.15)$$

Again, these coordinates are restricted to the south pole wedge. We can also define Kruskal coordinates which cover the entire Penrose diagram, see figure 2. As shown in appendix A this amounts to

$$e^{2\omega(x^+, x^-)} = \frac{4\ell^4}{(\ell^2 - x^+ x^-)^2}, \quad \Phi = 2\pi\alpha \frac{(\ell^2 + x^+ x^-)}{(\ell^2 - x^+ x^-)}. \quad (2.16)$$

The coordinate transformation that relates the Kruskal coordinates (x^+, x^-) to the static coordinates (σ^+, σ^-) is

$$x^\pm = \pm \ell e^{\pm \sigma^\pm / \ell}, \quad (2.17)$$

which illustrates the different roles these coordinate systems play for us. The transformation is the same relationship as between Rindler and Minkowski coordinates, such that indeed the coordinate systems (2.15) and (2.16) define different vacua.

In our approach we also care about the boundary dynamics of different solutions to (2.14). When considering the desired non-equilibrium state, we should be able to see at future infinity \mathcal{I}^+ that the entropy (2.6) has now become dynamical. The static patch (2.15) is not connected to the boundary, but it is connected via analytic continuation to the so-called Milne patch in the expanding region [33], see (A.17). The Milne solution is

$$e^{2\omega(y^+, y^-)} = \frac{1}{\sinh^2\left(\frac{y^+ + y^-}{2\ell}\right)}, \quad \Phi = 2\pi\alpha \frac{1}{\tanh\left(\frac{y^+ - y^-}{2\ell}\right)}. \quad (2.18)$$

In terms of the coordinates (τ, χ) used in (A.17), the lightcone coordinates y^\pm used in (2.18) are

$$y^\pm = \tilde{\tau} \pm \chi, \quad d\tau = \frac{d\tilde{\tau}}{\sinh \frac{\tilde{\tau}}{\ell}}. \quad (2.19)$$

As we will see in the next section, this geometry is of importance for our purposes as it captures the evolution of the entropy (2.6) at future infinity.

2.3 Boundary action and renormalised dilaton

We now turn to the boundary dynamics at \mathcal{I}^+ and the extrinsic curvature term of (2.11). In most of this section, we will use planar coordinates in order to make the analogy to [44] more apparent:

$$ds_2^2 = \frac{\ell^2(-d\eta^2 + dx^2)}{\eta^2}, \quad \Phi = -2\pi\alpha \frac{x}{\eta}. \quad (2.20)$$

Note that $\eta \leq 0$ and $x \geq 0$, with \mathcal{I}^+ located at $\eta = 0$, such that the dilaton is correctly positive. As \mathcal{I}^+ is a conformal boundary, we would like to cut off the space along a

boundary curve $(\eta(u), x(u))$. It is usually conjectured that the complete gravitational theory can be described by a quantum mechanical system at the conformal boundary; then u would correspond to the coordinate of this quantum mechanical boundary theory. It will play a special role in our setup as our results with respect to the entropy at future infinity are phrased in terms of this parameter. Following [33, 44] we set the following two boundary conditions

$$g_{uu} = \frac{\ell^2}{\epsilon^2}, \quad \Phi_b = \frac{\Phi_r}{\epsilon}. \quad (2.21)$$

For the partial reduction solutions we are considering, Φ_r generally takes on the form

$$\Phi_r = 2\pi\ell\alpha. \quad (2.22)$$

Solving (2.21) we get

$$K^{(2)} = \frac{1}{\ell} - \frac{\epsilon^2}{\ell} \{x(u), u\}, \quad (2.23)$$

such that the action (2.11) reduces to the effective boundary term

$$S_{\text{GH}} = \frac{1}{8\pi G} \int du \Phi_r \{x(u), u\}. \quad (2.24)$$

We can interpret (2.24) along the lines of [44]. The future boundary exhibits an asymptotic symmetry of reparametrisations of the coordinate $x(u)$, which may be understood as the gravitational degree of freedom of this two-dimensional system. By introducing the JT action, we explicitly break the symmetry and (2.24) may be considered the action of this ‘boundary graviton’. Variation of (2.24) with respect to the boundary mode $x(u)$ amounts to

$$-\frac{1}{8\pi G} \left(\Phi_r \{x(u), u\}' + 2\Phi_r' \{x(u), u\} + \Phi_r'' \right) = 0, \quad (2.25)$$

where $'$ denotes derivation with respect to u . We will ultimately be interested in a dynamical (renormalised) boundary dilaton Φ_r . To fully understand the background solutions, let us first consider constant Φ_r . Then (2.25) reduces to

$$\{x(u), u\}' = 0. \quad (2.26)$$

The associated conserved charge is given by [33, 44, 45]

$$K = -\frac{\Phi_r}{8\pi G} \{x, u\}. \quad (2.27)$$

One possible solution of (2.26) is given by

$$x(u) = 2\ell \tanh \frac{u}{2\ell} = \frac{\beta_{\text{dS}}}{\pi} \tanh \frac{\pi u}{\beta_{\text{dS}}}, \quad (2.28)$$

which just corresponds to the Milne solution (2.18). Note that with (2.22) and (2.28), (2.27) amounts to

$$K = \frac{S_{\text{dS},\alpha}}{2\beta_{\text{dS}}}. \quad (2.29)$$

Here we can see why the solution (2.28) (i.e., the metric (2.18)) is of special importance to us. The ADM quantity (2.29) is linked to the entropy (2.6) of the static observer, such that demanding dynamical behaviour of (2.27) at \mathcal{I}^+ conforms with the desired change in entropy. Hence, the sensitivity of the static patch entropy to the state of our matter fields in static coordinates will in section 3.1 translate to the sensitivity of (2.27) to the boundary flux at future infinity. A closer look at (2.27) leads to a further distinction compared to recent results on evaporating black holes in an AdS setting such as [15]. It is in general clear that allowing for non-equilibrium states should correspond to a dynamically evolving ADM quantity. For an asymptotically AdS₂ black hole it is reasonable to allow either a time-dependence of the Schwarzian or of the renormalised dilaton value in (2.27). Whereas the former choice corresponds to a time-dependent temperature and hence a dynamically evolving black hole mass as in [15], the latter amounts to a fixed temperature with a dynamically evolving angle (or equivalently a time-dependent dilaton) in three dimensions as in [31]. The former choice is not an option for a fixed de Sitter background, since a time-dependent temperature does not correspond to a change in integration constant but instead amounts to a shift away from a de Sitter geometry. Hence, we will consider the temperature to be fixed as in (2.4) and let the dilaton acquire dynamical behaviour.

3 Adding matter: a dynamical boundary dilaton

In this section we will consider adding matter to our configuration. In this way, we consider the observer inside the static patch to experience an incoming (net) positive energy flux. Solving the equations of motion for the boundary dilaton $\Phi_r \sim \alpha$ at \mathcal{I}^+ , we find a time-dependent $\alpha(u)$. Indeed, from the three-dimensional perspective we see that this corresponds to a shrinking gravitational system in the φ -direction: the cosmological horizon is evaporating. We also comment on the timescales relevant to our problem.

3.1 Matter and the Unruh state

We wish to consider a setup in which the size of the horizon decreases, such that the entropy (2.6) dynamically evolves. To be able to do so, we will have to specify a quantum state for the radiation. The state we want to consider is the Unruh-de Sitter state established in [40]. Since this state is less discussed in the literature, we will carefully define its construction.

As we are working in a semi-classical limit, we promote the stress tensor components to their expectation values $T_{\mu\nu} = \langle T_{\mu\nu} \rangle$. In a curved background, the stress tensor receives contributions from the Weyl anomaly. Our first task is to specify the components of the quantum stress tensor independently of the state. One approach is to demand conservation of the stress energy tensor as in [46, 47]

$$\nabla_\mu \langle T^{\mu\nu} \rangle = 0, \tag{3.1}$$

which allows to solve for the components in the general lightcone coordinates of (2.13)

$$\langle T_{x^\pm x^\pm}(x^\pm) \rangle = \frac{c}{12\pi} \left(\partial_\pm^2 \omega - \partial_\pm \omega \partial_\pm \omega \right) - \frac{c}{24\pi} t_{x^\pm x^\pm}(x^\pm) + \langle \tau_{x^\pm x^\pm} \rangle, \tag{3.2}$$

$$\langle T_{x^+ x^-}(x^+, x^-) \rangle = -\frac{c}{12\pi} \partial_+ \partial_- \omega. \tag{3.3}$$

Here, $\tau_{\mu\nu}$ refers to the (state-independent) contribution to the stress tensor in flat space. While the off-diagonal component (in lightcone coordinates) is completely fixed by the conformal anomaly, the diagonal components include state-dependent contributions: the two independent degrees of freedom $t_{x^\pm x^\pm}(x^\pm)$. The stress tensor naturally obeys the anomalous transformation law, which in our conventions is³

$$\langle T_{y^\pm y^\pm}(y^\pm) \rangle = \left(\frac{dx^\pm}{dy^\pm} \right)^2 \langle T_{x^\pm x^\pm}(x^\pm) \rangle - \frac{c}{24\pi} \{x^\pm, y^\pm\}, \quad (3.4)$$

with the functions $t_{x^\pm x^\pm}(x^\pm)$ changing accordingly,

$$t_{y^\pm y^\pm}(y^\pm) = \left(\frac{dx^\pm}{dy^\pm} \right)^2 t_{x^\pm x^\pm}(x^\pm) - \{x^\pm, y^\pm\}. \quad (3.5)$$

Specifying $t_{x^\pm x^\pm}(x^\pm)$ amounts to fixing a choice of vacuum, and hence a choice of thermal flux for the static patch observer. This determines the flux at future infinity \mathcal{I}^+ :

$$\langle T_{x^+ x^+} \rangle - \langle T_{x^- x^-} \rangle = \frac{c}{24\pi} (t_{x^- x^-} - t_{x^+ x^+}). \quad (3.6)$$

By fixing the two independent degrees of freedom, we can recover the standard Bunch-Davies vacuum, which is defined with respect to the Kruskal coordinates (2.16) to be

$$\langle T_{x^\pm x^\pm}(x^\pm) \rangle = 0. \quad (3.7)$$

Note that by use of (3.4) and (2.17) we can see that the Bunch-Davies state (3.7) corresponds to thermal equilibrium on the static patch:

$$\langle T_{\sigma^\pm \sigma^\pm}(\sigma^\pm) \rangle = \frac{\pi c}{12\beta_{\text{dS}}^2}. \quad (3.8)$$

At future infinity (3.7) corresponds to a zero net flux (3.6). Hence we must follow the approach of [40] and break the symmetry between incoming and outgoing flux on the static patch or equivalently allow for a net flux (3.6) at \mathcal{I}^+ . Our desired state corresponds to setting the vacuum with respect to the static coordinates for the left-moving and with respect to the Kruskal coordinates for the right-moving modes. Hence in static coordinates we find

$$\langle T_{\sigma^+ \sigma^+}(\sigma^+) \rangle = 0, \quad \langle T_{\sigma^- \sigma^-}(\sigma^-) \rangle = \frac{\pi c}{12\beta_{\text{dS}}^2}, \quad (3.9)$$

whereas in Kruskal coordinates this gives

$$\langle T_{x^+ x^+}(x^+) \rangle = -\frac{c}{48\pi(x^+)^2}, \quad \langle T_{x^- x^-}(x^-) \rangle = 0. \quad (3.10)$$

Note that the stress tensor (3.10) is singular at the past horizon and the NEC is violated as required by Hawking's area theorem [48, 49]. In figure 3 we summarise the fluxes in different patches.

³Note the non-standard minus for the Schwarzian transformation law and non-standard normalisation.

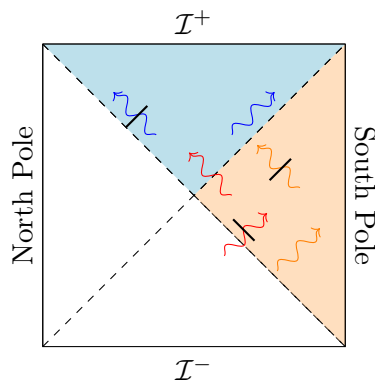


Figure 3. Penrose diagram of the Unruh state. The black bars denote zero one-point functions, whereas the arrows denote non-zero one-point functions of the stress tensor. Globally (red radiation), there are only left-moving modes and no right-moving modes. In the static patch (orange radiation), this corresponds to no outgoing radiation. This gets transferred to the Milne patch (blue radiation). As also elaborated upon in the main text, in global or Kruskal coordinates there is a flux of negative energy.

Since \mathcal{I}^+ is sensitive to the diagonal components of the stress tensor, it is sensitive to the flux (3.6) and hence also to the state of the quantum fields. By expressing the boundary matter action in terms of $x(u)$ we can see how (2.25) is modified (in addition, an intuitive derivation is given in [44]). For classically conformal matter we arrive at

$$\frac{1}{8\pi G_N} \left(\Phi_r \{x(u), u\}' + 2\Phi_r' \{x(u), u\} + \Phi_r'' \right) = \langle T_{x^-x^-}(u) \rangle - \langle T_{x^+x^+}(u) \rangle. \quad (3.11)$$

Here, we have a general differential equation relating the change of a previously conserved quantity (2.27) to a flux leaving \mathcal{I}^+ , expressed in general lightcone coordinates. Now, as elaborated upon in section 2.3, we are specifically interested in the solution (2.28) since the corresponding ADM quantity is related to the entropy of the static patch. Hence a flux as in (3.11) will give the desired evolution of the entropy. Therefore, we must actually consider the matter contribution to (3.11) with respect to the Milne coordinates. Due to the analytic continuation linking Milne and static coordinates, the stress tensor in terms of Milne coordinates is also given by (3.9). Note that in (3.11) the stress tensor components are given in terms of the boundary variable u . Therefore, if we now use (3.4), assume both the state (3.10) and no initial outgoing matter, for $u > 0$ we deduce [45]

$$\langle T_{x^+x^+}(u) \rangle = 0, \quad (3.12)$$

$$\langle T_{x^-x^-}(u) \rangle = -\frac{c}{24\pi} \{x, u\}, \quad (3.13)$$

and therefore also

$$\frac{1}{8\pi G_N} \left(\Phi_r \{x(u), u\}' + 2\Phi_r' \{x(u), u\} + \Phi_r'' \right) = -\frac{c}{24\pi} \{x(u), u\}. \quad (3.14)$$

For de Sitter spacetimes the temperature is an intrinsically fixed quantity, such that we may work with the simpler equation

$$\left(-4\frac{\pi^2}{\beta_{\text{dS}}^2}\Phi_r' + \Phi_r'''\right) = \frac{2cG\pi^2}{3\beta_{\text{dS}}^2}. \tag{3.15}$$

In principle (3.15) yields both homogeneous exponential and linear inhomogeneous solutions. As we are interested in the backreaction of the matter on the dilaton we work with the latter. Hence, we solve (3.15) as

$$\Phi_r(u) = 2\pi\ell \left(1 - \frac{cG}{12\pi\ell}u\right). \tag{3.16}$$

Here, we have imposed the condition $\Phi_r(u = 0) = 2\pi\ell$. We have determined the backreacted, renormalised dilaton value in terms of the Euclidean boundary time u of the quantum mechanical model living at future infinity.⁴ This means that we are reducing the dynamics of the gravity+CFT system living on two-dimensional de Sitter to the dynamical boundary function (3.16). Let us now make the connection to the higher-dimensional picture of figure 1. Note that (3.16) corresponds to

$$\alpha(u) = \left(1 - \frac{cG}{12\pi\ell}u\right). \tag{3.17}$$

Hence, at least at \mathcal{I}^+ we see that (3.16) may be understood as transparent boundary conditions for the flux moving along φ . Different phases of evaporation correspond to the evolution of the parameter α as given in (3.17). From (3.17) we determine the Page time, i.e., the value of u for which α equals 1/2:

$$u_{\text{Page}} = \frac{6\pi\ell}{cG}. \tag{3.18}$$

Moreover, (3.17) may also be understood as the evolution of the inverse of an effective Hubble parameter $\ell\dot{\alpha}(u)$,

$$\ell\dot{\alpha}(u) = -\frac{c}{6} \frac{1}{S_{\text{dS}}}, \tag{3.19}$$

such that the backreaction is suppressed by the entropy.

To conclude, we see that even though we set evaporating conditions on the two-dimensional spacetime, due to the nature of the dilaton, determining the backreaction on Φ_r immediately implies dynamical evolution in the three-dimensional description.

3.2 Estimates on the de Sitter lifetime

Any approach to de Sitter space should take into account the restrictions imposed on specific observers. More concretely, as we are interested in determining the evolution of the entropy of the radiation, we should always compare with possible bounds on the

⁴In the language of [21], the degree of freedom of the dot.

lifetime of de Sitter space as these might constrain up to which point we can trust the entropy computations of section 5. Here we give a general argument before moving to a bulk description in section 5.3.

The least restrictive timescale is the recurrence or Poincaré time. Following [3], we can view de Sitter in thermal equilibrium as a thermofield double state in analogy with the ideas of [50]. However, it can be shown that the assumption of finite entropy contradicts the algebra acting on the thermofield double state,⁵ which implies that the symmetry between different static patches is broken. This introduces a new timescale

$$t \sim \exp(S_{\text{dS}}), \tag{3.20}$$

indicating when the space may not be approximated by de Sitter anymore. However, as elucidated in the previous section, we are using an out-of-equilibrium state in which the de Sitter isometries are broken from the onset. This should drastically reduce any lifetime considerations to a timescale smaller than (3.20). It would be interesting to consider in detail how the argument leading to (3.20) has to be modified.

In [40] a bound on the lifetime in the Unruh-de Sitter state was given as

$$t \sim S_{\text{dS}}. \tag{3.21}$$

As also stated above, in this low dimensional setting we may think of (3.17) as determining the evolution of an effective Hubble parameter (3.19). As we recover the same behaviour demonstrated in [40] for the effective Hubble parameter, we consider the same bound. Hence, in our language the lifetime on dS in the Unruh state is given as

$$u \sim u_{\text{Page}}, \tag{3.22}$$

where we specified u_{Page} in (3.18). From the boundary perspective it might not be quite clear what effect should actually constrain the system to this timescale. However, in section 5.3 we will use a specific bulk argument first used in [39], which demonstrates the appearance of a trapped region at the time (3.22).

4 The static patch

So far we have restricted ourselves to the use of boundary calculations. However, as the static patch is ‘disconnected’ from future infinity by a cosmological horizon, it might not be immediately clear to what extent (3.17) may be applied inside the static patch and where exactly a thermal bath should be located for the static observer. We should therefore understand the properties of the dilaton inside the static patch. We will locate a non-gravitating region for which the dilaton notably exhibits the same behaviour as at \mathcal{I}^+ , which will justify the calculations of section 5.2.

⁵It may be also argued that for this reason for a single observer the Hilbert space only describes one side of the horizon. Only the horizon-invariant subalgebra would correspond to physical states [51].

4.1 The bulk dilaton solution

Let us start by stating the backreacted bulk dilaton solution. In JT gravity, backreaction effects are fully captured by the dilaton, such that we have to solve the equations (2.14) with the sources (3.3) and (3.10). Solving the set of differential equations gives

$$\begin{aligned} \Phi(x^+, x^-) = & \frac{a_1 x^- + a_2 x^+}{\ell^2 - x^+ x^-} + a_3 \left(1 - \frac{2\ell^2}{\ell^2 - x^+ x^-} \right) \\ & + \frac{cG}{6} \left(\frac{2\ell^2}{\ell^2 - x^+ x^-} - \frac{\ell^2 + x^+ x^-}{\ell^2 - x^+ x^-} \log \frac{x^+}{\ell} \right), \end{aligned} \tag{4.1}$$

where a_1, a_2, a_3 are integration constants. We wish to construct a solution that qualitatively matches the structure of (3.16). This means we want to recover the background solution (2.16), with a quantum correction enforcing a decreasing Gibbons-Hawking entropy. Hence, we fix the integration constants to $a_1 = 0 = a_2$ and $a_3 = -2\pi\alpha + \frac{cG}{6}$. Then we find

$$\Phi(x^+, x^-) = \frac{\ell^2 + x^+ x^-}{\ell^2 - x^+ x^-} 2\pi \left(\alpha - \frac{cG}{12\pi} \log \frac{x^+}{\ell} \right) + \frac{cG}{6}. \tag{4.2}$$

The parameter α of the background solution sets the value of the Gibbons-Hawking entropy. The structure in the brackets of (4.2) may be understood as this parameter α acquiring dynamical behaviour due to the backreaction of the quantum state. We can use the rescaling symmetry in (x^+, x^-) to set $\alpha = 1$ in (4.2); then, taking it to \mathcal{I}^+ we recover the behaviour (3.16) and hence also (3.17). The last constant term of (4.2) corresponds to a shift in the vacuum which already occurs for the Bunch-Davies state [35]. As this merely amounts to a rescaling of S^1 it is not interesting for our purposes, and we drop this term.

4.2 The cosmological horizon and quantum mechanics

In the static patch, the Unruh state (3.9) corresponds to incoming radiation. Therefore, a natural set of coordinates to describe the bulk dilaton solution inside the static patch is given by the incoming Eddington-Finkelstein coordinates (σ^+, r) with $\sigma^+ = t + r^*$ as in (2.15). In these coordinates, the two-dimensional metric is

$$ds^2 = - \left(1 - \frac{r^2}{\ell^2} \right) (d\sigma^+)^2 + 2d\sigma^+ dr. \tag{4.3}$$

The backreacted bulk dilaton (4.2) with $\alpha = 1$ takes on the form

$$\Phi(\sigma^+, r) = \frac{r}{\ell} 2\pi \left(1 - \frac{cG}{12\pi\ell} \sigma^+ \right). \tag{4.4}$$

As can be seen by the appearance of Φ in (2.11), in two dimensions Φ plays the role of the inverse of the gravitational coupling. Hence we can see by the structure of (4.4) that at the pole $r \rightarrow 0$ we arrive at a strongly coupled gravitational region. On the other hand, at the past cosmological horizon $\sigma^+ \rightarrow -\infty$, we find that gravity becomes weak. Hence, while naturally \mathcal{I}^+ plays a special role as gravity fully decouples there, here we have located a

second region inside the bulk for which the same logic holds. This weakly-gravitating or non-dynamical region will allow us to compute the entropy of radiation collected inside the static patch [52].

From (4.4) we can read off the backreacted value of α in the static patch (denoted α_s) by comparing to (2.10) (with $\phi = \frac{r}{\ell}$)

$$\alpha_s(\sigma^+) = 1 - \frac{cG}{12\pi\ell}\sigma^+ . \tag{4.5}$$

We see that we recover exactly the behaviour (3.16), but with the spacelike parameter u replaced by the null coordinate σ^+ . For an observer at the pole ($r = 0$), this reduces to genuine time-dependence as $\sigma^+(r = 0) = t$:

$$\alpha_{s,pole}(t) = 1 - \frac{cG}{12\pi\ell}t . \tag{4.6}$$

Note that while it is clear that merely taking the bulk solution (4.2) to the boundary \mathcal{I}^+ must give the same behaviour, as guaranteed by the equivalence of the Schwarzian description to the bulk equations (2.14), the behaviour exhibited in (4.5) and (4.6) is more pronounced. We can view (4.6) as the static patch counterpart of (3.16), and it is then tempting to think of this as the timelike realisation of the quantum mechanical model living at future infinity. This might be in line with a ‘stretched horizon’ static patch holography [53, 54], where the physics inside the static patch (i.e., the physics as experienced by an observer at $r = 0$) has a dual description in which the degrees of freedom are located at the ‘boundary’ of the static patch, i.e., the horizon. As the evaporation angle $2\pi\alpha \in [0, 2\pi)$ we see that the evaporation process is finite: the observer at the pole can collect radiation only for a finite time.

This is indeed the interpretation we will take: whereas it is the static patch observer at $r = 0$ who is collecting radiation, thereby invoking the dynamical behaviour of α , there is a dual description at the weakly-coupled past horizon. This, then, is the region where we will compute the entanglement entropy of the emitted radiation via the auxiliary, three-dimensional spacetime, where a dynamical α corresponds to a dynamical interface in the φ -direction. We will recap the logic in the next section, where we perform the aforementioned calculations.

5 Fine-grained entropy calculations

We are now in a position to calculate the fine-grained entropy of the radiation as a function of u at \mathcal{I}^+ and as a function of t at the past cosmological horizon in the static patch. These are the two regions of the two-dimensional de Sitter spacetime at which the gravitational dynamics reduce to quantum mechanical descriptions. At the two aforementioned decoupling regions we encounter a description in terms of a matter CFT coupled to the dilaton determined by backreaction. In our construction, we consider the dilaton to have a higher-dimensional origin, such that the transparency relates to the spherical coordinate φ ; this functions as an auxiliary system. This allows the calculation of the fine-grained entropy

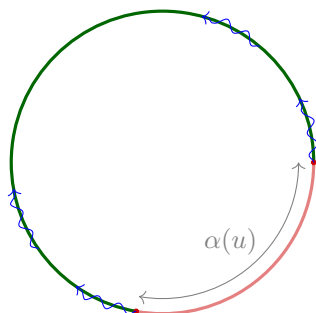


Figure 4. A constant χ slice of the (renormalised) cylinder at \mathcal{I}^+ of three-dimensional de Sitter in our partial reduction approach. In the two-dimensional picture the radiation ends up at \mathcal{I}^+ (red), before evaporating into the bath (green), which is located along a higher dimension (φ). The transfer of radiation from dynamical gravity to bath corresponds to (3.17). Note that as u increases, $\alpha(u)$ will decrease such that we are indeed modelling an evaporating system. We included the higher-dimensional de Sitter region in opaque red to clarify the entanglement structure.

of the two-dimensional system at the gravitationally decoupled regions to be performed via this auxiliary system. For both regions we use the higher-dimensional setting to first calculate the entanglement entropy in thermal equilibrium of a subregion with interval $\Delta\varphi$ and then by use of the solutions (3.17) and (4.5) we imbue the results with dynamical evolution determined by the backreaction, to obtain the desired out-of-equilibrium state.

5.1 Entropy computed at \mathcal{I}^+

Consider the three-dimensional Milne solution

$$ds^2 = -d\tau^2 + \sinh^2 \frac{\tau}{\ell} d\chi^2 + \ell^2 \cosh^2 \frac{\tau}{\ell} d\varphi^2, \tag{5.1}$$

and its partial reduction (A.18). The gravitational dynamics in the reduced de Sitter space (A.18) with the coordinates (τ, χ) reduce to that of a quantum mechanical boundary degree of freedom, namely (3.17). Note that this is in accordance with a dS/CFT picture [55]. At future infinity the induced metric is

$$ds^2 = \frac{1}{4} e^{2\tau^*/\ell} (d\chi^2 + \ell^2 d\varphi^2), \tag{5.2}$$

where τ^* denotes the asymptotic value $\tau \rightarrow \tau^* = \infty$. The setup at \mathcal{I}^+ is depicted in figure 4.

As we want to use the general formula for entanglement entropy on curved spacetimes Weyl-equivalent to flat spacetime, we define new coordinates

$$x = e^{\xi+i\varphi}, \quad \bar{x} = e^{\xi-i\varphi}, \tag{5.3}$$

where $\xi = \chi/\ell$. In these coordinates, (5.2) is given by

$$ds^2 = \frac{\ell^2}{\Omega^2} dx d\bar{x}, \quad \Omega = 2e^{-\tau^*/\ell} \sqrt{x\bar{x}}. \tag{5.4}$$

The matter (CFT) entropy in a region with general endpoints (x_1, \bar{x}_1) and (x_2, \bar{x}_2) now is

$$\begin{aligned}
 S_{\text{mat}} &= \frac{c}{6} \log \left[\frac{(x_1 - x_2)(\bar{x}_1 - \bar{x}_2)}{\Omega(x_1)\Omega(x_2)} \right] \\
 &= \frac{c}{6} \log \left[\frac{e^{2\tau^*/\ell}}{4} (2 \cosh(\xi_1 - \xi_2) - 2 \cos(\varphi_1 - \varphi_2)) \right].
 \end{aligned}
 \tag{5.5}$$

We are interested in calculating the matter entropy in the Unruh state (3.10), but from the three-dimensional point of view we can apply the standard formula in thermal equilibrium as in (5.5). The net flux corresponding to the Unruh state in 2D arises by imposing $\alpha(u)$ as in (3.17). Since in the auxiliary system we only consider separation in the direction of the dimensional reduction, we take $\chi_1 = \chi_2$ and $\Delta\varphi = 2\pi(1 - \alpha)$, such that we get

$$\begin{aligned}
 S_{\text{rad}} &= \frac{c}{6} \log \left[e^{2\tau^*/\ell} \sin^2 \Delta\varphi \right] \\
 &= \frac{c}{6} \log \left[\frac{4\ell^2}{\epsilon^2} \sin^2 \frac{\Phi_r}{2\ell} \right],
 \end{aligned}
 \tag{5.6}$$

where we collected the coordinate-dependent UV-divergences as $\epsilon = 2\ell e^{-\tau^*/\ell}$, in line with $\Phi_b = \frac{\Phi_r}{\epsilon}$ for the Milne coordinates (A.18). Writing (5.6) as a function of u , we find

$$\begin{aligned}
 S_{\text{rad}} &= \frac{1}{2G} \log \sin \frac{\Phi_r(u)}{2\ell} + \frac{1}{2G} \log \frac{2\ell}{\epsilon} \\
 &= \frac{1}{2G} \log \sin \pi \left(1 - \frac{cG}{12\pi\ell} u \right) + \frac{1}{2G} \log \frac{2\ell}{\epsilon},
 \end{aligned}
 \tag{5.7}$$

where we used $\frac{c}{3} = \frac{1}{2G(2)}$. Plotting (5.7) with an appropriate cut-off gives figure 5.

Let us postpone backreaction considerations and only comment on figure 5 for the moment. We can see that the entropy reaches the highest point at the Page time (3.18), after which it decreases. We take this to mean that the meta-observer located at \mathcal{I}^+ observes the evaporating geometry as a pure state. Moreover, note that we did not apply the formula (1.1) or demanded purity of some specific system. We arrive at a pure state of radiation without use of any involved argument. As a meta-observer at \mathcal{I}^+ is located behind the cosmological horizon, and thus has access to the entire history of their universe, for such an observer there is no naive division between interior and exterior subsystems. Hence, the formula (1.1) does not have to be applied.

However, we have pointed out a restriction due to the finite lifetime of this state in section 3.2. We will show in section 5.3 that a trapped surface forms at the Page time. As this complies with geodesic incompleteness, we do not consider the entropy curve after the Page time to be observationally meaningful as the radiation would not reach \mathcal{I}^+ . More accurately, it is most likely not even appropriate to speak of \mathcal{I}^+ after u_{Page} anymore due to the occurrence of a singularity. Hence, the meta-observer will not recover information. We still find the comments above on the role of the meta-observer valuable in the larger context of different observers in de Sitter spacetimes and the use of the island formula.

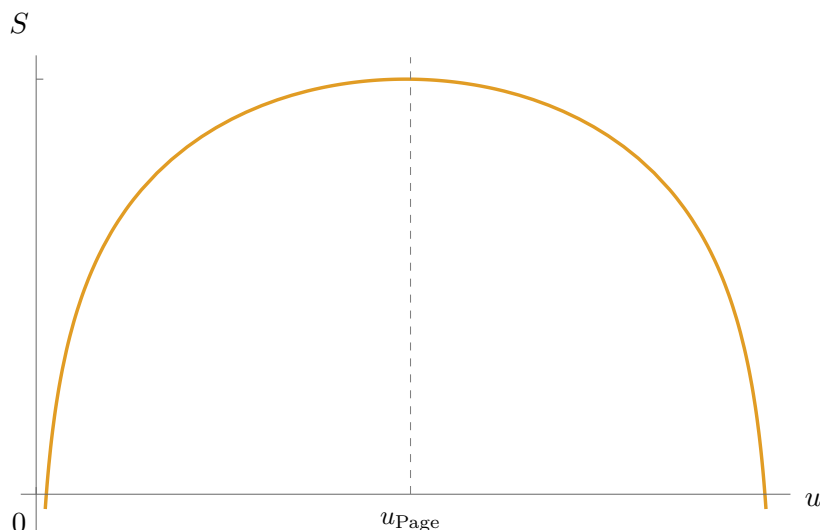


Figure 5. The radiation entropy collected at \mathcal{I}^+ . For this plot, we took the cut-off $\epsilon = 2\ell e^{-2GS_{\text{dS}}}$, and $\ell = G = 1$, which fixes $c = \frac{3}{2}$. The qualitative behaviour is the same for any c ; this just determines the range of u .

5.2 Entropy computed inside the static patch

Next, we will consider an observer at $r = 0$ collecting radiation coming from the past cosmological horizon; this corresponds indeed to the Unruh state, and evokes a dynamical backreacted dilaton (4.4). As explained in section 4, the two-dimensional gravitational system coupled to conformal matter on the reduced metric (2.15) can be described by a single degree of freedom close to the past cosmological horizon: the renormalised dilaton $\Phi_r(\sigma^+) = 2\pi\alpha(\sigma^+)$, where $\alpha(\sigma^+)$ is given in (4.5). In the three-dimensional geometry (2.3), this describes transparency in the auxiliary φ -direction. Thus, we will consider the entanglement entropy of a subsystem with interval $\Delta\varphi$ in thermal equilibrium before using (4.6) to imbue the time-dependence as seen by a static observer.

Recall that the collection of radiation happens at $r = 0$, i.e., in a thermal state, but we will take a stretched horizon point of view in which we use the ‘dual’ degree of freedom at the past horizon, which is a gravitationally weakly-coupled region. Within the three-dimensional auxiliary system there is only separation in the φ -direction between the subsystems, and the induced metric at the past horizon is flat. Thus we may use the standard thermal CFT result [56]:

$$S = \frac{c}{3} \log \sinh \frac{\pi}{\beta_{\text{dS}}} \ell \Delta\varphi + \frac{c}{3} \log \frac{r}{\ell}, \tag{5.8}$$

where $\Delta\varphi$ is a general angle separation and β_{dS} is the inverse of the dS intrinsic constant temperature given in (2.4). Note that $\beta_{\text{dS}} = 2\pi\ell$ such that the expression above actually simplifies; here we left β_{dS} to indicate thermal behaviour. The entropy (5.8) may be most conveniently derived by a holographic approach. As such the second term of (5.8) is the UV cut-off defined in the usual holographic manner ($r \rightarrow \frac{\ell^2}{\epsilon}$ with $\epsilon \rightarrow 0$).

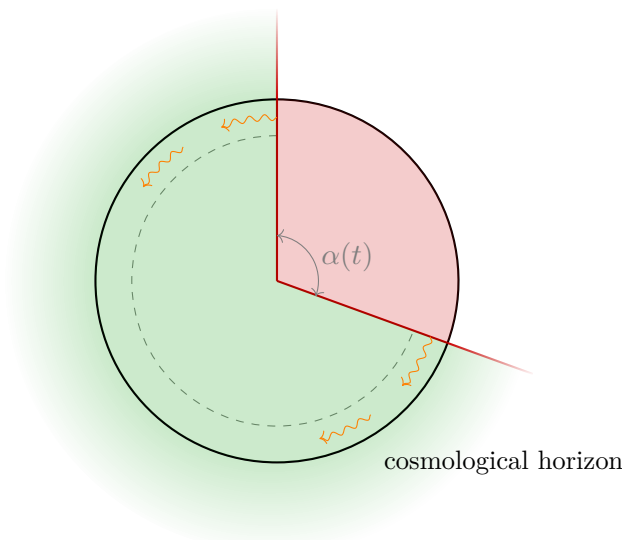


Figure 6. A timeslice of the three-dimensional static patch in our partial reduction approach. In the dual description, radiation moves along the stretched horizon. This has the effect of shifting the dividing line between bath and JT gravity. The entanglement between these two systems is a function of the angle φ (parametrised by α), which dynamically decreases during the evaporation process. We also indicated the part of the 3D geometry that has been reduced over, to clarify the entanglement structure.

Returning to the two-dimensional perspective, the angular interval of the bath is $\Delta\varphi = 2\pi(1 - \alpha)$, and the Unruh state gives a dynamical α . For the observer at the pole, we will use (4.6), such that the entropy (5.8) gives (using $\frac{c}{3} = \frac{1}{2G^{(2)}}$)

$$\begin{aligned}
 S_{\text{rad}} &= \frac{1}{2G} \log \sinh \frac{\pi}{\beta_{\text{dS}}} \frac{cG}{6} t + \frac{1}{2G} \log \frac{\ell}{\epsilon} \\
 &= \frac{1}{2G} \log \sinh \left(\frac{cG}{12\ell} t \right) + \frac{1}{2G} \log \frac{\ell}{\epsilon}.
 \end{aligned}
 \tag{5.9}$$

The expression (5.9) holds before the Page time. Comparing the expression in the second line of (5.9) to (5.7) clearly shows the thermal behaviour of the static patch compared to the non-thermal behaviour at future infinity. We can also see that at later times (before the Page time) the expression (5.9) exhibits linear behaviour in t .

While any considerations after the Page time are from a strictly observational perspective irrelevant just as for the meta-observer, they are still useful for our understanding. As stated previously, we are essentially working on a flat submanifold, with a non-gravitational system coupled to (4.6), such that we can use holographic arguments for the calculation of this specific entropy. The arguments of [31, 57] should also apply for this case; we briefly outline them here. In the large N limit, the entanglement entropy for a two-dimensional CFT at finite temperature can be evaluated using the RT formula in a BTZ geometry. In such a geometry, in general two potential minimal surfaces may be considered candidates for the RT surface as a function of the interval size, which in our language translates to a dependence on t . At early times a single connected component contributes, leading to the

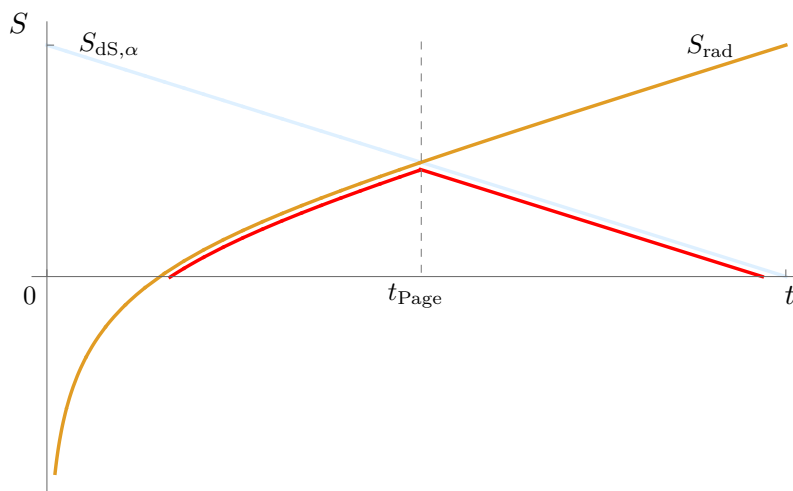


Figure 7. The decreasing de Sitter entropy (light blue) and the radiation entropy (orange) as collected inside the static patch. We took the cut-off ϵ such that the complement of the radiation entropy overlaps at early times with the decreasing de Sitter curve. To plot we set $\ell = G = 1$; then, $\epsilon = \sinh(\pi)\ell e^{-\pi}$. Note that the negative entropy values at early times are an effect of the finite cut-off and indicate that the computation should not be trusted before this timescale.

thermal expression (5.9). At late times (i.e., after the Page time) a phase transition occurs and there are in principle two disconnected contributions, one of which is disregarded by the demand of purity as in [31]. Thus, after the Page time we are still working with (5.8) but with the complementary interval

$$\Delta\varphi = 2\pi\alpha(t). \tag{5.10}$$

This leads to a unitary Page curve, plotted in figure 7: the static patch observer too would in principle see a pure state. For the static patch observer, this conclusion however requires formula (1.1) just as in [39]. Again, in practice catastrophic backreaction forbids information recovery and we should consider the curve to end at the Page time.

5.3 Backreaction considerations: formation of a trapped region

In section 3.2 we determined the time of destabilisation for the Unruh-de Sitter state to be set by the Page time (3.18). Here, we will explicitly show what is happening in the bulk, following the logic of [39]. For this we require the bulk dilaton solution (4.2). At the Page time, which corresponds to setting $\alpha = \frac{1}{2}$ in (4.2), we discover the existence of a trapped region. In this two-dimensional setting the expansion scalars translate to $\partial_{\pm}\Phi$; trapped regions are therefore defined as $\partial_{\pm}\Phi < 0$, which translates to

$$\begin{aligned} x^+ \left(cG((x^+x^-)^2 - \ell^4) + 2x^+x^-\ell^2 \left(6\pi - cG \log \frac{x^+}{\ell} \right) \right) &< 0, \\ x^+ \left(6\pi - cG \log \frac{x^+}{\ell} \right) &< 0, \end{aligned} \tag{5.11}$$

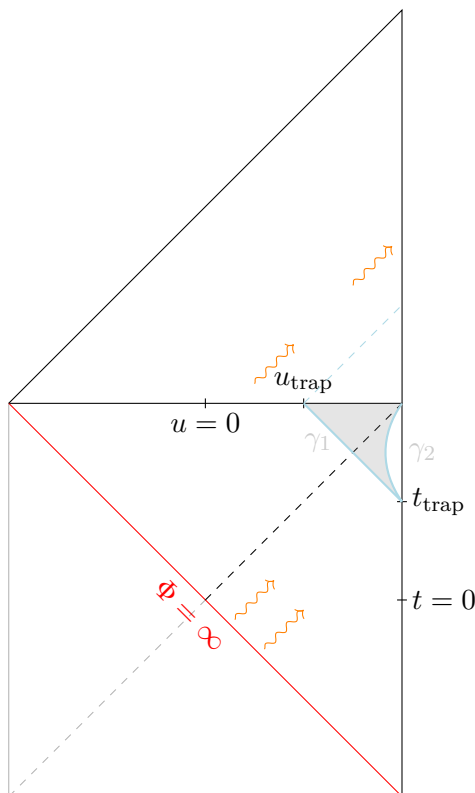


Figure 8. The lower half of the Penrose diagram is de Sitter space; indicated in red is the past singularity. The upper triangle is Minkowski space, which we drew to indicate the effect of the trapped region (shaded in gray) on what the meta-observer can see. The observer inside the static patch can collect radiation up to the Page time $t_{\text{Page}} = t_{\text{trap}}$, at which time the trapped region forms. Similarly, the meta-observer can see radiation from before u_{trapped} only.

respectively. These inequalities determine two curves bounding the trapped region. These curves are given by

$$\begin{aligned} \gamma_1 : \quad x^+ &= \ell \exp\left(\frac{6\pi}{cG}\right), \\ \gamma_2 : \quad x^- &= \frac{\ell^2}{cGx^+} \left(cG \log \frac{x^+}{\ell} - 6\pi - \sqrt{\left(6\pi - cG \log \frac{x^+}{\ell}\right)^2 + (cG)^2} \right). \end{aligned} \quad (5.12)$$

Equality $\partial_+ \Phi = 0 = \partial_- \Phi$ is obtained at the pole, $(x^+, x^-) = (x_{\gamma_1}^+, -\ell^2/x_{\gamma_1}^+)$. For a static observer at this pole, the trapped region occurs at the time

$$t > t_{\text{trapped}} = \frac{6\pi\ell}{cG} = t_{\text{Page}}, \quad (5.13)$$

with the analogous statement for the meta-observer in terms of u ; see figure 8. As can be seen explicitly in figure 8, the trapped region prevents the radiation from reaching the static patch observer for times $t > t_{\text{trapped}}$. Moreover, the same is true for the meta-observer at future infinity, who does not have access to radiation for $u > u_{\text{trapped}}$. However, the

Penrose-Hawking singularity theorem [58, 59] does not immediately apply to the trapped region described here, as the NEC is violated. It can be shown by use of the quantum singularity theorem [60] that for $u > u_{\text{trapped}}$ a (quantum) singularity forms at future infinity [39].

6 Discussion

In this section we will summarise our findings on a more conceptual level and elaborate on open questions. We conclude by commenting on inflationary scenarios in this setup.

In this paper, we considered a three-dimensional de Sitter geometry in a setup which naturally supplies a segmentation into dynamical gravity on dS_2 and an auxiliary system located in the direction of the partial reduction. Since we are interested in modelling an evaporation process, we added conformal matter to our theory. Putting dynamical gravity in an out-of-equilibrium quantum state then indeed furnishes a decreasing Gibbons-Hawking entropy due to backreaction effects. By analysing the behaviour of the backreacted dilaton solution, we discover two decoupling regions in which field theory descriptions arise. As should be expected, one of these regions is \mathcal{I}^+ , in line with [55]. Perhaps more surprisingly, the second region is inside the static patch at the past cosmological horizon, which we interpret in the holographic ‘stretched horizon’ picture of [53, 54]. In both regions we can thus calculate the fine-grained entropy of the collected radiation via field theory considerations.

6.1 Quantum mechanics and the island

Let us elaborate on this setup in the language of [61].⁶ We will use the region at \mathcal{I}^+ to be explicit, but analogous statements hold for the static patch. The gravitational dynamics of the two-dimensional de Sitter space (A.18) with coordinates (τ, χ) reduce to that of a quantum mechanical boundary degree of freedom. Since the dilaton can be given a three-dimensional interpretation as an angle, this can be interpreted as transparency along a third direction φ , such that we are coupling the single quantum mechanical boundary degree of freedom to a matter CFT. We can now consider an imaginary interface in this non-gravitational theory, which factorises the Hilbert space into two subsystems: the quantum mechanical boundary degree of freedom coupled to a part of the bath, and the remainder of the bath. It is the entanglement entropy between these two systems that we are calculating.

For the calculation at future infinity we recover a naturally pure evaporating process. The static observer, more akin to an asymptotic AdS observer, requires a more involved argument to furnish a unitary process. Our results for the static observer are in line with [39], in which a stretched horizon picture was advocated for this observer with the gravitational physics reducing to field theory considerations at the horizon. This is supported by our results. We can however even make a more general statement: at the past cosmological horizon we see a timelike realisation of the backreaction dynamics determined at \mathcal{I}^+ . A natural question to ask is how far this connection can be pushed. Although we believe these

⁶See section 5.4 of [61].

comments are important for our understanding of various observers in de Sitter space, for this quantum state, the main takeaway should still be that for both observers we finally arrive at a tragedy as neither can recover any information.

It is interesting to connect our construction to the more canonical island approach. For the BTZ construction of [31] it seems the island can be identified with the region bounded by the RT surface of the thermal bath within the gravitating region, which lies outside of the horizon. While our approach naturally introduces a thermal bath, it is not immediately clear how to pinpoint the location of the island for the de Sitter case, as was done in [39]. It would be interesting to explore this further. To do so, it is also important to connect our results to [37], in which three necessary criteria were constructed for the existence of an island. These implied that for pure de Sitter spacetimes there are no islands for an entangling region located at future infinity. To put our results into this context — and see how these conditions are evaded —, notice the following. First, we are considering a different quantum state: not the Hartle-Hawking/Bunch-Davies state but the Unruh-de Sitter state. Secondly, we find that the use of (1.1) is only required for the static observer, whereas the no-go conjecture of [37] considers a region at future infinity.

6.2 Information recovery

For evaporating black holes, small amounts of information thrown in after the Page time can be recovered from the Hawking radiation after waiting the so-called scrambling time $t \approx \frac{\beta}{2\pi} \log S_{\text{BH}}$ [62–64]. Does a similar story hold for the evaporating de Sitter horizon? Due to the occurrence of catastrophic backreaction at the Page time within our construction, this seems not to be the case. In [65, 66] a setup was presented in which recovery of information expelled through the cosmological horizon was analysed in the Bunch-Davies state using shock waves; and in [66] a concrete protocol was proposed for information transfer to the antipodal observer. The relevant timescale here, too, is the scrambling time. As at early times the Unruh-de Sitter state should be almost indistinguishable from the Bunch-Davies state, it might be expected that some form of information retrieval might be possible for (additional) information expelled through the cosmological horizon. It would be interesting to see if this expectation is indeed true and at which timescale this breaks down due to the deviation of the two quantum states.

6.3 Inflationary perspective

Finally, let us comment on inflationary physics. To do so, we use planar coordinates (2.20), and consider a scenario as explained in e.g. [67]. To the future of our de Sitter construction we glue flat space, corresponding to the old Universe in which gravitational effects can be neglected. This is also depicted in figure 8. Future infinity constitutes the reheating surface, the transitory region between the inflating and the old Universe. This would give a simple model for analysing primordial fluctuations. Let us not consider the full setup but only make some tentative comments up to \mathcal{I}^+ . The evaporating quantum state of (3.10) expressed in terms of (2.20) also leads to a net flux at future infinity. However, as the coordinates (2.20) are ground state solutions of the Schwarzian theory, the conserved ADM quantity (2.27) vanishes on-shell. Contrast this with both the Milne coordinates (2.18) and

the global coordinates (2.12) for which the ADM quantity (2.27) is related to the entropy of the cosmological horizon, such that the quantum state indeed captures the evaporating horizon. As already noted in [40], in the coordinates (2.20) the stress tensor components are well-defined within the entire planar patch. Hence, for these coordinates the Unruh state is a natural alternative to the Bunch-Davies state. It would be interesting to pursue this direction further. It would also be interesting to connect (2.29) with the results of [68] and to understand if a first law may be constructed, linking a variation of the conserved quantity K to a variation in the entropy $S_{\text{dS},\alpha}$.

In general, as inflation is a UV dependent problem, the island formula (1.1) may play a pivotal role in understanding inflationary scenarios via fine-grained entropy considerations. As such it is important to understand in what way non-perturbative effects of the replica wormhole type are realised in inflationary models and how this changes semi-classical expectations. A fruitful avenue could be to consider potential entropy paradoxes for various subregions of the gravitationally prepared state depicted in figure 8, as in [67]. In addition, for these inflationary setups it would be important to understand in how far higher-dimensional setups can evade the constraints of [37].

Acknowledgments

It is a pleasure to thank Jan Pieter van der Schaar for useful discussions and comments on a draft. JKK would furthermore like to thank Alexandros Kanargias and Stefan Förste for helpful discussions. Work of EPV and EV is supported by the Spinoza grant and the Delta ITP consortium, a program of the NWO that is funded by the Dutch Ministry of Education, Culture and Science (OCW). Work of JKK was supported in part by the Heising-Simons Foundation, the Simons Foundation, and National Science Foundation Grant No. NSF PHY-1748958. JKK also gratefully acknowledges support by the Graduate School of Physics and Astronomy (BCGS). JKK, EV and EPV would like to thank the Institute d'Études Scientifiques de Cargèse, where part of this work was conducted, for hospitality, and the attendees of the 2021 summer school 'Old and New Frontiers in Quantum Field Theory' for a stimulating atmosphere. JKK finally would like to thank the University of Amsterdam for hospitality during the completion of this work.

A Coordinate systems

In this appendix, we will for the sake of completeness give various two-dimensional coordinate systems for de Sitter space and the associated dilaton solutions. Note that the solutions we quote originate from dimensional reduction and not from an intrinsically two-dimensional setup. Concretely, this means that the dilaton solutions might differ from previous work on JT gravity in purely two-dimensional de Sitter.

Global coordinates. In global coordinates (T, θ) the metric and dilaton are

$$ds^2 = -dT^2 + \ell^2 \cosh^2 \frac{T}{\ell} d\theta^2, \quad \Phi = 2\pi\alpha \sin \theta \cosh \frac{T}{\ell}. \quad (\text{A.1})$$

Here, $\theta \in [0, \pi]$ and $T \in (-\infty, \infty)$. These coordinates are called global coordinates as they can be used to describe all of de Sitter space.

Global conformal coordinates. In global conformal coordinates (σ, θ) the metric and dilaton are given as

$$ds^2 = \frac{\ell^2}{\cos^2 \sigma} \left(-d\sigma^2 + d\theta^2 \right), \quad \Phi = 2\pi\alpha \frac{\sin \theta}{\cos \sigma}, \quad (\text{A.2})$$

where $\sigma \in (-\frac{\pi}{2}, \frac{\pi}{2})$. These coordinates cover the full Penrose diagram of de Sitter, figure 2. The transformation to go from global coordinates to global conformal coordinates is given by

$$\tan \frac{\sigma}{2} = \tanh \frac{T}{2\ell}. \quad (\text{A.3})$$

In terms of the Schwarzian equations of motion (2.26), (A.2) corresponds to

$$x(u) = 2\ell \tan \frac{u}{2\ell}. \quad (\text{A.4})$$

Planar coordinates. In the flat slicing the metric and dilaton are given by

$$ds^2 = -dt^2 + e^{2t/\ell} d\rho^2, \quad \Phi = 2\pi\alpha \frac{\rho}{\ell} e^{t/\ell}, \quad (\text{A.5})$$

where $\rho \geq 0$ and $t \in (-\infty, \infty)$. These coordinates cover half of the de Sitter Penrose diagram (static patch + future patch). The transformation between planar and global coordinates is given by

$$\begin{aligned} \rho &= \frac{\ell \cosh \frac{T}{\ell} \sin \theta}{\sinh \frac{T}{\ell} + \cos \theta \cosh \frac{T}{\ell}}, \\ e^{t/\ell} &= \sinh \frac{T}{\ell} + \cos \theta \cosh \frac{T}{\ell}. \end{aligned} \quad (\text{A.6})$$

Planar conformal coordinates. From the previous coordinate system, we can go to conformal time η via

$$\eta = -\ell e^{-t/\ell}, \quad (\text{A.7})$$

where $\eta \leq 0$ with equality at \mathcal{I}^+ . Then the metric and dilaton are given by

$$ds^2 = \frac{\ell^2}{\eta^2} \left(-d\eta^2 + dx^2 \right), \quad \Phi = -2\pi\alpha \frac{x}{\eta}, \quad (\text{A.8})$$

where we set $x = \rho$. These coordinates cover the same planar patch as the previous ones.

Note that we can combine the coordinate transformations (A.6), (A.3) and (A.7) to find a direct relation between planar conformal coordinates (η, x) and global conformal coordinates (σ, θ) :

$$\begin{aligned} \eta &= -\frac{\ell \cos \sigma}{\cos \theta + \sin \sigma}, \\ x &= \frac{\ell \sin \theta}{\cos \theta + \sin \sigma}. \end{aligned} \quad (\text{A.9})$$

Kruskal coordinates. We can extend the planar coordinates to cover the entire Penrose diagram by defining Kruskal coordinates as follows:

$$x^+ = \eta + x, \quad x^- = -\frac{\ell^2}{\eta - x}. \quad (\text{A.10})$$

Then the metric and dilaton are given by

$$ds^2 = -\frac{4\ell^4}{(\ell^2 - x^+x^-)^2} dx^+ dx^-, \quad \Phi = 2\pi\alpha \left(\frac{\ell^2 + x^+x^-}{\ell^2 - x^+x^-} \right). \quad (\text{A.11})$$

Static patch coordinates. The static patch coordinates are defined with respect to the Kruskal coordinates as

$$x^+ = \ell e^{t/\ell} \sqrt{\frac{\ell - r}{\ell + r}}, \quad x^- = -\ell e^{-t/\ell} \sqrt{\frac{\ell - r}{\ell + r}}. \quad (\text{A.12})$$

In terms of these coordinates, the metric and dilaton are

$$ds^2 = -\left(1 - \frac{r^2}{\ell^2}\right) dt^2 + \left(1 - \frac{r^2}{\ell^2}\right)^{-1} dr^2, \quad \Phi = 2\pi\alpha \frac{r}{\ell}. \quad (\text{A.13})$$

These coordinates only cover the static patch for an observer located at the south pole $r = 0$; their cosmological horizon is located at $r = \ell$.

We can also define the Kruskal coordinates via

$$x^\pm = \pm \ell e^{\pm \sigma^\pm / \ell}, \quad (\text{A.14})$$

where we introduced null coordinates

$$\sigma^\pm = t \pm r^*. \quad (\text{A.15})$$

Here, r^* is a tortoise coordinate

$$r^* = \int_0^r \frac{1}{f(r')} dr' = \ell \operatorname{arctanh} \left(\frac{r}{\ell} \right), \quad (\text{A.16})$$

which only holds for $r < \ell$ and hence only covers the static patch. Note that the south pole ($r = 0$) is at $r^* = 0$ and the cosmological horizon ($r = \ell$) at $r^* = \infty$. In terms of the null coordinates σ^\pm we recover the metric (2.15). Note that (A.14) is equivalent to the coordinate change between Rindler and Minkowski.

Milne coordinates. Finally, from the static patch coordinates we can analytically continue across the future horizon to describe the future or Milne patch:⁷

$$\tau = i\ell \arccos \frac{r}{\ell}, \quad \chi = t, \quad (\text{A.17})$$

which gives

$$ds^2 = -d\tau^2 + \sinh^2 \frac{\tau}{\ell} d\chi^2, \quad \Phi = 2\pi\alpha \cosh \frac{\tau}{\ell}. \quad (\text{A.18})$$

Unlike the static patch solution, the Milne solution does not exhibit time translation symmetry. However, they are essentially the same solutions connected by analytic continuation; in the two patches, the isometries are actualised in a different manner.

⁷Note that this continuation differs slightly from the one presented in [33]. We believe the one given here is correct.

Open Access. This article is distributed under the terms of the Creative Commons Attribution License ([CC-BY 4.0](https://creativecommons.org/licenses/by/4.0/)), which permits any use, distribution and reproduction in any medium, provided the original author(s) and source are credited.

References

- [1] G.W. Gibbons and S.W. Hawking, *Cosmological Event Horizons, Thermodynamics, and Particle Creation*, *Phys. Rev. D* **15** (1977) 2738 [[INSPIRE](#)].
- [2] E. Witten, *Quantum gravity in de Sitter space*, in *Strings 2001: International Conference*, Mumbai India (2001) [[hep-th/0106109](#)] [[INSPIRE](#)].
- [3] N. Goheer, M. Kleban and L. Susskind, *The Trouble with de Sitter space*, *JHEP* **07** (2003) 056 [[hep-th/0212209](#)] [[INSPIRE](#)].
- [4] M.K. Parikh and E.P. Verlinde, *de Sitter holography with a finite number of states*, *JHEP* **01** (2005) 054 [[hep-th/0410227](#)] [[INSPIRE](#)].
- [5] M.K. Parikh, I. Savonije and E.P. Verlinde, *Elliptic de Sitter space: $dS/Z(2)$* , *Phys. Rev. D* **67** (2003) 064005 [[hep-th/0209120](#)] [[INSPIRE](#)].
- [6] D. Anninos, F. Denef, R. Monten and Z. Sun, *Higher Spin de Sitter Hilbert Space*, *JHEP* **10** (2019) 071 [[arXiv:1711.10037](#)] [[INSPIRE](#)].
- [7] X. Dong, E. Silverstein and G. Torroba, *de Sitter Holography and Entanglement Entropy*, *JHEP* **07** (2018) 050 [[arXiv:1804.08623](#)] [[INSPIRE](#)].
- [8] H. Geng, S. Grieninger and A. Karch, *Entropy, Entanglement and Swampland Bounds in DS/dS* , *JHEP* **06** (2019) 105 [[arXiv:1904.02170](#)] [[INSPIRE](#)].
- [9] S. Ryu and T. Takayanagi, *Holographic derivation of entanglement entropy from AdS/CFT*, *Phys. Rev. Lett.* **96** (2006) 181602 [[hep-th/0603001](#)] [[INSPIRE](#)].
- [10] V.E. Hubeny, M. Rangamani and T. Takayanagi, *A Covariant holographic entanglement entropy proposal*, *JHEP* **07** (2007) 062 [[arXiv:0705.0016](#)] [[INSPIRE](#)].
- [11] N. Engelhardt and A.C. Wall, *Quantum Extremal Surfaces: Holographic Entanglement Entropy beyond the Classical Regime*, *JHEP* **01** (2015) 073 [[arXiv:1408.3203](#)] [[INSPIRE](#)].
- [12] T. Faulkner, A. Lewkowycz and J. Maldacena, *Quantum corrections to holographic entanglement entropy*, *JHEP* **11** (2013) 074 [[arXiv:1307.2892](#)] [[INSPIRE](#)].
- [13] T. Barrella, X. Dong, S.A. Hartnoll and V.L. Martin, *Holographic entanglement beyond classical gravity*, *JHEP* **09** (2013) 109 [[arXiv:1306.4682](#)] [[INSPIRE](#)].
- [14] G. Penington, *Entanglement Wedge Reconstruction and the Information Paradox*, *JHEP* **09** (2020) 002 [[arXiv:1905.08255](#)] [[INSPIRE](#)].
- [15] A. Almheiri, N. Engelhardt, D. Marolf and H. Maxfield, *The entropy of bulk quantum fields and the entanglement wedge of an evaporating black hole*, *JHEP* **12** (2019) 063 [[arXiv:1905.08762](#)] [[INSPIRE](#)].
- [16] A. Almheiri, R. Mahajan, J. Maldacena and Y. Zhao, *The Page curve of Hawking radiation from semiclassical geometry*, *JHEP* **03** (2020) 149 [[arXiv:1908.10996](#)] [[INSPIRE](#)].
- [17] D.N. Page, *Information in black hole radiation*, *Phys. Rev. Lett.* **71** (1993) 3743 [[hep-th/9306083](#)] [[INSPIRE](#)].

- [18] D.N. Page, *Time Dependence of Hawking Radiation Entropy*, *JCAP* **09** (2013) 028 [[arXiv:1301.4995](#)] [[INSPIRE](#)].
- [19] H. Geng et al., *Information Transfer with a Gravitating Bath*, *SciPost Phys.* **10** (2021) 103 [[arXiv:2012.04671](#)] [[INSPIRE](#)].
- [20] A. Laddha, S.G. Prabhu, S. Raju and P. Shrivastava, *The Holographic Nature of Null Infinity*, *SciPost Phys.* **10** (2021) 041 [[arXiv:2002.02448](#)] [[INSPIRE](#)].
- [21] A. Almheiri, R. Mahajan and J. Maldacena, *Islands outside the horizon*, [arXiv:1910.11077](#) [[INSPIRE](#)].
- [22] T.J. Hollowood and S.P. Kumar, *Islands and Page Curves for Evaporating Black Holes in JT Gravity*, *JHEP* **08** (2020) 094 [[arXiv:2004.14944](#)] [[INSPIRE](#)].
- [23] H.Z. Chen, Z. Fisher, J. Hernandez, R.C. Myers and S.-M. Ruan, *Evaporating Black Holes Coupled to a Thermal Bath*, *JHEP* **01** (2021) 065 [[arXiv:2007.11658](#)] [[INSPIRE](#)].
- [24] A. Almheiri, R. Mahajan and J.E. Santos, *Entanglement islands in higher dimensions*, *SciPost Phys.* **9** (2020) 001 [[arXiv:1911.09666](#)] [[INSPIRE](#)].
- [25] F.F. Gautason, L. Schneiderbauer, W. Sybesma and L. Thorlacius, *Page Curve for an Evaporating Black Hole*, *JHEP* **05** (2020) 091 [[arXiv:2004.00598](#)] [[INSPIRE](#)].
- [26] T. Anegawa and N. Iizuka, *Notes on islands in asymptotically flat 2d dilaton black holes*, *JHEP* **07** (2020) 036 [[arXiv:2004.01601](#)] [[INSPIRE](#)].
- [27] K. Hashimoto, N. Iizuka and Y. Matsuo, *Islands in Schwarzschild black holes*, *JHEP* **06** (2020) 085 [[arXiv:2004.05863](#)] [[INSPIRE](#)].
- [28] T. Hartman, E. Shaghoulian and A. Strominger, *Islands in Asymptotically Flat 2D Gravity*, *JHEP* **07** (2020) 022 [[arXiv:2004.13857](#)] [[INSPIRE](#)].
- [29] H. Geng and A. Karch, *Massive islands*, *JHEP* **09** (2020) 121 [[arXiv:2006.02438](#)] [[INSPIRE](#)].
- [30] M. Alishahiha, A. Faraji Astaneh and A. Naseh, *Island in the presence of higher derivative terms*, *JHEP* **02** (2021) 035 [[arXiv:2005.08715](#)] [[INSPIRE](#)].
- [31] E. Verheijden and E. Verlinde, *From the BTZ black hole to JT gravity: geometrizing the island*, *JHEP* **11** (2021) 092 [[arXiv:2102.00922](#)] [[INSPIRE](#)].
- [32] J. Cotler, K. Jensen and A. Maloney, *Low-dimensional de Sitter quantum gravity*, *JHEP* **06** (2020) 048 [[arXiv:1905.03780](#)] [[INSPIRE](#)].
- [33] J. Maldacena, G.J. Turiaci and Z. Yang, *Two dimensional Nearly de Sitter gravity*, *JHEP* **01** (2021) 139 [[arXiv:1904.01911](#)] [[INSPIRE](#)].
- [34] A. Blommaert, *Searching for butterflies in dS JT gravity*, [arXiv:2010.14539](#) [[INSPIRE](#)].
- [35] W. Sybesma, *Pure de Sitter space and the island moving back in time*, *Class. Quant. Grav.* **38** (2021) 145012 [[arXiv:2008.07994](#)] [[INSPIRE](#)].
- [36] V. Balasubramanian, A. Kar and T. Ugajin, *Islands in de Sitter space*, *JHEP* **02** (2021) 072 [[arXiv:2008.05275](#)] [[INSPIRE](#)].
- [37] T. Hartman, Y. Jiang and E. Shaghoulian, *Islands in cosmology*, *JHEP* **11** (2020) 111 [[arXiv:2008.01022](#)] [[INSPIRE](#)].
- [38] H. Geng, Y. Nomura and H.-Y. Sun, *Information paradox and its resolution in de Sitter holography*, *Phys. Rev. D* **103** (2021) 126004 [[arXiv:2103.07477](#)] [[INSPIRE](#)].

- [39] L. Aalsma and W. Sybesma, *The Price of Curiosity: Information Recovery in de Sitter Space*, *JHEP* **05** (2021) 291 [[arXiv:2104.00006](#)] [[INSPIRE](#)].
- [40] L. Aalsma, M. Parikh and J.P. Van Der Schaar, *Back(reaction) to the Future in the Unruh-de Sitter State*, *JHEP* **11** (2019) 136 [[arXiv:1905.02714](#)] [[INSPIRE](#)].
- [41] J.B. Hartle and S.W. Hawking, *Wave Function of the Universe*, *Phys. Rev. D* **28** (1983) 2960 [[INSPIRE](#)].
- [42] U.H. Danielsson, *Inflation, holography, and the choice of vacuum in de Sitter space*, *JHEP* **07** (2002) 040 [[hep-th/0205227](#)] [[INSPIRE](#)].
- [43] A. Almheiri and J. Polchinski, *Models of AdS_2 backreaction and holography*, *JHEP* **11** (2015) 014 [[arXiv:1402.6334](#)] [[INSPIRE](#)].
- [44] J. Maldacena, D. Stanford and Z. Yang, *Conformal symmetry and its breaking in two dimensional Nearly Anti-de-Sitter space*, *PTEP* **2016** (2016) 12C104 [[arXiv:1606.01857](#)] [[INSPIRE](#)].
- [45] J. Engelsöy, T.G. Mertens and H. Verlinde, *An investigation of AdS_2 backreaction and holography*, *JHEP* **07** (2016) 139 [[arXiv:1606.03438](#)] [[INSPIRE](#)].
- [46] S.M. Christensen and S.A. Fulling, *Trace Anomalies and the Hawking Effect*, *Phys. Rev. D* **15** (1977) 2088 [[INSPIRE](#)].
- [47] D. Lohiya, *Trace anomalies in a two-dimensional de sitter metric and black-body radiation*, *J. Phys. A* **11** (1978) 1335.
- [48] S.W. Hawking, *Gravitational radiation from colliding black holes*, *Phys. Rev. Lett.* **26** (1971) 1344 [[INSPIRE](#)].
- [49] R. Bousso and N. Engelhardt, *New Area Law in General Relativity*, *Phys. Rev. Lett.* **115** (2015) 081301 [[arXiv:1504.07627](#)] [[INSPIRE](#)].
- [50] J.M. Maldacena, *Eternal black holes in anti-de Sitter*, *JHEP* **04** (2003) 021 [[hep-th/0106112](#)] [[INSPIRE](#)].
- [51] M.K. Parikh and E.P. Verlinde, *de Sitter holography with a finite number of states*, *JHEP* **01** (2005) 054 [[hep-th/0410227](#)] [[INSPIRE](#)].
- [52] S. Raju, *Failure of the split property in gravity and the information paradox*, [arXiv:2110.05470](#) [[INSPIRE](#)].
- [53] L. Susskind, *de Sitter Holography: Fluctuations, Anomalous Symmetry, and Wormholes*, *Universe* **7** (2021) 464 [[arXiv:2106.03964](#)] [[INSPIRE](#)].
- [54] L. Susskind, L. Thorlacius and J. Uglum, *The Stretched horizon and black hole complementarity*, *Phys. Rev. D* **48** (1993) 3743 [[hep-th/9306069](#)] [[INSPIRE](#)].
- [55] A. Strominger, *The dS/CFT correspondence*, *JHEP* **10** (2001) 034 [[hep-th/0106113](#)] [[INSPIRE](#)].
- [56] P. Calabrese and J.L. Cardy, *Entanglement entropy and quantum field theory*, *J. Stat. Mech.* **0406** (2004) P06002 [[hep-th/0405152](#)] [[INSPIRE](#)].
- [57] N. Bao and H. Ooguri, *Distinguishability of black hole microstates*, *Phys. Rev. D* **96** (2017) 066017 [[arXiv:1705.07943](#)] [[INSPIRE](#)].
- [58] R. Penrose, *Gravitational collapse and space-time singularities*, *Phys. Rev. Lett.* **14** (1965) 57 [[INSPIRE](#)].

- [59] S.W. Hawking and G.F.R. Ellis, *The Large Scale Structure of Space-Time*, *Cambridge Monographs on Mathematical Physics*, Cambridge University Press, Cambridge U.K. (2011) [[INSPIRE](#)].
- [60] A.C. Wall, *The Generalized Second Law implies a Quantum Singularity Theorem*, *Class. Quant. Grav.* **30** (2013) 165003 [*Erratum ibid.* **30** (2013) 199501] [[arXiv:1010.5513](#)] [[INSPIRE](#)].
- [61] S. Raju, *Lessons from the information paradox*, *Phys. Rept.* **943** (2022) 2187 [[arXiv:2012.05770](#)] [[INSPIRE](#)].
- [62] P. Hayden and J. Preskill, *Black holes as mirrors: Quantum information in random subsystems*, *JHEP* **09** (2007) 120 [[arXiv:0708.4025](#)] [[INSPIRE](#)].
- [63] Y. Sekino and L. Susskind, *Fast Scramblers*, *JHEP* **10** (2008) 065 [[arXiv:0808.2096](#)] [[INSPIRE](#)].
- [64] S.H. Shenker and D. Stanford, *Black holes and the butterfly effect*, *JHEP* **03** (2014) 067 [[arXiv:1306.0622](#)] [[INSPIRE](#)].
- [65] E. Verheijden, *Traversable wormholes, shock waves, and de Sitter space*, MSc Thesis, University of Amsterdam, Amsterdam The Netherlands (2018).
- [66] L. Aalsma, A. Cole, E. Morvan, J.P. van der Schaar and G. Shiu, *Shocks and information exchange in de Sitter space*, *JHEP* **10** (2021) 104 [[arXiv:2105.12737](#)] [[INSPIRE](#)].
- [67] Y. Chen, V. Gorbenko and J. Maldacena, *Bra-ket wormholes in gravitationally prepared states*, *JHEP* **02** (2021) 009 [[arXiv:2007.16091](#)] [[INSPIRE](#)].
- [68] V. Balasubramanian, J. de Boer and D. Minic, *Mass, entropy and holography in asymptotically de Sitter spaces*, *Phys. Rev. D* **65** (2002) 123508 [[hep-th/0110108](#)] [[INSPIRE](#)].

Conclusion

8.1 Summary and Outlook

In this thesis we have studied different aspects of holographic approaches to quantum gravity. All but one publication relied on a specific two-dimensional model of quantum gravity, JT gravity. To begin with, in chapter 2 we introduced and constructed $\mathcal{N} = (2, 2)$ JT axial supergravity on an Euclidean AdS_2 background. The extrinsic supercurvature reduces to the $\mathcal{N} = 2$ super-Schwarzian action, hinting at a duality with the low-energy sector of the $\mathcal{N} = 2$ SYK model. In the following chapter 3, the aforementioned results are put to use. In the setting of 1/4 BPS black holes in AdS_4 as solutions of $\mathcal{N} = 2$ supergravity, we considered an s -wave reduction with an additional matter hypermultiplet in the near-horizon limit. We calculate the holographic four-point function of this theory and compare it with the same quantity in $\mathcal{N} = (2, 2)$ JT supergravity in the presence of gauged matter via the super-Schwarzian. While both, chapters 2 and 3 deal with the JT theory defined on the hyperbolic disk, in chapter 4 we work with the duality between JT gravity on an arbitrary hyperbolic Riemann surface and a specific double-scaled matrix model. More concretely, we consider deformations of the JT theory via topological gravity. By use of the KdV equation we work out the spectral form factor and observe how the deformations affect this quantity. We conclude by commenting on a proposed duality between Lorentzian dS_2 and an analytic continuation of the aforementioned double-scaled matrix integral, which relies on the moduli space volumes of hyperbolic Riemann surfaces with defect to be mere analytic continuations of those with geodesic boundaries. In chapter 5 we move on to the study of complexity in a holographic context. We consider Lloyd's bound, which is a fundamental upper bound on the computation speed, in the context of charged black holes. We show that while complexity as a holographic quantity penetrates the outer horizon of a charged black hole, in order to be compatible with Lloyd's bound it may not penetrate the inner horizon. In chapter 6 we move on to a fully non-perturbative definition of holographic complexity in terms of JT gravity. We describe a new approach based on a modified replica trick, which not only gives the late time expected plateau but also furnishes a variance which saturates. Moreover, the inclusion of EOW branes is also worked out. In the final, chapter 7, we concern ourselves with a cosmological setup. We consider a low-dimensional setting in which we set boundary conditions which correspond to an evaporating cosmological horizon. Remarkably, for this state, the past cosmological horizon becomes a holographic screen which is decoupled from gravity. We argue that there is no information recovery of the Hawking radiation.

Let us now understand what the results of this thesis in combination with the state of the field imply on a broader, conceptual level. What have we learned and what questions can we therefore extract?

1.) We have emphasised that JT gravity as first defined in [80] and extensively used in this thesis, can be identified with a specific double-scaled matrix model. This theory of two-dimensional gravity therefore is a (random matrix) ensemble. As such, we have also noted that $Z(\beta_1, \beta_2) \neq Z(\beta_1) \times Z(\beta_2)$. This of course is not in line with standard AdS/CFT. For example, type IIB string theory on $AdS_5 \times S^5$ is (expected to be in all detail) equivalent to $\mathcal{N} = 4$ super Yang-Mills, which clearly is not an ensemble-averaged theory. The duality between string theory on $AdS_3 \times S^3 \times T^4$ and a deformed symmetric product orbifold CFT $\text{Sym}^N(T^4)$ is another notable example [140–143]. How do we realign this with what we have seen and used in this thesis? We have exclusively used “bottom-up” constructions. These approaches are in some sense quite natural as they use a sum over all possible bulk geometries. Moreover, wormhole geometries destroy the factorisation of the boundary partition function but engender the correct statistical behaviour. We may therefore conclude that this approach furnishes averaged signals but does not see the random underlying noise. Concretely, for the spectral form factor one should expect large fluctuations around the plateau for example. This tension can be amplified. In the supergravity approximation to string theory, we can see wormholes contribute to both $AdS_5 \times S^5$ and $AdS_3 \times S^3 \times T^4$ [144–146]. This implies that string theory must modify the “bottom-up” proposal. It is usually believed (see for example [147]) that JT gravity might constitute an approximation to a unique, UV-complete theory for which the factorisation of the partition function is restored. This means that one should view JT gravity and in higher dimensions the Einstein-Hilbert action as mere effective theories, which only have access to averaged observables. Furthermore, while JT in itself from a merely two-dimensional standpoint might give correct statistical generalities with respect to the two-point function or calculations of entropy, it is not a theory with a unique, underlying spectrum. Therefore, the unique spectrum would have to be furnished from some higher-dimensional construction, for example string theory. The vague scenario outlined in [147] and made more concrete in [148], is the following. Starting from some concrete brane scenario in higher dimensions, one could imagine some low energy limit in which branes are integrated out. This open string language could then be rephrased in closed string language in terms of a potential $U(\phi_1, \phi_2, \dots)$, which would now include non-local interactions. This potential could then supply a unique Hamiltonian, for which the factorisation problem would then be resolved. It would be highly interesting to see if such intuition can be made more precise when starting from a higher-dimensional stringy setting. This would match brane configurations natural to string theory to a factorising theory of two-dimensional quantum gravity.

2.) In AdS_3 there might be more hope to make these somewhat vague statements more concrete. In AdS_3 , one could consider two different approaches in defining a path integral. Again, some effective approach based on a path integral with Einstein-Hilbert action or the tensionless stringy setting on $AdS_3 \times S^3 \times T^4$ mentioned above. How are these approaches related? It might be expected that (in some way deformed) Einstein-Hilbert on AdS_3 might correspond to some averaged version of the tensionless string, in which fine-grained degrees of freedom are lost and only averaged information is recovered. Therefore, that some deformed version of the $\text{Sym}^N(T^4)$ CFT is dual to an effective bulk gravitational theory. In this context it has been shown that topological gravity coupled to a specific $U(1)^4$ Chern-Simons theory amounts to a bulk dual of an averaged Narain family of torus CFTs [149]. More drastically, more recent results suggest that this can be generalised. Reference

[150] provides evidence that Einstein-Hilbert on AdS_3 is dual to an average over all two-dimensional large c conformal field theories.

3.) We have also argued in this thesis that the off-shell geometries used in [80] and therefore also in chapters 4 and 6 play an important role. In terms of the spectral form factor they correct the early time decay. More heuristically, we may say they introduce some discreteness, which furnishes the sine-Kernel result given explicitly in (1.69).¹ As elucidated in [79], while indeed these geometries are off-shell in the canonical ensemble, it can at least be shown that in the microcanonical ensemble the double-trumpet ($n = 2, g = 0$ in the partition function (1.81)) amounts to an actual solution. It is of course important to understand if in higher dimensions some argument can be made for the inclusion of similar geometries. One specific case was made in the reference [83]. There it was argued that in the canonical ensemble wormhole geometries may contribute to the Euclidean path integral as non-perturbative effects. These wormhole geometries are analogues of the double-trumpet of [79] and [80]. More specifically, such geometries are not saddlepoints of the Einstein-Hilbert action but so-called constrained instantons. It would seem at least naively feasible for the case of AdS_3 to argue that not only the double-trumpet contributes, but also a geometry which is topologically more complicated. For example one might hope that one could argue for the consideration of more complicated boundary topologies and more than two boundaries. This would then take on a heuristic form similar in nature to (1.81). However, this would require the use of more involved hyperbolic geometry. The author also believes that the distinction between the non-compact moduli space of hyperbolic Riemann surfaces and its Mumford-Deligne compactification plays an important role.

4.) In chapter 6 it was explained that the JT path integral allows for the calculation of non-perturbatively corrected complexity. As only hinted at in that chapter, it would seem that there should be an alternative formalism in which replicated geometries appear. This should be the case as the annealed result, which would amount to taking an expectation value and then the logarithm, does not agree with our quenched result. Or in the language of chapter 6, $\langle y \rangle^N \neq \langle y^N \rangle$. In the spirit of [136], this might imply some wormhole formalism with N geometries retaining a connection even after the limit $N \rightarrow 0$. This would already happen at the disk level, where the classical result is recovered (linear growth of complexity in time).

5.) In chapter 7 (see also introductory section 1.6) we have identified the cosmic horizon as a potentially holographic region of de Sitter spacetime. It is for this reason that reference [119] suggests a modified procedure in calculating the complexity of de Sitter. Assuming that some kind of holographic model lives at the de Sitter cosmic horizon, it is reasonable to calculate complexity with respect to this region. This implies that in the CV proposal geodesics must be anchored to the cosmic horizon. It would be interesting to try and use the technology of reference [100] and section 6 to calculate the result for the CV proposal anchored at the cosmic horizon including the higher topologies of JT gravity. How can this be done in de Sitter? It would seem feasible to use the analytic continuation of [151] (see reference [152] for use of this continuation in a two-dimensional context). This analytic continuation links Lorentzian de Sitter spacetime to hyperbolic spacetime. Determining the correct result would allow one to draw conclusions about the nature of the dual holographic model. Reference [119] suggests that the proposed hyperfast complexity growth implies a double-scaled SYK

¹ See also chapter 4.

model as a microscopic description of dS_3 .

Bibliography

- [1] R. Bousso, *The Holographic principle*, *Rev. Mod. Phys.* **74** (2002) 825, arXiv: [hep-th/0203101](#) (cit. on pp. 1, 7, 37).
- [2] L. D'Alessio, Y. Kafri, A. Polkovnikov and M. Rigol, *From quantum chaos and eigenstate thermalization to statistical mechanics and thermodynamics*, *Adv. Phys.* **65** (2016) 239, arXiv: [1509.06411 \[cond-mat.stat-mech\]](#) (cit. on p. 1).
- [3] V. Jahnke, *Recent developments in the holographic description of quantum chaos*, *Adv. High Energy Phys.* **2019** (2019) 9632708, arXiv: [1811.06949 \[hep-th\]](#) (cit. on p. 1).
- [4] G. Sárosi, *AdS₂ holography and the SYK model*, *PoS Modave2017* (2018) 001, arXiv: [1711.08482 \[hep-th\]](#) (cit. on pp. 1, 9).
- [5] P. Di Francesco, P. H. Ginsparg and J. Zinn-Justin, *2-D Gravity and random matrices*, *Phys. Rept.* **254** (1995) 1, arXiv: [hep-th/9306153](#) (cit. on pp. 1, 24, 25, 27).
- [6] L. Susskind, “Three Lectures on Complexity and Black Holes”, SpringerBriefs in Physics, Springer, 2018, arXiv: [1810.11563 \[hep-th\]](#) (cit. on pp. 1, 31, 32).
- [7] S. Chapman and G. Policastro, *Quantum computational complexity from quantum information to black holes and back*, *Eur. Phys. J. C* **82** (2022) 128, arXiv: [2110.14672 \[hep-th\]](#) (cit. on pp. 1, 30, 32).
- [8] I. C. M.A. Nielsen, *Quantum computation and quantum information* (cit. on pp. 1, 28, 30).
- [9] J. M. Maldacena, *The Large N limit of superconformal field theories and supergravity*, *Adv. Theor. Math. Phys.* **2** (1998) 231, arXiv: [hep-th/9711200](#) (cit. on pp. 2, 6, 7).
- [10] E. Witten, *Anti-de Sitter space, thermal phase transition, and confinement in gauge theories*, *Adv. Theor. Math. Phys.* **2** (1998) 505, ed. by L. Bergstrom and U. Lindstrom, arXiv: [hep-th/9803131](#) (cit. on pp. 2, 112).
- [11] S. S. Gubser, I. R. Klebanov and A. M. Polyakov, *Gauge theory correlators from noncritical string theory*, *Phys. Lett. B* **428** (1998) 105, arXiv: [hep-th/9802109](#) (cit. on p. 2).
- [12] E. Witten, *Anti-de Sitter space and holography*, *Adv. Theor. Math. Phys.* **2** (1998) 253, arXiv: [hep-th/9802150](#) (cit. on p. 2).
- [13] S. W. Hawking, *Gravitational radiation from colliding black holes*, *Phys. Rev. Lett.* **26** (1971) 1344 (cit. on pp. 2, 3).
- [14] J. D. Bekenstein, *Black holes and the second law*, *Lett. Nuovo Cim.* **4** (1972) 737 (cit. on p. 2).
- [15] J. D. Bekenstein, *Black holes and entropy*, *Phys. Rev. D* **7** (1973) 2333 (cit. on p. 2).

- [16] J. D. Bekenstein, *Generalized second law of thermodynamics in black hole physics*, *Phys. Rev. D* **9** (1974) 3292 (cit. on p. 2).
- [17] W. Israel, *Event horizons in static vacuum space-times*, *Phys. Rev.* **164** (1967) 1776 (cit. on p. 3).
- [18] W. Israel, *Event horizons in static electrovac space-times*, *Commun. Math. Phys.* **8** (1968) 245 (cit. on p. 3).
- [19] B. Carter, *Axisymmetric Black Hole Has Only Two Degrees of Freedom*, *Phys. Rev. Lett.* **26** (1971) 331 (cit. on p. 3).
- [20] S. W. Hawking, *Black holes in general relativity*, *Commun. Math. Phys.* **25** (1972) 152 (cit. on p. 3).
- [21] J. D. Bekenstein, *A Universal Upper Bound on the Entropy to Energy Ratio for Bounded Systems*, *Phys. Rev. D* **23** (1981) 287 (cit. on p. 3).
- [22] G. 't Hooft, *Dimensional reduction in quantum gravity*, *Conf. Proc. C* **930308** (1993) 284, arXiv: [gr-qc/9310026](https://arxiv.org/abs/gr-qc/9310026) (cit. on p. 3).
- [23] L. Susskind, *The World as a hologram*, *J. Math. Phys.* **36** (1995) 6377, arXiv: [hep-th/9409089](https://arxiv.org/abs/hep-th/9409089) (cit. on p. 3).
- [24] G. 't Hooft, *A Planar Diagram Theory for Strong Interactions*, *Nucl. Phys. B* **72** (1974) 461, ed. by J. C. Taylor (cit. on pp. 4, 5, 25).
- [25] D. Tong, *Gauge Theory*, URL: <https://www.damtp.cam.ac.uk/user/tong/gaugetheory/gt.pdf> (cit. on p. 5).
- [26] G. T. Horowitz and A. Strominger, *Black strings and P-branes*, *Nucl. Phys. B* **360** (1991) 197 (cit. on p. 5).
- [27] J. de Boer, L. Maoz and A. Naqvi, *Some aspects of the AdS / CFT correspondence*, *IRMA Lect. Math. Theor. Phys.* **8** (2005) 33, ed. by O. Biquard, arXiv: [hep-th/0407212](https://arxiv.org/abs/hep-th/0407212) (cit. on p. 6).
- [28] M. Banados, <http://web.physics.ucsb.edu/pasi/Banados.pdf> (cit. on p. 6).
- [29] L. Susskind and E. Witten, *The Holographic bound in anti-de Sitter space*, (1998), arXiv: [hep-th/9805114](https://arxiv.org/abs/hep-th/9805114) (cit. on pp. 6, 7).
- [30] S. W. Hawking, *Black hole explosions*, *Nature* **248** (1974) 30 (cit. on p. 8).
- [31] S. W. Hawking, *Particle Creation by Black Holes*, *Commun. Math. Phys.* **43** (1975) 199, ed. by G. W. Gibbons and S. W. Hawking, [Erratum: *Commun. Math. Phys.* 46, 206 (1976)] (cit. on p. 8).
- [32] J. M. Bardeen, B. Carter and S. W. Hawking, *The Four laws of black hole mechanics*, *Commun. Math. Phys.* **31** (1973) 161 (cit. on p. 8).
- [33] V. Arnold, *Mathematical Methods of Classical Mechanics* (cit. on p. 8).
- [34] A. I. Larkin and Y. N. Ovchinnikov, *Quasiclassical Method in the Theory of Superconductivity*, *Soviet Journal of Experimental and Theoretical Physics* **28** (1969) 1200 (cit. on p. 9).

-
- [35] S. H. Shenker and D. Stanford, *Multiple Shocks*, *JHEP* **12** (2014) 046, arXiv: [1312.3296 \[hep-th\]](#) (cit. on pp. 9, 16).
- [36] D. A. Roberts, D. Stanford and L. Susskind, *Localized shocks*, *JHEP* **03** (2015) 051, arXiv: [1409.8180 \[hep-th\]](#) (cit. on pp. 9, 10, 16).
- [37] S. H. Shenker and D. Stanford, *Stringy effects in scrambling*, *JHEP* **05** (2015) 132, arXiv: [1412.6087 \[hep-th\]](#) (cit. on pp. 9, 16).
- [38] J. M. Deutsch, *Eigenstate thermalization hypothesis*, *Reports on Progress in Physics* **81** (2018) 082001, URL: <https://doi.org/10.1088/1361-6633/aac9f1> (cit. on pp. 10, 11).
- [39] G. T. Horowitz and V. E. Hubeny, *Quasinormal modes of AdS black holes and the approach to thermal equilibrium*, *Phys. Rev. D* **62** (2000) 024027, arXiv: [hep-th/9909056](#) (cit. on pp. 11, 17).
- [40] D. Birmingham, I. Sachs and S. N. Solodukhin, *Conformal field theory interpretation of black hole quasinormal modes*, *Phys. Rev. Lett.* **88** (2002) 151301, arXiv: [hep-th/0112055](#) (cit. on p. 11).
- [41] E. Wigner, *Annals Math* **62** (1955) 548 (cit. on p. 11).
- [42] E. Wigner, *Annals Math* **65** (1957) 203 (cit. on p. 11).
- [43] *Annals Math* **67** (1958) 325 (cit. on p. 11).
- [44] F. J. Dyson, *Statistical theory of the energy levels of complex systems. I*, *J. Math. Phys.* **3** (1962) 140 (cit. on pp. 11, 18).
- [45] T. Guhr, A. Muller-Groeling and H. A. Weidenmuller, *Random matrix theories in quantum physics: Common concepts*, *Phys. Rept.* **299** (1998) 189, arXiv: [cond-mat/9707301](#) (cit. on p. 12).
- [46] Y. Alhassid, *The Statistical theory of quantum dots*, *Rev. Mod. Phys.* **72** (2000) 895, arXiv: [cond-mat/0102268](#) (cit. on pp. 12, 13).
- [47] V. E. Kravtsov, *Random matrix theory: Wigner-Dyson statistics and beyond: Lecture notes given at SISSA (Trieste, Italy)*, (2009), arXiv: [0911.0639 \[cond-mat.dis-nn\]](#) (cit. on p. 12).
- [48] A. Altland and M. R. Zirnbauer, *Nonstandard symmetry classes in mesoscopic normal-superconducting hybrid structures*, *Phys. Rev. B* **55** (2 1997) 1142, URL: <https://link.aps.org/doi/10.1103/PhysRevB.55.1142> (cit. on p. 13).
- [49] M. R. Zirnbauer, *Riemannian symmetric superspaces and their origin in random-matrix theory*, *J. Math. Phys.* **37** (1996) 4986, arXiv: [math-ph/9808012](#) (cit. on p. 13).
- [50] O. Bohigas, M. J. Giannoni and C. Schmit, *Characterization of chaotic quantum spectra and universality of level fluctuation laws*, *Phys. Rev. Lett.* **52** (1984) 1 (cit. on p. 13).
- [51] T. A. Brody et al., *Random matrix physics: Spectrum and strength fluctuations*, *Rev. Mod. Phys.* **53** (1981) 385 (cit. on p. 14).

- [52] B. M. Victor and T. M., *Level clustering in the regular spectrum*, Proc. R. Soc. Lond. A356:375–394 (1977) (cit. on p. 15).
- [53] M. Srednicki, *Chaos and Quantum Thermalization*, (1994), arXiv: [cond-mat/9403051](https://arxiv.org/abs/cond-mat/9403051) (cit. on p. 15).
- [54] M. Srednicki, *The approach to thermal equilibrium in quantized chaotic systems*, J.Phys.A **32** (1999) (cit. on p. 15).
- [55] M. Srednicki, *Thermal fluctuations in quantized chaotic systems*, J. Phys. A **29** (1996) L75, arXiv: [chao-dyn/9511001](https://arxiv.org/abs/chao-dyn/9511001) (cit. on p. 15).
- [56] S. H. Shenker and D. Stanford, *Black holes and the butterfly effect*, JHEP **03** (2014) 067, arXiv: [1306.0622](https://arxiv.org/abs/1306.0622) [hep-th] (cit. on p. 16).
- [57] J. Polchinski, *Chaos in the black hole S-matrix*, (2015), arXiv: [1505.08108](https://arxiv.org/abs/1505.08108) [hep-th] (cit. on p. 16).
- [58] J. Maldacena, S. H. Shenker and D. Stanford, *A bound on chaos*, JHEP **08** (2016) 106, arXiv: [1503.01409](https://arxiv.org/abs/1503.01409) [hep-th] (cit. on p. 16).
- [59] Y. Sekino and L. Susskind, *Fast Scramblers*, JHEP **10** (2008) 065, arXiv: [0808.2096](https://arxiv.org/abs/0808.2096) [hep-th] (cit. on p. 16).
- [60] J. M. Maldacena, *Eternal black holes in anti-de Sitter*, JHEP **04** (2003) 021, arXiv: [hep-th/0106112](https://arxiv.org/abs/hep-th/0106112) (cit. on pp. 16, 17, 173).
- [61] K. Papadodimas and S. Raju, *Local Operators in the Eternal Black Hole*, Phys. Rev. Lett. **115** (2015) 211601, arXiv: [1502.06692](https://arxiv.org/abs/1502.06692) [hep-th] (cit. on p. 17).
- [62] F. Wegner, *The mobility edge problem: Continuous symmetry and a conjecture*, Zeitschrift für Physik B Condensed Matter **35** (1979) 207, URL: <https://doi.org/10.1007/BF01319839> (cit. on p. 18).
- [63] K. B. Efetov, *Supersymmetry and theory of disordered metals*, Adv. Phys. **32** (1983) 53 (cit. on p. 18).
- [64] A. Altland and J. Sonner, *Late time physics of holographic quantum chaos*, SciPost Phys. **11** (2021) 034, arXiv: [2008.02271](https://arxiv.org/abs/2008.02271) [hep-th] (cit. on p. 18).
- [65] M. Mehta, *On the statistical properties of the level-spacings in nuclear spectra*, Nuclear Physics **18** (1960) 395, ISSN: 0029-5582, URL: <https://www.sciencedirect.com/science/article/pii/0029558260904132> (cit. on p. 18).
- [66] M. Gaudin, *Sur la loi limite de l'espacement des valeurs propres d'une matrice ale'atoire*, Nuclear Physics **25** (1961) 447, ISSN: 0029-5582, URL: <https://www.sciencedirect.com/science/article/pii/0029558261901766> (cit. on p. 18).
- [67] A. V. Andreev and B. L. Altshuler, *Spectral Statistics beyond Random Matrix Theory*, Phys. Rev. Lett. **75** (5 1995) 902, URL: <https://link.aps.org/doi/10.1103/PhysRevLett.75.902> (cit. on p. 18).

-
- [68] J. S. Cotler et al., *Black Holes and Random Matrices*, [JHEP 05 \(2017\) 118](#), [Erratum: [JHEP 09, 002 \(2018\)](#)], arXiv: [1611.04650 \[hep-th\]](#) (cit. on pp. [19](#), [20](#)).
- [69] R. Jackiw, *Lower Dimensional Gravity*, [Nucl. Phys. B 252 \(1985\) 343](#), ed. by R. Baier and H. Satz (cit. on p. [19](#)).
- [70] C. Teitelboim, *Gravitation and Hamiltonian Structure in Two Space-Time Dimensions*, [Phys. Lett. B 126 \(1983\) 41](#) (cit. on p. [19](#)).
- [71] J. Maldacena, D. Stanford and Z. Yang, *Conformal symmetry and its breaking in two dimensional Nearly Anti-de-Sitter space*, [PTEP 2016 \(2016\) 12C104](#), arXiv: [1606.01857 \[hep-th\]](#) (cit. on p. [19](#)).
- [72] J. Engelsöy, T. G. Mertens and H. Verlinde, *An investigation of AdS_2 backreaction and holography*, [JHEP 07 \(2016\) 139](#), arXiv: [1606.03438 \[hep-th\]](#) (cit. on p. [19](#)).
- [73] A. Almheiri and J. Polchinski, *Models of AdS_2 backreaction and holography*, [JHEP 11 \(2015\) 014](#), arXiv: [1402.6334 \[hep-th\]](#) (cit. on p. [19](#)).
- [74] D. Stanford and E. Witten, *Fermionic Localization of the Schwarzian Theory*, [JHEP 10 \(2017\) 008](#), arXiv: [1703.04612 \[hep-th\]](#) (cit. on pp. [20](#), [21](#)).
- [75] D. Bagrets, A. Altland and A. Kamenev, *Power-law out of time order correlation functions in the SYK model*, [Nucl. Phys. B 921 \(2017\) 727](#), arXiv: [1702.08902 \[cond-mat.str-el\]](#) (cit. on p. [20](#)).
- [76] T. G. Mertens, G. J. Turiaci and H. L. Verlinde, *Solving the Schwarzian via the Conformal Bootstrap*, [JHEP 08 \(2017\) 136](#), arXiv: [1705.08408 \[hep-th\]](#) (cit. on p. [20](#)).
- [77] A. Kitaev and S. J. Suh, *Statistical mechanics of a two-dimensional black hole*, [JHEP 05 \(2019\) 198](#), arXiv: [1808.07032 \[hep-th\]](#) (cit. on p. [20](#)).
- [78] Z. Yang, *The Quantum Gravity Dynamics of Near Extremal Black Holes*, [JHEP 05 \(2019\) 205](#), arXiv: [1809.08647 \[hep-th\]](#) (cit. on pp. [20](#), [35](#)).
- [79] P. Saad, S. H. Shenker and D. Stanford, *A semiclassical ramp in SYK and in gravity*, (2018), arXiv: [1806.06840 \[hep-th\]](#) (cit. on pp. [20](#), [23](#), [241](#)).
- [80] P. Saad, S. H. Shenker and D. Stanford, *JT gravity as a matrix integral*, (2019), arXiv: [1903.11115 \[hep-th\]](#) (cit. on pp. [20–23](#), [26](#), [33](#), [34](#), [240](#), [241](#)).
- [81] M. Mirzakhani, *Simple geodesics and Weil-Petersson volumes of moduli spaces of bordered Riemann surfaces*, [Invent. Math. 167 \(2006\) 179](#) (cit. on p. [22](#)).
- [82] B. Eynard and N. Orantin, *Weil-Petersson volume of moduli spaces, Mirzakhani's recursion and matrix models*, (2007), arXiv: [0705.3600 \[math-ph\]](#) (cit. on p. [22](#)).
- [83] J. Cotler and K. Jensen, *Gravitational Constrained Instantons*, [Phys. Rev. D 104 \(2021\) 081501](#), arXiv: [2010.02241 \[hep-th\]](#) (cit. on pp. [23](#), [241](#)).

- [84] M. R. Douglas and S. H. Shenker, *Strings in less than one dimension*, *Nuclear Physics B* **335** (1990) 635, ISSN: 0550-3213, URL: <https://www.sciencedirect.com/science/article/pii/055032139090522F> (cit. on p. 25).
- [85] E. Brezin and V. A. Kazakov, *Exactly Solvable Field Theories of Closed Strings*, *Phys. Lett. B* **236** (1990) 144 (cit. on p. 25).
- [86] D. J. Gross and A. A. Migdal, *Nonperturbative Two-Dimensional Quantum Gravity*, *Phys. Rev. Lett.* **64** (1990) 127, ed. by E. Brezin and S. R. Wadia (cit. on p. 25).
- [87] V. A. Kazakov, *The Appearance of Matter Fields from Quantum Fluctuations of 2D Gravity*, *Mod. Phys. Lett. A* **4** (1989) 2125, ed. by E. Brezin and S. R. Wadia (cit. on p. 26).
- [88] M. Staudacher, *The Yang-Lee edge singularity on a dynamical planar random surface*, *Nuclear Physics B* **336** (1990) 349, ISSN: 0550-3213, URL: <https://www.sciencedirect.com/science/article/pii/055032139090432D> (cit. on p. 26).
- [89] G. W. Moore, N. Seiberg and M. Staudacher, *From loops to states in 2-D quantum gravity*, *Nucl. Phys. B* **362** (1991) 665 (cit. on p. 26).
- [90] E. Witten, *On the Structure of the Topological Phase of Two-dimensional Gravity*, *Nucl. Phys. B* **340** (1990) 281 (cit. on p. 26).
- [91] E. Witten, *Two-dimensional gravity and intersection theory on moduli space*, *Surveys Diff. Geom.* **1** (1991) 243 (cit. on p. 26).
- [92] S. Aaronson, “The Complexity of Quantum States and Transformations: From Quantum Money to Black Holes”, 2016, arXiv: [1607.05256](https://arxiv.org/abs/1607.05256) [[quant-ph](https://arxiv.org/archive/quant)] (cit. on p. 27).
- [93] L. Susskind, *Computational Complexity and Black Hole Horizons*, *Fortsch. Phys.* **64** (2016) 24, [Addendum: *Fortsch.Phys.* 64, 44–48 (2016)], arXiv: [1403.5695](https://arxiv.org/abs/1403.5695) [[hep-th](https://arxiv.org/archive/hep)] (cit. on pp. 27, 32).
- [94] D. Stanford and L. Susskind, *Complexity and Shock Wave Geometries*, *Phys. Rev. D* **90** (2014) 126007, arXiv: [1406.2678](https://arxiv.org/abs/1406.2678) [[hep-th](https://arxiv.org/archive/hep)] (cit. on pp. 27, 32, 33).
- [95] A. R. Brown, D. A. Roberts, L. Susskind, B. Swingle and Y. Zhao, *Complexity, action, and black holes*, *Phys. Rev. D* **93** (2016) 086006, arXiv: [1512.04993](https://arxiv.org/abs/1512.04993) [[hep-th](https://arxiv.org/archive/hep)] (cit. on pp. 27, 32, 33).
- [96] A. R. Brown, D. A. Roberts, L. Susskind, B. Swingle and Y. Zhao, *Holographic Complexity Equals Bulk Action?*, *Phys. Rev. Lett.* **116** (2016) 191301, arXiv: [1509.07876](https://arxiv.org/abs/1509.07876) [[hep-th](https://arxiv.org/archive/hep)] (cit. on pp. 27, 32).
- [97] L. J. Boya, E. Sudarshan and T. Tilma, *Volumes of compact manifolds*, *Reports on Mathematical Physics* **52** (2003) 401, ISSN: 0034-4877, URL: [http://dx.doi.org/10.1016/S0034-4877\(03\)80038-1](http://dx.doi.org/10.1016/S0034-4877(03)80038-1) (cit. on p. 29).
- [98] A. Belin, R. C. Myers, S.-M. Ruan, G. Sárosi and A. J. Speranza, *Does Complexity Equal Anything?*, *Phys. Rev. Lett.* **128** (2022) 081602, arXiv: [2111.02429](https://arxiv.org/abs/2111.02429) [[hep-th](https://arxiv.org/archive/hep)] (cit. on p. 31).

-
- [99] D. Carmi, S. Chapman, H. Marrochio, R. C. Myers and S. Sugishita, *On the Time Dependence of Holographic Complexity*, **JHEP** **11** (2017) 188, arXiv: [1709.10184 \[hep-th\]](#) (cit. on p. 33).
- [100] L. V. Iliesiu, M. Mezei and G. Sárosi, *The volume of the black hole interior at late times*, (2021), arXiv: [2107.06286 \[hep-th\]](#) (cit. on pp. 33–35, 241).
- [101] P. Saad, *Late Time Correlation Functions, Baby Universes, and ETH in JT Gravity*, (2019), arXiv: [1910.10311 \[hep-th\]](#) (cit. on pp. 34, 35).
- [102] D. Harlow and D. Jafferis, *The Factorization Problem in Jackiw-Teitelboim Gravity*, **JHEP** **02** (2020) 177, arXiv: [1804.01081 \[hep-th\]](#) (cit. on p. 35).
- [103] A. H. Guth, *The Inflationary Universe: A Possible Solution to the Horizon and Flatness Problems*, **Phys. Rev. D** **23** (1981) 347, ed. by L.-Z. Fang and R. Ruffini (cit. on p. 35).
- [104] A. D. Linde, *A New Inflationary Universe Scenario: A Possible Solution of the Horizon, Flatness, Homogeneity, Isotropy and Primordial Monopole Problems*, **Phys. Lett. B** **108** (1982) 389, ed. by L.-Z. Fang and R. Ruffini (cit. on p. 35).
- [105] A. Albrecht and P. J. Steinhardt, *Cosmology for Grand Unified Theories with Radiatively Induced Symmetry Breaking*, **Phys. Rev. Lett.** **48** (1982) 1220, ed. by L.-Z. Fang and R. Ruffini (cit. on p. 35).
- [106] R. H. Dicke, P. J. E. Peebles, P. G. Roll and D. T. Wilkinson, *Cosmic Black-Body Radiation*, **Astrophys. J.** **142** (1965) 414 (cit. on p. 35).
- [107] S. Perlmutter et al., *Measurements of Ω and Λ from 42 high redshift supernovae*, **Astrophys. J.** **517** (1999) 565, arXiv: [astro-ph/9812133](#) (cit. on p. 35).
- [108] A. G. Riess et al., *Observational evidence from supernovae for an accelerating universe and a cosmological constant*, **Astron. J.** **116** (1998) 1009, arXiv: [astro-ph/9805201](#) (cit. on p. 35).
- [109] G. W. Gibbons and S. W. Hawking, *Cosmological Event Horizons, Thermodynamics, and Particle Creation*, **Phys. Rev. D** **15** (1977) 2738 (cit. on p. 35).
- [110] W. Fischler and L. Susskind, *Holography and cosmology*, (1998), arXiv: [hep-th/9806039](#) (cit. on p. 36).
- [111] R. Bousso, *A Covariant entropy conjecture*, **JHEP** **07** (1999) 004, arXiv: [hep-th/9905177](#) (cit. on pp. 36, 37).
- [112] A. C. Wall, *A proof of the generalized second law for rapidly changing fields and arbitrary horizon slices*, **Phys. Rev. D** **85** (2012) 104049, [Erratum: **Phys.Rev.D** 87, 069904 (2013)], arXiv: [1105.3445 \[gr-qc\]](#) (cit. on p. 37).
- [113] H. Casini, *Relative entropy and the Bekenstein bound*, **Class. Quant. Grav.** **25** (2008) 205021, arXiv: [0804.2182 \[hep-th\]](#) (cit. on p. 37).
- [114] R. Bousso, Z. Fisher, S. Leichenauer and A. C. Wall, *Quantum focusing conjecture*, **Phys. Rev. D** **93** (2016) 064044, arXiv: [1506.02669 \[hep-th\]](#) (cit. on p. 37).

- [115] R. Bousso, *Holography in general space-times*, **JHEP** **06** (1999) 028, arXiv: [hep-th/9906022](#) (cit. on pp. 38, 39).
- [116] J. M. Maldacena, *Non-Gaussian features of primordial fluctuations in single field inflationary models*, **JHEP** **05** (2003) 013, arXiv: [astro-ph/0210603](#) (cit. on p. 38).
- [117] A. Strominger, *The dS / CFT correspondence*, **JHEP** **10** (2001) 034, arXiv: [hep-th/0106113](#) (cit. on p. 38).
- [118] E. Witten, “Quantum gravity in de Sitter space”, *Strings 2001: International Conference*, 2001, arXiv: [hep-th/0106109](#) (cit. on p. 38).
- [119] L. Susskind, *Entanglement and Chaos in De Sitter Holography: An SYK Example*, (2021), arXiv: [2109.14104 \[hep-th\]](#) (cit. on pp. 38, 241).
- [120] S. Förste, J. Kames-King and M. Wiesner, *Towards the Holographic Dual of $N = 2$ SYK*, **JHEP** **03** (2018) 028, arXiv: [1712.07398 \[hep-th\]](#) (cit. on p. 41).
- [121] W. Fu, D. Gaiotto, J. Maldacena and S. Sachdev, *Supersymmetric Sachdev-Ye-Kitaev models*, **Phys. Rev. D** **95** (2017) 026009, [Addendum: *Phys.Rev.D* 95, 069904 (2017)], arXiv: [1610.08917 \[hep-th\]](#) (cit. on p. 41).
- [122] J. Gomis et al., *Anomalies, Conformal Manifolds, and Spheres*, **JHEP** **03** (2016) 022, arXiv: [1509.08511 \[hep-th\]](#) (cit. on p. 42).
- [123] S. Förste, A. Gerhardus and J. Kames-King, *Supersymmetric black holes and the $SJT/nSCFT_1$ correspondence*, **JHEP** **01** (2021) 186, arXiv: [2007.12393 \[hep-th\]](#) (cit. on p. 65).
- [124] P. Nayak, A. Shukla, R. M. Soni, S. P. Trivedi and V. Vishal, *On the Dynamics of Near-Extremal Black Holes*, **JHEP** **09** (2018) 048, arXiv: [1802.09547 \[hep-th\]](#) (cit. on p. 65).
- [125] K. Hristov and S. Vandoren, *Static supersymmetric black holes in AdS_4 with spherical symmetry*, **JHEP** **04** (2011) 047, arXiv: [1012.4314 \[hep-th\]](#) (cit. on p. 65).
- [126] S. L. Cacciatori and D. Klemm, *Supersymmetric $AdS(4)$ black holes and attractors*, **JHEP** **01** (2010) 085, arXiv: [0911.4926 \[hep-th\]](#) (cit. on p. 65).
- [127] S. J. Gates Jr., M. T. Grisaru and M. E. Wehlau, *A Study of general 2-D, $N=2$ matter coupled to supergravity in superspace*, **Nucl. Phys. B** **460** (1996) 579, arXiv: [hep-th/9509021](#) (cit. on p. 66).
- [128] S. Forste, H. Jockers, J. Kames-King and A. Kanargias, *Deformations of JT gravity via topological gravity and applications*, **JHEP** **11** (2021) 154, arXiv: [2107.02773 \[hep-th\]](#) (cit. on p. 111).
- [129] E. Witten, *Matrix Models and Deformations of JT Gravity*, **Proc. Roy. Soc. Lond. A** **476** (2020) 20200582, arXiv: [2006.13414 \[hep-th\]](#) (cit. on p. 111).
- [130] H. Maxfield and G. J. Turiaci, *The path integral of 3D gravity near extremality; or, JT gravity with defects as a matrix integral*, **JHEP** **01** (2021) 118, arXiv: [2006.11317 \[hep-th\]](#) (cit. on p. 111).

-
- [131] M. Alishahiha, S. Banerjee, J. Kames-King and E. Loos, *Complexity as a holographic probe of strong cosmic censorship*, *Phys. Rev. D* **105** (2022) 026001, arXiv: 2106.14578 [hep-th] (cit. on p. 157).
- [132] K. Papadodimas and S. Raju, *An Infalling Observer in AdS/CFT*, *JHEP* **10** (2013) 212, arXiv: 1211.6767 [hep-th] (cit. on p. 158).
- [133] K. Papadodimas and S. Raju, *State-Dependent Bulk-Boundary Maps and Black Hole Complementarity*, *Phys. Rev. D* **89** (2014) 086010, arXiv: 1310.6335 [hep-th] (cit. on p. 158).
- [134] M. Alishahiha, S. Banerjee and J. Kames-King, *Complexity via Replica Trick*, (2022), arXiv: 2205.01150 [hep-th] (cit. on p. 173).
- [135] I. Kourkoulou and J. Maldacena, *Pure states in the SYK model and nearly-AdS₂ gravity*, (2017), arXiv: 1707.02325 [hep-th] (cit. on p. 173).
- [136] N. Engelhardt, S. Fischetti and A. Maloney, *Free energy from replica wormholes*, *Phys. Rev. D* **103** (2021) 046021, arXiv: 2007.07444 [hep-th] (cit. on pp. 174, 241).
- [137] G. Penington, S. H. Shenker, D. Stanford and Z. Yang, *Replica wormholes and the black hole interior*, *JHEP* **03** (2022) 205, arXiv: 1911.11977 [hep-th] (cit. on p. 174).
- [138] J. Kames-King, E. M. H. Verheijden and E. P. Verlinde, *No Page curves for the de Sitter horizon*, *JHEP* **03** (2022) 040, arXiv: 2108.09318 [hep-th] (cit. on p. 205).
- [139] L. Aalsma, M. Parikh and J. P. Van Der Schaar, *Back(reaction) to the Future in the Unruh-de Sitter State*, *JHEP* **11** (2019) 136, arXiv: 1905.02714 [hep-th] (cit. on p. 205).
- [140] L. Eberhardt, M. R. Gaberdiel and R. Gopakumar, *The Worldsheet Dual of the Symmetric Product CFT*, *JHEP* **04** (2019) 103, arXiv: 1812.01007 [hep-th] (cit. on p. 240).
- [141] L. Eberhardt, M. R. Gaberdiel and R. Gopakumar, *Deriving the AdS₃/CFT₂ correspondence*, *JHEP* **02** (2020) 136, arXiv: 1911.00378 [hep-th] (cit. on p. 240).
- [142] A. Dei, M. R. Gaberdiel, R. Gopakumar and B. Knighton, *Free field world-sheet correlators for AdS₃*, *JHEP* **02** (2021) 081, arXiv: 2009.11306 [hep-th] (cit. on p. 240).
- [143] G. Giribet, C. Hull, M. Kleban, M. Porrati and E. Rabinovici, *Superstrings on AdS₃ at || = 1*, *JHEP* **08** (2018) 204, arXiv: 1803.04420 [hep-th] (cit. on p. 240).
- [144] J. M. Maldacena and L. Maoz, *Wormholes in AdS*, *JHEP* **02** (2004) 053, arXiv: hep-th/0401024 (cit. on p. 240).
- [145] N. Arkani-Hamed, J. Orgera and J. Polchinski, *Euclidean wormholes in string theory*, *JHEP* **12** (2007) 018, arXiv: 0705.2768 [hep-th] (cit. on p. 240).
- [146] D. Marolf and J. E. Santos, *AdS Euclidean wormholes*, *Class. Quant. Grav.* **38** (2021) 224002, arXiv: 2101.08875 [hep-th] (cit. on p. 240).

- [147] A. Blommaert and J. Kruthoff, *Gravity without averaging*, *SciPost Phys.* **12** (2022) 073, arXiv: [2107.02178 \[hep-th\]](#) (cit. on p. 240).
- [148] A. Blommaert, L. V. Iliesiu and J. Kruthoff, *Gravity factorized*, (2021), arXiv: [2111.07863 \[hep-th\]](#) (cit. on p. 240).
- [149] A. Maloney and E. Witten, *Averaging over Narain moduli space*, *JHEP* **10** (2020) 187, arXiv: [2006.04855 \[hep-th\]](#) (cit. on p. 240).
- [150] J. Chandra, S. Collier, T. Hartman and A. Maloney, *Semiclassical 3D gravity as an average of large- c CFTs*, (2022), arXiv: [2203.06511 \[hep-th\]](#) (cit. on p. 241).
- [151] J. Maldacena, *Vacuum decay into Anti de Sitter space*, (2010), arXiv: [1012.0274 \[hep-th\]](#) (cit. on p. 241).
- [152] J. Maldacena, G. J. Turiaci and Z. Yang, *Two dimensional Nearly de Sitter gravity*, *JHEP* **01** (2021) 139, arXiv: [1904.01911 \[hep-th\]](#) (cit. on p. 241).

List of Figures

1.1	The large n limit of a $SU(n)$ gluon propagator depicted in terms of double-line notation first introduced in [24]. Figure taken from [25].	5
1.2	Schematic depiction of $C(t)$ (as defined in (1.29)) for a chaotic system. Following a short "collusion time" $t_d \sim \beta$, $C(t)$ enters a regime of exponential Lyapunov growth. This ends at the scrambling time t_s (1.31). Thereafter $C(t)$ saturates to the late-time average. Figure taken from [4].	9
1.3	Here we see the <i>log-log</i> plot of the spectral form factor (as defined in (1.67)) for the SYK model [68]. More concretely, the parameters of the depicted SYK model are: $q = 4$, $N = 34$, $\beta\mathcal{J} = 5$, where q specifies the number of fermions (randomly) interacting with each other, N specifies the total number of fermions, β is the inverse temperature and finally J is the coupling. The x-axis labelling T refers to the time. Both a single SYK model sample (red) and a disorder average over 90 samples (black) are depicted. Figure taken from [68].	19
1.4	Depicted are the surfaces contributing to the single boundary partition function, which amounts to (1.82). These surfaces consist of one asymptotic boundary but an arbitrary genus g . Furthermore as the Euler characteristic is $\chi = 1 - 2g$, the weighting is $e^{(1-2g)S_0}$. Figure taken from [80].	21
1.5	Depiction of the contribution $Z_{g=2, n=1}$ to (1.81). The path integral over ϕ constrains in each topological class to $R = -2$ surfaces. The path integral over the metric reduces to an integral over metric fluctuations on the asymptotic boundary (pictured on the left here) and a finite-dimensional integral over geometric moduli. We may think of the entire surface as the trumpet glued to a Riemann surface with geodesic boundary of length b and $g = 2$. The gluing has two parameters, the length b and a twist, both of which have to be integrated over. This procedure leads for the case of a single boundary to the expression (1.82). Figure taken from [80].	22
1.6	Schematic depiction of the "pants" approach used in constructing hyperbolic Riemann surfaces with boundary and arbitrary genus. Each pair of pants amounts to a $g = 0$ surface with three geodesic boundaries. For the contributions to the path integral (1.80), the moduli space of bordered Riemann surfaces $\mathcal{M}_{g,n}(b_1, \dots, b_n)$ up to arbitrary values is required. While in principle this may be calculated via the integral over the so-called Weil-Petersson symplectic form (restricted to a fundamental domain), in the seminal result of [81], it was shown that these volumes obey a recursion relation. Figure taken from [80].	22
1.7	Depiction of Feynman diagrams corresponding to the theory defined in (1.91). The left panel shows the propagator and the right shows the vertex. Figure taken from [5].	24

1.8	Depiction of Feynman diagrams corresponding to the theory defined in(1.94). We are using a double-line representation of the matrix indices. On the left panel we see the propagator and on the right the vertex. Figure taken from [5].	25
1.9	A random matrix triangulisation of the theory of surfaces defined in (1.86) by the matrix integral (1.95). Figure taken from [5].	27
1.10	The Bloch sphere (Riemann sphere) geometrically represents the pure states of the qubit (1.105). Without loss of generality, north and south pole correspond to the mutually orthogonal states $ 0\rangle$ and $ 1\rangle$ respectively. Each point on the sphere represents a state of the two-dimensional system. Figure taken from [8].	28
1.11	Depiction of the evolution of complexity for a N qubit model with a k -local (chaotic) Hamiltonian under the assumption that $k \ll N$. We can imagine time going from left to right, therefore e^{iHt} acting on the system. The specific setting shown here, has $N = 6$ and $k = 2$ and there are no restrictions on spatial locality, therefore the system is all-to-all. Figure taken from [6].	31
1.12	Schematic depiction of the evolution of complexity for a chaotic system in time. We observe early linear growth exponential in the degrees of freedom and a late time saturation to a constant value. Quantum recurrence is expected to occur on a doubly exponential timescale [6, 7]. Figure taken from [7].	32
1.13	The three different surface topologies, which contribute to the calculation of $\langle \text{Tr}_B(\chi(x_1)\chi(x_2)) \rangle$ in the context of JT gravity. In red we see the boundary-to-boundary geodesic which furnishes these topologies in the path integral and leads to the moduli space structure of (1.130). Green depicts the asymptotic AdS boundary with graviton fluctuations. In purple we see the closed geodesics along which the wavefunctions are glued and therefore in the formula (1.130) amounts to the b_1 and b_2 integrations. Figure taken from [100].	34
1.14	There are four null hypersurfaces F_1, \dots, F_4 orthogonal to the spherical surface B . Whereas F_1 and F_3 exhibit negative expansion, F_2 and F_3 have positive expansion and are therefore not relevant to the entropy bound. F_1 and F_3 are denoted as light-sheets and may be used in (1.133). Figure taken from [1].	37
1.15	Penrose diagram of dS. The diagonal lines in the left panel are horizons dividing the spacetime into four regions corresponding to the different behaviour of changes to the area of S^{D-2} spheres. The legs of "wedges" indicate the direction of negative expansion. In the middle panel we see diagonal lines which correspond to a null foliation of spacetime in terms of past light cones of an observer on the north pole and future light cones for an observer on the south pole. We see that the projection, which runs along the tip of the nose gives two options for an holographic screen. In the middle we see that the spacetime may be projected onto a screen at both conformal boundaries \mathcal{I}^+ and \mathcal{I}^- or as in the panel on the right. Here, we see the north pole observer projected onto the cosmological horizon. Figure taken from [115].	39